

# Sunday

104<sup>th</sup> Scientific Assembly and Annual Meeting November 25–30 | McCormick Place, Chicago





#### PS10

#### **Opening Session**

Sunday, Nov. 25 8:30AM - 10:15AM Room: Arie Crown Theater



AMA PRA Category 1 Credits ™: 1.75 ARRT Category A+ Credit: 1.25

#### Participants

Vijay M. Rao, MD, Philadelphia, PA (*Presenter*) Nothing to Disclose Bruce R. Thomadsen, PhD, Madison, WI (*Presenter*) Nothing to Disclose Bojan D. Petrovic, MD, Glencoe, IL (*Presenter*) Nothing to Disclose

#### For information about this presentation, contact:

bpetrovic2@northshore.org

#### Sub-Events

# PS10A Presentation of the Outstanding Educator Award

Participants

David M. Yousem, MD, Baltimore, MD (*Recipient*) Royalties, Reed Elsevier; Speaker, American College of Radiology; Employee, Medicolegal Consultation; ; ;

For information about this presentation, contact:

dyousem1@jhu.edu

# PS10B Presentation of the Outstanding Researcher Award

Participants Carolyn C. Meltzer, MD, Atlanta, GA (*Recipient*) Nothing to Disclose

# For information about this presentation, contact:

cmeltze@emory.edu

- PS10C Dedication of the 2018 RSNA Meeting Program to the Memory of William G. Bradley Jr, MD, PhD (1948-2017), and Alexander R. Margulis, MD (1921-2018)
- PS10D President's Address: How Emerging Technology Will Empower Tomorrow's Radiologists to Provide Better Patient Care

Participants

Vijay M. Rao, MD, Philadelphia, PA (Presenter) Nothing to Disclose

David C. Levin, MD, Philadelphia, PA (Presenter) Consultant, HealthHelp, LLC; Board Member, Outpatient Imaging Affiliates, LLC

# Abstract

With rapid advances in artificial intelligence (AI) and related technologies, radiologists have an opportunity to improve the quality of care they provide to patients, as well as to increase their stature within the medical community and the personal and professional satisfaction they derive from their work. This is true not only in the United States but also around the world. With an aging population and continual growth in imaging procedures globally, a large amount of complex imaging data is available for data mining. AI will enable us to harness the data more effectively. Although AI algorithms for medical imaging are being developed at a fast pace across the globe, many questions remain unanswered regarding computer ethics, regulatory compliance and lack of standards. Digital extraction of quantitative features of lesions that reveal their underlying pathophysiology -- and perhaps even their genetic basis -- are the underpinnings of imaging biomarkers and radiomics. The science of radiology will be greatly enhanced if this potential is actually realized, but it will require a tremendous worldwide effort on the part of all in the field, as well as from organizations like RSNA that are dedicated to advancing the science. Radiologists will also have an opportunity to become integrators or aggregators of diagnostic data. The Interagency Working Group on Medical Imaging of the National Science and Technology Council has proposed the concept of the "diagnostic cockpit." In such a construct, recent findings from other imaging studies, lab results, other test results, key aspects of the patient history and physical exam, and patient demographics and risk factors are all extracted from the EMR, then aggregated to provide the greatest likelihood of not only a correct diagnosis but also a prediction of prognosis and response to personalized therapy. Who is better positioned to lead such an entity than radiologists? The time has come for radiologists to position themselves to provide such leadership in driving this field to the next level. Radiologists will have to increase their knowledge of all aspects of diseases and data science aside from just the imaging aspects. AI applications will provide benefits at every step of the life cycle of an imaging test by increasing the efficiency of the radiology department workflow in many ways, and it will free up some of the time radiologists now spend on image interpretation. That extra time should be spent on greater engagement with patients. This means discussing the imaging tests with them and taking on more responsibility for their total imaging care. Our colleagues in interventional radiology and breast imaging are already doing this, and the rest of the profession must follow suit. If tomorrow's radiologists can accomplish all this, they will become even more essential members of the clinical care team.

# PS10E Annual Oration in Diagnostic Radiology: Artificial Intelligence, Analytics, and Informatics: The Future is Here

Participants

Michael P. Recht, MD, New York, NY (*Presenter*) Nothing to Disclose David H. Kim, MD, Middleton, WI (*Introduction*) Shareholder, Cellectar Biosciences, Inc; Shareholder, Elucent Medical;

# Abstract

This is an exciting yet challenging time for Radiology. The transformation from a fee for service to a value driven health care system, the increasing sophistication and demands of our patients and referring physicians, the rapid advancements in imaging technology, and the explosive development of artificial intelligence/machine learning all promise significant disruptions to the current practice of Radiology. It is imperative that radiologists face these challenges head on in order to shape our future. To do that, we need to take the lead in utilizing informatics, analytics/business intelligence, and artificial intelligence/machine learning to enhance the value of imaging and radiologists. To demonstrate our value, radiologists must become more integrated into the clinical care team, and more visible and "user-friendly" to both referring physicians and our patients. This, however, is an ever more difficult proposition, due to the increasing demands on our time - for example, the demand for increased productivity, and increasing regulatory requirements - and due to the ongoing geographic dispersion of our practices. The development of several innovations in informatics has helped us meet this challenge. Some examples include virtual rounds and virtual consults, enhanced (multimedia) imaging reports, "collaborative" imaging pathways, radiology-pathology feedback loops, and, most recently, the development of a patient centric radiology mobile app. The use of business analytics and business intelligence is considered essential in most industries. Although the measurement of radiologists' productivity (RVUs) and turnaround times has become commonplace in our field, the use of more advanced metrics and analytics, such as equipment utilization, scheduling efficiency, cost-based accounting, on-time performance, referring physician referral patterns and satisfaction, and service-related costs have been rare in radiology departments. Even when used, the data are typically not real time, and their extraction and display requires the services of dedicated IT or analytics personnel. To truly derive value from data, it is necessary to ensure that the data is accurate, easily accessible, and most importantly, actionable. Examples of how this can be achieved to create value will be presented. The rapid development of artificial intelligence and machine learning is a ubiquitous topic both within the medical literature and at scientific meetings. While many have concentrated on the threat posed by artificial intelligence, others have stressed its potential both to increase the value of imaging and to enhance the radiologist's role in patient care. Examples of how artificial intelligence can be utilized to significantly improve the elements that comprise value in imaging - cost, guality, experience, outcome, appropriateness will be discussed.



# SPOI11

**Oncodiagnosis Panel: Oropharyngeal Cancer (Interactive Session)** 

Sunday, Nov. 25 10:45AM - 12:15PM Room: E451B



AMA PRA Category 1 Credits ™: 1.50 ARRT Category A+ Credit: 1.75

# Participants

James S. Welsh, MD, Aurora, IL (*Moderator*) Nothing to Disclose Christine M. Glastonbury, MBBS, San Francisco, CA (*Presenter*) Author with royalties, Reed Elsevier Upendra Parvathaneni, MBBS,FRANZCR, Seattle, WA (*Presenter*) Nothing to Disclose Michael K. Gibson, MD,PhD, Nashville, TN (*Presenter*) Advisory Board, Amgen Inc; Speaker, Bristol-Myers Squibb Company; ; Pierre Lavertu, MD, Cleveland, OH (*Presenter*) Nothing to Disclose

For information about this presentation, contact:

mike.gibson.1@vanderbilt.edu

christine.glastonbury@ucsf.edu

pierre.lavertu@uhhospital.org

# LEARNING OBJECTIVES

1) To present the rationale for changes in oropharyngeal cancer staging in the AJCC/UICC 8th edition. 2) To reinforce the necessity of a team approach to cancer management and the utility of the radiologist for aiding staging. 3) Be able to understand the relative roles of surgery and radiotherapy in the management of oropharyngeal cancer. 4) Be able to understand the role of transoral surgery (TORS) in the management of early oropharyngeal lesions. 5) To review and understand the roles of chemotherapy and biological therapy as radiosensitizers in treatment of orophryngeal cancer.



#### SSA01

# Breast Imaging (Update on Screening)

Sunday, Nov. 25 10:45AM - 12:15PM Room: E450A

# BR

AMA PRA Category 1 Credits ™: 1.50 ARRT Category A+ Credit: 1.75

#### **Participants**

Catherine S. Giess, MD, Wellesley, MA (*Moderator*) Nothing to Disclose Debra L. Monticciolo, MD, Temple, TX (*Moderator*) Nothing to Disclose

# Sub-Events

# SSA01-01 Interval Cancers in a Large Prospective Breast Tomosynthesis Screening Trial

Sunday, Nov. 25 10:45AM - 10:55AM Room: E450A

Participants

Kristin Johnson, MD, Lund, Sweden (*Presenter*) Nothing to Disclose Kristina Lang, MD,PhD, Malmo, Sweden (*Abstract Co-Author*) Travel support, Siemens AG Speaker, Siemens AG Debra M. Ikeda, MD, Stanford, CA (*Abstract Co-Author*) Scientific Advisory Board, Grail, Inc; Reviewer, Siemens AG Hanna Sartor, MD,PhD, Malmo, Sweden (*Abstract Co-Author*) Travel support, Siemens AG Speaker, Siemens AG Ingvar T. Andersson, MD, PhD, Malmo, Sweden (*Abstract Co-Author*) Nothing to Disclose Sophia Zackrisson, Malmo, Sweden (*Abstract Co-Author*) Speaker, AstraZeneca PLC; Speaker, Siemens AG; Travel support, AstraZeneca PLC; Travel support, Siemens AG

#### For information about this presentation, contact:

kristin.johnson@med.lu.se

# PURPOSE

To assess interval cancer rate in a large, prospective digital breast tomosynthesis (DBT) screening trial in comparison with a concurrent screening population and to assess tumor characteristics of interval cancers in DBT-screening.

# METHOD AND MATERIALS

The prospective \*\*\*\*Trial, comparing digital breast tomosynthesis (DBT) with digital mammography (DM) in 14,848 women has shown a significantly increased sensitivity with DBT. Interval cancer rate in the trial was compared with a concurrent screening population; i.e. women participating in DM screening at the same screening site during the same time period (2010-15, n=100,273 screens). Interval cancers and concurrent screens were identified through linkage with the Radiology Information System, the \*\*Cancer Registry and the National Quality Register Breast Cancer. Confidence intervals (CI) 95 % were calculated for rates and difference between rates. Tumor characteristics were retrieved from pathology reports and invasive cancers classified according to St Gallen subtypes.

#### RESULTS

In total, there were 22 interval cancers in the \*\*\*\*Trial. The interval cancer rate was 1.5 per 1000 screens [22/14,848] (95% CI 0.9-2.2) in the \*\*\*\*Trial and 1.8 per 1000 screens [179/100,273] (95% CI 1.5-2.1) in the concurrent population. Although the interval cancer rate was lower in the trial, the difference of 0.3 was not statistically significant (95 % CI -0.5-0.9). Among the interval cancers in the \*\*\*\*Trial, the mean cancer size was 17 mm (range 2-37 mm), 2 were DCIS (grade 2 and 3), 5 luminal A-like, 9 luminal B-like HER2-, 2 luminal B-like HER2+ and 4 triple negative.

#### CONCLUSION

The slightly lower interval cancer rate in the trial might indicate that DBT-screening leads to the detection of clinically relevant cancers. Still, a relatively large proportion of the interval cancers had unfavorable prognostic characteristics.

# **CLINICAL RELEVANCE/APPLICATION**

Analysis of interval cancers is important in order to elucidate the future value of DBT in screening.

# SSA01-02 Does Tomosynthesis Work For Everyone?

Sunday, Nov. 25 10:55AM - 11:05AM Room: E450A

Participants

Ethan O. Cohen, MD, Houston, TX (*Presenter*) Spouse, Consultant, Medtronic plc; Spouse, Consultant, Novo Nordisk AS; Spouse, Consultant, Eli Lilly and Company; Spouse, Consultant, AstraZeneca PLC Rachel E. Perry, MD, Birmingham, AL (*Abstract Co-Author*) Nothing to Disclose Ashmitha Srinivasan, MD, Houston, TX (*Abstract Co-Author*) Nothing to Disclose Hilda H. Tso, DO, Houston, TX (*Abstract Co-Author*) Nothing to Disclose Kanchan Phalak, MD, Houston, TX (*Abstract Co-Author*) Nothing to Disclose Michele D. Lesslie, DO, Bellaire, TX (*Abstract Co-Author*) Nothing to Disclose Karen E. Gerlach, MD, Houston, TX (*Abstract Co-Author*) Nothing to Disclose Jessica W. Leung, MD, Houston, TX (*Abstract Co-Author*) Scientific Advisory Board, Hologic, Inc; Speakers Bureau, Hologic, Inc; Speakers Bureau, FUJIFILM Holdings Corporation

For information about this presentation, contact:

ecohen@mdanderson.org

#### PURPOSE

To compare the performance of full-field digital screening mammograms (FFDM) with and without digital breast tomosynthesis (DBT) in women with and without breast implants.

# METHOD AND MATERIALS

An IRB-approved, HIPAA-compliant retrospective review was performed of 103,070 consecutive screening mammograms obtained from February 2011 through June 2014. Recall rates (RRs), cancer detection rates (CDRs), and positive predictive values for recall (PPV1s) were analyzed.

#### RESULTS

The following data compare FFDM and FFDM-DBT: 67,331 FFDM and 28,835 FFDM-DBT from women *without* implants yielded RRs of 8.0% and 6.3%, respectively (p<0.00001); CDRs of 4.1 and 5.0 per 1000 exams, respectively (p=0.07); and PPV1s of 5.1% and 8.0%, respectively (p<0.0001). 4325 FFDM and 2579 FFDM-DBT from women *with* implants yielded RRs of 5.2% and 4.1%, respectively (p=0.040); CDRs of 1.8 and 2.7 per 1000 exams, respectively (p=0.46); and PPV1s of 3.6% and 6.7%, respectively (p=0.25). The same data is also used to evaluate the effect of implants on screening: 67,331 FFDM *without* implants and 4325 FFDM *with* implants yielded RRs of 8.0% and 5.2%, respectively (p<0.00001); CDRs of 4.1 and 1.8 per 1000 exams, respectively (p<0.00001); and PPV1s of 5.1% and 3.6%, respectively (p=0.30). 28,835 FFDM-DBT *without* implants and 2579 FFDM-DBT *with* implants yielded RRs of 6.3 and 4.1, respectively (p<0.00001); CDRs of 5.0 and 2.7, respectively (p=0.11); and PPV1s of 8.0 and 6.7, respectively (p=0.63).

#### CONCLUSION

Tomosynthesis improves the performance of digital screening mammography, while the presence of implants reduces its performance. Specifically, tomosynthesis improved RRs, CDRs, and PPV1s for all women (*with* and *without* implants), though statistically significant differences were seen only for RRs in women *without* implants, RRs in women *with* implants, and PPV1s for women *without* implants. Implants were associated with decreased RRs, worse CDRs, and worse PPV1s for all screening exams (FFDM and FFDM-DBT), but statistically significant differences were seen only for RRs for all screening exams and CDR for FFDM. Further study with larger populations is warranted.

# **CLINICAL RELEVANCE/APPLICATION**

The benefit of tomosynthesis has been incompletely studied in screening mammography patients with implants. This research suggests that tomosynthesis is useful for screening women *with* implants in addition to those *without* implants.

# SSA01-03 Disparities in Screening Mammography Cost-Sharing and Utilization Before and After the Affordable Care Act (ACA) and the Revised USPSTF Guidelines

Sunday, Nov. 25 11:05AM - 11:15AM Room: E450A

#### Awards

# **Trainee Research Prize - Resident**

Participants

Soudabeh Fazeli Dehkordy, MD, MPH, San Diego, CA (Presenter) Nothing to Disclose

A. Mark Fendrick, MD, Ann Arbor, MI (*Abstract Co-Author*) Consultant, Abbott Laboratories; Consultant, AstraZeneca PLC; Consultant, sanofi-aventis Group; Consultant, F. Hoffmann-La Roche Ltd; Consultant, GlaxoSmithKline plc; Consultant, Merck & Co, Inc; Consultant, Neocure Group LLC; Consultant, Pfizer Inc; Consultant, POZEN Inc; Consultant, Precision Health Economics LLC; Consultant, The TriZetto Group, Inc; Consultant, Zanzors; Speakers Bureau, Merck & Co, Inc; Speakers Bureau, Pfizer Inc; Researcher, Abbott Laboratories; Researcher, AstraZeneca PLC; Researcher, sanofi-aventis Group; Researcher, Eli Lilly and Company; Researcher, F. Hoffmann-La Roche Ltd; Researcher, GlaxoSmithKline plc; Researcher, Merck & Co, Inc; Researcher, Novartis AG ; Researcher, Pfizer Inc

Sarah Bell, Ann Arbor, MI (*Abstract Co-Author*) Nothing to Disclose Emily Kobernik, Ann Arbor, MI (*Abstract Co-Author*) Nothing to Disclose Vanessa Dalton, MD, Ann Arbor, MI (*Abstract Co-Author*) Expert Witness, Bayer AG Ruth C. Carlos, MD, MS, Ann Arbor, MI (*Abstract Co-Author*) Nothing to Disclose

# For information about this presentation, contact:

sfazeli@ucsd.edu

# PURPOSE

To assess changes in screening mammography cost-sharing and utilization before and after the Affordable Care Act (ACA) and the revised USPSTF guidelines by race and income level.

# METHOD AND MATERIALS

We used patient-level analytic files between 2004 and 2014 from Optum<sup>™</sup> Clinformatics<sup>™</sup> Data Mart. We included women 40-74 years 1) without a history of breast cancer or mastectomy with 2) at least one year of continuous enrollment in a given plan, examining out-of-pocket payments and utilization for screening mammography. Trends for screening mammography utilization and cost sharing elimination over time by race and income level were visually inspected. We then specifically calculated the slopes and compared trends before and after 2009 and 2010 to assess the impact of ACA implementation and USPSTF guideline revisions on screening mammography cost sharing elimination and utilization.

#### RESULTS

We identified an average of 2,173,686 commercially insured women ages 40-74 years with at least 12 months of continuous enrollment in a given plan per year. Overall, an upward trend was seen in the proportion of women with zero cost sharing over time among all races and income level. Comparing trends for cost-sharing elimination before and after 2010, a statistically significant upward but small trend was found among all races and income levels with no racial or income disparities evident. Screening mammography utilization plateaued or showed a significant decline after 2009 in all income and racial groups except for African Americans in whom screening rates continued to increase after 2009.

# CONCLUSION

Impact of ACA cost-sharing elimination did not differ among various racial and income groups. Among our population of employerbased insured women, the racial gap in screening mammography appeared to have closed and potentially reversed among African American women.

# CLINICAL RELEVANCE/APPLICATION

It is important to continue monitoring screening mammography utilization as health care policies and guidelines change, as these changes may affect disparities in screening between different racial and income groups.

# **Honored Educators**

Presenters or authors on this event have been recognized as RSNA Honored Educators for participating in multiple qualifying educational activities. Honored Educators are invested in furthering the profession of radiology by delivering high-quality educational content in their field of study. Learn how you can become an honored educator by visiting the website at: https://www.rsna.org/Honored-Educator-Award/ Ruth C. Carlos, MD, MS - 2015 Honored EducatorRuth C. Carlos, MD, MS - 2018 Honored Educator

# SSA01-04 Screening Mammography: There is Value in Screening Women Aged 75 and Over

Sunday, Nov. 25 11:15AM - 11:25AM Room: E450A

Participants

Stamatia V. Destounis, MD, Scottsville, NY (*Presenter*) Research Grant, Hologic, Inc; Research Grant, Delphinus Medical Technologies, Inc

Andrea L. Arieno, BS, Rochester, NY (*Abstract Co-Author*) Nothing to Disclose Amanda Santacroce, Rochester, NY (*Abstract Co-Author*) Nothing to Disclose

For information about this presentation, contact:

sdestounis@ewbc.com

# PURPOSE

To review outcomes of screening mammography performed in women 75 and over to determine the rate of cancer diagnosed and associated histology and surgical excision performed.

# METHOD AND MATERIALS

Patients 75 years of age and over who presented for screening mammography and underwent biopsy with resultant malignant pathology were retrospectively collected and analyzed to record patient demographics, lesion information, pathology results and treatment. Cases of non-breast malignancy, cases of breast cancer diagnosed by modality other than mammography, and cases with missing or incomplete records were excluded.

# RESULTS

From 2007-2016 there were a total of 679,168 screening appointments, with 3,480 patients diagnosed with screen-detected cancers (5.1/1000). 68,218 (10%) screenings were performed in women aged 75 and over; 530 of these women were diagnosed with 560 breast cancers, for a cancer detection rate of 7.8/1000. Average patient age 80.3 (range 75-98). Lesions most frequently presented as a mass (74%). A large majority (81%) of the malignancies diagnosed were invasive; 55.7% grade 2 or 3. Positive lymph nodes were reported at surgical excision in 7.0% of patients. Tumor stage was largely stage 0 or 1 (64%); 12% were determined to be stage II or III. 98% of cancers were surgically excised; twelve cancers were not due to advanced patient age or overall degraded patient health.

# CONCLUSION

For the relatively small percentage of our screening population that women 75 and over comprise (10%), the patients diagnosed in this population made up 16% of all patients diagnosed with screen-detected cancers, a substantial cancer detection rate (7.8/1000). Most of the cancers diagnosed were low grade, a significant number were invasive (81%), over half were grade 2 or 3, and a majority were lower stage (0 or I). Most (98%) underwent surgical excision, suggesting that most women 75 and over are in good health and want to pursue surgical excision. Screening mammography should be performed in this age group given the incidence of breast cancer that exists.

# **CLINICAL RELEVANCE/APPLICATION**

Ongoing debate exists regarding the age to cease screening mammography, citing lack of research in the aging population. Our study demonstrates the value of screening women 75 and over.

# SSA01-05 Risk of Breast Cancer After a False-Positive Screening Mammogram in Relation to Mammographic Abnormality: Potential for Prevention?

Sunday, Nov. 25 11:25AM - 11:35AM Room: E450A

Participants

Rasika Rajapakshe, PhD, Kelowna, BC (*Presenter*) Nothing to Disclose Miao Hui, PhD, Singapore, Singapore (*Abstract Co-Author*) Nothing to Disclose Brenda A. Farnquist, MD, Chestnut Hill, MA (*Abstract Co-Author*) Nothing to Disclose Janette Sam, RT, Vancouver, BC (*Abstract Co-Author*) Nothing to Disclose Mikael Hartman, MD,PhD, Singapore, Singapore (*Abstract Co-Author*) Nothing to Disclose

#### For information about this presentation, contact:

#### rrajapak@bccancer.bc.ca

#### PURPOSE

False positive recall rates have consistently been identified as a harm of organized breast cancer screening. The extent to which these recalled women are at increased risk of future breast cancer remains unclear.

#### METHOD AND MATERIALS

All women who had two or more screening mammograms between 1988-2013 in a large organized breast screening program were included in the study. They were followed until a breast cancer diagnosis, last screen date +5 years, or end of follow-up on Dec 31, 2013, whichever came first. The relative risk (RR) of breast cancer for women with a false-positive test compared with women with negative tests was estimated with Poisson regression, adjusted for age, and five calendar periods.

#### RESULTS

A total of 772,289 women with 4.82 million screening mammograms and a median follow up of 11.8 years were included. There were 238,860 women with false positive findings and 26,950 cancers of which 16,084 screen detected and 10,866 non screen detected. The adjusted RR [Value (95% CI)] of breast cancer after the first false-positive test was 1.73(1.68-1.77) for all, 1.65(1.61-1.70) for invasive, and 2.13(2.01-2.27) for in situ cancers respectively. The RR remained increased beyond 8 years after the first false-positive test. Of the 5157 screen detected cancers after the first false positive test, 3358 (65%) were on the ipsilateral breast while 1799 (35%) were on the contralateral breast. Women with breast density >50% at the time of false positive test had a twofold risk of breast cancer; RR 2.07(1.99-2.14) while those with breast density <50% had a RR of 1.58(1.54-1.63). When stratified for mammographic features found on the first false positive mammogram, architectural distortion plus mass had the highest RR 4.68(3.16-6.93) for invasive cancers while calcifications alone and calcifications plus asymmetry had highest RR 5.57(4.88-6.36) and 4.07(2.49-6.66) for in situ cancers. These findings would require further validation.

# CONCLUSION

False positive mammogram correlates with an increased risk of developing breast cancer. Screen detected breast cancers post false positive mammogram most likely to occur in the ipsilateral breast.

#### **CLINICAL RELEVANCE/APPLICATION**

Mammographic features at the time of recall predict the risk of subsequent cancer and may warrant increased surveillance and/or chemo-prevention.

# SSA01-06 Stratification of Ductal Carcinoma in Situ in a Screening Population by Age and Grade Over a 16-Year Period

Sunday, Nov. 25 11:35AM - 11:45AM Room: E450A

Participants

Angela Sie, MD, Long Beach, CA (*Presenter*) Nothing to Disclose Gretchen M. Stipec, MD, Manhattan Bch, CA (*Abstract Co-Author*) Nothing to Disclose Maya S. Hsieh, MD, Long Beach, CA (*Abstract Co-Author*) Nothing to Disclose Ryan Kobayashi, Long Beach, CA (*Abstract Co-Author*) Nothing to Disclose Tiesha Jones, Long Beach, CA (*Abstract Co-Author*) Nothing to Disclose Stephen A. Feig, MD, Orange, CA (*Abstract Co-Author*) Nothing to Disclose

#### For information about this presentation, contact:

asie@memorialcare.org

#### PURPOSE

To determine if there is a correlation between age and grade of screening-detected ductal carcinoma in situ (DCIS).

# **METHOD AND MATERIALS**

We performed an IRB approved, retrospective review of screening-detected cases of DCIS at our large, community-based breast center, diagnosed between 2001 and 2016. All cases of DCIS diagnosed from 2001 through 2016 were collated. Odds ratios were produced from logistic regression analyses.

#### RESULTS

DCIS accounted for 20.9% (372/1781) of all cancers detected in our screening practice between 2001 and 2016. The total number of cases in our study was 372, with a mean age of 60.6 years, median age of 60.0 years, mean size of 2.1 cm, median size of 1.8 cm. Age distribution showed 31.7% (118/372) were <55 years old, and 68.3% (254/372) were >= 55 years old. The tumor grade was identified in 366 (98.4%) of the cases and included 6.8% (25/366) low grade, 46.4% (170/366) intermediate grade, and 46.7% (171/366) high grade. Mammographic findings were 80.9 % (301/372) calcifications and 16.9% (63/372) mass or focal asymmetry. Estrogen receptor (ER)/Progesterone receptor (PR) status was identified in 240 (64.5%) cases and included 81.3% (195/240) ER + and 72.9% (175/240) PR+ cases. Logistic regression analysis revealed that for each unit decrease in age, the odds ratio of intermediate versus low grade was 4 times higher (p=0.038), and high versus low grade was 5 times higher (p=0.009). No patient (0/19) under 45 years old had low grade DCIS. Younger women were slightly more likely to have DCIS that was ER+ and PR+.

#### CONCLUSION

The vast majority of screening-detected DCIS cases (93.1%) were intermediate or high grade. Younger patients had a statistically significant greater chance of intermediate or high grade DCIS versus low grade DCIS.

#### **CLINICAL RELEVANCE/APPLICATION**

Grade and age have an inverse relationship in the screening-detected DCIS at our institution during the 16 year period studied. Since screening- detected DCIS in younger patients tends to be high or intermediate grade, screening mammography in younger

patients remains clinically important.

# SSA01-07 Frequency and Cancer Yield of Probably Benign Breast Findings in Clinical Practice in the National Mammography Database (BI-RADS Category 3)

Sunday, Nov. 25 11:45AM - 11:55AM Room: E450A

Participants

Mai A. Elezaby, MD, Madison, WI (*Presenter*) Research Grant, Exact Sciences Corporation Colin Longhurst, Madison, WI (*Abstract Co-Author*) Nothing to Disclose Priyadarshini Karthik, Reston, VA (*Abstract Co-Author*) Nothing to Disclose Debapriya Sengupta, MBBS, MPH, Reston, VA (*Abstract Co-Author*) Nothing to Disclose Elizabeth S. Burnside, MD, MPH, Madison, WI (*Abstract Co-Author*) Dr. Burnside has a research grant from Hologic Margarita L. Zuley, MD, Pittsburgh, PA (*Abstract Co-Author*) Investigator, Hologic, Inc Wendie A. Berg, MD, PhD, Pittsburgh, PA (*Abstract Co-Author*) Nothing to Disclose Mythreyi Bhargavan-Chatfield, PhD, Reston, VA (*Abstract Co-Author*) Nothing to Disclose Judy Burleson, Reston, VA (*Abstract Co-Author*) Nothing to Disclose Cindy S. Lee, MD, Garden City, NY (*Abstract Co-Author*) Nothing to Disclose

# For information about this presentation, contact:

melezaby@uwhealth.org

# PURPOSE

The Breast Imaging Reporting and Data System (BI-RADS) assessment category 3 describes a probably benign finding with a low likelihood of malignancy of <= 2%. Since 2013, the BI-RADS Atlas discouraged its use at screening, which was reinforced in Medicare's pay-for-performance Physician Quality Reporting System (PQRS) initiative. However, there are sparse data on the frequency of use and cancer yield of BI-RADS 3 findings in clinical practice. This study assesses the frequency and cancer yield of probably benign findings in screening and diagnostic mammography in the National Mammography Database (NMD), which is the largest national database of mammography.

# METHOD AND MATERIALS

This HIPAA-compliant and IRB-exempt study retrospectively analyzed data from screening and diagnostic mammograms performed between 1/1/2009 and 12/31/2015 in the NMD. We calculated the overall frequency and cancer yield of BI-RADS 3 findings in screening and diagnostic mammography. Cancer yield is defined as the number of breast cancers diagnosed among women with probably benign findings within the study period. Exams with BI-RADS 3 findings but lacking biopsy or 12-month follow-up were excluded . Exams from NMD facilities contributing data for < 2 years were excluded to ensure adequate follow-up.

# RESULTS

Data from 6,421,365 screening and 1,264,929 diagnostic mammograms performed in 3,345,013 women at 261 NMD facilities in 31 states were analyzed. A total of 215,403 mammograms had probably benign findings, with frequency of 0.3% (20,060/6,421,365) in screening and 15% (193,850 /1, 264,929) in diagnostic mammograms. Among the 101,025 women with BI-RADS 3 findings and at least one follow up , 948 (0.94%, 95%CI 0.91, 1.03) women had a diagnosis of malignancy. Rates of BI-RADS 3 use were stable over the 6 calendar years analyzed.

#### CONCLUSION

A probably benign, BI-RADS 3, assessment was rarely used in screening but common in diagnostic mammography in the NMD. The overall cancer yield of probably benign findings was 0.94%, consistent with BI-RADS Atlas threshold of <= 2%. These results support use of probably benign assessment in clinical practice for findings with low risk of malignancy.

#### **CLINICAL RELEVANCE/APPLICATION**

In the NMD, BI-RADS 3 showed appropriately low cancer yield of 0.9%. Proper use of BI-RADS 3 helps reduce cost, morbidity and patient anxiety while increasing cost-effectiveness of screening.

# SSA01-08 Digital Breast Tomosynthesis Improves Performance Metrics of Screening Mammogram in Women Aged 40 to 54 Compared to Full Field Digital Mammogram

Sunday, Nov. 25 11:55AM - 12:05PM Room: E450A

Participants

Amir Imanzadeh, MD, Shelton, CT (*Presenter*) Nothing to Disclose Maryam Etesami, MD, New Haven, CT (*Abstract Co-Author*) Nothing to Disclose Sarvenaz Pourjabbar, MD, New Haven, CT (*Abstract Co-Author*) Nothing to Disclose Laura J. Horvath, MD, New Haven, CT (*Abstract Co-Author*) Nothing to Disclose Michelle Y. Giwerc, New Haven, CT (*Abstract Co-Author*) Nothing to Disclose Liane E. Philpotts, MD, New Haven, CT (*Abstract Co-Author*) Nothing to Disclose

For information about this presentation, contact:

amir.imanzadeh@yale.edu

#### PURPOSE

The starting age for screening mammogram has been a controversial subject mostly due to reported low cancer detection rate (CDR) and high false positive recall rate (RR) in younger women. However, digital breast tomosynthesis (DBT) may improve performance of screening mammogram and change the justification of screening guidelines. The purpose of this study is to compare the performance of screening mammogram in women aged 40-54 between full field digital mammogram (FFDM) and DBT.

#### **METHOD AND MATERIALS**

In an IRB approved study, we retrospectively analyzed screening mammograms performed in women aged 40-54 at 2 of our imaging

centers from August 2008 through April 2017. We included all FFDM screening mammograms performed before and all DBT screenings performed after installation of DBT at each site. DBT screening was offered to all women after installation at no additional charge. RR, CDR, and characteristics of screen-detected cancers were compared between FFDM and DBT screening in 3 age groups: 40-44 (group 1), 45-49 (group 2) and 50-54 (group 3).

#### RESULTS

16938 FFDM and 28313 DBT were performed in women aged 40-54. In FFDM, RR significantly decreased from group 1 (17.4%) to group 2 (14.0%) and group 3 (11.3%); however, in DBT screening, RR was only significantly decreased from group 1 (12.2%) to group 2 (9.1%) and there was no significant difference between group 2 and group 3 (8.4%). RR of all 3 age groups were significantly lower for DBT compared to FFDM. CDR per 1000 exams in FFDM was significantly lower in groups 1 and 2 (2.4 and 2.3) compared to group 3 (5.0), but in DBT, there was no significant difference in CDR among the 3 groups (3.0, 4.4, and 3.8 in groups 1,2, and 3, respectively). There was significant increase in CDR from FFDM to DBT in women aged 45-49 (p=0.03). The ratio of invasive to in-situ carcinomas were similar in FFDM and DBT subgroups.

# CONCLUSION

DBT screening decreases RR and increases CDR compared to FFDM in women aged 40-49, and more prominently for 45-49 age group. As a result, unlike FFDM, there is no significant difference in RR and CDR of ages 45-49 and 50-54 with DBT screening.

#### **CLINICAL RELEVANCE/APPLICATION**

Improved performance of DBT screening in women aged 40-49 compared to FFDM screening, may further justify recommendations for starting screening mammogram at younger age.

# SSA01-09 Six Years of Consecutive, Population-Based Screening with Digital Breast Tomosynthesis: Outcomes by Screening Year and by Screening Round

Sunday, Nov. 25 12:05PM - 12:15PM Room: E450A

Participants

Emily F. Conant, MD, Philadelphia, PA (*Presenter*) Grant, Hologic, Inc; Consultant, Hologic, Inc; Grant, iCAD, Inc; Consultant, iCAD, Inc; Speaker, iiCME

Samantha P. Zuckerman, MD, Philadelphia, PA (*Abstract Co-Author*) Nothing to Disclose Elizabeth S. McDonald, MD, Philadelphia, PA (*Abstract Co-Author*) Nothing to Disclose Susan Weinstein, MD, Philadelphia, PA (*Abstract Co-Author*) Nothing to Disclose Lauren Pantalone, BS, Philadelphia, PA (*Abstract Co-Author*) Nothing to Disclose Aimilia Gastounioti, Philadelphia, PA (*Abstract Co-Author*) Nothing to Disclose Despina Kontos, PhD, Philadelphia, PA (*Abstract Co-Author*) Nothing to Disclose Marie Synnestvedt, Philadelphia, PA (*Abstract Co-Author*) Nothing to Disclose Mitchell D. Schnall, MD, PhD, Philadelphia, PA (*Abstract Co-Author*) Nothing to Disclose Rebecca Hubbard, Philadelphia, PA (*Abstract Co-Author*) Nothing to Disclose

#### For information about this presentation, contact:

emily.conant@uphs.upenn.edu

#### PURPOSE

Digital breast tomosynthesis (DBT) improves screening outcomes by decreasing recalls and increasing cancer detection. However, most DBT studies have analyzed prevalence rather than incidence screening. We investigate outcomes from 6 years of consecutive DBT screening, at both the population level by year (DBT Y1-6) and patient level by round (DBT R1-6).

# METHOD AND MATERIALS

71535 consecutive DBT screens in 33245 women were performed from 10/2011 to 9/2017 with 31246, 17801, 11067, 6560, 3553, and 1308 screens in rounds 1-6, respectively. Recall rate % (RR), cancer detection (CDR), biopsy (BX) and false negative (FN) rates per 1000 screens for each year (DBTY1-Y6) and each round (R1-R6) were analyzed. Outcomes were compared the prior year of digital mammography (DM) screening (DMY0, n=10765). Cancer registry data was used to determine FN (defined as cancer diagnosed <1 yr after negative screen) for DMY0-DBTY5 and DBT R1-R5.

#### RESULTS

At the Population Level, RR for DBTY1-6 was lower than DMY0 (7.9 vs 10.4%). However, DBT RR increased in DBTY1-3 (8.8, 9.0, 9.2%) before decreasing in DBTY4-6 (7.1, 6.1, 7.4%). CDR increased in DBTY1-3 (5.5, 5.8, 6.5) then decreased in DBTY4-6 (6.3, 5.1, 5.5) however, DBT CDR was higher in each year than DMY0 (4.8). Invasive CDR for DBTY1-4 and DBTY6 (3.9, 4.5, 4.5, 4.9, respectively) were also higher than DM0 (3.4) however, DBTY5 was lower (2.9). BX increased from DMY0 of 1.9 to 2.2, 1.9, 2.0 in DBTY1-3; in DBTY4-6, BX rates were lower (1.5, 1.3, 1.5). FN remained without significant change from DMY0 (1.1) to DBT1-5 (0.5, 0.3, 0.4, 0.8, 1.0). By Screening Round, RR decreased from DBTR1 to R5 from 10.6, 7.0, 5.1, 4.5, 4.1 until R6= 4.2%. CDR for R1-6 were 6.4, 5.5, 6.1, 4.4, 4.2, 3.1, respectively. BX rate decreased after DBTR1 (2.5) for R2-6 (1.4, 1.4, 1.0, 0.8, 1.0). FN were 0.5, 0.5, 1.3, 0.6, 0.8 for R1-5. Whether by year or round, DBT PPV1 was higher than DM.

# CONCLUSION

At the population level, DBT screening had higher overall CDR and lower RR than DM with FN rates remaining relatively stable. Little data exists on outcomes by round of screening, however, our data may help guide DBT screening benchmarks.

# **CLINICAL RELEVANCE/APPLICATION**

Consecutive years of DBT screening show decreased recall and increased PPV1 compared to DM alone. Further long term DBT outcome data may help guide new, personalized screening algorithms by age, density and risk.

#### **Honored Educators**

Presenters or authors on this event have been recognized as RSNA Honored Educators for participating in multiple qualifying educational activities. Honored Educators are invested in furthering the profession of radiology by delivering high-quality educational content in their field of study. Learn how you can become an honored educator by visiting the website at:

https://www.rsna.org/Honored-Educator-Award/ Mitchell D. Schnall, MD, PhD - 2013 Honored Educator



#### SSA02

# Breast Imaging (Contrast Enhanced Spectral Mammography)

Sunday, Nov. 25 10:45AM - 12:15PM Room: E450B



AMA PRA Category 1 Credits ™: 1.50 ARRT Category A+ Credit: 1.75

#### **Participants**

John M. Lewin, MD, Denver, CO (*Moderator*) Nothing to Disclose Maxine S. Jochelson, MD, New York, NY (*Moderator*) Nothing to Disclose

# Sub-Events

# SSA02-01 Background Parenchymal Enhancement at Contrast-Enhanced Spectral Mammography (CESM) as a Breast Cancer Risk Factor

Sunday, Nov. 25 10:45AM - 10:55AM Room: E450B

Participants

Yael Yagil, MD, Ramat Gan, Israel (*Abstract Co-Author*) Nothing to Disclose Vera Sorin, BMedSc, Ramat Gan, Israel (*Presenter*) Nothing to Disclose Renata Faermann, MD, Tel Aviv, Israel (*Abstract Co-Author*) Nothing to Disclose Anat Shalmon, Ramat Gan, Israel (*Abstract Co-Author*) Nothing to Disclose Osnat Halshtok, MD, Ramat Gan, Israel (*Abstract Co-Author*) Nothing to Disclose Michael Gotlieb, MD, Ramat Gan, Israel (*Abstract Co-Author*) Nothing to Disclose Miriam Sklair-Levy, MD, Tel -Hashomer, Israel (*Abstract Co-Author*) Nothing to Disclose

# For information about this presentation, contact:

mirisklair@gmail.com

#### PURPOSE

To assess the extent of background parenchymal enhancement (BPE) at contrast-enhanced spectral mammography (CESM), interreader agreement in BPE classification, and correlation between BPE and breast cancer.

#### **METHOD AND MATERIALS**

Between 2012 and 2015 a total of 516 women underwent CESM imaging for screening and diagnostic purposes. BPE on CESM images was retrospectively, independently and blindly graded by 4 reviewers using the following scale: minimal, mild, moderate or marked. Inter-reader agreement was estimated using correlation coefficient (ICC). Associations between BPE and clinical factors, biopsy rate and histopathology results were examined using a multivariate logistic regression analysis.

# RESULTS

A total of 412 (80%) of women underwent CESM for screening purposes. Mean age was 53 (range 28-77) years and 86.2-94% had a breast density BI-RADS score of C-D. Most women (76.4-90.5%) had minimal or mild BPE at CESM. Overall inter-reader agreement on BPE scores was good (ICC 0.88, 95%CI 0.81-0.92). A total of 122 (24%) biopsies were performed with a malignant histopathology result in 45 (37%) cases. On a multivariate analysis BPE demonstrated a significant association with age (P=0.004, OR 0.942, 95%CI 0.905-0.981) and with biopsy performance rate (P=0.006, OR 2.646, 95%CI 1.319-5.307). Moderate or marked BPE was predictive of a malignant biopsy result (P=0.002, OR 3.105, 95%CI 1.541-6.259).

#### CONCLUSION

CESM BPE is correlated with age and biopsy rate. Moderate or marked BPE is associated with malignant biopsy results, and hence may predict an increased risk for breast cancer.

#### **CLINICAL RELEVANCE/APPLICATION**

CESM BPE grading may be used as an additional risk assessment tool for breast cancer.

# SSA02-02 Contrast Enhanced Digital Mammography (CEDM) Helps to Safely Reduce Benign Breast Biopsies

#### Sunday, Nov. 25 10:55AM - 11:05AM Room: E450B

# Participants

Margarita L. Zuley, MD, Pittsburgh, PA (*Presenter*) Investigator, Hologic, Inc David Gur, PhD, Pittsburgh, PA (*Abstract Co-Author*) Nothing to Disclose Uzma Waheed, MD, Pittsburgh, PA (*Abstract Co-Author*) Nothing to Disclose Marie A. Ganott, MD, Pittsburgh, PA (*Abstract Co-Author*) Nothing to Disclose Bronwyn Nair, MD, Sewickley, PA (*Abstract Co-Author*) Nothing to Disclose Christiane M. Hakim, MD, Pittsburgh, PA (*Abstract Co-Author*) Nothing to Disclose Gordon S. Abrams, MD, Pittsburgh, PA (*Abstract Co-Author*) Nothing to Disclose

#### For information about this presentation, contact:

#### zuleyml@upmc.edu

#### PURPOSE

One criticism of breast imaging is the harm caused by the relatively high rate of biopsy of benign breast lesions -- particularly BIRADS 4A and 4B lesions. The purpose of this project is to assess if CEDM during diagnostic evaluation could increase biopsy PPV for soft tissue density lesions by reducing benign biopsies while not impacting biopsy of cancers.

#### **METHOD AND MATERIALS**

This HIPPA compliant IRB approved protocol accrued 57 consenting women aged 34-74 (avg 49) years with 60 BIRADS 4A or 4B soft tissue lesions scheduled for ultrasound (US), stereotactic or tomosynthesis (DBT) directed biopsy from April 2016-November 2017. CEDM was performed immediately prior to biopsy. The cohort included 46 masses, 6 asymmetries and 8 distortions. Pathology confirmed 9 cancers and 51 benign concordant lesions. Four MQSA qualified radiologists reviewed and provided a BIRADS score 3 times for each lesion: first for mammography (M)/DBT only, next with US added and third with CEDM added. Readers recorded if the lesion enhanced, how enhancement compared to background and background parenchymal enhancement. Differences in BIRADS ratings were compared.

#### RESULTS

After M/DBT and US, prior to CEDM, 173/240 (72%) ratings were classified as > BIRADS 4. After viewing CEDM, 60 of these were re-classified as < BIRADS 3; a 35% average [range 0-59%] reduction in biopsy recommendation (p<0.05). Cancers enhanced in 32/36 (89%) ratings and 32/36 cancers were rated as BIRADS >4 before and after CEDM. Benign lesions enhanced in 77/204 (38%) (false positives). With US 3/36 cancer and 44/204 benign were converted to BIRADS>4 and 2/36 cancer and 10/204 benign to BIRADS <3 rating. With CEDM, 1/36 cancer and 8/204 benign were converted to BIRADS>4 and 1/36 cancer and 60/204 benign to BIRADS<3. Hence 1/36 cancer ratings (2.7%) were adversely affected (false negative) by CEDM.

# CONCLUSION

CEDM use during diagnostic evaluation of BIRADS 4A or 4B lesions may result in a significant increase in PPV with minimal impact on cancer diagnosis rates.

# **CLINICAL RELEVANCE/APPLICATION**

CEDM use during diagnostic evaluation of BIRADS 4A or 4B soft tissue lesions may significantly reduce the number of women recommended for benign biopsy while missing very few cancers.

# SSA02-03 Diagnostic Performance of Contrast-Enhanced Spectral Mammography for Suspicious Malignant Microcalcifications (BI-RADS 4)

Sunday, Nov. 25 11:05AM - 11:15AM Room: E450B

Participants

Rong Long, Beijing, China (*Presenter*) Nothing to Disclose Kun Cao, MD, Beijing, China (*Abstract Co-Author*) Nothing to Disclose Min Cao, MBBCh, MD, Beijing, China (*Abstract Co-Author*) Nothing to Disclose Haijiao Li, MD, Beijing, China (*Abstract Co-Author*) Nothing to Disclose Yingshi Sun, Beijing, China (*Abstract Co-Author*) Nothing to Disclose

# For information about this presentation, contact:

lucky\_6677@126.com

# PURPOSE

To assess the diagnostic performance of contrast-enhanced spectral mammography (CESM) for evaluation of suspicious malignant microcalcifications (BI-RADS 4) comparing with full-field digital mammography (FFDM).

#### **METHOD AND MATERIALS**

Patients with mammographic calcifications without associated mass or distortions and were originally reported as BI-RADS 4 during Jan 2015 to Jan 2018 were retrospectively collected. Lesions that proven through pathological diagnosis either by biopsy or operation were included in the study and grouped as FFDM or CESM according to the examination they received. The microcalcification morphology and associated enhancement (CESM group) were reviewed by two radiologists to analyse the accuracy of the diagnosis . Diagnostic accuracy was assessed respectively for FFDM and CESM versus the results of pathology. Statistical differences of the two methods were compared using Chi-square test.

#### RESULTS

48 lesions (13 malignant and 35 benign) from 48 patients were enrolled in FFDM group, and 31 lesions (10 malignant and 21 benign) from 30 patients were in CESM group. The diagnostic sensitivity, specificity, positive predictive value, negative predictive value and accuracy were 92.3%, 42.9%, 37.5%, 93.8% and 56.3% for FFDM group, and were 100%, 71.4%, 62.5%, 100% and 80.6% for CESM group, respectively. The specificity and accuracy of CESM were significantly higher than that of FFDM (p<0.05). All 10 cancers including 8 DCIS in CESM group were judged as enhancement (table 1).

# CONCLUSION

Comparing with FFDM, CESM improve the diagnostic performance on BI-RADS 4 mammographic calcifications, especially on specificity and overall accuracy. The detectability of all DCIS lesions in this small cohort may validate its potential use in previously "calcification only" disease, but still need further large sample to confirm.

#### **CLINICAL RELEVANCE/APPLICATION**

CESM improve the diagnostic performance on BI-RADS 4 mammographic calcifications, and decrease unnecessary biopsies.

# Quantitative Objective Evaluation of Contrast-Enhanced Spectral Mammogram in Predicting Response to Neo-Adjuvant Chemotherapy: A Comparative Study with RECIST 1.1 and Combined Evaluation Methods

Sunday, Nov. 25 11:15AM - 11:25AM Room: E450B

Amr F. Moustafa, MD, Cairo, Egypt (*Presenter*) Nothing to Disclose Rasha M. Kamal, MD, Cairo, Egypt (*Abstract Co-Author*) Nothing to Disclose Mohammed M. Gomaa, MD, Cairo, Egypt (*Abstract Co-Author*) Nothing to Disclose Shaimaa Mostafa, Giza, Egypt (*Abstract Co-Author*) Nothing to Disclose Roaa Mubarak, Cairo, Egypt (*Abstract Co-Author*) Nothing to Disclose Mohamed El-Adawy, Cairo, Egypt (*Abstract Co-Author*) Nothing to Disclose Ahmed Abdel-Latif, Cairo, Egypt (*Abstract Co-Author*) Nothing to Disclose Amany M. Helal, MD,PhD, Cairo, Egypt (*Abstract Co-Author*) Nothing to Disclose Mona A. Sakr, Cairo, Egypt (*Abstract Co-Author*) Nothing to Disclose

#### For information about this presentation, contact:

amrfaroukmoustafa@cu.edu.eg

#### PURPOSE

Initiating a new objective quantitative tool for evaluation of residual disease after neoadjuvant chemotherapy using CESM in comparison to RECIST 1.1 and combind evaluation methods.

#### **METHOD AND MATERIALS**

The study was approved by the ethical commitee of a multidisciplinary breast cancer hospital. It included 42 patients scheduled for receiving NAC. They underwent 2 CESM examinations; prior to and after NAC and maximum10 days prior to surgery. All patients were assessed using the RECIST 1.1 criteria, a combined approach (RECIST + qualitative subjective assessment) and a new quantitaive approach using an image analysis software (MATLAB and Simulink, Release 2013b). The technique consists of 3 main steps: 1-preprocessing 2. extracting the region of Interest (ROI) and 3- Assessing the response to chemotherapy depending on the analysis of the tumour number of pixels included within the ROI. The difference in the intensity of enhancmenet between the pre and post NAC enahncement is calculated and compared between the 3 assessment methods in correlation to postoperative pathology using the Miller-Payne grading. For statistical evaluation, patients were classified into responders and non-responders.

#### RESULTS

The calculated correlation coefficient when comparing the residual disease on CESM and Miller payne grade using RECIST 1.1, the combined approach and the proposd quantitative method was 0.59, 0.89 and 0.69 respectively. According to Miller Payne grading 39/42 cases were classified as responders (Miller payne III, IV, and V). Using the new quantitive approach all 39/39 cases (100%) were considered responders in comparison to 38/39 using the combined approach and 34/39 using the RECIST 1.1 criteria. The calculated sensitivity, positive and negative predictive values of the quantitative objective evaluation (100, 97.5,100 % respectively) was higher than the RECIST method (87.2%, 97.1% 28.6%) and the combined response method (97.4%,97.4% and 66.7%).

#### CONCLUSION

Quantitative objective analysis of CESM allows accurate objective evaluation of the response of breast cancer to chemotherapy and evaluation of residual tumor prior to surgery.

# CLINICAL RELEVANCE/APPLICATION

Objective analysis of CESM is an accurate tool for evaluation of the response of breast cancer post neo-adjuvant chemotherapy and is recommended as part of pre-operative work up

# SSA02-05 Diagnostic Value of Contrast-Enhanced Spectral Mammography in Comparison to MRI in a Population of Breast Lesions

```
Sunday, Nov. 25 11:25AM - 11:35AM Room: E450B
```

Participants

Dong Xing, MBBS, Yantai, China (*Abstract Co-Author*) Nothing to Disclose Xiaoxiao Chi I, Yantai, China (*Presenter*) Nothing to Disclose Jianjun Dong, Yantai, China (*Abstract Co-Author*) Nothing to Disclose Haizhu Xie, Yantai, China (*Abstract Co-Author*) Nothing to Disclose Amiee Chen, Shanghai, China (*Abstract Co-Author*) Nothing to Disclose Huizhi Cao, PhD, Beijing, China (*Abstract Co-Author*) Nothing to Disclose

# PURPOSE

To evaluate the diagnostic value between contrast-enhanced spectral mammography (CESM) and breast magnetic resonance imaging (MRI).

#### **METHOD AND MATERIALS**

Between July 2017 and February 2018, 235 patients who were suspected of breast abnormalities by clinical examination or mammography were underwent CESM and MRI examination. The image of CESM and MRI and the pathological specimens were analyzed. All lesions were evaluated independently by three experienced radiologists. Using histopathological results as the gold standard, the diagnostic performance of CESM and MRI were investigated. The areas under ROC curves was applied to analyze diagnostic efficiency. The data on maximum tumor size measurements were gathered on CESM and MRI. The Pearson's correlation coefficients and 95% confidents intervals between CESM vs. pathology and MRI vs. pathology were calculated.

#### RESULTS

263 breast lesions were found in 235 patients, in which 177 were malignant and 86 were benign. By evaluating the diagnostic value,

the sensitivity, positive prediction value, negative predictive value, and false-negative from CESM examination was comparable to that from MRI (91.5%,94.7%,83.7%,8.5% versus 91.5%,90.5%,82.1%,8.5%). Importantly, the accuracy and the specificity were higher for CESM than that for MRI (81%,89.5% Vs. 80.2%,71.7%) while the the false-positive was lower(10.5% Vs. 19.8%). The areas under ROC curves of CESM and MRI were 0.950 and 0.939, displaying the equivalent diagnostic efficiency (p=0.48). For the agreement between measurements, mean tumor size was 3.1 (range 0-16) cm for CESM and 3.4 (range0-17) cm for MRI compared with 3.2 (range 0-16) cm on histopathological results, the average difference of diameters between CESM, MRI and Histopathologic size was -0.01, -0.05cm, respectively, with 95% consistency interval range of -0.34 to 0.31, -0.87 to 0.22cm, respectively. The Pearson's correlation coefficients of CESM versus histopathology (r=0.774, p=0.000) was consistent with MRI (r=0.771, p=0.000).

# CONCLUSION

Our results show better accuracy, specificity and the lower false-positive of CESM in breast cancer detection than MRI. CESM displayed a good correlation with histopathology in assessing the lesion size of breast cancer, which is consistence with MRI.

# **CLINICAL RELEVANCE/APPLICATION**

CESM provides additional enhancement information for diagnosing breast lesions and measuring cancer sizes with high correlation to surgicohistology.

# SSA02-06 Usefulness of Low-Dose Perfusion Breast CT: Quantification of Tumor Vascularity and Prediction of Histologic Biomarkers in Invasive Breast Cancer

Sunday, Nov. 25 11:35AM - 11:45AM Room: E450B

Participants

Eun Kyung Park, MD,PhD, Ansan, Korea, Republic Of (*Presenter*) Nothing to Disclose Bo Kyoung Seo, MD, PhD, Ansan, Korea, Republic Of (*Abstract Co-Author*) Research Grant, Canon Medical Systems Corporation; Research Grant, Guerbet SA; Research Grant, Koninklijke Philips NV; Myoung-Ae Kwon, Ansan, Korea, Republic Of (*Abstract Co-Author*) Nothing to Disclose Chang Sub Ko, Ansan, Korea, Republic Of (*Abstract Co-Author*) Nothing to Disclose Jaehyung Cha, Seoul, Korea, Republic Of (*Abstract Co-Author*) Nothing to Disclose Kyu Ran Cho, MD, PhD, Seoul, Korea, Republic Of (*Abstract Co-Author*) Nothing to Disclose Ok Hee Woo, MD, Seoul, Korea, Republic Of (*Abstract Co-Author*) Nothing to Disclose

# For information about this presentation, contact:

seoboky@korea.ac.kr

# PURPOSE

To investigate the usefulness of low-dose perfusion breast computed tomography (CT) for quantification of tumor vascularity and for prediction of histologic biomarkers in invasive breast cancer.

# METHOD AND MATERIALS

This prospective study was approved by IRB with informed consent. A total of 139 patients with invasive breast cancers were enrolled. Low-dose perfusion CT was performed in the prone position with a spectral CT (iQon, Philips Healthcare) after contrast injection (Xenetix350, Guerbet). Effective dose was less than 1.2 mSv. Perfusion parameters were measured using a Philips Advanced Perfusion and Permeability application prototype in breast cancers, normal breast tissue, and fat; peak enhancement intensity (HU), perfusion on deconvolution model (mL/min/100/g), mean transit time (sec), time to peak (sec), blood volume (mL/100/g), permeability (mL/min/100/g), and blood volume permeability on Patlak model (mL/100/g). CT perfusion parameters of cancers and normal tissue or fat were compared using Mann-Whitney test. Correlation analysis was performed between CT perfusion parameters of cancers and histologic biomarkers including tumor grade, estrogen receptor (ER), progesterone receptor (PR), human epidermal growth factor receptor 2 (HER2), and Ki67 using Mann-Whitney or Kruskal-Wallis test.

#### RESULTS

In breast cancers, peak enhancement intensity, perfusion, blood volume, permeability, and blood volume permeability were significantly higher, and mean transit time, time to peak were shorter than those values in normal glandular tissues and fat (P<.001 for all). Peak enhancement intensity significantly increased in cancers with ER-, PR-, HER2+, Ki67+ or more than 20 mm (P<.05 for all). Time to peak decreased in cancers with ER-, PR-, HER2+, Ki67+, high grade, or more than 20 mm (P<.05 for all). Blood volume permeability increased in cancers with ER-, PR-, HER2+, Ki67+, or high grade (P<.05 for all). HER2-enriched cancers showed higher peak enhancement intensity and blood volume permeability than luminal type cancers (P<.02 for all).

#### CONCLUSION

Low-dose perfusion breast CT can be useful in quantifying tumor vascularity and predicting prognostic biomarkers of invasive breast cancer.

# **CLINICAL RELEVANCE/APPLICATION**

Low-dose perfusion breast CT can be used to quantify tumor vascularity and to predict biomarkers of invasive breast cancer and for patients who have difficulty with magnetic resonance imaging.

# SSA02-07 Contrast-Enhanced Cone-Beam Breast-CT without Prior Non-Contrast Scan: Can We Reduce Radiation Exposure While Maintaining Diagnostic Accuracy?

Sunday, Nov. 25 11:45AM - 11:55AM Room: E450B

Participants

Susanne Wienbeck, MD, Goettingen, Germany (*Presenter*) Nothing to Disclose Uwe Fischer, MD, Goettingen, Germany (*Abstract Co-Author*) Nothing to Disclose Joachim Lotz, MD, Gottingen, Germany (*Abstract Co-Author*) Nothing to Disclose Johannes Uhlig, Goettingen, Germany (*Abstract Co-Author*) Nothing to Disclose

#### For information about this presentation, contact:

# susanne.wienbeck@med.uni-goettingen.de

#### PURPOSE

Contrast-enhanced cone-beam breast-CT (CE-CBCT) is a novel breast imaging technique with comparably high radiation dose. The current diagnostic standard includes one non-contrast scan (NC-CBCT) followed by intravenous contrast media injection and a contrast-enhanced scan (CE-CBCT). Performing only the CE-CBCT scan might reduce radiation exposure. Our study aims to evaluate whether CE-CBCT alone is comparable to combined NC + CE-CBCT regarding diagnostic accuracy while reducing radiation exposure.

# **METHOD AND MATERIALS**

This prospective IRB-approved study included 48 women (61 breasts, 100 lesions) with median age 57.9 years (IQR: 49-66 years) and BI-RADS 4/5 lesions diagnosed on mammography/ultrasound in ACR density types c/d breasts. Two blinded breast radiologists read CE-CBCT alone versus NC-CBCT + CE-CBCT in consensus. Intra-observer variability was assessed by one reader performing independent double reading. Sensitivity, specificity and AUC were measured separately for CE-CBCT alone versus NC + CE-CBCT.

# RESULTS

Of 100 lesions, 51 were rated as malignant, 6 as high risk and 43 as benign. Histopathological assessment was performed in 63 breast lesions and imaging follow-up over at least 1 year in another 37 lesions. Diagnostic accuracy for both CBCT approaches was comparable: AUC, sensitivity and specificity showed no significant differences comparing CE-CBCT alone versus NC + CE-CBCT (AUC: 0.84 vs. 0.83, p=0.643; sensitivity: 0.89 vs. 0.85, p=0.158; specificity: 0.73 vs. 0.76, p=0.655). Inter- and intra-observer agreement on BI-RADS readings were excellent (ICC=0.76, ICC=0.83, respectively). Radiation dose was significantly lower for CE-CBCT alone versus NC + CE-CBCT (median average glandular radiation dose 5.9 mGy vs. 11.7 mGy, p<0.001).

# CONCLUSION

The diagnostic accuracy of CE-CBCT alone is comparable to that of combined NC + CE-CBCT in ACR type c/d breast. At the same time, CE-CBCT significantly reduces radiation exposure to the breast. Further research is warranted to confirm these findings in a larger and generalizable population.

# **CLINICAL RELEVANCE/APPLICATION**

Assessment of CE-CBCT alone yields comparable diagnostic accuracy to combined NC + CE-CBCT and reduces radiation exposure by up to 50%. Additional acquisition of NC-CBCT might therefore be unnecessary.

# SSA02-08 Automatic Classification of Breast Lesions in Contrast Mammography Using Deep Learning in Conjunction with Multimodal Information: BIRADS Lexicon Features and Raw Image Features

#### Sunday, Nov. 25 11:55AM - 12:05PM Room: E450B

#### Participants

Shaked Rose Perek, BSC, Tel Aviv, Israel (*Abstract Co-Author*) Nothing to Disclose Miriam Sklair-Levy, MD, Tel - Hashomer, Israel (*Presenter*) Nothing to Disclose Gali Zimmerman Moreno, PhD, Ramat Gan, Israel (*Abstract Co-Author*) Nothing to Disclose Arnaldo Mayer, PhD, Ramat Gan, Israel (*Abstract Co-Author*) Nothing to Disclose Anat Shalmon, Ramat Gan, Israel (*Abstract Co-Author*) Nothing to Disclose Osnat Halshtok, MD, Ramat Gan, Israel (*Abstract Co-Author*) Nothing to Disclose Renata Faermann, MD, Tel Aviv, Israel (*Abstract Co-Author*) Nothing to Disclose Michael Gotlieb, MD, Ramat Gan, Israel (*Abstract Co-Author*) Nothing to Disclose Yael Yagil, MD, Ramat Gan, Israel (*Abstract Co-Author*) Nothing to Disclose

#### For information about this presentation, contact:

mirisklair@gmail.com

#### PURPOSE

To assess the combined usage of BIRADS lexicon and pixel data for multimodal automatic classification of breast lesions in dual energy contrast enhanced spectral mammography (CESM) and evaluate its potential for biopsy sparing in benign breast lesion.

# METHOD AND MATERIALS

130 biopsy proven CESM breast lesions, (65 benign and 65 malignant) were manually contoured and described by the BIRADS lexicon. BIRADS data was encoded by a binary vector for each lesion which, together with the lesion pixels, formed a multimodal representation. A deep neural network was designed to process pixel data from its entry layer and merge it with BIRADS data in its deepest layers to better balance between low-level pixel information and high-level BIRADS data that need to be merged. The network was validated in a 5-folds cross-validation (CV) scheme, to tell apart benign/malignant lesions. In each fold, a different subset of 25 lesions was used for testing, and the rest for training. This CV was conducted using 3 different configurations, in order to assess and compare the contributions of different information modalities. (a) BIRADS-only classifier using SVM (BOC), (b) pixel-only network (PON), (c) and the multimodal BIRADS+pixels network (MBPN).

# RESULTS

The results are shown in Fig.1, where blue is benign and red is malignant. The classification score (y axis) reflects malignancy probability. We seek a threshold, below which there are only benign lesions, so that no malignancy is missed, i.e. sensitivity=100% (green line Fig.1). With this condition in mind, the maximal specificities (SP) are: (a) BIRADS only, SP=12%; (b) pixel-only network, SP=37%; (c) multimodal BIRADS and pixel network (MBPN), SP=60%. This means that with MBPN we can safely spare unnecessary biopsy for 60% of benign lesions without missing any malignancies.

#### CONCLUSION

This research showed that the combined usage of BIRADS data, provided by the radiologist, with pixel data extracted from CESM strongly improves the specificity obtained for automatic lesion classification on pixel or BIRADS data alone.

#### **CLINICAL RELEVANCE/APPLICATION**

Multimodal lesion classification in CESM may significantly reduce benign breast biopsies, thus reducing cost and improving patient experience.

# SSA02-09 Preoperative Diagnosis of Metastatic Axillary Sentinel Lymph Nodes in Breast Cancer with Quantitative Parameters Derived from Dual-Energy Spectral CT

Sunday, Nov. 25 12:05PM - 12:15PM Room: E450B

Participants Chushan Zheng, Guangzhou, China (*Presenter*) Nothing to Disclose Xiang Zhang, Guangzhou, China (*Abstract Co-Author*) Nothing to Disclose Jun Shen, MD, Guagnzhou, China (*Abstract Co-Author*) Nothing to Disclose

# PURPOSE

The purpose of this study was to evaluate the diagnostic performance of gemstone spectral imaging (GSI) quantitative parameters derived from dual-energy spectral computed tomography (DEsCT) for the preoperative diagnosis of metastatic sentinel lymph nodes (SLNs) in patients with breast cancer.

# METHOD AND MATERIALS

This prospective study was approved by the ethics committee, and all patients provided written informed consent. From June 2015 to December 2017, dual-phasic contrast-enhanced DEsCT was performed in 193 female patients with breast cancer. Quantitative GSI and morphological parameters were compared between metastatic and non-metastatic SLNs. The quantitative parameters were fitted to univariate and multiple logistic regression models. Their diagnostic abilities were analyzed by receiver operating characteristic curves and compared by the McNemar test.

#### CONCLUSION

DEsCT can be used as a complementary means for the preoperative identification of SLN metastases in patients with breast cancer.

#### **CLINICAL RELEVANCE/APPLICATION**

The slope of the Hounsfield unit curve in venous phase derived from dual-energy spectral CT, can be used to differentiate metastatic from non-metastatic axillary sentinel lymph nodes of breast cancer.



#### SSA03

# Science Session with Keynote: Cardiac (Coronary CTA: Flow and Fractional Flow Reserve)

Sunday, Nov. 25 10:45AM - 12:15PM Room: S404AB



AMA PRA Category 1 Credits ™: 1.50 ARRT Category A+ Credit: 1.75

FDA Discussions may include off-label uses.

#### Participants

Belinda D'Souza, MD, New York, NY (Moderator) Nothing to Disclose

U. Joseph Schoepf, MD, Charleston, SC (*Moderator*) Research Grant, Astellas Group; Research Grant, Bayer AG; Research Grant, Siemens AG; Research support, Bayer AG; Consultant, Guerbet SA; Consultant, General Electric Company; Consultant, HeartFlow, Inc: Consultant, Bayer AG; Consultant, Siemens AG; :

Inc; Consultant, Bayer AG; Consultant, Siemens AG; ; ; Bernd J. Wintersperger, MD, Toronto, ON (*Moderator*) Speaker, Siemens AG; Research support, Siemens AG; Institutional research agreement, Siemens AG; Speaker, Bayer AG

# Sub-Events

SSA03-01 The Relationship of Coronary Endothelial Shear Stress (ESS) at Baseline and Hyperemia, and Its Association to Invasive Fractional Flow Reserve (FFR) and Computed Tomography Angiography FFR (CT-FFR)

Sunday, Nov. 25 10:45AM - 10:55AM Room: S404AB

#### Awards

# **Trainee Research Prize - Medical Student**

Participants

Anji Tang, Boston, MA (*Presenter*) Nothing to Disclose Andreas Giannopoulos, MD, Zurich, Switzerland (*Abstract Co-Author*) Nothing to Disclose Frank J. Rybicki III, MD, PhD, Ottawa, ON (*Abstract Co-Author*) Medical Director, Imagia Cybernetics Inc Dimitris Mitsouras, PhD, Boston, MA (*Abstract Co-Author*) Research Grant, Canon Medical Systems Corporation;

# For information about this presentation, contact:

dmitsouras@alum.mit.edu

#### PURPOSE

Low baseline ESS promotes development of high-risk plaque features. High ESS in one CTA-based hyperemic simulation technology (Heartflow FFRCT) was also recently shown to predict invasive FFR<=0.8. We determined the relationship of resting to hyperemic ESS using non-proprietary CTA-based rest/stress simulation algorithms, and whether flow state affects the ability of ESS to predict FFR<=0.8. Neither of these relationships have been previously assessed for data derived entirely from CTA.

#### **METHOD AND MATERIALS**

Computational fluid dynamics (CFD) was performed for 63 adults from CTA prior (<90d) to invasive FFR. Rest-state CFD used only CTA data (myocardial mass, Murray's law). Stress CFD coupled the epicardial arteries to a microvascular resistance model using 1/4 the resistance values obtained by the rest CFD. Only commercial CTA segmentation and CFD software was used. Rest and stress ESS at relevant locations (eg, coronary segments, across lesion, min lumen diameter, every 3 mm, min/max ESS) were compared (t-test) between FFR<=0.8 vs >0.8 vessels. Receiver operating characteristic area-under-the-curve (AUC) to predict FFR<=0.8 in all vessels was compared for diameter stenosis (%DS) and plaque volume (%PV) by CTA, CT-FFR, and rest and stress ESS.

#### RESULTS

In vessels where CT-FFR differed <0.05 from FFR (ie, stress CFD matched the patient's true hyperemic conditions), most ESS metrics differed significantly for FFR<=0.8 vs >0.8 vessels, eg lesion rest ESS=4.2 vs 1.9 Pa (p=0.012) and stress ESS=17.0 vs 9.6 (p=0.001), or, maximum ESS (rest: 9.5 vs 4.1, p=0.001; stress: 37.0 vs 19.6, p<0.001). Notably, the minimum ESS did not differ for FFR<=0.8 vs >0.8 vessels (rest p=0.184, stress p=0.454), but the location of minimum ESS differed in 31 of 40 vessels between rest and stress. AUC to detect FFR<=0.8 was 0.57 for CTA %DS, 0.74 for %PV, 0.9 for CT-FFR, and 0.86 for rest and 0.85 for stress ESS across the lesion. The AUC of rest and stress ESS was not inferior to that of CT-FFR (p=0.446); CT-FFR statistically significantly improved only upon the AUC of %PV.

# CONCLUSION

High ESS across a lesion at either baseline or hyperemia is associated with lesion-specific ischemia, and both have similar diagnostic accuracy as CT-FFR to detect FFR<=0.8. Low ESS regions differ between rest and stress.

#### **CLINICAL RELEVANCE/APPLICATION**

ESS from CTA can detect lesion-specific ischemia similarly to CT-FFR, with or without the need to simulate hyperemia.

#### **Honored Educators**

Presenters or authors on this event have been recognized as RSNA Honored Educators for participating in multiple qualifying educational activities. Honored Educators are invested in furthering the profession of radiology by delivering high-quality educational content in their field of study. Learn how you can become an honored educator by visiting the website at: https://www.rsna.org/Honored-Educator-Award/ Frank J. Rybicki III, MD, PhD - 2016 Honored Educator

# SSA03-02 Comparison Between Stress Cardiac Computed Tomography Perfusion versus Fractional Flow Reserve CT Derived in the Evaluation of Suspected Coronary Artery Disease: PERFECTION Prospective Study

Sunday, Nov. 25 10:55AM - 11:05AM Room: S404AB

# Participants

Andrea Baggiano, Milan, Italy (*Abstract Co-Author*) Nothing to Disclose Margherita Soldi, Milan, Italy (*Abstract Co-Author*) Nothing to Disclose Giuseppe Muscogiuri, MD, Charleston, SC (*Presenter*) Nothing to Disclose Andrea Guaricci, MD, Foggia, Italy (*Abstract Co-Author*) Nothing to Disclose Marco Guglielmo, Milan, Italy (*Abstract Co-Author*) Nothing to Disclose Daniele Andreini, MD, Milan, Italy (*Abstract Co-Author*) Nothing to Disclose Daniele Andreini, MD, Milan, Italy (*Abstract Co-Author*) Nothing to Disclose Edoardo Conte, Milan, Italy (*Abstract Co-Author*) Nothing to Disclose Edoardo Conte, Milan, Italy (*Abstract Co-Author*) Nothing to Disclose Marca D. Annoni, MD, Milan, Italy (*Abstract Co-Author*) Nothing to Disclose Maria E. Mancini, Milan, Italy (*Abstract Co-Author*) Nothing to Disclose Alberto Formenti, Milan, Italy (*Abstract Co-Author*) Nothing to Disclose Mauro Pepi, Milan, Italy (*Abstract Co-Author*) Nothing to Disclose Gianluca Pontone, MD, Milan, Italy (*Abstract Co-Author*) Nothing to Disclose Mauro Pepi, Milan, Italy (*Abstract Co-Author*) Nothing to Disclose Mauro Pepi, Milan, Italy (*Abstract Co-Author*) Nothing to Disclose Gianluca Pontone, MD, Milan, Italy (*Abstract Co-Author*) Nothing to Disclose Gianluca Pontone, MD, Milan, Italy (*Abstract Co-Author*) Nothing to Disclose Gianluca Pontone, MD, Milan, Italy (*Abstract Co-Author*) Nothing to Disclose Gianluca Pontone, MD, Milan, Italy (*Abstract Co-Author*) Speakers Bureau, General Electric Company Consultant, General Electric Company Research Consultant, HeartFlow, Inc Speakers Bureau, HeartFlow, Inc Speakers Bureau, Medtronic plc Speakers Bureau, Baver AG

#### For information about this presentation, contact:

andrea.baggiano@gmail.com

#### PURPOSE

The PERFECTION study is a longitudinal, prospective and consecutive cohort study to compare the feasibility and accuracy of FFRCT versus stress-CTP for the diagnosis of functionally significant CAD.

#### **METHOD AND MATERIALS**

One-hundred-forty-seven consecutive symptomatic patients (Mean age:  $65.8\pm9.2$ ; Male: 105) for chest pain who were referred for non-emergent, clinically indicated ICA plus invasive FFR were enrolled. The primary endpoint was to compare the diagnostic accuracy of cCTA versus cCTA+FFRCT versus cCTA+stress-CTP for the detection of significant CAD in a vessel and patients-based analysis defined by ICA with an invasive FFR <= 0.80 or coronary artery stenoses >= 80% or totally occluded vessels.

#### RESULTS

Rest cCTA was successfully performed in all patients, FFRCT was performed in 143 out of 147 patients and stress-CTP was performed in 144 out of 147 patients. cCTA demonstrated a vessel and patient-based sensitivity (SE), specificity (SP), negative predictive value (NPV), positive predictive value (PPV) and diagnostic accuracy (ACC) of 99%, 76%, 100%, 61%, 82% and 95%, 54%, 94%, 63%, 74%, respectively. The diagnostic performance of integrated protocol of rest cCTA+FFRCT showed a vessel and patient-based SE, SP, NPV, PPV and ACC of 88%, 94%, 95%, 84%, 92% and 90%, 85%, 92%, 83%, 87%, respectively. Finally, the diagnostic performance of integrated protocol of rest cCTA+FFRCT showed a vessel and patient based SE, SP, NPV, PPV and ACC of 72%, 95%, 97%, 87%, 94% and 98%, 87%, 99%, 86%, 92%, respectively. Both FFRCT and stress-CTP significantly improved SP, PPV and overall ACC in both per-vessel and per-patient based model when added to cCTA, while no differences were found between cCTA+FFRCT versus cCTA+stress CTP.

#### CONCLUSION

Both FFRCT and stress-CTP are valid tool in addition to cCTA to evaluate the functional relevance of CAD. Based on these results, in patients with suspected CAD, cCTA alone or with integrated FFRCT might be sufficient to exclude relevant stenosis with the advantage to require a single acquisition with a low radiation exposure and low amount of contrast agent. Nevertheless, it might be reasonable to combine stress-CTP data in some patients with positive integrated cCTA+FFRCT exam thanks to the better specificity.

#### **CLINICAL RELEVANCE/APPLICATION**

FFRCT and CTP in addition to cCTA can be helpful to evaluate the functional relevance of CAD

# SSA03-03 CT Myocardial Perfusion Imaging and CT Angiography-Derived Coronary Fractional Flow Reserve for the Prediction of Major Adverse Cardiac Events in Patients with Coronary Artery Disease

Sunday, Nov. 25 11:05AM - 11:15AM Room: S404AB

Participants

Marly van Assen, MSc, Charleston, SC (*Presenter*) Nothing to Disclose
Carlo N. De Cecco, MD, PhD, Atlanta, GA (*Abstract Co-Author*) Research Grant, Siemens AG
Marwen Eid, MD, Charleston, SC (*Abstract Co-Author*) Nothing to Disclose
Maximilian J. Bauer, Charleston, SC (*Abstract Co-Author*) Nothing to Disclose
Marco Scarabello, MD, Milan, Italy (*Abstract Co-Author*) Nothing to Disclose
U. Joseph Schoepf, MD, Charleston, SC (*Abstract Co-Author*) Research Grant, Astellas Group; Research Grant, Bayer AG; Research Grant, Siemens AG; Research support, Bayer AG; Consultant, Guerbet SA; Consultant, General Electric Company; Consultant, HeartFlow, Inc; Consultant, Bayer AG; Consultant, Siemens AG; ;
Francesco Lavra, MD, Cagliari, Italy (*Abstract Co-Author*) Nothing to Disclose
Philipp L. von Knebel Doeberitz, MD, Charleston, SC (*Abstract Co-Author*) Research Grant, Siemens AG

Domenico Mastrodicasa, MD, Charleston, SC (*Abstract Co-Author*) Nothing to Disclose Matthijs Oudkerk, MD, PhD, Groningen, Netherlands (*Abstract Co-Author*) Nothing to Disclose Rozemarijn Vliegenthart, MD, PhD, Groningen, Netherlands (*Abstract Co-Author*) Instutional Research Grant, Siemens AG Taylor M. Duguay, Charleston, SC (*Abstract Co-Author*) Nothing to Disclose

#### For information about this presentation, contact:

schoepf@musc.edu

#### PURPOSE

To determine the prognostic value of dynamic CT perfusion imaging (CTMPI) and CT coronary angiography (CCTA)-derived fractional flow reserve (CT-FFR) for the prediction of major adverse cardiac events (MACE).

#### **METHOD AND MATERIALS**

Data was included from four institutions using patients who underwent CCTA and stress dynamic CTMPI on a 3rd generation dualsource CT system with a follow up period of 18 months or until MACE occurred. On-site CT-FFR was computed for each coronary artery. Using CTMPI data, a myocardial blood flow (MBF) index was calculated, for which each vessel territory was normalized to global MBF. The lowest CT-FFR and MBF index was recorded for each patient. The prognostic value of CTA, CT-FFR, MBF index, as well as the combination of the three was evaluated for the prediction of MACE using binary logistic regression and measures of diagnostic accuracy.

#### RESULTS

Of the 81 total patients included, 25 (31%) experienced MACE during the follow up period. CCTA alone had an area under the curve (AUC) of 0.655 for predicting MACE, with a corresponding sensitivity and specificity of 56% and 75%, respectively. The CT-FFR AUC for the prediction of MACE was 0.703 with a sensitivity and specificity of 64% and 80%, respectively. The optimal threshold computed with the Youden index was 0.75. Dynamic CTMPI had an AUC of 0.812 using the index MBF with a sensitivity and specificity of 88% and 75%, respectively. Using the Youden index, the optimal threshold for index MBF was 0.88. In cases with a negative CTMPI and positive CT-FFR, index MBF was most predictive of outcome (83% of patients). The combination of CCTA, CT-FFR, and CTMPI resulted in an improved AUC of 0.857 compared to CT-FFR and CTMPI alone.

#### CONCLUSION

Combined CT-FFR and dynamic CTMPI analysis based on cardiac CT imaging is a promising approach for the prediction of MACE in patients with coronary artery disease. While both techniques individually demonstrate good diagnostic accuracy, an integrated approach using both modalities improved the diagnostic accuracy for predicting MACE.

#### **CLINICAL RELEVANCE/APPLICATION**

This study shows the benefit of a combined CT-FFR/CTMPI approach to predict MACE. The correct identification of patients at risk of MACE can improve the efficiency and cost-effectiveness of treatment.

# SSA03-04 Machine Learning Based CT-FFR Integrating With Quantitative Myocardial Mass Subtended By Coronary Stenosis Outperforms Plaque Features for Predicting Hemodynamical Significance of Lesions

Sunday, Nov. 25 11:15AM - 11:25AM Room: S404AB

Participants

Mengmeng Yu, MA, Shanghai, China (*Presenter*) Nothing to Disclose Jiayin Zhang, MD, Shanghai, China (*Abstract Co-Author*) Nothing to Disclose

# For information about this presentation, contact:

radiologistmoon@163.com

# PURPOSE

To study the diagnostic performance of the ratio of subtended myocardial mass to the minimal lumen diameter (MLD) at coronary computed tomographic angiography (CCTA) and machine learning based CT-FFR for differentiating functionally significant from insignificant lesions, with reference to fractional flow reserve (FFR).

# **METHOD AND MATERIALS**

Patients who underwent both coronary CTA and FFR measurement at invasive coronary angiography (ICA) within 2 weeks were retrospectively included in our study. CT-FFR, subtended myocardial mass (V sub), percentage of V sub, V ratio/MLD, along with other parameters, including minimal luminal area (MLA), MLD, lesion length (LL), diameter stenosis, area stenosis, plaque burden, and remodeling index, low attenuation plaque, napkin-ring sign, spotty calcification of lesions were recorded. Lesions with FFR <= 0.8 were considered to be functionally significant.

#### RESULTS

One hundred and seventy-two patients with 196 lesions were ultimately included for analysis. The LL, diameter stenosis, area stenosis, plaque burden, V sub, V ratio and V ratio/MLD were all significantly longer or larger in the group of FFR <= 0.8 (p < 0.001 for all), while smaller MLA, MLD and CT-FFR value were also noted (p < 0.001 for all). There were no significant differences between the hemodynamic significant subgroup and insignificant subgroup with respect to the risky plaque features. The area under the curve (AUC) of V ratio/MLD was comparable to that of CT-FFR (AUC=0.84 vs 0.88; p=0.28) and was significantly better than other parameters and for diagnosing functionally significant stenosis. For vessels with CT-FFR values below 0.70, 0.70 to 0.79, 0.80 to 0.89, and above 0.89, diagnostic accuracy of CT-FFR was 92.6%(25/27), 61.8%(34/55), 83.9%(47/56), 94.8%(55/58), respectively. For lesions with CT-FFR values ranging from 0.70 to 0.79, the accuracy could be improved to 80.0% (44/55) if these lesions were evaluated with Vratio/ MLD instead of CT-FFR.

#### CONCLUSION

The "grey-zone" lesions, which have CT-FFR values ranging from 0.7 to 0.8, showed lower diagnostic performance. A stepwise

approach, reserving Vratio/ MLD for "grey-zone" lesions instead of CT-FFR, can improve diagnostic accuracy.

# **CLINICAL RELEVANCE/APPLICATION**

integrating ML based CT-FFR and V ratio/MLD allowed the most accurate discrimination between flow-limiting and non flow-limiting coronary lesions.

# SSA03-05 Coronary Computed Tomography Angiography-Derived Fractional Flow Reserve in Anomalous Origin of the Right Coronary Artery from the Left Coronary Sinus

Sunday, Nov. 25 11:25AM - 11:35AM Room: S404AB

Participants

Chunxiang Tang, MS, Nanjing, China (*Abstract Co-Author*) Nothing to Disclose Meng Jie Lu, Nanjing, China (*Presenter*) Nothing to Disclose U. Joseph Schoepf, MD, Charleston, SC (*Abstract Co-Author*) Research Grant, Astellas Group; Research Grant, Bayer AG; Research Grant, Siemens AG; Research support, Bayer AG; Consultant, Guerbet SA; Consultant, General Electric Company; Consultant, HeartFlow, Inc; Consultant, Bayer AG; Consultant, Siemens AG; ; ; Maximilian J. Bauer, Charleston, SC (*Abstract Co-Author*) Nothing to Disclose John W. Nance JR, MD, Charleston, SC (*Abstract Co-Author*) Nothing to Disclose Parkwood Griffith, Charleston, SC (*Abstract Co-Author*) Nothing to Disclose Chang Sheng Zhou, BS, Nanjing, China (*Abstract Co-Author*) Nothing to Disclose Fan Zhou, Nanjing, China (*Abstract Co-Author*) Nothing to Disclose Jing Yan, Shanghai, China (*Abstract Co-Author*) Nothing to Disclose Guang Ming Lu, MD, PhD, Nanjing, China (*Abstract Co-Author*) Nothing to Disclose Long Jiang Zhang, MD, PhD, Nanjing, China (*Abstract Co-Author*) Nothing to Disclose

# PURPOSE

To examine fractional flow reserve derived from computed tomographic angiography (FFRCT) in patients with anomalous origin of the right coronary artery from the left coronary sinus with interarterial courses (AORLIC), its relationship with patient demographics, anatomical features of AORLIC on coronary computed tomographic angiography (CCTA) images, and its clinical relevance.

#### METHOD AND MATERIALS

Ninety-four patients with AORLIC who underwent CCTA were retrospectively included. Anatomic features (including RCA ostium location relationship with the pulmonary valve [high or low interarterial courses], takeoff angle, degree of stenosis, etc.) associated with abnormal FFRCT values (<0.8) on CCTA were analyzed. Patient demographics and anatomical data were analyzed using binary logistic regression analysis. Receiver operating characteristic analyses were performed to describe the diagnostic performance in detecting AORLIC with normal or abnormal FFRCT values.

# RESULTS

Compared to patients with normal FFRCT values, more patients with high interarterial courses and greater proximal RCA stenosis were found to have abnormal FFRCT values (all P < 0.05). AORLIC with high interarterial courses was found to be the main contributor to abnormal FFRCT values (odds ratios =4.61, 95% confidence interval [CI], 1.51-14.08; P=0.007). The corresponding sensitivity and specificity for predicting abnormal FFRCT were 57.4% and 76.6%, respectively (area under the curve=0.670, 95% CI: 0.560-0.781). AORLIC patients with abnormal FFRCT values showed a higher prevalence of typical angina (19.1% vs 4.3%, P=0.025) and atypical angina (23.4% vs 6.4%, P=0.026) compared to patients with normal FFRCT values.

#### CONCLUSION

AORLIC patients with abnormal FFRCT values have a higher prevalence of high interarterial courses, typical angina, and atypical angina than patients with normal FFRCT values.

#### **CLINICAL RELEVANCE/APPLICATION**

Patients with AORLHIC were more likely to have abnormal FFRCT, showing a higher prevalence of typical angina and atypical angina compared to patients with normal FFRCT values. Thus, this noninvasive FFRCT method may have potential to identify patients at risk for sudden cardiac death.

# SSA03-06 Building-Block-Based 3D Deep Learning: Fully Automated Estimation of Fractional Flow Reserve from Coronary CT Angiography

Sunday, Nov. 25 11:35AM - 11:45AM Room: S404AB

Participants

Kanako K. Kumamaru, MD, PhD, Tokyo, Japan (*Presenter*) Nothing to Disclose Yujiro Otsuka, Tokyo, Japan (*Abstract Co-Author*) Nothing to Disclose Shinichiro Fujimoto, Tokyo, Japan (*Abstract Co-Author*) Nothing to Disclose Yuko Kawaguchi, Tokyo, Japan (*Abstract Co-Author*) Nothing to Disclose Etsuro Kato, Tokyo, Japan (*Abstract Co-Author*) Nothing to Disclose Kazuhisa Takamura, Tokyo, Japan (*Abstract Co-Author*) Nothing to Disclose Chihiro Aoshima, Tokyo, Japan (*Abstract Co-Author*) Nothing to Disclose Hiroyuki Daida, Tokyo, Japan (*Abstract Co-Author*) Nothing to Disclose Yosuke Kogure, MD, Tokyo, Japan (*Abstract Co-Author*) Nothing to Disclose Shigeki Aoki, MD, PhD, Tokyo, Japan (*Abstract Co-Author*) Nothing to Disclose

#### For information about this presentation, contact:

k-kumamaru@juntendo.ac.jp

#### PURPOSE

To evaluate the accuracy of a building-block-based fully automated 3D deep-learning model for estimating fractional flow reserve

(FFR) from whole coronary CT angiography (CCTA) data, with catheter FFR as the reference standard.

# METHOD AND MATERIALS

This HIPAA-compliant, IRB-approved retrospective study of 1052 consecutive patients (mean age, 63 ± 17 years) included 131 patients whose CCTA studies showed 30%-90% stenosis in at least one segment and underwent catheter FFR, and 921 patients who underwent clinically indicated CCTA without catheter FFR. We designed a fully automated building-block-based 3D deep-learning model that inputs whole CCTA data and outputs FFR without requiring any manual segmentations. The model was trained with all 1052 CCTAs. The model comprised lumen extraction, residual extraction, and prediction blocks. In the first and second blocks, a conditional generative adversarial network and a 3D convolutional ladder network, respectively, were used to extract specific features from the CCTA by eliminating image inputs less related to FFR estimation. The prediction block estimated FFR via two independent neural networks with integrated virtual adversarial training and a self-consistency check to reduce overfitting. We used Monte Carlo cross-validation to evaluate the accuracy of the deep-learning model for estimating FFR, with catheter FFR as the reference standard.

# RESULTS

Abnormal catheter FFR values (<=0.8) were observed in 55% of the labeled data (72/131). The deep-learning FFR achieved area under the curve (AUC) of the receiver-operating curve of 0.72 for detection of abnormal FFR, which is significantly higher than for CTA > 50% stenosis (AUC = 0.56). The deep-learning FFR model achieved 76% accuracy for detecting abnormal FFR, with sensitivity of 86.2% (95%CI: 80.5%-90.7%) and specificity of 61.2% (52.4%-69.5%).

#### CONCLUSION

The building-block-based 3D deep-learning model, performing fully automatic estimation of FFR from whole cardiac CT data, achieved accuracy of 76% for the detection of abnormal FFR.

#### **CLINICAL RELEVANCE/APPLICATION**

Our deep-learning model estimates FFR without time-consuming vessel segmentation and may greatly improve the clinical workflow when selecting patients suitable for revascularization procedures.

#### SSA03-07 Prediction of Lesion-Specific Ischemia from Machine Learning-Derived Fractional Flow Reserve

Sunday, Nov. 25 11:45AM - 11:55AM Room: S404AB

# Participants

Hyun Jung Koo, MD, Seoul, Korea, Republic Of (*Presenter*) Nothing to Disclose Joon-Won Kang, MD, Seoul, Korea, Republic Of (*Abstract Co-Author*) Nothing to Disclose Young-Hak Kim, Seoul, Korea, Republic Of (*Abstract Co-Author*) Nothing to Disclose Dong Hyun Yang, MD, Seoul, Korea, Republic Of (*Abstract Co-Author*) Nothing to Disclose

# For information about this presentation, contact:

donghyun.yang@gmail.com

# PURPOSE

This study evaluate the diagnostic performances of machine learning-based model for predicting fractional flow reserve (ML-FFR) and computed tomography (CT) derived-FFR (CT-FFR) in patients with coronary artery diseases with reference standard of invasive FFR.

## METHOD AND MATERIALS

In 472 patients with coronary artery diseases, CT angiography (CTA) and invasive coronary angiography were performed with FFR in 555 lesions. CTA data were visually analyzed to evaluate the location, stenosis degrees and plaque types, and analyzed by semiautomated software to quantify computational fluid dynamics (CFD)-based CT-derived FFR. The trained ML-FFR at each point along the centerline of the coronary tree, was obtained by automated feature selection and model building from quantitative CTA. Correlation between CT-FFR and ML-FFR was obtained. The diagnostic performance of CFD-based CT-FFR and ML-FFR were compared using invasive FFR as reference standard.

#### RESULTS

A total of 270 lesions showed ischemia by invasive FFR (FFR <= 0.80). The correlation between CFD-based CT-FFR and ML-FFR was high (r= 0.60 - 0.99, P<0.001). CT-FFR showed moderate to high sensitivity and specificity for all lesions including left main, left anterior descending, left circumflex and right coronary arteries (Sensitivity: 55.4 - 83.3; specificity 65.1 - 73.9). For intermediate (visual stenosis grading 30-80%) lesions and tandem lesions, moderate sensitivity and specificity were observed (sensitivity: 65.1 and 62.5; specificity: 70.7 and 58.0, respectively). ML-FFR showed comparable results to CT-FFR for all lesions (Sensitivity: 57.1 - 83.3; specificity 66.5 - 77.3), and also in intermediate or tandem lesions (sensitivity: 65.1 and 62.5; specificity: 71.3 and 59.1, respectively). Compared with the CFD-based CT-FFR, the time to perform ML-FFR was shortened to a few seconds.

# CONCLUSION

ML-FFR showed comparable results to CFD-based CT-FFR for the prediction of lesion-specific ischemia confirmed by invasive FFR.

# **CLINICAL RELEVANCE/APPLICATION**

ML-FFR can be used as additional information after obtaining CTA for evaluation of coronary artery stenosis with equivalent diagnostic performance of CFD-based CT-FFR.

# SSA03-08 Cardiac Keynote Speaker: Value of CTA for Fractional Flow Reserve

Sunday, Nov. 25 11:55AM - 12:15PM Room: S404AB

#### Participants

U. Joseph Schoepf, MD, Charleston, SC (*Presenter*) Research Grant, Astellas Group; Research Grant, Bayer AG; Research Grant, Siemens AG; Research support, Bayer AG; Consultant, Guerbet SA; Consultant, General Electric Company; Consultant, HeartFlow,

Inc; Consultant, Bayer AG; Consultant, Siemens AG; ; ;

For information about this presentation, contact:

schoepf@musc.edu



#### SSA04

Science Session with Keynote: Cardiac (Nonischemic Cardiomyopathies)

Sunday, Nov. 25 10:45AM - 12:15PM Room: S404CD



AMA PRA Category 1 Credits ™: 1.50 ARRT Category A+ Credit: 1.75

**FDA** Discussions may include off-label uses.

#### Participants

Karen G. Ordovas, MD, San Francisco, CA (*Moderator*) Advisor, Arterys Inc Scott R. Akers, MD, PhD, Philadelphia, PA (*Moderator*) Nothing to Disclose

# Sub-Events

SSA04-01 Cardiac Keynote Speaker: Prognostic Role of MR Imaging in Nonischemic Myocardial Disease

Sunday, Nov. 25 10:45AM - 11:05AM Room: S404CD

Participants

Karen G. Ordovas, MD, San Francisco, CA (Presenter) Advisor, Arterys Inc

# SSA04-03 Prevalence, CMR Characteristics, and Outcomes of Hypertrophic Cardiomyopathy with Restrictive Phenotype

Sunday, Nov. 25 11:05AM - 11:15AM Room: S404CD

Participants

Shuang Li, Beijing, China (*Presenter*) Nothing to Disclose Bailing Wu, Hubei, China (*Abstract Co-Author*) Nothing to Disclose Gang Yin SR, BS, Beijing, China (*Abstract Co-Author*) Nothing to Disclose Lei Song, Beijing, China (*Abstract Co-Author*) Nothing to Disclose Yong Jiang, Beijing, China (*Abstract Co-Author*) Nothing to Disclose Jinghan Wang, Beijing, China (*Abstract Co-Author*) Nothing to Disclose Shihua Zhao, Beijing, China (*Abstract Co-Author*) Nothing to Disclose Minjie Lu, MD, PhD, Beijing, China (*Abstract Co-Author*) Nothing to Disclose

#### For information about this presentation, contact:

coolkan@163.com

# PURPOSE

Previous reports indicated that there was a subgroup of HCM with restrictive phenotype, which was defined by restrictive filling and reduced diastolic volumes. However, the CMR characteristics and prognosis of the restrictive phenotype has not been systematically investigated. The aim of this project was to investigate the prevalence, clinical significance, CMR characteristics and outcomes of hypertrophic cardiomyopathy (HCM) with restrictive phenotype .

#### **METHOD AND MATERIALS**

A total of 2892 consecutive patients with HCM were evaluated to identify individuals who fulfilled diagnostic criteria for restrictive phenotype. 32 patients of HCM with restrictive phenotype and 32 age and gender matched patients with typical non obstructive HCM were retrospectively enrolled.

# RESULTS

The left and right atrium diameter were  $55.4\pm4.8$  mm and  $61.4\pm8.7$  mm, which were significantly larger than those of the controls (p<0.001); The left ventricular end-diastolic volume index, the cardiac index, and the left heart ejection fraction of patients with restrictive phenotype were all significantly less than those of the controls. The segments with late gadolinium enhancement(LGE) were 7.8±2.4 in restrictive phenotype group, which were significantly greater than controls (4.6±2.3, p=0.004). The 62-month survival rate was 54.1% in HCM with restrictive phenotype, compared with 91.7% in control group.

# CONCLUSION

Restrictive phenotype is a special subtype of HCM. The MR features of this phenotype include mild-to-moderate left ventricular hypertrophy, severely enlarged atria, normal or small ventricles, pericardial effusion and a wide range of LGE. These patients have severe clinical symptoms and poor prognosis. MRI shows high diagnostic value in the identification of this phenotype.

#### **CLINICAL RELEVANCE/APPLICATION**

MRI shows high diagnostic value in the identification of hypertrophic cardiomyopathy with restrictive phenotype and will help indicate patients' prognosis.

# **Renal Disease**

Sunday, Nov. 25 11:15AM - 11:25AM Room: S404CD

Participants Yi Zhang, MS, Chengdu, China (*Presenter*) Nothing to Disclose Zhigang Yang, MD, Chengdu, China (*Abstract Co-Author*) Nothing to Disclose Huayan Xu, Chengdu, China (*Abstract Co-Author*) Nothing to Disclose Wanlin Peng, MS, Chengdu, China (*Abstract Co-Author*) Nothing to Disclose Yingkun Guo, Chengdu, China (*Abstract Co-Author*) Nothing to Disclose

#### For information about this presentation, contact:

loselien@live.cn

# PURPOSE

This study aimed to investigate the subclinical myocardial deformation of left ventricle (LV) in end stage renal disease (ESRD) patients by cardiac magnetic resonance (CMR) tissue tracking and explore its prediction of HF.

# METHOD AND MATERIALS

Sixty-two consecutive ESRD patients with preserved LV ejection fraction (LVEF>50%) and 21 age- and sex- matched healthy volunteers were prospectively recruited and underwent 3.0T CMR examination. A series of SSFP cine sequence, including short axis, horizontal 4-chamber and vertical 2-chamber long axis were scanned. LV function variables were measured. LV myocardial strain parameters such as global peak strain (PS), peak strain rate, peak velocity indices were automatically computed. After examination, patients were followed up for a duration of 11-30 months to assess HF outcome by phone contact.

# RESULTS

ESRD patients with preserved LVEF had decreased radial, circumferential and longitudinal PS compared with normal controls (42.11±12.53% vs. 48.01±11.22%, -17.89±2.73% vs. -19.67±2.23%, -15.25±2.49% vs. -17.18±2.52%; respectively, all P<0.05). After a 11-30-month follow-up, 30 of 62 patients had HF. By analyzing myocardial strain data, it showed that ESRD patients suffered from HF was already found to have lower values of PS in three directions than both normal controls and patients free from HF (all P<0.05). The global circumferential and longitudinal PS were proven to be significant risk factors of HF (OR 1.294, 1.228; 95% confidence interval 1.100-1.522, 1.035-1.457; respectively, all P<0.05). A significantly lower survival rate and higher risk of HF were displayed in patients with circumferential and longitudinal PS lower than the median value. Cut-off values of PS -18.78% for circumferential and -14.54% for longitudinal to discriminate HF outcome was identified with relatively high sensitivity and specificity (AUC of 0.840, 0.821, respectively).

#### CONCLUSION

CMR tissue tracking provided subclinical and prognostic information to predict HF in ESRD patients before notably decreased LVEF. LV global circumferential and longitudinal PS were demonstrated to be independent risk factors of HF in ESRD patients.

# **CLINICAL RELEVANCE/APPLICATION**

Our study proved the ability of CMR tissue tracking parameters to provide subclinical and prognostic information to predict heart failure in ESRD patients before notably decreased LVEF which may give a guidance of appropriate and early cardiovascular treatment.

# SSA04-05 Value of Fractal Analysis in Identification and Further Discrimination of Isolated Left Ventricular Non-Compaction and Dilated Cardiomyopathy by Cardiac Magnetic Resonance

Sunday, Nov. 25 11:25AM - 11:35AM Room: S404CD

#### Participants

Lianggeng Gong, Nanchang, China (*Abstract Co-Author*) Nothing to Disclose Tian Zheng, Nanchang, China (*Presenter*) Nothing to Disclose Qian Zou, Nanchang, China (*Abstract Co-Author*) Nothing to Disclose Hongye Zou, Nanchang, China (*Abstract Co-Author*) Nothing to Disclose Wei Zhou, Nanchang City, China (*Abstract Co-Author*) Nothing to Disclose Shuhao Li, MMed, Nanchang, China (*Abstract Co-Author*) Nothing to Disclose

For information about this presentation, contact:

zhengt1116@163.com

#### PURPOSE

The aim of this study was to compare cardiac magnetic resonance imaging (MRI) features between isolated left ventricular noncompaction (IVNC) and dilated cardiomyopathy(DCM).

# **METHOD AND MATERIALS**

A consecutive series of 35 patients with IVNC (males,n=23) and 30 patients with DCM (males,n=21) from a tertiary university hospital were reviewed. 20 healthy volunteers (males,n=13) were selected as control group. All groups were matched for age, gender, and body surface area. The degree of LV trabeculation was evaluated by a semi-automatic tool based on fractal analysis (FA). The resulting FD is a unitless measure value of how completely the object fills space. Myocardial deformation and Left ventricular (LV) function was assessed by feature tracking.

#### RESULTS

IVNC group had higher max apical FD and mean global FD than DCM group (max apical FD: $1.433\pm0.074$  vs.  $1.341\pm0.062$ ,P < 0.001; mean global FD: $1.323\pm0.036$  vs. $1.267\pm0.041$ , p<0.001, respectively). FDs show positively correlation with the ratio of NC/C. Compared with controls, both patient groups showed significantly reduced strain and strain rate values of all LV segments. Of note, The global longitudinal strain value of the left ventricle (GPSL) was different in the IVNC group -6.49(-11.41, -4.90) and the

DCM group -4.61(-5.87, -3.61) (P < 0.01). and Left ventricular (LV) function. The diagnostic accuracy is equivalent in univariable, but the accuracy is higher when using FDs in coordination with myocardial deformation(AUC=0.93,CI 95% [0.86; 0.98], P<0.001).

# CONCLUSION

Fractal analysis can measure quantitatively the extent of non-compacted myocardium of the left ventricle, and have a definite value in the identification of pathological non-compacted myocardium and normal trabeculation. Fractal dimension combined with myocardial strain is a superior predictor of distinguishing IVNC from DCM.

#### **CLINICAL RELEVANCE/APPLICATION**

(dealing with isolated ventricular non-compaction) 'Fractal analysis based on Cine MR studies has a definite value in the identification of pathological non-compacted myocardium and normal trabeculation .'

# SSA04-06 Native T1 Mapping Distinguishes Patients with Arrhythmogenic Right Ventricular Cardiomyopathy from Control Subjects

Sunday, Nov. 25 11:35AM - 11:45AM Room: S404CD

#### Participants

Mimount Bourfiss, Utrecht, Netherlands (*Presenter*) Nothing to Disclose Niek H. Prakken, MD,PhD, Amersfoort, Netherlands (*Abstract Co-Author*) Nothing to Disclose Jeroen F. van der Heijden, Utrecht, Netherlands (*Abstract Co-Author*) Nothing to Disclose Ihab R. Kamel, MD, PhD, Baltimore, MD (*Abstract Co-Author*) Research Grant, Siemens AG Stefan L. Zimmerman, MD, Ellicott City, MD (*Abstract Co-Author*) Project consultant, Siemens Healthcare; Research grant, American Heart Association; Folkert Asselbergs, MD,PhD, Utrecht, Netherlands (*Abstract Co-Author*) Nothing to Disclose Tim Leiner, MD, PhD, Utrecht, Netherlands (*Abstract Co-Author*) Speakers Bureau, Koninklijke Philips NV Research Grant, Bayer AG Birgitta K. Velthuis, MD, Utrecht, Netherlands (*Abstract Co-Author*) Nothing to Disclose Anneline S. te Riele, MD, Utrecht, Netherlands (*Abstract Co-Author*) Nothing to Disclose

#### PURPOSE

Arrhythmogenic right ventricular cardiomyopathy (ARVC) is an inherited heart disease characterized by fibrofatty replacement of the myocardium. Native T1 mapping is a promising technique to quantify changes in cardiac microstructure on cardiac magnetic resonance imaging (CMR). We aimed to analyze the diagnostic value of native T1 mapping in ARVC.

#### **METHOD AND MATERIALS**

We analyzed short-axis cine 1.5 Tesla CMR images obtained using a MOLLI sequence in 51 subjects (15 ARVC patients fulfilling the 2010 diagnostic Task Force Criteria, 23 phenotype negative ARVC relatives, and 13 control subjects with right ventricular outflow tract ventricular tachycardia [RVOT VT]). Global and regional fibrosis of the left ventricle (LV) were measured as native T1 times using cvi42 (version 5.6.6, Calgary, Canada). LV segmentation was according to the 16-segment American Heart Association recommendation. We also assessed dispersion of regional T1 times, defined as the standard deviation of regional T1 times within the same patient over all analyzed segments. Diagnostic performance was assessed using ROC curve analysis.

#### RESULTS

Mean age was  $39\pm17$  years and 49%(25/51) were male. Mean global native T1 times were not significantly different among ARVC patients ( $1061\pm40$ ms p=0.085) and relatives ( $1053\pm23$ ms p=0.181) compared to controls ( $1038\pm27$ ms). However, in comparison to controls ( $67\pm12$ ), the dispersion of regional T1 times was significantly higher in ARVC patients ( $91\pm32$ ms p=0.014) and relatives ( $77\pm15$ ms p=0.044). This was reflected in longer regional T1 times in the basal (p=0.037) and mid (p=0.013) segments in ARVC patients; and only in the basal (p=0.042) segment in relatives. More specifically, ARVC patients had longer posterolateral, inferior and anterior T1 times (p<=0.027) while relatives had longer posterolateral and inferior T1 times (p<=0.009) compared to controls. ROC analyses revealed the highest AUC for the diagnosis of ARVC using posterolateral native T1 time in both ARVC patients (AUC=0.794) and relatives (AUC=0.790).

#### CONCLUSION

Native T1 mapping distinguishes ARVC patients and at-risk relatives from RVOT VT controls using regional (posterolateral and inferior) T1 times.

# CLINICAL RELEVANCE/APPLICATION

Early detection of ARVC is pertinent as life-threatening ventricular arrhythmias can occur. Native T1 mapping has a possible role in differentiating ARVC patient and at-risk relatives from controls.

#### **Honored Educators**

Presenters or authors on this event have been recognized as RSNA Honored Educators for participating in multiple qualifying educational activities. Honored Educators are invested in furthering the profession of radiology by delivering high-quality educational content in their field of study. Learn how you can become an honored educator by visiting the website at: https://www.rsna.org/Honored-Educator-Award/ Ihab R. Kamel, MD, PhD - 2015 Honored EducatorStefan L. Zimmerman, MD - 2012 Honored EducatorStefan L. Zimmerman, MD - 2015 Honored Educator

# SSA04-07 The Study of T1-Mapping and Extracellular Volume (ECV) Quantification of Myocardial Fibrosis Caused by Iron Deposited in a Pig Model

Sunday, Nov. 25 11:45AM - 11:55AM Room: S404CD

Participants Peng Peng, Nanning, China (*Presenter*) Nothing to Disclose Liling Long, MD, Nanning, China (*Abstract Co-Author*) Nothing to Disclose De Lin Zhong, Nanning, China (*Abstract Co-Author*) Nothing to Disclose

#### For information about this presentation, contact:

# PURPOSE

To explore the relationship between myocardial extracellular volume(ECV) and myocardial fibrosis index--collagen volume fraction(CVF) using an iron overloaded pig model by 3T MRI.

# **METHOD AND MATERIALS**

27 pigs underwent iron dextran loading from 1 to 15 weeks. 4 controls were studied as well. T1 values were measured using a ShMOLLI sequence at 3T. Gd-DTPA was used to enhance. Measured the T1 values of the ventricular septum and left ventricular blood pool at the short axial slices of the papillary muscle respectively at plain scan and enhanced scan at the time of 20 minutes after injecting Gd-DTPA contrast medium, then calculated the ECV. Ex vivo cardiac pathology was obtained for all pigs studied. Pathological fibrosis index-collagen volume fraction(CVF) was acquired. Postmortem assessments of cardiac iron concentration(CIC) was conducted in an atomic absorption spectrophotometer. MRI measures were fitted against CVF using linear regression for the first 22 pigs. The remaining 5 were used to test the accuracy of the derived model.

#### RESULTS

In the experimental pigs, as dextran iron injection increased over time, the cardiac iron content increased, and myocardial collagen fibrils increased accordingly. ECV was linearly correlated to CVF (r= 0.990) in this study at 3T. By regression, the linear equations were determined as Y=-0.010+0.467X (F=1139.33,P<0.001) (Y:CVF, X:ECV). In the 5 test pigs, the predicted CVFs using the derived equations agreed well with the results quantified by pathology.

#### CONCLUSION

ECV are highly correlated with CVF in a novel iron overloaded pigs model. MRI quantification of myocardial fibrosis caused by iron deposited is feasible at 3T.

# **CLINICAL RELEVANCE/APPLICATION**

Used MRI method to assess the degree of myocardial fibrosis caused by iron deposited in iron overloaded patients and developed a reliable and noninvasive techniques to measure myocardial fibrosis.

# SSA04-08 Texture Analysis of Magnetic Resonance T1 Mapping with Dilated Cardiomyopathy: A Machine Learning Approach

Sunday, Nov. 25 11:55AM - 12:05PM Room: S404CD

Participants

Xiaoning Shao, Zhengzhou, China (*Abstract Co-Author*) Nothing to Disclose Yingjie Sun, Luohe, China (*Abstract Co-Author*) Nothing to Disclose Wenbo Zhang, Zhengzhou, China (*Abstract Co-Author*) Nothing to Disclose Yong Zhang, DO, Zhengzhou, China (*Abstract Co-Author*) Nothing to Disclose Zhifeng Kou, PhD, Detroit, MI (*Abstract Co-Author*) Nothing to Disclose Jingliang Cheng, MD,PhD, Zhengzhou, China (*Abstract Co-Author*) Nothing to Disclose Jingjing Liu, Zhengzhou, China (*Presenter*) Nothing to Disclose

# For information about this presentation, contact:

xiaoningshao@163.com

#### PURPOSE

Diagnosis of dilated cardiomyopathy is a challenge in clinical radiology. We want to find out whether texture analysis parameters on magnetic resonance T1 mapping can be helpful for the diagnosis of dilated cardiomyopathy (DCM).

# **METHOD AND MATERIALS**

We screened 50 dilated cardiomyopathy cases retrospectively and recruited 24 healthy controls prospectively between March 2015 and July 2017. T1 maps were acquired using Modified Look-Locker Inversion Recovery (MOLLI) sequence at 3.0 T MR scanner. Endocardium and epicardium were drawn on short-axis slices of T1 maps by an experienced radiologist. Twelve histogram parameters and five gray-level co-occurrence matrix (GLCM) features were extracted during texture analysis. Differences in texture features between DCM patients and healthy controls were evaluated by T-tests. Support vector machine (SVM) was used to calculate the diagnosis accuracy of those texture parameters. Schematic diagram of this study is shown on figure one.

# RESULTS

Most histogram features were higher in DCM group as compared to healthy control, and nine of them had significant differences between DCM group and healthy control. As for GLCM features, energy, correlation, and homogeneity were higher in DCM group than that of the healthy control. Also, Entropy and contrast were lower in DCM group. Entropy, contrast, and homogeneity had significant differences between two groups. The diagnosis accuracy using SVM classifier with all those histogram features and GLCM features was 0.85±0.07.

#### CONCLUSION

A computer-based texture analysis and machine learning approach of T1 mapping could provide an objective tool for the diagnosis of dilated cardiomyopathy.

#### **CLINICAL RELEVANCE/APPLICATION**

Texture analysis of T1 mapping could provide an objective tool for the diagnosis of dilated cardiomyopathy.

# SSA04-09 Fully Automated Diagnosis of Cardiomyopathy from Cardiac MR Imaging Using Convolutional Neural Networks

Participants Dermot Mallon, MBChB, London, United Kingdom (*Presenter*) Nothing to Disclose Antonio de Marvao, MBChB, London, United Kingdom (*Abstract Co-Author*) Nothing to Disclose Carlo Biffi, BSC, London, United Kingdom (*Abstract Co-Author*) Nothing to Disclose Jinming Duan, PhD, London, United Kingdom (*Abstract Co-Author*) Nothing to Disclose Ghalib Bello, PhD, London, United Kingdom (*Abstract Co-Author*) Nothing to Disclose Timothy Dawes, London, United Kingdom (*Abstract Co-Author*) Nothing to Disclose Georgia Doumou, BSC, London, United Kingdom (*Abstract Co-Author*) Nothing to Disclose Stuart A. Cook, MRCP, PhD, London, United Kingdom (*Abstract Co-Author*) Nothing to Disclose Declan P. O'Regan, FRCR, London, United Kingdom (*Abstract Co-Author*) Nothing to Disclose

# For information about this presentation, contact:

dmallon@ic.ac.uk

# PURPOSE

Primary cardiomyopathies are diseases of the myocardium that are characterized by remodeling of the left ventricle and impaired cardiac function. Dilated cardiomyopathy (DCM) is a leading cause of heart failure while hypertrophic cardiomyopathy (HCM) is a common cause of sudden death. Diagnosis is made on imaging criteria but relies on manual volumetric analysis of the data and requires expertise to differentiate from other conditions which mimic cardiomyopathy. Deep learning approaches have shown promise in image classification tasks, and here we designed and evaluated a convolutional neural network (CNN) for fully-automated diagnosis of cardiomyopathy in a large sample of cardiac magnetic resonance (CMR) datasets.

# **METHOD AND MATERIALS**

The study cohort consisted of 1,069 adult participants: 311 patients with DCM, 396 patients with HCM and 362 healthy volunteers (HV) matched by gender, age and body surface area. All subjects had a conventional CMR including retrospectively-gated cine imaging. The 4-chamber cine sequence was used for analysis and passed to a 6-layer convolutional neural network implemented in TensorFlow. Five convolutional layers, with between 64 and 128 nodes, were followed by a fully-connected 128-node layer. A predicted classification was obtained from an output later with a SoftMax activation function. The model was trained over 100 epochs using a Titan X GPU. Four-fold cross validation was performed with results reported as mean accuracy.

#### RESULTS

All subjects were included in the analysis. Processing time per subject was approximately 2 seconds. In total 80/82 DCM, 84/97 HCM and 87/87 HV participants were correctly classified in the held-out data. Overall, 251/266 participants were correctly classified (94.3%).

# CONCLUSION

Cardiomyopathy can be diagnosed with a high degree of accuracy through direct analysis of time-resolved CMR imaging using a CNN. This includes correctly excluding disease in every healthy adult. Future work will include simultaneous analysis of cine sequences in different cardiac planes and external validation of the model on an independent cohort.

#### **CLINICAL RELEVANCE/APPLICATION**

These findings demonstrate the potential of an automated method to efficiently and objectively diagnose cardiomyopathy on cardiac MRI.



#### SSA05

# Chest (Emphysema/COPD)

Sunday, Nov. 25 10:45AM - 12:15PM Room: E451A



AMA PRA Category 1 Credits <sup>™</sup>: 1.50 ARRT Category A+ Credit: 1.75

#### Participants

Carole A. Ridge, MD, Dublin 7, Ireland (*Moderator*) Nothing to Disclose Beth Zigmund, MD, Haddonfield, NJ (*Moderator*) Consultant, BioVentrix, Inc

# Sub-Events

# SSA05-01 High-Resolution Chest CT Imaging of the Lung: Impact of High Matrix Reconstruction and Photon-Counting-Detector CT

Sunday, Nov. 25 10:45AM - 10:55AM Room: E451A

Participants

David J. Bartlett, MD, Rochester, MN (*Presenter*) Nothing to Disclose Chi Wan Koo, MD, Rochester, MN (*Abstract Co-Author*) Nothing to Disclose Brian J. Bartholmai, MD, Rochester, MN (*Abstract Co-Author*) License agreement, ImBio, LLC; Scientific Advisor, ImBio, LLC; Scientific Advisor, Bristol-Myers Squibb Company Kishore Rajendran, PhD, Rochester, MN (*Abstract Co-Author*) Nothing to Disclose Jayse Weaver, Rochester, MN (*Abstract Co-Author*) Nothing to Disclose Joel G. Fletcher, MD, Rochester, MN (*Abstract Co-Author*) Grant, Siemens AG; Consultant, Medtronic plc; ; Ahmed Halaweish, PhD, Rochester, MN (*Abstract Co-Author*) Employee, Siemens AG Shuai Leng, PHD, Rochester, MN (*Abstract Co-Author*) License agreement, Bayer AG Cynthia H. McCollough, PhD, Rochester, MN (*Abstract Co-Author*) Research Grant, Siemens AG

For information about this presentation, contact:

fletcher.joel@mayo.edu

#### PURPOSE

To evaluate the impact of 1024 matrix size and photon-counting-detectors (PCDs) relative to 512 matrix size and energyintegrating-detectors (EIDs) for chest CT.

# METHOD AND MATERIALS

22 adult patients undergoing clinically indicated chest CT received dose-matched PCD CT after written informed consent. 1.5 mm images were reconstructed at a 1mm overlap with our routine clinical kernel (B46) at both 512 and 1024 matrix sizes for EID scans. For PCD, B46 and an additional sharp kernel (Q65, not available for EID) was reconstructed at a 1024 matrix. Two chest radiologists compared only the right lung of B46/EID/1024; B46/PCD/1024 and Q65/PCD/1024 images in a side-by-side fashion to the routine clinical B46/EID/512 images, noting the highest level bronchus clearly identified in each lobe. The 3rd and 4th order bronchi were specifically evaluated and any lung nodules were compared to the B46/EID/512 images using a 5 point Likert scale (+2 = improved detection confidence, +1=preferred but no confidence change, 0 = similar, -1=worse but no confidence change, -2=worse with decreased confidence). Statistical analysis was performed using a Wilcoxon signed rank test with a p <0.05 considered significant.

# RESULTS

Compared to B46/EID/512, readers detected higher order bronchi using Q65/PCD/1024 images for every lung lobe (p<0.002). For B46/EID/1024 reconstruction, higher order bronchi were only significantly better seen in the right middle lobe (p=0.007). Readers were able to better identify bronchial walls of the 3rd and 4th order bronchi better using Q65/PCD/1024 (mean Likert-scores of 1.1 and 1.5), which was significantly higher compared to B46/EID/1024 or B46/PCD/1024 (mean difference 0.8; p<0.0001). Of 49 non-calcified pulmonary nodules (8 part solid, 41 solid), Q65/PCD/1024 had a slightly but significantly higher mean visualization score of 0.8 compared to 0 for B46/EID/1024 and 0.2 for B46/PCD/1024 (p<0.0002).

#### CONCLUSION

Lung PCD-CT with 1024 matrix using a sharp Q65 kernel increase visualization of higher order bronchi and bronchial walls without compromising nodule detection. Softer kernels and further work are needed to examine the internal density characteristics of nodules at PCD-CT.

# **CLINICAL RELEVANCE/APPLICATION**

PCD-CT with 1024 matrix improves visualization of medium and small bronchi compared to current routine chest CT, creating an opportunity for radiologists to better characterize lung pathology.

# SSA05-02 Normalized Emphysema Score Progression: An Improved CT Biomarker for Mortality

Sunday, Nov. 25 10:55AM - 11:05AM Room: E451A

Participants

Anton Schreuder, MD, Nijmegen, Netherlands (Presenter) Nothing to Disclose

Colin Jacobs, PhD, Nijmegen, Netherlands (Abstract Co-Author) Research Grant, MeVis Medical Solutions AG

Leticia Gallardo Estrella, MSc, Nijmegen, Netherlands (Abstract Co-Author) Nothing to Disclose

Cornelia M. Schaefer-Prokop, MD, Nijmegen, Netherlands (*Abstract Co-Author*) Advisory Board, Riverain Technologies, LLC Wataru Fukumoto, Hiroshima, Japan (*Abstract Co-Author*) Nothing to Disclose

Mathias Prokop, PhD, Nijmegen, Netherlands (*Abstract Co-Author*) Speakers Bureau, Bracco Group; Speakers Bureau, Bayer AG; Research Grant, Canon Medical Systems Corporation; Speakers Bureau, Canon Medical Systems Corporation; Research Grant, Siemens AG; Speakers Bureau, Siemens AG; Departmental spinoff, Thirona; Departmental licence agreement, Varian Medical Systems, Inc; ;

Bram Van Ginneken, PhD, Nijmegen, Netherlands (*Abstract Co-Author*) Stockholder, Thirona BV; Co-founder, Thirona BV; Research Grant, Varian Medical Systems, Inc; Research Grant, Canon Medical Systems Corporation

#### For information about this presentation, contact:

anton.schreuder@radboudumc.nl

## PURPOSE

Normalized emphysema score (normES) is a protocol-robust and validated CT biomarker for mortality. We aimed to improve mortality prediction by modelling its change over time.

# METHOD AND MATERIALS

CT scans from all 1810 deceased participants from the National Lung Screening Trial were selected. Of these, 445 died from lung cancer. A random selection of 4190 surviving participants were sampled with replacement up to 24432 to approximate the full cohort. The normES was obtained by computing the emphysema scores after resampling, normalization, and bullae cluster analysis. The reference models contained solely the baseline (T0) normES. To investigate if progression of emphysema provides additional information, normES from the first (T1) and second annual screening rounds (T2) and normES progression (normESprog) were added to the base model. normESprog was calculated by subtracting the T0 log(normES) from the T1 or T2 log(normES) and dividing by the time in between. Proportional hazard models predicting all-cause and lung cancer mortality were compared by calculating the continuous net reclassification improvement (NRI) for each year of follow-up.

# RESULTS

The analysis of T0 and T1 data was performed on 22695 samples; 3547 lacked T0 or T1 scans, or had corrupted data. NRI improvement for all-cause and lung cancer mortality prediction compared to the base models were 4.5% (95%CI: -7.3 to 8.4%) and 4.1% (-9.3 to 14.6%) 3 years after baseline, 6.1% (-5.3 to 9.4%) and 0.1% (-7.1 to 12.2%) after 5 years, and 6.1% (-6.2 to 8.7%) and -0.4% (-5.6 to 11.3%) after 7 years, respectively. When modelling the T0 to T2 interval, another 2603 samples were excluded. For all-cause mortality, the 3, 5, and 7 year time points showed respective NRI improvements of -0.5% (-6.7 to 8.0%), 10.8% (5.5% to 14.7%), and 12.2% (7.1% to 15.6%). Improvements in lung cancer mortality prediction were -6.1% (-24.0 to 12.6%), 19.6% (10.6 to 29.2%), and 24.1% (15.4% to 31.7%), respectively. All hazard models had a logrank test p<.001.

#### CONCLUSION

Two normES measurements are better than one at predicting mortality over longer periods of time. The time between normES measurements should be sufficiently distant to account for the slow progression of emphysema.

# **CLINICAL RELEVANCE/APPLICATION**

Normalized emphysema score progression is an automatic emphysema quantification method which can better predict the long-term mortality than a single baseline measurement.

# SSA05-03 Comparison of Two Independent Visual Assessment Protocols for the Detection of Emphysema in the National Lung Screening Trial Cohort

Sunday, Nov. 25 11:05AM - 11:15AM Room: E451A

Participants

Tyler Sevco, MD, Ann Arbor, MI (*Presenter*) Nothing to Disclose Joseph K. Leader, Pittsburgh, PA (*Abstract Co-Author*) Nothing to Disclose David Wilson, Pittsburgh, PA (*Abstract Co-Author*) Nothing to Disclose Carl R. Fuhrman, MD, Pittsburgh, PA (*Abstract Co-Author*) Nothing to Disclose

For information about this presentation, contact:

tsevco22@gmail.com

#### PURPOSE

To investigate the variability in assessing the presence of emphysema in a lung cancer screening population using low-dose CT scans and compare this to rates of spirometry-detected airflow obstruction.

# METHOD AND MATERIALS

Baseline low-dose CT scans from 6,352 NLST participants enrolled in the CT arm who also underwent spirometry were evaluated. Emphysema was visually assessed in NLST as present or absent. In our study, two readers visually assessed CT scans using a modified NETT protocol that divided the lung into upper, middle, and basal zones and graded emphysema as none (0%), trace (1-25%), mild (25-50%), moderate (50-75%), or severe (75%+). In this protocol, a subject was scored as positive if any region was scored trace or greater. Results were compared to emphysema and spirometry data from the Pittsburgh Lung Screening Study (PLuSS).

#### RESULTS

Among the 6,352 subjects, emphysema was identified in 55.4% (3518/6352) of subjects in NLST and 40.4% (2566/6352) of subjects using our protocol (agreement Kappa=0.4990). Emphysema severity in the current study was reported as none, trace, mild, moderate, and severe in 59.6%, 27.4%, 7.0%, 4.1%, and 1.9% of the subjects, respectively. Inter-reader agreement for the presence of emphysema between the two readers in our study in 200 CT scans was moderate to substantial (K=0.6073). Using the McNemar test statistic, there was a statistically significant difference between our visual assessment of emphysema and the NLST assessment of emphysema (p < 0.001). Spirometry-detected airflow obstruction was reported in 32.0% of the NLST subjects. In PLuSS (n=3638), emphysema and airflow obstruction were identified in 42.5% and 42.7% of the subjects, respectively.

# CONCLUSION

Our study revealed a significant disagreement in emphysema assessment between two independent visual interpretations of lowdose CT scans. The discrepancy between emphysema and airflow obstruction (55.4% versus 32.0%) in the NLST-ACRIN subcohort appears to be from overdetection of emphysema. Our visual emphysema assessment of NLST CT scans is more consistent with rates of spirometry-detected airflow obstruction and with previously published rates of emphysema in lung cancer screening populations.

# **CLINICAL RELEVANCE/APPLICATION**

Since emphysema is recognized as a significant risk factor for lung cancer, our study demonstrates the need to standardize and improve emphysema assessment in low-dose lung cancer screening CT scans.

# SSA05-04 Visual Presence of Emphysema Predicts Progression of Emphysema and Air Trapping in Cigarette Smokers

Sunday, Nov. 25 11:15AM - 11:25AM Room: E451A

#### Participants

Bilal El Kaddouri, MD, Brussels, Belgium (*Presenter*) Nothing to Disclose Matthew J. Strand, Denver, CO (*Abstract Co-Author*) Nothing to Disclose Stephen Humphries, Denver, CO (*Abstract Co-Author*) Research Consultant, PAREXEL International Corporation; Research Consultant, Veracyte, Inc; Research Consultant, Boehringer Ingelheim GmbH; Research Grant, Siemens AG Jean-Paul Charbonnier, MSc, Nijmegen, Netherlands (*Abstract Co-Author*) Employee, Thirona BV Eva M. van Rikxoort, PhD, Nijmegen, Netherlands (*Abstract Co-Author*) Stockholder, Thirona BV Co-founder, Thirona BV David A. Lynch, MBBCh, Denver, CO (*Abstract Co-Author*) Research support, Siemens AG; Research Consultant, PAREXEL International Corporation; Research Consultant, Boehringer Ingelheim GmbH; Research Consultant, F. Hoffmann-La Roche Ltd; Research Consultant, Veracyte, Inc;

# For information about this presentation, contact:

belkaddo@ulb.ac.be

# PURPOSE

Visual categorization of emphysema on CT has been shown to correlate with symptomatic impairment and with mortality. However, the relationship between presence of emphysema and subsequent progression of disease has not previously been evaluated.

# METHOD AND MATERIALS

We studied 4126 subjects enrolled in the COPDGene study, who had visual CT scores at baseline, and quantitative inspiratory and expiratory CT at baseline and at 5 years. Trained research analysts performed visual classification of parenchymal emphysema on baseline volumetric CT scans of these subjects using the Fleischner Society classification system. Each scan was independently evaluated by two analysts; discordances between analysts were adjudicated by a thoracic radiologist. Statistical analysis used a linear mixed model, adjusted for age, height, gender, race, smoking status, scanner make, and reconstruction algorithm, with dependent variables being inspiratory lung density at 15th percentile (adjusted for lung volume) as a measure of emphysema, and % of lung voxels < -856 HU on expiratory CT (LAA-856) as a measure of air trapping. Analysis was stratified by presence or absence of COPD at baseline.

# RESULTS

In subjects with COPD, those with parenchymal emphysema at baseline showed a lung density decline of 4.7 g/l (95% CI 3.9, 5.4, p<0.0001), compared with 1.4 g/l (0.5, 2.4, p=0.003) for those without emphysema. For subjects without COPD, corresponding values were 4.0 (3.2, 4.9, p<0.0001) and 0.8 (0.25, 1.4. p=0.005). In subjects with COPD, those with baseline emphysema showed increase of 3.8% (2.9, 4.6, p<0.0001) in LAA-856, compared with 0.5% (-0.6, 1.5, n.s.) for those without. For subjects without COPD, those with emphysema had an increase in LAA-856 of 1.7% (1.1, 2.4, p<0.0001), while those without emphysema had a slight decrease of 0.5% (0.1, 0.9, p=0.01).

# CONCLUSION

The presence of parenchymal emphysema at baseline is associated with a higher rate of progression in emphysema and air trapping at 5 year follow-up, in cigarette smoking subjects with and without COPD.

# **CLINICAL RELEVANCE/APPLICATION**

The presence of visible emphysema on CT in cigarette smokers is an important predictor of subsequent progression.

# SSA05-05 3D Oxygen-Enhanced MRI at 3T System versus Thin-Section CT: Quantitative Capability for Pulmonary Functional Loss Assessment and Clinical Stage Classification in Smokers

Sunday, Nov. 25 11:25AM - 11:35AM Room: E451A

Participants

Yoshiharu Ohno, MD, PhD, Kobe, Japan (*Presenter*) Research Grant, Canon Medical Systems Corporation; Research Grant, Koninklijke Philips NV; Research Grant, Bayer AG; Research Grant, DAIICHI SANKYO Group; Research Grant, Fuji Pharma Co, Ltd; Research Grant, Guerbet SA;

Masao Yui, Otawara, Japan (*Abstract Co-Author*) Employee, Canon Medical Systems Corporation Yu Chen, MENG, Beijing, China (*Abstract Co-Author*) Employee, Canon Medical Systems Corporation Yuji Kishida, MD,PhD, Kobe, Japan (*Abstract Co-Author*) Nothing to Disclose Shinichiro Seki, Kobe, Japan (*Abstract Co-Author*) Research Grant, Canon Medical Systems Corporation Katsusuke Kyotani, RT,MSc, Kobe, Japan (*Abstract Co-Author*) Nothing to Disclose Takeshi Yoshikawa, MD, Kobe, Japan (*Abstract Co-Author*) Research Grant, Canon Medical Systems Corporation Takamichi Murakami, MD, PhD, Osakasayama, Japan (*Abstract Co-Author*) Nothing to Disclose

For information about this presentation, contact:

yosirad@kobe-u.ac.jp

# PURPOSE

To prospectively and directly compare the quantitative capability for pulmonary functional loss assessment and clinical stage classification between 3D oxygen-enhanced MR imaging (O2-enhanced MRI) and thin-section CT in smokers.

#### **METHOD AND MATERIALS**

Twenty consecutive smokers (12 men and 8 women; age rang 56-85 years) underwent 3D O2-enhanced MRI, thin-section CT and pulmonary function test (FEV1/FVC%, %FEV1% and %DLCO/VA). All smokers were classified into four stages ('Without COPD', 'Mild COPD', 'Moderate COPD', 'Severe or very severe COPD') according to the GOLD guideline. For 3D O2-enhanced MRI in each smoker, 3D Fast Field Echo sequence with variable flip angles was performed with and without 100% oxygen inhalation at a 3T MR system. With non-rigid registration software, regional T1 value change map was generated from O2-enhanced MR data by pixel by pixel analyses. Then, ROIs were placed over the lung on all slices, and averaged to determine mean T1 value change ( $\Delta$ T1) in each subject. On quantitative CT in each subject, percentage of low attenuation area within entire lung (LAA%) was also measured. To compare the capability for pulmonary functional loss assessment, both indexes were correlated with each parameter. Then, both indexes were compared four clinical stages by Tukey's HSD test. Finally, discrimination analyses were performed, and accuracy was compared each other by McNemar's test.

# RESULTS

 $\Delta$ T1 and LAA% were significantly correlated with FEV1/FVC% ( $\Delta$ T1: r=-0.70, p=0.0006; LAA%: r=-0.75, p=0.0002), %FEV1 ( $\Delta$ T1: r=-0.84, p<0.0001; LAA%: r=-0.67, p=0.0013) and %DLCO/VA ( $\Delta$ T1: r=-0.69, p=0.0009; LAA%: r=-0.63, p=0.0029).  $\Delta$ T1 had significant difference between 'Severe or very severe COPD' group and others (p<0.05), although LAA% had significant difference between 'Severe or very severe COPD' (p<0.05) or 'Mild COPD' (p<0.05) groups. Discrimination accuracies of  $\Delta$ T1 (73.7 [14/19] %) was significantly higher than that of LAA% (42.1 [8/19] %, p=0.03).

# CONCLUSION

3D O2-enhanced MRI has a better capability for pulmonary functional loss assessment and clinical stage classification in smokers than quantitative CT.

#### **CLINICAL RELEVANCE/APPLICATION**

3D O2-enhanced MRI has a better capability for pulmonary functional loss assessment and clinical stage classification in smokers than quantitative CT.

# SSA05-07 Using Deep Learning to Predict Emphysema in Early Lung Cancer Screening Low-Dose CT Scan

Sunday, Nov. 25 11:45AM - 11:55AM Room: E451A

#### Participants

John H. Lee, PhD, Chicago, IL (*Presenter*) Nothing to Disclose

Artit C. Jirapatnakul, PhD, New York, NY (Abstract Co-Author) Nothing to Disclose

Rowena Yip, MPH, New York, NY (Abstract Co-Author) Nothing to Disclose

Claudia I. Henschke, MD, PhD, New York, NY (Abstract Co-Author) Nothing to Disclose

David F. Yankelevitz, MD, New York, NY (Abstract Co-Author) Royalties, General Electric Company; Stockholder, Accumetra; Advisory Board, GRAIL

Maryellen L. Giger, PhD, Chicago, IL (*Abstract Co-Author*) Stockholder, Hologic, Inc; Shareholder, Quantitative Insights, Inc; Shareholder, QView Medical, Inc; Co-founder, Quantitative Insights, Inc; Royalties, Hologic, Inc; Royalties, General Electric Company; Royalties, MEDIAN Technologies; Royalties, Riverain Technologies, LLC; Royalties, Mitsubishi Corporation; Royalties, Canon Medical Systems Corporation

#### For information about this presentation, contact:

jhl33@uchicago.edu

#### PURPOSE

The patients who are recommended for annual lung cancer screening are at a higher risk for other cardiopulmonary diseases. Therefore, it would be beneficial to use the low-dose CT scans (LDCT) to identify other conditions. This work aims to demonstrate the feasibility of using deep learning method to identify findings, specifically emphysema.

#### METHOD AND MATERIALS

The dataset consists of 860 cases of LDCT scans from a lung screening program. Emphysema was identified on each scan as none, mild, moderate, or severe. To evaluate the effect of potential labeling error caused by per case rating system, three different approaches were taken: 1) using the entire lung region, 2) using only the top 50% of the lung since emphysema due to smoking tends to affect the upper lobes more than the lower lobes, and 3) using only the bottom 50% of the lung as a control. Deep learning consisted of feature extraction using a pre-trained VGG-19 network followed by a support vector machine binary classifier that predicted the presence of emphysema (none vs. moderate and severe). The predictions were first performed on a per slice basis and averaged to acquire per case prediction. The area under the receiver operating characteristic curve (AUC) was used to evaluate the performance.

Per slice prediction for the entire lung region, the top 50%, and the bottom 50% produced an AUC of 0.76 (SE: 0.01), 0.77 (0.01), and 0.74 (0.01), respectively. Per case prediction produced an AUC of 0.84 (0.03), 0.83 (0.03), and 0.80 (0.03). The higher AUCs for per case prediction demonstrates that aggregating the predictions on slices help reduce the effect of labeling errors. The AUCs for the bottom 50% are lower, but still on par, which is likely due to the fact emphysema does not completely spare the bottom lobes.

# CONCLUSION

We have demonstrated the potential of transfer learning to predict the presence of emphysema on LDCT scans. Fine-tuning work is currently on-going, and given the high performance already achieved with transfer learning, fine-tuning is likely to achieve even higher performance.

# **CLINICAL RELEVANCE/APPLICATION**

LDCT provides an opportunity to identify other pathologies that may otherwise go undiagnosed. Having a suite of algorithms that automatically searches for multiple incidental findings has the potential to increase efficiency and prevent missing important findings.

# SSA05-08 Inspiratory/Expiratory Xenon-Enhanced Area-Detector CT with and without 3D Motion Analysis: Capability for Pulmonary Functional Loss Assessment and Clinical Stage Classification of COPD

Sunday, Nov. 25 11:55AM - 12:05PM Room: E451A

Participants

Yoshiharu Ohno, MD, PhD, Kobe, Japan (*Presenter*) Research Grant, Canon Medical Systems Corporation; Research Grant, Koninklijke Philips NV; Research Grant, Bayer AG; Research Grant, DAIICHI SANKYO Group; Research Grant, Fuji Pharma Co, Ltd; Research Grant, Guerbet SA; Yasuko Fujisawa, MS, Otawara, Japan (*Abstract Co-Author*) Employee, Canon Medical Systems Corporation Naoki Sugihara, MENG, Otawara, Japan (*Abstract Co-Author*) Employee, Canon Medical Systems Corporation Yuji Kishida, MD,PhD, Kobe, Japan (*Abstract Co-Author*) Nothing to Disclose Shinichiro Seki, Kobe, Japan (*Abstract Co-Author*) Research Grant, Canon Medical Systems Corporation Takeshi Yoshikawa, MD, Kobe, Japan (*Abstract Co-Author*) Research Grant, Canon Medical Systems Corporation Hisanobu Koyama, MD,PhD, Osaka, Japan (*Abstract Co-Author*) Nothing to Disclose

Takamichi Murakami, MD, PhD, Osakasayama, Japan (Abstract Co-Author) Nothing to Disclose

# For information about this presentation, contact:

yosirad@kobe-u.ac.jp

# PURPOSE

To prospectively evaluate the utility of 3D lung motion assessment on inspiratory/expiratory xenon-enhanced area-detector CT (Xe-enhanced ADCT) for pulmonary functional loss assessment and clinical stage evaluation of chronic obstructive pulmonary disease (COPD).

#### **METHOD AND MATERIALS**

Twenty-eight consecutive patients with and without COPD (18 men and 10 women; mean age, 72 years old) prospectively underwent inspiratory/expiratory Xe-enhanced ADCT examinations as well as pulmonary function tests. Then, all patients were classified by GOLD classification as follows: 'Without COPD', 'Mild COPD', 'Moderate COPD' and 'Severe or Very Severe COPD'. In each subject, Xe-enhanced ADCT data was transferred to our proprietary software to generate xenon ventilation maps such as wash-in (WI), wash-out (WO) and ventilation ratio (VR: VR=[WI-WO]/WI) maps as well as 3D motion magnitude maps at X-, Y- and Z-axes as well as expansion rate (ER) map by Jacobian method by pixel-by-pixel analyses. Then, each regional index was assessed by ROI measurements, and each final value was determined as averaged value. To determine the relationship between xenon ventilation- and 3D motion-based indexes, Pearson's correlations were performed. Then, step-wise regression analyses were performed between all indexes and %FEV1. Finally, discrimination accuracies were performed among xenon-ventilation indexes, 3D-moion based indexes and combined method by McNema's test.

#### RESULTS

WO had significant and correlations with X, Y and Z-axis motion magnitudes (-0.53 CONCLUSION

3D lung motion assessment is useful for pulmonary functional loss and clinical stage classification of COPD, when applied with inspiratory/expiratory Xe-enhanced ADCT.

# CLINICAL RELEVANCE/APPLICATION

Inspiratory/expiratory xenon-enhanced area-detector CT with 3D lung motion assessment is more useful than that without 3D lung motion assessment for pulmonary functional loss and clinical stage classification of COPD.

# SSA05-09 A Convolutional Neural Network Approach to Imaging-Based Pulmonary Measurements in COPD Patients

Sunday, Nov. 25 12:05PM - 12:15PM Room: E451A

# Awards

# Student Travel Stipend Award

Participants

Tara A. Retson, MD, PhD, San Diego, CA (*Presenter*) Nothing to Disclose Kang Wang, MD,PhD, San Diego, CA (*Abstract Co-Author*) Nothing to Disclose Kevin Blansit, MS,BS, La Jolla, CA (*Abstract Co-Author*) Nothing to Disclose Naeim Bahrami, PhD, MSc, San Diego, CA (*Abstract Co-Author*) Nothing to Disclose Evan Masutani, La Jolla, CA (*Abstract Co-Author*) Nothing to Disclose Andrew C. Yen, MD, San Diego, CA (*Abstract Co-Author*) Nothing to Disclose Seth J. Kligerman, MD, Denver, CO (*Abstract Co-Author*) Nothing to Disclose Albert Hsiao, MD, PhD, La Jolla, CA (*Abstract Co-Author*) Founder, Arterys, Inc; Consultant, Arterys, Inc; Consultant, Bayer AG; Research Grant, General Electric Company;

For information about this presentation, contact:

tretson@ucsd.edu

#### PURPOSE

Chronic obstructive pulmonary disease (COPD) affects over 16 million Americans and 251 million people worldwide. Multiple patterns of pathology exist, and imaging measurements are increasingly important for identifying COPD subtypes and prognosis. We hypothesized that a convolutional neural network (CNN) could predict volumetric measurements relating to pulmonary function, based on a subset of chest CT images.

# METHOD AND MATERIALS

With HIPAA compliance and IRB approval, we retrospectively identified inspiratory CT scans for 160 COPD patients from our institution enrolled in the COPDGene multicenter study. We used a CNN based on VGG19 to develop regression-based inference predictions of total lung capacity (TLC), functional residual capacity (FRC), and percentage of emphysema. Measurement of these parameters was obtained previously as part of the larger COPDGene dataset, and has been discussed by other groups. A subset of 10 equally spaced axial chest images were selected from the full chest CT and used to train the network, with assessment by five fold cross validation. Correlations between CNN and ground truth are given as R2, and bias was assessed with Bland-Altman plot analysis.

# RESULTS

CNN predicted measurements of TLC were correlated with those from the COPDGene dataset with an R2 value of 0.86 (slope 1.10), and mean difference of 0.14L  $\pm$  0.57L. FRC was correlated with an R2 value of 0.84 (slope 1.26), and mean difference of -0.06L  $\pm$  0.56L. Percent emphysema was correlated at an R2 value of 0.82 (slope 1.04), and mean difference of 0.15%  $\pm$  3.34%.

#### CONCLUSION

Here we show the ability of a CNN to produce well correlated predictions of pulmonary volume measurements, inferred from a subset of chest CT images. Refinement of this CNN can expand it to additional structures or volumes, and may allow automation of quantitative pulmonary function measurements and volumes to streamline disease monitoring.

# **CLINICAL RELEVANCE/APPLICATION**

We present a convolutional neural network capable of making well-correlated, inference-based, predictions of pulmonary volume measurements in COPD patients, based on a subset of 10 chest CT slices.



#### SSA06

# Science Session with Keynote: Emergency Radiology (Imaging Algorithms, Modalities and Techniques)

Sunday, Nov. 25 10:45AM - 12:15PM Room: S405AB



AMA PRA Category 1 Credits ™: 1.50 ARRT Category A+ Credit: 1.75

# Participants

Ferco H. Berger, MD, Toronto, ON (*Moderator*) Nothing to Disclose Jeremy R. Wortman, MD, Boston, MA (*Moderator*) Nothing to Disclose Howard P. Forman, MD, New Haven, CT (*Moderator*) Nothing to Disclose

#### Sub-Events

# SSA06-01 Emergency Radiology Keynote Speaker: Impact of Dual Energy CT on ED Workflow and Downstream Utilization

Sunday, Nov. 25 10:45AM - 10:55AM Room: S405AB

Participants Jeremy R. Wortman, MD, Boston, MA (*Presenter*) Nothing to Disclose

# **Honored Educators**

Presenters or authors on this event have been recognized as RSNA Honored Educators for participating in multiple qualifying educational activities. Honored Educators are invested in furthering the profession of radiology by delivering high-quality educational content in their field of study. Learn how you can become an honored educator by visiting the website at: https://www.rsna.org/Honored-Educator-Award/ Jeremy R. Wortman, MD - 2017 Honored Educator

# SSA06-02 Acute Pancreatitis: A Quantitative Analysis of Iodine with Dual-Energy Spectral Computed Tomography

Sunday, Nov. 25 10:55AM - 11:05AM Room: S405AB

Participants Wei Wei, Hefei, China (*Presenter*) Nothing to Disclose

# For information about this presentation, contact:

weiweill@126.com

#### PURPOSE

To investigate the correlation between iodine concentration and clinical severity of acute pancreatitis (AP) through the quantitative evaluation with dua-energy spectral computed tomography (DESCT), so as to find out an effective imaging technology in the evaluation of clinical severity of AP.

# **METHOD AND MATERIALS**

Sixty patients with AP confirmed clinically (AP group) and 30 patients with normal pancreas (control group) were retrospectively analyzed. All the patients underwent enhanced CT scan in the spectral imaging mode. Iodine concentration and normalized iodine concentration (NIC) were respectively measured during arterial phase and portal phase in the material-decomposition images by using a spectral imaging viewer (GSI Viewer).

# RESULTS

Iodine concentration and NIC were significantly higher in the control group than in the AP group (P<0.05, P<0.001). In the AP group, according to Ranson grading, 24 patients were in the mild grade, 20 patients were moderate, and 16 patients were severe. Iodine concentration and NIC decreased along with the increase of their Ranson grade. There were significant difference in iodine concentration and NIC among the three subgroups (iodine concentration on arterial phase: F=8.776, P<0.01; iodine concentration on portal phase: F=4.019, P<0.05; NIC on arterial phase: F=12.700, P<0.001; NIC on portal phase: F=8.732, P<0.01). Iodine concentration and NIC on arterial and portal phases in the mild grade group were both significantly higher than those in the moderate grade group (P<0.05); however, iodine concentration on arterial and portal phases, and NIC on arterial phase in the severe grade group were significantly lower than those in the moderate grade group (P<0.05).

# CONCLUSION

DESCT can analyze hemodynamic changes in AP quantitatively, which is of great value in evaluating changes in AP of each grade.

# CLINICAL RELEVANCE/APPLICATION

The quantitative evaluation of iodine with dua-energy spectral computed tomography (DESCT) provide a new method for the prognosis of patients with acute pancreatitis.

# **Room Patients**

Sunday, Nov. 25 11:05AM - 11:15AM Room: S405AB

Participants Jeremy R. Wortman, MD, Boston, MA (*Presenter*) Nothing to Disclose Ellen X. Sun, MD, Boston, MA (*Abstract Co-Author*) Nothing to Disclose Jennifer W. Uyeda, MD, Boston, MA (*Abstract Co-Author*) Consultant, Allena Pharmaceuticals, Inc; Invited Speaker, Siemens AG Roger Lacson, Boston, MA (*Abstract Co-Author*) Nothing to Disclose Daniel I. Glazer, MD, Boston, MA (*Abstract Co-Author*) Nothing to Disclose Aaron D. Sodickson, MD,PhD, Boston, MA (*Abstract Co-Author*) Institutional research agreement, Siemens AG; Speaker, Siemens AG; Speaker, General Electric Company Daniel A. Souza, MD, Boston, MA (*Abstract Co-Author*) Nothing to Disclose PURPOSE

To assess the diagnostic performance of DECT characterization of incidental, indeterminate renal lesions detected on routine contrast-enhanced CT in ER patients, using reference standard of renal mass protocol CT or MRI.

# **METHOD AND MATERIALS**

The study cohort included patients with an indeterminate lesion on portal venous phase DECT (homogeneous lesion of greater than 20 HU, or complex cystic lesion), with reference standard imaging (renal mass protocol CT or MRI) of the lesion performed within 2 years. All DECT scans were performed in the ER setting on the same dual source DECT scanner. Two radiologists with DECT experience used DECT post-processed iodine selective images to characterize lesions as: definitely non-enhancing, equivocal/possible enhancement, or definitely enhancing; readers also measured iodine concentration within lesions. Two expert abdominal radiologists evaluated reference standard imaging of each lesion, categorizing each as definitely non-enhancing (Bosniak I and II cysts), equivocal/possible enhancement (Bosniak IIF or other lesions needing follow up), and definitely enhancing (solid mass, Bosniak III/IV cysts).

#### RESULTS

66 lesions were included in the study cohort, on reference standard imaging 44 were non-enhancing (11 Bosniak I and 33 Bosniak II cysts) and 22 were lesions with equivocal or definite enhancement (7 Bosniak IIF cysts, 3 Bosnaik III cysts, 3 Bosniak IV cysts, 9 solid masses). Qualitative assessment of lesions as enhancing on by DECT readers on iodine selective images had a sensitivity of 100%, specificity of 43%, positive predictive value of 47%, negative predictive value of 100%, and accuracy of 62%.

# CONCLUSION

Characterizing incidental indeterminate renal lesions on portal venous phase DECT as non-enhancing with DECT post-processing was successfully able to exclude enhancement in these lesions (NPV of 100%), indicating that incidental lesions without enhancement on DECT are highly likely to be Bosniak I or II cysts. However, the specificity and positive predictive value of enhancement seen on DECT were relatively low. Further research is needed to assess methods to mitigate false positive enhancement with DECT.

# **CLINICAL RELEVANCE/APPLICATION**

Qualitative assessment of enhancement of incidental renal lesions with DECT had a high negative predictive value, indicating that lesions without enhancement on DECT post-processed images are highly likely to be Bosniak I or II cysts.

# **Honored Educators**

Presenters or authors on this event have been recognized as RSNA Honored Educators for participating in multiple qualifying educational activities. Honored Educators are invested in furthering the profession of radiology by delivering high-quality educational content in their field of study. Learn how you can become an honored educator by visiting the website at: https://www.rsna.org/Honored-Educator-Award/ Jeremy R. Wortman, MD - 2017 Honored EducatorAaron D. Sodickson, MD,PhD - 2014 Honored EducatorAaron D. Sodickson, MD,PhD - 2017 Honored EducatorAaron D. Sodickson, MD,PhD - 2018 Honored Educator

# SSA06-04 The Impact of Socioeconomic Status on CT-Imaging and Management of Acute Appendicitis

#### Sunday, Nov. 25 11:15AM - 11:25AM Room: S405AB

Participants

Diana Dinh, MD, Boston, MA (Presenter) Nothing to Disclose Matthew Hartman, BS, Boston, MA (Abstract Co-Author) Nothing to Disclose Nicholas Wilson, MD , Boston, MA (Abstract Co-Author) Nothing to Disclose Nemil Shah, MD, Boston, MA (Abstract Co-Author) Nothing to Disclose Douglas Barnes, MS, Charlestown, MA (Abstract Co-Author) Nothing to Disclose Curtis Hon, Boston, MA (Abstract Co-Author) Nothing to Disclose Neha Khemani, Boston, MA (Abstract Co-Author) Nothing to Disclose Hyunjoong Kim, Boston, MA (Abstract Co-Author) Nothing to Disclose Claire Lis, BS, Boston, MA (Abstract Co-Author) Nothing to Disclose Stephen J. Raulli, BS, MS, Lexington, MA (Abstract Co-Author) Nothing to Disclose Christina A. Snyder, MS, BS, Boston, MA (Abstract Co-Author) Nothing to Disclose Brian Williams, BS, Boston, MA (Abstract Co-Author) Nothing to Disclose Alexandra Gero, MPH, Boston, MA (Abstract Co-Author) Nothing to Disclose Mustafa Qureshi, Boston, MA (Abstract Co-Author) Nothing to Disclose Heidi Wing, Boston, MA (Abstract Co-Author) Nothing to Disclose Tracey Dechert, MD, Boston, MA (Abstract Co-Author) Nothing to Disclose Stephan W. Anderson, MD, Cambridge, MA (Abstract Co-Author) Nothing to Disclose Christina A. LeBedis, MD, Boston, MA (Abstract Co-Author) Nothing to Disclose

# PURPOSE

To assess the impact of socioeconomic status on CT findings and the management of acute appendicitis.

## **METHOD AND MATERIALS**

Informed consent was waived for this IRB-approved, HIPAA compliant, retrospective study of 18-64 year old patients with acute appendicitis at our institution by MDCT from 1/1/2006-12/31/2016 (n=1886). Insurance, race/ethnicity, primary language, and education level were obtained from the electronic medical record. Multivariate linear regression was performed to determine crude and adjusted parameter estimates for length of stay. For each metric, the estimates generated from linear regression are interpreted as difference in length of stay associated with one unit change in each covariate. Logistic regression models were run and crude and adjusted odds ratio (OR) were calculated for each categorical outcome. A P value of less than 0.05 was considered statistically significant for all analyses. Statistical computations were performed on SAS 9.3 system (SAS Institute, Cary, NC).

## RESULTS

Free care/Medicaid/Medicare subjects had 0.4 days increase in length of stay as compared to private insurance (p=0.039). Free care/Medicaid/Medicare subjects were also found to have increase odds of surgical site infection or re-operation (OR=1.93, 95% CI= 1.03-3.63, p=0.041), as compared to private insurance patients. Hispanics were associated with lower odds of complicated CT findings (OR=0.55, 95% CI=0.335-0.898, p=0.017), and both Hispanic and Blacks had lower odds of perforation, abscess, or gangrene by intraoperative report (OR=0.67, 95% CI=0.47-0.97, p=0.035; OR=0.68, 95% CI=0.48-0.97, p=0.033, respectively), as compared to Whites. There were no statistically significant differences in CT findings, length of stay, or post-operative complication by primary language or education level.

## CONCLUSION

Acute appendicitis is a common emergent illness presenting across the socioeconomic spectrum. Free care, Medicaid and Medicare patients have increased length of stay and increased odds of post-operative complication. Hispanics show lower odds of complicated CT findings on initial presentation. Hispanics and Blacks have lower odds of having complicated intraoperative findings.

## **CLINICAL RELEVANCE/APPLICATION**

Further investigation on the impact of socioeconomic status within radiology and the potential for radiologists to join the fight in combating health disparity are necessary to eliminate health inequality.

#### **Honored Educators**

Presenters or authors on this event have been recognized as RSNA Honored Educators for participating in multiple qualifying educational activities. Honored Educators are invested in furthering the profession of radiology by delivering high-quality educational content in their field of study. Learn how you can become an honored educator by visiting the website at: https://www.rsna.org/Honored-Educator-Award/ Stephan W. Anderson, MD - 2018 Honored Educator

# SSA06-05 Virtual Monoenergetic Dual-Energy CT for Evaluation of Hepatic and Splenic Lacerations

Sunday, Nov. 25 11:25AM - 11:35AM Room: S405AB

## Awards

# Student Travel Stipend Award

Participants

Ellen X. Sun, MD, Boston, MA (*Presenter*) Nothing to Disclose Jeremy R. Wortman, MD, Boston, MA (*Abstract Co-Author*) Nothing to Disclose Jennifer W. Uyeda, MD, Boston, MA (*Abstract Co-Author*) Consultant, Allena Pharmaceuticals, Inc; Invited Speaker, Siemens AG Roger Lacson, Boston, MA (*Abstract Co-Author*) Nothing to Disclose Aaron D. Sodickson, MD, PhD, Boston, MA (*Abstract Co-Author*) Institutional research agreement, Siemens AG; Speaker, Siemens AG; Speaker, General Electric Company

#### PURPOSE

To evaluate the utility of virtual monoenergetic imaging in assessing splenic and hepatic lacerations and to determine the optimal energy level to maximize laceration contrast-to-noise ratio.

# METHOD AND MATERIALS

We retrospectively examined 26 contrast-enhanced abdominal CT studies performed on a dual-source dual-energy CT (DECT) scanner in our Emergency Department from 2013 to 2017, with liver and/or splenic lacerations. All studies included portal venous phase imaging acquired simultaneously at low (80 or 100 kVp) and high (140 kVp with tin filtration) energy levels. Conventional 120 kVp-equivalent mixed images were generated for routine review by blending the low and high energy acquisitions. Virtual monoenergetic reconstructions were retrospectively generated in 10 keV steps from 40-90 keV. Liver or splenic laceration attenuation, background parenchymal attenuation and noise were measured on each set of monoenergetic and mixed images. Injury-to-parenchyma contrast and contrast-to-noise ratios (CNR) were calculated. Differences between CNR of monoenergetic series and mixed images were assessed with a paired t-test.

# RESULTS

Liver laceration was identified in 17 patients, and splenic laceration in 10 patients. Background noise was lower at higher monoenergetic levels, with the lowest noise seen at 90 keV, equivalent to that of mixed images (8.26 for 90 keV and 8.66 for mixed, p=0.035). For liver and splenic lacerations, CNR at 40-60 keV was higher than that of mixed images. Injury-to-parenchyma CNR was highest at 40 keV, significantly higher than mixed images (mean CNR 6.14 for 40 keV, 5.48 for mixed, p=0.024). Subgroup analysis of liver and splenic lacerations demonstrated a significant improvement in CNR at 40 keV compared with mixed images for splenic lacerations (5.89 vs. 4.98, p=0.036); for liver lacerations, the increased CNR at 40 keV compared with mixed images was not statistically significant (6.29 vs. 5.77, p=0.2).

## CONCLUSION

With DECT virtual monoenergetic imaging, the optimal energy level for assessing liver and splenic lacerations was 40 keV, which showed improved injury-to-parenchyma CNR compared with traditional polyenergetic reconstructions.

#### **CLINICAL RELEVANCE/APPLICATION**

Virtual monoenergetic imaging at low keV can improve contrast to noise ratio of hepatic and splenic lacerations, which may improve

detectability of subtle injuries and aid radiologists in classifying these injuries.

#### **Honored Educators**

Presenters or authors on this event have been recognized as RSNA Honored Educators for participating in multiple qualifying educational activities. Honored Educators are invested in furthering the profession of radiology by delivering high-quality educational content in their field of study. Learn how you can become an honored educator by visiting the website at: https://www.rsna.org/Honored-Educator-Award/ Jeremy R. Wortman, MD - 2017 Honored EducatorAaron D. Sodickson, MD,PhD - 2014 Honored EducatorAaron D. Sodickson, MD,PhD - 2017 Honored EducatorAaron D. Sodickson, MD,PhD - 2018 Honored Educator

## SSA06-06 Emergency Department Would Become the New Diagnostic Center if the Trend in National Imaging Utilization Continues

Sunday, Nov. 25 11:35AM - 11:45AM Room: S405AB

Participants

Santosh K. Selvarajan, MD, Philadelphia, PA (Presenter) Nothing to Disclose

For information about this presentation, contact:

santosh.rad@gmail.com

#### PURPOSE

Policymakers and payers have been concerned with the rapid growth in imaging utilization particularly in the Emergency Departments. Our purpose is to study the trends in utilization of imaging in EDs in recent years, by modality. Secondly, to determine the specialty of the interpreting physicians.

#### **METHOD AND MATERIALS**

The nationwide Medicare Part B Physician/Supplier Procedure Summary Master Files for 2004-2016 were the data source. CPT codes for plain radiography (XR), non-cardiac ultrasound (US), CT, MRI, and nuclear medicine (NM) were aggregated by modality. Medicare's place-of-service codes were used to identify those exams done during ED visits, and its specialty codes were used to determine which specialties did the interpretations. Trends from 2004 to 2016 were assessed.

#### RESULTS

Between 2004 and 2016 in the ED, the utilization of CT increased from 2,842,446 in 2004 to 7,705,340 in 2016 (+103%). MRI studies increased from 69,000 to 286,000 (+204%). The number of non-cardiac ultrasounds grew from 408,000 to 1,024,809 (+151%). The radiographs performed grew from 9,471,777in 2004 to 13,177,023 in 2016 (+31%). The Nuclear Medicine studies showed a slight numerical decline, from 106,792 in 2004 to 65,985 in 2010 (-25%), but this was largely due to code bundling that occurred in myocardial perfusion imaging in 2010. Nuclear Medicine studies slightly increased from 65,985 in 2010 to 78,000 in 2016 (+11%). In each of the first 4 modalities, growth was steady and progressive with no evidence of slowing even after code bundling for CT abdomen and pelvis. Radiologists' share of the interpretations in 2016 were: CT 99%, MRI 99%, XR 98%, US 87.5%, NM 95%

## CONCLUSION

The utilization of imaging in EDs grew substantially from 2004 to 2016 in comparision to the utilization in other places where imaging is performed. The largest numerical increases were seen in CT and XR. Radiologists strongly predominate in interpreting in all modalities.

## **CLINICAL RELEVANCE/APPLICATION**

The progressive growth of utilization is of concern and suggests that more interdepartmental cooperation is needed for appropriate use of imaging in EDs.

# SSA06-07 The Value of the Radiologist as Consultant to Improve Patient Care in the Emergency Department

Sunday, Nov. 25 11:45AM - 11:55AM Room: S405AB

Participants

Sarvenaz Pourjabbar, MD, New Haven, CT (*Presenter*) Nothing to Disclose Joseph J. Cavallo, MD, New Haven, CT (*Abstract Co-Author*) Nothing to Disclose Amir Imanzadeh, MD, Shelton, CT (*Abstract Co-Author*) Nothing to Disclose Scott Blanchette, New Haven, CT (*Abstract Co-Author*) Nothing to Disclose Kevin Connell, New Haven, CT (*Abstract Co-Author*) Nothing to Disclose Syed A. Bokhari, MD, New Haven, CT (*Abstract Co-Author*) Nothing to Disclose

# For information about this presentation, contact:

sarvenaz.pourjabbar@yale.edu

#### PURPOSE

In the emergency department (ED), imaging studies are requested by a wide spectrum of healthcare providers, many of whom are not educated in the finer details of imaging protocols. This lack of expertise leads to suboptimal diagnostic imaging; this results in decreased diagnostic accuracy, unnecessary cost and added radiation, among other potential inefficiencies. While order entry algorithms been implemented, they are not a comprehensive solution. This study demonstrates the value of radiologists' input on diagnostic imaging at the time of order entry.

## **METHOD AND MATERIALS**

Contrast enhanced CT/CT Angiogram (CTA) exams ordered in our ED are subject to validation by radiologist/radiology physician assistant. If the ordered study is deemed to be suboptimal, the provider is contacted and better options are discussed. Subsequently, the optimal study is protocolled. Per IRB, this quality improvement study was not subject to review. Ordered CT/CTA exams of the chest, abdomen or pelvis were reviewed over the course of 90 ED shifts (10pm-7am) spanning from 9/2017-3/2018. Total CT exam orders placed and the number of exams that were ultimately modified were recorded.

#### RESULTS

During the study, 631 eligible exam orders were reviewed. 14% (88/631) of the requests were modified. Of these modifications, 15% (13/88) were cancellations. In 84% (63/75) of alterations, contrast was improperly used. Suggested order alterations were more often related to oral contrast (52%, 38/75) than intravenous contrast (31%, 23/75). The anatomic area scanned was changed in 15% (11/75) of modified exams. In 13% (10/75) of modified exams, the type of study was changed entirely (Fig. 1).

## CONCLUSION

In the era of value-based health care, it is essential to tailor patients' imaging to address specific clinical questions. Our results demonstrate that approximately 14% of diagnostic CT orders requested in the ED are not optimized. Most commonly, mistakes are related to contrast. Having radiology staff available to identify suboptimal diagnostic CT orders can add value to patient care by optimizing contrast protocols, ensuring the clinical question will be addressed and avoiding redundant examinations.

## **CLINICAL RELEVANCE/APPLICATION**

In the ED, active monitoring of CT scan requests by a radiologist/trained radiology staff can further optimize diagnostic imaging, despite the availability of clinical decision support.

# SSA06-08 National Trends of Non-Cardiac Ultrasound in the Emergency Department: What's the Contribution of Non-Radiologists?

Sunday, Nov. 25 11:55AM - 12:05PM Room: S405AB

#### Participants

Santosh K. Selvarajan, MD, Philadelphia, PA (Presenter) Nothing to Disclose

#### For information about this presentation, contact:

santosh.rad@gmail.com

## PURPOSE

The Accreditation council for Graduate Medical Education (ACGME) requires Point of Care Ultrasound (POCUS) training to be part of Emergency Medicine. Our purpose was to determine recent trends in Non-cardiac ultrasound utilization in Emergency Departments. Secondly, assess the contribution of Non-Radiologists interpretations from 2004 to 2016.

## **METHOD AND MATERIALS**

The Medicare Physician/Supplier Procedure Summary Master Files for 2004-2016 were used. The codes for ED Ultrasound were selected for 2004 and 2016. The procedure volumes in ED settings were calculated. Then Medicare provider specialty codes were used to identify those exams interpreted by Radiologists and other specialties.

#### RESULTS

The number of non-cardiac ultrasounds grew from 408,000 in 2004 to 1,024,809 in 2016 (+151%). Radiologists interpreted 87.5% of all ED non-cardiac ultrasounds. The vascular surgeons and emergency physicians interpreted 4% each, cardiologists and other surgical subspecialties interpreted the remaining 4.5%. There is 181% increase in the studies interpreted by vascular surgeons (15820 in 2004 to 44,369 in 2016), 1117% increase in the studies interpreted by emergency physicians (3459 in 2004 to 41400 in 2016), 26% increase by surgical specialties (14502 in 2004 to 18351 in 2016), and 140% increase by cardiologists (5270 in 2004 to 12470 in 2016).

# CONCLUSION

The utilization of non-cardiac ultrasound grew substantially from 2004 to 2016. Radiologists continue to predominate in interpreting ED ultrasounds. There is small but substantial growth of emergency physicians and vascular surgeons' interpretations. Although much small in number the interpretations by cardiologists and other surgical specialties have also slowly increased.

## **CLINICAL RELEVANCE/APPLICATION**

Although Non-Radiologists interpreting non-cardiac Emergency ultrasound has slowly grown, future studies are needed to assess the complexity of studies interpreted by them.

## SSA06-09 Tiered Response Algorithm for Endovascular Management of Traumatic Hemorrhage

Sunday, Nov. 25 12:05PM - 12:15PM Room: S405AB

Participants Bahman Sadeghi, MD, Orange, CA (*Presenter*) Nothing to Disclose Hanna Javan, MD, Orange, CA (*Abstract Co-Author*) Nothing to Disclose Kari J. Nelson, MD, Orange, CA (*Abstract Co-Author*) Nothing to Disclose Dayantha Fernando, MD, Orange, CA (*Abstract Co-Author*) Nothing to Disclose James Katrivesis, MD, Yorba Linda, CA (*Abstract Co-Author*) Nothing to Disclose Eric Kuncir, MD, Orange, CA (*Abstract Co-Author*) Nothing to Disclose Michael Lekewa, Orange, CA (*Abstract Co-Author*) Nothing to Disclose Nadine Abi-Jaoudeh, MD, Orange, CA (*Abstract Co-Author*) Research collaboration, Koninklijke Philips NV; Research collaboration, Teclison Cherry Pharma Inc; Research support, SillaJen, Inc

#### For information about this presentation, contact:

bsadeghi@uci.edu

# PURPOSE

Hemorrhagic shock represents the second-leading cause of early death in traumatic injury with endovascular therapy as an integral part of the therapeutic armamentarium. The emphasis on a rapid response is balanced with the judicious utilization of resources that led to the creation of a tiered algorithm. The purpose of this study is to assess the efficacy of such a response for the

management of non-operative traumatic hemorrhage.

### **METHOD AND MATERIALS**

A retrospective review of after-hour trauma activations was performed at a level 1 trauma center from July 2015 to July 2017. Activation of the interventional team was initiated either immediately ("EmboNow"), prior to imaging review and attending interventional radiologist (IR) approval, or after review and discussion with IR ("EmboSoon"). The need for transfusion and overall technical clinical success (defined as lack of re-intervention) were collected. Length of stay (LOS) and overall mortality, as well as overall morbidity, was evaluated. Pearson chi-square and Wilcoxon Rank-Sum (WRS) analyses were performed on various parameters to determine the significant clinical efficacy of a tiered response system.

## RESULTS

A total of 73 trauma activations with EmboNow (n=27) and EmboSoon (n=46) occurred in the study time frame. Of the EmboSoon activations, 28 instances did not require the mobilization of the team and 3 instances required the mobilization of the team but did not progress to intervention. No significant difference was determined when assessing the necessity of hemostatic intervention within the groups. Of the cases requiring embolization (n=31), no difference in the clinical success rate was noted. Overall mortality for the EmboNow and EmboSoon groups was not significantly different, 3.7% and 6.7%, respectively. Also, no significant difference observed between the response groups for average LOS, EmboNow = 10.1 days and EmboSoon = 13.3 days.

# CONCLUSION

A tiered response algorithm did not increase overall mortality nor length of stay in patients who ultimately underwent embolization but prevented unnecessary mobilization in 28 cases.

# CLINICAL RELEVANCE/APPLICATION

Efficient use of IR resources as well as cooperation and communication among a multidisciplinary trauma team is essential to improve and maintain high-quality clinical services, and to get the best clinical outcomes in management of traumatic hemorrhage.



## SSA07

# Science Session with Keynote: Gastrointestinal (Radiomics)

Sunday, Nov. 25 10:45AM - 12:15PM Room: N226



AMA PRA Category 1 Credits ™: 1.50 ARRT Category A+ Credit: 1.75

#### **Participants**

Alexander R. Guimaraes, MD, PhD, Portland, OR (*Moderator*) Consultant, Agfa-Gevaert Group Aya Kamaya, MD, Stanford, CA (*Moderator*) Nothing to Disclose Aliya Qayyum, MD, MBBS, Houston, TX (*Moderator*) Spouse, Founder, In Context Reporting

#### Sub-Events

# SSA07-01 Gastrointestinal Keynote Speaker

Sunday, Nov. 25 10:45AM - 10:55AM Room: N226

Participants

Alexander R. Guimaraes, MD, PhD, Portland, OR (Presenter) Consultant, Agfa-Gevaert Group

# **Honored Educators**

Presenters or authors on this event have been recognized as RSNA Honored Educators for participating in multiple qualifying educational activities. Honored Educators are invested in furthering the profession of radiology by delivering high-quality educational content in their field of study. Learn how you can become an honored educator by visiting the website at: https://www.rsna.org/Honored-Educator-Award/ Alexander R. Guimaraes, MD, PhD - 2018 Honored Educator

# SSA07-02 Added Value of Radiomic Analysis in Gadoxetic Acid-Enhanced MRI for Prediction of Postoperative Early and Late Recurrence of Single Hepatocellular Carcinoma

Sunday, Nov. 25 10:55AM - 11:05AM Room: N226

Participants

Sungwon Kim, MD, Seoul, Korea, Republic Of (*Abstract Co-Author*) Nothing to Disclose Jaeseung Shin, Seoul, Korea, Republic Of (*Presenter*) Nothing to Disclose Jin-Young Choi, Seoul, Korea, Republic Of (*Abstract Co-Author*) Nothing to Disclose Myeong-Jin Kim, MD, PhD, Seoul, Korea, Republic Of (*Abstract Co-Author*) Nothing to Disclose

# For information about this presentation, contact:

dinbe@yuhs.ac

## PURPOSE

To evaluate the added value of the radiomic model in predicting early and late recurrence after resection in a single HCC of less than 5 cm using preoperative gadoxetic acid-enhanced MRI, compared to clinical-only model.

# METHOD AND MATERIALS

This retrospective study included 214 patients with surgically resected and pathologically confirmed single HCC (<5cm; 1-2cm [n = 47]; 2-5cm [n = 167]) between January 2010 and December 2015 who underwent preoperative gadoxetic acid-enhanced MR imaging. All prediction models were made with training set and performance was evaluated with temporally independent validation set (training set vs. validation set; 1-5cm, 162 vs 52; 2-5cm, 128 vs. 39). Independent predictors for early and late disease-free survival (DFS) in clinicopathologic information were identified using the Cox regression model, respectively. Three dimensional radiomic features for predicting DFS were selected in each early (<2 years) and late period (2-5 years). A combined radiomic-clinical model (CMB) and a clinical-only model (CLN) were created using a random survival forest and additional values of radiomic features were evaluated using bootstrapping method (n = 1000) in each of the following conditions: early DFS vs. late DFS; tumor size 1-2cm vs. 2-5cm; all combinations of the three dynamic phases (arterial, portal, hepatobiliary phase); the peritumoral border extension included in the radiomic feature extraction (0mm vs. 3mm vs. 5mm).

# RESULTS

The combined radiomic-clinical model showed a higher C-index than the clinical-only model in the prediction of early DFS but showed a lower C-index than the clinical-only model in the prediction of late DFS. The combined model using the radiomic features from 2-5cm size tumors, all three phases, 3mm peritumoral border extension showed the highest C-index value (CMB, C-index 0.716 [0.627-0.799]; CLN, C-index 0.696 [0.557-0.799]).

#### CONCLUSION

Radiomic features combined with clinical factors may improve the prediction of postoperative early recurrence of HCC, but they do not affect the prediction of late recurrence.

## **CLINICAL RELEVANCE/APPLICATION**

Combined analysis of radiomic and clinicopathologic features may influence the postoperative management of patients by increasing the predictive power of postoperative early recurrence of HCC.

# SSA07-03 Auto-Encoder and Multilayer Perceptron Assisted Radiomics Approach for Prediction of Early Intrahepatic Recurrence After Radiofrequency Ablation in Hepatocellular Carcinoma

Sunday, Nov. 25 11:05AM - 11:15AM Room: N226

Participants

Cheyu Hsu, MD, Taipei, Taiwan (*Presenter*) Nothing to Disclose Kao-Lang Liu, MD, Taipei, Taiwan (*Abstract Co-Author*) Nothing to Disclose Shihmin Lin, MD, Taoyuan, Taiwan (*Abstract Co-Author*) Nothing to Disclose Po-Ting Chen, MD, Taipei City, Taiwan (*Abstract Co-Author*) Nothing to Disclose Weichung Wang, Taipei, Taiwan (*Abstract Co-Author*) Nothing to Disclose Sung-Hsin Kuo, MD, PhD, Taipei, Taiwan (*Abstract Co-Author*) Nothing to Disclose

For information about this presentation, contact:

codiwa@gmail.com

# PURPOSE

After radiofrequency ablation (RFA), > 50% of early stage hepatocellular carcinoma (HCC) patients undergo intrahepatic recurrence (IHR) within 2-3 years. To optimize the selection of most profitable patients to receive RFA, better prediction algorithms are needed to identify early IHR after RFA. Radiomics allows noninvasively extracting three-dimensional and quantitative features of tumor phenotypes from radiographic images. Recent advances in deep neural network also provide powerful tools for features selection and classification. The present study aims to combine those approaches to establish prediction model to identify patients with a low predicted IHR and suitable for RFA as first-line treatment.

#### **METHOD AND MATERIALS**

Patients who initially underwent RFA for single nodular HCC <= 5 cm with Child-Pugh grade A or B were included. A total of 6568 triphasic CT-based features of pretreatment tumors were obtained from 176 patients in the experimental cohort (EC). A Radiomic based prediction model (RPM), trained with variational autoencoder (VAE) and multilayer perceptron (MLP), was developed to predict the 2-year IHR, and validated in an independent validation cohort (VC) of 57 HCC patients. Imaging traits including tumor encapsulation, tumor necrosis, lack of fast wash-in or wash-out, multi-segment involvement were analyzed and correlated to the neurons of the encoder layers as an approach to explain the black box of hidden layers.

## RESULTS

The VAE, with 16 neurons in encoder layers, held the task of noise reduction for high dimensional radiomic features, and MLP, with 4 hidden layers, was used to train the model. The RPM, trained with 1,711,457 parameters, outperformed the traditional volumetric predictors of maximal tumor diameter in the prediction of 2-year IHR, with a C-index of 0.757 / 0.707 (EC / VC), compared to 0.540 / 0.510. Imaging traits of tumor necrosis and lack of fast wash-in were associated with neuron\_A and neuron\_B in the encoder layers. Multivariate analysis showed only RPM and pre-RFA AFP level were significantly associated with 2-year IHF.

# CONCLUSION

The radiomics approach provides a novel and convenient way to predict 2-year IHR in patients with early stage HCC who received RFA. The VAE and MLP help denoise high dimensional data and shed the light on the explanation of deep neural network.

## **CLINICAL RELEVANCE/APPLICATION**

The RPM will select most profitable patients to receive RFA

# SSA07-04 Development of a Liver Tumor Diagnosis Tool with Deep Neural Networks: Radiologist-Level Performance with Artificial Intelligence

Sunday, Nov. 25 11:15AM - 11:25AM Room: N226

Participants

Charlie Hamm, Berlin, Germany (*Presenter*) Nothing to Disclose Clinton Wang, New Haven, CT (*Abstract Co-Author*) Nothing to Disclose Lynn J. Savic, New Haven, CT (*Abstract Co-Author*) Nothing to Disclose Marc Ferrante, MD, N New Hyde Pk, NY (*Abstract Co-Author*) Nothing to Disclose Isabel T. Schobert, New Haven, CT (*Abstract Co-Author*) Nothing to Disclose Todd Schlachter, MD, Farmington, CT (*Abstract Co-Author*) Nothing to Disclose Ming De Lin, PhD, New Haven, CT (*Abstract Co-Author*) Nothing to Disclose Ming De Lin, PhD, New Haven, CT (*Abstract Co-Author*) Nothing to Disclose Jeffrey C. Weinreb, MD, New Haven, CT (*Abstract Co-Author*) Nothing to Disclose Jeffrey C. Weinreb, MD, New Haven, CT (*Abstract Co-Author*) Consultant, Bracco Group; Author, Siemens AG Julius Chapiro, MD, New Haven, CT (*Abstract Co-Author*) Research Grant, Koninklijke Philips NV; Research Grant, Guerbet SA; Consultant, Guerbet SA; Consultant, Eisai Co, Ltd Brian S. Letzen, MD, New Haven, CT (*Abstract Co-Author*) Nothing to Disclose

# For information about this presentation, contact:

julius.chapiro@yale.edu

## PURPOSE

To develop and evaluate the performance of a 3D deep convolutional neural network (CNN) system compared to board-certified radiologists in automatically classifying hepatic lesions on contrast-enhanced multi-phasic magnetic resonance images (MRI).

# METHOD AND MATERIALS

This IRB-approved, HIPAA-compliant analysis included 296 patients with a total of 494 focal hepatic lesions of different entities

(simple cyst, hemangioma, focal nodular hyperplasia, hepatocellular carcinoma [HCC], intrahepatic cholangiocarcinoma, and colorectal carcinoma metastasis). Lesions were defined on T1-weighted MRI scans (arterial, portal venous, delayed phase) and divided into training (n=434) and test sets (n=60). The training set was provided to a 3D CNN to learn how to classify each lesion type. The system's performance on the test set was compared with that of two board-certified radiologists.

#### RESULTS

Over 20 iterations, the CNN model achieved an overall average accuracy of 92%, a sensitivity (Sn) of 92%, and a specificity (Sp) of 98%. The model showed the lowest performance for colorectal carcinoma metastasis (89% Sn, 98% Sp) while the highest performance was achieved in classifying simple cysts (99% Sn, 100% Sp). The model's performance in a single run on the test set showed an average Sn of 90% and Sp of 98% across the six lesion types, compared to an average Sn of 82.5% and Sp of 96.5% for the radiologists. Specifically, the model achieved a 90% Sn for classifying HCC compared to 65% for radiologists. The model showed a true positive rate of 93.5% and false positive rate of 1.6% for HCC classification, with a receiver operating characteristic area under the curve (AUC) of 0.992. The model computation time per lesion was 1 millisecond.

## CONCLUSION

This novel 3D CNN system demonstrates the feasibility of AI decision-support to accurately classify several classes of liver lesions on multi-phasic MRI, providing a tool to potentially augment radiologists' performance and efficiency.

# CLINICAL RELEVANCE/APPLICATION

As the volume demands of radiology increase, a synergistic workflow that combines a radiologist's experience and intuition with the computational power of AI may enhance efficiency and quality.

#### **Honored Educators**

Presenters or authors on this event have been recognized as RSNA Honored Educators for participating in multiple qualifying educational activities. Honored Educators are invested in furthering the profession of radiology by delivering high-quality educational content in their field of study. Learn how you can become an honored educator by visiting the website at: https://www.rsna.org/Honored-Educator-Award/ Jeffrey C. Weinreb, MD - 2018 Honored Educator

# SSA07-05 Utility of Radiomics Analysis of Gadoxetic Acid-Enhanced Hepatobiliary Phase MR Images: A Noninvasive Method for Accurate Diagnosis and Staging of Hepatic Fibrosis

Sunday, Nov. 25 11:25AM - 11:35AM Room: N226

Participants

Hyo Jung Park, MD, Seoul, Korea, Republic Of (*Presenter*) Nothing to Disclose Seung Soo Lee, MD, Seoul, Korea, Republic Of (*Abstract Co-Author*) Nothing to Disclose Bum-Woo Park, BA, Seoul, Korea, Republic Of (*Abstract Co-Author*) Nothing to Disclose Jessica Yun, Seoul, Korea, Republic Of (*Abstract Co-Author*) Nothing to Disclose

For information about this presentation, contact:

happyeahj@gmail.com

# PURPOSE

To develop and validate a radiomics-based index for staging liver fibrosis using gadoxetic acid-enhanced hepatobiliary phase (HBP) MR images.

# METHOD AND MATERIALS

The institutional review board approved the study, and informed consent was waived. A total of 436 patients with pathologically proven liver fibrosis and gadoxetic acid-enhanced liver MR imaging preceding less than 3 months of histopathologic analysis were included (132, 22, 53, 77, 153 for fibrosis grade 0, 1, 2, 3, 4, respectively). The subjects were randomly divided into the development and test cohorts at a ratio of 3:1. Feature extraction was performed from HBP images, and extracted features included 8 histogram features and 35 high-order textural features. For feature selection and modeling for binary decision to discriminate F0-2 vs. F3-4, we used a logistic regression with elastic net regularization. Performance of the selected model in diagnosing significant fibrosis (>= F2), advanced fibrosis (>= F3), and cirrhosis (F4) was evaluated using the AUROC in the test cohort, and was compared with serum markers (APRI and FIB-4).

#### RESULTS

Radiomic fibrosis index had significant positive correlation with the pathologic fibrosis stage (p=0.735, P<.001). In the test cohort, AUROCs of the model were 0.9, 0.89, and 0.91 for diagnosing significant fibrosis, advanced fibrosis and cirrhosis, respectively. The Obuchowski index, a weighted average of the AUROC values obtained for all pairs of fibrosis stages, was 0.864 (62% CI, 0.819-0.909) in radiomics model, significantly higher than those of APRI (0.604, P<.001) and FIB-4 (0.621, P<.001). Using the threshold values for radiomic fibrosis index determined in the development cohort, the sensitivities of 78.9% - 92.1%, specificities of 75.4% - 82.0%, and accuracies of 80.3% - 81.3% were achieved for diagnosing significant fibrosis, advanced fibrosis, and cirrhosis in the test cohort.

# CONCLUSION

Radiomics analysis of HBP images of gadoxetic acid-enhanced MRI can provide accurate diagnosis and staging of liver fibrosis.

# **CLINICAL RELEVANCE/APPLICATION**

Radiomics analysis of HBP images has a potential usefulness for the noninvasive and accurate diagnosis and staging of hepatic fibrosis.

# SSA07-06 Application Value of Radiomics Features Based on Monochromatic Images of Spectrum CT in the Pathological Grading of Gastric Adenocarcinoma

Sunday, Nov. 25 11:35AM - 11:45AM Room: N226

Participants

Yue Lv, Dalian, China (*Presenter*) Nothing to Disclose Ailian Liu, MD, Dalian, China (*Abstract Co-Author*) Nothing to Disclose Jinghong Liu, MD, PhD, Dalian, China (*Abstract Co-Author*) Nothing to Disclose Yijun Liu, Dalian, China (*Abstract Co-Author*) Nothing to Disclose Chen Lihua, Dalian, China (*Abstract Co-Author*) Nothing to Disclose Jingjun Wu, Dalian, China (*Abstract Co-Author*) Nothing to Disclose Xinying Li, Dalian, China (*Abstract Co-Author*) Nothing to Disclose Yan Guo, Shenyang, China (*Abstract Co-Author*) Nothing to Disclose Xin Li, Shanghai, China (*Abstract Co-Author*) Nothing to Disclose

## For information about this presentation, contact:

lvyue\_dl@163.com

#### PURPOSE

To evaluate the clinical value of radiomics features based on monochromatic images of spectrum CT in the pathological grading of gastric adenocarcinoma.

# METHOD AND MATERIALS

Retrospectively 196 patients with gastric adenocarcinoma who underwent upper or total abdominal GSI scanning using the Discovery 750 CT machine were collected, who were divided into poorly differentiated group (Group A) and moderately-well differentiated group (Group B) according to pathological results. High-quality, standardized venous phase single-energy images of 70 keV were obtained from the AW4.6 workstation, and then radiomics features based on the monochromatic images were extracted and a Logistic regression model was established by the dimensionality-reduced features. The efficacy of the Logistic regression model was evaluated by the receiver operating characteristic curve (ROC) and its accuracy was verified. At the same time, the grading results and performance of conventional energy spectrum parameters were compared and analyzed.

#### RESULTS

The grading efficacy of the normalized iodine (water) concentration of conventional spectral parameters was 0.668. The area under the ROC curve (AUC) of the Logistic regression model was 0.872 (sensitivity was 73.3% and specificity was 83.3%) and the diagnostic accuracy was 78.3%.

#### CONCLUSION

Radiomics features based on the single-source dual-energy CT monochromatic images can non-invasively differentiate gastric adenocarcinoma from poorly differentiated and moderately-well differentiated tumors. Its efficacy is better than that of conventional spectral CT.

# **CLINICAL RELEVANCE/APPLICATION**

Radiomics features based on the single-source dual-energy CT monochromatic images can provide more quantitativeand repeatable information for clinical treatment options and preoperative evaluations.

# SSA07-07 Multi-Feature Based CT Radiomic Signature Peroperatively Predicts Lymph Node Metastasis in Advanced Gastric Cancer

Sunday, Nov. 25 11:45AM - 11:55AM Room: N226

Participants

Mengjie Fang, Beijing, China (*Presenter*) Nothing to Disclose Di Dong, PhD, Beijing, China (*Abstract Co-Author*) Nothing to Disclose Zaiyi Liu, MD, Guangzhou, China (*Abstract Co-Author*) Nothing to Disclose Lei Tang, MD, Beijing, China (*Abstract Co-Author*) Nothing to Disclose Jie Tian, PhD, Beijing, China (*Abstract Co-Author*) Nothing to Disclose

For information about this presentation, contact:

fmj5mj@gmail.com

#### PURPOSE

To investigate whether the method of deep learning could improve the performance of radiomic features, and to build a radiomic signature for preoperative prediction of lymph node metastasis (LNM) in patients with advanced gastric cancer (AGC).

# METHOD AND MATERIALS

In this ethical-approved retrospective study, we collected a primary cohort consisting of 110 patients from Center 1 and a validation cohort consisting of 121 patients from Center 2. A total of 521 features were extracted from venous-phase CT images. The features could be divided into two groups: deep learning features and conventional hand-crafted features. Based on the whole feature set and the hand-crafted-only feature set respectively, RELIEFF and support vector machine model were implemented to select key features and build two radiomic signatures to yield quantitative risk for LNM. The predictive performances of the signatures were evaluated by receiver operator characteristics analysis and accuracy analysis in the external validation cohort.

#### RESULTS

Combining the deep learning features and conventional features, the multi-feature based CT radiomic signature outperformed the conventional signature (area under the curve: 0.799 vs. 0.735 in the external validation cohort). It showed powerful predictive ability of discriminate non-NO patients from NO patients with accuracies of 0.764 (95% confidence interval [CI]: 0.673-0.839) and

0.736 (95% CI: 0.648-0.812) in the primary and validation cohorts respectively.

# CONCLUSION

Taking advantages of the novel deep learning method and the conventional machine learning method, radiomic signature could serve as a useful tool for preoperative LNM status prediction in patients with AGC.

# CLINICAL RELEVANCE/APPLICATION

Multi-feature based CT radiomic signature has potential in the preoperative non-invasive prediction of lymph node metastasis and facilitate the clinical strategy.

# SSA07-08 Correlation Analysis of Spectral CT Parameters and K-ras Gene Mutation in Colorectal Cancer

Sunday, Nov. 25 11:55AM - 12:05PM Room: N226

Participants

Dan Wang, Lanzhou, China (*Presenter*) Nothing to Disclose Junlin Zhou, Lanzhou, China (*Abstract Co-Author*) Nothing to Disclose

### PURPOSE

To evaluate the relationship between K-ras mutation of colorectal cancer and the quantitative parameters and qualitative parameters with spectral CT.

## METHOD AND MATERIALS

A retrospective analysis of 66 cases of colorectal adenocarcinoma with K-ras mutation confirmed by surgical or endoscopic biopsy was performed by spectral CT dual-phase enhanced scans. The relationship between K-ras mutation and the qualitative and quantitative parameters of CT was statistically analyzed. The CT qualitative evaluation included the location of the tumor, the thickening of the intestinal wall, the infiltration of perienteral fat, and the enlargement of the lymph nodes; the parameters of the CT quantitative assessment include the 40~140keV single energy CT, the iodine (water) concentration, the water(iodine) concentration, the normalized iodine concentration(NIC) and the spectrum curve slope in the arterial and venous phase. The slope is calculated according to the following formula: slope = (CT40keV-CT100keV) /60. Chi-square test was used to statistically analyze the correlation between CT qualitative signs and K-ras mutation status. Independent sample t-test was used for statistical analysis to evaluate the correlation between spectral CT features and K-ras mutations.

#### RESULTS

K-ras mutations were positive in 32 (48%) of the 66 patients. The colorectal cancer patients with K-ras mutation were multiple in the right hemicolon(x2=8.09,P=0.007), eccentric thickening(x2=12.17,P=0.001), and more perienteric lymph nodes(x2=12.17,P=0.001), which were not related to the degree of fat infiltration around the lesions, and the extent of perianal invasion(P>0.05). The iodine concentration(t=-3.47,P=0.002), NIC(t=-3.18,P=0.004), the slope of the spectrum curve(t=-3.58,P=0.001) and the CT value of the low energy level (40-70 keV) (P<0.05) in arterial phase were increased in the K-ras mutation-type colorectal cancer patients than the wild-type ones.

## CONCLUSION

K-ras mutations in colorectal cancer correlated with a part of spectral CT quantitative parameters and qualitative parameters.

#### **CLINICAL RELEVANCE/APPLICATION**

K-ras mutations could be initially judged by qualitative and quantitative parameters of spectral CT.

# SSA07-09 MRI-Based Radiomics Analysis for Predicting KRAS Mutation in Patients with Rectal Cancer

Sunday, Nov. 25 12:05PM - 12:15PM Room: N226

Participants

Huanhuan Liu, Shanghai, China (*Presenter*) Nothing to Disclose Caiyuan Zhang, MD, Shanghai, China (*Abstract Co-Author*) Nothing to Disclose Jinning Li, BMedSc, Shanghai, China (*Abstract Co-Author*) Nothing to Disclose Xin Li, Shanghai, China (*Abstract Co-Author*) Nothing to Disclose Dengbin Wang, Shanghai, China (*Abstract Co-Author*) Nothing to Disclose

For information about this presentation, contact:

liuhuanhuan0117@163.com

## PURPOSE

Genetic profiling of tumors is important for personalized treatment through the development of targeted therapies. For patients with suspected or proven metastatic rectal cancer, the identification of KRAS/NRAS/BRAF mutations is of great significance. Either of the mutations predicts a lack of response to cetuximab and panitumumab, which is important for the individual treatment strategy. Therefore, our study was to investigate the value of radiomics analysis for predicting KRAS mutation in patients with rectal cancer.

# **METHOD AND MATERIALS**

A total of 128 patients with histopathologically confirmed rectal cancer who underwent preoperative MR imaging and postoperative KRAS mutation test without any preoperative chemoradiotherapy were divided into the primary cohort (n=89) and the validation cohort (n=39). MRI-based radiomics features were extracted from oblique axial T2-weighted images. The independent two-sample t test, Kruskal-Wallis test, and Pearson correlation analysis were used for features selection. A radiomics signature was built and multivariable logistic regression analysis was used to develop the radiomics model including radiomics features and independent clinico-radiologic risk factors. The performance of the radiomics model was assessed by the receiver operating characteristic curve (ROC) and decision curve analysis.

A total of 385 radiomic features were extracted from each patient, and 12 radiomics features were selected for the radiomics signature. The radiomics signature was significantly associated with KRAS mutation (P<0.001). The areas under the ROCs were 0.845 in the primary cohort and 0.767 in the validation cohort. Decision curve analysis confirmed the clinical utility of the radiomics model. The clinical background and tumor MRI-staging showed no significant correlation with KRAS mutation.

# CONCLUSION

The MRI-based radiomics model could be used to predict the KRAS mutation in patients with rectal cancer, which could be helpful for individual treatment strategy.

# **CLINICAL RELEVANCE/APPLICATION**

(dealing with MRI-based radiomics ) "The MRI-based radiomics model could be used to predict the KRAS mutation in patients with rectal cancer, which could be helpful for individual treatment strategy"



#### SSA08

# Science Session with Keynote: Gastrointestinal (Crohn's Disease and Small Bowel)

Sunday, Nov. 25 10:45AM - 12:15PM Room: N227B



AMA PRA Category 1 Credits ™: 1.50 ARRT Category A+ Credit: 1.75

## Participants

Joel G. Fletcher, MD, Rochester, MN (*Moderator*) Grant, Siemens AG; Consultant, Medtronic plc; ; Tracy A. Jaffe, MD, Durham, NC (*Moderator*) Nothing to Disclose Aoife Kilcoyne, MBBCh, Boston, MA (*Moderator*) Nothing to Disclose

#### Sub-Events

# SSA08-01 Crohn's Disease Evaluation with Diffusion Weighted Imaging

Sunday, Nov. 25 10:45AM - 10:55AM Room: N227B

Participants

Nicholas K. Cheung, MBBS, Hobart, Australia (*Presenter*) Nothing to Disclose Andrew J. Halliday, MBBS, Hobart, Australia (*Abstract Co-Author*) Nothing to Disclose Aditya Varma, MBBS, Hobart, Australia (*Abstract Co-Author*) Nothing to Disclose

#### PURPOSE

Diffusion-weighted-imaging (DWI) is increasingly used for Crohn's disease (CD) evaluation. Sensitivity and specificity rates are however heterogeneous1-5, and only two series to-date reported paediatric CD results4,6. We report one of the largest series for DWI evaluation of adult and pediatric CD.

#### **METHOD AND MATERIALS**

Between 2014 and 2016, 77 patients (18 pediatrics) underwent DWI for CD. All had histopathological confirmation within 28 days. Two radiologists were presented random DWI sequences, to evaluate bowel segments for disease activity, based subjectively on "greater-than-normal visual diffusion-restriction", followed objectively by mean minimum-ADC values. Sensitivity/specificity for detection and inter-observer reliability were recorded. Differences in ADC values calculated with unpaired t-test.

#### RESULTS

Both radiologists had 99% sensitivity and specificity (kappa 0.98) in terminal ileitis detection. Minimum mean ADC values were  $1.3\pm0.4\times10$ -3mm2/s. Overall specificity rates of 75% in determining colonic involvement. The greatest disparity was within the sigmoid, with 68% specificity. Moderate inter-observer reliability achieved (kappa 0.40). ADC values significantly differed between true and false positive colonic segments (Mean ADC  $1.08\pm0.4\times10$ -3mm2/s vs.  $1.84\pm0.55\times10$ -3mm2/s, p<0.0001). Overall results were similar for the pediatric subgroup.

## CONCLUSION

We achieved a 99% diagnostic rate of CD affected terminal ileum. Low specificity and interobserver reliability for CD affected colon, however, ADC quantitative values improved diagnostic accuracy and correlation.

## SSA08-02 High Spatiotemporal Resolution Free-Breathing Quantitative Bowel Perfusion Imaging

Sunday, Nov. 25 10:55AM - 11:05AM Room: N227B

Participants

Verena Obmann, MD, Cleveland, OH (*Presenter*) Nothing to Disclose Kun Yang, Cleveland, OH (*Abstract Co-Author*) Nothing to Disclose Satyam Ghodasara, MD, Cleveland, OH (*Abstract Co-Author*) Research support, Siemens AG Katherine Wright, Cleveland, OH (*Abstract Co-Author*) Research support, Siemens AG Marcie Stopchinski, Cleveland, OH (*Abstract Co-Author*) Nothing to Disclose Yong Chen, Cleveland, OH (*Abstract Co-Author*) Nothing to Disclose Ananya Panda, MD, MBBS, Rochester, MN (*Abstract Co-Author*) Support, Siemens AG Maneesh Dave, Cleveland, OH (*Abstract Co-Author*) Nothing to Disclose Vikas Gulani, MD, PhD, Cleveland, OH (*Abstract Co-Author*) Research support, Siemens AG; Licensed Technology, Siemens Healthineers - both myself and my spouse. MR Fingerprinting, on which we are both inventors, has been licensed by Siemens.

#### For information about this presentation, contact:

verena.obmann@case.edu

#### PURPOSE

This study shows that 3D through-time spiral GRAPPA can be used to acquire DCE-MRI data of the bowel with a high spatiotemporal resolution without a need for breath-holding, and enables quantitative perfusion analysis of the entire bowel.

## **METHOD AND MATERIALS**

3D DCE-MRI data of the bowel was obtained from 7 patients with Crohn disease undergoing MRE exam at 1.5T (Siemens Aera). A total of 50 coronal volumes were acquired continuously over the course of approximately 1.5 minutes after the injection of 0.1 mmol/kg gadobenate dimeglumine (3ml/s) with a temporal resolution of 1.6s while the patients breathed freely. Each volume included 40 slices with an in-plane matrix size of 272×272, in-plane resolution of 1.5 mm, and an uninterpolated slice thickness of 4 mm. Conventional qualitative MRI findings were recorded. The Tofts model was used to quantitatively characterize contrast enhancement in the bowel. Multislice ROIs were drawn in the bowel wall as well as in the aorta to calculate the arterial input function. Ktrans and ve were quantified by fitting the mean signal within each ROI from the bowel to the model.

## RESULTS

This acquisition technique allowed for full coverage of the entire abdomen. Mean age was 40.1 years (range 19-68 years) in 3 male and 4 female patients. 2 showed active inflammatory changes while 5 did not exhibit evidence of active disease at the time of examination. All inflamed bowel segments showed mural thickening and increased contrast enhancement. Quantified perfusion properties for segments with active inflammation were in mean  $0.096\pm0.045$  (0.044-0.123) compared to non-affected segments  $0.019\pm0.033$  (0.002-0.099) for Ktrans and  $0.476\pm0.212$  (0.337-0.724) vs.  $0.223\pm0.319$  (0.068-0.232) for ve.

## CONCLUSION

This study shows that free-breathing, high spatiotemporal resolution, and quantitative 3D DCE-MRI of the bowel is feasible with spiral GRAPPA leading to accurate characterization of the early arterial portions of the bowel contrast enhancement time course. Although evaluated in a limited number of patients, perfusion metrics already demonstrate separation of normal and inflamed bowel wall.

# **CLINICAL RELEVANCE/APPLICATION**

Spiral GRAPPA allows for quantitative perfusion assessment of the intestine without preselecting specific loops as the entire abdomen is covered. This sequence can be used for future therapy response assessment trials.

# SSA08-03 Tagged Cine-MRI for the Assessment of Caloric Stimulation of Small Bowel Motility

Sunday, Nov. 25 11:05AM - 11:15AM Room: N227B

#### Participants

Catharina S. de Jonge, MSc, Amsterdam, Netherlands (*Presenter*) Nothing to Disclose Andre M. Sprengers, PhD, Nijmegen, Netherlands (*Abstract Co-Author*) Nothing to Disclose Kyra L. van Rijn, MD, Amsterdam, Netherlands (*Abstract Co-Author*) Nothing to Disclose Aart J. Nederveen, PhD, Amsterdam, Netherlands (*Abstract Co-Author*) Nothing to Disclose Jaap Stoker, MD, PhD, Amsterdam, Netherlands (*Abstract Co-Author*) Research Consultant, Robarts Clinical Trials, Inc

## PURPOSE

Continuously tagged imaging for the assessment of motility in the small bowel region has been demonstrated as an alternative to other more established MRI techniques. Providing its own contrast and the possibility to monitor motility during free-breathing, this technique can assess motility at frequencies as low as 2 contractions per minute (cpm), this is the slow wave, motility pattern range. This study aims to validate a clinically feasible test for small bowel motility assessment in the low frequency range using tagged cine-MRI before and after a 300-kCal meal.

## METHOD AND MATERIALS

After ±11h overnight fasting, 16 healthy subjects (9 males, median age 25, range 19-37y) underwent a free-breathing, tagged cine-MRI to capture global small bowel motility. Each subject underwent i) baseline motility scan ii) food challenge with Nutridrink iii) post-challenge scan iv) second post-challenge scan (after ±20 minutes). Motility was quantified within a region of interest covering the small bowel, using a validated frequency analysis technique for measuring the spectral power of the strain, referred to as 'motility score'. Motility score was assessed in 20 frequency intervals between 1-20 cpm.

#### RESULTS

The motility score was consistently higher in the low frequency regime (1-10cpm) right after caloric intake, this regime is consistent with the stomach and bowel frequencies (3-12 cpm). The difference between baseline motility score and directly after drinking was significant in the low range intervals 2-4cpm and 6-8cpm. The difference between the motility score directly after drinking and  $\pm 20$  minutes after drinking was significant in the low range intervals 1-4cpm. No significant changes were observed in the breathing range.

# CONCLUSION

This study demonstrates the continuously tagged imaging sequence and quantification method is capable of assessing changes in motility patterns in high detail during free breathing. The method is non-invasive and independent of preparation, enabling monitoring in both fasted and fed state. This indicates that it can be used to perform stimulation tests to measure response in various frequency intervals and with that assess (patho)physiology in the gastrointestinal tract.

# **CLINICAL RELEVANCE/APPLICATION**

Continuously tagged MR imaging is capable of non-invasively assessing small bowel motility in high detail during free breathing, providing a tool to explore (patho)physiology in fasted and fed state.

# SSA08-04 Value of Spectral Computed Tomography Imaging For Evaluation of Intestinal Activity and in Crohn's Disease

Sunday, Nov. 25 11:15AM - 11:25AM Room: N227B

Participants Yu Zhang, MS, Wuhan, China (*Presenter*) Nothing to Disclose Hongran Liu, MD, Wuhan, China (*Abstract Co-Author*) Nothing to Disclose Jing Li, Wuhan, China (*Abstract Co-Author*) Nothing to Disclose Cen Chen, Wuhan, China (*Abstract Co-Author*) Nothing to Disclose Xin Li, MD,PhD, wuhan, China (*Abstract Co-Author*) Nothing to Disclose Ping Han, MD, Wuhan, China (*Abstract Co-Author*) Nothing to Disclose

For information about this presentation, contact:

octopussss1988@163.com

## PURPOSE

To investigate the clinical value of spectral CT imaging in assessing the activity of Crohn's disease compared with the simple endoscopic score (SES).

# METHOD AND MATERIALS

50 patients suspected to have Crohn's disease received both colonoscopy and contrast enhanced computed tomographic enterography (CTE) were involved in this study. The interval time between the two examinations was less than one week. All patients were scanned on a GE Discovery 750 HDCT scanner using GSI spectral imaging mode. The portal-phase monochromatic images from 40 to 140kev and iodine-based material decomposition images were reconstructed after scan. Reconstructed images data were processed with GSI Viewer for analysis. According to the SES-CD (Simple Endoscopic Score for Crohn's Disease)scores, 50 patients were divided into 4 groups(GroupA:Score=0-2,n=6;GroupB:Score=3-6,n=12;GroupC:Score=7-15,n=17;GroupD:Score>=16,n=15). Three different locations of suspicious area of the small bowel were selected from each patient. The spectral curve slope and its mean value were calculated under 40-70KeV; the iodine concentrations and effective atomic number of the involved bowel wall in material decomposition images were measured; the CT value of 50KeV images were measured; the variance analysis was used for the iodine concentration and spectral curve slope comparison among the four groups.

#### RESULTS

The spectral curve slopes(-1.58 $\pm$ 0.48,-2.17 $\pm$ 0.66,-3.18 $\pm$ 1.07,-3.97 $\pm$ 0.65)and iodine concentrations (8.02 $\pm$ 1.70,12.33 $\pm$ 2.23,17.84 $\pm$ 4.40,22.24 $\pm$ 3.61),CT value of 50 KeV (60.41 $\pm$ 1.60,72.67 $\pm$ 3.23,111.66 $\pm$ 4.21,140.57 $\pm$ 4.01)and effective atomic number (7.78 $\pm$ 0.07,8.12 $\pm$ 0.09,8.45 $\pm$ 1.21,8.77 $\pm$ 1.01)of four groups were found statistically significant different (P<0.01);the spectral curve slopes,iodine concentrations,CT value of 50KeV,effective atomic number among Group A,Group C and Group D were statistically different(P<0.05);Group B,Group C and Group D were statistically different(P<0.05).

#### CONCLUSION

The spectral curve slope, the iodine concentration, the CT value of 50KeV and effective atomic number of the small bowel derived from spectral CT imaging can be used to evaluate the activity of Crohn's disease.

#### **CLINICAL RELEVANCE/APPLICATION**

Spectral CT had sensitivity in detecting intestinal activity and severity of CD, which could be an alternative choice in evaluation of CD. The purpose of this study was to establish the standards of evaluating the activity of Crohn's disease using spectral CT in the future.

# SSA08-05 Eliminating Unnecessary Anatomic Coverage Allows for Significant Radiation Dose Savings in Follow-Up Outpatient CT Enterographies of Young Crohn's Adults

Sunday, Nov. 25 11:25AM - 11:35AM Room: N227B

Awards

## **Student Travel Stipend Award**

Participants David C. Wang, MD, Toronto, ON (*Presenter*) Nothing to Disclose Sarah A. Johnson, MD, Toronto, ON (*Abstract Co-Author*) Nothing to Disclose Nasir M. Jaffer, MD, Toronto, ON (*Abstract Co-Author*) Nothing to Disclose Luis S. Guimaraes, MD, Toronto, ON (*Abstract Co-Author*) Nothing to Disclose

## PURPOSE

To determine the minimal Z-axis coverage necessary to include all relevant extra-intestinal (EI) findings and the entire bowel in follow up CT enterographies (CTEs) of young Crohn's (CD) outpatients, and the potential radiation dose savings in eliminating unnecessary Z-coverage in this young population, where significant EI findings are rare and dose savings are beneficial.

## **METHOD AND MATERIALS**

All outpatient CTEs of 18-40 years old CD patients performed from January to December 2016 were included. Two abdominal radiologists in consensus noted the most inferior vertebral level - superior endplate (SE) - that would include: 1) entire small bowel (SB), 2) all diseased SB, 3) all diseased colon, and 4) EI findings. Total Z-axis coverage and the distance from the top of the scan to each SE was measured. The percentage of potential dose savings based on the percentage of unnecessary Z-axis coverage was calculated.

#### RESULTS

80 scans were included. All diseased colon and the entire SB was always inferior to the SE of T12. All diseased SB segments were inferior to L2. 9% had potentially significant EI findings: 1 pneumonia (T11), 1 focal biliary dilatation (T12), 2 chronic mesenteric venous thrombosis (L1 and L3), 2 sacroiliitis (S1) and 1 peripheral nerve sheath tumor (S5). However, only the pneumonia had management implications. Mean dose savings - with standard deviation (SD) and confidence intervals (CI) - achieved by starting the scan at T12, L1 and L2 would be 15.3% (SD: 4.1, 95%CI: 14.5 - 16.2), 21.5% (SD: 3.9; 95% CI: 20.6 to 22.4) and 28.4% (SD: 3.6; 95% CI: 27.6 - 29.2), respectively.

#### CONCLUSION

L2 was the cutoff to include all diseased small bowel segments, creating a potential for mean dose savings of 28% in this population. While T12 was the cutoff to include the entire SB (dose reduction of 15%), new proximal SB disease on follow up scans is very rare and was never found above L2 in our population. T12 was also the cutoff that included all EI findings except a

pneumonia, with no additional clinically significant EI findings above L2. There is an opportunity for 15-28% mean dose reduction on CTEs just by excluding unnecessary anatomic coverage.

# **CLINICAL RELEVANCE/APPLICATION**

In a population that particularly benefits from dose reduction (young Crohn's adults), the dose of follow-up CTEs can be significantly reduced by eliminating unnecessary anatomic coverage.

# SSA08-06 Evaluation of Bowel Fibrosis in Crohn's Disease Combining Diffusion Kurtosis and Intravoxel Incoherent Motion MR Imaging: Correlation with Surgical Histopathology

Sunday, Nov. 25 11:35AM - 11:45AM Room: N227B

Participants

Li Huang, Guangzhou, China (*Presenter*) Nothing to Disclose Xuehua Li II, Guangzhou, China (*Abstract Co-Author*) Nothing to Disclose Zhongwei Zhang, MD, PhD, Gainesville, FL (*Abstract Co-Author*) Nothing to Disclose Siyun Huang, MD, Guangzhou, China (*Abstract Co-Author*) Nothing to Disclose Mengchen Zhang, Guangzhou, China (*Abstract Co-Author*) Nothing to Disclose Xu Yan, Shanghai, China (*Abstract Co-Author*) Employee, Siemens AG Ziping Li, MD, PhD, Guangzhou, China (*Abstract Co-Author*) Nothing to Disclose

## For information about this presentation, contact:

guitar\_sun@163.com

## PURPOSE

To assess the utility combining diffusion kurtosis imaging (DKI) and intravoxel incoherent motion (IVIM) Imaging for grading the degrees of the intestinal fibrosis in Crohn's disease (CD), using surgical histopathology as the reference standard.

# METHOD AND MATERIALS

21 CD patients underwent both elective surgery and diffusion weighted imaging (b values of 0-2000 s/mm2). Apparent diffusion coefficients (ADCs) was calculated using b values of 100-1000 s/mm2. Diffusion coefficients (Dapp) and kurtosis (Kapp) on DKI maps (b values of 0, 600, 1000, 1500 and 2000 s/mm2) and pesudodiffusion coefficient (D\*) and perfusion fraction (f) on IVIM maps (b values of 0,10, 20, 40, 60, 80, 100, 150, 300, 600 and 1000 s/mm2) were measured region-by-region with surgical specimens. Resected bowel tissues were scored from 1 to 3 for histologic fibrosis.The parameters f, ADCs, and Kapp were combined to provide a single diagnostic grade compared with the fibrosis score.

### RESULTS

67 surgical specimens were evaluated and included none-mild (n=28), moderate (n=21) and severe (n=18) fibrosis. Significant differences were found between none-mild and both moderate and severe fibrotic segments for ADCs, Dapp, Kapp and f (P<0.05). They had similar correlation with histologic fibrosis scores (r: 0.644 for Kapp, -0.522 for Dapp, -0.635 for f, -0.601 for ADCs, all P<0.05). D\* did not correlate with histological fibrosis. High accuracy for differentiating moderate-severe fibrotic from none-mild fibrotic segments (AUC: 0.826 for Kapp, 0.791 for Dapp, 0.860 for f, 0.806 for ADCs) was showed by ROC analysis and the thresholds of 0.336 for f, 1.177 mm2/s for ADCs and 0.787 for Kapp were found with sensitivity of 92.61%, 84.6% and 89.7%, and specificity of 82.50%, 71.4%, 75%, respectively. The integrated score combined f, ADCs and Kapp thresholds was found a good correlation with histological fibrosis (r: 0.817, P<0.05). And AUC for differentiating moderate-severe fibrotic from none-mild fibrotic segments was 0.889 (P<0.001) with 94.40% sensitivity and 85.21% specificity.

#### CONCLUSION

DKI and IVIM can both detect varying degrees of bowel fibrosis in CD. Combination of DKI and IVIM parameters appears to improve diagnostic accuracy and the performance was better than single parameter of DKI or IVIM.

# **CLINICAL RELEVANCE/APPLICATION**

Combination of DKI and IVIM parameters appears to improve diagnostic accuracy compared with single parameter for detecting bowel fibrosis in CD.

# SSA08-07 Comparison of Three Magnetization Transfer Ratio Parameters for the Assessment of Bowel Wall Fibrosis in Crohn's Disease

Sunday, Nov. 25 11:45AM - 11:55AM Room: N227B

Participants

Jixin Meng, Guangzhou, China (*Presenter*) Nothing to Disclose Xuehua Li II, Guangzhou, China (*Abstract Co-Author*) Nothing to Disclose Siyun Huang, MD, Guangzhou, China (*Abstract Co-Author*) Nothing to Disclose Mengchen Zhang, Guangzhou, China (*Abstract Co-Author*) Nothing to Disclose Canhui Sun, MD, PhD, Guangzhou, China (*Abstract Co-Author*) Nothing to Disclose Ziping Li, MD, PhD, Guangzhou, China (*Abstract Co-Author*) Nothing to Disclose

## PURPOSE

Magnetization transfer ratio (MTR) and normalized MTR derived from MT-MRI has been reported as two promising parameters to quantitatively detect bowel fibrosis in Crohn's disease (CD). However, the use of these two parameters for grading bowel fibrosis has not consider the presence of slightly increasing MTR in normal bowel wall due to the existence of intestine smooth muscle. Hence, we establish a new MTR index which includes the element from normal bowel wall. The aim of this study was to compare the efficacy of the three MTR indices for the assessment of bowel wall fibrosis in CD and then select an optimal index for the clinical application, using surgical histopathology as the reference standard.

# METHOD AND MATERIALS

Abdominal MT imaging of 20 consecutive CD patients were analyzed before selective operation. The MTR. normalized MTR (MTR in

affected bowel wall+MTR in skeletal muscle), and new MTR ( [MTR in affected bowel wall-MTR in normal bowel wall]+ [MTR in skeletal muscle- MTR in normal bowel wall]) were calculated. Region-by-region correlations between MT imaging and surgical specimen were performed, and Masson staining was using to manifest the histologic degree of fibrosis. Spearman rank correlation, one-way ANOVA test, and receiver operating characteristic curve were used for statistical analysis.

# RESULTS

63 fibrotic intestinal segments from 20 CD patients were included in this study. Normalized MTR showed the strongest correlation with bowel fibrosis score (r=0.700,P <0.001), followed by new MTR (r=0.695,P<0.001) and MTR (r=0.590,P<0.001). The significant differences in MTR (F=23.13,P<0.001), normalized MTR (F=21.073,P<0.001) and new MTR (F=10.577,P<0.001) were found among mild, moderate and severe bowel fibrosis, respectively. MTR (AUC=0.959, P<0.001) and normalized MTR (AUC=0.933, P<0.001) had similar accuracy for differentiating moderate-severe from mild bowel fibrosis, followed by new MTR (AUC=0.883, P=0.002).

#### CONCLUSION

MTR, normalized MTR and new MTR are all able to detect and grade intestinal fibrosis in CD. Normalized MTR may be slightly superior to both MTR and new MTR and be an optimal index to quantitatively reflect the severity of bowel fibrosis with a simple calculation.

## **CLINICAL RELEVANCE/APPLICATION**

The normalized MT ratio might be the relatively preferable indicator for assessing intestinal fibrosis in CD patients, which contributes to guiding further clinical treatment.

# SSA08-08 Natural History of Inflammatory Strictures in Small Bowel (SB) Crohn's Disease in the Setting of Anti-TNF Therapy

Sunday, Nov. 25 11:55AM - 12:05PM Room: N227B

#### Participants

David J. Bartlett, MD, Rochester, MN (*Presenter*) Nothing to Disclose Shannon P. Sheedy, MD, Rochester, MN (*Abstract Co-Author*) Nothing to Disclose Jay P. Heiken, MD, Rochester, MN (*Abstract Co-Author*) Patent agreement, Guerbet SA; Patent agreement, Bayer AG Parakkal Deepak, MBBS, Rochester, MN (*Abstract Co-Author*) Advisory Board, Pfizer Inc; Advisory Board, Johnson & Johnson; Speakers Bureau, AbbVie Inc; Research Grant, Takeda Pharmaceutical Company Limited Joel G. Fletcher, MD, Rochester, MN (*Abstract Co-Author*) Grant, Siemens AG; Consultant, Medtronic plc; ; David Bruining, MD, Rochester, MN (*Abstract Co-Author*) Research Grant, Given Imaging Ltd Consultant, Bracco Group Jeff L. Fidler, MD, Rochester, MN (*Abstract Co-Author*) Nothing to Disclose

## For information about this presentation, contact:

fletcher.joel@mayo.edu

## PURPOSE

To examine the natural history of Crohn's small bowel (SB) strictures, examining both the need for subsequent surgery as well as their development from active inflammation, in Crohn's disease (CD) patients treated with anti-TNF therapy.

# METHOD AND MATERIALS

Adult CD patients with SB strictures (luminal narrowing + proximal SB dilation) underwent serial CTE/MRE during anti-TNF therapy. Every stricture was examined by a GI radiologist for the severity of inflammation with associated imaging findings, penetrating disease, and other complications. Numerous morphological measurements were obtained (wall thickness, length, proximal SB dilation), and various ratios of these measurements were calculated. Patients were categorized into groups based on time of stricture development (baseline CTE/MRE vs. subsequent) and surgical outcome (surgical resection vs. observation).

# RESULTS

58 CD patients (age 44±15; 27 females) with 74 strictures underwent CTE/MRE (47/11). 39 strictures (33 patients) underwent surgery (mean time of 2.7years) and 35 strictures (25 patients), who were observed for a mean of 5.3 years. Strictures going to surgery were associated with enteric fistulas [38% (15/39) vs. 11% (4/35)], perienteric edema [44%(17/39) vs. 23%(8/35)], and chronic mesenteric vein occlusion [12%(4/33) vs. 4%(1/25(4%)]. Stricture morphologic measurements and ratios were similar among the surgery and observation groups. There were 57 strictures (42 patients) at baseline and 17 strictures (16 patients) that developed on subsequent exams. Prior to stricture development, involved SB segments had less pronounced wall thickness (5.5 vs.7.8 mm), length of involvement (9.6 vs. 12.4 cm), and less inflammation compared to appearance at time of stricture development. New strictures had less pronounced wall thickness (7.8 vs. 9.2mm) and less penetrating disease [6% (1/17) vs. 35% (20/57)] than established strictures.

# CONCLUSION

Strictures undergoing subsequent resection were associated with penetrating disease, perienteric edema, and mesenteric vein occlusion. Development of strictures from inflamed segments and subsequent development of penetrating complications is consistent with current concepts of CD progression.

# **CLINICAL RELEVANCE/APPLICATION**

Strictures associated with penetrating disease, perienteric inflammation, and mesenteric vein occlusion are more likely to undergo surgery.

# SSA08-09 Gastrointestinal Keynote Speaker: Crohn Disease

Sunday, Nov. 25 12:05PM - 12:15PM Room: N227B

# Participants

Joel G. Fletcher, MD, Rochester, MN (Presenter) Grant, Siemens AG; Consultant, Medtronic plc; ;



#### SSA09

# **Gastrointestinal (Machine Learning)**

Sunday, Nov. 25 10:45AM - 12:15PM Room: N228



AMA PRA Category 1 Credits ™: 1.50 ARRT Category A+ Credit: 1.75

#### Participants

Dushyant V. Sahani, MD, Boston, MA (*Moderator*) Research support, General Electric Company Medical Advisory Board, Allena Pharmaceuticals, Inc

Andrew D. Smith, MD, PhD, Birmingham, AL (*Moderator*) President and Owner, Radiostics LLC; President and Owner, eRadioMetrics LLC; President and Owner, Liver Nodularity LLC; President and Owner, Color Enhanced Detection LLC; Patent holder Khaled M. Elsayes, MD, Ann Arbor, MI (*Moderator*) Nothing to Disclose David Fuentes, Houston, TX (*Moderator*) Nothing to Disclose

#### Sub-Events

## SSA09-01 Automated Liver Lesion Segmentation Using Deep Learning

Sunday, Nov. 25 10:45AM - 10:55AM Room: N228

Participants

Sean Sall, San Francisco, CA (Presenter) Researcher, Arterys Inc

Jesse Lieman-Sifry, San Francisco, CA (Abstract Co-Author) Researcher, Arterys Inc

Felix Lau, San Francisco, CA (Abstract Co-Author) Researcher, Arterys Inc

Claude B. Sirlin, MD, San Diego, CA (*Abstract Co-Author*) Research Grant, Gilead Sciences, Inc; Research Grant, General Electric Company; Research Grant, Siemens AG; Research Grant, Bayer AG; Research Grant, ACR Innovation; Research Grant, Koninklijke Philips NV; Research Grant, Celgene Corporation; Consultant, General Electric Company; Consultant, Bayer AG; Consultant, Boehringer Ingelheim GmbH; Consultant, AMRA AB; Consultant, Fulcrum Therapeutics; Consultant, IBM Corporation; Consultant, Exact Sciences Corporation; Advisory Board, AMRA AB; Advisory Board, Guerbet SA; Advisory Board, VirtualScopics, Inc; Speakers Bureau, General Electric Company; Author, Medscape, LLC; Author, Resoundant, Inc; Lab service agreement, Gilead Sciences, Inc; Lab service agreement, ICON plc; Lab service agreement, Intercept Pharmaceuticals, Inc; Lab service agreement, Shire plc; Lab service agreement, Takeda Pharmaceutical Company Limited; Lab service agreement, sanofi-aventis Group; Lab service agreement, Johnson & Johnson; Lab service agreement, NuSirt Biopharma, Inc; Contract, Epigenomics; Contract, Arterys Inc Albert Hsiao, MD,PhD, La Jolla, CA (*Abstract Co-Author*) Founder, Arterys, Inc; Consultant, Arterys, Inc; Consultant, Bayer AG; Research Grant, General Electric Company;

Daniel Golden, PhD, San Francisco, CA (Abstract Co-Author) Employee, Arterys Inc

## For information about this presentation, contact:

sean@arterys.com

## PURPOSE

To develop an automated deep learning-based method for liver lesion segmentation on MRI scans in order to enable more efficient quantification of lesion size and measurement of growth over time.

## METHOD AND MATERIALS

We utilize 1,312 annotated lesions from 607 unique abdominal MRI studies and 393 unique patients. DICOM images and lesion locations were collected as part of standard clinical care. Identified lesions were segmented manually on multiphasic contrastenhanced series by annotators trained in liver lesion segmentation. The median lesion diameter was 15.8 mm, while the median lesion volume was 1.469 mL. We designate an 80%-10%-10% split between the training, validation, and testing sets. We report all metrics on the test set. We use a fully-convolutional neural network that operates on 3D patches, centered on the lesion of interest. The network is a variant of the ENet segmentation architecture.

#### RESULTS

Our automated contouring method achieved a median volume error of 0.277 mL and a median LLD error of 2.01 mm. The median LLD error is significantly below the LI-RADS 'threshold growth' threshold (5.0mm).

#### CONCLUSION

Our automated lesion segmentation method yields a low median LLD error, demonstrating that our estimates may be used as part of a semi-automated clinical workflow in which the clinician may review and modify the segmentations. Additionally, we demonstrate that automated volumetric estimates are feasible from MRI and, with further validation, may provide a viable method of tracking tumor volume over time.

## **CLINICAL RELEVANCE/APPLICATION**

An automated liver lesion segmentation system may improve radiologist accuracy and efficiency in quantifying lesion size and measuring growth over time.

# SSA09-03 Convolutional Neural Networks Permit Estimation of Whole-Liver Hepatic Proton-Density Fat Fraction from Single or Dual-Echo Chemical-Shift-Encoded MRI

Sunday, Nov. 25 11:05AM - 11:15AM Room: N228

## Awards

## **Student Travel Stipend Award**

Participants

Kang Wang, MD, PhD, San Diego, CA (Presenter) Nothing to Disclose Tara A. Retson, MD, PhD, San Diego, CA (Abstract Co-Author) Nothing to Disclose Jonathan C. Hooker, BS, San Diego, CA (Abstract Co-Author) Nothing to Disclose Naeim Bahrami, PhD, MSc, San Diego, CA (Abstract Co-Author) Nothing to Disclose Kevin Blansit, MS, BS, La Jolla, CA (Abstract Co-Author) Nothing to Disclose Evan Masutani, La Jolla, CA (Abstract Co-Author) Nothing to Disclose Claude B. Sirlin, MD, San Diego, CA (Abstract Co-Author) Research Grant, Gilead Sciences, Inc; Research Grant, General Electric Company; Research Grant, Siemens AG; Research Grant, Bayer AG; Research Grant, ACR Innovation; Research Grant, Koninklijke Philips NV; Research Grant, Celgene Corporation; Consultant, General Electric Company; Consultant, Bayer AG; Consultant, Boehringer Ingelheim GmbH; Consultant, AMRA AB; Consultant, Fulcrum Therapeutics; Consultant, IBM Corporation; Consultant, Exact Sciences Corporation; Advisory Board, AMRA AB; Advisory Board, Guerbet SA; Advisory Board, VirtualScopics, Inc; Speakers Bureau, General Electric Company; Author, Medscape, LLC; Author, Resoundant, Inc; Lab service agreement, Gilead Sciences, Inc; Lab service agreement, ICON plc; Lab service agreement, Intercept Pharmaceuticals, Inc; Lab service agreement, Shire plc; Lab service agreement, Enanta; Lab service agreement, Virtualscopics, Inc; Lab service agreement, Alexion Pharmaceuticals, Inc; Lab service agreement, Takeda Pharmaceutical Company Limited; Lab service agreement, sanofi-aventis Group; Lab service agreement, Johnson & Johnson; Lab service agreement, NuSirt Biopharma, Inc; Contract, Epigenomics; Contract, Arterys Inc Albert Hsiao, MD, PhD, La Jolla, CA (Abstract Co-Author) Founder, Arterys, Inc; Consultant, Arterys, Inc; Consultant, Bayer AG; Research Grant, General Electric Company;

#### For information about this presentation, contact:

kaw016@ucsd.edu

#### PURPOSE

Confounder-corrected, chemical-shift-encoded (CSE) MRI with 6-echo acquisitions accurately quantifies hepatic proton-density fat fraction (PDFF). However, 6-echo acquisition increases scan time, might result in motion artifact, and limits image resolution of PDFF maps. This study assessed the feasibility of estimating PDFF from the first echo or first 2 echoes of 6-echo CSE MRI using a convolutional neural network (CNN).

## **METHOD AND MATERIALS**

In this IRB-approved and HIPPA-compliant study, we retrospectively identified 355 liver 3T MR exams that included a magnitudebased PDFF sequence comprising 6 gradient-echo images at sequential nominally out- and in-phase echo times. A non-linear fitting algorithm was used to reconstruct the PDFF maps pixel-by-pixel (6-echo PDFF). Using 310 image datasets selected at random, we trained a CNN to estimate 6-echo PDFF maps using only the first echo (1-echo PDFF) or the first two echoes (2-echo PDFF). We tested the CNN in the other 45 PDFF acquisitions. On each axial image containing liver, the liver was segmented and the average PDFF values across all liver pixels was calculated. Per-image mean hepatic 1-echo PDFF and 2-echo PDFF were compared with 6echo PDFF using Pearson correlation and Bland-Altman analyses.

### RESULTS

A total of 1065 images were analyzed. Per-image 6-echo PDFF values ranged from 0% to 43%, while R2\* ranges from 33 to 195 s-1. Correlations were high for 1-echo vs. 6-echo PDFF (R2=0.99, slope=0.96, intercept=-0.04) and for 2-echo vs. 6-echo PDFF (R2=0.99, slope=0.98, intercept = 0.29). Compared to the the 6-echo method, the 1-echo method showed minimal PDFF overestimation (bias of 0.56%, p<0.01) while the 2-echo method showed minimal PDFF underestimation (bias = -0.12%, p<0.001); 95% limits of agreement were [-1.3%, 2.4%] for 1-echo and [-1.15%, 0.91%] for 2-echo PDFF.

#### CONCLUSION

A CNN can accurately estimate hepatic PDFF from either the first or first two echoes of a magnitude-based CSE PDFF sequence in livers without substantial iron overload. Further work is required to determine whether these results are generalizable for other pulse sequences, scan parameters or concurrent pathology.

# **CLINICAL RELEVANCE/APPLICATION**

CNN-based whole-liver PDFF estimation from single or two-echo acquisitions might reduce scan time and enable broader clinical use of quantitative fat fraction measurement.

# SSA09-04 A New Multi-Model Machine Learning Framework to Improve Hepatic Fibrosis Grading Using Ultrasound Elastography Systems from Different Vendors

Sunday, Nov. 25 11:15AM - 11:25AM Room: N228

Participants

Isabelle Durot, MD, Stanford, CA (*Presenter*) Nothing to Disclose Alireza Akhbardeh, PhD, Stanford, CA (*Abstract Co-Author*) Nothing to Disclose Hersh Sagreiya, MD, Palo Alto, CA (*Abstract Co-Author*) Nothing to Disclose Andreas M. Loening, MD, PhD, Stanford, CA (*Abstract Co-Author*) Research Grant, Koninklijke Philips NV Consultant, ReCor Medical, Inc

Daniel L. Rubin, MD, MS, Stanford, CA (Abstract Co-Author) Nothing to Disclose

For information about this presentation, contact:

durot@stanford.edu

PURPOSE

To show that the diagnostic performance of point shear wave elastography (pSWE) and two-dimensional shear wave elastography (2DSWE) for grading liver fibrosis using shear wave velocity (SWV) combined with a new machine learning (ML) technique, can be as accurate as magnetic resonance elastography (MRE) and can be applied to ultrasound systems from different vendors.

## **METHOD AND MATERIALS**

This IRB-approved retrospective study included two patient groups with chronic liver disease: 1) 123 patients undergoing pSWE (Siemens S2000) and MRE; and 2) 60 patients undergoing 2DSWE (Philips Epiq7) and MRE. For Siemens data, accuracy of median SWV to differentiate clinically non-significant from significant fibrosis was calculated using the published cutoff value of 1.34 m/s, with MRE-based fibrosis grading used as the standard. Next, for both groups, in a technique not using any published US elastography cutoff values, median SWV and true labels from MRE-based grading were input to the Matlab perfcurve function to generate a receiver-operating characteristic (ROC) curve and calculate area-under-the-curve (AUC). Finally, in both groups, four ML algorithms - support vector machines (SVM), logistic regression, naïve Bayes, and quadratic discriminant analysis - using ten SWV measurements as inputs were trained with MRE as the gold standard to obtain MRE-equivalent binary fibrosis grading; scores from the ML algorithms were input into the Matlab perfcurve function to generate ROC AUC, and results were validated using two-fold cross validation.

#### RESULTS

The performance of median SWV to differentiate clinically non-significant and significant fibrosis (with MRE as the gold standard) was fair for pSWE with the published cutoff value for Siemens (accuracy 55.4%); moderate for Siemens (AUC: 0.73) and Philips (AUC: 0.71) without using a cutoff value; and excellent for an SVM ML algorithm in both groups (Siemens: AUC: 0.96; Philips: AUC: 0.97).

#### CONCLUSION

The results from Siemens and Philips data suggest that a multi-vendor ML-based algorithm can grade liver fibrosis using ultrasound elastography with excellent diagnostic performance, comparable to MRE. SVMs outperformed the current standard of assessment, median SWV.

#### **CLINICAL RELEVANCE/APPLICATION**

The new ML algorithm may be applied to systems from different vendors after validation, providing more comparable and accurate fibrosis grading.

#### **Honored Educators**

Presenters or authors on this event have been recognized as RSNA Honored Educators for participating in multiple qualifying educational activities. Honored Educators are invested in furthering the profession of radiology by delivering high-quality educational content in their field of study. Learn how you can become an honored educator by visiting the website at: https://www.rsna.org/Honored-Educator-Award/ Daniel L. Rubin, MD, MS - 2012 Honored EducatorDaniel L. Rubin, MD, MS - 2013 Honored Educator

# SSA09-05 A 3D Deep Neural Network for Liver Volumetry in Contrast-Enhanced MRI

Sunday, Nov. 25 11:25AM - 11:35AM Room: N228

Participants

Niklas Verloh, MD, Regensburg, Germany (*Presenter*) Nothing to Disclose Hinrich B. Winther, MD, Hannover, Germany (*Abstract Co-Author*) Nothing to Disclose Christian Hundt, DIPLPHYS,PhD, Mainz, Germany (*Abstract Co-Author*) Nothing to Disclose Kristina I. Ringe, MD, Hannover, Germany (*Abstract Co-Author*) Nothing to Disclose Frank K. Wacker, MD, Hannover, Germany (*Abstract Co-Author*) Nothing to Disclose Bertil Schmidt, Mainz, Germany (*Abstract Co-Author*) Nothing to Disclose Michael Haimerl, Regensburg, Germany (*Abstract Co-Author*) Nothing to Disclose Lukas Beyer, MD, Regensburg, Germany (*Abstract Co-Author*) Nothing to Disclose Christian R. Stroszczynski, MD, Regensburg, Germany (*Abstract Co-Author*) Nothing to Disclose Philipp Wiggermann, Regensburg, Germany (*Abstract Co-Author*) Nothing to Disclose

#### For information about this presentation, contact:

niklas.verloh@klinik.uni-regensburg.de

#### PURPOSE

To establish a fully automatic 3D deep learning liver segmentation-system for contrast-enhanced liver MRI.

# METHOD AND MATERIALS

Data-sets of Gd-EOB-DTPA-enhanced liver MR images of 100 patients have been selected. The ground truth segmentation of the liver parenchyma in the hepatobiliary phase was performed manually by a resident physician with five years of experience. The dataset was split into a training/validation set (n = 75) and a testing set (n = 25). The artificial neural network (ANN) used in this study is based on 3D-Unet (Cicek et al. 2016, arxiv: 1606.06650). The trained ANN was used to perform a fully automatic image segmentation of the testing set.

#### RESULTS

The ANN accomplishes a Dice index of  $95.1\pm2.3$  % (mean  $\pm$  std), an overlap of  $90.8\pm3.9$  % and a volume difference of  $3.8\pm6.8$ %.

#### CONCLUSION

This study demonstrates a 3D neural network, which is able to provide a fully automatic segmentation scheme for MRI Images. It is able to segment the liver parenchyma with high precision.

# **CLINICAL RELEVANCE/APPLICATION**

The 3D neural network provides an accurate automatic liver segmentation in MRI; hence it would serve as a useful tool for

radiologists for treatment planning, especially for patients undergoing liver surgery.

# SSA09-06 Machine Learning for Rapid Assessment of Outcomes of an Ultrasound Screening and Surveillance Program in Patients at Risk for Hepatocellular Carcinoma

Sunday, Nov. 25 11:35AM - 11:45AM Room: N228

Participants

Hailey Choi, MD, San Francisco, CA (*Presenter*) Nothing to Disclose Imon Banerjee, PhD, Stanford, CA (*Abstract Co-Author*) Nothing to Disclose Hersh Sagreiya, MD, Palo Alto, CA (*Abstract Co-Author*) Nothing to Disclose Aya Kamaya, MD, Stanford, CA (*Abstract Co-Author*) Nothing to Disclose Daniel L. Rubin, MD, MS, Stanford, CA (*Abstract Co-Author*) Nothing to Disclose Terry S. Desser, MD, Stanford, CA (*Abstract Co-Author*) Nothing to Disclose

## For information about this presentation, contact:

hailey.choi@ucsf.edu

## PURPOSE

To determine large-scale retrospective outcomes of surveillance ultrasound exams in high-risk populations according to the American College of Radiology (ACR) Ultrasound Liver Imaging Reporting and Data System (LI-RADS) classification.

## METHOD AND MATERIALS

13,860 ultrasound screening and surveillance exams from 4830 subjects performed between 2007-2017, pre-dating ultrasound LI-RADS recommendations, were assessed. Using more recent reports from May 2017-June 2018, which contained ultrasound LI-RADS specifications (1744 reports), a scalable ensemble machine learning approach was utilized to create a model that can infer ultrasound LI-RADS categories from neural word embedding analysis of the report body text. The model assigned ultrasound LI-RADS categories to the older, free-text reports (12,116 reports). Subjects who underwent serial surveillance exams were identified, and the labeled dataset was assessed for changes in LI-RADS categories over time.

#### RESULTS

2270 subjects had at least 2 exams. Subjects underwent an average of 5 exams, with mean screening interval of 13 months; mean follow-up duration was 43 months. When applied to the free-text reports, our model scored an average of 0.74 precision, 0.64 recall, and 0.66 F1-score, based on a validation set of 215 reports retrospectively categorized by 2 readers. According to the model's predictions, 1909 (84%) subjects remained in the same LI-RADS category over time: 1875 of these subjects remained in US-1 category, while 26 persisted as US-2; 2 patients had 2 exams each, which were both US-3. 205 (9%) progressed from US-1 to US-2. 95 (4%) alternated between US-1 and US-2. 61 (3%) subjects progressed to US-3 category was US-3.

# CONCLUSION

Machine learning enables large-scale retrospective longitudinal evaluation of relatively recent ACR Ultrasound LI-RADS guidelines. Based on our model's predictions, 3% of patients in our cohort developed suspicious lesions to warrant further work-up.

# **CLINICAL RELEVANCE/APPLICATION**

Our experience is the first large-scale assessment of ACR Ultrasound LI-RADS categories with longitudinal outcomes. Although retrospective, our long-term longitudinal data will be helpful in validating and improving current ACR Ultrasound LI-RADS recommendations, as well as in assessing clinical outcomes of HCC surveillance programs.

#### **Honored Educators**

Presenters or authors on this event have been recognized as RSNA Honored Educators for participating in multiple qualifying educational activities. Honored Educators are invested in furthering the profession of radiology by delivering high-quality educational content in their field of study. Learn how you can become an honored educator by visiting the website at: https://www.rsna.org/Honored-Educator-Award/ Daniel L. Rubin, MD, MS - 2012 Honored EducatorDaniel L. Rubin, MD, MS - 2013 Honored Educator

# SSA09-08 Deep Learning with Convolutional Neural Network for Histopathological Classification of Pancreatic Neuroendocrine Neoplasms: A Preliminary Study

Sunday, Nov. 25 11:55AM - 12:05PM Room: N228

Participants

Yanji Luo, Guangzhou, China (*Presenter*) Nothing to Disclose Huanhui Xiao, Guangzhou, China (*Abstract Co-Author*) Nothing to Disclose Shiting Feng, MD, Guangzhou, China (*Abstract Co-Author*) Nothing to Disclose Ziping Li, MD, PhD, Guangzhou, China (*Abstract Co-Author*) Nothing to Disclose Bingsheng Huang, Shenzhen, China (*Abstract Co-Author*) Nothing to Disclose

# For information about this presentation, contact:

luoyanji163@163.com

#### PURPOSE

To evaluate the efficacy of deep convolutional neural network (DCNN) for the pathological classification of pancreatic neuroendocrine neoplasms (P-NENs) on contrast agent-enhanced computed tomography.

#### **METHOD AND MATERIALS**

One hundred and three patients (poor-differentiated [G3], n=19; well-differentiated [G1+G2], n=84) preoperatively investigated by multi spiral computed tomography (MSCT) and subsequently with histopathological proven P-NENs were enrolled. The 103 datasets

were normalized and augmented by multiple preprocessing techniques (rotated, contrast enhanced and noise-added images), and were split into training (81.6%), validation (5.8%), and test set (12.6%) with 8-fold cross validation. The DCNN with the residual learning framework (ResNet), was used to classify the images as having manifestations of poor- or well-differentiated P-NENs. The DCNN was composed of fifty convolutional, one maxpooling, one global average pooling and two fully connected layers. Training and testing were performed eight times. Accuracy, sensitivity, and specificity for categorizing poor- and well-differentiated P-NENs with DCNN model and the area under the receiver operating characteristic curve for poor- versus well-differentiated P-NENs were calculated.

## RESULTS

The accuracy, sensitivity, and specificity of classifying poor- and well-differentiated P-NENs were 80.6%, 79.0%, and 81.0%, respectively. The area under the receiver operating characteristic curve for differentiating histopathological grading of P-NENs was 0.79.

# CONCLUSION

Deep learning with DCNN showed high diagnostic performance in differentiating histopathological classification of P-NENs at dynamic CT images.

## **CLINICAL RELEVANCE/APPLICATION**

The proposed framework could assist the radiologists in differentiating histopathological grading of P-NENs from contrast agentenhanced CT images and provide prognostic information with regard to patients' outcome.

# SSA09-09 Hepatic Steatosis Classification Using Deep Learning with Ultrasonic Radio-Frequency Data

#### Sunday, Nov. 25 12:05PM - 12:15PM Room: N228

Participants

Aiguo Han, PhD, Urbana, IL (Presenter) Nothing to Disclose

Rohit Loomba, MD, MSc, La Jolla, CA (*Abstract Co-Author*) Grant, Adheron; Grant, Arora; Grant, Bristol-Myers Squibb Company; Grant, DAIICHI SANKYO Group; Grant, Galectin; Grant, Galmed Pharmaceuticals Ltd; Grant, General Electric Company; Grant, GENFIT SA; Grant, Gilead Sciences, Inc; Grant, Immuron Ltd; Grant, Intercept Pharmaceuticals, Inc; Grant, Janseen Inc; Grant, Kinemed; Grant, Madrigal Pharmaceuticals, Inc; Grant, Merck & Co, Inc; Grant, NGM Biopharmaceuticals, Inc; Grant, Promega Corporation Inc; Grant, Siemens AG; Grant, Sirius; Grant, Tobira Therapeutics, Inc

Claude B. Sirlin, MD, San Diego, CA (*Abstract Co-Author*) Research Grant, Gilead Sciences, Inc; Research Grant, General Electric Company; Research Grant, Siemens AG; Research Grant, Bayer AG; Research Grant, ACR Innovation; Research Grant, Koninklijke Philips NV; Research Grant, Celgene Corporation; Consultant, General Electric Company; Consultant, Bayer AG; Consultant, Boehringer Ingelheim GmbH; Consultant, AMRA AB; Consultant, Fulcrum Therapeutics; Consultant, IBM Corporation; Consultant, Exact Sciences Corporation; Advisory Board, AMRA AB; Advisory Board, Guerbet SA; Advisory Board, VirtualScopics, Inc; Speakers Bureau, General Electric Company; Author, Medscape, LLC; Author, Resoundant, Inc; Lab service agreement, Gilead Sciences, Inc; Lab service agreement, ICON plc; Lab service agreement, Intercept Pharmaceuticals, Inc; Lab service agreement, Shire plc; Lab service agreement, Takeda Pharmaceutical Company Limited; Lab service agreement, sanofi-aventis Group; Lab service agreement, Johnson & Johnson; Lab service agreement, NuSirt Biopharma, Inc; Contract, Epigenomics; Contract, Arterys Inc John Erdman, Urbana, IL (*Abstract Co-Author*) Nothing to Disclose

Michael P. Andre, PhD, La Jolla, CA (Abstract Co-Author) Researcher, Siemens AG

William D. O'Brien JR, PhD, Urbana, IL (Abstract Co-Author) Research Grant, Siemens AG

For information about this presentation, contact:

han51@illinois.edu

## PURPOSE

To develop a deep learning framework that uses radio-frequency (RF) ultrasound data for settings-independent information extraction, and assess its accuracy for classifying hepatic steatosis in adults with known/suspected nonalcoholic fatty liver disease (NAFLD).

## **METHOD AND MATERIALS**

This was an IRB-approved, HIPPA-compliant prospective study of adults with known/suspected NAFLD. Ultrasound liver images (right lobe) and the underlying raw RF data were acquired intercostally by 2 sonographers using 4C1 and 6C1HD transducers from Siemens S3000. System settings were adjusted for each participant. Twenty liver images for each transducer were acquired for each participant. Gated RF lines from a fixed region of interest were preprocessed and used to train a deep convolutional neural network (CNN) for hepatic steatosis classification, with histology as the reference standard. No effort was made to correct for instrumentation settings. Five-fold cross validation was used for training and test. The model outputs from individual RF lines of all images were aggregated to yield a classification for a patient. As a comparison, B-mode images were graded by 8 radiologists based on their overall impression of hepatic steatosis.

## RESULTS

Forty patients (sex: 16M, 24F; age: 55.5±12.3 yo; BMI: 30.2±5.4 kg/m2) were included, of which 22 had no/mild steatosis (grade 0: N=2; grade 1: N=20) and 18 had moderate/severe steatosis (grade 2: N=12; grade 3: N=6). The CNN achieved 80±5% cross-validated accuracy (72±9% sensitivity, 86±4% specificity) for identifying patients with grade 2 or 3 steatosis. By comparison, radiologists' overall impression (grade 2 or 3) for the 6C1HD transducer achieved 68% accuracy (83% sensitivity, 57% specificity) and the overall impression for the 4C1 transducer achieved 72% accuracy (77% sensitivity, 68% specificity) for the same classification.

#### CONCLUSION

A CNN can automatically classify human patients as having or not having moderate/severe steatosis based on RF lines acquired during liver ultrasounds using variable instrumentation settings. Preliminary findings suggest the CNN may outperform specificity of expert radiologists.

Deep learning using the RF lines acquired during liver ultrasounds could assist radiologists in automatic hepatic steatosis classification.



#### SSA10

# Genitourinary (Multi-Parametric Prostate MRI)

Sunday, Nov. 25 10:45AM - 12:15PM Room: N229



AMA PRA Category 1 Credits ™: 1.50 ARRT Category A+ Credit: 1.75

## Participants

Temel Tirkes, MD, Indianapolis, IN (*Moderator*) Nothing to Disclose Nicola Schieda, MD, Ottawa, ON (*Moderator*) Nothing to Disclose B. Nicolas Bloch, MD, Vienna, Austria (*Moderator*) Nothing to Disclose

#### Sub-Events

# SSA10-01 DWI of the Prostate: Do We Still Need to Acquire High B Value > 1000 S/Mm<sup>2</sup>?

Sunday, Nov. 25 10:45AM - 10:55AM Room: N229

Participants

Salma Jendoubi, Paris, France (*Presenter*) Nothing to Disclose Sarah Montagne, Paris, France (*Abstract Co-Author*) Nothing to Disclose Mathilde Wagner, MD, PhD, Paris, France (*Abstract Co-Author*) Consultant, Canon Medical Systems Corporation Malek Ezziane, Paris, France (*Abstract Co-Author*) Nothing to Disclose Julien Mespoulet, Paris, France (*Abstract Co-Author*) Nothing to Disclose Candice Estellat, Paris, France (*Abstract Co-Author*) Nothing to Disclose Eva Comperat, Paris, France (*Abstract Co-Author*) Nothing to Disclose Olivier Cussenot, Paris, France (*Abstract Co-Author*) Nothing to Disclose Amandine Baptiste, Paris, France (*Abstract Co-Author*) Nothing to Disclose Raphaele M. Renard Penna, Paris, France (*Abstract Co-Author*) Nothing to Disclose

For information about this presentation, contact:

jendoubisalma@gmail.com

#### PURPOSE

To compare performances of computed high b-value Diffusion Weighted Images (cDWI) derived from low b-value DWI and acquired high b-value DWI (aDWI), in image quality overall and prostate cancer (PCa) detection rate

# METHOD AND MATERIALS

A total of 124 men with suspected PCa underwent diagnosis multi-parametric prostate MRI on a 3.0T MR system (SIGNATM Architect, GE healthcare) using a 32-channel phased-array torso coil. MRI protocol included 3DT2w, high resolution Fov Optimized and Constrained Undistorted Single-Shot (FOCUSTM) DWI with b-values of 100, 400, 800 and 2000 s/mm<sup>2</sup> and dynamic contrast enhanced images. cDWIs were derived from the three lower b-value DWI using a mono-exponential diffusion decay. MRI images were prospectively analyzed by one expert radiologist who provided the PI-RADS score and retrospectively by five observers (4 radiologists and 1 technician) who independently rated cDWIs (2000 and 2500 s/mm2) and aDWI (2000 s/mm2) on a 5-point scale regarding subjective image quality features (distortion, ghosting, suppression of benign prostate, anatomic clarity, rectal preparation). The 4 radiologists assessed tumor detection, conspicuity and contrast ratio with both sequences. SNR was measured in detected tumor and geometric distortion was analyzed on T2W and DWIs (diameter of the prostate from the left to the right and from anterior to posterior)

## RESULTS

cDWI demonstrated higher rating for image quality (p < 0.001). Prostate volume >50cc and rectal preparation significantly improved image quality for all DWIs with decrease distortion (p < 0.015). In patients with biopsy (n=63), no significant differences were found for tumor detection rate, however cDWI improved SNR and lesion conspicuity (p < 0.001)

#### CONCLUSION

Using cDWI can provide a substantial reduction in acquisition time while improving image quality. Overall quality of diffusion weighted imaging is dependent of an adequate rectal preparation

#### **CLINICAL RELEVANCE/APPLICATION**

This post-processing technique may in practice improve visual conspicuity of tumors while maintaining high quality images, without requiring any increase in exam time

# SSA10-02 Accurate Localization and Grading of Prostate Cancer with Diffusion Histology Imaging

Sunday, Nov. 25 10:55AM - 11:05AM Room: N229

Sheng-Kwei Song, PhD, Saint Louis, MO (*Abstract Co-Author*) Nothing to Disclose Qingsong Yang, Shanghai, China (*Abstract Co-Author*) Nothing to Disclose Joshua Lin, Saint Louis, MO (*Abstract Co-Author*) Nothing to Disclose Jianping Lu, MD, Shanghai, China (*Abstract Co-Author*) Nothing to Disclose Chunyu Song, St Louis, MO (*Abstract Co-Author*) Nothing to Disclose Joseph E. Ippolito, MD, PhD, Saint Louis, MO (*Abstract Co-Author*) Nothing to Disclose

## For information about this presentation, contact:

ze-zhong@wustl.edu

## PURPOSE

Prostate cancer (PCa) is the leading malignancy and second most common cause of death for American man. Multiparametric MRI has been employed to aid PCa diagnosis despites its significant false positive rate. The misdiagnoses are most likely caused by confounding prostatitis and/or benign prostatic hyperplasia (BPH). Non-invasive PCa grading methods has yet been developed for clinical applications. A novel diffusion histology imaging (DHI) has been developed and applied to accurately detect and grade prostate cancer.

#### **METHOD AND MATERIALS**

In vivo (262 patients) and ex vivo DHI (67 prostatectomy specimens from 22 patients) was performed. Logistic regression was used to distinguish among different tissue types. Support vector machine (SVM) algorithm was employed to construct predictive models for PCa grading.

# RESULTS

Prostate diffusion-weighted MRI signals were modeled as a linear combination of an anisotropic diffusion tensor and a spectrum of isotropic diffusion tensors. Inflammatory cells, cancer cells, stromal cells and luminal structures in prostate can be detected, distinguished, and quantified as DHI-derived anisotropic and isotropic diffusion signatures. A 3D-rendered prostate from DHI was obtained from a 58-year old patient (Fig 1A). Suspicious peripheral zone PCa (pink), Transition zone BPH (gold), and peripheral zone inflammation (blue-green) was identified. In prostatectomy specimens and living subjects, DHI exhibited great sensitivity and specificity in distinguishing PCa from benign peripheral zone prostate tissues (AUC 0.955 ex vivo; AUC 1 in vivo), benign central gland (AUC 0.955 in vivo), stromal BPH (AUC 0.965 ex vivo) and BPH (AUC 0.920 ex vivo). DHI predictive model presented high overall prediction accuracy on both Gleason scores (86.4% ex vivo and 88.6% in vivo), and NCCN risk categorization (87.9% in vivo), respectively (Fig. 1B). DHI showed much better prostatic tissue classification and tumor grades prediction than ADC did (Fig. 1B).

# CONCLUSION

DHI assesses various intra-gland structures of prostate, accurately localizing and grading PCa.

# **CLINICAL RELEVANCE/APPLICATION**

Results suggest that DHI may potentially localize and grade PCa. If validated, DHI could be used to detect and grade PCa either guiding or even replacing needle biopsy. It can be used in PCa treatment stratification and monitoring, and active surveillance.

# SSA10-03 Comparison of Apparent Diffusion Coefficient (ADC) Ratio to Conventional Calculated High B Value ADC for Discrimination of Gleason 3+3 and >= 3+4 Prostate Cancer in 224 Patients with 3T MRI with Whole Mount Histopathology Correlation

Sunday, Nov. 25 11:05AM - 11:15AM Room: N229

Participants

Amirhossein Mohammadian Bajgiran, MD, Los Angeles, CA (*Presenter*) Nothing to Disclose Sohrab Afshari Mirak, MD, Los Angeles, CA (*Abstract Co-Author*) Nothing to Disclose Sepideh Shakeri, Los Angeles, CA (*Abstract Co-Author*) Nothing to Disclose Ely R. Felker, MD, Los Angeles, CA (*Abstract Co-Author*) Nothing to Disclose Anthony Sisk, DO, Los Angeles, CA (*Abstract Co-Author*) Nothing to Disclose Robert E. Reiter, MD, Los Angeles, CA (*Abstract Co-Author*) Nothing to Disclose David S. Lu, MD, Los Angeles, CA (*Abstract Co-Author*) Nothing to Disclose Johnson; Research Grant, Johnson & Johnson; Consultant, Bayer AG; Research Grant, Bayer AG; Speaker, Bayer AG Steven S. Raman, MD, Santa Monica, CA (*Abstract Co-Author*) Nothing to Disclose

#### For information about this presentation, contact:

ambajgiran@ucla.edu

## PURPOSE

To determine the performance of 3T MRI apparent diffusion coefficient (ADC) ratio with coventional high B value ADC for detection of high Gleason Score (GS) prostate cancer (PCa) using whole-mount histopathology (WMHP) as a reference.

# METHOD AND MATERIALS

In this HIPAA-compliant, IRB-approved study, the cohort included 224 men with 249 unilateral PCa lesions with both 3T mpMRI and WMHP before and after robotic prostatectomy from NOV 2009 to NOV 2017. All studies were peformed on 3T scanners and ADC maps were derived from four b value combinations (0, 50, 500, 800) and calculated b= 1200. On an independent workstation, regions of interest (ROIs) were placed on individual WMHP verified lesions to calculate mean high b value ADC (ADC tumor\_mean), lowest mean high b value ADC subregion within each PCa lesion (ADC tumor\_min) and within uninvolved non tumor containing regions of the same zone to calculate background ADC (ADC benign) and the ADC ratio (ADC ratio (ADC tumor\_mean or ADC tumor\_min) divided by ADC benign)). The performance of individual ADC measurements in discriminating low GS (3+3) from high GS (>=3+4) PCa on WMHP was assessed using the area under the receiver operating characteristic (ROC) and area under curve (AUC) and using Spearman's rho coefficient.

The mean ADC was 1.573, 1.014 and  $0.921 \times 10(-3)$ mm2/sec for normal (ADC benign), mean PCa lesion (ADC tumor\_mean) and lowest ADC PCa subregion (ADC tumor\_min), respectively. The association between ADC measurements and GS showed a significant negative correlation (P=0.001) with Spearman's rho for ADC\_tumor\_mean (-0.268), ADC tumor\_min (-0.267) and ADC ratio (-0.366). ADC ratio had the best overall correlation with GS>= 3+4 compared with other ADC measurements. On ROC analysis, the AUCs were 0.703, 0.709 and 0.781 for ADC tumor\_mean, ADC tumor\_min and ADC ratio respectively for discriminating GS 3+3 from >= 3+4 PCa lesions on WMHP.

# CONCLUSION

Compared with mean and minimal tumor ADC measurements, ADC ratio had the best AUC for discrimination of GS >= 3+4 from GS=3+3 PCa on 3T MRI with WMHP correlation.

# CLINICAL RELEVANCE/APPLICATION

The ADC ratio as an intrapatient-normalized diagnostic tool may provide a more robust predictor for detection of GS >= 3+4 compared to GS == 3+3 lesions compared with tumor ADC alone.

# SSA10-04 3T MRI Restriction Spectrum Imaging versus ADC in Determining and Grading Prostate Cancer in Correlation to High Gleason score and Suspicious PI-RADS v2 Scores Using Whole Mount Histopathology

Sunday, Nov. 25 11:15AM - 11:25AM Room: N229

Participants

Sepideh Shakeri, Los Angeles, CA (*Presenter*) Nothing to Disclose Sohrab Afshari Mirak, MD, Los Angeles, CA (*Abstract Co-Author*) Nothing to Disclose Amirhossein Mohammadian Bajgiran, MD, Los Angeles, CA (*Abstract Co-Author*) Nothing to Disclose Ely R. Felker, MD, Los Angeles, CA (*Abstract Co-Author*) Nothing to Disclose Preeti Ahuja, PhD, Los Angeles, CA (*Abstract Co-Author*) Nothing to Disclose David S. Karow, MD, PhD, San Diego, CA (*Abstract Co-Author*) Nothing to Disclose Nathan White, PhD, San Diego, CA (*Abstract Co-Author*) Nothing to Disclose Kyunghyun Sung, PhD, Los Angeles, CA (*Abstract Co-Author*) Nothing to Disclose Steven S. Raman, MD, Santa Monica, CA (*Abstract Co-Author*) Nothing to Disclose

For information about this presentation, contact:

sshakeri@mednet.ucla.edu

# PURPOSE

To compare restriction spectrum imaging (RSI), a multidirectional high b value technique with -conventional apparent diffusion coefficient (ADC) for detection of aggressive prostate cancer (PCa) (Gleason score (GS) > 3+4) & high suspicion Prostate Imaging Reporting and Data System version2 score (PI-RADSv2) (4&5) using whole mount histopathology (WMHP) as the gold standard.

# METHOD AND MATERIALS

In this IRB approved, HIPAA compliant study, the study cohort included 77 men with both 3T- multiparametric MRI (mpMRI) & WMHP. RSI was processed from 32 direction high b value sequences & distortion was corrected using alternating phase-encode. A genitourinary (GU) pathologist marked all WMHP PCa lesions individually then a GU radiologist calculated the corresponding ROIs on RSI and ADC map by placing the ROI on PCa target & control adjacent tumor free peripheral zone (PZ) matched to WMHP. Paired Wilcoxon sign rank test was used to determine case and control correlations. Bootstrap methods was performed to determine differences between RSI & ADC in tumor grading. 2 sided p-value < 0.05 was considered significant by using SAS version 9.4.

# RESULTS

In 77 men with 235 ROIs (158 PCa & 77 control) the PCa GS & PIRADS v2 scores were: 75.2% primary GS 3 & 24.8% primary GS 4. PIRADS v2 scores were 3 (16.5 %) and 4 & 5 (83.5 %). Mean RSI z score and mean ADC values in PCa & normal controls were 3.4 (-1.7 -13.6) & -0.72(-1.8 - 4.8) respectively & 1022.6 (453-1961) & 1429.3(1042-2176) respectively. The mean PCa values correlated to the control values for both RSI z-score & ADC (p<0.0001). There was positive correlation between RSI z-score & GS in all groups (3+3, 3+4 & >=4+3), significant between (GS 3+3 & GS >=4+3 (p=0.0003, r=0.29)) and also in all PIRADSv2 scores, significant between 3&5(p=0.0001, r=0.45)). The ADC value in PCa was inversely significant in all GS (p<0.0001, r= -0.46). RSI outperformed ADC in determining the PCa compared to control PZ regardless of the Gleason or PIRADSv2 score (AUC 0.95 vs 0.82 (p<0.0001)).

# CONCLUSION

RSI is positively correlated with aggressive PCa and it outperformed ADC in determining PCa from non-cancerous regions. It may have a complementary role in predicting cancer scoring.

# **CLINICAL RELEVANCE/APPLICATION**

RSI can be used as a complementary imaging in predicting Prostate cancer aggressivness

# SSA10-05 Improving Workup of MRI-Detected PI-RADS 4&5 Lesions by Using Quantitative ADC Measurements to Obviate Unnecessary MRI Guided Biopsies

Sunday, Nov. 25 11:25AM - 11:35AM Room: N229

Participants

Stephan H. Polanec, MD, Vienna, Austria (*Presenter*) Nothing to Disclose
Hubert Bickel, MD, Vienna, Austria (*Abstract Co-Author*) Nothing to Disclose
Thomas H. Helbich, MD, Vienna, Austria (*Abstract Co-Author*) Research Grant, Medicor, Inc Research Grant, Siemens AG Research
Grant, C. R. Bard, Inc
Georg J. Wengert, MD, Vienna, Austria (*Abstract Co-Author*) Nothing to Disclose
Katja Pinker-Domenig, MD, Vienna, Austria (*Abstract Co-Author*) Nothing to Disclose

Mathias Lazar, MD, Vienna, Austria (*Abstract Co-Author*) Nothing to Disclose Martin Susani, Vienna, Austria (*Abstract Co-Author*) Nothing to Disclose Shahrokh F. Shariat, Vienna, Austria (*Abstract Co-Author*) Nothing to Disclose Paola Clauser, MD, Vienna, Austria (*Abstract Co-Author*) Nothing to Disclose Pascal A. Baltzer, MD, Vienna, Austria (*Abstract Co-Author*) Nothing to Disclose

#### For information about this presentation, contact:

stephan.polanec@meduniwien.ac.at

## PURPOSE

To assess whether quantitative ADC measurements derived from Diffusion-Weighted Imaging (DWI) may obviate unnecessary biopsies in MRI-detected PI-RADS 4 & 5 lesions.

# METHOD AND MATERIALS

This IRB-approved, retrospective study investigated 101 PI-RADS 4 & 5 prostate lesions (52 malignant, 49 benign) verified by in bore MRI-guided biopsy in 101 men (mean age, 62.8y). Two experienced uroradiologists independently and repeatedly measured minimum, mean, and maximum Apparent Diffusion Coefficient (ADC) from diffusion-weighted imaging (DWI) measurements (TR/TE 3300/60ms; GRAPPA 2, spectrally adiabatic inversion recovery [SPAIR] fat suppression; b-values of 0, 100, 400, and 800sec/mm2; six diffusion directions, bipolar diffusion sampling, acquisition time, 4:34min, 20 slices at 3.6 mm; matrix 160) by placing a two-dimensional region-of-interest around the lesions which were subsequently subjected to targeted MRI-guided biopsy. Readers were blinded to clinical information but localized the lesions based on the documented needle position during biopsy. Receiver operating characteristic (ROC) statistics were used to analyze diagnostic performance, and reproducibility statistics were calculated.

#### RESULTS

Minimum ADC values showed the best diagnostic performance (overall AUC R1: 0.801; R2: 0.796 peripheral zone AUC R1:0.814, R2: 0.805; transitional zone AUC R1:0.786, R2:0.779) and the tightest limits of interreader agreement (-8.6 to 9.9%). Thresholds to rule-in and rule-out any prostate cancer (PCa) were identified. Applying these 32,7% (16/49) of unnecessary biopsies could have been avoided.

## CONCLUSION

The application of quantitative ADC measurements in MRI-detected PI-RADS 4 & 5 lesions may be used to avoid unnecessary MRI-guided biopsies.

## **CLINICAL RELEVANCE/APPLICATION**

In time of increasing healthcare costs, and decreasing healthcare budgtes it is important to devolop strategies to avoid unnecessary prostate biopsies in patients with MRI suspicious PI-RADS 4 and 5 lesions.

# SSA10-06 Clinically Significant Prostate Cancers with an Early Enhancement Effect on Prostate Dynamic Contrast-Enhanced MRI: Association with Clinical and Histopathological Characteristics

Sunday, Nov. 25 11:35AM - 11:45AM Room: N229

Participants

Ayumu Kido, Kurashiki, Japan (*Presenter*) Nothing to Disclose Tsutomu Tamada, MD,PhD, Kurashiki, Japan (*Abstract Co-Author*) Nothing to Disclose Naoki Kanomata, Kurashiki, Japan (*Abstract Co-Author*) Nothing to Disclose Takeshi Fukunaga, Kurashiki, Japan (*Abstract Co-Author*) Nothing to Disclose Hidemitsu Sotozono, MD, Kurashiki, Japan (*Abstract Co-Author*) Nothing to Disclose Akihiko Kanki, MD, Kurashiki, Japan (*Abstract Co-Author*) Nothing to Disclose Akira Yamamoto, MD, Kurashiki, Japan (*Abstract Co-Author*) Nothing to Disclose Yoshiko Ueno, MD, PhD, Kobe, Japan (*Abstract Co-Author*) Nothing to Disclose

#### For information about this presentation, contact:

ttamada@med.kawasaki-m.ac.jp

## PURPOSE

To determine the clinical, histopathological, and imaging features of clinically significant prostate cancer (csPC) with an early enhancement effect (EEE) on dynamic contrast-enhanced MRI (DCE-MRI).

## METHOD AND MATERIALS

Eighty-eight prostate cancer patients with 127 csPCs (>0.5 cc with Gleason score (GS) =6 or >5 mm in diameter with GS>6) undergoing 3-T multiparametric MRI including T2-weighted imaging (T2WI), diffusion-weighted imaging (DWI), and DCE-MRI before radical prostatectomy were included. Two radiologists independently assigned each lesion a score of 1 to 5 for T2WI and DWI, negative (none (EEE score 0) or weak (score 1)) or positive (moderate (score 2) or strong (score 3)) EEE for DCE-MRI, and overall PI-RADS assessment category according to PI-RADS v2. Mean tumor apparent diffusion coefficients (ADCs) were also measured.

#### RESULTS

A total of 38 lesions (29.9%) had no EEE (non-EEE group), and 89 (70.1%) had the EEE (EEE group). The tumor detection rate of csPCs using DCE-MRI was 80.7% (71/88 patients) in the patient-based analysis. In the comparison between the groups, PSA, tumor size, Gleason score (GS) grade, and frequency of tumors with GS>3+4 were significantly higher in the EEE group than in the non-EEE group (P = 0.015 to 0.046). Tumor ADCs were significantly lower in the EEE group than in the non-EEE group (P = 0.001). In addition, the T2WI score, DWI score, and PI-RADS assessment category were significantly higher in the EEE group than in the non-EEE group (P < 0.001 to = 0.001). There were no significant differences in age, PSA density, prostate volume, tumor location (peripheral zone/transition zone), frequency of tumors with GS>3+3, D'Amico risk classification, and pathological T stage (pT2/pT3) (P = 0.059 to 0.963). The EEE score was significantly higher for tumors with GS >3+4 (n=43) than for tumors with GS = 3+3 (n=31) or tumors with GS = 3+4 (n=53) (P = 0.003 and 0.022, respectively). However, there was no significant difference in the EEE score between tumors with GS = 3+4 (P = 0.437).

#### CONCLUSION

These observations suggest that csPCs with the EEE tend to be larger, more aggressive, and have higher cellularity, and the EEE may be a new predictor for differentiating between low and intermediate-risk PCs vs. high-risk PCs. However, csPCs with the EEE were easy to detect on T2WI and DWI.

#### **CLINICAL RELEVANCE/APPLICATION**

The EEE on DCE-MRI may be a new predictor for risk stratification in PC.

# SSA10-07 Different Methods of AIF (Arterial Input Function) Acquirement for Quantitative Analysis of Dynamic Contrast-Enhanced MRI for Prostate Cancer Detection

Sunday, Nov. 25 11:45AM - 11:55AM Room: N229

Participants

Farid Ziayee, Dusseldorf, Germany (*Presenter*) Nothing to Disclose Lars Schimmoeller, MD, Dusseldorf, Germany (*Abstract Co-Author*) Nothing to Disclose Tim Ullrich, Duesseldorf, Germany (*Abstract Co-Author*) Nothing to Disclose Christian Arsov, MD, Duesseldorf, Germany (*Abstract Co-Author*) Nothing to Disclose Hans-Joerg Wittsack, PhD, Duesseldorf, Germany (*Abstract Co-Author*) Nothing to Disclose Gerald Antoch, MD, Duesseldorf, Germany (*Abstract Co-Author*) Nothing to Disclose

## For information about this presentation, contact:

farid.ziayee@med.uni-duesseldorf.de

## PURPOSE

Primary aim of this study was to analyze if quantitative DCE allows distinction of prostate cancer (PCa) and healthy tissue in peripheral and transition zone (PZ, TZ) with use of three different methods for the determination of the arterial input function (AIF). Reproducibility of quantitative perfusion analysis of DCE requires a standardized AIF acquisition.

#### **METHOD AND MATERIALS**

We analyzed multiparametric MRI of 50 consecutive patients retrospectively with three different methods of AIF determination, either by defining a region of interest in an artery (AIFm), by use of an automated algorithm (AIFa) or thirdly with a populationbased AIF (AIFp). Quantitative perfusion parameters Ktrans, ve and kep in PCa, PZ and TZ for the three different AIFs were examined.

#### RESULTS

In all three AIF methods, Ktrans and kep were significantly higher in PCa than in TZ (p<0.003), whereas ve was only significant in AIFp (p=0.002 in AIFp, p= 0.114 in AIFm, p=0.087 in ve). Results for PCa and PZ were significant in all methods and all quantitative parameters (p < 0.04). Values for Ktrans demonstrated narrowest confidence interval between the 3 methods. Overlapping of results was smallest in Ktrans. Values between AIFa and AIFm were similar whereas values for AIFp deviated considerably from AIFa and AIFm. However Spearman test showed good correlation of values for Ktrans between all methods (p>0.7). AIFa showed a success rate of 98% in finding the artery.

#### CONCLUSION

Prostate cancer can be distinguished in PZ and TZ with quantitative perfusion parameters of Toft's model independently from AIF acquisition method. AIFa is a recommendable, user-independent automatic method to determine quantitative perfusion parameters allowing an objective measurement and saving interactive time for the radiologist. Ktrans appears to be a more promising quantitative parameter for PCa detection than ve and/or kep.

#### **CLINICAL RELEVANCE/APPLICATION**

As an easily reproducible, simpe and fast method automated AIF can be implented as the standard method of AIF acquisition for quantitative DCE evaluation. Ktrans can facilitate PCa detection in both, TZ and PZ.

# SSA10-08 Accuracy of IMPROD Pre-Biopsy Biparametric MRI for the Detection of Prostate Cancer in Men before Their First Biopsy: Correlation with Whole Mount Prostatectomy Sections and Implication for Focal Therapy

Sunday, Nov. 25 11:55AM - 12:05PM Room: N229

Participants

Ivan Jambor, MD, PhD, Turku, Finland (*Presenter*) Speakers Bureau, Koninklijke Phillips NV Pekka Taimen, Turku, Finland (*Abstract Co-Author*) Nothing to Disclose Aida K. Kiviniemi, MD, Turku, Finland (*Abstract Co-Author*) Nothing to Disclose Janne Verho, MD, Jyvaskyla, Finland (*Abstract Co-Author*) Nothing to Disclose Otto Ettala, Turku, Finland (*Abstract Co-Author*) Nothing to Disclose Kari Syvanen, Turku, Finland (*Abstract Co-Author*) Nothing to Disclose Esa Kahkonen, Turku, Finland (*Abstract Co-Author*) Nothing to Disclose Jani Saunavaara, Turku, Finland (*Abstract Co-Author*) Nothing to Disclose Peter Bostrom, Turku, Finland (*Abstract Co-Author*) Nothing to Disclose Hannu J. Aronen, MD, PhD, Kuopio, Finland (*Abstract Co-Author*) Nothing to Disclose

#### PURPOSE

To evaluate accuracy of high quality IMPROD biparametric prostate MRI (bpMRI) for prostate cancer in men before their first biopsy who subsequently underwent prostatectomy.

#### **METHOD AND MATERIALS**

Forty-five men with elevated PSA (2.5 - 10.0 ng/ml) underwent bpMRI examination prior their first biopsy at 3 Tesla and subsequent prostatectomy within 4 months of bpMRI. bpMRI consisted of T2-weighted imaging (T2w) and three separate diffusion weighted imaging acquisitions with acquisition time under 15 minutes (IMPROD trial protocol, http://petiv.utu.fi/improd). All bpMRI were reported by one reader before biopsy and each suspicion lesion was manually delineated on axial T2w images. Following completion of the study, radiologist in conjunction with pathologist delineated cancer areas on axial T2w images using whole mount prostatectomy, following semi-automatic co-registration, as ground true. Accuracy, expressed as area under receiver operating characteristic curve (AUC), of prospectively reported manual cancer segmentations was evaluated on interpolated isotropic voxel size of 1mm3.

## RESULTS

In total 55 lesions with diameter >5 mm or any Gleason grade 4 were identified in 45 men and 4, 25, 10, 7, 9 lesions belong to ISUP Groups 1 (Gleason score <=6), 2 (Gleason 3+4=7), 3 (Gleason 4+3=7), 4 (Gleason score 8), 5 (Gleason scores 9 and 10), respectively. Prostate cancer was multifocal in 27 (60%, 27/34) men with additional 26 cancer lesions with Gleason score <=6 and diameter <=5 mm. Nine men (20%, 9/45) had more than one lesion with diameter > 5 mm or any Gleason grade 4. Seven lesions (13%, 7/55) were not identified on prebiopsy bpMRI, of those 4, 1, 1, and 1 belong to ISUP Groups 1, 2, 3 and 4, respectively. AUC (95% confidence interval on lesion level) on 1 mm3 isotropic voxel size for all lesions and ISUP Groups 1, 2, 3, 4, 5 were 0.70 (0.50 - 0.89) and 0.55 (0.50 - 0.70), 0.72 (0.51 - 0.88), 0.75 (0.65 - 0.84), 0.66 (0.54 - 0.73), 0.71 (0.50 - 0.89), respectively.

## CONCLUSION

High quality prebiopsy bpMRI enabled detention of 87% of lesions with diameter >5 mm or any Gleason grade 4. However, only limited accuracy on isotropic 1mm3 voxel was achieved potentially limiting focal therapy planning.

## **CLINICAL RELEVANCE/APPLICATION**

High quality prebiopsy biparametric MRI has high accuracy on lesion level for prostate cancer with diameter >5 mm or any Gleason grade 4. However, accuracy on isotropic 1 mm3 voxel level is limited.

# SSA10-09 Prostate Cancer Detection on 3T Multiparametric Magnetic Resonance Imaging: The Impact of Tumor Focality

Sunday, Nov. 25 12:05PM - 12:15PM Room: N229

Participants

David C. Johnson, Los Angeles, CA (*Abstract Co-Author*) Nothing to Disclose Sohrab Afshari Mirak, MD, Los Angeles, CA (*Presenter*) Nothing to Disclose Lorna Kwan, Los Angeles, CA (*Abstract Co-Author*) Nothing to Disclose Amirhossein Mohammadian Bajgiran, MD, Los Angeles, CA (*Abstract Co-Author*) Nothing to Disclose Sepideh Shakeri, Los Angeles, CA (*Abstract Co-Author*) Nothing to Disclose Leonard S. Marks, MD, Los Angeles, CA (*Abstract Co-Author*) Nothing to Disclose Leonard S. Marks, MD, Los Angeles, CA (*Abstract Co-Author*) Speaker, Avero Diagnostics; Investigator, Actavis, Inc; Investigator, Indevus Pharmaceuticals Inc; Investigator, Light Sciences Corporation; Investigator, Hologic, Inc; Investigator, Danaher Corporation; Investigator, GlaxoSmithKline plc; Investigator, Allergan, Inc; Investigator, GTx, Inc; Advisor, Indevus Pharmaceuticals Inc; Advisor, Hologic, Inc; Advisor, GlaxoSmithKline plc; Advisor, GTx, Inc Robert E. Reiter, MD, Los Angeles, CA (*Abstract Co-Author*) Nothing to Disclose Steven S. Raman, MD, Santa Monica, CA (*Abstract Co-Author*) Nothing to Disclose

# For information about this presentation, contact:

safsharimirak@mednet.ucla.edu

#### PURPOSE

To analyze the performance of 3 Tesla multiparametric magnetic resonance imaging (3T mpMRI) of the prostate for detection of prostate cancer (CaP) and identify predictors of tumor detection with particular attention to the effect of tumor focality.

#### **METHOD AND MATERIALS**

Retrospective review of prospectively maintained database of patients undergoing 3T mpMRI prior to radical prostatectomy for CaP at a single institution from 2010-2018. Radiographic lesions were assigned a suspicion score according to the Prostate Imaging-Reporting and Data System version 2 and compared to whole mount prostatectomy specimens to determine per-lesion detection by 3T mpMRI. Clinical and pathologic predictors of tumor detection were identified through multivariable analysis. Clinically significant CaP was defined as Gleason score of at least 7.

## RESULTS

588 patients underwent mpMRI prior to radical prostatectomy for CaP with a total of 1213 unique pathologic cancer foci (88% intermediate or high risk), of which, 541 were detected by mpMRI for an overall sensitivity of 45% (95% CI 42%, 47%). 685 unique radiographic regions of interest were identified, of which, 132 were not associated with a pathologic lesion (false positive rate: 19%, 95% CI 16%, 22%) and 12 corresponded to the same pathologic lesion as another region of interest, for a positive predictive value of 81%. Nearly 2/3 of patients had multifocal CaP. Multifocality was associated with decreased detection of the index tumor (80% vs 66% of index tumors identified in solitary vs multifocal CaP, p<0.001). The majority (74%) of missed solitary tumors and a significant percentage (31%) of missed multifocal tumors were clinically significant. On multivariate analysis, smaller tumor size, lower PSA density, not using an endorectal coil, lower gleason score, non-index lesion status, pathologic stage, and multifocality were associated with lower detection rates for both any cancer and clinically significant CaP.

## CONCLUSION

Pre-operative mpMRI miss a significant proportion of CaP foci. Clinicopathologic factors, including tumor focality, affect the accuracy of mpMRI, which must be understood when considering focal therapies.

## **CLINICAL RELEVANCE/APPLICATION**

An improved understanding of the factors affecting CaP detection on 3T mpMRI is necessary as this imaging modality is increasingly incorporated into screening, diagnosis, and treatment planning.



#### SSA11

# Genitourinary (Gynecologic Malignancy)

Sunday, Nov. 25 10:45AM - 12:15PM Room: N230B



AMA PRA Category 1 Credits ™: 1.50 ARRT Category A+ Credit: 1.75

#### Participants

Katherine E. Maturen, MD, Ann Arbor, MI (*Moderator*) Royalties, Reed Elsevier; Royalties, Wolters Kluwer nv; Consultant, Allena Pharmaceuticals, Inc;

Nicole M. Hindman, MD, New York, NY (Moderator) Nothing to Disclose

#### Sub-Events

# SSA11-01 Histogram Analysis of Apparent Diffusion Coefficients for Predicting Pelvic Lymph Node Metastasis in Patients with Uterine Cervical Cancer

Sunday, Nov. 25 10:45AM - 10:55AM Room: N230B

Participants

Jiyeong Lee, MD, Seoul, Korea, Republic Of (*Presenter*) Nothing to Disclose Chan Kyo Kim, MD, PhD, Seoul, Korea, Republic Of (*Abstract Co-Author*) Nothing to Disclose Jae-Hun Kim, PhD, Seoul, Korea, Republic Of (*Abstract Co-Author*) Nothing to Disclose Sung Yoon Park, Seoul, Korea, Republic Of (*Abstract Co-Author*) Nothing to Disclose Jung Jae Park, Daejeon, Korea, Republic Of (*Abstract Co-Author*) Nothing to Disclose

## For information about this presentation, contact:

Jiyeong25.lee@samsung.com

#### PURPOSE

Preoperative prediction of lymph node (LN) metastasis in uterine cervical cancer remains a challenge. We aimed to investigate the value of apparent diffusion coefficient (ADC) histogram analysis in predicting pelvic LN metastasis in patients with uterine cervical cancer undergoing surgery.

## **METHOD AND MATERIALS**

Our retrospective study included 162 cervical cancer patients (mean age, 47.7 years; range, 26-81 years) who received radical abdominal hysterectomy with pelvic LN dissection. All enrolled patients underwent routine pelvic 3T-MRI including diffusion-weighted imaging. The ADC histogram for the tumor was generated using in-house software and several histogram parameters were obtained. For predicting pelvic LN metastasis, clinical parameters (age, FIGO stage, tumor antigen [TA]-4, and histologic type) and imaging parameters (tumor size, maximal and short diameter of LN, MRI T-stage, and ADC histogram parameters) were evaluated using logistic regression analysis.

#### RESULTS

At histopathological findings, pelvic LN metastasis occurred in 50 patients (30.9%). In patients with LN metastasis, all ADC histogram parameters were significantly different from those without LN metastasis (all p < 0.05), except maximum, skewness, uniformity and entropy. At receiver operating characteristic (ROC) curve analysis, the area under the ROC curve of the 97.5th ADC percentile (ADC97.5) was 0.782, which was the greatest among other imaging and clinical variables. At univariate analysis, maximal and short diameters of LN, MRI T-stage, TA-4, tumor size and ADC97.5 were significantly associated with pelvic LN metastasis. However, the ADC97.5 was the only independent predictor of pelvic LN metastasis (odd ratio, 0.995; p < 0.001) (Table 1).

## CONCLUSION

As an imaging marker, the ADC97.5 from histogram analysis appears to be useful for the prediction of pelvic LN metastasis in patients with uterine cervical cancer undergoing surgery.

#### **CLINICAL RELEVANCE/APPLICATION**

Preoperative ADC histogram analysis may be a useful tool to predict pelvic lymph node metastasis in patients with uterine cervical cancer, which may be helpful for clinical decision-making.

# SSA11-03 Differentiation of Gynecological Sarcoma From Leiomyoma: Predictive Performance Comparison Between Radiologists and Radiomic Analysis

Sunday, Nov. 25 11:05AM - 11:15AM Room: N230B

Participants Huihui Xie, Beijing, China (*Presenter*) Nothing to Disclose Xiaodong Zhang, MD, PhD, Beijing, China (*Abstract Co-Author*) Nothing to Disclose Xiaoying Wang, MD, Beijing, China (*Abstract Co-Author*) Nothing to Disclose

## For information about this presentation, contact:

## xiehuiui1030@163.com

#### PURPOSE

To explore qualitative MRI features associated with gynecological sarcoma (GS). To build a predictive radiomic model, compare its performance with experienced radiologists.

## **METHOD AND MATERIALS**

78 patients (29 GSs, 49 leiomyomas) imaged with MRI prior to surgery were included in this retrospective study. One reader evaluated their clinical data and MRI reports and marked the index lesion. Two readers blindedly evaluated each index lesion for qualitative MRI features, included: (a) intratumor hemorrhage; (b) increased vascularity; (c) intratumor necrosis; (d) tumor borderline; (e) tumor shape; and (f) uterine cavity. Association were evaluated with Fisher's exact test. The MATLAB toolbox Radiomics was used for radiomic analysis. 4 non-texture features and 43 texture features were extracted. Univariate association between all features was explored using Spearman's rank correlation. Multivariate imbalanced-adjusted logistic regression model involved bootstrap resampling was used for prediction model construction. A predictive model was evaluated using a nest cross-validation scheme. The predictive performance was evaluated by area under the receiver-operating characteristic curve.

#### RESULTS

Patients with GSs were older than patients with leiomyomas, p < 0.0001. 3 MRI features (intratumor hemorrhage, indistinct borderline and uninterrupted uterine cavity) were associated with GS, p < 0.0001. The AUC of predictive performance based on MRI reports made by experienced radiologists was 0.793, sensitivity :58.6%, specificity: 100%, accuracy: 84.6%. 5 radiomic features differed significantly between GS and leiomyoma were: 'Energy-GLCM-S1Q2N1', 'GLN-GLSZM-S6Q1N4', 'LGZE-GLSZM-S6Q2N3', 'Solidity', and 'SRLGE-GLRLM-S6Q1N2'. p < 0.0001. The highest AUC was 0.91, sensitivity :82%, specificity: 84%, accuracy: 83%.

## CONCLUSION

Patients' age and three MRI features were significantly correlated with GS. Radiomic model triumphed over experience radiologists on the differentiation of GS and leiomyoma.

# **CLINICAL RELEVANCE/APPLICATION**

Although several features at MRI can raise suspicion of a uterine sarcoma, it is difficult to differentiate from benign leiomyoma and can result in inappropriate treatment and poor prognosis.

# SSA11-04 Amide Proton Transfer MR Imaging of Uterine: Comparison between Malignant and Benign Lesions

#### Sunday, Nov. 25 11:15AM - 11:25AM Room: N230B

Participants

Yonglan He, MD, Beijing, China (*Presenter*) Nothing to Disclose Chengyu Lin, Beijing, China (*Abstract Co-Author*) Nothing to Disclose Yafei Qi I, MD, Beijing, China (*Abstract Co-Author*) Nothing to Disclose Xiaoqi Wang, Beijing, China (*Abstract Co-Author*) Nothing to Disclose Hailong Zhou, Beijing, China (*Abstract Co-Author*) Nothing to Disclose Zhengyu Jin, Beijing, China (*Abstract Co-Author*) Nothing to Disclose Huadan Xue, MD, Beijing, China (*Abstract Co-Author*) Nothing to Disclose

# For information about this presentation, contact:

ylhe\_526@163.com

# PURPOSE

To evaluate the capability of amide proton transfer (APT) MR imaging for the differentiation of uterine malignant tumor from benign lesions.

# METHOD AND MATERIALS

Between October 2017 and April 2018, 58 patients with suspicious uterine lesions underwent APT MR imaging on a 3T MR scanner (Ingenia, Philips Healthcare, the Netherlands). The APT values (in percentage, representing the magnetization transfer ratio asymmetry in z-spectrum) were calculated based on images acquired from 3D TSE sequence with dual RF transmits interleave labelling. The APT values were measured on 12 lesions of pathologically confirmed endometrial adenocarcinoma, 29 lesions of leiomyomas and 21 lesions of adenomyosis with typical MR manifestation, 20 regions of normal uterine myometrium. Bonferroni's multiple comparisons test was used to compare the differences among different types of uterine lesions. Receiver operating characteristic (ROC) analyses were performed to computationally determine each feasible threshold value, sensitivity and specificity were assessed.

## RESULTS

The APT values of endometrial adenocarcinoma, leiomyomas, adenomyosis, and normal uterine myometrium were  $2.816\pm0.153$ ,  $1.504\pm0.156$ ,  $1.798\pm0.083$ ,  $1.917\pm0.121$ (mean $\pm$ standard error of mean), respectively. Statistical significant differences had been found between endometrial adenocarcinoma and leiomyomas (p<0.0001, 95%CI  $0.275\sim1.524$ ), endometrial adenocarcinoma and adenomyosis (p=0.0002, 95%CI  $0.400\sim1.637$ ), endometrial adenocarcinoma and normal uterine myometrium (p=0.0012, 95%CI  $0.275\sim1.524$ ). Area under the curve of ROC analysis for differentiating endometrial adenocarcinoma from leiomyomas and adenomyosis was 0.925 and 0.968, respectively. The feasible threshold values of each group were determined as 2.37 and 2.375, with sensitivity of 83.33% and 83.33%, specificity of 89.66% and 95.24%, respectively. There were no significant differences among the APT values of leiomyomas, adenomyosis and normal myometrium.

# CONCLUSION

Endometrial adenocarcinoma showed significant higher APT values than that of leiomyomas, adenomyosis, and normal uterine myometrium. There were no significant differences among APT values of uterine benign lesions and normal myometrium.

#### **CLINICAL RELEVANCE/APPLICATION**

This first attempt of APT imaging study in common uterine lesions showed the feasibility of APT weighted MRI in differential diagnosis between uterine malignant and benign lesions.

# SSA11-05 PET-MRI Value for Endometrial Adenocarcinoma Staging: Initial Experience

Sunday, Nov. 25 11:25AM - 11:35AM Room: N230B

Participants

Ingrid Faouzi, BMBS, Paris, France (*Presenter*) Nothing to Disclose Sophie Egels, Paris, France (*Abstract Co-Author*) Nothing to Disclose Dris Kharroubi, Paris, France (*Abstract Co-Author*) Nothing to Disclose Yasmina Badachi, MD, Paris, France (*Abstract Co-Author*) Nothing to Disclose Philippe Maksud, Paris, France (*Abstract Co-Author*) Nothing to Disclose Catherine Uzan, Paris, France (*Abstract Co-Author*) Nothing to Disclose Olivier Lucidarme, MD, Paris, France (*Abstract Co-Author*) Nothing to Disclose Olivier Lucidarme, MD, Paris, France (*Abstract Co-Author*) Speaker, Bracco Group; Speaker, F. Hoffmann-La Roche Ltd; Speaker, Boehringer Ingelheim GmbH; Mathilde Wagner, MD, PhD, Paris, France (*Abstract Co-Author*) Consultant, Canon Medical Systems Corporation

#### For information about this presentation, contact:

mathilde.wagner@aphp.fr

#### PURPOSE

To assess the performance of a positron emission tomography - magnetic resonance imaging (PET-MRI) examination for endometrial adenocarcinoma staging.

## **METHOD AND MATERIALS**

Consecutive patients with a PET-MRI examination for endometrial adenocarcinoma staging and surgery were included. One pair of radiology/nuclear medicine physicians and one resident with experience in MRI and PET analyzed the PET-MR images. The examination included images focused on the uterus (axial diffusion-weighted, axial/sagittal T2-weighted, axial/sagittal post gadolinium T1-weighted and PET images) and whole-body acquisitions (axial diffusion-weighted, axial pre and post-contrast T1-weighted and PET images). The percentage of accurate assessment of deep myometrial invasion, nodal invasion and metastases (per patient) of 5 sets of images (1=T2+diffusion images; 2=T2+diffusion+PET images; 3=T2+diffusion+post-contrast T1 images; 4=post-contrast+PET images; 5=everything) were assessed using surgical, pathological and follow-up data as gold standard.

#### RESULTS

Twenty-one patients (67±8 yo) with endometrial adenocarcinoma were included. Eleven patients had a myometrial invasion deeper than 50%, 5 patients had a nodal invasion, 4 patients had a proven metastasis. The mean delay between surgery and the PET-MRI examination was 12.5 days. T2 and diffusion-weighted images allowed the highest number of correct staging of the deep myometrial invasion (17/21, 81%, without any false negative case). Adding the post-contrast images or the PET images increased the number of false positive cases. The nodal invasion assessment varied between readers and sets of images, from 50 to 81% of accurate staging. The metastatic staging was correct in 86-95% of the cases.

#### CONCLUSION

Adding PET images to MR images does not seem to improve imaging diagnosis performance for deep myometrial invasion assessment of endometrial adenocarcinoma.

## **CLINICAL RELEVANCE/APPLICATION**

T2 and diffusion-weighted imaging seems to be the best combination for deep myometrial invasion assessment of endometrial adenocarcinoma. The adjunction of post-contrast or PET images does not improve the accuracy.

# SSA11-06 Prediction of Malignancy in Adnexal Incidentalomas Detected on Computed Tomography: A Machine-Learning Approach

Sunday, Nov. 25 11:35AM - 11:45AM Room: N230B

Participants

Celine D. Alt, MD, Duesseldorf, Germany (*Abstract Co-Author*) Nothing to Disclose Gerald Antoch, MD, Duesseldorf, Germany (*Presenter*) Nothing to Disclose Sophie Heueveldop, Dusseldorf, Germany (*Abstract Co-Author*) Nothing to Disclose Simon B. Eickhoff, Dusseldorf, Germany (*Abstract Co-Author*) Nothing to Disclose

# PURPOSE

To establish a machine-learning algorithm to predict indication for surgery and malignancy of adnexal incidentalomas detected on computed tomography (CT).

# **METHOD AND MATERIALS**

The institution database was searched from January 2013 to July 2016 for women who underwent abdominal CT scans for any indication. All patients with an adnexal lesion visible on CT and histopathological verification were included retrospectively. The institutional ethics committee approved this study and granted a waiver of informed consent. 286 adnexal lesions in 230 women were included. Based on different CT features an automated random-forest classifier was developed to predict clinical decisions and outcomes. Following development, model performance was tested on a different data set by cross-validation. Decision forests were trained and evaluated for their out-of-sample performance with respect to three different aims: (i) which tumors are radiologically conspicuous (from the group of all incidentalomas); (ii) which tumors are recommended for surgery (from the group selected in (i)); (iii) which were histologically confirmed to be malignant (from the group selected in (ii)).

The study cohort included 69% benign, 29% malignant, and 2% benign non-ovarian or secondary metastatic lesions. Balanced accuracies for the out-of-sample predictions were (i) 96%, (ii) 87%, and (iii) 79%. Relevant features were found to be maximum diameter, homogeneous content, septa, nodules, lipid content, solid portion, liquid content, fractal anisotropy, and box-volume.

## CONCLUSION

Standardized description of radiological features of adnexal lesions in combination with machine-learning algorithms allows a reliable prediction whether an individual patient will be recommended for surgery by the subsequent gynecological evaluation and even allows to predict the outcome of the histopathological result. The proposed prediction model gives radiologists a simple algorithm for decision making in adnexal incidentalomas with respect to the necessity of further evaluation.

#### **CLINICAL RELEVANCE/APPLICATION**

An accurate assessment of an adenexal incidentaloma with a correct identification of malignancy, while avoiding unnecessary intervention for benign lesions, is crucial regarding clinical management.

# SSA11-07 Comparison of Signal Intensity Ratio and ADC in Characterization of Solid Adnexal Masses on Diffusion-Weighted MR Imaging

Sunday, Nov. 25 11:45AM - 11:55AM Room: N230B

Participants

Amal A. Al-Rashid, MBBS, MD, Doha, Qatar (*Abstract Co-Author*) Nothing to Disclose Mohammed A. Sabawi, MBBCh, Doha, Qatar (*Abstract Co-Author*) Nothing to Disclose Sulafa A. Ibrahim, MBBS, Doha, Qatar (*Abstract Co-Author*) Nothing to Disclose Hanan Sherif, MD, Doha, Qatar (*Abstract Co-Author*) Nothing to Disclose Ahmed-Emad Mahfouz, MD, Doha, Qatar (*Abstract Co-Author*) Nothing to Disclose Laith E. Abandeh, MD, Doha, Qatar (*Presenter*) Nothing to Disclose

#### For information about this presentation, contact:

mahfouzae@yahoo.com

#### PURPOSE

To assess the value of signal intensity ratio versus apparent diffusion coefficient (ADC) in differentiation of benign and malignant adnexal masses on diffusion-weighted images.

#### **METHOD AND MATERIALS**

Thirty five patients with pathologically-proven solid adnexal lesions (21 malignant and 14 benign) have been examined by an identical protocol of magnetic resonance (MR) imaging, including DWI with b values of 0 and 800 s/mm2 and gadolinium-enhanced MR images. Signal intensity was measured on the b0 and b800 images by operator-determined region of interest at the same location of the lesion and the signal intensity ratio (SIR b800/b0) was calculated. ADC value was measured at the same location of the lesion. Measurements were done in the part of the lesion corresponding to enhancing part of the lesion on the gadolinium-enhanced images. Statistical analysis was done by generating receiver operator characteristic (ROC) curve and calculating the area under the curve (AUC).

#### RESULTS

The sensitivity, specificity, positive predictive value, negative predictive value and accuracy for diagnosis of malignancy using a cut-off value of  $1.385 \times 10^{-3}$  mm2/s for ADC were 78.95%, 37.50%, 75%, 42.86% and 66.67% respectively. Using SIR b800/b0 cut-off value of 0.33 (which is the corresponding ratio for the ADC cut-off value) the sensitivity, specificity, positive predictive value, negative predictive value and accuracy for diagnosis of malignancy were 100.00%, 75.00%, 90.48 %, 100.00% and 92.59% respectively. AUC for the ROC curves have been 0.6176 for the ADC and 0.8722 for the SIR (p < 0.02).

# CONCLUSION

The use of SIR b800/b0 has improved the accuracy of differentiation of malignant and benign adnexal masses in comparison to the use of ADC on diffusion-weighted MR images.

## **CLINICAL RELEVANCE/APPLICATION**

In addition to other imaging features, diffusion-weighted imaging is quite useful for differentiation of benign and malignant adnexal masses. The use of manually obtained signal intensity ratio b800/b0 instead of the machine-generated ADC values increases the accuracy of this method.

# SSA11-08 Adnexal Mass Staging CT with a Disease-Specific Structured Report Compared to Simple Structured Report

Sunday, Nov. 25 11:55AM - 12:05PM Room: N230B

Participants

Andrea Franconeri, MD, Pavia, Italy (*Presenter*) Nothing to Disclose Johannes Boos, MD, Dusseldorf, Germany (*Abstract Co-Author*) Nothing to Disclose Jieming Fang, Boston, MA (*Abstract Co-Author*) Nothing to Disclose Anuradha S. Shenoy-Bhangle, MD, Boston, MA (*Abstract Co-Author*) Nothing to Disclose Michele Perillo, MD, FRCPC, Montreal, QC (*Abstract Co-Author*) Nothing to Disclose Catherine J. Wei, MD, PhD, Boston, MA (*Abstract Co-Author*) Nothing to Disclose Leslie A. Garrett, Boston, MA (*Abstract Co-Author*) Nothing to Disclose Katharine Esselen, Boston, MA (*Abstract Co-Author*) Nothing to Disclose Liu W. Fong, Boston, MA (*Abstract Co-Author*) Nothing to Disclose Olga R. Brook, MD, Boston, MA (*Abstract Co-Author*) Nothing to Disclose

## For information about this presentation, contact:

#### afrancon88@gmail.com

## PURPOSE

To assess a disease-specific structured template for CT staging of ovarian malignancy compared to a simple structured report

## **METHOD AND MATERIALS**

This is a HIPAA-compliant, IRB-approved study with waiver of informed consent. An adnexal mass-specific structured reporting CT template was developed in collaboration between gyneco-oncologists and diagnostic radiologists. The study population included 24 consecutive women who had a staging CT prior to undergoing debulking surgery for a primary ovarian malignancy. Subjective evaluation by gyneco-oncologists and objective evaluation by radiologists for the presence of 19 key imaging features were performed to assess the clarity and usefulness for procedural planning of the disease-specific structured report (dsSR) and the simple structured report (sSR). Accuracy, sensitivity, and specificity were assessed using operating room notes and pathology reports as the reference standard.

## RESULTS

Fewer key features were missing from dsSR than sSR:  $0.2\pm0.8$  (range 0-2) vs.  $10.2\pm1.7$  (range 7-14), respectively (p<0.0001). Compared to sSR, gynecologists deemed dsSR more helpful ( $4.3\pm0.7$  vs.  $3.7\pm0.8$ , p<0.0001) and easier to understand ( $4.3\pm0.6$  vs.  $3.9\pm0.7$ , p=0.0057) (on a scale 0-5, 0 not helpful/very difficult to understand; 5 extremely helpful/very clear to understand). Gyneco-oncologists reported a higher rate of potential to modify their surgical approach based on dsSR (33-42%) compared to sSR (13-17%) (p=0.004).

## CONCLUSION

Disease-specific structured reports were more reliable than simple structured reports in describing key imaging features essential for procedural planning. dsSR was described as more helpful and easier to understand and more likely to lead to modification of the surgical approach by gyneco-oncologists compared to sSR.

# **CLINICAL RELEVANCE/APPLICATION**

Disease-specific structured report is more helpful than simple structured reports for planning gynecological surgery, is easier to understand, and misses fewer imaging descriptors essential for procedural planning.

# SSA11-09 MRI Evaluation of Vulvar Cancer in Fresh Radical Local Excision Specimens for Cancer Localization and Prediction of the Surgical Tumor-free Margins

## Sunday, Nov. 25 12:05PM - 12:15PM Room: N230B

Participants

Jan Heidkamp, Nijmegen, Netherlands (*Presenter*) Nothing to Disclose Petra Zusterzeel, Nijmegen, Netherlands (*Abstract Co-Author*) Nothing to Disclose Ilse Van Engen - Van Grunsven, Nijmegen, Netherlands (*Abstract Co-Author*) Nothing to Disclose Christiaan G. Overduin, MSc, Nijmegen, Netherlands (*Abstract Co-Author*) Nothing to Disclose Andor Veltien, Nijmegen, Netherlands (*Abstract Co-Author*) Nothing to Disclose Arie Maat, Nijmegen, Netherlands (*Abstract Co-Author*) Nothing to Disclose Maroeska M. Rovers, PhD, Nijmegen, Netherlands (*Abstract Co-Author*) Nothing to Disclose Jurgen J. Futterer, MD, PhD, Nijmegen, Netherlands (*Abstract Co-Author*) Research Grant, Siemens AG

#### PURPOSE

In the surgical treatement of vulvar squamous-cell carcinoma (VSCC) tumour free margins of >=8 mm are considered adequate. The purpose of this study was to investigate the feasibility of ex vivo MRI in localizing VSCC and assess the surgical tumor-free margins in fresh radical local excision (RLE) specimens to guide the surgeon during surgical resections.

# METHOD AND MATERIALS

Nine patients with biopsy-proven VSCC and scheduled for RLE were prospectively included. Intact fresh specimens were scanned using a 7T preclinical MR-scanner. Whole-mount H&E-stained slides were obtained every 3 mm and correlated with ex vivo MRI. A pathologist annotated VSCC and minimal tumor-free margins (3-, 9 o'clock, basal) on the digitalized histological slides. Both an observer with knowledge of histology (the non-blinded annotation) and a radiologist blinded to histology (the blinded annotation) performed annotation of the same features on ex vivo MRI. Linear correlation and agreement (Bland-Altman analysis) of the ex vivo MRI measurements with histology were assessed. Diagnostic performance for VSCC localization and identification of margins <8 mm were expressed in PPV and NPV.

#### RESULTS

In 153 matched ex vivo MRI slices, the observer correctly identified 79/91 margins as <8 mm (PPV, 87%) and 110/124 margins as >=8 mm (NPV, 89%). The radiologist correctly annotated absence of VSCC in 73/81 (NPV, 90%) and presence in 65/72 (PPV, 90%) slices. Sixty-four of 90 margins were correctly identified as <8 mm (PPV, 71%) and 83/102 margins as >=8 mm (NPV, 81%). Both non-blinded annotations were linearly correlated and demonstrated good agreement with histology. Compared to the non-blinded annotation, the linear correlation between ex vivo MRI and histology was less strong and the Bland-Altman 95% limits of agreement were wider in the blinded annotation.

## CONCLUSION

Accurate localization of VSCC and measurements of the surgical tumour free margins in fresh WLE specimens using ex vivo MRI is technically feasible. The high NPV and PPV for localization of VSCC and identification of margins <8 mm demonstrate clinical applicability of the technique.

# **CLINICAL RELEVANCE/APPLICATION**

Perioperative information on the margin status of RLE specimens provided by ex vivo MRI could assist the surgeon in achieving adequate surgical margins and prevent subsequent secondary treatment.



#### SSA12

Science Session with Keynote: Informatics (Artificial Intelligence in Radiology: Cutting Edge Deep-Learning)

Sunday, Nov. 25 10:45AM - 12:15PM Room: S406B



AMA PRA Category 1 Credits ™: 1.50 ARRT Category A+ Credit: 1.75

FDA Discussions may include off-label uses.

#### Participants

George L. Shih, MD, MS, New York, NY (*Moderator*) Consultant, Image Safely, Inc; Stockholder, Image Safely, Inc; Consultant, MD.ai, Inc; Stockholder, MD.ai, Inc;

An Tang, MD, Montreal, QC (*Moderator*) Research Consultant, Imagia Cybernetics Inc; Speaker, Siemens AG; Speaker, Eli Lilly and Company

Synho Do, PhD, Boston, MA (Moderator) Nothing to Disclose

#### Sub-Events

# SSA12-01 Informatics Keynote Speaker: Cutting Edge AI in Radiology

Sunday, Nov. 25 10:45AM - 10:55AM Room: S406B

Participants

An Tang, MD, Montreal, QC (*Presenter*) Research Consultant, Imagia Cybernetics Inc; Speaker, Siemens AG; Speaker, Eli Lilly and Company

#### For information about this presentation, contact:

an.tang@umontreal.ca

#### **Honored Educators**

Presenters or authors on this event have been recognized as RSNA Honored Educators for participating in multiple qualifying educational activities. Honored Educators are invested in furthering the profession of radiology by delivering high-quality educational content in their field of study. Learn how you can become an honored educator by visiting the website at: https://www.rsna.org/Honored-Educator-Award/ An Tang, MD - 2018 Honored Educator

## SSA12-02 Predicting Thyroid Nodule Malignancy with Efficient Convolutional Neural Networks

Sunday, Nov. 25 10:55AM - 11:05AM Room: S406B

Awards

**Trainee Research Prize - Medical Student** 

Participants

Ian Pan, MA, Providence, RI (*Presenter*) Nothing to Disclose Matthew T. Stib, MD, Providence, RI (*Abstract Co-Author*) Nothing to Disclose William D. Middleton, MD, Saint Louis, MO (*Abstract Co-Author*) Nothing to Disclose Derek Merck, PhD, Providence, RI (*Abstract Co-Author*) Nothing to Disclose Michael D. Beland, MD, Providence, RI (*Abstract Co-Author*) Research Grant, Canon Medical Systems Corporation; Consultant, General Electric Company

#### For information about this presentation, contact:

ian\_pan@brown.edu

## PURPOSE

Various sonographic features of thyroid nodules have been described, and classification systems (i.e., TI-RADS) have been developed to aid radiologists in determining which suspicious nodules require fine needle aspiration (FNA). This study aims to improve our predictive ability by training convolutional neural networks (CNNs) to discriminate between pathology-confirmed benign and malignant thyroid nodules using ultrasound images.

## **METHOD AND MATERIALS**

Our dataset consisted of 151 malignant and 500 benign thyroid nodules from 571 patients, where each nodule contributed 1 longitudinal and 1 transverse ultrasound view. Preprocessing included cropping the nodule of interest and resizing the image to 224 x 224 pixels. The data were divided into 10 training/validation/test folds following a stratified 80%/10%/10% split with no patient overlap. CNNs based on the MobileNet architecture were initialized with pretrained ImageNet weights. A fully-connected layer was first trained for 10 epochs, and the entire network was fine-tuned for 20 epochs. Data were sampled to achieve 50%/50% class balance for each epoch. Data augmentation probability, dropout probability, and learning rate were tuned via randomized search with 60 iterations. Weights with the highest area under the ROC curve (AUC) during validation were used for testing. A malignancy score is determined for each nodule by averaging the predictions for each view across 3 models.

#### RESULTS

Our model achieved a mean AUC of 0.863 (95% CI: 0.827, 0.898). The median malignancy scores for benign and malignant nodules were 0.162 and 0.618, respectively. With 5 strata, (0-0.2, 0.2-0.4, 0.4-0.6, 0.6-0.8, 0.8-1.0), 5.94%, 18.2%, 29.5%, 65.7%, and 81.4% of nodules in each respective stratum were malignant, compared to an overall malignancy rate of 23.2%. At a threshold of 0.10, the model reduces the number of negative FNAs by 36% while maintaining 95% sensitivity.

## CONCLUSION

CNNs fine-tuned on limited data can accurately predict the malignancy potential of sonographically suspicious thyroid nodules. Larger datasets would likely further improve the performance of our classifier. External validation studies are necessary to verify the generalizability of this approach.

# CLINICAL RELEVANCE/APPLICATION

CNN malignancy scores calculated from thyroid ultrasound images can be combined with a radiologist's interpretation for improved stratification of nodules to reduce the number of unnecessary FNAs.

# SSA12-03 A Deep-learning Method for Fast Detection of Rib Fracture in CT Images: Effect of Computer-Aided Diagnosis to Radiologists

Sunday, Nov. 25 11:05AM - 11:15AM Room: S406B

## Participants

Xiaodong LI, Linyi, China (Presenter) Nothing to Disclose

# For information about this presentation, contact:

## lxd2018rsna@163.com

## CONCLUSION

2 reading modes of CAD(CR, SR) can significantly increase the sensitivities of RFD of radiologists. The reading time is shorter by CR than by SR.CR mode can be used as the first option to detect rib fracture by radiologists.

#### Background

To assess the effect of rib fracture computer-aided diagnosis(CAD) on diagnosis of radiologist.

## **Evaluation**

85 trauma CTs(50 males) with follow-up review CTs were included in the retrospective study.All trauma CTs were subjected to CAD system to generate rib fracture bounding box. The procedure of the CAD system contains ribs segmentation, centerline extraction, rib fracture detection(RFD) based on deep learning algorithm(Faster RCNN), false positive removal and rib fracture localization. 2 senior(NO.1,2) and 2 junior radiologists(NO.3,4) independently evaluated the data using 3 reading modes(without CAD, CR, SR). The fracture line or bone callus growth is the criterion for determining the rib fracture. The follow-up review CTs verified the diagnosis of rib fracture and established the reference standard[1]. All fractures detected by the 4 readers were compared to the reference standard.  $\chi^2$  test and rank-sum test were performed to test whether there was significant difference between sensitivities and reading times of 3 reading modes. Abbreviations: without CAD: Radiologists independently evaluated the data as a first reader and then apply the CAD system as a second reader(SR) to review the results.

#### Discussion

The reference standard identified 281 rib fractures in 85 patients. The sensitivity of RFD with SR 97.2%(273/281;P<0.001) and CR 96.4%(271/281;P<0.001) were significantly higher than that of without CAD 89.7%(252/281). There was no significant sensitivity difference between CR and SR(P>0.3). Senior and junior radiologists used CAD as CR or SR and there was no significant sensitivity difference between 2 modes(P=0.067,P=0.067). Reading time was significantly shorter for CR(98s) compared to that of without CAD(148s;P<0.001) and SR(169s;P<0.001). Reading time of the 3 modes was less in the senior group than in the junior group with significant differences(P<0.001).

# SSA12-04 Highly Sensitive Identification and Delineation of Hemorrhagic Stroke Lesion Using Cascaded Deep Learning Model

Sunday, Nov. 25 11:15AM - 11:25AM Room: S406B

## Participants

Junghwan Cho, PhD, Lowell, MA (*Presenter*) Nothing to Disclose Manohar Karki, Lowell, MA (*Abstract Co-Author*) Nothing to Disclose Eunmi Lee, Lowell, MA (*Abstract Co-Author*) Nothing to Disclose Jong Kun Kim, MD,PhD, Daegu, Korea, Republic Of (*Abstract Co-Author*) Nothing to Disclose Ki-Su Park, MD,PhD, Daegu, Korea, Republic Of (*Abstract Co-Author*) Nothing to Disclose Dong Eun Lee, MD, Daegu, Korea, Republic Of (*Abstract Co-Author*) Nothing to Disclose Jae Young Choe, MD, Daegu, Korea, Republic Of (*Abstract Co-Author*) Nothing to Disclose Sinyoul Park, MD,PhD, Daegu, Korea, Republic Of (*Abstract Co-Author*) Nothing to Disclose Suk Hee Lee, MD, Daegu, Korea, Republic Of (*Abstract Co-Author*) Nothing to Disclose Suk Hee Lee, MD, Daegu, Korea, Republic Of (*Abstract Co-Author*) Nothing to Disclose Jeoungwoo Sim, MD, Daegu, Korea, Republic Of (*Abstract Co-Author*) Nothing to Disclose Jeoungwoo Son, MD, Gimcheon, Korea, Republic Of (*Abstract Co-Author*) Nothing to Disclose Jeong Ho Lee, MD,PhD, Daegu, Korea, Republic Of (*Abstract Co-Author*) Nothing to Disclose

#### CONCLUSION

A cascaded deep learning model was developed to identify and delineate hemorrhagic stroke lesion, obtaining overall sensitivity accuracy for classification with 97.91% and segmentation with 83.43%, respectively.

Highly accurate and timely detection of intracranial hemorrhagic stroke is a critical clinical issue for diagnosis decision and treatment in emergency room. Deep learning is a promising approach to solve delayed and missed diagnosis of stroke accident. Accordingly, we developed a cascaded deep learning model trained by a series of different CT window settings as a preprocessing step. It consists of two convolution neural networks (CNNs) for identifying bleeding or not and fully convolutional networks (FCNs) for delineating their lesions.

## **Evaluation**

For this study, we acquired 135,000 CT images from 5,650 patients including 3,000 non-bleeding and 2,650 bleeding. In case of bleeding, five subtypes of intracranial hemorrhage (intraventricular, intraparenchymal, subarachnoid, epidural, and subdural hemorrhage) were well labeled by experts. At first, a cascaded deep learning model was trained to identity whether there is bleeding or not and 5-fold cross validation was conducted. We evaluated sensitivity accuracy by the cascaded model, enabling to review the negative case by the second CNN trained with more narrow window width (40/40 [level/width]) in case that CT image is recognized as negative by the first CNN trained with default brain window setting (50/100). It results in increasing around 1% sensitivity (97.91%) while preserving specificity (98.76%). To delineate lesion of bleeding, the FCNs was trained with 33,300 CT slices using DGX-1 system. We achieved overall precision accuracy ranging from 70% to 90% and recall accuracy ranging from 62% to 88% at different Dice coefficient threshold as true positive decision.

#### Discussion

In diagnostic accuracy, there is a tradeoff between sensitivity and specificity. But while preserving specificity, the cascaded deep learning model can increase sensitivity in diagnosis of hemorrhagic stroke. It has the capability to help doctors inform any suspected cases.

# SSA12-05 Differentiation of Hepatic Masses in Abdominal CT Images Using Texture-Aware Convolutional Neural Networks with Texture Image Patches

Sunday, Nov. 25 11:25AM - 11:35AM Room: S406B

Participants

Hansang Lee, Daejeon, Korea, Republic Of (*Presenter*) Nothing to Disclose Helen Hong, PhD, Seoul, Korea, Republic Of (*Abstract Co-Author*) Nothing to Disclose Heejin Bae, Seoul, Korea, Republic Of (*Abstract Co-Author*) Nothing to Disclose Sungwon Kim, MD, Seoul, Korea, Republic Of (*Abstract Co-Author*) Nothing to Disclose Joonseok Lim, MD, Seoul, Korea, Republic Of (*Abstract Co-Author*) Nothing to Disclose Junmo Kim, Seoul, Korea, Republic Of (*Abstract Co-Author*) Nothing to Disclose

#### For information about this presentation, contact:

hlhong@swu.ac.kr

hlhong@swu.ac.kr

# CONCLUSION

Our method can be applied to the differentiation of various subtypes of hepatic masses including cyst and hemangioma, and early diagnosis of hepatic cancer.

#### Background

Differentiation of hepatic masses into benign and malignant classes in CT images is an important task for early diagnosis and surgical decision of hepatic cancer. In the cases of small masses, acquisition of intensity and texture features is difficult, making the differentiation challenging. Thus, we propose a deep convolutional neural network (CNN) classification of hepatic masses using texture image patch (TIP) generation to enhance the classification efficiency in small masses.

#### **Evaluation**

Our method was evaluated on a dataset consisting of 349 abdominal CT scans including 576 benign and 210 malignant masses. Each mass was manually segmented by the radiologist. In TIP generation, the patches representing only the internal texture of the masses were created by filling the square patch with the segmented mass regions repeatedly. These TIPs have the effect of reflecting the texture information to CNN regardless of the original size of masses. Using these TIPs, the transfer learning (TL) was performed on the ImageNet pre-trained AlexNet to classify the patches into benign or malignant classes. To improve the classification efficiency, we re-trained the random forest (RF) classifier on the deep features extracted from the last feature layer of TL-AlexNet. In experiments, our framework was trained on 390 images(b282, m108), validated on 160 images(b113, m47), and tested on 236 images(b181, m55). The proposed method achieved the accuracy of 87.7% where the comparative methods achieved the accuracies of 83.5%, 80.1%, and 85.2%, without TIP, TL, and RF, respectively.

#### Discussion

Our TIPs improve the learning efficiency of CNN by augmenting the texture information of small masses and allowing the CNN to focus on the texture information. The TL also plays an important role in learning important imaging features for differentiating the hepatic masses. Instead of obtaining the CNN-classified outputs, re-training the RF classifier on the deep features improves the specificity of the proposed method by enhancing the malignancy detection.

# SSA12-06 GrayNet: Medical Generic Image Representations for Deep Learning System of Urinary Stone Detection

Sunday, Nov. 25 11:35AM - 11:45AM Room: S406B

Participants Hyunkwang Lee, Boston, MA (*Presenter*) Nothing to Disclose Anushri Parakh, MBBS, MD, Boston, MA (*Abstract Co-Author*) Nothing to Disclose Sehyo Yune, MD, MPH, Boston, MA (*Abstract Co-Author*) Nothing to Disclose Jeong Hyun Lee, MD, Seoul, Korea, Republic Of (*Abstract Co-Author*) Nothing to Disclose Myeongchan Kim, MD, Boston, MA (*Abstract Co-Author*) Nothing to Disclose Isabelle Hartnett, Boston, MA (*Abstract Co-Author*) Nothing to Disclose Dushyant V. Sahani, MD, Boston, MA (*Abstract Co-Author*) Research support, General Electric Company Medical Advisory Board, Allena Pharmaceuticals, Inc Synho Do, PhD, Boston, MA (*Abstract Co-Author*) Nothing to Disclose

# For information about this presentation, contact:

hyunkwanglee@seas.harvard.edu

#### PURPOSE

The performance of deep-learning based image analysis model developed from an institution is not guaranteed to be achieved when deployed in another if the institutions use different imaging systems with varying scan acquisition and reconstruction settings. We established a pretrained model enriched with medical generic image representations extracted from GrayNet, a dataset for human anatomy recognition with 23 labels and evaluated benefits of GrayNet pretrained models for detecting urinary stones.

#### METHOD AND MATERIALS

GrayNet contains 322 IV contrast-enhanced whole body CT scans with 120,182 axial slices obtained by CT scanners from two manufacturers (171 from GE and 151 from Siemens). The corresponding virtual unenhanced CT images were generated with a customized transform function. All slices were annotated as 23 radiologist-established anatomical labels. We randomly selected 40 cases for validation and the remainings were used for training of a deep convolutional neural network, Inception-v3. The best model, selected based on validation loss, was reserved as a pretrained model for urinary stone detection. Patients who underwent unenhanced CT scans from two manufacturers (GE and Siemens) for suspected urolithiasis were identified and categorized according to presence (n=128) or absence (n=161) of urinary stones, and then split into train, validation, and test subsets. Inception-v3 models initialized with random, ImageNet, and GrayNet pretrained weights were trained on training datasets from a single manufacturer and both. The optimal models were evaluated on test datasets. Area under the ROC curve (AUC) was measured for evaluation metric.

## RESULTS

The performance of the GrayNet model trained on the GE dataset showed higher AUC (0.893) than the ImageNet model (0.833) when tested on the Siemens dataset. Similar trend was observed when models trained on the Siemens dataset and tested on the GE dataset (0.917 from GrayNet, 0.854 from ImageNet). When trained on the combined dataset, the GrayNet model obtained higher AUC than those of ImageNet and random models.

#### CONCLUSION

The GrayNet pretrained weights enabled better generalization performance, compared to the models initialized with ImageNet pretrained and random weights.

# **CLINICAL RELEVANCE/APPLICATION**

The GrayNet pretrained weights enriched with generic medical image representations can be used as a baseline for deep learning systems for a successful deployment in varying settings.

## **Honored Educators**

Presenters or authors on this event have been recognized as RSNA Honored Educators for participating in multiple qualifying educational activities. Honored Educators are invested in furthering the profession of radiology by delivering high-quality educational content in their field of study. Learn how you can become an honored educator by visiting the website at: https://www.rsna.org/Honored-Educator-Award/ Dushyant V. Sahani, MD - 2012 Honored EducatorDushyant V. Sahani, MD - 2015 Honored EducatorDushyant V. Sahani, MD - 2016 Honored EducatorDushyant V. Sahani, MD - 2017 Honored Educator

# SSA12-07 Deep Learning of Clinically Relevant Chest X-Ray Findings on the Combination of Three Large Datasets

Sunday, Nov. 25 11:45AM - 11:55AM Room: S406B

#### Participants

Satyananda Kashyap, PhD, San Jose, CA (*Abstract Co-Author*) Nothing to Disclose Mehdi Moradi, PhD, San Jose, CA (*Abstract Co-Author*) Employee, IBM Corporation Alexandros Karargyris, San Jose, CA (*Abstract Co-Author*) Employee, IBM Corporation Joy T. Wu, MBChB,MPH, San Jose, CA (*Abstract Co-Author*) Employee, IBM Corporation Murray A. Reicher, MD, Rancho Santa Fe, CA (*Abstract Co-Author*) Chief Medical Officer, Merge Healthcare Incorporated Board Member, Merge Healthcare Incorporated Co-CEO, Health Companion, Inc Former Chairman, DR Systems, Inc Tanveer Syeda-Mahmood, PhD, San Jose, CA (*Presenter*) Employee, IBM Corporation

#### For information about this presentation, contact:

mmoradi@us.ibm.com

mmoradi@us.ibm.com

#### CONCLUSION

We have presented a network trained on the largest collection of chest X-ray images with visually observable radiological findings that performs at similar accuracy to networks developed with 14 NIH labels.

## Background

Despite deep learning networks now becoming the de facto method of image classification, their relevance to radiologists is limited by the semantics of label used for training such networks. Recent use of image labels such as pneumonia that are not diagnosable from imaging alone have raised concerns on the utility of the networks. We develop a new classifier for chest X-ray images by training it on labels that derived from visually observable radiological findings. We form a new combined data set of 335,688 images from three sources, namely, PLCO Chest X-rays [Gohagan 2000]), Cancer Screening Trial, National Institute of Health (ChestXray14 dataset [Wang 2017]) and the Indiana University dataset [Demner-Fushman 2016]. The 49 original labels assigned to these combined datasets were mapped to the corresponding visually observable findings and regrouped into 20 finding labels. For example, 'consolidation, pneumonia, infiltration, and infiltrate' were all mapped to 'alveolar opacity'. The consolidated dataset with the new labels was used to train a DenseNet121 network architecture [Huang 2016], with 512x512 size input images preprocessed with histogram equalization and intensity normalization.

## **Evaluation**

The dataset was divided to 80% training and 20% validation. The areas under the ROC curve for the 20 findings are: Alveolar opacity: 0.81, Hernia: 0.84, Pneumothorax: 0.86, Atelectasis: 0.87, Aortic atherosclerosis and/or Carotid artery calcification: 0.90, Bone Lesion: 0.77, Enlarged cardiac silhouette: 0.86, Enlarged Hilum: 0.75, Findings consistent with granulomatous disease: 0.76, Hyperaeration: 0.79, Increased reticular markings: 0.71, Mass and/or Nodule: 0.64, Pleural effusion: 0.92, Pleural mass and/or thickening: 0.71, Spinal degenerative changes: 0.89, Tortuous Aorta: 0.89, Vascular redistribution: 0.85, Catheter and/or Tube: 0.89, Missing plus NA: 0.82, Other: 0.69.

#### Discussion

Label validation particulalry in 'no finding' labels from NIH dataset is under way.

# SSA12-08 Automatic Classification and Reporting of Multiple Common Thorax Diseases Using Chest Radiographs

Sunday, Nov. 25 11:55AM - 12:05PM Room: S406B

Participants

Xiaosong Wang, PhD, Bethesda, MD (*Presenter*) Nothing to Disclose Yifan Peng, Bethesda, MD (*Abstract Co-Author*) Nothing to Disclose Le Lu, Bethesda, MD (*Abstract Co-Author*) Employee, NVIDIA Corporation Zhiyong Lu, Bethesda, MD (*Abstract Co-Author*) Nothing to Disclose Ronald M. Summers, MD, PhD, Bethesda, MD (*Abstract Co-Author*) Royalties, iCAD, Inc; Royalties, Koninklijke Philips NV; Royalties, ScanMed, LLC; Research support, Ping An Insurance Company of China, Ltd; Researcher, Carestream Health, Inc; Research support, NVIDIA Corporation; ; ; ;

For information about this presentation, contact:

xiaosong.wang@live.com

#### PURPOSE

Chest radiographs are one of the most common radiological exams in daily clinical routines. Reporting thorax diseases using chest radiographs is often an entry-level task for radiologist trainees, but it remains a challenging job for learning-oriented machine intelligence. It's due to the shortage of large-scale well-annotated medical image datasets and lack of techniques that can mimic the high-level reasoning of human radiologists. In this work, we show that clinical free-text radiological reports can be utilized as a priori knowledge for tackling these two difficult problems.

## METHOD AND MATERIALS

We used a hospital-scale chest radiograph dataset, which consists of 112,120 frontal-view radiographs of 30,805 patients. 14 disease labels observed in images were mined using natural language processing techniques, i.e., atelectasis, cardiomegaly, effusion, infiltrate, mass, nodule, pneumonia, pneumothorax, consolidation, edema, emphysema, fibrosis, pleural thickening, and hernia. We propose a novel text-image embedding neural network (illustrated in the attached figure) for extracting the distinctive image and text representations. Multilevel attention models are integrated into an end-to-end trainable architecture for highlighting the meaningful text words and image regions. We first apply this combined convolutional and recurrent neural network (CNN-RNN) to classify the image by using both image features and text embeddings from associated reports. Furthermore, we transform the framework into a radiograph reporting system by taking only images as input and turning RNN into a generative model.

## RESULTS

The proposed framework achieves high accuracy  $(0.96\pm0.03 \text{ in AUCs})$  in disease classification using both images and reports on an unseen and hand-labeled dataset (OpenI, 3,643 images). When using only the images as input, the system can also produce significantly improved results  $(0.80\pm0.07 \text{ in AUCs})$  compared to the state-of-the-art  $(0.74\pm0.08)$  with a p-value=0.0005. The figure shows sample classification results with generated reports (attended words in red).

## CONCLUSION

We illustrate a framework for fully-automated classification and reporting of common thorax diseases in chest radiographs and demonstrate its superior performance compared to the state-of-the-art.

# **CLINICAL RELEVANCE/APPLICATION**

The proposed multi-purpose CADx system can be applied for automatic classification and reporting of common thoracic diseases as a second opinion.

# SSA12-09 Deep-learning for Distal Radius Fracture Detection in X-Ray Imaging

Sunday, Nov. 25 12:05PM - 12:15PM Room: S406B

Participants

Maximilian Russe, MD, Freiburg, Germany (*Presenter*) Nothing to Disclose Mathias F. Langer, MD, PhD, Freiburg, Germany (*Abstract Co-Author*) Nothing to Disclose Elmar C. Kotter, MD, MSc, Freiburg, Germany (*Abstract Co-Author*) Editorial Advisory Board, Thieme Medical Publishers, Inc

#### PURPOSE

Development of a robust algorithm for fracture detection of the distal radius in x-ray imaging for the use in an emergency department.

#### **METHOD AND MATERIALS**

Anterior-posterior x-ray images of the wrist from 2013-2017 were classified for fracture or absence of fracture by a consensus reading from a junior and a senior radiologist. Secondary reading was performed by a certified Msk radiologist. 1900 cases were exported for the deep learning study. Data leakage was excluded using only first-time images of the patients. Images where separated into 1351 images for training and 449 for validation. Besides the validation sample for the CNN learning, a separate analysis of the final model was performed using a separate test sample, containing 50 images with and without fractures. For the development of the deep learning model an established Convulsive neuronal network (CNN), GoogLeNet was used. Due network specifications an images distortion using a smashing transformation to 256\*256 pixels was needed. The data was augmented using vertical flipping and up to +/- 10° rotation. No manual segmentation or image correction was made. Deep learning was performed by using Torch on Nvidia DIGITS with a standard workplace graphic unit (Nvidia Quadro P4000). Following parameters where used: 1000 training and validation epochs. AdaGrad was used as solver type and the initial learning rate was 0.01.

## RESULTS

The training of the CNN took 4.34h of processing time. Final image processing of all 100 test images took 17 seconds. An overall accuracy of the validation sample was achieved with a final value of 94.2%, the overall accuracy of the separate test sample is 90%. The per-class accuracy in the validation sample was for fractures 87.5% and for no fractures 96.4% in the test sample 86% and 94%. These values are comparable and so overfitting of the CNN can be excluded.

## CONCLUSION

The created algorithm shows a good detection rate for distal radius fractures. An exclusion of fracture was performed with even a higher accuracy. These results are promising for preliminary classification of x-rays within a clinical setting.

## **CLINICAL RELEVANCE/APPLICATION**

X-ray reading is still a relevant task for fracture detection, fracture detection algorithms can be used to reduce the work load and already could be used for prioritizing work load. Instant preliminary fracture detection can be achieved with this deep learning model and easily implemented in clinical routine.



#### SSA13

# Molecular Imaging (Brain)

Sunday, Nov. 25 10:45AM - 12:15PM Room: S504CD



AMA PRA Category 1 Credits ™: 1.50 ARRT Category A+ Credit: 1.75

**FDA** Discussions may include off-label uses.

#### Participants

Peter Herscovitch, MD, Bethesda, MD (*Moderator*) Nothing to Disclose Dima A. Hammoud, MD, Bethesda, MD (*Moderator*) Nothing to Disclose

# Sub-Events

# SSA13-01 Template-Enhanced ZTE Attenuation Correction for Brain FDG-PET/MR Imaging

Sunday, Nov. 25 10:45AM - 10:55AM Room: S504CD

Participants

Tetsuro Sekine, MD, PhD, Tokyo, Japan (*Presenter*) Nothing to Disclose Bradley J. Kemp, PhD, London, ON (*Abstract Co-Author*) Nothing to Disclose Sandeep Kaushik, MS, Bangalore, India (*Abstract Co-Author*) Employee, General Electric Company Florian Wiesinger, Garching bei Munchen, Germany (*Abstract Co-Author*) Employee, General Electric Company Gaspar Delso, PhD, Cambridge, United Kingdom (*Abstract Co-Author*) Employee, General Electric Company;

## For information about this presentation, contact:

tetsuro.sekine@gmail.com

## PURPOSE

The impact of MR-based attenuation correction on PET quantitation accuracy is an ongoing cause of concern for advanced brain research with PET/MR. The purpose of this study was to evaluate a new, template-enhanced zero-echo-time (ZTE) attenuation correction method for PET/MR scanners.

## **METHOD AND MATERIALS**

30 subjects underwent a clinically-indicated 18F-FDG-PET/CT, followed by PET/MR on a GE SIGNA PET/MR. For each patient, a 42second ZTE sequence was used to generate two attenuation maps: one with the standard ZTE segmentation-based method; and another with a modification of the method, wherein pre-registered anatomical templates and CT data were used to enhance the segmentation. CT data, was used as gold standard. Reconstructed PET images were qualified visually and quantified in 68 volumesof-interest using a standardized brain atlas.

## RESULTS

Attenuation maps were successfully generated in all cases, without manual intervention or parameter tuning. The PET bias with template-enhanced ZTE attenuation correction was measured to be  $-0.9\% \pm 0.9\%$ , compared with  $-1.4\% \pm 1.1\%$  with regular ZTE attenuation correction. In terms of absolute bias, the new method yielded  $1.1\% \pm 0.7\%$ , compared with  $1.6\% \pm 0.9\%$  with regular ZTE. Statistically significant bias reduction was obtained in the frontal region (from -2.0% to -1.0%), temporal (from -1.2% to -0.2%), parietal (from -1.9% to -1.1%), occipital (from -2.0% to -1.1%) and insula (from -1.4% to -1.1%).

#### CONCLUSION

These results indicate that the co-registration of pre-recorded anatomical templates to ZTE data is feasible in clinical practice and can be effectively used to improve the performance of segmentation-based attenuation correction.

## **CLINICAL RELEVANCE/APPLICATION**

The accuracy of PET/MR attenuation correction based on zero echo time (ZTE) data can be increased with the incorporation of registered anatomical priors in the segmentation procedure.

# SSA13-02 Advantages of 325ps Time-of-Flight Digital Photon Counting PET/CT in Low Dose Brain PET Performance for Assessing Breast Cancer Metastasis

Sunday, Nov. 25 10:55AM - 11:05AM Room: S504CD

Participants

Jun Zhang, PhD, Columbus, OH (*Presenter*) Nothing to Disclose Katherine Binzel, PhD, Columbus, OH (*Abstract Co-Author*) Nothing to Disclose Michelle I. Knopp, Columbus, OH (*Abstract Co-Author*) Nothing to Disclose Maryam Lustberg, Columbus, OH (*Abstract Co-Author*) Nothing to Disclose Michael V. Knopp, MD, PhD, Columbus, OH (*Abstract Co-Author*) Nothing to Disclose

### PURPOSE

To evaluate the feasibility and advantages of 325ps time-of-flight (TOF) digital photon counting (DPC) PET in low dose FDG brain PET performance in patients with breast cancer.

## METHOD AND MATERIALS

18 low dose (3.1±0.2mCi) brain FDG-PET scans from 0-75min of 9 patients (BMI=33±6) were performed on a 325ps DPC PET/CT (Philips Vereos) to assess neurometabolic changes for breast cancer before and after chemotherapy (interval=77±10 days). 5 groups of PET reconstructions (10, 5, 2, 1 and 0.5 min) centered at 65min p.i. were performed in 3D-OSEM (2mm-isotropic) w (TOF) and w/o (nTOF). All data were co-registered and normalized based on a 43 normal FDG brain database with 90 neuro-anatomic regions created using MIMSoftware and Brain Atlas Mapping (1,620 regions total). SUV and Z-Score were calculated. NEMA phantom (6 spheres with contrast ratio of 4, 0.5-10min) and 3D-Hoffman phantom (0.5-10min, 0.6-2mCi FDG) were scanned.

# RESULTS

NEMA TOF PET revealed 1.0-0.7 recovery coefficients for 6 spheres 37-10mm, with an average of 0%, 0%, 6%, 14%, 30% and 46% higher SUVmax than nTOF's, across all PET (10-0.5min). Visually, Hoffman phantom and patient data consistently revealed more robust image quality with improved details and better contrast on TOF than nTOF. No brain tumors were identified on patients. Quantitatively, an average SUVmean difference (1±3%, 1±3%, 0±2%, 2±4% and 2±5%, TOF vs nTOF) was obtained for PET 10-0.5min. Significant differences in region-based therapy response (p<0.05) were found between TOF and nTOF for PET <=2min. Robust Z-Scores (<=10% variance) were found on TOF PET when reducing from 10 to 1min. TOF PET demonstrated better adaptability than nTOF to scan time and dose reduction in image quality and quantification (details given at RSNA).

## CONCLUSION

Compared to current standard of care FDG brain PET (10-13mCi, 10min), this low dose (3mCi) brain PET study with scan time reduction (10-0.5min) demonstrated advantages of the solid state 325ps DPC PET technology. The new technology advances neuro PET with more precise imaging of the brain enabled by the excellent TOF capability.

#### **CLINICAL RELEVANCE/APPLICATION**

Time-of-flight improvement (325ps) enabled by the new generation solid state DPC PET/CT has advantages in improving robustness of brain neuro PET acquisitions even under low dose and short scan time.

# SSA13-03 The Association Between Perihematomal Edema and Iron Deposition Using Diffusion Tensor Imaging and T2\* Mapping after Experimental Intracerebral Hemorrhage

Sunday, Nov. 25 11:05AM - 11:15AM Room: S504CD

#### Awards

# **Trainee Research Prize - Medical Student**

Participants

Xiaoxin Liu, Yinchuan, China (*Presenter*) Nothing to Disclose Chunhua Wang, MD, Chengdu, China (*Abstract Co-Author*) Nothing to Disclose Yushu Chen, BSc, Chengdu, China (*Abstract Co-Author*) Nothing to Disclose Lei Wang, BA, Chengdu, China (*Abstract Co-Author*) Nothing to Disclose Li Song, Chengdu, China (*Abstract Co-Author*) Nothing to Disclose Ruzhi Zhang, BSC, Chengdu, China (*Abstract Co-Author*) Nothing to Disclose Xuejun Ping, Yinchuan, China (*Abstract Co-Author*) Nothing to Disclose Fabao Gao, MD, PhD, Chengdu, China (*Abstract Co-Author*) Nothing to Disclose

## PURPOSE

This study aimed to explore the relationship between iron deposition and perihematomal edema after intracerebral hemorrhage (ICH) by diffusion tensor imaging (DTI) and T2\* mapping.

# METHOD AND MATERIALS

14 male SD rats were included in ICH group. 6 rats were included as normal controls. In ICH group, 40  $\mu$ L of autologous blood was injected into the right basal ganglia to mimic spontaneous ICH. All rats underwent T2WI, DTI and T2\* mapping on a 7.0 T animal MRI. The time points of scan of DTI and T2\* mapping were days 1, 3, and 7. We used T2WI images scanned at 3-6 h after ICH to measure the initial hematoma. Abnormal mean diffusivity (MD) value and volume were calculated by MD maps. T2\* value and abnormal T2 \* value volume were measured using T2\* mapping maps.

## RESULTS

In ICH group, the initial hematoma was  $19.14 \pm 8.151 \ \mu$ L. The T2\* values were  $21.23 \pm 2.40 \ ms$ ,  $20.62 \pm 2.96 \ ms$ , and  $17.97 \pm 2.54 \ ms$  at 1d, 3d and 7d after ICH in the ipsilateral side and were  $32.47 \pm 2.11 \ ms$ ,  $32.51 \pm 2.74 \ ms$ , and  $32.43 \pm 3.71 \ ms$  in the contralateral side. In normal control group, T2\* value was  $32.73 \pm 2.55 \ ms$  in the ipsilateral side and was  $33.07 \pm 2.16 \ ms$  in the contralateral side. The T2\* value in the ipsilateral side in ICH group were significant lower than normal control group at 1d, 3d and 7d after ICH, respectively (all P < 0.001). There were no significant differences in T2\* value between the contralateral side and normal group (all P > 0.05). The volumes of abnormal T2\* value were  $30.93 \pm 18.55 \ \mu$ L,  $25.30 \pm 9.27 \ \mu$ L, and  $31.50 \pm 10.58 \ \mu$ L and the volumes of abnormal MD were  $48.86 \pm 31.51 \ \mu$ L,  $64.30 \pm 64.72 \ \mu$ L, and  $30.63 \pm 24.99 \ \mu$ L at 1d, 3d and 7d after ICH. A positive correlation was observed between abnormal T2\* volume and abnormal MD volume at 1d after ICH (r = 0.92, P < 0.001).

## CONCLUSION

There was a positive correlation between abnormal T2\* volume and abnormal MD volume at 1d after ICH. DTI and T2\* mapping has the potential to explore the relationship between perihematomal edema and iron overload after ICH.

#### **CLINICAL RELEVANCE/APPLICATION**

DTI and T2\* mapping can not only diagnose the edema and iron overload in hematoma and perihematomal area after ICH, but also explore the relationship between iron deposition and perihematomal edema.

# SSA13-04 Imaging Type-Three Diabetes in an Alzheimer's Disease Animal Model: A Preliminary Mouse Study

Sunday, Nov. 25 11:15AM - 11:25AM Room: S504CD

## Participants

Val J. Lowe, MD, Rochester, MN (*Abstract Co-Author*) Research Grant, General Electric Company; Research Grant, Siemens AG; Research Grant, Eli Lilly and Company; Advisory Board, Merck & Co, Inc Tyler J. Bruinsma, BA, Rochester, MN (*Presenter*) Nothing to Disclose

#### For information about this presentation, contact:

vlowe@mayo.edu

#### PURPOSE

Investigating the brain distribution of iodine-125 labeled insulin (125I-Insulin) by dynamic single photon emission computed tomography/computed tomography (SPECT/CT) in mice with and without metabolic syndrome and/or Alzheimer's disease (AD).

#### **METHOD AND MATERIALS**

Six-month-old APP/PS1 mice (n=6) and wild type (WT) littermates (n=6) were split into two groups. Half were fed a high fat diet (HFD) while half were fed a regular chow diet (RCD) for four months. Insulin tolerance tests were performed at 1 and 4 months after feeding began. A bolus injection of 125I-Insulin was administered via the femoral vein and each mouse was imaged with SPECT/CT. Regions of interest were drawn around the brain and standard uptake values (SUV) were calculated. Following the imaging protocol, mice were perfused with PBS and individual brain regions and peripheral organs were harvested and assayed for 125I activity in a dual channel gamma counter. One-way ANOVA, repeated measures ANOVA, and Student's t-test were used to assess the significance of results.

## RESULTS

Blood glucose levels in HFD mice showed diminished response to insulin compared to RCD littermates (p<0.001). APP/PS1 mice on both HFD and RCD showed attenuated reductions in blood glucose during the insulin tolerance test (p<0.02). The HFD mice had significantly higher brain 125I-Insulin SUV at all time points as compared to RCD mice (p<0.005). In the RCD cohort, WT mice showed greater brain SUV than the APP/PS1 mice between 30-60 minutes (p<0.005). Post-perfusion gamma counts revealed significantly lower retention of 125I-insulin in the eyes and brains of HFD mice as compared to RCD mice (p<0.05).

## CONCLUSION

Although, HFD causes peripheral insulin resistance in both WT and APP/PS1 mice, the imaging showed an unexpected increase in these mice. In contrast, lower insulin retention post-mortem was seen in both WT and APP/S1 mice on HFD. Greater peripheral insulin resistance and lower brain insulin retention in APP/PS1 mice compared to WT mice suggests the impairment of insulin delivery that triggers 'type-three diabetes' in the AD brain. Further work is necessary to better understand the brain kinetics of insulin.

### **CLINICAL RELEVANCE/APPLICATION**

Insulin molecular imaging is a promising new frontier for elucidating the underlying connection between AD and insulin resistance.

## SSA13-05 Imaging Amyloid Plaques Without Contrast Agent

Sunday, Nov. 25 11:25AM - 11:35AM Room: S504CD

Participants

Eshan Dahal, Silver Spring, MD (*Abstract Co-Author*) Nothing to Disclose Bahaa Ghammraoui, Silver Spring, MD (*Abstract Co-Author*) Nothing to Disclose Aldo Badano, PhD, Silver Spring, MD (*Presenter*) Nothing to Disclose

#### PURPOSE

PET is clinically used to quantify brain amyloid load in vivo in Alzheimer's disease (AD) patients, but requires the use of amyloidspecific radiotracer and provides no information on plaque structure. We study small-angle x-ray scattering (SAXS) imaging for structural characterization of amyloid plaques in human brains and quantification of the amyloid load without contrast agent. Experimental SAXS images of an amyloid plaque model and Monte Carlo simulations of diagnostic energy x-ray transport in a human head digital model are reported to determine SAXS system design choices for amyloid imaging.

## **METHOD AND MATERIALS**

SAXS measurements were performed using a point collimation mode and monochromatic x-ray beam. Simulations of a SAXS-CT geometry in a voxelized human head (MIDA model) were performed using a publicly available GPU-accelerated Monte Carlo radiation transport tool. SAXS-CT images of the brain with varying amyloid load at relevant q angles were reconstructed using filtered back projection (FBP).

## RESULTS

SAXS measurements of amyloid fibrils pellet show strong scattering with distinct peaks around 6.4 and 13.4 nm-1 due to the ßsheet fibrillar structure. SAXS is capable of detect amyloid plaques without any contrast agent based on their scattering signature. SAXS-CT simulations performed on a human head digital model with inserted amyloid plaques show feasible detection of plaques as small as 2 mm. More realistic SAXS-CT simulation requires measured cross-section models of amyloid in the brain with different mass fraction of plaques. This allows optimizing the SAXS imaging system to detect micrometer-sized amyloids near 6.4 nm-1.

#### CONCLUSION

Our results showcase the potential of SAXS imaging method to image amyloid plaques in the human brain and to quantify amyloid load without using contrast agent.

#### **CLINICAL RELEVANCE/APPLICATION**

SAXS may surpass the amyloid imaging performance of PET if it can detect and image amyloids in the early stage of plaques

deposition in AD patients with an effective radiation dose of 10 mSv or lower.

# SSA13-06 Features of Corticospinal Tract Using Diffusion Tensor Imaging After Experimental Intracerebral Hemorrhage

Sunday, Nov. 25 11:35AM - 11:45AM Room: S504CD

Participants

Chunhua Wang, MD, Chengdu, China (*Abstract Co-Author*) Nothing to Disclose Xiaoxin Liu, Yinchuan, China (*Presenter*) Nothing to Disclose Li Song, Chengdu, China (*Abstract Co-Author*) Nothing to Disclose Ruzhi Zhang, BSC, Chengdu, China (*Abstract Co-Author*) Nothing to Disclose Yushu Chen, BSc, Chengdu, China (*Abstract Co-Author*) Nothing to Disclose Fabao Gao, MD, PhD, Chengdu, China (*Abstract Co-Author*) Nothing to Disclose

## PURPOSE

To dynamically evaluate the effect of hematoma on corticospinal tract (CST) after intracerebral hemorrhage (ICH) by diffusion tensor imaging (DTI).

## **METHOD AND MATERIALS**

29 male SD rats were injected with 40uL of autologous blood from tail in the right basal ganglia. DTI sequence was scanned on 7.0T MRI at day 1 (D1), day 3 (D3), day 7 (D7), day 14 (D14), day 21 (D21) and day 28 (D28) after ICH. Sham and normal controls underwent the same scan. The initial hematoma volume was obtained from T2WI images (3-6h after ICH). Mean diffusivity (MD), axial diffusivity (AD), radial diffusivity (RD) and fractional anisotropy (FA) were obtained from DTI maps. The regions of interest included cerebral peduncle (CP) and pyramidal tract (PY). Modified neurological severity score (mNSS) was used to evaluate the neurological function of rats.

## RESULTS

FA values of ipsilateral CP in ICH group were significant lower than in sham group at D1, D3, D7, D14 and D21 (all p < 0.05). FA values of ipsilateral CP in ICH group at D3, D7 were significant lower than normal controls (both p < 0.01). MD of ipsilateral CP in ICH group at D1 was significant higher than sham group and at D28 was significantly lower than sham group (both p < 0.05). AD of ipsilateral CP at D7 and D28 in ICH group was significantly lower than in normal group (both p < 0.05). RD of ipsilateral CP in ICH group was higher than sham group at D1 and D3 and lower at D28 (all p < 0.05). No significant differences were found in DTI parameters in ipsilateral and contralateral PYs between ICH group was ham group, and among different time points and normal controls (all p > 0.05). The scores of mNSS in ICH group were significantly greater than in sham group (all p < 0.05). The score of mNSS in ICH group at D1 was significantly greater than other time points (all p < 0.05).

## CONCLUSION

DTI parameters of ipsilateral CP were abnormal, whereas no changes in DTI parameters of PY were found in ICH model induced by 40uL autologous blood. DTI has the potential to detect dynamically the effect of hematoma on CST.

## **CLINICAL RELEVANCE/APPLICATION**

DTI reveals the changes of CST in parameters after ICH at basal ganglia.

# SSA13-07 The rCBV with Contrast Leakage Correction Improves the Correlation Between MR Perfusion Weighted Imaging and Fluorine-18-Deoxyglucose Positron Emission Tomography in Patients with Brain Tumors

Sunday, Nov. 25 11:45AM - 11:55AM Room: S504CD

Participants Xiang Liu, MD, Rochester, NY (*Presenter*) Nothing to Disclose Wei Tian, MD, PhD, Rochester, NY (*Abstract Co-Author*) Nothing to Disclose Henry Z. Wang, MD, PhD, Pittsford, NY (*Abstract Co-Author*) Consultant, VirtualScopics, Inc

#### For information about this presentation, contact:

Xiang\_Liu@URMC.Rochester.edu

## PURPOSE

Tumor angiogenesis and tumor metabolite are important for clinical management for patients with brain tumors. Although rCBV without contrast leakage-correction is the most widely used imaging parameter of MR dynamic susceptibility contrast perfusion weighted imaging (DSC-PWI), the rCBV with contrast leakage-correction was reported to have better accuracy in the evaluation of tumor hemodynamic abnormality. The purpose of this study is to compare the correction between these two rCBV parameters and fluorine-18-deoxyglucose (FDG) positron emission tomography (PET).

# METHOD AND MATERIALS

85 paired MR DSC-PWI and FDG-PET examinations in 65 patients with brain tumors, including high grade gliomas, brain metastases and cerebral lymphomas, were enrolled in this study. The interval between MR DSC-PWI and FDG-PET examinations ranged from 0 to 13 days in 72 paired MR DSC-PWI and FDG-PET examinations, another 13 paired stable post-surgical scans were acquired within 28 days. The rCBV maps without and with contrast leakage correction were generated using FDA-approved GE BrainStat and NordicICE programs. Two neruoradiologists measured the maximal rCBV ratio and the tumor versus normal tissue count ratio (TNR) in the "hot" ROIs. The correlation between maximal rCBV ratio of rCBV without and with contrast leakage correction and TNR was evaluated with Spearman Rank correlation analysis, and the difference between these two correlations was assessed with paired ttest.

## RESULTS

The mean maximal rCBV ratio of rCBV with contrast leakage correction (1.65±1.38) were higher than rCBV without contrast leakage

correction ( $1.02 \pm 0.876$ , p=0.03). The rCBV with contrast leakage correction has better correlation with FDG-PET-TNR (Correlation coefficient =0.618, p<0.001) than rCBV without contrast leakage correction (Correlation coefficient =0.436, p=0.018), p<0.001.

## CONCLUSION

The rCBV with contrast leakage correction shows better correlation with FDG-PET-TNR. Combing different MR-DSC-PWI and FDG-PET parameters could provide comprehensive information of tumor hemodynamic change and tumor metabolic abnormality.

#### **CLINICAL RELEVANCE/APPLICATION**

The rCBV with contrast leakage correction shows better correlation with FDG-PET-TNR. Combing different MR-DSC-PWI and FDG-PET parameters could provide comprehensive information of tumor hemodynamic change and tumor metabolic abnormality.

# SSA13-08 Peptide Functionalized Nano-Inhibitors Restrain Brain Tumor Growth by Blocking cMET Signaling

Sunday, Nov. 25 11:55AM - 12:05PM Room: S504CD

Participants

Yingwei Wu, MD, Shanghai, China (*Presenter*) Nothing to Disclose Qi Fan, Shanghai, China (*Abstract Co-Author*) Nothing to Disclose Xiaofeng Tao, Shanghai, China (*Abstract Co-Author*) Nothing to Disclose

For information about this presentation, contact:

wuyw0103@hotmail.com

#### PURPOSE

To determine therapeutic effect of peptide functionalized NP in restraining brain tumor growth by blocking cMET Signaling

## **METHOD AND MATERIALS**

A dendrimer-based nanoinhibitor(Den-CMBP) has been developed using MET targeted cMBP peptides conjugated on G4 dendrimer. Binding affinity of Den-CMBP and free CMBP was evaluated using Surface Plasmon Resonance(SPR) Technology. Cellular responses including cell apoptosis, viability, proliferation were evaluated by treatment with Den-CMBP at various concentrations.GBM rodent models were developed by U87-MG cells implantation. Expression of cMET and downstream signature proteins were tested in U87-MG tumor cells and U87-induced mice models by Western blotting analysis. Mice bearing GBM tumors were treated with Den-CMBP, free CMBP and PF-04217903, a small molecular MET inhibitor, respectively. In-vivo MRI was used to assess tumor volume pre and post treatment. Immunofluorescence staining was performed to evaluate MET immnuno-activity post treatment. Survival was calculated for three sub-groups.

#### RESULTS

Compared to the free cMBP peptide(KD =  $3.964 \times 10-7$  M), the binding affinity of the nanoinhibitor increased three-order of multitude to  $1.316 \times 10-10$  M due to the multivalent effect. Nanoinhibitor efficiently blocked MET signaling with remarkably reduced levels of phosphorylated MET and its downstream signaling proteins in GBM tumor models and U87MG cell culture. In vivo T2-weighted MRI showed significant tumor growth restraint post treatment of nanoinhibitor. The volumes of tumor treated with DencMBP1 were recorded as 0.019, 0.408, and 3.659 mm3 at 7, 15 and 21 days, which decreased 63.5%, 80.0% and 78.3% respectively compared to the control group. No obvious therapeutic effect was observed after administration of free cBMP peptide, nanoinhibitor attenuated glioma growth by inhibiting MET downstream signaling. Median survival was extended to 35 days with treatment of nano inhibitors.

# CONCLUSION

Overall, this work developed a dendrimer based MET targeted nanoinhibitor that effectively inhibits glioma growth by blocking MET downstream signaling, which would provide an alternative therapeutic strategy for tumor therapy.

## **CLINICAL RELEVANCE/APPLICATION**

The multivalency of dendrimer based NPs would help to decrease dosage and side-effects as well.

# SSA13-09 Dynamic Cell Tracking with Time-Lapse MRI: The Temporal Window for Detection of Inflammatory Disease

Sunday, Nov. 25 12:05PM - 12:15PM Room: S504CD

Awards

## **Trainee Research Prize - Resident**

Participants

Max Masthoff, MD, Muenster, Germany (*Presenter*) Nothing to Disclose Sandra Gran, Muenster, Germany (*Abstract Co-Author*) Nothing to Disclose Xueli Zhang, Muenster, Germany (*Abstract Co-Author*) Nothing to Disclose Lydia Wachsmuth, Muenster, Germany (*Abstract Co-Author*) Nothing to Disclose Anne Helfen, MD, Muenster, Germany (*Abstract Co-Author*) Nothing to Disclose Walter L. Heindel, MD, Muenster, Germany (*Abstract Co-Author*) Nothing to Disclose Lydia Sorokin, Muenster, Germany (*Abstract Co-Author*) Nothing to Disclose Johannes Roth, MD, Muenster, Germany (*Abstract Co-Author*) Nothing to Disclose Michel Eisenblaetter, MD, Muenster, Germany (*Abstract Co-Author*) Nothing to Disclose Moritz Wildgruber, MD, PhD, Munster, Germany (*Abstract Co-Author*) Nothing to Disclose Cornelius Faber, Muenster, Germany (*Abstract Co-Author*) Nothing to Disclose

#### PURPOSE

While several imaging techniques apply various approaches for cell tracking, the actual dynamic process remained concealed for non-invasive imaging in deep tissue until recently. With the concept of time lapse MRI, real time tracking of individual cells has

become possible. Here, we investigate which velocity range of cell motility can be resolved and investigate time Lapse MRI to track immune cell motility in a model of multiple sclerosis.

# METHOD AND MATERIALS

A time lapse MRI protocol using a T2\*w gradient echo sequence with a single frame scan-time of 8min12s was developed on a 9.4T small-animal MRI. Movies were composed of images from 20 repetitions. Phantom scans were performed on Resovist-labelled monocytes. In vivo scans were performed in healthy (n=6) and experimental autoimmune encephalomyelitis (EAE, n=14) mice (C57BL/6J) injected i.v. with Resovist 24h prior to MRI. Simulations were performed with a synthetic phantom reproducing the observed contrast of one labelled cell. Motion was simulated by composing synthetic k space data with different fractions obtained from different positions of the synthetic cell.

## RESULTS

Phantom and in vivo scans confirmed that labelled immune cells could be tracked in the brain. Simulations showed that moving cells up to velocities of  $1\mu$ m/s were detectable. In EAE mice significantly reduced numbers of in vivo labelled immune cells were observed as compared to naïve mice (253±29, n=6 vs 31±6, n=14). In EAE mice significant differences were observed before (45±9, n=6) versus after onset (21±4, n=8) of symptoms.

## CONCLUSION

Time lapse MRI proofed sensitive enough to detect "patrolling" immune cells along the endothelium. With the start of the leucocyteadhesion cascade in inflammation, cells start "rolling" with a higher velocity, resulting in less detected cells in EAE. Thus, time lapse MRI enables for assessing immune cell dynamics non-invasively and may serve as a tool for detection or monitoring of an inflammatory response prior to onset of clinical symptoms.

## **CLINICAL RELEVANCE/APPLICATION**

Time lapse MRI may be a versatile tool for studying onset and type of innate immune response by non-invasive, real-time imaging of dynamic immune cells in the brain.



#### SSA14

## Musculoskeletal (Bone Marrow and Neoplasms)

Sunday, Nov. 25 10:45AM - 12:15PM Room: E353C



AMA PRA Category 1 Credits ™: 1.50 ARRT Category A+ Credit: 1.75

FDA Discussions may include off-label uses.

#### Participants

Luca Maria Sconfienza, MD, PhD, Milano, Italy (*Moderator*) Travel support, Bracco Group; Travel support, Esaote SpA; Travel support, ABIOGEN PHARMA SpA; Speakers Bureau, Fidia Pharma Group SpA Reto Sutter, MD, Zurich, Switzerland (*Moderator*) Nothing to Disclose

#### Sub-Events

# SSA14-01 MR-Based Assessment of Bone Marrow Fat in a Population-Based Cohort Study: Comparison of Different Methods and Association to Physical Activity

Sunday, Nov. 25 10:45AM - 10:55AM Room: E353C

Participants

Robert C. Bertheau, MD, Heidelberg, Germany (*Presenter*) Nothing to Disclose Roberto Lorbeer, Greifswald, Germany (*Abstract Co-Author*) Nothing to Disclose Johanna Nattenmueller, MD, Heidelberg, Germany (*Abstract Co-Author*) Nothing to Disclose Elke Wintermeyer, Tuebingen, Germany (*Abstract Co-Author*) Nothing to Disclose Christopher Schuppert, Heidelberg, Germany (*Abstract Co-Author*) Nothing to Disclose

Birgit Linkohr, Neuherberg, Germany (Abstract Co-Author) Nothing to Disclose

Juergen Machann, MD, Tuebingen, Germany (Abstract Co-Author) Nothing to Disclose

Hans-Ulrich Kauczor, MD, Heidelberg, Germany (Abstract Co-Author) Research Grant, Siemens AG Research Grant, Bayer AG

Speakers Bureau, Boehringer Ingelheim GmbH Speakers Bureau, Siemens AG Speakers Bureau, Koninklijke Philips NV Speakers Bureau, Bracco Group Speakers Bureau, AstraZeneca PLC

Annette Peters, Neuherberg, Germany (Abstract Co-Author) Nothing to Disclose

Fabian Bamberg, MD, Tuebingen, Germany (*Abstract Co-Author*) Speakers Bureau, Bayer AG ; Speakers Bureau, Siemens AG ; Research Grant, Siemens AG

Christopher L. Schlett, MD, MPH, Heidelberg, Germany (Abstract Co-Author) Nothing to Disclose

## For information about this presentation, contact:

robert.bertheau@med.uni-heidelberg.de

## PURPOSE

We aimed to compare different MRI-based assessments of bone marrow adipose tissue (MAT) at different anatomic locations and its correlation with physical activity.

#### **METHOD AND MATERIALS**

As part of the population-based KORA study, largely healthy subjects underwent whole-body MR imaging including a 2-point-T1-DIXON-VIBE (2pDIXON) sequence (entire body) and a multi-echo DIXON (ME) sequence (upper abdomen). MAT was quantified in the L1 and L2 vertebrae using both sequences, in the femoral necks using the 2pDIXON. In the 2pDIXON, MAT percentage was calculated as the mean value of the fat image divided by the sum of the mean values of the fat and water image. In the ME sequence, MAT percentage was directly derived from the output images, which accounted for R2\*. Physical activity was determined by standardized questionnaire.

#### RESULTS

A total of 385 subjects (96%) were included in the analysis (56±9.1yrs, 58% male); with an evenly distributed physical activity pattern (29% >2h/week; 31% 1h/week; 15% 1h/week (irregularly); 26% no physical activity). Based on the 2pDIXON, MAT was 52.6±10.2% in L1, 56.2±10.3% in L2, 87.4±5.9% in the right and 87.2±5.9% in the left femur neck, while in the ME sequence MAT was significantly lower (43.0±8.0% and 44.1±7.9%, for L1 and L2, all p<0.001; respectively). Both MAT measurements in the vertebrae were strongly correlated (r: 0.81 to 0.93), in contrast, correlation of MAT between vertebrae and femoral necks was weak (r: 0.36 to 0.46). All vertebral bone marrow fat measurements were inversely associated with high physical activity (>2h/w), but no correlation was found with the femoral necks (all p>=0.35). Strongest association was observed for L1, derived from the 2pDixon ( $\beta$ = 3.9, p=0.005). This association remained significant when adjusted for age, gender and waist circumference (p=0.005). Also, high reproducibility, assessed in a subset of 30 subjects, was observed in the 2pDIXON measurement at L1 (ICC for inter- and intra-reader: 0.92 and 0.90).

#### CONCLUSION

Physical activity was negatively correlated with MAT in the L1, L2 vertebrae but not with the femoral necks. 2pDIXON depicted that correlation better than the ME sequence.

MAT is centrally involved in many metabolic processes and may serve as a proxy for bone health/disease, e.g. osteoporosis. Its different dependence on physical activity at different body locations may contribute to a better understanding of related pathophysiology.

# SSA14-02 Application of Texture Analysis in the Differential Diagnosis of Osteoblastic Metastases and Enostoses: Comparison with CT Attenuation Measurements

Sunday, Nov. 25 10:55AM - 11:05AM Room: E353C

Participants

Seong Woo Jeon, MD, Suwon, Korea, Republic Of (*Presenter*) Nothing to Disclose Kyu-Sung Kwack, MD, PhD, Suwon, Korea, Republic Of (*Abstract Co-Author*) Nothing to Disclose Sunghoon Park, MD, Suwon, Korea, Republic Of (*Abstract Co-Author*) Nothing to Disclose

## PURPOSE

The purpose of this study was to investigate the role of CT texture in distinguishing between osteoblastic metastases from enostoses and to compare the results with CT attenuation values.

## **METHOD AND MATERIALS**

The study group comprised 32 patients with 64 sclerotic bone lesions found at CT (41 enostoses in 24 patients and 23 metastases in 8 patients). For each lesions in spine, CT texture analysis was performed by drawing a region of interest on axial CT slices. The histogram parameters (mean, SD, kurtosis, entropy, and skewness) were acquired using a research software 'TexRAD'. The diagnostic performances of mean CT attenuation values and texture analysis for differentiating osteoblastic metastases from enostoses were evaluated.

## RESULTS

Mean CT attenuation values had the best diagnostic performance with an ROC AUC (Az) of 0.953 among all parameters. Among CT texture analysis parameters to differentiate osteoblastic metastases and enostoses, the kurtosis had the highest ROC (Az = 0.787) than the entrophy (Az = 0.763) and skewness (Az = 0.691). The combination of mean attenuation and CT texture analysis parameters had poorer performance than mean CT attenuation values alone.

## CONCLUSION

Using texture analysis does not improve diagnostic performance in the differentiation of osteoblastic metastases and enostoses in the spine.

#### **CLINICAL RELEVANCE/APPLICATION**

CT texture analysis may have a spectrum of potential application in lesion characterization for some tumor types. However, based on our data, we cannot recommend adding CT texture analysis to differentiate osteoblastic metastases of the spine.

# SSA14-03 Differentiation of Osteomyelitis from Reactive Osteitis in the Patients with Diabetic Foot Using Multivariable Logistic Regression Analysis

Sunday, Nov. 25 11:05AM - 11:15AM Room: E353C

Participants

Yong-ho Jang, MD, Suwon, Korea, Republic Of (*Presenter*) Nothing to Disclose Kyu-Sung Kwack, MD, PhD, Suwon, Korea, Republic Of (*Abstract Co-Author*) Nothing to Disclose Sunghoon Park, MD, Suwon, Korea, Republic Of (*Abstract Co-Author*) Nothing to Disclose

## PURPOSE

To retrospectively investigate the differentiating magnetic resonance (MR) imaging findings between osteomyelitis and reactive osteitis in the patients with diabetic foot.

# METHOD AND MATERIALS

From November 2015 to March 2018, 118 patients who underwent MRI of the foot for evaluation of suspected osteomyelitis were included in this study. Primary (signal intensity, distribution, and pattern on the T1-weighted images, signal intensity on the T2-weighted images, and concordance of marrow signal intensity) and secondary MR imaging signs (cortical interruption, cellulitis, ulcer, soft tissue abscess, and gangrene) were retrospectively reviewed. To identify the MR features differentiating osteomyelitis from reactive osteitis and to evaluate their differentiating accuracy, multivariate regression and receiver operating characteristic (ROC) curve analysis were performed.

#### RESULTS

On MRI findings, signal intensity, distribution, and pattern on the T1-weighted images, signal intensity on the T2-weighted images, concordance of marrow signal intensity, cortical interruption, ulcer, soft tissue abscess, and gangrene were significantly different between two groups (p < 0.05). Multivariate regression analysis showed that the bright T2 signal intensity (OR 17.7, p < 0.001) and deep ulcer (OR 5.6, p = 0.009) were major factors associated with osteomyelitis. The area under the ROC curve of predicted probabilities for the combination of these factors was 0.879.

# CONCLUSION

In the patients with diabetic foot, osteomyelitis can be accurately distinguished from reactive osteitis by the bright T2 signal intensity and deep ulcer.

## **CLINICAL RELEVANCE/APPLICATION**

Identification and application of these MR features are important to analyzing radiological imaging in the patients with the diabetic foot and can help the radiologist to differentiate osteomyelitis from reactive osteitis

# SSA14-04 Predicting Osteomyelitis in Patients with Equivocal MRI Findings

#### Participants

Alessandra J. Sax, MD, Philadelphia, PA (*Presenter*) Nothing to Disclose William B. Morrison, MD, Philadelphia, PA (*Abstract Co-Author*) Consultant, AprioMed AB; Patent agreement, AprioMed AB; Consultant, Zimmer Biomet Holdings, Inc; Consultant, Samsung Electronics Co, Ltd; Consultant, Medical Metrics, Inc Adam C. Zoga, MD, Philadelphia, PA (*Abstract Co-Author*) Nothing to Disclose Johannes B. Roedl, MD, PhD, Philadelphia, PA (*Abstract Co-Author*) Nothing to Disclose Jeffrey A. Belair, MD, Philadelphia, PA (*Abstract Co-Author*) Nothing to Disclose Ethan J. Halpern, MD, Philadelphia, PA (*Abstract Co-Author*) Nothing to Disclose

#### For information about this presentation, contact:

alisax87@gmail.com

#### PURPOSE

Specificity of MRI in diagnosing osteomyelitis (OM) in the diabetic foot with ulceration is confounded by high frequency of equivocal findings (abnormal signal on T2fs/STIR sequences with normal signal on T1w sequences). We sought to determine the strongest risk factors for development of osteomyelitis in this setting.

#### **METHOD AND MATERIALS**

We analyzed MR exams of diabetic patients with pedal ulcers and suspected osteomyelitis who were indeterminate for OM based on discordant bone marrow signal (normal T1, abnormal T2fs/STIR) adjacent to the ulcer. Follow-up imaging and/or surgical results determined outcome (OM or non-OM). Ulcers were categorized based on surface area and depth (distance to bone). Patterns of marrow edema (subcortical vs medullary) were recorded. The ratio of marrow to joint fluid signal on T2fs/STIR sequences was measured. Statistical analysis was performed with a two-sample t-test and a Cox proportional hazard model.

#### RESULTS

60 MR exams were identified. 26 showed resolution of marrow findings (no osteomyelitis) and 34 progressed to osteomyelitis. Marrow ROI/joint fluid ratios averaged 65% (39-87%) in the OM group, and 45% (17-97%) in the non-OM group, p < .001. ROI ratios > 53% had a 6.5-fold increased risk of osteomyelitis, p < .001. Proximity to bone averaged 6mm in the OM group and 9mm in the non-OM group, p = .02. Ulcer size averaged 4 cm2 in the OM group versus 2.4 cm2 in the non-OM group, p = .07. Ulcers greater than 3cm2 had a 2-fold increase in the risk of osteomyelitis, p = .04.

## CONCLUSION

High bone marrow/joint fluid signal ratio on T2fs/STIR images was the strongest risk factor for development of osteomyelitis, with a ratio > 53% portending an 6.5-fold increased risk of osteomyelitis. Ulcer size and depth to bone are weaker predictors for the development of osteomyelitis.

#### **CLINICAL RELEVANCE/APPLICATION**

Diabetes affects 9.3% of US citizens, 25% of which develop a foot ulcer, the most significant risk factor for amputation. A test that could accurately predict early osteomyelitis in this population would significantly reduce morbidity.

# SSA14-05 Assessment of Early Treatment Response by MRI in Multiple Myeloma: Comparative Study of Whole-Body MRI and Lumbar Spinal MRI

Sunday, Nov. 25 11:25AM - 11:35AM Room: E353C

Participants

Miyuki Takasu, MD, Hiroshima, Japan (*Presenter*) Nothing to Disclose Yuji Akiyama, Hiroshima, Japan (*Abstract Co-Author*) Nothing to Disclose Kazushi Yokomachi, PhD, Hiroshima, Japan (*Abstract Co-Author*) Nothing to Disclose Tomoyo Fuji, Hiroshima, Japan (*Abstract Co-Author*) Nothing to Disclose Shota Kondo, Hiroshima, Japan (*Abstract Co-Author*) Nothing to Disclose Hiroaki Sakane, MD, Hiroshima, Japan (*Abstract Co-Author*) Nothing to Disclose Chihiro Tani, MD, Hiroshima, Japan (*Abstract Co-Author*) Nothing to Disclose Kazuo Awai, MD, Hiroshima, Japan (*Abstract Co-Author*) Nothing to Disclose Kazuo Awai, MD, Hiroshima, Japan (*Abstract Co-Author*) Nothing to Disclose Kazuo Awai, MD, Hiroshima, Japan (*Abstract Co-Author*) Nothing to Disclose Kazuo Awai, MD, Hiroshima, Japan (*Abstract Co-Author*) Research Grant, Canon Medical Systems Corporation; Research Grant, Hitachi, Ltd; Research Grant, Fujitsu Limited; Research Grant, Bayer AG; Research Grant, DAIICHI SANKYO Group; Research Grant, Eisai Co, Ltd; Medical Advisory Board, General Electric Company; ;

#### PURPOSE

This study compared remission status at completion of chemotherapy with changes in MRI biomarkers obtained from whole-body diffusion-weighted imaging (wb-DWI) and lumbar spinal chemical shift imaging soon after induction of chemotherapy, and compared the predictive value of the MRI biomarkers for complete response (CR).

## METHOD AND MATERIALS

Forty-two patients with symptomatic myeloma were examined before and after two cycles of chemotherapy using a 3-T MRI system (Ingenia; Philips Healthcare). For wb-DWI, coronal images were acquired by free-breathing single-shot echo-planar DWI with b-values of 0 and 1000. Total tumor volume (tTV) was obtained by semi-automatic segmentation of wb-DWI using a discriminant analysis method. The threshold for positive bone marrow (BM) involvement was an apparent diffusion coefficient (ADC) >0.55×10-3mm2/s according to a previous report. The mean fat fraction (FF) was calculated from the BM of the L1 to L3 vertebrae without a focal lesion using the coronal 3D 2-point mDIXON quant sequence. Coronal wb-T1 weighted, axial wb-T2 weighted, sagittal spinal STIR, and T1-weighted images were acquired. Serological data were also obtained. At the completion of chemotherapy, the patients were categorized into a CR group (n=12) or a non-CR group (n=30).

#### RESULTS

No significant differences in the baseline serological- and MRI-derived indices were observed between groups. At the second

examination, tTV, M protein, and B2-microglobulin were significantly decreased and 75th percentiles of ADC and FF were significantly increased in the CR group. The general linear model demonstrated that percentage changes in FF and M protein contributed significantly to the achievement of CR (P=0.01, P=0.03, respectively). AUCs of ROC curves were 0.876 for FF and 0.843 for M protein.

## CONCLUSION

Early change in the FF of lumbar BM soon after induction of chemotherapy was a significant predictor of CR. Total TV obtained by wb-DWI did not prove to be a significant predictor of CR. The sensitivity of FF in the lumbar BM for identification of CR was higher than M protein.

# **CLINICAL RELEVANCE/APPLICATION**

Early change in the FF of lumbar BM soon after induction of chemotherapy is a predictor of CR, suggesting that lumbar spinal MRI can be used to predict remission status.

# SSA14-06 MRI Radiomics in the Longitudinal Analysis of Desmoid Fibromatosis Undergoing Systemic Therapy

Sunday, Nov. 25 11:35AM - 11:45AM Room: E353C

Participants

Ty K. Subhawong, MD, Miami, FL (*Presenter*) Research Consultant, Arog Pharmaceuticals, Inc Katharina Feister, Miami, FL (*Abstract Co-Author*) Nothing to Disclose Kevin M. Sweet, MD, Miami, FL (*Abstract Co-Author*) Nothing to Disclose Jorge Monge Urrea, Miami, FL (*Abstract Co-Author*) Nothing to Disclose Peter Demaria, Miami, FL (*Abstract Co-Author*) Nothing to Disclose Robert Hsu, Miami, FL (*Abstract Co-Author*) Nothing to Disclose Heath Catoe, Miami, FL (*Abstract Co-Author*) Nothing to Disclose Ahmet M. Bagci, Miami, FL (*Abstract Co-Author*) Nothing to Disclose Noam Alperin, PhD, Miami, FL (*Abstract Co-Author*) Nothing to Disclose Breelyn A. Wilky, MD, Miami, FL (*Abstract Co-Author*) Research support, Merck & Co, Inc; Consultant, Novartis AG; Consultant, Johnson & Johnson; Consultant, Eli Lilly and Company

## For information about this presentation, contact:

tsubhawong@miami.edu

## PURPOSE

Desmoid-type fibromatosis exhibits unique morphological changes on MRI in response to systemic therapy. We sought to quantify the longitudinal changes in appearance of treated tumors to better elucidate the relationship between morphological and textural imaging features.

## METHOD AND MATERIALS

This IRB-approved retrospective study included 16 extra-abdominal lesions in 11 subjects (mean age 37 years), 6 females and 5 males. Therapeutic regimens included cytotoxic chemotherapy (n=7), tyrosine kinase inhibitor (n=2), tamoxifen (n=3), and NSAIDS (n=2). Tumors were segmented using 3D-Slicer, and features were extracted with the Radiomics extension; data included tumor shape, signal intensity (tumor: muscle enhancement ratio), and image texture. Response was classified at the lesional level by RECIST1.1 maximum diameter (Dmax) thresholds for progressive disease (>20% increase from nadir, PD), partial response (>30% decrease from baseline, PR), or otherwise stable disease (SD).

#### RESULTS

The 16 lesions were followed for mean of 5.1 years (range 9 months -14 yrs); this included a total of 100 distinct timepoints. Baseline mean Dmax=10 cm (range 4.2-173 cm), volume 176 cc (range 8-796 cc), and mean enhancement ratio 1.8 (range 0.9-4.0). By RECIST1.1 6 lesions remained stable, 6 lesions showed PD (median progression free survival 1.8 yrs). Only 4 lesions (25%) achieved PR (median time to PR 3.9 yrs), while 13/16 (81%) showed a drop in enhancement ratio (mean -46% from baseline). 12/16 (75%) tumors exhibited at least >20% drop from baseline (median 2.6 yrs). Dmax correlated poorly with enhancement ratio (r=0.09). A random effects GLS regression model containing shape-based, first-order, and textural features established skewness (p=0.008), minor axis length (p=0.04), and run entropy (p=0.05) as significant independent predictors of contrast enhancement ratio.

## CONCLUSION

Most desmoid fibromatoses show substantial decreased enhancement after systemic treatment despite relative stability in size. Desmoid segmentation enables identification of radiomic biomarkers that reflect clinically relevant longitudinal changes in tumor phenotype.

## **CLINICAL RELEVANCE/APPLICATION**

Consistent and durable decreases in tumor enhancement support augmenting or replacing size-based with signal-based imaging response criteria for desmoid tumors undergoing systemic therapy.

# SSA14-07 Differentiating Lipomatous Masses with High-Resolution 1H MRS Metabolites: Do Benign Lipomas and Atypical Lipomatous Tumors Have a Distinct Metabolic Signature?

Sunday, Nov. 25 11:45AM - 11:55AM Room: E353C

Participants

Santosh M. Bharti, Baltimore, MD (*Abstract Co-Author*) Nothing to Disclose Brett A. Shannon, MD, Baltimore, MD (*Abstract Co-Author*) Nothing to Disclose Carol Morris, MD, Baltimore, MD (*Abstract Co-Author*) Nothing to Disclose Adam Levin, Baltimore, MD (*Abstract Co-Author*) Nothing to Disclose Zaver M. Bhujwalla, PhD, Baltimore, MD (*Abstract Co-Author*) Nothing to Disclose Laura M. Fayad, MD, Baltimore, MD (*Abstract Co-Author*) Nothing to Disclose

## Ty K. Subhawong, MD, Miami, FL (Presenter) Research Consultant, Arog Pharmaceuticals, Inc

# For information about this presentation, contact:

lfayad1@jhmi.edu

## PURPOSE

Adipocytic tumors represent a spectrum of neoplastic disease from benign lipomas and variants, to atypical lipomatous tumors (ALTs) and liposarcomas. Some liposarcomas are suspected to arise through dedifferentiation of ALTs. The distinction of liposarcomas and premalignant ALTs can be a diagnostic challenge, as can the distinction of ALTs and lipoma variants (lipomas without pure lipid composition), with implications for surgical and clinical management. The purpose of this study is to identify metabolic biomarkers for adipocytic tumors, for accurate tumor classification.

## METHOD AND MATERIALS

In a prospective study, de-identified human surgical samples were collected from subjects who underwent surgical resection of indeterminate adipocytic tumors (those with imaging features atypical for simple lipomas). Tissue samples were snap frozen and stored at -80°C until 1H MRS analysis. Dual phase solvent extraction was performed on approximately 300 mg of tumor tissue. The water phase was separated, freeze-dried, and reconstituted in 600ul D2O PBS for MRS analysis. All MR spectra were acquired on an Avance III 750 MHz (17.6T) Bruker NMR spectrometer. Computational modeling of pattern recognition based cluster analysis was utilized to look for significant differences in metabolic signatures between the adipocytic tumor types.

## RESULTS

Tissue specimens from lipoma variants (n=6), ALTs (n=5) and adjacent non-involved subcutaneous normal fat (n=7) were examined using 1H MRS. Quantitative metabolite information is shown in figures 1A-B. The metabolic heatmap (Figure 1A) identifies the metabolic patterns of ALTs compared to lipoma variants and normal fat. A significant increase in several metabolite levels, including lactate, was observed in ALTs compared to lipomas and normal fat. Cluster analysis (Figure 1B) showed significant differences between normal fat, lipoma variants and ALTs.

#### CONCLUSION

Our preliminary data support investigating the use of high resolution 1H MRS of adipocytic tumors for differentiating between tumor subtypes and for understanding malignant progression.

#### CLINICAL RELEVANCE/APPLICATION

These results provide new insights into the metabolic differences between benign and premalignant tissue that may be exploited for formulating treatment plans and ultimately, metabolism-based therapeutic strategies.

## SSA14-08 Radiomic Analysis of Peripheral Nerve Sheath Tumors Accurately Predicts Benign versus Malignant Status

Sunday, Nov. 25 11:55AM - 12:05PM Room: E353C

Participants

Alexander T. Mazal, BS, Dallas, TX (*Presenter*) Nothing to Disclose Liyuan Chen, Dallas, TX (*Abstract Co-Author*) Nothing to Disclose Feng Poh, MBBS,FRCR, Singapore, Singapore (*Abstract Co-Author*) Nothing to Disclose Jing Wang, PhD, Dallas, TX (*Abstract Co-Author*) Nothing to Disclose Parham Pezeshk, MD, Dallas, TX (*Abstract Co-Author*) Nothing to Disclose Oganes Ashikyan, MD, Dallas, TX (*Abstract Co-Author*) Nothing to Disclose Michael R. Folkert, MD,PhD, Dallas, TX (*Abstract Co-Author*) Travel support, Varian, Inc; Research Grant, Augmenix, Inc Avneesh Chhabra, MD, Dallas, TX (*Abstract Co-Author*) Consultant, ICON plc; Author with royalties, Wolters Kluwer nv; Author with royalties, Jaypee Brothers Medical Publishers Ltd

#### For information about this presentation, contact:

avneesh.chhabra@utsouthwestern.edu

#### PURPOSE

To evaluate whether radiomic analysis can accurately differentiate benign (BPNST) versus malignant peripheral nerve sheath tumors (MPNSTs), and compare it to the expert radiologist interpretation.

## **METHOD AND MATERIALS**

44 patients with histologically confirmed PNSTs were identified from the institutional electronic data base. Fat suppressed T2W (fsT2W) imaging in isolation and all imaging combined including contrast (mimicking a routine setting) were used for Radiomic analysis and by two experienced musculoskeletal radiologists. Regions of interest (ROIs) corresponding to the tumor boundaries were contoured by a different experienced musculoskeletal radiologist using VelocityTM software (Varian Medical Systems). For system training, volumetric ROIs extracted from fsT2W images of 25 tumors (16 benign, 9 malignant) were used for the proposed Convolutional Neural Network (CNN), which included 7 convolution, 3 max-pooling and 2 fully connected layers. Data augmentation by rotating 3D images and Synthetic Minority Over-sampling technique (SMOTE) were employed to balance and increase training samples. The CNN was tested using 15 unknown tumors and evaluated for accuracy. Following which, two blinded radiologists in two diferent settings- fsT2W images (set 1) and all imaging sequences together (set 2) evaluated the same testing cases into benign versus malignant tumors. The accuracy of the CNN models was compared with radiologists. Statistical tests included Area Under the Curve (AUC) and Fisher's Exact Test.

## RESULTS

The CNN model using fsT2W predicted benign versus malignant among PNSTs with an accuracy and AUC of 87% and 0.89, compared to the accuracy and AUC of 73%, 0.83 and 93%, 0.83 for the radiologists 1 and 2, respectively (p>0.05). The accuracy and AUC of radiologists 1 and 2, and CNN using all sequences including contrast imaging (mirroring the routine setting) was 71%, 0.81 and 71%, 0.70, and 93%, 0.94, respectively.

## CONCLUSION

Radiomic analysis accurately differentiates benign versus malignant PNSTs and may serve as a powerful adjunctive measure during diagnosis of these neoplasms.

# **CLINICAL RELEVANCE/APPLICATION**

Given the morbidity and mortality associated with MPNSTs, the high accuracy of radiomics is likely to be extremely valuable in their diagnostic work-up. Further study with larger cohorts can determine whether radiomics may aid in classification among BPNST subtypes, such as neurofibroma, schwannoma, and perineurioma.

## SSA14-09 Grading of Soft Tissue Sarcoma by Using 3T MR Imaging Texture Analysis

Sunday, Nov. 25 12:05PM - 12:15PM Room: E353C

Participants

Ji Hyun Hong, MD, Seoul, Korea, Republic Of (*Presenter*) Nothing to Disclose Won-Hee Jee, MD, Seoul, Korea, Republic Of (*Abstract Co-Author*) Research Grant, Bayer AG; Chan-Kwon Jung, Seoul, Korea, Republic Of (*Abstract Co-Author*) Nothing to Disclose Joon-Yong Jung, MD, Seoul, Korea, Republic Of (*Abstract Co-Author*) Nothing to Disclose Yohan Son, Seoul, Korea, Republic Of (*Abstract Co-Author*) Nothing to Disclose Seung Han Shin, Seoul, Korea, Republic Of (*Abstract Co-Author*) Nothing to Disclose Yang-Guk Chung, MD, Seoul, Korea, Republic Of (*Abstract Co-Author*) Nothing to Disclose

# For information about this presentation, contact:

whjee12@gmail.com

## PURPOSE

To determine the value of 3T magnetic resonance (MR) imaging texture analysis to differentiate high-grade from low-grade soft tissue sarcoma.

## **METHOD AND MATERIALS**

The institutional review board approved this retrospective study and informed consent was waived. Forty-eight patients with soft tissue sarcoma who had undergone 3T MR imaging including contrast-enhanced (CE) imaging were included in this study. Texture analysis of whole tumor volume on T1- and T2-weighted images and fat-suppressed CE T1-weighted images were performed using Multiparametric toolbox. Histogram features (mean intensity, standard deviation (SD), skewness and kurtosis) and gray-level co-occurrence matrix features (Difference entropy, Difference variance, contrast, entropy) were compared between high-grade (grades 2 and 3) and low-grade (grade 1) soft tissue sarcoma using Mann-Whitney U test. The receiver operating characteristic curves with areas under the curve (AUC) for all parameters were obtained.

#### RESULTS

There were 11 patients with low-grade sarcomas and 37 patients with high-grade sarcomas: grade 2 (n = 10) and grade 3 (n = 27). T1 mean, T2 mean, T1 SD and CE T1 skewness were significantly lower in high-grade than low-grade sarcomas: 510.6 vs 761.3; 637.8 vs 850.0; 90.6 vs 142.9; 0.12 vs 0.63 (P= < .05), respectively. CE T1 mean, T2 skewness and CE T1 Difference variance were significantly higher in high-grade than low-grade sarcomas: 619.0 vs 385.9; 0.404 vs -0.425; 0.232 vs 0.175 (P= < .05), respectively. AUCs of above parameters except T1 mean were over 0.7: 0.725 (95% CI, 0.573-0.876) in T2 mean; 0.752 (95% CI, 0.568-0.936) in CE T1 mean; 0.737 (95% CI, 0.568-0.906) in T1 SD; 0.722 (95% CI, 0.557-0.887) in T2 skewness; 0.722 (95% CI, 0.560-0.885) in CE T1 skewness; 0.706 (95% CI, 0.526-0.887) in CE T1 Difference variance. AUC of T1 mean was 0.698 (95% CI, 0.489-0.907).

## CONCLUSION

Texture analysis based on 3T MR imaging may be reliable to differentiate between high-grade and low-grade soft tissue sarcomas.

# **CLINICAL RELEVANCE/APPLICATION**

MR imaging texture analysis may help predict grade of soft tissue sarcoma.



#### SSA15

# Musculoskeletal (Lower Extremity)

Sunday, Nov. 25 10:45AM - 12:15PM Room: E353B



AMA PRA Category 1 Credits ™: 1.50 ARRT Category A+ Credit: 1.75

#### Participants

Karen C. Chen, MD, Providence, RI (*Moderator*) Nothing to Disclose Matthew D. Bucknor, MD, San Francisco, CA (*Moderator*) Nothing to Disclose

## Sub-Events

# SSA15-01 MRI-Based 3D Models of the Pelvis Can Replace CT-Based 3D Models for Range of Motion Analysis in Femoroacetabular Impingement

Sunday, Nov. 25 10:45AM - 10:55AM Room: E353B

Participants

Florian Schmaranzer, Bern, Switzerland (*Presenter*) Nothing to Disclose Celia Degonda, Bern, Switzerland (*Abstract Co-Author*) Nothing to Disclose Till Lerch, Bern, Switzerland (*Abstract Co-Author*) Nothing to Disclose Jennifer L. Cullmann, Bern, Switzerland (*Abstract Co-Author*) Nothing to Disclose Johannes T. Heverhagen, MD, PhD, Bern, Switzerland (*Abstract Co-Author*) Research Grant, Bracco Group; Research Grant, Guerbet SA; Research Grant, Siemens AG; Speaker, Bayer AG Klaus A. Siebenrock, MD, PhD, Bern, Switzerland (*Abstract Co-Author*) Nothing to Disclose Moritz Tannast, MD, Bern, Switzerland (*Abstract Co-Author*) Nothing to Disclose Guoyan Zheng, PhD, Bern, Switzerland (*Abstract Co-Author*) Nothing to Disclose

# PURPOSE

Although femoroacetabular impingement (FAI) describes a dynamic osseous abutment of the femur against the acetabulum, current standard imaging assessment is static. Recently CT-based impingement analysis was introduced whereas MRI would offer a radiation-free alternative. Thus we asked (1) what is the mean distance between surface points of 3D pelvis models derived from CT/MRI; (2) whether impingement free range of motion correlates between CT and MRI; (3) and whether zones of impingement match for 3D models based on CT and MRI?

#### **METHOD AND MATERIALS**

IRB-approved comparative, retrospective study of 20 symptomatic hips with FAI. 3D CT scans (isovoxel: 1mm3) of the entire pelvis and the distal femoral condyles were obtained. Preoperative MR arthrograms of the hip were obtained including 0.8mm3 isovoxel T1 3D VIBE- and 1mm3 isovoxel 3D T1 VIBE DIXON sequences of the entire pelvis and the distal femoral condyles. Threshold-based manual segmentation was performed using commercial software (AMIRA). Both 3D models were compared with inhouse developed software which includes two specific algorithms for detection of the acetabular rim and for detection of the center of roation. We calculated (1) percentage of the surface points with < 1mm difference between the CT-/MR-based 3D models; (2) assessed correlation of impingement-free range of motion (in: flexion; extension; internal rotation 90° of flexion; external rotation in 90° of flexion; abduction; adduction) between CT and MRI and (3) compared location of impingement zones between CT and MRI using the clock-face system which divides the femur and acetabulum into 12 'hour' positions.

#### RESULTS

(1) 83% and 79% of the surface points of the proximal femur respectively of the acetabulum differed <1mm between the CT-based and MRI-based 3D models. (2) Correlation for the range of motion values was excellent (spearman rho=0.993, p<0.05) between CT and MRI. (3) Location of impingement did not differ between CT-based and MRI-based range of motion analysis in 12/12 acetabular and 11/12 femoral clock-face positions.

#### CONCLUSION

MRI-based 3D models of the pelvis can replace CT-based 3D models for range of motion analysis in femoroacetabular impingement

#### **CLINICAL RELEVANCE/APPLICATION**

3D-MRI based impingement analysis of the hip is a further step towards non-invasive, personalized surgical planning of FAI especially for complex deformities such as abnormal femoral torsion.

# SSA15-02 Does 3DMR Provide Equivalent Information as 3DCT for the Pre-Operative Evaluation of Adult Hip Pain Conditions of Femoroacetabular Impingement and Hip Dysplasia?

Sunday, Nov. 25 10:55AM - 11:05AM Room: E353B

Awards Student Travel Stipend Award

Participants

Kevin Yan, BA, Dallas, TX (*Presenter*) Nothing to Disclose Yin Xi, PhD, Dallas, TX (*Abstract Co-Author*) Nothing to Disclose Chayanit Sasiponganan, Dallas, TX (*Abstract Co-Author*) Nothing to Disclose Joseph S. Zerr, MD, Dallas, TX (*Abstract Co-Author*) Nothing to Disclose Joel Wells, MD,MPH, Dallas, TX (*Abstract Co-Author*) Nothing to Disclose Avneesh Chhabra, MD, Dallas, TX (*Abstract Co-Author*) Nothing to Disclose Avneesh Chhabra, MD, Dallas, TX (*Abstract Co-Author*) Consultant, ICON plc; Author with royalties, Wolters Kluwer nv; Author with royalties, Jaypee Brothers Medical Publishers Ltd

#### For information about this presentation, contact:

Kevin.Yan@UTSouthwestern.edu

## PURPOSE

Femoroacetabular impingement (FAI) and hip dysplasia (HD) are frequently evaluated by isotropic CT (3DCT) for preoperative planning at the expense of radiation. The aim was to determine if isotropic MRI (3DMR) imaging can provide similar quantitative and qualitative morphological information as 3DCT.

## **METHOD AND MATERIALS**

25 consecutive patients with a final diagnosis of FAI or HD were retrospectively selected from December 2016-December 2017. Two readers (R1, R2) performed quantitative angular measurements on 3DCT and 3DMR, blinded to the diagnosis and each other's measurements. 3DMR and 3DCT of the hips were qualitatively and independently evaluated by a radiologist (R3), surgeon (R4), and fellow (R5). Interobserver and intermodality comparisons were performed.

## RESULTS

Quality was good to excellent on all 3DCT and 3DMR reconstructions. The ICC was good to excellent for all measurements between R1 and R2 (ICC: 0.60-0.98) and the majority of intermodality measurements for R1 and R2. Average inter-reader and inter-modality PABAK showed good to excellent agreement for qualitative reads. On CT, all alpha angles (AA) were significantly lower in dysplasia patients than in cam patients (p<0.05). Lateral center-edge angle (LCEA) at the anterior, center, and posterior acetabulum were significantly lower in dysplasia than in cam patients (p<0.05). On MR, AA at 12, 1, and 2 o'clock, and LCEA at center were significantly lower in dysplasia patients than in cam patients (p<0.05).

#### CONCLUSION

Strong interobserver and intermodality correlations of hip morphology suggest that 3DMR has good potential to replace 3DCT and serve as a one-stop modality for bone and soft tissue characterizations in the pre-operative evaluation of FAI and HD.

## **CLINICAL RELEVANCE/APPLICATION**

In patients with symptomatic FAI and HD, 3DMR can replace 3DCT in the pre-operative evaluation, thereby reducing radiation, time, cost, and discomfort for the patients.

# SSA15-03 MR Texture Analysis of Acetabular Subchondral Bone Can Discriminate Between Normal and Cam Positive Hips

Sunday, Nov. 25 11:05AM - 11:15AM Room: E353B

Participants

Taryn Hodgdon, MD, Ottawa, ON (*Presenter*) Nothing to Disclose Rebecca Thornhill, PhD, Ottawa, ON (*Abstract Co-Author*) Nothing to Disclose Gerd Melkus, PhD, Ottawa, ON (*Abstract Co-Author*) Nothing to Disclose Nicholas James, Ottawa, ON (*Abstract Co-Author*) Nothing to Disclose Paul E. Beaule, MD, Ottawa, ON (*Abstract Co-Author*) Nothing to Disclose Kawan S. Rakhra, MD, Ottawa, ON (*Abstract Co-Author*) Nothing to Disclose

### PURPOSE

To assess whether texture analysis of acetabular subchondral bone on MRI can differentiate between normal and cam positive hips.

#### **METHOD AND MATERIALS**

IRB-approved, retrospective case-control study analyzing MR images in subjects with and without cam morphology of the proximal femur (n=68: 19 controls, 25 asymptomatic cam and 24 symptomatic cam-FAI). All subjects underwent unilateral 1.5T hip MRI. The acetabular subchondral bone was contoured manually as a volume of interest (VOI) on sagittal PD images. 3D histogram and second order texture features were evaluated for the global acetabular VOI for each subject using MaZda (v4.6). Differences between controls and asymptomatic or symptomatic cam hips were explored using Mann-Whitney U tests with post-hoc Bonferroni correction. Intra-acetabular variations in texture were assessed by subdividing each VOI into anterior and posterior segments in the sagittal plane and into medial, middle, and lateral segments in the coronal plane, generating 6 ROIs. Between groups and within-subjects differences in texture features were assessed using mixed model ANOVAs. Features were used to train a series of gradient boosted regression trees; for each, 500 hyperparameter configurations were selected at random. 10-fold, stratified cross-validation was then performed and the accuracy of the 10 forests for identifying cam positive hips was averaged.

#### RESULTS

Both asymptomatic and symptomatic cam-FAI hips demonstrated higher gray-level variance and lower kurtosis compared to controls (p=0.003 for each). Gray-level co-occurrence features f3, f4, and f7 were significantly higher in cam positive hips compared to controls (p=0.003 for each). Sub-region analysis revealed no significant interactions between subject group and ROI. The post-validation classification accuracy achieved by each gradient boosted tree model was 72% (control vs asymptomatic) and 79% (control vs symptomatic cam-FAI).

## CONCLUSION

Texture features extracted from MRI can detect subtle differences in subchondral bone architecture between controls and cam positive hips, regardless of patient symptom status.

#### **CLINICAL RELEVANCE/APPLICATION**

The texture profile of acetabular subchondral bone in cam positive hips is significantly different from controls in all regions. This suggests there are extra-articular structural changes occurring globally within the acetabular subchondral bone of patients with cam morphology regardless of symptom status.

## SSA15-04 Postoperative, Traction MR Arthrography in Patients with Persisting Pain After Hip Arthroscopy for FAI Reveals Unexpected High Prevalence of Osseous Deformities and Intra-Articular Lesions Due to Under-/ or Overcorrection

Sunday, Nov. 25 11:15AM - 11:25AM Room: E353B

Participants

Florian Schmaranzer, Bern, Switzerland (*Presenter*) Nothing to Disclose Till Lerch, Bern, Switzerland (*Abstract Co-Author*) Nothing to Disclose Markus Hanke, Bern, Switzerland (*Abstract Co-Author*) Nothing to Disclose Klaus A. Siebenrock, MD, PhD, Bern, Switzerland (*Abstract Co-Author*) Nothing to Disclose Moritz Tannast, MD, Bern, Switzerland (*Abstract Co-Author*) Nothing to Disclose Petr Vavron, St. Johann in Tirol, Austria (*Abstract Co-Author*) Nothing to Disclose Benjamin Henninger, MD, Innsbruck, Austria (*Abstract Co-Author*) Nothing to Disclose Ehrenfried Schmaranzer, St. Johann in Tirol, Austria (*Abstract Co-Author*) Nothing to Disclose

#### PURPOSE

Numbers of hip arthroscopies for FAI correction have risen exponentially, leading to an increase of patients with persistent pain who undergo postoperative MR imaging. To assess prevalence of new/residual (1) osseous deformities, (2) intra-articular lesions and (3) progression of osteoarthritis in symptomatic patients undergoing pre- and postoperative MR imaging after hip arthroscopy.

#### **METHOD AND MATERIALS**

IRB-approved, retrospective study. Between 2010-17, 806 patients underwent arthroscopic FAI correction and/or labrum surgery. Database was reviewed for symptomatic patients with complete radiographs and traction MR arthrography (MRA) of the hip (1.5 T) obtained before and after hip arthroscopy according to the routine protocol. 49 patients were included: mean age  $29 \pm 10$  years, 67% female. Traction was applied using a MR-compatible traction device with weight-adaption. One reader assessed pre- and postoperative images. (1) Acetabular coverage (LCE<25° = dysplasia, LCE>39° = pincer deformity) and Tönnis osteoarthritis (OA) grade were assessed on AP pelvic views. Cam deformity was defined (a>60°) on radial MR images. Femoral torsion measurements were only available for postoperative MRI (low/high torsion: <5°/>30°). (2) Presence of residual tears-, retears of the labrum, capsular adhesions/defects was assessed on traction MRA. (3) OA progression on traction MRA was defined as new acetabular/femoral cartilage lesions and osteophytes formation.

# RESULTS

(1) Preoperatively 42 (86%) hips showed deformities: 2 (4%) dysplastic-, 11 (22%) pincer- and 39 (80%) cam deformities. Postoperatively 39 (80%) hips showed deformities; 9 (18%) dysplastic-, 8 (16%) pincer-, 20 (41%) cam deformity, 4 (8%) hips with torsion <5°, 10 (20%) hips with torsion >30°. (2) Postoperatively 14 (29%) cases with residual-, 12 (24%) cases with labrum retears were observed. 6 (12%) hips had capsular adhesions, 22 (45%) had capsular defects. (3) Radiographic OA progression was observed in 5 (10%) hips, in 14 (30%) hips on traction MRA.

#### CONCLUSION

Prevalence of osseous deformities due to over- or undercorrection and intra-articular lesions is high after failed hip arthroscopy. Traction MRA was useful for detection of OA progression.

#### **CLINICAL RELEVANCE/APPLICATION**

Identification of osseous over-/undercorrection after failed hip arthroscopy is essential because open surgical approaches must be considered for correction of dysplasia and abnormal femoral torsion.

## SSA15-05 Comparison of Lateral Centre Edge Angle and Sourcil Angle Measurements on "Ghost" 3D Volume Rendered CTs and Plain Radiographs

Sunday, Nov. 25 11:25AM - 11:35AM Room: E353B

#### Awards

#### **Student Travel Stipend Award**

Participants Madhvi Patel, BSC, MBBS, London, United Kingdom (*Presenter*) Nothing to Disclose Martin Siebachmeyer, London, United Kingdom (*Abstract Co-Author*) Nothing to Disclose Myriam Guessoum, London, United Kingdom (*Abstract Co-Author*) Nothing to Disclose Jonathan Hutt, London, United Kingdom (*Abstract Co-Author*) Nothing to Disclose Nikolaos Papadakos, Tooting, United Kingdom (*Abstract Co-Author*) Nothing to Disclose

#### For information about this presentation, contact:

madhvi.patel@stgeorges.nhs.uk

## PURPOSE

Comparison of lateral centre edge angle and sourcil angle measurements on "Ghost" 3D volume rendered CTs and plain radiographs.

## **METHOD AND MATERIALS**

A retrospective single-centre observational study evaluating the degree of agreement between measurements of lateral centre edge angle on CT and plain radiographs in 50 hips. Measurements of LCEA and sourcil angle were made on AP radiographs and 'Ghost' CT. All patients who were under orthopaedic investigation for femoro-acetabular impingement, had both a pelvic radiograph

and CT of at least one hip were included. Patients with severe anatomic deformity or those who were post-operative were excluded from the study. A paired sample t-test was performed to determine if there was a significant difference between measurements on plain radiograph and 'Ghost' CT, with the null hypothesis stating no significant difference.

## RESULTS

On plain film the mean of the LCEA was 31.60, standard deviation = 8.254; and on CT "Ghost" images the mean LCEA was 30.96, standard deviation = 8.315 (paired t-test: p < .002). The confidence interval is 0.25 to 1.03. On plain film the mean of the Sourcil angle was 6.20, standard deviation = 4.848; and on CT "Ghost" images the mean of LCEA was 6.76, standard deviation = 4.841 (paired t-test: p < .016). The confidence interval is -1.19 to -1.17. The results show that there is a statistical difference between measurements of LCE and sourcil angles made on plain radiographs and CT, but the confidence interval is small. We can be 95% sure that the true mean angle lies within a range of 1.28 degrees for lateral centre edge angle and a range of 0.02 degrees for the sourcil angle.

## CONCLUSION

Although there is a statistical difference between measurements of LCE and sourcil angles made on plain radiographs and "Ghost" CT the narrow confidence interval infers that the difference is actually quite small and in clinical practice this would be clinically insignificant. This would preclude the need for plain radiographs and reduce the radiation dose in young patients who ultimately require CT imaging as part of their femoro-acetabular impingement workup.

## **CLINICAL RELEVANCE/APPLICATION**

Measurements of LCEA and sourcil angles on 'Ghost CT' are clinically indifferent and can be used to preclude the need for plain radiographs in the work up of FAI in young patients with hip pain.

## SSA15-06 The Puck Stops Here: An Adaptive Response of the Hip Observed with MRI and Unique to Super External Rotators

Sunday, Nov. 25 11:35AM - 11:45AM Room: E353B

Participants

Matthew Bober, MD, Philadelphia, PA (*Presenter*) Nothing to Disclose Adam C. Zoga, MD, Philadelphia, PA (*Abstract Co-Author*) Nothing to Disclose

For information about this presentation, contact:

matthew.bober@jefferson.edu

#### PURPOSE

Overhead athletes rely on extreme ranges of motion to excel in their respective fields, leading to structural changes including capsular and osseous overgrowth, which in turn contribute to overuse lesions including SLAP and unique impingement syndromes. Super external hip rotators, in particular hockey goalies, similarly rely on tremendous ranges of motion to excel at their avocation. We sought to compare hip capsule thickness in hockey goalies with age and gender matched controls in order to describe MRI findings of adaptive response of the hip.

## METHOD AND MATERIALS

Retrospective cohort study examining the hip capsule thickness of hockey goalies with other male athletes aged matched at 20-30 years. Capsule thickness was used as a marker for adaptive response at the hip as this was described previously with adaptive response in the shoulder. Power analysis was performed and determined that a sample size of 17 was selected for each group. Measurements were performed at the anterior, middle, and posterior capsule regions on coronal non-fat saturated T1 MRI images at the level of the femoral head and neck. A two tailed t-test was then conducted to analyze the two groups.

#### RESULTS

The hip capsule was statistically thicker in super external rotators at each region when compared with other age matches athletic males. The average capsule thickness at the femoral head in the control group ranged from 8 - 9 mm and in the goalies group from 10 - 12 mm (p values ranged from 0.001 and 0.007). At the femoral neck, the control group capsule thickness was between 11 - 13 mm compared to 16 - 18 mm for the super external rotators (p-values between 0.002 and 0.01).

## CONCLUSION

Hip super external rotating hockey goalies have a thicker hip capsule than their age and gender matched controls at both the level of the femoral head and neck.

#### **CLINICAL RELEVANCE/APPLICATION**

Hip super external rotators adapt with capsular thickening, which may predispose to hip pathology known to be prevalent in such athletes such as femoroacetabular impingement, labral tears, and early osteoarthritis. This adaptive hip capsular thickening should be observed at MRI, and should be correlated with other pathologies on a larger scale with a goal of prevention and early intervention.

# SSA15-07 Diagnostic Performance of Magnetic Resonance Imaging in Detecting Syndesmotic Injuries: A Meta-Analysis

Sunday, Nov. 25 11:45AM - 11:55AM Room: E353B

Participants

Delaram Shakoor, MD, Baltimore, MD (Presenter) Nothing to Disclose

Lew Schon, MD, Baltimore, MD (*Abstract Co-Author*) Royalties, DJO, LLC; Royalties, Arthrex, Inc; Royalties, DARCO International, Inc; Royalties, Gerson Lehrman Group, Inc; Royalties, Zimmer Biomet Holdings, Inc; Royalties, Reed Elsevier; Speakers Bureau, Tornier, Inc; Speakers Bureau, Zimmer Biomet Holdings, Inc; Speakers Bureau, BioMimetic Therapeutics, Inc; Consultant, Zimmer Biomet Holdings, Inc; Consultant, BioMimetic Therapeutics, Inc; Consultant, Guidepoint Global, LLC; Consultant, Gerson Lehrman Group, Inc; Consultant, Tornier, Inc; Consultant, Wright Medical Technology, Inc; Consultant, Royer Medical, Inc; Consultant, Carestream Health, Inc; Stockholder, Tornier, Inc; Stockholder, Royer Medical, Inc; Stockholder, Bioactive Surgical, Inc; Stockholder, HealthpointCapital; Research support, Royer Medical, Inc; Research support, Zimmer Biomet Holdings, Inc; Research support, Tornier, Inc; Research support, Arthrex, Inc; Research support, SpineSmith LP; Research support, BioMimetic Therapeutics, Inc; Support, Bioactive Surgical, Inc; Support, Educational Concepts in Medicine, LLC; Support, Smith & Nephew plc; Support, OrthoHelix Surgical Designs, Inc; Support, Chesapeake Surgical Biocomposites; Support, Olympus Corporation; Support, Omega Surgical Instruments Ltd

Cesar de Cesar Netto, Baltimore, MD (*Abstract Co-Author*) Consultant, Cuervebeam; Stock Options, Cuervebeam; Consultant, Ossio Greg Osgood, Baltimore, MD (*Abstract Co-Author*) Grant, Carestream Health, Inc

Barbar Shafiq, Baltimore, MD (Abstract Co-Author) Nothing to Disclose

James R. Ficke, Baltimore, MD (Abstract Co-Author) Nothing to Disclose

Sahar Jalali-Farahani, MD, MPH, Philadelphia, PA (Abstract Co-Author) Nothing to Disclose

Shadpour Demehri, MD, Baltimore, MD (Abstract Co-Author) Research support, General Electric Company ; Research Grant, Carestream Health, Inc; Consultant, Toshiba Corporation

## For information about this presentation, contact:

sdemehr1@jhmi.edu

## PURPOSE

Distal tibiofibular syndesmotic injuries are common and occur in association with ankle sprains and ankle fractures. There are conflicting reports in the literature regarding the diagnostic performance of magnetic resonance (MR) imaging in detecting these injuries. Therefore, in this meta-analysis we intend to determine diagnostic performance of MR-imaging in detecting syndesmotic injuries, using open or arthroscopic surgery as the standard of reference.

# **METHOD AND MATERIALS**

A comprehensive literature search (until March 2018) was performed and original research studies reporting diagnostic performance of MRI and MR arthrography (MRA) in detecting syndesmotic injuries were included. Pooled values of sensitivity and specificity were calculated using fixed or random effect models based on the level of heterogeneity.

#### RESULTS

Out of 421 identified records, seven studies (309 MRI examinations) were included. Two studies (65 ankles) also reported the results of indirect MRA (iMRA) while other two studies (53 ankles) reported the results of direct MRA. There was no publication bias according to Deeks funnel plot asymmetry test (P=0.2) and meta-funnel. Pooled values of sensitivity were 89% [95% confidence interval (CI): 84%-94%] for non-enhanced MRI, 91% (CI: 79%-98%) for iMRA and 92% (CI: 73%-99%) for MRA. Pooled values of specificity of MRI, iMRA and MRA were 88% (CI: 82%-93%), 91% (CI: 82%-96%) and 67% (CI: 35%-90%), respectively. High degree of heterogeneity was observed in all modalities (I2 >50%). Comparing diagnostic odds ratios (DOR) of MRI with iMRA yielded no significant result (relative DOR (rDOR):0.41, P=0.5). No significant difference was observed between DORs of MRI and MRA (rDOR: 1.76, P=0.4). There was no significant difference between DORs of iMRA and MRA (rDOR: 7.69, P=0.2).

## CONCLUSION

MRI, iMRA and MRA can accurately detect syndesmotic injuries. The specificity of MRA appeared to be lower when compared to MRI and iMRA.

# **CLINICAL RELEVANCE/APPLICATION**

With high diagnostic performance of conventional non-enhanced MRI, using intravenous or intraarticular gadolinium may not improve the diagnostic performance of MRI examinations.

# SSA15-08 Scanned versus Fused-Reconstructed Oblique MR-Images for Assessment of the Ankle Syndesmosis: Diagnostic Performance and Reader Agreement

# Sunday, Nov. 25 11:55AM - 12:05PM Room: E353B

Participants

Peter Dankerl, MD, Erlangen, Germany (*Presenter*) Nothing to Disclose Hannes Seuss, Erlangen, Germany (*Abstract Co-Author*) Nothing to Disclose Matthias Hammon, MD,PhD, Erlangen, Germany (*Abstract Co-Author*) Nothing to Disclose Frank W. Roemer, MD, Erlangen, Germany (*Abstract Co-Author*) Officer, Boston Imaging Core Lab, LLC; Research Director, Boston Imaging Core Lab, LLC; Shareholder, Boston Imaging Core Lab, LLC Rafael Heiss, Erlangen, Germany (*Abstract Co-Author*) Speakers Bureau, Siemens AG Manuel Schmidt, MD, Erlangen, Germany (*Abstract Co-Author*) Nothing to Disclose Alexander Cavallaro, MD, Erlangen, Germany (*Abstract Co-Author*) Nothing to Disclose Rolf Janka, MD, PhD, Erlangen, Germany (*Abstract Co-Author*) Nothing to Disclose Michael Uder, MD, Erlangen, Germany (*Abstract Co-Author*) Speakers Bureau, Bracco Group Speakers Bureau, Siemens AG Speakers Bureau, Bayer AG Research Grant, Siemens AG

## For information about this presentation, contact:

peter.dankerl@uk-erlangen.de

## PURPOSE

To evaluate the diagnostic performance and reader agreement of a novel image reconstruction method enabling fusion of standard two-dimensional transversal and coronal images into oblique images for the assessment of the ankle syndesmosis.

# METHOD AND MATERIALS

We evaluated 40 magnetic resonance imaging examinations of patients with ankle sprains (16 with ruptures and 24 without) for the presence of anterior inferior tibiofibular ligament rupture. For all patients, an oblique-fusion reconstruction (OFR) was created in comparable fashion to the scanned oblique proton density weighted turbo spin echo (PDwTSE) sequence. Image reconstruction was performed with dedicated software enabling image fusion from standard transversal 3 mm PDwTSE and coronal sequences with fat suppression. The resulting fused images were used as the source for the reconstruction of OFR images. To evaluate diagnostic

performance, three readers with different levels of experience independently read the scanned images once and the fused images twice. We analyzed sensitivity, specificity, negative and positive predictive values, accuracy and agreement.

# RESULTS

The experienced reader misinterpreted one OFR as false negative, demonstrating a sensitivity of 0.97 and specificity of 1.00. The intermediate reader had perfect accuracy. The inexperienced reader diagnosed two false positive ruptures (specificity: 0.92) in his first, and missed three ruptures (sensitivity: 0.81) in his second read. No differences were significant. Intrareader agreement was 0.95, 1.00 and 0.74 and interreader agreement was 0.90.

## CONCLUSION

The proposed OFR enables reliable detection of anterior inferior tibiofibular ligament rupture with excellent inter- and intrareader agreement, making conventional scanning of oblique images redundant.

# **CLINICAL RELEVANCE/APPLICATION**

Presented method enables the creation of additional MRI sequences in a totally different orientation from routine 2D images. Thereby scanning of e.g. oblique images is redundant and MRI scanning time - in our case 28% can be saved.

# SSA15-09 Tarsal Coalition and the Accessory Anterolateral Facet

Sunday, Nov. 25 12:05PM - 12:15PM Room: E353B

Participants

Mashya T. Abbassi, MD, Richmond, VA (*Presenter*) Nothing to Disclose Josephina A. Vossen, MD, PhD, Richmond, VA (*Abstract Co-Author*) Nothing to Disclose Peter J. Haar, MD, PhD, Richmond, VA (*Abstract Co-Author*) Nothing to Disclose Kevin B. Hoover, MD, PhD, Richmond, VA (*Abstract Co-Author*) Nothing to Disclose

# PURPOSE

The accessory anterolateral talar facet (AALTF) is an anatomic variant that can cause peroneal spastic flatfoot in adolescents and accessory talar facet impingement (ATFI) in adults. The purpose of this study was to assess the relationship between AALTF and tarsal coalitions.

# METHOD AND MATERIALS

Retrospective analysis of consecutive patients undergoing MRI ankle over a 2-year period (01/2014 to 12/2015) at our institution was performed. This study received IRB approval and complied with HIPAA guidelines. We reviewed MRIs for presence of AALTF and tarsal coalition. The criteria for identifying AALTF on MRI was facet articulation spreading contiguously from the posterior facet of the talus anterior to the lateral process of the talus. Presence of a tarsal coalition was assessed using MRI, allowing differentiation between types of coalition (cartilaginous, fibrous and osseous). Exclusion criteria were prior surgery, recent trauma, or abnormalities preventing visualization of the talocalcaneal joint.

# RESULTS

Of the 391 patients (137 men, 254 women; mean age 45 years) included in this study, 3.6% (14/391) had an AALTF. Of these patients, 29% (4/14) had a tarsal coalition, of which 3 were talocalcaneal (1 osseous, 1 fibrous and 1 cartilaginous) and 1 was calcaneonavicular (fibrous). Of the patients without an AALTF, 2% (9/377) had a tarsal coalition, of which 7 were calcaneonavicular (4 fibrous and 3 cartilaginous), 2 were talocalcaneal (1 osseous, 1 fibrous). One-tailed chi-square tests of independence with Yates correction and odds ratio (OR) calculations were performed to examine the relation between the AALTF and the presence of a tarsal coalition. For the relationship between AALTF and tarsal coalition,  $\chi 2 = 21.2$  (df, 1; n = 391; p < 0.0001; OR 16.3; 95% CI, 4.3-62.1).

## CONCLUSION

Our study showed a significant relationship between the presence of an AALTF and tarsal coalition. Our findings indicate that MRI is a valuable test for identifying comorbid findings of AALTF in patients.

## **CLINICAL RELEVANCE/APPLICATION**

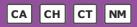
The accessory anterolateral talar facet (AALTF) is an anatomic variant that can cause peroneal spastic flatfoot and accessory talar facet impingement (ATFI). Our study showed a significant relationship between the presence of an AALTF and tarsal coalition. Patients undergoing resection for tarsal coalition should be evaluated for AALTF, in order to improve pre-operative planning and postsurgical outcome.



#### SSA16

Nuclear Medicine (Chest and Cardiovascular Nuclear Imaging)

Sunday, Nov. 25 10:45AM - 12:15PM Room: S505AB



AMA PRA Category 1 Credits ™: 1.50 ARRT Category A+ Credit: 1.75

#### Participants

Ukihide Tateishi, MD,PhD, Tokyo, Japan (*Moderator*) Nothing to Disclose Phillip J. Koo, MD, Phoenix, AZ (*Moderator*) Advisory Board, Bayer AG; Advisory Board, Johnson & Johnson; ; ; ;

## Sub-Events

# SSA16-01 Association Between Asynchrony and Stenoses in Apparently Normal Coronary Arteries

Sunday, Nov. 25 10:45AM - 10:55AM Room: S505AB

Participants

Andrew Van Tosh, MD, Roslyn, NY (*Abstract Co-Author*) Grant, Astellas Group David Cooke, Atlanta, GA (*Abstract Co-Author*) Royalties, Syntermed, Inc Christopher J. Palestro, MD, New Hyde Park, NY (*Abstract Co-Author*) Nothing to Disclose Kenneth Nichols, PhD, New Hyde Park, NY (*Presenter*) Royalties, Syntermed, Inc;

For information about this presentation, contact:

knichols@northwell.edu

#### PURPOSE

Left ventricular (LV) arteries are considered abnormal if stenosis > 70%, but lesser stenoses may be concerning. Our study was undertaken to determine the % of cases in which stenoses are < 70% & perfusion images suggest apparently normal (ApNI) arteries, yet myocardial flow reserve (MFR) is abnormally low, & whether PET parameters predict magnitude of stenosis.

#### **METHOD AND MATERIALS**

Data were analyzed of 105 pts evaluated by Rb-82 rest/regadenoson-stress PET/CT & arteriography, which measured % stenoses. Global ejection fractions (EFs) & regional summed stress score (SSS) & summed rest score (SRS) of relative myocardial perfusion were assessed. Rest & stress systolic & diastolic asynchrony (Asynch) was assessed by a medical imaging physicist who visually scored phase histograms & phase polar maps within a coronary territory using a 5-point scale (0 = normal to 4 = markedly asynchronous extensive territory), based on phase polar maps being out of phase from expected contraction patterns of normal pts. Absolute myocardial blood flow (MBF) was quantified from rebinned first pass dynamic transit images of the Rb-82 bolus injection through the heart chambers, with myocardial flow reserve (MFR) computed as stress-MBF/rest-MBF. ApNI arteries were defined as those with SRS < 4 & SSS < 4 & stenosis < 70%. Following convention, abnormal regional MFR was defined as < 2.0.

#### RESULTS

Among 315 arteries, 174 had undetectable stenosis, 72 ranged from 25-69% & 69 ranged from 70-100%. Among all arteries, 162 were ApNI with higher MFR than the other 153 arteries ( $2.65\pm1.34$  versus  $1.96\pm1.26$ , p < 0.0001). Nonetheless, 35% (56/162) of ApNI arteries had abnormally low MFR < 2.0 (mean =  $1.50\pm0.31$ ). For all arteries, magnitude of % stenosis was most strongly associated with magnitude of Asynch (r = 0.50, p < 0.0001), & significantly associated with stress MBF (r = -0.25, p < 0.0001), SSS (r = 0.24, p < 0.0001), SRS (r = 0.17, p = 0.002), & MFR (r = -0.18, p = 0.002). For ApNI arteries, % stenosis was associated with magnitude of Asynch (r = 0.34, p < 0.0001).

#### CONCLUSION

In arteries that are apparently normal by relative perfusion assessment & by conventional arteriographic criteria, MFR can nonetheless by abnormally low, with stenoses < 70% associated with regional asynchrony.

# **CLINICAL RELEVANCE/APPLICATION**

It is advisable to measure regional MFR & regional asynchrony for pts with suspected CAD.

# SSA16-02 Evaluation of Role of F-18 FDG Cardiac PET and Tc-99m Sestamibi Myocardial Perfusion Imaging in Assessing the Therapeutic Benefit in Patients with Coronary Artery Disease and Left Ventricular Systolic Dysfunction

Sunday, Nov. 25 10:55AM - 11:05AM Room: S505AB

Participants

Ankur Pruthi, New Delhi, India (*Abstract Co-Author*) Nothing to Disclose Ritu Verma, New Delhi, India (*Presenter*) Nothing to Disclose Harsh Mahajan, MD, MBBS, New Delhi, India (*Abstract Co-Author*) Nothing to Disclose Vidur Mahajan, MBBS, New Delhi, India (*Abstract Co-Author*) Nothing to Disclose Ethel S. Belho, New Delhi, India (*Abstract Co-Author*) Nothing to Disclose

## For information about this presentation, contact:

vidur@mahajanimaging.com

#### PURPOSE

To evaluate the therapeutic benefit with revascularization and optimal medical treatment (OMT) in patients diagnosed with hibernating myocardium on myocardial perfusion imaging (MPI) using F-18 FDG cardiac PET

## **METHOD AND MATERIALS**

59 consecutive patients (43 males, 16 females, Mean Age  $60.7 \pm 9.4$  years) with CAD and LV systolic dysfunction who underwent myocardial viability imaging for revascularization work-up and were diagnosed with hibernating myocardium were enrolled in this study. Patients were later treated with either revascularization or OMT and were followed for a median duration of 7.7 months for assessing the therapeutic benefit. Therapeutic benefit was assessed under 3 categories (a) Improvement in functional class (b) Adverse cardiac-events and (c) Improvement in LV function and myocardial perfusion on follow-up resting 99mTc-sestamibi myocardial perfusion imaging.

## RESULTS

29 patients underwent revascularization (49%) and 25 patients received OMT (42%). Five patients were lost to follow-up. Patients were matched for baseline characteristics in both treatment arms. On follow-up, significant improvement was noted in NYHA functional class and CCS angina class post-revascularization. No such improvement was noted in the OMT group. The cardiac-event rate of patients in OMT group was significantly higher than that of patients in revascularization group (36% vs. 10.3 %; p = 0.046). At 1 year of follow-up, event-free survival in revascularization group was significantly superior compared to OMT group (83.8% vs. 50.8%; p = 0.039). On follow-up resting MPI scan, mean improvement in LVEF in revascularization group was significantly higher than in OMT group (6.0% vs. 1.4%; p=0.04).

#### CONCLUSION

Myocardial viability imaging is a sensitive modality to identify hibernating myocardium in patients with CAD and LV dysfunction and predicting its recovery following revascularization, thereby guiding the optimal treatment strategy for these patients.

## **CLINICAL RELEVANCE/APPLICATION**

Myocardial viability imaging should be performed prior to revascularization in patients with coronary artery disease with leftventricular dysfunction to help predict recovery post-treatment.

## SSA16-03 A Comparative Analysis of Myocardial Perfusion on Gated SPECT versus Coronary Atherosclerosis and Calcium Score on 64-Slice CT

Sunday, Nov. 25 11:05AM - 11:15AM Room: S505AB

Participants

Parul Mohan, MBBS, MD, New Delhi, India (*Abstract Co-Author*) Nothing to Disclose Harsh Mahajan, MD, MBBS, New Delhi, India (*Presenter*) Nothing to Disclose Upendra Kaul, MBBS, MD, New Delhi, India (*Abstract Co-Author*) Nothing to Disclose

## For information about this presentation, contact:

drparulmohan@gmail.com

#### PURPOSE

The aim of the current study was to compare the results of 64-slice CT and gated SPECT on a regional basis (per vessel distribution territory) in patients with known or suspected CAD.

## METHOD AND MATERIALS

Three hundred and seventy five patients underwent both gated SPECT for myocardial perfusion imaging and 64-slice CT for coronary calcium scoring and coronary angiography. The coronary calcium score was determined for each coronary artery. Coronary arteries on multislice CT angiography were classified as having no CAD, insignificant stenosis (<50% luminal narrowing), significant stenosis, or total or subtotal occlusion (>90% luminal narrowing).Gated SPECT findings were classified as normal or abnormal (reversible or fixed defects) and were allocated to the territory of one of the various coronary arteries.

#### RESULTS

In coronary arteries with a calcium score of 10 or less, the corresponding myocardial perfusion was normal in 96 %. In coronary arteries with extensive calcifications (score > 400), the percentage of vascular territories with normal myocardial perfusion was lower, 48%. Similarly, in most of the normal coronary arteries on 64-slice CT angiography, the corresponding myocardial perfusion was normal on SPECT in >94%. In contrast, the percentage of normal SPECT findings was significantly lower in coronary arteries with obstructive lesions (<57%) or with total or subtotal occlusions (<10%) (P < 0.01). Nonetheless, only 42% of vascular territories with normal perfusion corresponded to normal coronary arteries on multislice CT angiography, whereas insignificant and significant stenosis were present in, respectively, 40% and 18% of corresponding coronary arteries.

# CONCLUSION

Although a relationship exists between the severity of CAD on multislice CT and myocardial perfusion abnormalities on SPECT, analysis on a regional basis showed only moderate agreement between observed atherosclerosis and abnormal perfusion. Accordingly, 64-slice CT and gated SPECT provide complementary rather than competitive information, and further studies should address how these two modalities can be integrated to optimize patient management.

## **CLINICAL RELEVANCE/APPLICATION**

Accordingly, 64-slice CT and gated SPECT provide complementary rather than competitive information.

# SSA16-04 The Association of Carotid Plaque 18F-FDG and 18F-Naf Uptake on PET Scan with Symptomatic Carotid Artery Disease: A Systematic Review and Meta-Analysis

Sunday, Nov. 25 11:15AM - 11:25AM Room: S505AB

Participants Salama Chaker, New York, NY (*Presenter*) Nothing to Disclose Khalid Al-Dasuqi, MD, New York, NY (*Abstract Co-Author*) Nothing to Disclose Hediyeh Baradaran, MD, New York, NY (*Abstract Co-Author*) Nothing to Disclose Michelle Demetres, New York, NY (*Abstract Co-Author*) Nothing to Disclose Diana Delgado, MS, New York, NY (*Abstract Co-Author*) Nothing to Disclose Ajay Gupta, MD, New York, NY (*Abstract Co-Author*) Nothing to Disclose

For information about this presentation, contact:

mhc2002@qatar-med.cornell.edu

#### PURPOSE

We sought to investigate the ability of 18F-FDG and 18F-NaF PET imaging to identify vulnerable carotid plaques and predict stroke recurrence in the setting of recent cerebrovascular accidents by performing a systematic review.

# METHOD AND MATERIALS

We performed this study according to the Meta-Analysis of Observational Studies in Epidemiology (MOOSE) group and the Preferred Reporting Items for Systematic Reviews and Meta-Analyses (PRISMA) statement guidelines. We performed a systematic review of Ovid MEDLINE, Ovid EMBASE, and the Cochrane Library Databases yielding a total of 4,144 unique articles for screening after deduplication. These were screened for peer-reviewed journal articles that examined the association between carotid plaque tracer uptake and recent or future ischemic events such as strokes, transient ischemic attacks and retinal artery embolisms. Screened articles were then adjudicated as meeting inclusion criteria by two independent readers.

#### RESULTS

Fourteen articles were included for subsequent analysis. Of those, 11 articles analyzed 18F-FDG uptake in recently symptomatic carotid arteries as compared to asymptomatic carotid arteries. Two of these studies analyzed 18F-NaF uptake as well. The remaining 3 articles investigated the risk of stroke recurrence associated with 18F-FDG uptake. The existing literature demonstrates significant heterogeneity in the PET protocols, reported tracer uptake metrics, and thresholds for positive uptake.

## CONCLUSION

Our systematic review revealed a growing body of literature supporting 18F-FDG's utility in predicting future stroke recurrence and its modest ability in discerning symptomatic from asymptomatic carotid plaques. Additional studies are needed to elucidate the role of 18F-NaF as compared to 18F-FDG imaging. Further work is needed to define more standardized approaches for PET image acquisition and imaging analysis in order to improve the generalizability of this technique to detect high-risk carotid plaques.

## **CLINICAL RELEVANCE/APPLICATION**

Carotid atherosclerosis is responsible for 15% of ischemic strokes. Further work is needed to investigate the utility of 18F-FDG and 18F-NaF PET imaging in detecting high-risk carotid plaques.

## SSA16-05 Provider Utilization Trends for Elective Myocardial Perfusion Imaging

Sunday, Nov. 25 11:25AM - 11:35AM Room: S505AB

Participants

Sarah I. Kamel, MD, Philadelphia, PA (*Presenter*) Nothing to Disclose Charles M. Intenzo, MD, Philadelphia, PA (*Abstract Co-Author*) Nothing to Disclose Laurence Parker, PhD, Philadelphia, PA (*Abstract Co-Author*) Nothing to Disclose David C. Levin, MD, Philadelphia, PA (*Abstract Co-Author*) Consultant, HealthHelp, LLC; Board Member, Outpatient Imaging Affiliates, LLC

## For information about this presentation, contact:

sarah.kamel@jefferson.edu

## PURPOSE

To analyze trends in performance of elective stress nuclear myocardial perfusion imaging (MPI) modalities in the Medicare population.

## METHOD AND MATERIALS

The nationwide Medicare Part B fee-for-service databases for 2004-2016 were reviewed. CPT codes relevant to stress MPI were selected: planar and single photon emission computed tomography (SPECT), and positron emission computed tomography (PET). The databases indicate procedure volume for each code, and these were used to calculate utilization rates per 1,000 Medicare beneficiaries. Elective MPI exams were identified by using place-of-service codes for private offices and hospital outpatient departments (HOPDs). The specialty of the performing physician was determined using Medicare physician specialty codes. Because the Medicare Part B databases are complete population counts, sample statistics are not required.

#### RESULTS

Elective standard (STD) MPI (both planar imaging and SPECT) utilization peaked in 2006 at 74 studies per 1,000 beneficiaries and then progressively decreased to 45 by 2016 (-36%). In 2004, cardiologists' share of elective STD MPI had been 79%, and this steadily increased in subsequent years to 87% in 2016. Cardiologists perform elective STD MPI mostly in private offices where

utilization peaked in 2008 at 50 studies per 1,000 and then declined to 22 in 2016 (-56%). In HOPDs, utilization by cardiologists has increased over the period of the study from 7 studies to 15 (+120%). Utilization in private offices and HOPDs by radiologists has declined from 13 in 2004 to 6 in 2016 (-58%). Elective PET MPI, less frequently used at 3 studies per 1,000 in 2016, maintained an overall net upward trend since 2005, and most of this growth reflected increasing use by cardiologists (90% share in 2016).

## CONCLUSION

In the Medicare population, the overall use of elective STD MPI is declining, however cardiologists are performing an increasing market share in the outpatient setting. A shift in place-of-service has been noted with fewer studies performed in private offices and increasing numbers performed in HOPDs. PET MPI utilization, while still not widespread, has grown over the period of the study, reflecting an increasing use by cardiologists.

## **CLINICAL RELEVANCE/APPLICATION**

Cardiologists maintain an increasing share in utilization of elective standard and PET MPI.

#### SSA16-06 Medium and Large Vessel Vasculitis: Recognizing Patterns on FDG PET-CT

Sunday, Nov. 25 11:35AM - 11:45AM Room: S505AB

#### Participants

Nikhil Seniaray, New Delhi, India (*Abstract Co-Author*) Nothing to Disclose Ritu Verma, New Delhi, India (*Presenter*) Nothing to Disclose Harsh Mahajan, MD, MBBS, New Delhi, India (*Abstract Co-Author*) Nothing to Disclose Vidur Mahajan, MBBS, New Delhi, India (*Abstract Co-Author*) Nothing to Disclose Ethel S. Belho, New Delhi, India (*Abstract Co-Author*) Nothing to Disclose P. S. Gupta, New Delhi, India (*Abstract Co-Author*) Nothing to Disclose Vanshika Gupta, New Delhi, India (*Abstract Co-Author*) Nothing to Disclose Ankur Pruthi, New Delhi, India (*Abstract Co-Author*) Nothing to Disclose

#### For information about this presentation, contact:

vidur@mahajanimaging.com

#### PURPOSE

The diagnosis of medium to large-vessel vasculitis and the assessment of its activity and extent remain challenging. We assess the clinical utility of FDG PET CT in patients with suspected medium and large vessel vasculitis to evaluate the pattern and extent of vessel involvement.

## METHOD AND MATERIALS

100 consecutive patients (64 males and 36 females) with suspected medium and large-vessel vasculitis were evaluated with FDG PET/CT. FDG uptake in the major vessels was visually graded using a four-point scale and quantified with standardised uptake values (SUV max). Patients were further sub-divided into three groups: (a) steroid-naive medium to large-vessel vasculitis (N=34, 69% of total positive patients), (b) vasculitis on steroid treatment (N=15, 30.6% of total positive patients) and (c) no evidence of vasculitis (N=51). Analysis of variance and linear regression were used to investigate the association of FDG uptake with clinical parameters.

#### RESULTS

FDG-PET revealed pathological findings in 49 of 100 patients. FDG PET/CT was positive (visual uptake >2; equal to or greater than liver) in all patients with steroid-naive medium to large-vessel vasculitis. The thoracic aorta, the carotid and the subclavian arteries were most frequently involved. In these patients, SUVmax values were significantly higher than in the other groups.

#### CONCLUSION

FDG PET is a sensitive and specific imaging tool for medium and large vessel vasculitis, especially when performed in steroid naive patients. It increases the overall diagnostic accuracy and has an impact on the clinical management in a significant proportion of patients.

#### **CLINICAL RELEVANCE/APPLICATION**

FDG-PET should be used in diagnosis and characterisation of medium and large vessel vasculitis to determine optimal treatment methodologies.

# SSA16-07 Assessing the Feasibility of 18F-Naf PET/CT to Detect the Atherosclerotic Calcification of Aortic Wall in Rheumatoid Arthritis Patients

Sunday, Nov. 25 11:45AM - 11:55AM Room: S505AB

Participants

Siavash Mehdizadeh Seraj, MD, Philadelphia, PA (*Presenter*) Nothing to Disclose William Y. Raynor, Philadelphia, PA (*Abstract Co-Author*) Nothing to Disclose Abdullah Al-Zaghal, MD, Philadelphia, PA (*Abstract Co-Author*) Nothing to Disclose Pegah Jahangiri, MD, Philadelphia, PA (*Abstract Co-Author*) Nothing to Disclose Mohsen Khosravi, MD, MPH, Philadelphia, PA (*Abstract Co-Author*) Nothing to Disclose Thomas J. Werner, Philadelphia, PA (*Abstract Co-Author*) Nothing to Disclose Joshua Baker, MD, Philadelphia, PA (*Abstract Co-Author*) Nothing to Disclose Abass Alavi, MD, Philadelphia, PA (*Abstract Co-Author*) Nothing to Disclose Stephen J. Hunt, MD,PhD, Philadelphia, PA (*Abstract Co-Author*) Consultant, Amgen Inc; Consultant, BTG International Ltd

#### For information about this presentation, contact:

siavash.mehdizadehseraj@uphs.upenn.edu

PURPOSE

Rheumatoid arthritis (RA) has long been associated with increased risk for atherosclerosis. 18F-sodium fluoride (NaF) is a PET tracer that detects calcium deposition in the early stages of atherosclerotic plaque formation. We aimed to assess whether NaF-PET/CT can sensitively discriminate aorta calcification between RA patients and normal subjects.

# METHOD AND MATERIALS

Fifteen RA patients (11 men, 4 women; mean age 53.8±10.8 y, range 25-64) and fifteen healthy controls (11 men, 4 women; mean age 53.5±11.2 y, range 25-64) were included in this study. Controls were matched to patients by sex and age (±5 years). All subjects in this study underwent NaF-PET/CT scanning 90 minutes after NaF tracer administration. Using OsiriX software, regions of interest were manually drawn around the abdominal aorta wall starting superiorly with the first axial slice containing the left kidney, ending with the last slice before the aortic bifurcation. The global mean standardized uptake value (global SUVmean) was obtained and compared between RA patients and healthy subjects. An unpaired t-test assessed the difference in means of RA group and controls, and a ROC analysis assessed discrimination.

## RESULTS

The global SUVmean of RA patients ranged from 0.88 to 2.35, and from 0.79 to 1.47 in healthy controls. Furthermore, average global SUVmean scores among RA patients was significantly greater than that of healthy controls. ( $1.62\pm0.49$  and  $1.04\pm0.16$ , respectively, P<0.01). ROC analysis revealed fair discrimination between the two groups (AUC = 0.77).

## CONCLUSION

Our findings indicate that global assessment with NaF-PET/CT is a feasible technique to detect active vascular calcification in the abdominal aorta. Discriminant validity was observed by assessing a known co-morbidity of RA and comparing RA to non-RA. Further studies are needed to validate this technique to diagnose and monitor patients at high risk for atherosclerosis.

## **CLINICAL RELEVANCE/APPLICATION**

Global assessment with NaF-PET/CT can determine the degree of active vascular calcification, which can help diagnose, monitor, and assess treatment response in atherosclerosis.

# SSA16-08 F-18 FLT PET/CT for Therapeutic Monitoring in Patients with Cardiac Sarcoidosis: Comparison with F-18 FDG PET/CT

Sunday, Nov. 25 11:55AM - 12:05PM Room: S505AB

## Participants

Takashi Norikane, Kita-gun, Japan (*Presenter*) Nothing to Disclose Yuka Yamamoto, MD, PhD, Kagawa, Japan (*Abstract Co-Author*) Nothing to Disclose Takahisa Noma, Kita, Japan (*Abstract Co-Author*) Nothing to Disclose Hiroaki Dobashi, MD, Kita-gun, Japan (*Abstract Co-Author*) Nothing to Disclose Yoshihiro Nishiyama, MD, Kagawa, Japan (*Abstract Co-Author*) Nothing to Disclose

#### PURPOSE

F-18 fluorodeoxyglucose (FDG) PET has been used in sarcoidosis including cardiac involvement for therapeutic monitoring. However, it can be challenging because it accumulates physiologically in normal myocardium. The purpose of this study was to evaluate the ability of F-18 fluorothymidine (FLT) PET for therapeutic monitoring in patients with cardiac sarcoidosis, in comparison with FDG.

## **METHOD AND MATERIALS**

FLT and FDG PET/CT studies were performed before and after immunosuppressive therapy in 6 patients with newly diagnosed cardiac sarcoidosis. The patients had fasted for at least 18 h before FDG PET/CT, but were given no special dietary instructions before FLT PET/CT. Uptake of FLT and FDG was examined visually and semiquantitatively using maximal standardized uptake value (SUV).

#### RESULTS

Before therapy, all patients had both cardiac and extra-cardiac thoracic sarcoidosis. Fifteen lesions in cardiac region and 22 lesions in extra-cardiac region were visually detected on both FLT and FDG PET/CT. After therapy, 10 and 8 lesions in cardiac region and 15 and 11 lesions in extra-cardiac region showed no increased uptake on FLT and FDG PET/CT, respectively. On after therapy FLT scan, all SUV for each lesion were lower than those on before therapy FLT scan, and the mean SUVs in cardiac and extra-cardiac lesions decreased significantly (p<0.001 and p<0.001, respectively). On after therapy FDG scan, all SUV for each lesion were also lower than those on before therapy SUVs in cardiac and extra-cardiac lesions also decreased significantly (p<0.001 and p<0.001, respectively). The mean SUV reductions in cardiac and extra-cardiac lesions on FLT scan were 53% and 57%, respectively. The mean SUV reductions in cardiac and extra-cardiac lesions on FDG scan were 57% and 55%, respectively. No significant difference in SUV reduction was found between FLT and FDG scans.

#### CONCLUSION

This preliminary study indicates that FLT PET/CT, even without the usually necessary fasting, may have the potential to identify the therapeutic response in patients with cardiac sarcoidosis as well as FDG PET/CT.

## **CLINICAL RELEVANCE/APPLICATION**

FLT PET/CT, even without the usually necessary fasting, may have the potential to identify the therapeutic response in patients with cardiac sarcoidosis.

# SSA16-09 Feasibility of Using Global Lung FDG Uptake in COPD Patients on PET/CT to Assess the Correlation Between Pulmonary Parenchymal Inflammation and Pulmonary Function Test Indices as well as Emphysema Severity

Sunday, Nov. 25 12:05PM - 12:15PM Room: S505AB

Kamyar Pournazari, MD,MSc, Philadelphia, PA (*Presenter*) Nothing to Disclose Esha S. Kothekar, MD, Philadelphia, PA (*Abstract Co-Author*) Nothing to Disclose Abdullah Al-Zaghal, MD, Philadelphia, PA (*Abstract Co-Author*) Nothing to Disclose Siavash Mehdizadeh Seraj, MD, Philadelphia, PA (*Abstract Co-Author*) Nothing to Disclose Mohsen Khosravi, MD, MPH, Philadelphia, PA (*Abstract Co-Author*) Nothing to Disclose Thomas J. Werner, Philadelphia, PA (*Abstract Co-Author*) Nothing to Disclose Abass Alavi, MD, Philadelphia, PA (*Abstract Co-Author*) Nothing to Disclose Drew A. Torigian, MD, MA, Philadelphia, PA (*Abstract Co-Author*) Co-founder, Quantitative Radiology Solutions LLC

## For information about this presentation, contact:

pegah.jahangiri@uphs.upenn.edu

## PURPOSE

The purpose of this study was to determine the relationship between the degree of pulmonary parenchymal inflammation measured from FDG-PET/CT with the degree of emphysema and also with PFT indices in chronic obstructive pulmonary disease (COPD) patients based on image segmentation and partial volume correction.

# METHOD AND MATERIALS

56 COPD patients (51 men; median age 64) who underwent 18F-fluorodeoxyglucose-positron emission tomography/computed tomography (FDG-PET/CT) were studied. Lung parenchymal volume (L), macroscopic emphysema volume (E) and non-emphysematous lung parenchyma mean attenuation (A) were measured from CT images. Uncorrected maximum standardized uptake value of lung (USUVmax) was measured from PET/CT images. A first level of partial volume correction was then applied to account for varying amounts of macroscopic emphysema (CSUVmax) followed by a second level of correction to account for the mixture of air and lung parenchyma at the microscopic level (CCSUVmax). Correlation of fraction of emphysema(F=E/L) with USUVmax, CSUVmax, CCSUVmax were tested using Pearson correlation and linear regression statistical tests. Pearson correlation and linear regression statistical tests were applied to test the correlations of USUVmax, CSUVmax, and CCSUVmax with FEV1/FVC ratio.

# RESULTS

Lung USUVmax and CSUVmax were not significantly correlated with fraction of emphysema (r=0.03, p=0.831 and r=0.18, p=0.292, respectively). However, CCSUVmax was significantly positively correlated with fraction of emphysema (r=0.47, p=0.013). Lung CSUVmax and CCSUVmax were significantly negatively correlated with FEV1/FVC ratio (r=-0.49, p=0.026 and r=-0.71, p<0.001, respectively), whereas there was no significant correlation between lung USUVmax and FEV1/FVC ratio (r=-0.25, p=0.073).

## CONCLUSION

These data demonstrate that the degree of pulmonary inflammation increases with the degree of emphysema severity and that patients with lower FEV1/FVC ratios have greater degrees of pulmonary parenchymal inflammation based on FDG-PET/CT quantitative assessment. These correlations are more statistically significant when pulmonary FDG uptake is corrected for the partial volume effect, which shows the importance of partial volume correction for accurate quantification of lung disease severity.

# **CLINICAL RELEVANCE/APPLICATION**

Measurement of pulmonary FDG uptake on PET/CT may therefore be useful in the diagnostic and response assessment of patients with COPD.



#### SSA17

Neuroradiology/Head and Neck (Head and Neck Tumors: State-of-the-Art Imaging)

Sunday, Nov. 25 10:45AM - 12:15PM Room: E350



AMA PRA Category 1 Credits ™: 1.50 ARRT Category A+ Credit: 1.75

FDA Discussions may include off-label uses.

#### Participants

Suresh K. Mukherji, MD, Northville, MI (*Moderator*) Nothing to Disclose Edward P. Quigley III, MD,PhD, Salt Lake City, UT (*Moderator*) Nothing to Disclose

# Sub-Events

# SSA17-01 Is Gadolinium Needed for the MRI Surveillance of Vestibular Schwannomas?

Sunday, Nov. 25 10:45AM - 10:55AM Room: E350

Participants

Peter Brown, MBChB, BSc, Leeds, United Kingdom (*Presenter*) Nothing to Disclose David J. Saunders, BMBCh, FRCR, Leeds, United Kingdom (*Abstract Co-Author*) Nothing to Disclose Jeremy A. Macmullen-Price, MBChB, FRCR, Edinburgh, United Kingdom (*Abstract Co-Author*) Nothing to Disclose Sonal K. Verma, MD, Leeds, United Kingdom (*Abstract Co-Author*) Nothing to Disclose Phil Ayres, Leeds, United Kingdom (*Abstract Co-Author*) Nothing to Disclose Caroline Tait, Leeds, United Kingdom (*Abstract Co-Author*) Nothing to Disclose Ceryl Harwood, Leeds, United Kingdom (*Abstract Co-Author*) Nothing to Disclose Ian Craven, Sheffield, United Kingdom (*Abstract Co-Author*) Nothing to Disclose Stuart Currie, FRCR,MD, Leeds, United Kingdom (*Abstract Co-Author*) Nothing to Disclose

### PURPOSE

The aim of this study was to test the hypothesis that high-resolution, T2-weighted magnetic resonance imaging (HRT2-MRI) is an acceptable alternative to gadolinium-enhanced T1-weighted MRI (Gd-MRI) in the assessment of size of vestibular schwannomas (VS). Current VS surveillance requires a minimum of 6 scans to demonstrate no interval growth. Proof of this hypothesis may allow a change in practice to performing VS surveillance imaging with HRT2-MRI rather than the current standard of T1-Gd MRI, a change that could have potential health and economic benefits; given the costs and potential complications from repeat gadolinium administration.

# METHOD AND MATERIALS

Two neuroradiologists independently performed single dimension intra-canalicular measurements with, or without additional intracisternal measurements (depending on the tumour extension) on axial images of 50 VS imaged with HRT2-MRI and Gd-MRI. Paired student t-tests (alpha = 0.05) were used to determine whether differences in the mean tumour measurements between HRT2-MRI and Gd-MRI were statistically significant. Intraclass and interclass correlation coefficients (ICC) were calculated to determine intraand interobserver reliability. Bland-Altman plots were used to evaluate the level of agreement between VS measurements obtained on HRT2-MRI and Gd-MRI.

#### RESULTS

There was no statistically significant difference in the mean diameter of VS size, measured on HRT2-MRI and Gd-MRI for both neuroradiologists (p=0.28 & p=0.74 for observer 1 and 2 respectively). Interobserver reliability between the neuroradiologists demonstrated excellent correlation for both imaging techniques (ICC=0.99 for HRT2-MRI and Gd-MRI). Intraobserver reliability was also excellent (ICC>=0.98 for both observers measuring on HRT2-MRI and Gd-MRI). Bland-Altman plots showed the differences between the two sequences were within limits of agreement for both observers.

## CONCLUSION

This study supports the use of HRT2-MRI alone for the surveillance of known VS.

# CLINICAL RELEVANCE/APPLICATION

High resolution T2 MRI shows good agreement with gadolinium-enhanced T1 MRI in measurement of vestibular schwannomas which could have health and economic benefits in their surveillance.

# SSA17-02 Histogram Analysis of Diffusion Kurtosis Imaging for Differentiating Malignant from Benign Masses in Head and Neck Region

Sunday, Nov. 25 10:55AM - 11:05AM Room: E350

Participants Hao Hu, Nanjing, China (*Presenter*) Nothing to Disclose Gao Ma, Nanjing, China (*Abstract Co-Author*) Nothing to Disclose Xiao-Quan Xu, Nanjing, China (*Abstract Co-Author*) Nothing to Disclose

#### PURPOSE

To evaluate the diagnostic performance of histogram parameters derived from diffusion kurtosis imaging (DKI) for differentiating malignant from benign masses in head and neck region.

## **METHOD AND MATERIALS**

Our study retrospectively enrolled 80 patients with head and neck masses who had undergone DKI scan for pre-treatment evaluation. Patients were grouped into malignant group (n=64) and benign group (n=16). Apparent diffusion for Gaussian distribution (Dapp) and apparent kurtosis coefficient (Kapp) were generated. Histogram parameters, including mean, median, 10th, 90th percentiles, skewness and kurtosis of Dapp and Kapp were calculated. Independent-sample t test and Mann-Whitney U test were used to compare the differences of quantitative parameters between two study groups. Differentiating performances of significant parameters were determined by using receiver operating characteristic (ROC) curve analyses. Multivariable stepwise logistic regression was used to identify independent predictors of malignancy

#### RESULTS

Malignant group showed significantly lower Dapp-10th, Dapp-mean, Dapp-median and Dapp-90th, while higher Kapp-10th, Kappmean, Kapp-median and Kapp-90th than benign group (All Ps<0.001). Dapp-10th demonstrated significantly higher differentiating performance than Dapp-mean (P=0.039), while Kapp-90th also demonstrated significantly higher differentiating performance than Kapp-mean (P=0.008). Dapp-10th was the only independent predictor of malignancy, with a sensitivity of 0.813, and a specificity of 1.000 at a cut-off value of 0.989×10-3 mm2/s.

#### CONCLUSION

Histogram analysis of DKI holds promising for exhibiting the difference of tumor heterogeneity between malignant and benign head and neck masses. Dapp-10th may be the promising imaging biomarker for predicting malignant tumor in head and neck region.

## **CLINICAL RELEVANCE/APPLICATION**

To assist in the differentiation of head and neck mass lesions.

# SSA17-03 Texture Analysis of Diffusion-Weighted Imaging in Head and Neck Squamous Cell Carcinoma: Diagnostic Value for Nodal Metastasis

Sunday, Nov. 25 11:05AM - 11:15AM Room: E350

#### Participants

Jung Hyun Park, MD, Bundang, Korea, Republic Of (*Presenter*) Nothing to Disclose Yun Jung Bae, MD, Seongnam-si, Korea, Republic Of (*Abstract Co-Author*) Nothing to Disclose Byungse Choi, MD,PhD, Seongnam-Si, Korea, Republic Of (*Abstract Co-Author*) Nothing to Disclose Leonard Sunwoo, MD, Seongnam, Korea, Republic Of (*Abstract Co-Author*) Nothing to Disclose Jae Hyoung Kim, Seongnam, Korea, Republic Of (*Abstract Co-Author*) Nothing to Disclose Cheolkyu Jung, MD, Chungcheongbuk-do, Korea, Republic Of (*Abstract Co-Author*) Nothing to Disclose

For information about this presentation, contact:

nadine16jhp@gmail.com

## PURPOSE

To evaluate the diagnostic performance of texture features of diffusion-weighted imaging (DWI) in differentiating metastasis from benign lymph nodes (LNs) in head and neck squamous cell cancer (SCC).

## METHOD AND MATERIALS

Between June, 2016 and February, 2018, thirty-six patients with pathologically proven head and neck SCC were included in this study. All patients underwent preoperative magnetic resonance imaging (MRI) including DWI and conventional imaging at 3T. Total 204 MRI-detected LNs including 176 subcentimeter normal-sized LNs were assigned to the metastatic or benign groups according to the pathology. Texture features including histogram and gray-level matrices were derived by drawing region-of-interest on LNs while excluding necrosis on apparent diffusion coefficient maps. Texture features between metastasis and benign LNs were compared using independent t-test, and hierarchical cluster analysis was performed to identify correlations between features. Multivariate logistic regression and receiver operating characteristic analysis were performed to assess diagnostic performance for metastatic LNs.

## RESULTS

Total 83 out of 204 LNs in all-size were confirmed as metastasis; 58 out of 176 normal-sized LNs were metastasis. Three discriminative texture features for differentiating metastasis from benign LNs were complexity (all-size, P<.001, odds ratio [OR] 1.0000022, 95% confidence interval [CI] 1.000001-1.000004; normal-size, P=.001, OR, 1.000002, 95% CI, 1.0000008-1.000004), normalized energy (P=.014, OR 1.000002, 95% CI 1.0000004-1.000004; P=.001, OR 1.000002, 95% CI 1.0000009-1.000004) and roundness (P=.008, OR 103.56, 95% CI 3.35-3675.25; P=.008, OR 116.88, 95% CI 3.39-4675.74). Area under the curves (AUCs) for diagnosing metastasis in all-sized and normal-sized LNs were 0.829 and 0.767 regarding complexity, 0.699 and 0.685 regarding normalized energy, and 0.699 and 0.685 regarding roundness. The combination of three features resulted in higher AUC values of 0.836 and 0.781, respectively.

# CONCLUSION

Texture analysis of DWI can be useful in diagnosing nodal metastasis in head and neck SCC, especially in normal -sized LNs.

## **CLINICAL RELEVANCE/APPLICATION**

Texture analysis of diffusion-weighted imaging can be useful in differentiating benign and metastatic lymph nodes in head and neck squamous cell cancer.

# SSA17-04 Treatment Response Assessment of Nasopharyngeal Carcinoma Based on Diffusion Kurtosis Imaging

Participants Ning Tu, Wuhan, China (*Presenter*) Nothing to Disclose Guangyao Wu SR, MD,PhD, Wuhan, China (*Abstract Co-Author*) Nothing to Disclose Xiangyu Wang, Wuhan, China (*Abstract Co-Author*) Nothing to Disclose Panying Wang, MD, Shenzhen, China (*Abstract Co-Author*) Nothing to Disclose

## For information about this presentation, contact:

tuning@whu.edu.cn

## PURPOSE

The prediction of treatment response is important in planning and modifying the chemoradiation therapy regimen. This study aimed to explore the quantitative indices for treatment response assessment of nasopharyngeal carcinoma (NPC) based on diffusion kurtosis imaging(DKI).

### **METHOD AND MATERIALS**

Thirty-six patients with initial diagnosis of locally advanced NPC and DKI acquisitions before and after neoadjuvant chemotherapy (NAC) were enrolled. Patients were divided into respond (RP) and non-respond (NRP) groups and residual (RD) and non-residual (NRD) groups after NAC and radiation therapy(RT). Histogram parameters (10th, 25th, 50th, 75th, 90th percentile, mean, standard deviation, skewness, and kurtosis) of DKI-derived parameters (ADC, D, K) were calculated. Intraclass correlation coefficient (ICC), Kolmogorov-Smirnov test, Student's t-test or Mann-Whitney U test, receiver operating characteristic curve (ROC) and Delong tests were performed.

#### RESULTS

Most of the parameters have good to excellent consistency (ICC: 0.675-0.998). The pre- and post-ADC (10th, 25th, 50th), D (10th, 25th, 50th) and K (50th) were significantly different between RP and NRP, while the pre- and post- ADC (10th, 50th), D (25th, 50th) and K (75th, 90th) were significantly different between RD and NRD (all P<0.05). ROC analysis indicated that setting pre-D50th=0.875mm2/s as the cut-off value could obtain optimal diagnostic performance for the prediction of NAC treatment response, while post-K90th=1.035 is optimal for prediction of RT response.

#### CONCLUSION

DKI derived parameters can be used as promising quantitative biomarkers in prediction of NAC and RT treatment response in locally advanced NPC patients.

# **CLINICAL RELEVANCE/APPLICATION**

DKI derived parameters can be used as promising quantitative biomarkers in prediction of NAC and RT treatment response in locally advanced NPC patients.

# SSA17-05 Differential Diagnosis of Nasopharyngeal Carcinoma and Nasopharyngeal Lymphoma Based on DCE-MRI and DWI

Sunday, Nov. 25 11:25AM - 11:35AM Room: E350

Participants

Chengru Song, Zhengzhou, China (*Presenter*) Nothing to Disclose Jingliang Cheng, MD,PhD, Zhengzhou, China (*Abstract Co-Author*) Nothing to Disclose Yong Zhang, DO, Zhengzhou, China (*Abstract Co-Author*) Nothing to Disclose

#### PURPOSE

To evaluate the utility of dynamic contrast-enhanced MRI and diffusion weighted imaging (DWI) in the differentiation of nasopharyngeal carcinoma (NPC) and nasopharyngeal lymphoma (NPL).

#### **METHOD AND MATERIALS**

Fifty-two patients with pathologically confirmed NPC and 43 patients with NPL were recruited and underwent conventional MRI and dynamic contrast-enhanced MRI. The MR signals, time signal-intensity curves(TIC) types, time to peak(TTP), enhancement peak(EP), maximum contrast enhancement ratio(MCER), washout ratio(WR), ADC and relative ADC value of all the subjects were calculated and analyzed, thereafter, inter-group comparison was performed. The threshold values of TTP, EP, MCER, WR, ADC and rADC for differentiating NPC from NPL were determined using a receiver operating characteristic curve (ROC) analysis.

#### RESULTS

For NPC group, 40 cases (76.19%) demonstrated obvious heterogeneous enhancement. The mean TTP, EP, MCER and WR were (48.29±12.20)s, 1475.38±77.76, (136.89±24.41)% and 16.81±8.36, respectively. For NPL group, 38 cases (88.89%) demonstrated obvious homogeneous enhancement. The mean TTP, EP, MCER and WR were (63.21±14.29)s, 1161.82±64.04, (113.47±28.52)% and 7.39±6.21, respectively. The ADC value and rADC value were (842.34±94.66)×10-6 mm2·s-1 and 0.74±0.08 in NPC, whereas (652.15±83.47)×10-6 mm2·s-1 and 0.56±0.08 in NPL. The differences of TTP, EP, MCER, WR, ADC, rADC between NPC and NPL were statistically significant (P<0.05). The TTP of NPC was lower than that of NPL, whereas the opposite for the remaining parameters. ADC and rADC value reveled the highest diagnostic efficiency in differentiating NPC from NPL, while rADC was even slightly superior to ADC. The best differentiate threshold value of ADC and rADC were 736.5×10-6mm2·s-1, 634.0×10-6mm2·s-1, respectively. While the areas under the ROC curve (AUC), sensitivity, specificity and Youden index of ADC and rADC were 0.943, 0.909, 0.852, 0.761, and 0.951, 0.955, 0.852, 0.77, respectively.

## CONCLUSION

Dynamic contrast-enhanced MRI and DWI are effective in differentiating NPC from NPL. ADC and rADC value reveled the highest diagnostic efficiency.

## **CLINICAL RELEVANCE/APPLICATION**

Dynamic contrast-enhanced MRI and DWI can be applied in the differential diagnosis of NPC from NPL.

# SSA17-06 Deep Learning-Based Computer-Aided Diagnosis System for Diagnosis of Cervical Lymph Node Metastasis from Thyroid Cancer on Computed Tomography: A Pilot Study

Sunday, Nov. 25 11:35AM - 11:45AM Room: E350

Participants

Eun Ju Ha, Suwon, Korea, Republic Of (*Presenter*) Nothing to Disclose Jeong Hoon Lee, Seoul, Korea, Republic Of (*Abstract Co-Author*) Nothing to Disclose

## PURPOSE

Surgical extent of thyroid cancer relies on the accurate preoperative detection of lymph node metastasis. Therefore, contrastenhanced computed tomography (CT) is recommended as an adjunct to ultrasonography for patients with clinical suspicion for advanced disease. The purpose of this study was to develop the computer-aided diagnosis (CAD) system to differentiate metastatic lymph nodes on preoperative CT.

#### **METHOD AND MATERIALS**

From May 2013 to July 2017, we enrolled 995 lymph nodes seen on CT, which were confirmed by fine-needle aspiration or surgery. The datasets were split into training (543 benign and 244 metastatic lymph nodes), validation (52 benign and 52 metastatic lymph nodes), and test (52 benign and 52 metastatic lymph nodes). Using the GoogLeNet-Class Activation Map model, we developed a CAD system to differentiate the metastatic lymph nodes. We evaluated the diagnostic performance of this CAD system in our test set.

#### RESULTS

In the test set, the sensitivity, specificity, and accuracy of our model for predicting cervical lymph node metastasis were 84.62%, 96.15%, and 90.38%, respectively. The area under the receiver operating characteristic curve was 0.912 for the CAD system.

#### CONCLUSION

We developed a deep learning-based CAD system for differentiation of lymph nodes metastasis from thyroid cancer on preoperative CT. This CAD system is highly accurate and may be used as an adjunctive tool for preoperative diagnosis of lymph node metastasis.

## CLINICAL RELEVANCE/APPLICATION

This study is an initial report to develop a deep learning-based CAD system for diagnosis of metastatic cervical lymph nodes on preoperative CT.

# SSA17-07 Therapy Effects of Advanced Laryngeal Squamous Cell Carcinoma: Evaluated Using MTRasym3.5ppm in Magnetic Resonance Amide Proton Transfer Images

Sunday, Nov. 25 11:45AM - 11:55AM Room: E350

Participants

Xiaojie Luo, MD, Beijing, China (*Presenter*) Nothing to Disclose Lu Yu, BS, Beijing, China (*Abstract Co-Author*) Nothing to Disclose Min Chen, MD, PhD, Beijing, China (*Abstract Co-Author*) Nothing to Disclose

#### PURPOSE

The accurate evaluation of the therapeutic effects of advanced laryngeal squamous cell carcinoma (LSCC) remains challenging. In this study, we determined the value of MTRasym3.5ppm derived from amide proton transfer weighted for predicting the therapeutic effects of advanced LSCC and to provide valuable evidence for early judgement of the tumour's response to therapy in clinical practice.

## **METHOD AND MATERIALS**

We prospectively analysed 41 patients with pathologically confirmed LSCC. All patients were underwent MRI on the neck before therapy. Amide Proton Transfer (APT) images (saturation time 0.8 s, saturation power 2  $\mu$ T) was performed under 3.0 Tesla MR scanner. APT images were calculated using magnetization transfer ratio asymmetry at 3.5ppm with respect to water. 19 of 41 patients showed complete remission (CR), and 22 showed non-complete remission (NCR).

#### RESULTS

The mean of MTRasym3.5ppm in the CR group were significantly lower than the NCR group (P<0.05). There were no significant differences for T stage, treatment modality between two groups (P>0.05). The 2-year cumulative recurrence rate of patients with higher MTRasym3.5ppm values was significantly higher than that of patients with lower MTRasym3.5ppm values (P<0.05), while the 2-year survival rate of those patients was not significantly different (P>0.05).

# CONCLUSION

APT could easily identify CR patients and potentially help to choose the appropriate treatment regimen for advanced LSCC.

# **CLINICAL RELEVANCE/APPLICATION**

MTRasym3.5ppm derived from amide proton transfer weighted for predicting the therapeutic effects of advanced LSCC

# SSA17-08 Computer-Aided Diagnosis System for Thyroid Nodules Seen on Ultrasonography: Diagnostic Performance and Reproducibility Based on Operator Experience

Sunday, Nov. 25 11:55AM - 12:05PM Room: E350

Yoon Joo Cho, Suwon, Korea, Republic Of (*Presenter*) Nothing to Disclose Eun Young Jeong, Suwon, Korea, Republic Of (*Abstract Co-Author*) Nothing to Disclose Seon Young Park, MD, Suwon, Korea, Republic Of (*Abstract Co-Author*) Nothing to Disclose Hye Lin Kim, MD, Suwon, Korea, Republic Of (*Abstract Co-Author*) Nothing to Disclose

## For information about this presentation, contact:

radhej@naver.com

#### PURPOSE

To evaluate the diagnostic performance and reproducibility of a computer-aided diagnosis (CAD) system for thyroid cancer diagnosis using ultrasonography (US) based on the operator's experience

### **METHOD AND MATERIALS**

Between July 2016 and October 2016, 76 consecutive patients with 100 thyroid nodules (>= 1.0 cm) were prospectively included. An experienced radiologist performed the US examinations with a real-time CAD system integrated into the US machine, and three operators with different levels of US experience (0-5 years) independently applied the CAD system. We compared the diagnostic performance of the CAD system based on the operators' experience and calculated the interobserver agreement for cancer diagnosis and in terms of each US descriptor.

## RESULTS

The sensitivity, specificity, positive predictive value (PPV), negative predictive value (NPV), and accuracy of the CAD system were 88.6, 83.9, 81.3, 90.4, and 86.0%, respectively. The sensitivity and accuracy of the CAD system were not significantly different from those of the radiologist (P > 0.05); while the specificity was higher for the experienced radiologist (P = 0.016). For the less-experienced operators, the sensitivity was 68.8-73.8%, specificity 74.1-88.5%, PPV 68.9-73.3%, NPV 72.7-80.0%, and accuracy 71.0-75.0%. The less-experienced operators showed lower sensitivity and accuracy than those for the experienced radiologist (all P < 0.05). The interobserver agreement was good for the final diagnosis and each US descriptor; however, the margin and composition remained moderate agreement.

#### CONCLUSION

The CAD system may have a potential role in the thyroid cancer diagnosis. However, operator dependency still remains and needs improvement.

#### **CLINICAL RELEVANCE/APPLICATION**

1. The sensitivity and accuracy of the CAD system did not differ significantly from those of the experienced radiologist (88.6% vs. 84.1%, P=0.687; 86.0% vs. 91.0%, P=0.267) while the specificity was significantly higher for the experienced radiologist (83.9% vs. 96.4%, P=0.016). 2. However, the diagnostic performance varied according to the operator's experience (sensitivity 70.5-88.6%, accuracy 72.0-86.0%) and they were significantly lower for the less-experienced operators than for the experienced radiologist (all P<0.05). 3. The interobserver agreement was good for the final diagnosis and each US descriptor; however, the margin and composition remained moderate agreement.

# SSA17-09 Detection of Parathyroid Adenomas with Wide-Beam Multiphase CT: Towards a True Four-Dimensional Visualization Technique with Quantitative Analysis of Perfusion Parameters

Sunday, Nov. 25 12:05PM - 12:15PM Room: E350

Participants Steven Raeymaeckers, Jette, Belgium (*Presenter*) Nothing to Disclose Yannick De Brucker IV, Jette, Belgium (*Abstract Co-Author*) Nothing to Disclose Tim I. Vanderhasselt, MD, Brussels, Belgium (*Abstract Co-Author*) Nothing to Disclose Johan de Mey, MD, PhD, Jette, Belgium (*Abstract Co-Author*) Nothing to Disclose

#### For information about this presentation, contact:

Steven.Raeymaeckers@uzbrussel.be

#### PURPOSE

Diagnosis of a parathyroid adenoma on CT is typically based upon features obtained from three consecutive phases: Low attenuation (NECT) Arterial peak enhancement Rapid washout of contrast in venous phase However, if timing of these phases is not optimal, wash-in or wash-out phenomena can appear less conspicuous or could even be missed. In this ethical compliant study we explore the possibility of using a multiphase (16x) technique in continuous axial scanning mode in order to perform quantitative perfusion analysis.

#### **METHOD AND MATERIALS**

Up to date, we included 13 patients with suspected primary hyperparathyroidism (i.e. an elevated serumlevel of calcium and raised levels of parathyroid hormone) prior to surgery. Continuous axial scanning (Revolution CT, GE Healthcare) was performed over a fixed 8 cm volume (100 kVp, 0.625 mm) with following temporal scan protocol: Non-contrast scan Contrast administration (90 mL, 6 mL/s) followed by 20 sec delay 11 phases with a 2-second interphase delay 4 phases with a 10-second interphase delay The following perfusion parameters were considered in the normal thyroid, parathyroid and lymph nodes: maximum peak enhancement (HUmax), mean blood flow (MBF) and volume (MBV), time to peak (TTP) and mean slope of increase (MSI).

#### RESULTS

In all but 2 patients the enlarged parathyroid can be visualized. Parathyroid adenomas show a different enhancement pattern compared to the thyroid, with an obvious wash-in of contrast. Most adenomas show an obvious wash-out of contrast. Normal cervical lymph nodes show a continuous and shallow increase of enhancement. HUmax of visualised adenomas is well above the normal thyroid gland (mean 474 vs 332 HU). MBF in the adenoma is 93% higher compared to the thyroid (mean 507,5 vs 263 mL/100g/min). Similarly MBV is increased with 69% (mean 21.6 vs 12.8 mL/100g). Adenomas demonstrate earlier peak enhancement, at 29.6s versus 31.6s for the thyroid. MSI is significantly steeper for the adenomas compared with normal thyroid tissue. Mean dose length product was  $530\pm238$  mGycm

# CONCLUSION

Quantitative analysis of perfusion parameters obtained by multiphase CT can be used for detection and differentiation of parathyroid adenomas.

# **CLINICAL RELEVANCE/APPLICATION**

Improved detection and differentiation of parathyroid adenomas is a key factor in the diagnosis and treatment of primary hyperparathyroidism.



#### SSA18

# Neuroradiology (White Matter Diseases: Beyond Bright T2)

Sunday, Nov. 25 10:45AM - 12:15PM Room: E352



AMA PRA Category 1 Credits ™: 1.50 ARRT Category A+ Credit: 1.75

#### Participants

Aaron S. Field, MD, PhD, Madison, WI (*Moderator*) Research Grant, General Electric Company Peter B. Barker, DPhil, Baltimore, MD (*Moderator*) Speakers Bureau, Koninklijke Philips NV

# Sub-Events

# SSA18-01 The Automatic Differential Diagnosis of Multiple Sclerosis and Cerebral Small Vessel Disease

Sunday, Nov. 25 10:45AM - 10:55AM Room: E352

Participants

Daniel Eftekhari, MSc, BEng, Toronto, ON (*Presenter*) Nothing to Disclose Pascal N. Tyrrell, PhD, Toronto, ON (*Abstract Co-Author*) Chief Science Officer, AceAge Inc; Research Consultant, Novo Nordish Anne L. Martel, PhD, Toronto, ON (*Abstract Co-Author*) Co-founder, Pathcore Inc; Officer, Pathcore Inc; Alan R. Moody, MD, Toronto, ON (*Abstract Co-Author*) Nothing to Disclose Richard Aviv, MBBCh, FRCR, Toronto, ON (*Abstract Co-Author*) Nothing to Disclose

# For information about this presentation, contact:

daniel.eftekhari@mail.utoronto.ca

## PURPOSE

Multiple sclerosis (MS) and cerebral small vessel disease (SVD) may be difficult to distinguish using only neuroimaging and clinical presentation. As early diagnosis and treatment is associated with better long-term outcome in both diseases, and the societal and monetary cost for both diseases is potentially high, particularly for misdiagnosis in MS, we developed an accurate and automatic diagnostic algorithm to differentiate relapsing-remitting MS (RRMS) and SVD using neuroimaging and clinical presentation.

## **METHOD AND MATERIALS**

Statistical and machine learning algorithms, including a mixture of *t*-distributions and a novel spatial heuristic algorithm, were developed for the segmentation of white matter hyperintensities and T1 black holes on FLAIR and T1 W MRI sequences. Combined spatial probability maps of RRMS and SVD lesion masks were subsequently developed using a derivation set of patients. A novel cross entropy image distance metric, which is insensitive to co-registration and anatomical differences between patients, was used to quantify the similarity of new cases to each disease. Bayesian learning algorithms using non-informative priors were trained using these neuroimaging features in combination with clinical presentation. Model hyperparameters were tuned using Monte Carlo cross validation.

#### RESULTS

The dataset consists of 39 RRMS (median age 48 (31 - 60), 12 M, 27 F) and 72 SVD patients (median age 73 (52 - 86), 44 M, 28 F). An intraclass correlation coefficient (two-way random effects, absolute agreement, single measures) of 0.952 (95% CI [0.902, 0.976]) between total lesion volume for the automatic segmentations and RRMS ground truth tracings was obtained. The segmentation algorithms provide the additional benefit of being blind to disease ground truth, and are robust to varying MRI acquisition parameters. The model consisting of both neuroimaging and clinical features achieved 95% sensitivity and 99% specificity in distinguishing RRMS from SVD. This was a significant improvement on models developed using neuroimaging and clinical presentation in isolation.

# CONCLUSION

Future directions include using additional predictors thought to distinguish the diseases in the predictive models, and extending the model to multi-disease classification.

## **CLINICAL RELEVANCE/APPLICATION**

As the misdiagnosis rate for MS is 5-10%, and the societal and monetary cost of both diseases is high, this work has real potential for clinical impact.

# SSA18-02 Diffusion Basis Spectrum Imaging (DBSI) Quantitatively Assesses Axonal Protection of FTY720 in Mice with Optic Neuritis

Sunday, Nov. 25 10:55AM - 11:05AM Room: E352

Participants Ruimeng Yang, MD,PhD, Guangzhou, China (*Abstract Co-Author*) Nothing to Disclose Tsen-Hsuan Lin, Saint Louis, MO (*Abstract Co-Author*) Nothing to Disclose Jie Zhan, St Louis, MO (*Abstract Co-Author*) Nothing to Disclose Chunyu Song, St Louis, MO (*Abstract Co-Author*) Nothing to Disclose Zezhong Ye, St. Louis, MO (*Abstract Co-Author*) Nothing to Disclose Peng Sun, PhD, Saint Louis, MO (*Presenter*) Nothing to Disclose Sheng-Kwei Song, PhD, Saint Louis, MO (*Abstract Co-Author*) Nothing to Disclose

For information about this presentation, contact:

yangrm0708@gmail.com

#### PURPOSE

Diffusion basis spectrum imaging (DBSI) has been introduced to overcome the limitations of diffusion tensor imaging (DTI) to accurately detect and distinguish confounding neuropathologies in MS[1, 2, 3]. Optic neuritis is frequently the first symptom of MS. Fingolimod (FTY720) was the first FDA-approved oral agent for treating MS[4]. Although its anti-inflammatory effect is clear, neuroprotection, which is highly associated with neurological function, remains uncertain. This study investigates whether FTY720 treatment protects optic nerve axons from EAE mice with optic neuritis using in vivo DBSI.

## **METHOD AND MATERIALS**

EAE was induced in C57BL/6 mice as previously reported. Daily clinical score and visual acuity (VA) were assessed. When VA <= 0.25 cycle/degree, mice were alternately assigned to receive daily gavage of either FTY720 (1 mg/kg bw) or the same amount of saline for 10 consecutive weeks. MRI experiments were performed on a 4.7 T small-animal scanner. For each EAE mouse, baseline DBSI was performed two weeks prior to immunization with follow-up scans at 2, 6 and 10 weeks post-treatment. The 25-direction diffusion-weighted imaging acquisition was performed with TR = 1500 ms, TE = 35 ms, NE = 2, FOV = 22.5 × 22.5 mm2, matrix size = 192 × 192, slice thickness = 0.8 mm, max. b value = 2,200 s/mm2,  $\Delta$  = 18 ms,  $\delta$  = 6 ms. The total scan time = 2 hr 4 min. Mice were perfusion fixed immediately after final in vivo DBSI for immunohistochemical assessment of axonal injury/loss, demyelination and cellular inflammation.

#### RESULTS

Compared with saline-treated group, FTY720 treatment slowed VA deterioration and protected against inflammation, demyelination, and axonal injury/loss as seen by in vivo DBSI-derived neuroimaging biomarkers, validated by post-DBSI immunohistochemical analysis.

#### CONCLUSION

Current results suggest that FTY720 reduce axonal loss in EAE mouse optic nerve. This may be direct or indirect based on its antiinflammatory effects. We propose that DBSI could serve as a non-invasive biomarker to monitor disease progress and validate treatment efficacy for MS patients.

# **CLINICAL RELEVANCE/APPLICATION**

Results support that DBSI derived pathological metrics can be used to assess the therapeutic efficacy of disease modifying therapies in MS and potentially other diseases.

# SSA18-03 Whole Brain Adiabatic T1rho and Relaxation Along a Fictitious Field Imaging in Healthy Volunteers and Patients with Multiple Sclerosis: Initial Findings

Sunday, Nov. 25 11:05AM - 11:15AM Room: E352

Participants

Harri Merisaari, Turku, Finland (*Abstract Co-Author*) Nothing to Disclose Aida K. Kiviniemi, MD, Turku, Finland (*Abstract Co-Author*) Nothing to Disclose Eero Rissanen, Turku, Finland (*Abstract Co-Author*) Nothing to Disclose Marko Pesola, Kotka, Finland (*Abstract Co-Author*) Nothing to Disclose Timo Liimatainen, PhD, Kuopio, Finland (*Abstract Co-Author*) Nothing to Disclose Laura Airas, Turku, Finland (*Abstract Co-Author*) Nothing to Disclose Hannu J. Aronen, MD, PhD, Kuopio, Finland (*Abstract Co-Author*) Nothing to Disclose Ivan Jambor, MD, PhD, Turku, Finland (*Presenter*) Speakers Bureau, Koninklijke Phillips NV

## PURPOSE

To evaluate feasibility of whole brain adiabatic T1p and Relaxation Along a Fictitious Field (RAFF) imaging in healthy volunteers and patients with multiple sclerosis (MS).

## **METHOD AND MATERIALS**

Twenty-eight healthy volunteers (24 - 69 years) and nine patients (35- 45 years) with relapsing-remitting MS provided written informed consent and underwent MRI examination performed using a clinical 3 Tesla MR scanner as a part of an ongoing single institutional clinical trial. Relaxation Along a Fictitious Field in second rotating frame of reference (RAFF2) was performed using RF peak amplitude of 11.74  $\mu$ T and pulse train durations of 0, 45, 90 ms. The adiabatic T1p data sets were obtained using hyperbolic secant (HS) pulses with the RF peak amplitude of 13.50  $\mu$ T and pulse train duration of 0, 72ms, and 144 ms. The parametric maps of TRAFF and T1p were calculated using two parameter monoexponential model. Semi-automatic segmentation of MS lesions, white matter (WM), and gray matter (GM) was performed based on T1 and FLAIR weighted images. Mean TRAFF and T1p in normal-appearing WM, GM, and lesions were compared within and between subject groups by using analysis of variance.

## RESULTS

The number of healthy volunteers in 20-29, 30-39, 40-49, 50-59, 60-69 age groups was 7, 5, 6, 6, 4, respectively. The differences in the median relaxation values between the age groups did not reach the level of statistical significance. Similarly, Pearson correlation coefficients were not statistically significant for any of the relaxation parameters. In contrast, statistically significant differences in TRAFF and T1p values were present between the tissue types in MS patients.

## CONCLUSION

Statistically significant differences were present in TRAFF and T1p values between normal-appearing WM, GM, and lesions in patients with MS. Theses encouraging preliminary results support further instigation of RAFF for the evaluation of MS.

#### **CLINICAL RELEVANCE/APPLICATION**

Relaxation Along a Fictitious Field (RAFF) is a novel promising imaging method for evaluation of patients with multiple sclerosis.

# SSA18-04 MRI Findings in Tumefactive Demyelinating Lesions: A Systematic Review and Meta-Analysis

Sunday, Nov. 25 11:15AM - 11:25AM Room: E352

Participants Chan Park, Gwangju, Korea, Republic Of (*Presenter*) Nothing to Disclose Chong Hyun Suh, MD, Seoul, Korea, Republic Of (*Abstract Co-Author*) Nothing to Disclose Ho Sung Kim, Seoul, Korea, Republic Of (*Abstract Co-Author*) Nothing to Disclose

#### PURPOSE

We aimed to evaluate conventional and advanced MRI findings for the diagnosis of tumefactive demyelinating lesions (TDL) and determine the diagnostic performance of MRI for differentiating TDL from primary brain tumor.

# METHOD AND MATERIALS

A systematic search of Ovid-MEDLINE and EMBASE up to December 6, 2017, was conducted to find relevant studies. The pooled incidence of conventional MRI TDL findings was obtained with the inverse variance method for calculating weights and the DerSimonian-Liard random-effects model. Pooled sensitivity and specificity were obtained using a bivariate random-effects model.

#### RESULTS

Eighteen eligible studies with 325 TDL patients were included. The pooled incidence of open ring or incomplete rim enhancement was 36% (95% CI, 25-47%), which was significantly higher than the incidence of closed ring or complete rim enhancement (13% [95% CI, 6-21%]; p = 0.0013). The pooled incidences of T2 hypointense rim, absent or mild mass effect, and absent or mild perilesional edema were 46% (95% CI, 25-68%), 64% (95% CI, 42-87%), and 55% (95% CI, 27-82%), respectively. Open ring or incomplete rim enhancement showed high specificity (98-100%). On advanced MRI, TDL showed a high apparent diffusion coefficient, peripheral restricted diffusion, and low cerebral blood volume. The pooled sensitivity and specificity of MRI for differentiating TDL from primary brain tumor were 89% (95% CI, 82-93%) and 94% (95% CI, 89-97%), respectively.

## CONCLUSION

Conventional MRI findings may help differentiate TDL from primary brain tumor, although further study is needed to determine the added value of advanced MRI.

#### **CLINICAL RELEVANCE/APPLICATION**

Conventional MRI findings may help differentiate TDL from primary brain tumor.

# SSA18-05 In-Vivo Tissue Marker of Neuro-Inflammation is Associated with WMH Burden: A Multimodal PET-MR stu

Sunday, Nov. 25 11:25AM - 11:35AM Room: E352

Participants

Hongyu An, DSc, St. Louis, MO (*Presenter*) Research Grant, Siemens AG Chunwei Ying, St. Louis, MO (*Abstract Co-Author*) Nothing to Disclose Yasheng Chen, St. Louis, MO (*Abstract Co-Author*) Nothing to Disclose Jon J. Christensen, Saint Louis, MO (*Abstract Co-Author*) Nothing to Disclose Qing Wang, PhD, St. Louis, MO (*Abstract Co-Author*) Nothing to Disclose Lisa Cash, St. Louis, MO (*Abstract Co-Author*) Nothing to Disclose Jin-Moo Lee, MD, PhD, St. Louis, MO (*Abstract Co-Author*) Nothing to Disclose Andria Ford, St. Louis, MO (*Abstract Co-Author*) Nothing to Disclose Tammie S. Benzinger, MD,PhD, Saint Louis, MO (*Abstract Co-Author*) Research Grant, Eli Lilly and Company Investigator, Eli Lilly and Company Investigator, F. Hoffmann-La Roche Ltd

#### For information about this presentation, contact:

hongyuan@wustl.edu

## PURPOSE

White matter hyperintensities (WMH) on FLAIR have been widely observed in patients with cerebral small vessel disease (CSVD) and Alzheimer's disease (AD). WMH is strongly associated with progression to dementia. The pathogenesis of WMH is poorly understood. Animal models and post-mortem human brain studies have suggested a role of neuro-inflammation in WMH. However, there is no in vivo data from patients to provide direct evidence. In addition, it is unclear whether amyloid deposition, a hallmark pathological feature of AD, may be directly linked to WMH. In this study, we evaluated whether neuroinflammation and amyloid deposition are associated with WMH burden using PET-MR imaging.

#### **METHOD AND MATERIALS**

18 elderly subjects (11 females, age: 76 [69, 82] (Median [interquartile range IQR])) underwent serial PET and MR scans. 11C-PK11195 PET images were acquired to estimate neuroinflammation. In addition, 11C-PiB PET to measure amyloid deposition, were acquired 19 [14, 22] (Median [IQR]) months prior to the 11C-PK11195 scans from the same patients. WMH lesions were manually outlined using FLAIR images to obtain WMH volumes (VWMH). MR T1w MPRage images were used for brain tissue segmentation. Standardized uptake value ratio (SUVR) maps were obtained using cerebellum gray matter as a reference. Linear regression was performed between VWMH vs. 11C-PK11195 SUVR in WM and GM, VWMH vs. 11C-PiB uptake, and VWMH vs. age, respectively.

## RESULTS

VWMH across the elderly cohort was 8.4 ml [4.6ml 24.5ml]. 5 patients had a clinical dementia rating (CDR) score greater than 0.5 (CDR=0.5, n=3, CDR=1, n=2). 11C-PK11195 SUVR within WM, but not GM, was linearly associated with VWMH (R=0.54, P=0.022), suggestive of WM neuro-inflammation (Figure). Interestingly, amyloid deposition was not associated with VWMH (R=0.11, P=0.67).

As expected, age was linearly associated with VWMH (R=0.51, P=0.029).

## CONCLUSION

Our results demonstrate that selective WM 11C-PK11195 uptake is associated with WMH burden, suggesting neuro-inflammation as a mechanism underlying CSVD and vascular cognitive impairment. In contrast, amyloid deposition is not associated with WMH.

# CLINICAL RELEVANCE/APPLICATION

Selectively elevated PET 11C-PK11195 uptake within white matter demonstrates that neuro-inflammation is an important pathogenic factor in patients with white matter hyperintensity.

# SSA18-06 Automated Brain Volumetry of Neuromyelitis Optica Spectrum Disorders: Inter-Scanner Variability in White Matter Hyperintensities Segmentations, and Volumetric Differences Compared with Multiple Sclerosis

Sunday, Nov. 25 11:35AM - 11:45AM Room: E352

Participants

Chunjie Guo, Changchun, China (*Presenter*) Nothing to Disclose Shi L. Lin, Hong Kong, Hong Kong (*Abstract Co-Author*) Director, BrainNow Medical Technology Limited Leongtim Wong, Hong Kong, Hong Kong (*Abstract Co-Author*) Nothing to Disclose Huimao Zhang, Changchun, China (*Abstract Co-Author*) Nothing to Disclose

## For information about this presentation, contact:

guochunjie@hotmail.com

#### PURPOSE

To verify AccuBrain is a robust software for white matter lesions (WMLs) and brain volumetric segmentation in neuromyelitis optica spectrum disorders (NMOSD), and to distinguish NMOSD from multiple sclerosis (MS) in neuroimaging.

## METHOD AND MATERIALS

30 NMOSD and 30 MS patients well matched on age and gender from 3D images protocol at the same scanner were recruited in the first study on evaluating brain volumetric and WML differences. In addition, 6 of the NMOSD subjects agreed to enroll in a prospective study on inter-scanner variability and were scanned at 5 different scanners within 24 hours. 2D FLAIR images were obtained from all the sites, while one 3T scanner was also used to acquire 3D T1W and FLAIR images Two automated segmentation software, AccuBrain and lesion segmentation tool (LST) toolbox for SPM were used in WMLs segmentation to assess inter-scanner repeatability. To evaluate the volumetric and WML differences between NMOSD and MS, AccuBrain was used to perform automated segmentation and quantification of WML volumes, regional brain volumes and atrophy. Coefficient of variation (CV) was calculated to assess the effect of scanners on the variability in lesion segmentation, and two-sample t test was used to evaluate the differences of each regional volumetric measure between NMOSD and MS.

#### RESULTS

The mean inter-scanner CV of WML volume is  $14.6\% \pm 8.4\%$  when using AccuBrain, which is smaller compared to that of  $23.6\% \pm 11.2\%$  when using LST. In the brain volumetric analysis from 3D T1WI, although NMOSD and MS generally presented similar brain atrophy pattern, we found that they differ significantly in the thalamus-proper, lateral ventricle and third ventricle. In the WML analysis from 3D FLAIR images, significant volume difference was found between NMOSD and MS in white matter hyperintensities, which can be illustrated in the WML prevalence maps from the voxel-based lesion-symptom mapping (VLSM) analysis, with MS group having more WMLs situated over the posterior horns of the lateral ventricles.

# CONCLUSION

AccuBrain is a robust software for calculating WMLs in NMOSD patients in multicenter and longitudinal studies. In addition, NMOSD differs from MS not only in brain atrophy pattern, but also in WML volume and location, and AccuBrain is a suitable software for analysis.

#### **CLINICAL RELEVANCE/APPLICATION**

AccuBrain is a robust software for calculating WMLs and brain volumetric segmentation in NMOSD and MS patients.

# SSA18-07 Diagnostic Accuracy of the Post-Contrast Double Inversion Recovery (DIR) T2 Sequence and Its Double Inversion Time Influence on the Multiple Sclerosis (SM) Plaque Signal

Sunday, Nov. 25 11:45AM - 11:55AM Room: E352

Participants

Bilal A. Al-Badayneh, MBBS, San Giovanni Rotondo , Italy (*Presenter*) Nothing to Disclose Marco Perri, MD, San Giovanni Rotondo, Italy (*Abstract Co-Author*) Nothing to Disclose Daniela Grasso, MD, Manfredonia, Italy (*Abstract Co-Author*) Nothing to Disclose Rosario Balzano, Foggia, Italy (*Abstract Co-Author*) Nothing to Disclose Annuziata Russo, Barletta, Italy (*Abstract Co-Author*) Nothing to Disclose Annalisa Simeone, San Giovanni Rotondo, Italy (*Abstract Co-Author*) Nothing to Disclose Giuseppe Guglielmi, MD, Foggia, Italy (*Abstract Co-Author*) Nothing to Disclose Teresa Popolizio, San Giovanni Rotondo, Italy (*Abstract Co-Author*) Nothing to Disclose

## For information about this presentation, contact:

marco-perri@tiscali.it

# PURPOSE

To assess the diagnostic accuracy of the DIR T2 sequence in recognizing relapsing or clinically suspicious active MS plaques by using the influence of double inversion time on the scan signal obtained after administered paramagnetic MDC.

## METHOD AND MATERIALS

A total of Forty patients with clinically classified MS disease underwent brain magnetic resonance examinations. All the exams were performed using MR 3T scanner, with standard protocol and use of magnetic susceptibility weighted image sequences (SWI) with subsequent acquisition of Magnetization Prepared Rapid Gradient-Echo (MPRAGE T1) and pre and post-contrast DIR sequences. Two neuroradiologists, blinded on the degree of the clinical status of the disease, evaluated with final consent all the images to identify the presence or absence of lesion enhancements.

# RESULTS

Fourteen out of 40 patients did not show active plaques in the post-contrastographic sequences during remission; SWI only confirmed the presence of iron deposition as a biomarker of the disease. A total of 35 enhanced lesions were detected in 26 patients. The MPRAGE T1 sequences detected 29 lesions (82.8% of the total) in 22 patients; all these lesions showed a reduction in the signal in the post-contrastographic DIR sequences, while the same sequence after MDC showed 6 (17.2%) new cortical lesions active with signal increase in the remaining 4 patients.

## CONCLUSION

Our results demonstrate that the DIR post-contrast sequence has a higher diagnostic accuracy than post-contrast T1-weighted sequences in detecting different degrees of inflammation of MS plaques.

#### **CLINICAL RELEVANCE/APPLICATION**

The Double Inversion Time of DIR sequence is able to visualize different active degree of MS plaques. We believe this MRI findings can detect minimal relapse or remission of the disease and can be a useful tool for evaluate treatment response.

# SSA18-08 Two-Tiered MRI Workup to Rule Out Multiple Sclerosis (MS) Based on Specialty of Referring Physician

Sunday, Nov. 25 11:55AM - 12:05PM Room: E352

Participants Khashayar Rafatzand, MD, Worcester, MA (*Presenter*) Nothing to Disclose Farshad Safaei, Montreal, QC (*Abstract Co-Author*) Nothing to Disclose Masoumeh Kazemi Zanjani, Montreal, QC (*Abstract Co-Author*) Nothing to Disclose

For information about this presentation, contact:

khashayar.rafatzand@umassmemorial.org

#### PURPOSE

To determine cost-effectiveness of a two-tiered MRI protocol for MS based on specific referral patterns.

## **METHOD AND MATERIALS**

Data was extracted from PACS & RIS in a community hospital July 2011-August 2017. <u>INCLUSION</u>: 1. Patients referred for MRI of brain. 2. 'rule-out MS'; <u>EXCLUSION</u>: 1. Previous/known MS, 2. Prior abnormal MRI. <u>MRI protocols</u>: screening (MRIScrC-=Ax FLAIR, Sag Proton-density, Sag T2) vs diagnostic (MRIDxC+=Sag T1 Ax T2, Ax FLAIR, Ax T2\*, Ax DWI, Ax T1 pre-contrast, Ax T1 post-contrast, Sag 3D T1 post-contrast). <u>MRI results</u>: 1. Negative = Normal or not suspicious for demyelination. 2. Positive = Suspicious for demyelinating disease: call back required for the traditional MRI. <u>Technical MRI parameters</u>: 1. Sequence list 2. Allocated MRI time 3. Presence or absence of contrast <u>Referring MD info</u> 1. Neurologist vs. Non-neurologist <u>Patient demographics</u>: 1. Age, Gender, Disposition (Outpatient, ER, Inpatient) <u>Resources & costs identified</u>: MRI operations cost (including scan time, room time, technologist time, secretary time), Radiologist professional fees, contrast cost (IV equipment & MRI contrast), Renal function testing for MRIDxC+, patient visit (parking). <u>Three scenarios were simulated</u>: A) All patients undergo MRIDxC+ (similar to most regional practices). B) All patients underwent MRIScrC-. Patients with positive results called back for MRIDxC+. C) Patients referred by non-neurologists followed pathway A.

#### RESULTS

343 patients were included. (Table 1). <u>MRI results were positive</u> in 9/52 (%17.3) of neurologists' and 31/291 (%10.6) of nonneurologists' patients (p= 0.029). <u>MRI exam time</u>: MRIScrC- 20-minutes, MRIDxC+ 35-minutes. <u>Costs</u>: MRI operations (\$65.6/hour), radiologist fees (\$105/case), contrast (\$17.17), Renal testing (\$41.28), patient visit (\$20/visit). <u>MRI cost in each scenarios</u>: A) \$241.95, B)\$161.47 (%66.7 of A), C) \$175.7 (%72.6 of A). <u>Total savings in B and C</u>: \$27604.64, \$22723.75.

# CONCLUSION

We have demonstrated a higher pre-test probablity for abnormal MRI results based on referring physician's speciality (neurologists in case of MS). A two-tiered MRI protocoling system based on referral source has not been described, and in this population & practice led to significant cost-savings.

## **CLINICAL RELEVANCE/APPLICATION**

Referral patterns should be considered in application of targeted MRI workup strategies.

## SSA18-09 Iron Deposition and Thickness Changes in the Optic Radiation in Relapsing-Remitting Multiple Sclerosis: An Enhanced T2\*-Weighted Angiography Imaging Study

Sunday, Nov. 25 12:05PM - 12:15PM Room: E352

Participants Chun Zeng, Chongqing, China (*Presenter*) Nothing to Disclose Yongmei Li, Chongqing, China (*Abstract Co-Author*) Nothing to Disclose Han Yongliang, Chongqing, China (*Abstract Co-Author*) Nothing to Disclose

#### PURPOSE

relapsing-remitting multiple sclerosis (RRMS) by enhanced T2\*-weighted angiography imaging (ESWAN).

## **METHOD AND MATERIALS**

Fifty-one RRMS patients (42 patients with a disease duration  $[DD] \ge 2$  years [group Mor], 9 patients with a DD < 2 years [group Les]) and 51 healthy controls (group Con) underwent conventional MRI and ESWAN at 3.0 T. Mean phase value (MPV) of the OR was measured on the phase image, and thickness and signal changes were observed on the magnitude image.

#### RESULTS

Group Mor had the lowest MPV. In group Mor, 28 patients with bilateral OR lesions showed bilateral OR thinning with a heterogeneous signal, 14 patients with unilateral OR lesions showed ipsilateral OR thinning with a heterogeneous signal. In the remaining nine patients without OR lesions, bilateral OR showed a normal appearance. In the patients, a negative correlation was found between DD and OR thickness and a positive correlation was found between MPV and OR thickness.

#### CONCLUSION

We confirmed iron deposition in the OR in RRMS patients, and the OR thickness was lower in the patients than in the controls.

#### **CLINICAL RELEVANCE/APPLICATION**

3D-ESWAN can detect iron deposition in the OR in RRMS patients from the early stage of the disease, and the thickness of the OR in patients with a longer DD is lower than that in the controls. Thus, iron deposition in the OR is more pronounced in the early stage and occurs independent of its morphology.



#### SSA19

## Neuroradiology (Cognitive and Psychiatric Disorders)

Sunday, Nov. 25 10:45AM - 12:15PM Room: E351

# NR

AMA PRA Category 1 Credits ™: 1.50 ARRT Category A+ Credit: 1.75

FDA Discussions may include off-label uses.

#### Participants

Ronald L. Wolf, MD, PhD, Philadelphia, PA (*Moderator*) Nothing to Disclose Takashi Yoshiura, MD, PhD, Kagoshima, Japan (*Moderator*) Nothing to Disclose

# Sub-Events

# SSA19-01 Combination of Quantitative Tau Deposition on THK-5351 PET Imaging and Structural Volumetry to Improve Diagnosis in Alzheimer's Disease Spectrum

Sunday, Nov. 25 10:45AM - 10:55AM Room: E351

Participants

Minjae Kim, Seoul, Korea, Republic Of (*Abstract Co-Author*) Nothing to Disclose Sang Joon Kim, MD, Seoul, Korea, Republic Of (*Abstract Co-Author*) Nothing to Disclose Ji Eun Park, Seoul, Korea, Republic Of (*Abstract Co-Author*) Nothing to Disclose Woo Hyun Shim, Seoul, Korea, Republic Of (*Abstract Co-Author*) Nothing to Disclose Jessica Yun, Seoul, Korea, Republic Of (*Abstract Co-Author*) Nothing to Disclose Younghee Yim, MD, Chuncheon-si, Korea, Republic Of (*Presenter*) Nothing to Disclose

#### For information about this presentation, contact:

manzae.kim@gmail.com

# PURPOSE

The purpose of this study was to determine whether quantitative measurement of tau deposition from [18F]THK-5351 positron emission computed tomography (Tau PET) can improve diagnosis of Alzheimer's disease spectrum with well-defined structural volumetry on MRI.

# METHOD AND MATERIALS

From a prospective database in a multicenter study (NCT02656498), 113 subjects who had both baseline structural MRI and Tau PET within 6 month interval were included. There were 32 normal controls (NC), 55 mild cognitive impairment (MCI), and 26 Alzheimer's disease (AD) patients, and all institutions received IRB approval. Hippocampal volume was quantified from FDA-approved software for automated volumetric MRI analysis (Neuroquant) using T1-weighted-images. Standardized uptake value ratio (SUVr) was calculated from Tau PET images for 6 composite FreeSurfer-derived regions-of-interests (ROIs) approximating the anatomical definitions of in-vivo Braak stage 6 regions (Braak ROIs). Analysis of variance was performed to determine locations for structural volumetry analysis. Diagnostic performance of Tau PET ROIs and structural volumetry were compared using the area under the receiver-operating characteristic curve (AUROC).

## RESULTS

Compared with NC, MCI and AD showed significantly lower hippocampal volume (mean±standard deviation, NC, 7.14±0.84; MCI, 5.99±1.18; AD, 5.90±1.30mm3, P=0.01) and AD showed lower anterior cingulate volume (NC, 6.09±0.85; MCI, 6.00±0.76; AD, 5.43±0.91mm3, P=0.006). The diagnostic performance of structural volumetry (hippocampus and anterior cingulate) was higher than Braak ROIs in diagnosing AD from MCI (volumetry AUROC 0.70, 0.57-0.83 vs. Tau PET AUROC, 0.60, 0.48-0.71) or in diagnosing AD from NC (volumetry AUROC 0.84, 0.73-0.94 vs. Tau PET AUROC, 0.78, 0.65-0.87). Adding Braak ROIs significantly improved diagnostic performance in distinguishing AD from MCI (AUROC 0.81, 0.70-0.92, P<0.01) as well as AD from NC (AUROC, 0.93, 0.87-0.99, P <0.05) than using structural volumetry or Tau PET alone.

#### CONCLUSION

Quantitative analysis of tau deposition improved the diagnostic performance compared to structural volumetry alone in diagnosis of Alzheimer's disease spectrum, especially in diagnosis of Alzheimer's disease.

# **CLINICAL RELEVANCE/APPLICATION**

Differentiating AD from MCI still remains as a diagnostic challenge in clinical practice and adding quantitative Tau deposition using Braak ROIs may become a potentially useful imaging biomarker.

## SSA19-02 White Matter Cellularity Change Correlates with CSF B-Amyloid in Preclinical Alzheimer's Disease

Sunday, Nov. 25 10:55AM - 11:05AM Room: E351

Qing Wang, PhD, St. Louis, MO (Presenter) Nothing to Disclose

Suzanne Schindler, St Louis, MO (Abstract Co-Author) Nothing to Disclose

Anne Fagan, PhD, Saint Louis, MO (*Abstract Co-Author*) Consultant, F. Hoffmann-La Roche Ltd Consultant, IBL International Corp John Morris, Saint Louis, MO (*Abstract Co-Author*) Research support, Eli Lilly and Company Consultant, Eli Lilly and Company Yong Wang, PhD, St. Louis, MO (*Abstract Co-Author*) Consultant, Medtronic plc

Tammie S. Benzinger, MD, PhD, Saint Louis, MO (*Abstract Co-Author*) Research Grant, Eli Lilly and Company Investigator, Eli Lilly and Company Investigator, F. Hoffmann-La Roche Ltd

# PURPOSE

Innate immune cells, particularly microglia and astrocytes, have been reported to mediate the inflammatory response in Alzheimer disease (AD) and are considered to be an important contributor to AD pathogenesis. In the AD brain, AB deposition and neurofibrillary tangles provide obvious stimuli for neuroinflammation. This study aims to investigate the relationship between CSF B-amyloid (AB42) (a marker of AB deposition) and white matter cellularity change (reflecting immune cell activation) in preclinical AD using a diffusion MRI based method, neuro-inflammation imaging (NII).

## METHOD AND MATERIALS

CSF samples from 143 participants (average age  $65.0 \pm 8.2$ ) with normal cognition underwent analysis for AB42, total tau (tTau) and phosphotau 181 (pTau) with Roche Elecsys assays performed on the automated Roche cobas e 601 analyzer. NII was acquired with multi-b value scheme (bmax =1400s/mm2 and 23 directions). NII cell diffusivity (reflecting inflammatory cell activation) and cell fraction (reflecting inflammatory cell infiltration) was quantified by solving the NII model. The whole brain voxel-wise DTI-indices was analyzed using Tract Based Spatial Statistics (TBSS) (available in FSL).

#### RESULTS

NII cell diffusivity and cell fraction in major WM tracts was negatively correlated with CSF levels of A642 (Fig. 1 and 2). As an estimate of effect size, partial correlations were also examined between the NII imaging marker and CSF A642. When controlling with age, gender and APOE  $\epsilon$ 4 genotype, the partial correlations with CSF A642 was rpartial = -0.34 (P < 0.001) for NII cell diffusivity in the genu of corpus callosum (Fig. 1B) and rpartial = -0.30 (P < 0.001) for NII cell fraction in the posterior lateral capsule (Fig. 2B). Positive correlation between NII cell diffusivity with CSF tTau and pTau in the corpus callosum was observed.

# CONCLUSION

The significant negative correlations between NII cellularity and CSF A $\beta$ 42 suggest NII may be used to track the immune cell activation associated with abnormal  $\beta$ -amyloid accumulation. NII holds promise to noninvasively study the role of inflammation during AD progression and the effect of treatments targeting immune response.

# **CLINICAL RELEVANCE/APPLICATION**

Neuro-inflammation imaging holds promise to noninvasively study the role of inflammation during Alzheimer disease progression and the effect of treatments targeting immune response.

# SSA19-03 Correlation of Lobar Cerebral Microbleeds with Amyloid, Perfusion, and Metabolism in Alzheimer's Disease

Sunday, Nov. 25 11:05AM - 11:15AM Room: E351

#### Participants

Nasim Sheikh Bahaei, MD, FRCR, Irvine, CA (*Presenter*) Nothing to Disclose Roido Manavaki, Cambridge, United Kingdom (*Abstract Co-Author*) Nothing to Disclose Seyed Ahmad Sajjadi, MD,PhD, Irvine, CA (*Abstract Co-Author*) Nothing to Disclose Andrew N. Priest, DPhil, Cambridge, United Kingdom (*Abstract Co-Author*) Nothing to Disclose John T. O'Brien, MBBS, Cambridge, United Kingdom (*Abstract Co-Author*) Nothing to Disclose Jonathan H. Gillard, MD, Cambridge, United Kingdom (*Abstract Co-Author*) Consultant, GlaxoSmithKline plc

## For information about this presentation, contact:

nasim\_sh@me.com

## PURPOSE

Despite the well-documented relationship between lobar CMBs (ICMB) and Alzheimer's disease (AD), there is limited knowledge about the role of ICMB in AD pathology. To understand the nature of this relationship, we investigated the association between ICMB and total and regional amyloid load, perfusion and metabolism.

# METHOD AND MATERIALS

Participants with AD, Mild cognitive impairment (MCI) and age-matched healthy controls were recruited through well-established memory services. Detailed cognitive assessments and cardiovascular (CV) history and risk factors were recorded. All participants were imaged with Pittsburg-Compound B (PiB)-, Fludeoxyglucose (FDG)-PET followed by 3T MRI with susceptibility-weighted-imaging (SWI). Early frames of PiB-PET (1-8 min) were utilized to estimate perfusion and late frames (40-70 min) to measure amyloid burden. FDG emission data was acquired from 60-90 minutes after injection. PET uptake was presented as standardized uptake value ratio (SUVR) using cerebellum as reference. Presence of ICMB in each anatomical region was documented and the association between ICMB and PET uptake in each lobe was measured using multiple regression models. The mean of PET SUVRs was also compared between groups using t-test.

#### RESULTS

In multiple regressions models adjusting for sex, age, education, CV risk factors and clinical diagnosis, presence of ICMB was associated directly with total (p<0.001) and regional (p=0.01) late PiB and inversely with early PiB uptakes (p=0.04). In MCI group, participants with ICMB had higher perfusion (p=0.001) and metabolism (0.03) compared to MCI without ICMB, while AD individuals with ICMB had lower perfusion (p=0.03) than those with no ICMB and no significant difference in their metabolism. Presence of ICMB also weakened the association between perfusion and metabolism (R2 =0.2 versus R2 =0.49).

#### CONCLUSION

There is a significant relationship between ICMBs and various markers of AD pathology. ICMB has spatial association with AB load and complex effect on perfusion and metabolism.

## **CLINICAL RELEVANCE/APPLICATION**

ICMB could exacerbate and accelerate the neurodegenerative process in AD by affecting perfusion and metabolism. Regional association between ICMB and amyloid burden in PET suggests vascular amyloid could represent total amyloid load.

# SSA19-04 Mismatch of Perfusion and Brain Function in Type 2 Diabetes with Normal Cognition: Potential Compensation for Cognitive Impairment?

Sunday, Nov. 25 11:15AM - 11:25AM Room: E351

Participants

Ying Yu, Xian, China (*Presenter*) Nothing to Disclose Qian Sun, Xian, China (*Abstract Co-Author*) Nothing to Disclose Jin Zhang, Xian, China (*Abstract Co-Author*) Nothing to Disclose Bo Hu, MD, Xian, China (*Abstract Co-Author*) Nothing to Disclose Yang Yang, Xian, China (*Abstract Co-Author*) Nothing to Disclose Xin Zhang, Xian, China (*Abstract Co-Author*) Nothing to Disclose Yu-Jie Dai, Xian, China (*Abstract Co-Author*) Nothing to Disclose Yu-Jie Dai, Xian, China (*Abstract Co-Author*) Nothing to Disclose Lin-Feng Yan, Xi'an, China (*Abstract Co-Author*) Nothing to Disclose Si-Jie Xiu, Xian, China (*Abstract Co-Author*) Nothing to Disclose Si-Jie Xiu, Xian, China (*Abstract Co-Author*) Nothing to Disclose Si-Jie Xiu, Xian, China (*Abstract Co-Author*) Nothing to Disclose Yu-Chuan Hu, Xi'an, China (*Abstract Co-Author*) Nothing to Disclose Xiao-Cheng Wei, Beijing, China (*Abstract Co-Author*) Nothing to Disclose Zhongqiang Shi, Xi an, China (*Abstract Co-Author*) Nothing to Disclose Wen Wang, Xi'an, China (*Abstract Co-Author*) Nothing to Disclose Guang-Bin Cui, MD, Xian, China (*Abstract Co-Author*) Nothing to Disclose

For information about this presentation, contact:

yqlmn@126.com

#### PURPOSE

Type 2 diabetes mellitus (T2DM) is associated with increased risk of cognitive impairment and dementia, for which the disturbance in cerebral perfusion is an important etiology. The aim of this study is to explore the effect of T2DM on the coupling between cerebral blood flow (CBF) and cortical activation and its potential contribution to cognitive function.

#### **METHOD AND MATERIALS**

A total of 36 T2DM patients with normal cognition and 36 sex- and age-matched healthy subjects underwent arterial spin labeling imaging to compute CBF, resting-state functional MR (fMR) to identify the CBF-related network, and to calculate indicators of cortical activations, including functional connectivity strength (FCS), functional connectivity (FC) between region with decreased CBF and the whole brain, mean amplitude of low-frequency fluctuation (mALFF) and mean regional homogeneity (mReHo) of regions within CBF-related network. The CBF-cortical activation correlation coefficients, the so called CBF-cortical activation coupling, of regions in CBF-related network and its relationship with cognitive performance were compared between the 2 groups.

## RESULTS

T2DM patients with normal cognition showed significantly reduced CBF in the rostroventral area of the left inferior parietal lobule, whereas increased FCS in left dorsal caudate. In T2DM patients, significantly increased CBF-related FCs were predominantly located in cognitive- and executive-related brain regions, including the middle frontal gyrus (MFG), fusiform gyrus (FuG), superior parietal lobule (SPL), and inferior parietal lobule (IPL). The CBF-FC coupling at IPL, SPL, and CBF-mReHo coupling at MFG were significantly increased in T2DM patients. FCs of CBF-related network was positively correlated with global cognition, whereas negatively correlated with episodic memory and executive function across all subjects.

## CONCLUSION

Our findings demonstrated that the mismatched decreased CBF accompanied by increased FCs in CBF-related network plays a complementary role in T2DM patients with normal cognition. Increased neurovascular coupling might be a possible neuropathological mechanism of the preservation of cognitive function in T2DM patients.

#### **CLINICAL RELEVANCE/APPLICATION**

CBF and CBF-related FCs from fMR play a complementary role in early T2DM and are recommended as powerful biomarkers to explore the neuropathological mechanism of cognitive impairment and preservation.

## SSA19-05 The Cortical-Limbic Structural Covariance Network as an Early Predictive Bio-Signature for Cognitive Impairment in Parkinson's Disease

Sunday, Nov. 25 11:25AM - 11:35AM Room: E351

Participants

Yueh-Sheng Chen, MD, Kaohsiung, Taiwan (*Presenter*) Nothing to Disclose Meng-Hsiang Chen, Kaohsiung, Taiwan (*Abstract Co-Author*) Nothing to Disclose Kun-Hsien Chou, Taipei, Taiwan (*Abstract Co-Author*) Nothing to Disclose Cheng-Hsien Lu, Kaohsiung, Taiwan (*Abstract Co-Author*) Nothing to Disclose Chih Ying Lee, Kaohsiung, Taiwan (*Abstract Co-Author*) Nothing to Disclose Wei-Che Lin, MD, Kaohsiung, Taiwan (*Abstract Co-Author*) Nothing to Disclose

## PURPOSE

In the present study, we sought to identify the epicenter and its associated structural network that targeted the cognitive

impairments in Parkinson's disease (PD). We then tested whether alterations of the structural network would predict future cognitive decline in PD patients.

# METHOD AND MATERIALS

One hundred and one patients with PD (subgrouping into 3 groups [PD-normal (PDN), PD-mild cognitive impairment (PDMCI), PDdementia (PDD)]) and 58 normal control volunteers underwent comprehensive neuropsychological testing and T1W volumetric MRI scans. Epicenters were identified by voxel-wise group comparison between PDN and PDD. Gray matter structural covariance network (SCN) were constructed using the epicenters as seeds. The SCN volume corrected by total intracranial volume was calculated in each individual to reflect the SCN integrity. The PDN group had follow-up neuropsychological testing one year after the initial exam to assess the status of conversion into cognitive impairment.

## RESULTS

Bilateral amygdala and hippocampus were significantly atrophied in PDD as compared to PDN group. Analysis of bilateral amygdala/hippocampus SCN showed decreasing volume in PDD and PDMCI as compared to PDN group. The PDD group showed stronger covariance strength in the left prefrontal cortex as compared to the PDN group. The lower volume of bilateral amygdala/hippocampus SCN were associated with poorer cognitive function in all domains while lower volume in the prefrontal cortex was associated with poorer cognitive function and executive function domain. Smaller volume of bilateral amygdala/hippocampus SCN and left prefrontal cortex in the PDN patients can predict the conversion into PDMCI at one-year follow-up.

## CONCLUSION

The cortico-limbic system is important in cognitive decline in PD patients. The atrophy of amygdala/hippocampus SCN and increased co-atrophy of the prefrontal cortex can early predict MCI conversion in PD patients with normal cognition.

## **CLINICAL RELEVANCE/APPLICATION**

The analysis of cortical-limbic structural covariance network alteration can early predict MCI conversion in PD patients with normal cognition.

## SSA19-06 Repetitive Transcranial Electrical Stimulation Produces Enhanced Resting Cerebral Perfusion in the Locus Coeruleus

Sunday, Nov. 25 11:35AM - 11:45AM Room: E351

Participants

Matthew S. Sherwood, PhD, Dayton, OH (*Presenter*) Research Consultant, DCS Corporation Aaron Madaris, MS, BEng, Fairborn, OH (*Abstract Co-Author*) Intern, DCS Corporation Casserly Mullenger, MPH, Beavercreek, OH (*Abstract Co-Author*) Nothing to Disclose R. A. McKinley, PhD, Wright-Patterson AFB, OH (*Abstract Co-Author*) Nothing to Disclose

For information about this presentation, contact:

matthew.sherwood.7.ctr@us.af.mil

# PURPOSE

To evaluated the effect of repetitive left prefrontal transcranial electrical stimulation (TES) on cerebral perfusion (i.e., cerebral blood flow, CBF).

## METHOD AND MATERIALS

11 healthy, active-duty, Air Force military members completed 3 experimental sessions on 3 consecutive days. Transcranial DC stimulation, a form of TES, was utilized to deliver 2mA to the left prefrontal cortex (approximately F3) for 30 min at each session. Stimulation began concurrently with a 30 min laboratory vigilance task. The cathode was placed on the contralateral bicep. Preand post-stimulation MRI acquisitions were conducted at each session. The MRI procedure included a 3D pseudo-continuous arterial spin labeling sequence to acquire resting CBF. A control group consisting of 9 subjects performed the same procedures except sham stimulation was provided (30 s of stimulation followed by 19.5 min of no stimulation). CBF maps were created from the raw ASL data using proton density maps and a single-compartment perfusion model. The CBF maps were registered to a reference space. Permutation testing compared changes in CBF from session 1 pre-stimulation to session 3 post-stimulation between groups and within-groups on a voxel-wise basis using 500,000 permutations. The permutation test results were cluster-corrected for multiple comparisons.

#### RESULTS

Widespread increases in perfusion, indicative of increased metabolism, were observed in the active stimulation group; however, general decreases were observed in a matched group receiving sham TES. Furthermore, perfusion increased significantly more in the active stimulation group across many areas of the brain. These increases originated in the locus coeruleus (LC) and spread extensively to regions in the neocortex supporting functions such as object recognition and top-down attentional modulation.

#### CONCLUSION

Altered CBF in the LC is indicative of enhanced metabolic activity as cerebral perfusion is neurovascularly coupled with glucose metabolism. This finding increases our understanding of the broad behavioral effects that have been demonstrated using left prefrontal TES.

## **CLINICAL RELEVANCE/APPLICATION**

Altered production of norepinephrine has been linked with many neurologic disorders including Parkinson's disease, major depression disorder, and attention deficit hyperactivity disorder. Our findings implicate the potential for left prefrontal TES in the treatment of such disorders.

# SSA19-07 Tract Based Spatial Statistics in Persons who Will Develop Alzheimer's Dementia: A Study from the Alzheimer's Disease Neuroimaging Initiative (ADNI)

Participants Cyrus Raji, MD,PhD, St. Louis, MO (*Presenter*) Consultant, Brainreader ApS Maxwell B. Wang, BS, San Francisco, CA (*Abstract Co-Author*) Nothing to Disclose Erin Moe, BA, San Francisco, CA (*Abstract Co-Author*) Nothing to Disclose Eva M. Palacios, San Francisco, CA (*Abstract Co-Author*) Nothing to Disclose Pratik Mukherjee, MD, PhD, San Francisco, CA (*Abstract Co-Author*) Research Grant, General Electric Company Medical Adivisory Board, General Electric Company

## For information about this presentation, contact:

cyrusraji@gmail.com

## PURPOSE

To quantify differences in diffusion tensor imaging of persons who decline from normal cognition to Alzheimer's dementia compared to controls who do not develop dementia.

## **METHOD AND MATERIALS**

All subjects were from ADNI2 (n = 20). Average age was 73.4  $\pm$  3.9 years with age range 68.2-83.7 years. All subjects were age and gender-matched for comparison. The sample was 60% women and 40% men. Each subject received 3T MR imaging on either a Siemens or GE scanner for T1 volumetric imaging, MP-RAGE for Siemens or SPGR for GE. All DTI scans were obtained on a 3T GE scanner. Raw T1 and DTI DiCOM images were converted to NiFTI file format. Each scan was visually inspected for gross artifacts. Images were corrected for motion, eddy currents and skull-stripped using the fMRI software library (FSL). Fractional anisotropy (FA), mean diffusivity (MD), axial diffusivity and radial diffusivity (RD) maps were also obtained via FSL's dtifit and FSLmaths tools and visualized for errors. Data were then processed through FSL's tract-based spatial statistics (TBSS) with default parameters. FA, MD, RD, and axial diffusivity values were extracted.

#### RESULTS

Of the 20 subjects, 10 experienced longitudinal cognitive decline and 10 remained cognitively normal. Of the 10 converters, 80% were MCI at baseline and converted to AD and of these 50% declined after 6 months and another 50% declined after 12 months. Of the remaining two converters, one declined from normal to mild cognitive impairment (MCI) to AD after 24 months and another subject experienced a similar trajectory after 48 months. Comparing global DTI metrics, there was a trend towards statistical significance with respect to lower global mean FA in converters compared to non-converters (t = -.43, p = .07). However, voxel wise analyses with TBSS showed statistically significant reductions in frontal white matter tracts in converters compared to non-converters as shown in Figure 1 (red arrows). There were no statistically significant differences in other global DTI metrics including RD, MD, and axial diffusivity.

#### CONCLUSION

Diffusion weighted MR imaging identifies quantifiable differences between AD converters compared to non-converters.

#### **CLINICAL RELEVANCE/APPLICATION**

Identification of non-invasive quantitative neuroimaging biomarkers that predict cognitive decline to Alzheimer's dementia is important for determining persons who may benefit from drug trials or modification of risk factors.

#### SSA19-08 MR Differences of Cerebral Small Vessel Diseases in AD and MCI Patients

Sunday, Nov. 25 11:55AM - 12:05PM Room: E351

Participants

Yuhan Jiang, Dalian, China (*Abstract Co-Author*) Nothing to Disclose Yanwei Miao, Dalian, China (*Abstract Co-Author*) Nothing to Disclose Jin Shang, Dalian, China (*Abstract Co-Author*) Nothing to Disclose Yiwei Che, Dalian, China (*Abstract Co-Author*) Nothing to Disclose Peipei Chang, Dalian, China (*Abstract Co-Author*) Nothing to Disclose Ailian Liu, MD, Dalian, China (*Abstract Co-Author*) Nothing to Disclose Lijun Wang, Dalian, China (*Presenter*) Nothing to Disclose

For information about this presentation, contact:

jiangyuhan0728@163.com

#### PURPOSE

To evaluate and compare MRI manifestations of cerebral small vessel diseases (SCVD)among Alzheimer's disease (AD), mild cognitive impairment (MCI) patients and healthy controls (HC), and then to analyze the correlation between CSVD and cognitive score.

## **METHOD AND MATERIALS**

Twenty-four AD patients (12 men and 12 women; mean age, 73.08±8.39 yrs) and twenty-four cases of MCI (11 men and 13 women; mean age, 70.08±8.5 yrs) were participated into this study. Twenty-two volunteers without cognitive dysfunction were also recruited as controls (11 men and 11 women; mean age, 71.01±8.10 yrs). Their age, gender and education matched in three groups. All subjects underwent conventional sequences (including T1WI, T2WI and T2 Flair) and SWI on 3.0T MRI scanner. Enlarged perivascular spaces (EPVS) were counted and scored in basal ganglia (BG) and centrum semiovale (CS). Moreover, cerebral microbleeds (CMBs) and lacunar infarction (LI) were also counted, whileas white matter hyperintensity lesions(WMH) were graded and recorded. The Kruskal-Wallis test and Kolmogorov-Smirnov Z test were used to compare the ranked data between groups. Correlation between SCVD and MMSE were assessed by spearman correlation analysis.

#### RESULTS

In the BG, EPVS scores increased in AD group (2.08±0.77) than in MCI (1.29±0.46) and controls(1.09±0.29)(P<0.01); no difference

was found between EPVS scores in MCI and controls (P>0.05). In the CS, EPVS scores in AD group (2.87 $\pm$ 0.79) and MCI group (2.12 $\pm$ 0.53) were significantly higher than that in controls (1.36 $\pm$ 0.49) (P<0.01). There was no difference of cerebral microbleeds between three groups (P>0.05). The periventricular WMH and deep WMH in the AD group increased than in the controls (P<0.05). Compared to MCI group, AD group showed more severe in the periventricular WMH (P<0.01). The incidence of LI was most in AD group (58.3%, 14/24), in turn in MCI group (29.2%, 7/24) and in controls (18.2%, 4/22, P<0.05). In all data, EPVS in BG and CS, periventricular and deep WMH showed the negative correlation with MMSE score (r=-.072, -0.31, -0.56, -0.40; all P <0.05).

## CONCLUSION

CSVD is more common in AD than in MCI patients, and EPVS and WMH have significant effect on cognitive impairment.

# **CLINICAL RELEVANCE/APPLICATION**

CSVD is common in AD patients and is associated with the clinical status.

# SSA19-09 Altered Functional and Effective Connectivity Patterns Based on the Subregion of Hippocampus in Young Apoeɛ4 Carriers: A Three-Year Follow-Up Study

Sunday, Nov. 25 12:05PM - 12:15PM Room: E351

Participants Li Juan Zheng, MS, Nanjing, China (*Presenter*) Nothing to Disclose Long Jiang Zhang, MD, PhD, Nanjing, China (*Abstract Co-Author*) Nothing to Disclose Guang Ming Lu, MD, PhD, Nanjing, China (*Abstract Co-Author*) Nothing to Disclose

# For information about this presentation, contact:

18502524467@163.com

# PURPOSE

To determine whether the functional and effective connectivity based on the subregions of hippocampus altered in young APOE4 carriers with follow-up.

## **METHOD AND MATERIALS**

Resting-state functional MRI data and neuropsychological scales were obtained for APOE4 (with the age 24.0±3.2 years old, 7 female and 6 male) and APOE3 carriers (with the age 22.9±1.6 years old, 12 female and 7 male) at baseline and three-year followup. The hippocampi were divided along the A-P axis, into three equal sections (sub1/2/3 respectively stands for the anterior, middle and posterior part of the hippocampus). The hippocampus- and sub- based functional connectivity (FC) patterns were compared by mixed effect analysis and further post-hoc analysis. The effective connectivity (EC) patterns among the altered regions, affected by APOE4-by-time interaction, were examined in APOE4 groups at baseline and follow-up. The correlation analysis was conducted between the values of altered FC or EC and neuropsychological scales

## RESULTS

The APOE4-by-time interaction effect was evident in FC between sub3(L) and left middle and superior temporal gyrus (MTG/STG), sub2(R) and MTG/STG(L), and sub3(R) and anterior cingulate cortex(ACC). The Post-hoc analysis revealed decreased FC in sub3(L)-MTG/STG(L), sub3(R)-ACC, and increased FC in sub2(R)-MTG/STG(L) in APOE4 group at baseline when compared with APOE3 group. The APOE4 group at follow-up showed increased FC in sub3(L)-MTG/STG(L), sub3(R)-ACC and decreased FC in sub2(R)-MTG/STG(L) (all P<0.05, corrected by Gaussian random field with voxel-size P<0.01 and cluster-size P<0.05). The FC in sub3(L)-MTG/STG(L) at baseline and sub2(R)-MTG/STG(L) at follow-up correlated with the scores of scales both in APOE3 and APOE4 group. Besides, the APOE4 group showed increased EC separately from sub2(L) and MTG/STG(L) to sub3(L) among altered regions (the bilateral sub2/3, MTG/STG(L) and ACC). The values of changes in EC from MTG/STG(L) to sub3(L) positively correlated with the changed scores of delayed recall test (all P<0.05).

#### CONCLUSION

The left posterior part of hippocampus might be most vulnerable and susceptible to early modulation of interaction of APOE4 by time, which might be used as the longitudinal imaging-derived-phenotype in APOE 4 carriers.

## **CLINICAL RELEVANCE/APPLICATION**

providing a new biomarker to predict the early neuroimaging alteration in the young carriers.



#### SSA20

# Physics (Ultrasound in Imaging and Radiation Therapy)

Sunday, Nov. 25 10:45AM - 12:15PM Room: S102CD



AMA PRA Category 1 Credits ™: 1.50 ARRT Category A+ Credit: 1.75

FDA Discussions may include off-label uses.

#### Participants

Flemming Forsberg, PhD, Philadelphia, PA (*Moderator*) Research Grant, Canon Medical Systems Corporation; Research Grant, General Electric Company; Research Grant, Siemens AG; Research Grant, Lantheus Medical Imaging, Inc Thaddeus A. Wilson, PhD, Madison, WI (*Moderator*) Nothing to Disclose

#### Sub-Events

# SSA20-01 Parametric Mapping of the Prostate with Contrast-Enhanced Subharmonic Imaging

Sunday, Nov. 25 10:45AM - 10:55AM Room: S102CD

Participants

Bradley Freid, Philadelphia, PA (*Abstract Co-Author*) Nothing to Disclose Ethan J. Halpern, MD, Philadelphia, PA (*Abstract Co-Author*) Nothing to Disclose Venkat Masarapu, MD, Philadelphia, PA (*Abstract Co-Author*) Nothing to Disclose Priscilla Machado, MD, Philadelphia, PA (*Abstract Co-Author*) Nothing to Disclose Edouard J. Trabulsi, MD, Philadelphia, PA (*Abstract Co-Author*) Consultant, Intuitive Surgical, Inc Stockholder, Intuitive Surgical, Inc Consultant, Amgen Inc Speaker, Amgen Inc Consultant, Johnson & Johnson Speaker, Johnson & Johnson Flemming Forsberg, PhD, Philadelphia, PA (*Presenter*) Research Grant, Canon Medical Systems Corporation; Research Grant, General Electric Company; Research Grant, Siemens AG; Research Grant, Lantheus Medical Imaging, Inc

#### For information about this presentation, contact:

flemming.forsberg@jefferson.edu

## PURPOSE

To prospectively evaluate different quantitative parameters from contrast-enhanced transrectal subharmonic imaging (SHI) for the diagnosis of prostate cancer with histopathology as the reference standard.

#### **METHOD AND MATERIALS**

Fifty-five male patients scheduled for a transrectal systematic prostate biopsy were enrolled in this IRB-approved study. A 12-core sextant biopsy was done in each subject along with up to 6 additional targeted biopsies. Subjects were imaged with a transrectal IC5-9D ultrasound (US) transducer on a modified Logiq E9 system (GE Healthcare; Milwaukee, WI) operating in SHI mode (transmit/receive: 7.0/3.5 MHz). Two vials of the US contrast agent Definity (Lanteus Medical Imaging; N. Billerica, MA) diluted in 50 mL of saline were infused over 10 minutes. Images were obtained with transverse sweeps though the prostate using conventional US, color and power Doppler, as well as contrast harmonic imaging (HI), and SHI. Microbubble destruction pulses followed by motion-compensated maximum intensity projection (MIP) was evaluated in combination with HI and SHI. Imaging modes were rated on a five-point scale (1-5; benign to definitely malignant) for each sextant. Using MIP time intensity curves, parametric maps were generated at each biopsy location for the peak intensity (PI), time to peak (TTP), and estimated perfusion (EP as the slope of the wash-in). Parameters were compared to biopsy results.

#### RESULTS

Prostate cancer was found in 55 of 660 cores (8.33%) from 24 of the 55 subjects (43.64%). No significant difference between benign and malignant biopsy specimens were demonstrated for TTP ( $3.01 \pm 1.52$  vs  $3.18 \pm 1.56$  s; p=0.44). Two quantitative SHI parameters showed a significant difference between benign and malignant biopsy cores: EP ( $25.69 \pm 8.74$  vs  $30.09 \pm 10.23$  a.u./s; p=0.0007) and PI ( $123.85 \pm 16.02$  vs  $129.66 \pm 17.38$  a.u.; p=0.014).

#### CONCLUSION

Quantitative SHI demonstrates significantly higher EP and PI at sites with prostate cancer.

# **CLINICAL RELEVANCE/APPLICATION**

SHI appears to improve the diagnosis of prostate cancer relative to conventional transrectal US.

# SSA20-02 Ultrasonic Spectrum Analysis of the RF Time Series Can Early Predict the Tumor Response to Chemotherapy in Preclinical Breast Cancer Models

Sunday, Nov. 25 10:55AM - 11:05AM Room: S102CD

Yini Huang, MD, Guangzhou, China (*Abstract Co-Author*) Nothing to Disclose Jianhua Zhou, MD, Guangzhou, China (*Abstract Co-Author*) Nothing to Disclose Longhui Cao, Guangzhou, China (*Abstract Co-Author*) Nothing to Disclose Jianwei Wang, Guangzhou, China (*Abstract Co-Author*) Nothing to Disclose Chunyi Lin, Guangzhou, China (*Abstract Co-Author*) Nothing to Disclose Qing Li, Guangzhou, China (*Abstract Co-Author*) Nothing to Disclose Xueyi Zheng, Guangzhou, China (*Abstract Co-Author*) Nothing to Disclose Yun Wang, Guangzhou, China (*Abstract Co-Author*) Nothing to Disclose

## For information about this presentation, contact:

lifei@sysucc.org.cn

#### PURPOSE

This study was aimed to assess whether ultrasonic spectrum analysis of radiofrequency (RF) time series using a clinical ultrasound system allows for the early prediction of the tumor response to chemotherapy in human breast cancer xenografts that imitate clinical responding and nonresponding tumors.

#### **METHOD AND MATERIALS**

Clinically responding (n=20; MCF-7) and nonresponding (n=20; MBA-MD-231) breast cancer xenografts were established in 40 nude mice. Ten mice from each group received either chemotherapy (adriamycin, 4 mg/kg) or saline as controls. Each tumor was imaged longitudinally with a clinical ultrasound scanner at baseline (day 0) and subsequently on days 2, 4, 6, 8 and 12 following treatment, and the corresponding RF time-series data were collected. Changes in six RF time-series parameters (slope, intercept, S1, S2, S3 and S4) were compared with the measurement of the tumor cell density, and their prediction performances of the treatment response were analyzed.

#### RESULTS

Adriamycin significantly inhibited tumor growth and decreased the cancer cell density in responders (P < 0.001) but not in nonresponders (P > 0.05). Fold changes of slope were significantly increased in responders two days after adriamycin treatment (P = 0.002), but not in nonresponders (P > 0.05). Early changes in slope on day 2 could predict the treatment response in 100% of both responders (95% CI, 62.9-100.0%) and nonresponders (95% CI, 88.4-100%).

#### CONCLUSION

Ultrasonic RF time series allowed for the monitoring of the tumor response to chemotherapy and could further serve as biomarkers for the early prediction of treatment outcomes.

# **CLINICAL RELEVANCE/APPLICATION**

Because ultrasound imaging provided several major benefits such as the relatively low cost, portability and repeatability, and lack of radiation risks, our study built the foundation of further translational research to assess the clinical application of the RF time series to predict the treatment response in cancer patients without using any contrast agents.

# SSA20-03 Electric-Field Induced Acoustic Tomography (EfAT) for In-Situ Monitoring of Tumor Ablation during Irreversible/Reversible Electroporation

Sunday, Nov. 25 11:05AM - 11:15AM Room: S102CD

Participants

Ali Zarafshani, Norman, OK (*Abstract Co-Author*) Nothing to Disclose Siqi Wang, Norman, OK (*Abstract Co-Author*) Nothing to Disclose Bin Zheng, PhD, Pittsburgh, PA (*Abstract Co-Author*) Nothing to Disclose Liangzhong Xiang, PhD, Norman, OK (*Presenter*) Nothing to Disclose

#### For information about this presentation, contact:

a.zarafshani@ou.eduxianglzh@ou.edu

#### PURPOSE

High intensity ultra-short pulsed electric fields applied across a cell to increase the membrane permeability, allowing non-permeant drugs, genes access (or tumor ablation) through the formation of nano-scale pores in the cell membrane, known as reversible (or irreversible in the case where nano-scale defects in the cell membrane is used for tumor ablation instead of drugs/genes delivery). For physicians, real-time monitoring of cancer treatment and characterization of the delivered electric field is very important for treatment planning and therapy efficacy monitoring. Many techniques i.e. MRI or MREIT are suggested to characterize this process, but currently cannot monitor the process during pulse delivery in real time and mostly used for pre-and post-stimulation exposure.

## **METHOD AND MATERIALS**

A new imaging technique based on flow of electric field induced acoustic tomography is reported. The absorbed electric energy around the subject under test raises its temperature, thus leading to expansion effects. The expansion, then induces acoustic tomography images which can be acquired outside the body and consequently be used for real-time characterization and monitoring the electroporation process. These acoustic images made through the high-intensity and ultra-short pulsed electric fields that used in the electroporation process where combines the advantages of high-contrast electric field distribution and high-ultrasonic spatial resolution.

#### RESULTS

We captured different acoustic signals and corresponding ultrasonic images by changing the location of electric distribution in scale of mm and varying the electric field intensity ( $\mu$ s-ns 20kVcm-1-63kVcm-1) applied in irreversible and reversible electroporation process. The experimental results demonstrated a linear correlation between the measured acoustic signals and the intensity of the electric field.

# CONCLUSION

The study results indicate that this new technique can potentially be used for monitoring the electric field distribution as a noninvasive, label-free technique for real-time, in situ monitoring of electroporation-based technologies for treatment and ablation cancer.

#### **CLINICAL RELEVANCE/APPLICATION**

for ECT and NIIRE, the treatment efficiency is correlated to electric field distribution. To ensure adequate electric field coverage of the treated tumor EfAT to mapping the eletric field distribution is used for treatment plannning and therapy efficacy monitoring in the clinic.

# SSA20-04 Accuracy of Volumetric Measurements in the Breast: A Study of Comparing Ultrasound Tomography and Hand-Held Ultrasound

Sunday, Nov. 25 11:15AM - 11:25AM Room: S102CD

Participants

Rajni Natesan, MD, MBA, Houston, TX (*Presenter*) Officer, QT Ultrasound Labs Bilal Malik, PhD,MS, Novato, CA (*Abstract Co-Author*) Employee, QT Ultrasound Labs Lauralyn R. Markle, MD, Laguna Niguel, CA (*Abstract Co-Author*) Consultant, QT Ultrasound Labs Vashita Dhir, MD, Beverly Hills, CA (*Abstract Co-Author*) Consultant, QT Ultrasound, LLC Robin Terry, Novato, CA (*Abstract Co-Author*) Employee, QT Ultrasound, LLC

#### PURPOSE

This study assessed the accuracy of volumetric measurements acquired with ultrasound tomography (UST). UST imaging generates 3D speed-of-sound maps that can identify tissue types and measure lesion volumes. Since tumor volume doubling time is associated with growth rate and tumor biology, accurate measurement of tumor volume is critical for oncologic diagnosis, staging, and treatment.

## **METHOD AND MATERIALS**

Six cylindrical agar phantoms were imaged using UST and hand-held ultrasound (HHUS). Each phantom contained 4 embedded "lesions" composed of irregular-shaped chicken breast with known volumes ranging from 1.3 cm<sup>3</sup> to 7.4 cm<sup>3</sup>. Two board-certified breast imaging fellowship-trained radiologists independently performed blind interpretations of the UST and HHUS phantom images and calculated 24 lesion volumes. UST volumes were calculated with automated segmentation software (QT Ultrasound, Novato, CA). HHUS lesions were measured in 3 dimensions (a, b, c) and their volumes were calculated using 2 volume formulas: (1) (4/3)nr3 (with r = average of a, b, and c); and (2) ( $\pi/6$ )abc. These calculations were then statistically analyzed to determine the volumetric measurement accuracy of both UST and HHUS as compared to known true volumes calculated by water displacement methods.

## RESULTS

The average lesion volume calculated from UST images was  $3.93 \ 1.55 \ cm3$  and from HHUS was  $6.39 \ 2.61 \ cm3$  (sphere) or  $5.65 \ 2.39 \ cm3$  (ellipsoid), compared to the true average of  $3.98 \ 1.47 \ cm3$ . HHUS volumes were significantly larger than the true volumes with a mean over-estimation of  $62.8\% \ 36.9\% \ cm3$  (sphere) or  $43.3\% \ 32.6\% \ cm3$  (ellipsoid), whereas UST volumes agreed with the truth within measurement errors. Interobserver agreement was substantial (ICC = 0.95).

#### CONCLUSION

This study demonstrates that UST can accurately measure the volume of irregular-shaped masses, with superior accuracy than HHUS.

# **CLINICAL RELEVANCE/APPLICATION**

Ultrasound tomography can accurately measure tumor volume, demonstrating its potential utility in guiding oncologic management and treatment.

# SSA20-05 Evaluating Ductal Carcinoma in situ Progression via Tissue Oxygenation and Perfusion Using Photoacoustic and Contrast-Enhanced US

Sunday, Nov. 25 11:25AM - 11:35AM Room: S102CD

Participants

Ryan Margolis, Philadelphia, PA (Presenter) Nothing to Disclose

John R. Eisenbrey, PhD, Philadelphia, PA (*Abstract Co-Author*) Support, General Electric Company Support, Lantheus Medical Imaging, Inc

Flemming Forsberg, PhD, Philadelphia, PA (*Abstract Co-Author*) Research Grant, Canon Medical Systems Corporation; Research Grant, General Electric Company; Research Grant, Siemens AG; Research Grant, Lantheus Medical Imaging, Inc

Ji-Bin Liu, MD, Philadelphia, PA (Abstract Co-Author) Nothing to Disclose

Corinne Wessner, Philadelphia, PA (Abstract Co-Author) Nothing to Disclose

Kibo Nam, PhD, Philadelphia, PA (Abstract Co-Author) Nothing to Disclose

Maria Stanczak, MS, Philadelphia, PA (Abstract Co-Author) Nothing to Disclose

For information about this presentation, contact:

ryanamargolis@gmail.com

# PURPOSE

To investigate tissue oxygenation and perfusion as predictors of the aggressiveness of ductal carcinoma in situ (DCIS) as well as the influence of physical exercise on these parameters as well.

#### **METHOD AND MATERIALS**

Twenty FVB/NJ and 10 Tg(C3-1-TAg)cJeg mice (Jackson, Laboratories, Bar Harbor, ME) were evenly split into active and control subgroups, where the active group had access to a Fisher Science exercise wheel. Changes in mammary gland vascularity and perfusion were monitored with a Vevo 2100 LAZR scanner (FujiFilm VisualSonics, Toronto, Canada) using a LZ-250 PA probe.

Photoacoustic imaging was used to measure tissue oxygenation. To assess perfusion quantification, each mouse received a retroorbital bolus injection of 10  $\mu$ L of 3-4  $\mu$ m sized microbubbles (Advanced Microbubble Laboratories, Boulder, CO). Imaging of the mammary gland was performed weekly over 6 weeks and the mice were weighed biweekly. Offline analysis was performed using Vevo CQ software.

## RESULTS

For the FVB/NJ mice, weekly weight changes were lower for the active group than the control group  $(0.43\pm0.70 \text{ g vs. } 0.99\pm2.31 \text{ g}, p = 0.002)$ . Conversely, changes in oxygenation were higher for the active group than the control group  $(11.16\pm19.30\% \text{ vs.} 7.77\pm26.73; p=0.38)$ . There were no statistical differences for contrast wash-in rates (a measure of perfusion), or area under the curve between the two groups (p>0.25). For the SV40 Tag mice that naturally develop breast tumors, the weight changes were lower for the active group than control group  $(1.71\pm1.34 \text{ g vs. } 2.57\pm1.51 \text{ g}, p=0.0056)$ . There was also a statistical significant decrease in oxygenation in the exercise group compared to the control group  $(-19.37\pm26.88\% \text{ vs. } 20.21\pm29.55\%; p<0.001)$ . Similarly, there were no statistical differences between the wash-in rate or area under the curve between the two groups (p>0.26).

## CONCLUSION

Preliminary results indicate differences in tissue oxygenation between the FVB/NJ and SV40 Tag mice may become a predictive precursor for DCIS progression. The influence of exercise was shown by the weight changes, but the influence on DCIS progression is still being investigated.

## **CLINICAL RELEVANCE/APPLICATION**

This study may potentially minimize breast cancer overtreatments by predicting the aggressiveness of DCIS in humans via tissue oxygenation measurements using ultrasound.

## SSA20-06 A New Microfluidic Setup to Adjust Objectively 2D and 4D DCE-US Presets as an Alternative to Preclinical Studies

Sunday, Nov. 25 11:35AM - 11:45AM Room: S102CD

Participants

Virginie Grand-Perret, MSc, Villejuif, France (*Presenter*) Nothing to Disclose Ning Yao, Villejuif, France (*Abstract Co-Author*) Nothing to Disclose Ingrid Leguerney, Villejuif, France (*Abstract Co-Author*) Nothing to Disclose Baya Benatsou, Villejuif, France (*Abstract Co-Author*) Nothing to Disclose Philippe De-Vomocourt, DPhil, Ile-de-France, France (*Abstract Co-Author*) Nothing to Disclose Nathalie B. Lassau, MD, PhD, Villejuif, France (*Abstract Co-Author*) Nothing to Disclose Stephanie Pitre-Champagnat, Villejuif, France (*Abstract Co-Author*) Nothing to Disclose

#### For information about this presentation, contact:

virginie.grand-perret@u-psud.fr

## PURPOSE

Ultrasound tumor microvascularization assessment is a promising biomarker of patient response to anti-angiogenic drugs. Quantitative DCE-US imaging lacks dedicated phantoms featuring small vessels in order to optimize the image acquisition and define the preset parameters objectively. We propose a microfluidic setup dedicated to methodological development, and we compare it to a preclinical study on mice.

#### **METHOD AND MATERIALS**

*Microfluidic setup* The phantom was a 2.5x5x1cm3 block featuring cylindrical channels of diameters ranging from 145 to 450 µm. Sonovue (Bracco) was driven through the channels with very high reliability by a MFCS-EZ microfluidic flow controller (Fluigent SA, France). Flow rate was measured in real-time by a dedicated platform. An Aplio500 ultrasound scanner (Toshiba Medical Systems, Japan) with 2D and 4D 12MHz probes was used to acquire Contrast Harmonic Imaging (CHI) raw data. Quantification was made using UltraExtend FX software (Toshiba). The main parameters studied were mechanical index (MI), frequency (F), frame rate (fps), 4D volume angle (vol). *Preclinical study* 5 mice were imaged using the same 2D and 4D 12 MHz probes and injected with 100 µL Sonovue. 180 seconds raw data clips centered on the kidney were acquired and quantified using the scanner software. The same parameters were studied as on the microfluidic setup.

#### RESULTS

*Microfluidic setup* A new generation of microflow phantom enabled the precise control of 60-120 µL/min flow rates by a microfluidic pressure controller with a stable flow and under 5% variation over 3 minutes. After confirming the lack of microbubble destruction by the flow controller, the effects of MI, F, fps and vol were individually quantified. The best setup for optimal signal over noise ratio was MI 0.18, F h8.0 MHz, 4 fps, vol 30°. *Preclinical study* The best setup parameters were confirmed on the acquisitions on mice, however the in vivo variability of perfusion quantification was higher.

## CONCLUSION

The microfluidic setup we developed can be used to perform reproducible tests and set up acquisition parameters objectively in DCE-US imaging modes. It is an alternative approach to preclinical studies, and is more objective than in vivo models.

#### **CLINICAL RELEVANCE/APPLICATION**

The new microfluidic setup was relevant to set up DCE-US imaging mode parameters in an objective way and to adjusting the presets in DCE-US 2D and 4D.

# SSA20-07 Simultaneous MR and Ultrasound Image Acquisition in a Human Using a Hands-Free, MR-compatible, Volumetric Ultrasound Transducer for Image Guided Radiation Therapy

Sunday, Nov. 25 11:45AM - 11:55AM Room: S102CD

Participants Bryan Bednarz, PhD, Madison, WI (Presenter) Nothing to Disclose Warren Lee, Niskayuna, NY (Abstract Co-Author) Nothing to Disclose David M. Mills, PhD, Niskayuna, NY (Abstract Co-Author) Nothing to Disclose David Shoudy, Niskayuna, NY (Abstract Co-Author) Nothing to Disclose Heather Chan, Niskayuna, NY (Abstract Co-Author) Nothing to Disclose Aqsa Patel, Niskayuna, NY (Abstract Co-Author) Nothing to Disclose James Sabatini, Niskayuna, NY (Abstract Co-Author) Nothing to Disclose Eric Fiveland, MS, Niskayuna, NY (Abstract Co-Author) Nothing to Disclose Bo Wang, Niskayuna, NY (Abstract Co-Author) Nothing to Disclose Jihmli Mitra, Niskayuna, NY (Abstract Co-Author) Nothing to Disclose Shourya Sarcar, Niskayuna, NY (Abstract Co-Author) Nothing to Disclose Tim Fiorillo, Niskayuna, NY (Abstract Co-Author) Employee, General Electric Company Kwok Pong Chan, Niskayuna, NY (Abstract Co-Author) Employee, General Electric Company Alan B. McMillan, PhD, Madison, WI (Abstract Co-Author) Nothing to Disclose James H. Holmes, PhD, Madison, WI (Abstract Co-Author) Institutional research agreement, General Electric Company Spouse, Employee, Standard Imaging, Inc Wesley Culberson, PhD, Madison, WI (Abstract Co-Author) Nothing to Disclose Charles Matrosic, MS, Madison, WI (Abstract Co-Author) Nothing to Disclose Michael F. Bassetti, MD, Madison, WI (Abstract Co-Author) Research Grant, Merck KGaA; Research Grant, AstraZeneca PLC; Andrew Shepard, Madison, WI (Abstract Co-Author) Nothing to Disclose Sydney Jupitz, Madison, WI (Abstract Co-Author) Nothing to Disclose Patrick Hill, PhD, Madison, WI (Abstract Co-Author) Nothing to Disclose James A. Zagzebski, PhD, Madison, WI (Abstract Co-Author) Consultant, Gammex Sunnuclear; ;;; Scott Smith, Niskayuna, NY (Abstract Co-Author) Nothing to Disclose Thomas K. Foo, PhD, Niskayuna, NY (Abstract Co-Author) Employee, General Electric Company

For information about this presentation, contact:

bbednarz2@wisc.edu

#### CONCLUSION

These first human images demonstrate that the hands-free, electronically steerable e4D transducer can acquire ultrasound images during a MR acquisition without impacting either the MR or ultrasound images quality. This technology may be applied to other image-guided procedures (e.g. proton therapy, biopsies, and drug delivery).

#### Background

This work addresses the need for a cost-effective and non-invasive real-time motion management platform for radiotherapy. We have developed the first ever hands-free, MR-compatible, electronically-steered, and real-time volumetric (e4D) ultrasound probe that will be used to directly track tumor or vessel motion during radiation therapy. The ultrasound images acquired during treatment will be coupled to a pre-treatment training image set consisting of a simultaneous 4D ultrasound and 4D MRI acquisition. The images will be rapidly matched using advanced signal processing algorithms, allowing for the display and verification of MR-based tumor/organ motion in real-time from an ultrasound acquisition.

## **Evaluation**

The transducer contains 18,000 piezoelectric elements and beam forming and data acquisition electronics in the transducer housing. Currently, the probe is designed to have a maximum imaging depth of 15 cm, with 2 mm lateral resolution at 7 cm. The transducer acquires a 3D electronically-steered volume (4 vps) with a maximum sweep angle of 300. Simultaneous MR and ultrasound images were acquired on a healthy volunteers liver using a GE 3T MR750 scanner. A fast spoiled gradient echo (FSPGR) multi-phase 2D sagittal acquisition with temporal acquisition of 4 fps was used for imaging. A 32-channel cardiac phased-array receiver coil was used with the transducer positioned under anterior elements. Ultrasound images were acquired in harmonic mode (1.7/3.3 MHz) at a rate of 4 fps using the transducer and a GE Vivid E95 system. Images were co-analyzed using MIM Maestro.

#### Discussion

No significant artifacts were detected during the acquisition of the MR and ultrasound images. Some low level susceptibility artifacts near the transducer in the MR image was detected, but this was well-contained within 1-2 cm of the surface and did not adversely effect the image quality.

# SSA20-08 Optimization of a Subharmonic Dynamic Contrast-Enhanced Ultrasound Technique for Liver Tumor Imaging

Sunday, Nov. 25 11:55AM - 12:05PM Room: S102CD

## Participants

Jacinta Browne, PhD, Dublin 8, Ireland (*Presenter*) Nothing to Disclose Aoife Ivory, Dublin, Ireland (*Abstract Co-Author*) Nothing to Disclose Andrew Fagan, Rochester, MN (*Abstract Co-Author*) Nothing to Disclose

For information about this presentation, contact:

jacinta.browne@dit.ie

#### PURPOSE

Conventional dynamic contrast-enhanced ultrasound (DCE-US) detects the first harmonic signal component arising mainly from the contrast agent (CA) microbubbles perfusing through the tissue, although the tissue itself also generates harmonics. Subharmonic

(SH) signal detection holds significant potential for increasing the sensitivity of tumor detection in the liver as only the CA generates subharmonics. This paper describes the optimization of the SH-DCE-US technique via bench-level experiments and its translation to a clinical scanner.

## METHOD AND MATERIALS

Experiments were performed to maximize the signal from a commercial CA (SonoVue®, Bracco, Switzerland; default and an altered bubble size distribution) using a home-built microbubble characterization system with variable control over transmit beam center frequency and number of cycles. The optimal transmit beam parameters were translated to a commercial scanner (Aixplorer, Supersonic Imagine, France). A novel perfusion phantom, comprising different compartments mimicking healthy, diseased and necrotic tissue regions, was developed and used to validate the new technique on the scanner.

## RESULTS

The maximum SH signal was measured for a transmit beam of 3 cycles centered at 1.9 MHz (i.e. SH signal at 0.95 MHz) for the native CA (57% bubble volume 4-10 $\mu$ m). The optimal transmit frequency increased to a more useful range of 2.3-2.5 MHz (SH signal at 1.15-1.25 MHz) in an altered CA with reduced polydispersity ((1-4 $\mu$ m; 99%/82% bubble count/volume, respectively). DCE time-intensity curves were produced on the clinical scanner using these optimal transmit beam parameters with the perfusion phantom, with improved quantification at depth of the microbubble signal using the new SH technique.

## CONCLUSION

Optimal transmit beam parameters have been established for maximizing the SH signal in DCE-US scanning of the liver. Furthermore, a simple alteration of the CA's polydispersity shifted the optimal SH detection frequency above 1 MHz, which is the typical lower-frequency limit for curvilinear probes used for liver scanning. Improvements were demonstrated using a novel perfusion phanton.

## CLINICAL RELEVANCE/APPLICATION

This paper demonstrates an optimized dynamic contrast-enhanced liver ultrasound imaging technique, using subharmonic signal detection with an easily-altered microbubble contrast agent formulation.

# SSA20-09 US-Triggered Antibiotic Release from Novel Spinal Fusion Hardware

Sunday, Nov. 25 12:05PM - 12:15PM Room: S102CD

#### Participants

Lauren J. Jablonowski, PhD, Philadelphia, PA (Presenter) Nothing to Disclose

Cemile Basgul, Philadelphia, PA (Abstract Co-Author) Nothing to Disclose

Daniel W. MacDonald, Philadelphia, PA (Abstract Co-Author) Nothing to Disclose

Noreen J. Hickok, PhD, Philadelphia, PA (*Abstract Co-Author*) Researcher, Zimmer Biomet Holdings, Inc, Inc; Researcher, Synergy Technologies, Inc; Research collaboration, Acuitive Technologies, Inc

Steven M. Kurtz, PhD, Philadelphia, PA (*Abstract Co-Author*) Exponent; Active Implants Corporation; B. Braun Melsungen AG; Celanese; Ceramtec; Johnson & Johnson; DJO GLobal, Inc; Ferring Group; Formae; Kyocera Medical; Medtronic plc; Simplify Medical; Smith & Nephew plc; Stelkast; Stryker Corporation; Wright Medical Technology, Inc; Zimmer Biomet Holdings, Inc; Invibio; Reed Elsevier

Flemming Forsberg, PhD, Philadelphia, PA (*Abstract Co-Author*) Research Grant, Canon Medical Systems Corporation; Research Grant, General Electric Company; Research Grant, Siemens AG; Research Grant, Lantheus Medical Imaging, Inc

## For information about this presentation, contact:

lauren.jablonowski@jefferson.edu

# PURPOSE

To determine optimal acoustic parameters for destruction of a polymeric membrane surrounding a prophylactic-containing spinal reservoir. The long-term goal is to achieve ultrasound (US)-triggered release of antibiotics from within this spinal spacer to prevent post-surgical infection.

# METHOD AND MATERIALS

Polylactic acid (PLA)-coated, methylene blue (MeB)-loaded polyether ether ketone (PEEK) spacers (0.785cm3) with a drug-loading reservoir were created in our labs. Coated spacers were submerged in water and insonated for 10 minutes using a Logiq E9 scanner (GE Healthcare, Waukesha, WI) with a C1-6 curvilinear probe, using power Doppler to rupture the PLA coating for MeB release. Frequencies evaluated were 1.7, 2.5, and 3.6 MHz, pulse repetition frequencies (PRFs) tested were 0.1, 3.5, and 6.4 kHz, and acoustic output (AO) powers tested were 30, 60, and 100%. MeB release was evaluated qualitatively against known MeB concentration standards immediately following insonation and again after 24 hours. Results were collected in triplicate and compared with a one-way ANOVA.

## RESULTS

Membrane rupture increases with lower frequencies, but no significant difference was observed in release from the spacers at the frequencies evaluated (70-100% cumulative release, p=0.48). Therefore, 1.7 MHz was selected as optimal. This frequency was maintained, while PRF was varied. A PRF of 0.1 kHz resulted in significantly less immediate release (17.5 $\pm$ 1.3%; p=0.021), but no difference was seen between PRFs of 3.5 kHz (32.5 $\pm$ 2.5%) and 6.4kHz (36.3 $\pm$ 5.4%, p>0.99). AO power was varied with 1.7 MHz and PRF 6.4 kHz. There was no significant difference in release between the AO powers (p>0.08). Uninsonated controls exhibited only 1.3 $\pm$ 1.2% immediate release (p=0.031), and 6.8 $\pm$ 2.8% cumulative release (p=0.021), confirming US-triggered release as opposed to passive leakage.

## CONCLUSION

This study determined scanning parameters appropriate for US-triggered release of encapsulated prophylactics, as a first step towards deployment of this drug delivery system.

## **CLINICAL RELEVANCE/APPLICATION**

This system will aggressively combat post-surgical bacterial infection with great versatility in applications for wide clinical impact.



#### SSA21

## Physics (Dual-Energy/Spectral CT)

Sunday, Nov. 25 10:45AM - 12:15PM Room: S103AB



AMA PRA Category 1 Credits ™: 1.50 ARRT Category A+ Credit: 1.75

**FDA** Discussions may include off-label uses.

#### Participants

Cynthia H. McCollough, PhD, Rochester, MN (Moderator) Research Grant, Siemens AG

Timothy P. Szczykutowicz, PhD, Madison, WI (*Moderator*) Equipment support, General Electric Company; License agreement, General Electric Company; Founder, Protocolshare.org LLC; Medical Advisory Board, medInt Holdings, LLC; Co-owner, LiteRay Medical LLC

# Sub-Events

## SSA21-01 DXA-like Quantification of Bone Mineral Density using Dual-Layer Spectral CT Scout Scans

Sunday, Nov. 25 10:45AM - 10:55AM Room: S103AB

Participants

Alexis Laugerette, Munich, Germany (*Presenter*) Nothing to Disclose Benedikt J. Schwaiger, MD, Munich, Germany (*Abstract Co-Author*) Nothing to Disclose Kevin M. Brown, MS, Cleveland, OH (*Abstract Co-Author*) Employee, Koninklijke Philips NV Lena Frerking, Hamburg, Germany (*Abstract Co-Author*) Researcher, Koninklijke Philips NV Felix K. Kopp, Munich, Germany (*Abstract Co-Author*) Nothing to Disclose Kai Mei, Munich, Germany (*Abstract Co-Author*) Nothing to Disclose Thorsten Sellerer, MSc, Garching bei Munchen, Germany (*Abstract Co-Author*) Nothing to Disclose Jan S. Kirschke, MD, Muenchen, Germany (*Abstract Co-Author*) Speakers Bureau, Koninklijke Philips NV Thomas Baum, MD, Munich, Germany (*Abstract Co-Author*) Nothing to Disclose Daniela Pfeiffer, MD, Munich, Germany (*Abstract Co-Author*) Nothing to Disclose Alexander A. Fingerle, MD, Munchen, Germany (*Abstract Co-Author*) Nothing to Disclose Ernst J. Rummeny, MD, Munich, Germany (*Abstract Co-Author*) Nothing to Disclose Roland Proksa, Hamburg, Germany (*Abstract Co-Author*) Nothing to Disclose Portar J. Rummeny, MD, Munich, Germany (*Abstract Co-Author*) Nothing to Disclose Praze Figffer, MD, Munich, Germany (*Abstract Co-Author*) Nothing to Disclose Ernst J. Rummeny, MD, Munich, Germany (*Abstract Co-Author*) Nothing to Disclose Roland Proksa, Hamburg, Germany (*Abstract Co-Author*) Employee, Koninklijke Philips NV Franz Pfeiffer, Munich, Germany (*Abstract Co-Author*) Nothing to Disclose Peter B. Noel, PhD, Munich, Germany (*Abstract Co-Author*) Nothing to Disclose

#### For information about this presentation, contact:

alexis.laugerette@tum.de

#### PURPOSE

Scout scans are a mandatory part of CT examinations, but do not -yet- provide quantitative information. Purpose of this study was to develop and evaluate a method for areal bone mineral density (aBMD) measurement based on dual-layer spectral CT scout scans.

#### **METHOD AND MATERIALS**

A post-processing algorithm using a pair of 2D virtual mono-energetic scout images (VMSIs) was established in order to semiautomatically compute aBMD at the spine. The method was assessed based on repetitive measurements of the standardized European spine phantom (ESP) at the standard scout scan tube current (30 mA), at other tube currents (10 to 200 mA), as well as with fat-equivalent extension rings simulating different patient habitus, and was compared to dual-energy X-ray absorptiometry (DXA). In two female patients, the feasibility of the method was assessed in-vivo for vertebrae L1 to L4 and the results were compared to age-matched reference values. Finally, BMD was determined in a female patient population (n=31, age range 22-87 years old) with the proposed method, and T-scores were derived from the measurements, taking a young subset of the population as the reference.

# RESULTS

Derived from standard scout scans, aBMD values measured with the proposed method highly correlated with DXA measurements (r=0.9925), and mean accuracy (DXA: 4.12%, Scout: 1.60%) and precision (DXA: 2.64%, Scout: 2.03%) were comparable. In particular, the scout scan-based method performed better than DXA at low BMD values (accuracy DXA: 8.3%, Scout:4.79%). Moreover, when assessed at different tube currents, aBMD values did not differ significantly (p>=0.20 for all), suggesting that the presented method could be applied to scout scans with different settings. Finally, data derived from sample patients as well as first T-score representations agreed well with BMD values and T-score trend from a reference age-matched population.

# CONCLUSION

Based on dual-layer spectral CT scout scans, aBMD measurements were fast and reliable and highly correlated with DXA measurements. First measurements on patients were promising. Considering the number of CT acquisitions performed worldwide, this method could allow truly opportunistic osteoporosis screening at a larger scale.

#### **CLINICAL RELEVANCE/APPLICATION**

Dual-layer spectral CT frontal scout scans could provide fast and quantitative DXA-like BMD assessment at the spine and allow large-scale, opportunistic osteoporosis screening.

## SSA21-02 Spectral CT Metal Artifact Reduction

Sunday, Nov. 25 10:55AM - 11:05AM Room: S103AB

Participants

Taly G. Schmidt, PhD, Milwaukee, WI (*Abstract Co-Author*) Research Grant, General Electric Company Rina F. Barber, PhD, Chicago, IL (*Abstract Co-Author*) Nothing to Disclose Emil Y. Sidky, PhD, Chicago, IL (*Presenter*) Nothing to Disclose

## For information about this presentation, contact:

tal.gilat-schmidt@marquette.edu

## PURPOSE

To evaluate a novel Spectral CT metal artifact reduction method through simulations and phantom experiments using a photoncounting detector.

# METHOD AND MATERIALS

The proposed constrained 'one-step' Spectral CT Image Reconstruction (cOSSCIR) method addresses beam hardening due to metal by directly estimating basis material maps uisng a polyenergetic x-ray transmission model. The proposed method enables masking energy windows corrupted by metal on a ray-by-ray basis, for example masking only the lowest energy window in some rays while using information from higher energy windows. The cOSSCIR algorithm includes constraints that mitigate undersampling artifacts that occur when unreliable measurements through metal are masked. A Spectral CT acquisition of a pelvic phantom with Co-Cr-Mo hip prostheses was simulated with four energy windows. An experimental Spectral CT acquisition was performed with a CdTe photon-counting detector, three energy windows, and a phantom with and without metal. For both simulations and experiments, a weighted mask was applied to remove projection data corrupted by metal. cOSSCIR reconstruction was performed by decomposing into bone, water, and copper material maps and then combining the maps to form an effective monoenergetic image. Images were also reconstructed using filtered backprojection (FBP) with and without the Normalized Metal Artifact Reduction (NMAR) technique. CT number error in the region between the metal implants was compared.

## RESULTS

In the simulation study, the cOSSCIR algorithm reduced the CT number error in the metal artifact streaking region to less than 1 HU error. In the experimental study, the CT number error was 7 HU for cOSSCIR reconstruction with weighted mask, 60 HU for cOSSCIR without masking, 40 HU for FBP +NMAR, and 212 HU error for FBP. The cOSSCIR images did not contain streak artifacts seen in the NMAR images.

## CONCLUSION

The proposed Spectral CT metal artifact reduction method reduced shading artifacts to <1 HU error in simulations and 7 HU error in experiments, without introducing residual streak artifacts.

#### **CLINICAL RELEVANCE/APPLICATION**

Metal artifacts in CT images obscure structures, alter CT numbers, challenge diagnosis, and impede radiation therapy planning. The proposed method, which could also be applied to dual-KV systems, corrects metal artifacts without knowledge of the implant material.

# SSA21-03 Areal Bone Mineral Density Estimation Using Dual-Energy Computed Tomography Topograms

Sunday, Nov. 25 11:05AM - 11:15AM Room: S103AB

Participants

Tristan Nowak, Forchheim, Germany (*Abstract Co-Author*) Grant, Siemens AG Bernhard Schmidt, PhD, Forchheim, Germany (*Presenter*) Employee, Siemens AG Natalia Saltybaeva, PhD, Zurich, Switzerland (*Abstract Co-Author*) Nothing to Disclose Thomas G. Flohr, PhD, Forchheim, Germany (*Abstract Co-Author*) Employee, Siemens AG Hatem Alkadhi, MD, Zurich, Switzerland (*Abstract Co-Author*) Nothing to Disclose

## PURPOSE

Dual-Energy X-ray absorptiometry (DXA) is in wide clinical use for the diagnosis and monitoring of osteoporosis. Using DXA, a good estimation of areal bone mineral density (aBMD) can be extracted from two images acquired with different X-ray spectra by subtracting the influence of soft tissue on the total X-ray absorption and isolating the absorption of carbonated hydroxyapatite (HA). Since most clinically performed CT scans include a topogram as a 2D overview image, it would be beneficial to also employ these images for the diagnostic purpose of an aBMD estimation. A prerequisite for this approach is the acquisition of dual-energy topograms, either sequentially, or ideally, using a single scan. In this work, we compared quality and dose of aBMD measurements from a standard DXA (bone densitometry) scan with sequentially acquired dual-energy topograms.

## METHOD AND MATERIALS

Two anterior-posterior (AP) topograms of a BMD calibration spine phantom (European Spine Phantom, QRM GmbH, Möhrendorf, Germany) were sequentially acquired using a dual source SOMATOM Force CT System (Siemens Healthcare GmbH, Forchheim Germany). In order to maximize spectral separation, tube voltages of 70 kV without and 150 kV with added tin filtration were chosen at tube current time products of 70 and 75 mAs, respectively. The phantom consists of water-equivalent plastic with diameters of 260 mm (lateral) and 180 mm (AP) and holds three anthropomorphic vertebrae, L1-L3, of varying HA content (50, 100 and 200 mg/cm<sup>3</sup>) in the spongious part of the bone. A custom tool was developed to subtract soft tissue and create aBMD density maps from the input topograms. Deviations from the known aBMD values of 0.5, 1.0 and 1.5 g/cm<sup>2</sup> of the AP projections of vertebrae L1-L3 were evaluated.

#### RESULTS

The extracted values for vertebrae L1-L3 from the generated aBMD maps were in good agreement with the ground truth. The mean areal densities and standard deviations for L1, L2 and L3 were 0.493  $\pm$  0.05, 1.01  $\pm$  0.04 and 1.52 g/cm<sup>2</sup>  $\pm$  0.03, respectively.

## CONCLUSION

Especially with regard to the advent of energy-discriminating, photon-counting detectors, the work presented here shows a promising new domain for spectrally acquired topograms. This technique might serve as an alternative to using dedicated DXA scanners.

## CLINICAL RELEVANCE/APPLICATION

Areal bone mineral density measurement is feasible via topograms with sufficient energy separation acquired via dual-energy CT.

# SSA21-04 Monochromatic CT Image Reconstruction via Deep Learning

Sunday, Nov. 25 11:15AM - 11:25AM Room: S103AB

Participants

Wenxiang Cong, Albany, NY (*Abstract Co-Author*) Nothing to Disclose Ge Wang, PhD, troy, NY (*Abstract Co-Author*) Nothing to Disclose Hongming Shan, Troy, NY (*Presenter*) Research Grant, General Electric Company

#### PURPOSE

Develop a deep-learning-based algorithm to achieve monochromatic CT image reconstruction from current-integrating raw data.

## **METHOD AND MATERIALS**

In clinical CT, with a polychromatic x-ray source, raw data are collected in the current-integrating mode. This physical process is accurately described by an energy-dependent non-linear integral model. However, the non-linear model is too complicated to be directly solved for the image reconstruction, and often approximated as a linear integral model known as the Radon/X-ray transform, which basically ignores energy-dependent information. This model mismatch leads to inaccurate quantification of an attenuation image and significant beam-hardening artifacts. Here, we develop a deep-learning-based approach to address the mismatch between the computational process and the physical model. Our method learns a nonlinear transformation from big data to correct measured raw data in accordance with line integrals at a pre-specified monochromatic energy. A multi-layer perceptron (MLP) neural network is designed for this purpose, consisting of four layers, one input layer, two hidden layers, and one output layer. The sigmoid function is used for non-linear activation. The neural network is trained with the ADAM optimization. The training procedure is programmed in Python and the TensorFlow framework on a computer with a NVIDIA Titan XP GPU of 12 GB memory. A set of clinical dual-energy CT datasets of the human abdomen, collected on a GE Discovery CT750 scanner, are used in the training and testing stages to demonstrate the feasibility of the proposed methodology.

#### RESULTS

The optimization of the neural network has an excellent converging performance, achieving a high accuracy in the monochromatic projection estimation with a relative error of less than 0.2%, overcoming beam hardening effectively.

#### CONCLUSION

Our approach is capable of learning a nonlinear transformation from big data, making a step forward towards monochromatic imaging directly from single-spectrum energy-integrating data. This is a potential cost-effective alternative to dual-energy CT.

## **CLINICAL RELEVANCE/APPLICATION**

The deep-learning-based reconstruction method may perform monochromatic CT imaging, allowing for applications in lesion detection and tissue characterization, and proton therapy.

# SSA21-05 Evaluation of a Spectral Imaging Metal Artifact Reduction Algorithm Using a Novel Image Quality Phantom

Sunday, Nov. 25 11:25AM - 11:35AM Room: S103AB

Participants

Hilde K. Andersen, MSc, Oslo, Norway (*Presenter*) Nothing to Disclose Anette Aarsnes, Oslo, Norway (*Abstract Co-Author*) Nothing to Disclose Hildur Olafsdottir, Salem, NY (*Abstract Co-Author*) Research funded, Image Owl, Inc Joshua Levy, Salem, NY (*Abstract Co-Author*) Stockholder, The Phantom Laboratory President, The Phantom Laboratory Stockholder, Image Owl, Inc David J. Goodenough, PhD, Myersville, MD (*Abstract Co-Author*) Consultant, The Phantom Laboratory Anne C. Martinsen, Oslo, Norway (*Abstract Co-Author*) Nothing to Disclose

#### PURPOSE

To evaluate the performance of a spectral imaging metal artifact reduction algorithm (GSI-MAR) using a novel phantom.

## **METHOD AND MATERIALS**

A Catphan phantom with a CTP682 module (The Phantom Laboratory, Salem, NY, USA) was scanned on a GE Revolution 16 CT scanner (GE Healthcare, Milwaukee, WI, USA) with and without body annulus and with inserts of stainless steel, titanium and PMMA (control). Metal inserts had diameters of 0.5' and 0.25'. Spectral imaging scans were reconstructed in mono-energetic levels of 55 keV, 68 keV and 90 keV, with filtered back-projection (FBP), FBP with metal artifact reduction (MAR), 50% iterative reconstruction (ASIR-V) and 50% ASIR-V with MAR. Standard deviation (SD) as measures of streaking was derived from ROIs surrounding the inserts and in the outer part of the phantom. Low contrast detectability (LCD) close to the inserts was evaluated by two human observers. MTF and NPS were measured for all series.

Titanium did only introduce streaking close to the large insert. Stainless steel introduced large streaking artifacts. For the large titanium insert, MAR reduced SD from 23HU to 11HU without ring, and from 159HU to 14HU with ring. For the large stainless steel insert, MAR reduced SD from 61HU to 10HU without ring, and from 436HU to 23HU with ring. For the control, SD was 4HU without ring and 10HU with ring (all at 68 keV, same trend for 55 and 90 keV). Without the ring, LCD was close to the level of the control for the small inserts and the large titanium insert. For the large stainless steel insert, LCD decreased for 55 and 90 keV, and MAR improved LCD but not to the level of 68 keV and the control. With the ring, LCD decreased for all energies and inserts. For stainless steel, 90 keV had the best LCD, MAR improved LCD for 55 and 68 keV, but only to the level of 90 keV. For titanium, 68 keV had the best LCD, and MAR improved LCD for the small insert. Analyses of NPS and MTF are work in progress.

## CONCLUSION

GSI-MAR reduced streaks from titanium and stainless steel and improved LCD close to metal. Optimal energy level and effect of MAR depends on metal type and size, as well as patient size.

## **CLINICAL RELEVANCE/APPLICATION**

The performance of new metal artifact reduction algorithms in CT for different metals is not known. Catphan CTP682 module with metal inserts proved useful in evaluation of one such algorithm, GSI-MAR.

## SSA21-06 Limits for Detecting Low Concentrations of Iodine with Dual-Energy Computed Tomography

Sunday, Nov. 25 11:35AM - 11:45AM Room: S103AB

Participants

Megan C. Jacobsen, BA, Houston, TX (*Presenter*) Nothing to Disclose Erik N. Cressman, MD, Houston, TX (*Abstract Co-Author*) Nothing to Disclose Xinhui Duan, PhD, Dallas, TX (*Abstract Co-Author*) Nothing to Disclose Dianna D. Cody, PhD, Houston, TX (*Abstract Co-Author*) In-kind support, General Electric Company; Reviewer, ACR CT accreditation program; Researcher, Gammex, Inc Dawid Schellingerhout, MD, Houston, TX (*Abstract Co-Author*) Nothing to Disclose Rick R. Layman, PhD, Houston, TX (*Abstract Co-Author*) Researcher, Siemens AG

#### PURPOSE

Multiple studies in the literature have proposed diagnostic thresholds based on Dual-Energy Computed Tomography (DECT) iodine maps. However, it is critical to determine the minimum detectable iodine concentration for DECT systems to establish the clinical significance of various measured quantities for these image types.

#### **METHOD AND MATERIALS**

Seven serial dilutions of iohexol were made with concentrations from 0.03 to 2.0 mg iodine/mL in 50 mL centrifuge tubes. The dilutions and one blank with distilled water were scanned five times each in two scatter conditions: a 20.0 cm diameter (Head) phantom and a 30.0 cm x 40.0 cm elliptical (Body) phantom. We utilized six scanners from three vendors, including fast-kVp switching, dual-source, dual-layer detector, and split-filter DECT. Scan parameters and dose were matched as closely as possible across systems, and iodine maps were reconstructed using each vendor's software. Regions-of-Interest were placed centrally within each vial on the iodine map. Mean and standard deviation were calculated across the five scan acquisitions, and linear calibration curves were calculated for each scanner. Using standard analytical methods, the signal region corresponding to a 95% likelihood of measuring only water was defined as the Limit of Blank (LOB). Subsequently, the Limit of Detection (LOD) in the signal domain was defined as the LOB plus 1.645 times the standard deviation of the 0.5 mg/mL vial and was converted to a concentration using the calibration curves.

#### RESULTS

We found that the range of LOD was 0.021 - 0. 257 mg iodine/mL in the head phantom and 0.113 - 0.547 mg iodine/mL in the body phantom. Higher kVp levels on a given system generally performed better than lower kVp settings in the body phantom.

#### CONCLUSION

DECT systems available in today's marketplace can detect iodine concentrations as low as 0.113 mg I/mL in an anthropomorphic body phantom, which corresponds to an enhancement of approximately 2.8 HU at 120-kVp.

#### **CLINICAL RELEVANCE/APPLICATION**

DECT iodine quantification is a potential imaging biomarker, and we define detection limits for iodine measurements across multiple DECT systems, under which iodine cannot be reliably detected.

# SSA21-07 Radiation Dose Efficiency of Multi-Energy CT for Simultaneous Imaging of Multiple Contrast Agents

Sunday, Nov. 25 11:45AM - 11:55AM Room: S103AB

Participants

Liqiang Ren, PhD, Rochester, MN (*Presenter*) Nothing to Disclose Kishore Rajendran, PhD, Rochester, MN (*Abstract Co-Author*) Nothing to Disclose Michael R. Bruesewitz, Rochester, MN (*Abstract Co-Author*) Nothing to Disclose Joel G. Fletcher, MD, Rochester, MN (*Abstract Co-Author*) Grant, Siemens AG; Consultant, Medtronic plc; ; Shuai Leng, PHD, Rochester, MN (*Abstract Co-Author*) License agreement, Bayer AG Cynthia H. McCollough, PhD, Rochester, MN (*Abstract Co-Author*) Research Grant, Siemens AG Lifeng Yu, PhD, Chicago, IL (*Abstract Co-Author*) Nothing to Disclose

For information about this presentation, contact:

yu.lifeng@mayo.edu

# PURPOSE

Multi-energy CT (MECT) has been proposed for imaging multiple contrast agents simultaneously, which may allow multi-phase data

to be acquired in one single scan, potentially reducing radiation dose. This work aims to evaluate the dose efficiency of MECT in two potential applications: iodine/gadolinium (I/Gd) for liver imaging and iodine/bismuth (I/Bi) for small bowel imaging.

# METHOD AND MATERIALS

Dose efficiency was experimentally evaluated for I/Gd and for I/Bi by comparing a single-scan MECT (MECT\_1s) protocol and a traditional two-scan single-energy CT (SECT\_2s) protocol. For SECT\_2s, an abdominal phantom containing two sets of I samples was designed to mimic enhancement at late arterial and portal-venous phases. For MECT\_1s, I/Gd samples were used, with I enhancement corresponding to the late arterial phase and Gd enhancement to the portal-venous phase. Data were acquired on a SECT (120kV) for SECT\_2s, and on a dual-energy CT (DECT: 80/Sn150kV or 90/Sn150kV) or a photon-counting-detector (PCD) CT (140kV [25 50 75 90keV]) for MECT\_1s, with the total radiation dose from the two scan protocols matched. A generic image-based material decomposition method was used to determine the densities of I/Gd/water, based on which CT biphasic images were synthesized. The noise levels on the original images acquired with the SECT\_2s protocol and the synthesized images generated with the MECT\_1s protocol were compared. The dose efficiency for I/Bi was evaluated in a similar way except for the phantom design. For SECT\_2s, a different abdominal phantom was used, containing one set of I samples and one set of Bi samples mimicking the arterial and enteric enhancement, respectively. For MECT\_1s, I/Bi samples was used.

#### RESULTS

For I/Gd, the noise level with the MECT\_1s protocol was 500-1600% higher than that with the SECT\_2s protocol, given the same total dose. For I/Bi, the noise level with the MECT\_1s protocol was 110-230% higher.

#### CONCLUSION

Single-scan MECT imaging using two contrast agents (I/Gd and I/Bi) is intrinsically dose inefficient compared with traditional multiple SECT scans, particularly for I/Gd. The dose efficiency of MECT is highly dependent on the contrast materials used for a particular application.

#### **CLINICAL RELEVANCE/APPLICATION**

Use of a single-scan MECT protocol for multi-phase liver and small bowel CT imaging is very dose inefficient compared with a traditional dual-scan SECT protocol.

# SSA21-08 Liver Lesion Localization and Classification with Convolutional Neural Networks Comparing Conventional and Spectral Computed Tomography

Sunday, Nov. 25 11:55AM - 12:05PM Room: S103AB

Participants

Julia Fokuhl, Munich, Germany (*Abstract Co-Author*) Nothing to Disclose Shadi Albarqouni, Garching, Germany (*Abstract Co-Author*) Nothing to Disclose Manuel Schultheiss, Munich, Germany (*Abstract Co-Author*) Nothing to Disclose Stefanie Beck, MSc, Munich, Germany (*Abstract Co-Author*) Nothing to Disclose Felix K. Kopp, Munich, Germany (*Abstract Co-Author*) Nothing to Disclose Daniela Pfeiffer, MD, Munich, Germany (*Abstract Co-Author*) Nothing to Disclose Julia Dangelmaier, MD, Munich, Germany (*Abstract Co-Author*) Nothing to Disclose Gregor Pahn, DIPLPHYS, Heidelberg, Germany (*Abstract Co-Author*) Nothing to Disclose Andreas Sauter, MD, Munich, Germany (*Abstract Co-Author*) Nothing to Disclose Alexander A. Fingerle, MD, Munchen, Germany (*Abstract Co-Author*) Nothing to Disclose Ernst J. Rummeny, MD, Munich, Germany (*Abstract Co-Author*) Nothing to Disclose Nassir Navab, PhD, Garching, Germany (*Abstract Co-Author*) Nothing to Disclose Preter B. Noel, PhD, Munich, Germany (*Abstract Co-Author*) Nothing to Disclose

For information about this presentation, contact:

peter.noel@tum.de

#### PURPOSE

To localize and classify hepatic lesions with convolutional neural networks (CNNs) and evaluate the performance for different conventional and spectral computed tomography (CT) data.

## METHOD AND MATERIALS

Contrast-enhanced liver CTs of 172 patients (33 with cysts, 57 with hypodense metastases and 82 healthy) were collected from a dual-layer spectral CT. Automatic liver segmentation was used. The localization and classification tasks were split into two stages: The first CNN was trained to localize hepatic lesions and produce heatmaps showing the location. Only the disease type and no segmentation ground truth was needed for the training. The heatmaps were used to automatically cut a region of interest (ROI) around the predicted lesion. In the second stage, the ROIs were used to train an additional CNN for the classification between healthy, cyst and metastasis. The final evaluation was performed on previously un-seen patient data. All experiments were compared for conventional CT data, reconstructed virtual monoenergetic images (VMIs) and iodine concentration maps. The classification performance was evaluated with precision, recall, accuracy and F1-score. The localization results on the test set were compared to the segmentation ground truth. The distance between lesion predictions and true lesions and the localization accuracy were evaluated.

## RESULTS

The classification of the first CNN for healthy vs. lesion achieved a recall of 0.890, 0.855, 0.798, 0.874, 0.822 for 40 keV, 70 keV and 100 keV VMIs, iodine maps and conventional images, respectively. The localization accuracy and distance between true and predicted lesions presented the best results for low energy VMIs (40 - 70 keV) and iodine maps, outperforming the conventional data. The classification of ROIs into three classes reached the highest accuracy with 70 keV VMIs (84.5 %) compared to conventional data (83.5 %).

#### CONCLUSION

Using CNNs to localize locions, but POTs and norform locion electification offers a robust automatic workflow. Low energy V/MTs show

osing CNNS to localize lesions, cut ROIS and perform lesion classification oriers a robust automatic worknow. Low energy VMIS show several benefits compared to conventional CT: Small lesions were detected with higher accuracies, heatmap results were more reliable and metastases and cysts were classified better.

## **CLINICAL RELEVANCE/APPLICATION**

Using convolutional neural networks and spectral CT data for the automatic localization and classification of hepatic lesions has the potential to significantly aid the diagnostic decision process.

# SSA21-09 Realistic Liver Tissue Surrogates for CT Phantom Studies Can Accurately Quantify the Benefits and Limitations of? Reduced kV Imaging in CT

Sunday, Nov. 25 12:05PM - 12:15PM Room: S103AB

Participants

Andre Euler, MD, Durham, NC (Presenter) Fellowship funded, General Electric Company

Justin B. Solomon, PhD, Durham, NC (*Abstract Co-Author*) License agreement, Sun Nuclear Corporation; License agreement, 12 Sigma Technologies

Paul Fitzgerald, Niskayuna, NY (Abstract Co-Author) Employee, General Electric Company

Ehsan Samei, PhD, Durham, NC (*Abstract Co-Author*) Research Grant, General Electric Company; Research Grant, Siemens AG; Advisory Board, medInt Holdings, LLC; License agreement, 12 Sigma Technologies; License agreement, Gammex, Inc Rendon C. Nelson, MD, Durham, NC (*Abstract Co-Author*) Research Consultant, General Electric Company; Research Consultant, Nemoto Kyorindo Co, Ltd; Consultant, VoxelMetrix, LLC; Co-owner, VoxelMetrix, LLC; Advisory Board, Bracco Group; Advisory Board, Guerbet SA; Research Grant, Nemoto Kyorindo Co, Ltd; Speakers Bureau, Bracco Group; Royalties, Wolters Kluwer nv

# PURPOSE

To assess the utility of a liquid tissue surrogate for the liver (LTSL) to emulate the CT attenuation characteristics of contrastenhanced liver parenchyma and lesions as a function of tube potential, lesion contrast, phase of enhancement, and phantom size.

## **METHOD AND MATERIALS**

A 3D-printed, fillable phantom was used to emulate liver parenchyma and focal lesions. First, we compared the CT attenuation of LTSL-iodine and water-iodine solutions at 80, 100, 120, 140 kV to published patient data. Based on these results, we emulated liver parenchyma in late arterial phase (LA: +92HU at 120kV) and portal venous phase (PV: +112HU at 120kV) using LTSL-iodine. Additional LTSL-iodine solutions emulated hyperattenuating lesions during the LA-phase (lesion-to-parenchyma contrast (CLP) = +5 to +50HU) and hypoattenuating lesions during the PV-phase (CLP = -5 to -50HU). Fat-equivalent plastic rings emulated medium and large patients. Each combination of CLP, phase of enhancement, and phantom size was imaged at 80, 100, 120, 140 kV at constant radiation dose. CT attenuation, CLP, and CNRLP were assessed. A theoretical model estimated CT attenuation, CLP, and CNRLP as a function of tube potential and lesion contrast which was compared to the measured data.

## RESULTS

LTSL-iodine more accurately emulated the CT attenuation of contrast-enhanced liver parenchyma compared to water-iodine solutions. The theoretical model was confirmed by the empirical measurements using LTSL-iodine solutions: CT attenuation, CLP, and CNRLP increased when the tube potential decreased (P<0.001). This trend was independent of lesion contrast, phase of enhancement, and phantom size. The absolute improvement in CLP and CNRLP at reduced tube potentials, however, was inversely related to the magnitude of CLP at 140kV.

# CONCLUSION

LTSL accurately emulated the CT attenuation characteristics of contrast-enhanced liver parenchyma and lesions at different tube potentials, lesion contrast, and phase of parenchymal enhancement. The relative improvement in CLP and CNRLP at reduced tube potentials was independent of lesion contrast, phase, and phantom size while the absolute improvement decreased for low-contrast lesions.

# CLINICAL RELEVANCE/APPLICATION

Liquid tissue surrogates offer a promising tool for liver emulation in multi-energy CT phantom studies. Low contrast lesions, which are most difficult to detect in clinical routine, benefit less from low kV-imaging than high contrast lesions.



#### SSA22

## Physics (Image Processing in Imaging and Radiation Therapy)

Sunday, Nov. 25 10:45AM - 12:15PM Room: S103CD



AMA PRA Category 1 Credits ™: 1.50 ARRT Category A+ Credit: 1.75

FDA Discussions may include off-label uses.

#### Participants

Maryellen L. Giger, PhD, Chicago, IL (*Moderator*) Stockholder, Hologic, Inc; Shareholder, Quantitative Insights, Inc; Shareholder, QView Medical, Inc; Co-founder, Quantitative Insights, Inc; Royalties, Hologic, Inc; Royalties, General Electric Company; Royalties, MEDIAN Technologies; Royalties, Riverain Technologies, LLC; Royalties, Mitsubishi Corporation; Royalties, Canon Medical Systems Corporation

Robert Jeraj, PHD, Madison, WI (*Moderator*) Founder, AIQ Services Baowei Fei, PhD, Cleveland, OH (*Moderator*) Nothing to Disclose

#### Sub-Events

## SSA22-01 CNN-based Image Super-Resolution for CT Slice Thickness Reduction using Paired CT Scans for Improving Robustness of Computer-aided Nodule Detection System

Sunday, Nov. 25 10:45AM - 10:55AM Room: S103CD

Participants

Kyu-Hwan Jung, PhD, Seoul, Korea, Republic Of (*Presenter*) Stockholder, VUNO Inc Woong Bae, Seoul, Korea, Republic Of (*Abstract Co-Author*) Nothing to Disclose Seungho Lee, Seoul, Korea, Republic Of (*Abstract Co-Author*) Nothing to Disclose Gwangbeen Park, Seoul, Korea, Republic Of (*Abstract Co-Author*) Nothing to Disclose Hyunho Park, Seoul, Korea, Republic Of (*Abstract Co-Author*) Employee, VUNO Inc Sang Min Lee, MD, Seoul, Korea, Republic Of (*Abstract Co-Author*) Nothing to Disclose

#### For information about this presentation, contact:

khwan.jung@vuno.co

## PURPOSE

To evaluate the effectiveness of a slice thickness reduction technique in computed tomography(CT) scans using convolutional neural network(CNN)-based super-resolution(SR) network for improving the sensitivity of lung nodule detection in thick section CT scans.

#### **METHOD AND MATERIALS**

We collected 100 sets of CT scans with identical acquisition protocols that were differentiated only by the slice thickness (1mm, 3mm, and 5mm). By employing CNN-based SR network, we trained the model to learn the residuals between synthesized thin section slices and real thin section slices. We used 80 sets of CT scans for training, 5 sets for the validation and the remaining 10 sets were used for quantitative evaluation. We separately collected 100 sets of CT scans (also with 1mm, 3mm, and 5mm slice thickness) with one biopsy-confirmed nodule per scan(46 solid nodules and 54 non-solid nodules, size ranges 6-12mm) to evaluate the effectiveness of the slice thickness reduction techniques for improving the lung nodule detection performance in thick section CT scans. The computer-aided detection(CAD) system used for the evaluation of lung nodule detection performance was internally developed with LUNA16 dataset, which contains 888 CT scans with slice thickness less than 3mm.

#### RESULTS

When slice thickness was reduced from 3mm to 1mm, the peak signal-to-noise ratio(PSNR) and structural similarity index(SSIM) were 30.9624 and 0.8142 respectively; when slice thickness was reduced from 5mm to 1mm PSNR and SSIM were 29.2620 and 0.7439 respectively. In the nodule detection task, all solid and non-solid nodules were detected by the CAD system using 1mm slice thickness scans(100.0% recall). However, 2 solid nodules were missed when using 3mm slice thickness scans (95.7% recall) while their corresponding synthetic 1mm scans improved the recall to 97.8% (1 missed solid nodule). Recall of scans with 5mm slice thickness was 89.1% and 85.2% while their synthetic 1mm scans improved the recall to 100.0% and 96.3% for solid and non-solid nodules respectively.

# CONCLUSION

Our CNN-based SR method generates synthetic thin section slices from thick section slices which improve lung nodule detection performance using CAD.

## **CLINICAL RELEVANCE/APPLICATION**

Robustness to acquisition protocol is essential for reliable lung CAD systems. Our slice thickness reduction technique may improve the robustness of CAD systems when applied to CT scans with various slice thickness.

## SSA22-02 An Image Enhancement System for Disease Diagnosis

Participants

Timothy Perk, Madison, WI (*Presenter*) Nothing to Disclose Robert Jeraj, PHD, Madison, WI (*Abstract Co-Author*) Founder, AIQ Services

#### For information about this presentation, contact:

perk@wisc.edu

## PURPOSE

Varying background intensity levels in medical images increases the difficulty of reading images and of identifying abnormal image regions. Windowing and leveling techniques are performed on the entire image, which fails to account for regional differences in image intensity. A method which normalizes image regions by expected image intensity in that particular region could improve diagnostic accuracy of scans.

## **METHOD AND MATERIALS**

This technique is demonstrated for 18F-NaF PET/CT scans of 37 metastatic prostate cancer patients with a total of 1,751 bone lesions. Each image was divided into 19 skeletal regions, such as the humeri, ribs, or ilium, and thresholds were determined for each region. For this work, statistically optimized regional thresholding (SORT) determined thresholds by performing ROC optimization to determine detection thresholds in each bone region that maximize combined sensitivity and specificity for the detection of bone lesions. Finally, image voxels in each region were normalized by dividing the intensity values by the corresponding regional threshold. The detection rate and visibility of lesions was compared between the SORT normalized image and the image windowed at the lesion detection threshold recommended in literature (SUV=10 g/mL).

## RESULTS

SORT windowed images, which used 18 different normalization values (SUV range: 3-13 g/mL), improve detection of lesions with higher sensitivity (96% for SORT, 83% for SUV=10 g/mL) while retaining high specificity (97% for SORT, 97% for SUV=10 g/mL). Regional normalization images increased the visibility of lesions by reducing the number of adjustments to windowing required and setting background across the image to values lower than 1.

## CONCLUSION

Region-specific windowing of medical images can not only make an image easier for radiologists to read, but also assist in the identification of abnormal image regions, effectively reducing the amount of time required to read medical images. Regional windowing in this work was performed using thresholds optimized for disease detection; however, thresholds could be derived from other techniques, such as population mean healthy uptake in a region.

## **CLINICAL RELEVANCE/APPLICATION**

Unlike traditional windowing or leveling, region-specific windowing can account for regional differences across an image, thus reducing the amount of time and effort required to read medical images.

# SSA22-03 Evaluation of an Automated Deformable Mapping Technique with and Without External Fiducial Markers to Relate Corresponding Lesions in Digital Breast Tomosynthesis and Automated Breast Ultrasound Images

Sunday, Nov. 25 11:05AM - 11:15AM Room: S103CD

Participants

Crystal Green, MENG, Ann Arbor, MI (Presenter) Nothing to Disclose

Mitchell M. Goodsitt, PhD, Ann Arbor, MI (*Abstract Co-Author*) Investigator, General Electric Company; Research collaboration, General Electric Company

Jasmine H. Lau, Ann Arbor, MI (Abstract Co-Author) Nothing to Disclose

Kristy K. Brock, PhD, Houston, TX (Abstract Co-Author) License agreement, RaySearch Laboratories AB

Cynthia Davis, Niskayuna, NY (Abstract Co-Author) Nothing to Disclose

Paul L. Carson, PhD, Ann Arbor, MI (Abstract Co-Author) Research collaboration, General Electric Company Research collaboration, Light Age, Inc

# For information about this presentation, contact:

canngree@umich.edu

#### PURPOSE

To test an automated deformable mapping method for registering corresponding lesions in digital breast tomosynthesis (DBT) and automated breast ultrasound (ABUS) images with and without the use of external fiducial markers.

#### **METHOD AND MATERIALS**

A CIRS multi-modality breast phantom containing 20 lesions was employed and imaged with DBT (upright positioning with craniocaudal (CC) compression and mediolateral oblique (MLO) compression), and ABUS (supine positioning with anterior-to-chest wall compression). Eight external fiducial markers (gel pads containing 1-mm glass beads) were attached to the surface of the breast phantom prior to the imaging. The reconstructed images were segmented using manual (ABUS) and semi-automated (DBT) techniques. An automated mapping method generates, deforms, and relates the resulting models of the breast for registration of lesions between the DBT (CC or MLO) and ABUS image sets. Performance was assessed by the number of matched paired lesions and measures of the distances between the centers of mass (dCOM) of corresponding lesions.

#### RESULTS

The maximum number of lesions that could be matched was 18 because 2 of the 20 lesions were too close to the chest wall to be visible in the reconstructed DBT images. For mapping of DBT-CC to ABUS without markers, 14 of the 18 lesions were matched and the mean dCOM was  $13.64 \pm 6.25$  mm. With markers, 17 of the 18 lesions were matched and the mean dCOM was  $12.83 \pm 6.03$ 

mm. For mapping of DBT-MLO to ABUS without markers, 8 of the 18 lesions were matched and the mean dCOM was  $9.32 \pm 2.82$  mm. With markers, 17 of the 18 lesions were matched and the mean dCOM was  $12.25 \pm 5.75$  mm.

# CONCLUSION

This work demonstrates the potential for using this deformable mapping technique to identify related lesions between two DBT views and ABUS images. This method shows improved lesion correlation with the use of external fiducial markers. This should improve radiologists' characterization of breast lesions which should reduce patient callbacks and unnecessary biopsies. Future work will include an IRB-approved proof of concept study with patient data for registration between DBT and ABUS images.

### **CLINICAL RELEVANCE/APPLICATION**

This works demonstrates the use of an automated deformable registration technique between two DBT views and ABUS images and shows potential in improving the characterization of breast lesions between these modalities.

## SSA22-04 Medical Image Fusion Using M-Band Wavelet Transform for Radiotherapy

Sunday, Nov. 25 11:15AM - 11:25AM Room: S103CD

Participants

Satishkumar Chavan, Mumbai, India (*Abstract Co-Author*) Nothing to Disclose Abhijit D. Pawar, MD, Pune, India (*Abstract Co-Author*) Nothing to Disclose Sanjay Talbar, Nanded, India (*Presenter*) Nothing to Disclose

For information about this presentation, contact:

abhijitpawar.rad@gmail.com

#### CONCLUSION

The fused images using proposed method provides the best out of both CT and MRI. The proposed fusion scheme has potential application in precise localization and delineation of lesions in treatment planning of radiotherapy.

#### Background

Radiation oncologists need information from both the Computed Tomography (CT)and Magnetic Resonance Imaging (MRI) sequences for precise outlining of tumour in radiotherapy. The proposed work aims to create new enriched image using medical image fusion of CT and MRI slices. The spectral features from source slices are extracted using M-band Wavelet Transform (MBWT).MBWT is separable, orthogonal transform with a perfect reconstruction property. It provides high directional sensitivity and finer spectral resolution. The average for low frequency subbands and maxima for high frequency subbands are used as fusion rules. The inverse transform reconstructs visually enriched fused image.This fused image is an excellent assistance to the radiation oncologist for delineation of tumour to prepare precise treatment plan.

#### **Evaluation**

In this work, total 39 sets of CT and MRI slices are used. The qualitative evaluation of the work is done in context with visual perception, contrast enhancement, confidence to lesion delineation and usefulness in treatment planning. Three expert radiologists rated fused images on the scale of 0 (poor) to 4 (excellent). The quantitative evaluation involves fusion metrics viz.entropy (En), image quality index (IQI), edge quality index (EQI), and mean structural similarity index measure (mSSIM) which are useful for quality, similarities with source images, and edge preservation.

## Discussion

The fused images using proposed method provide better retention of the anatomical structures and visualization of lesions as compared to the state of art wavelet techniques as presented in Figure 1. The average score by three radiologists for fused images using presented work is 3.87. In quantitative evaluation, the fusion parameters are calculated and they give highest values for all the fused images using proposed method which indicate that proposed technique outperforms over other fusion techniques.

# SSA22-05 Using Texture Analysis to Optimize Reconstruction Parameters

```
Sunday, Nov. 25 11:25AM - 11:35AM Room: S103CD
```

Participants Kenneth Nichols, PhD, New Hyde Park, NY (*Presenter*) Royalties, Syntermed, Inc; Christopher Caravella, New Hyde Park, NY (*Abstract Co-Author*) Nothing to Disclose Christopher J. Palestro, MD, New Hyde Park, NY (*Abstract Co-Author*) Nothing to Disclose

## For information about this presentation, contact:

knichols@northwell.edu

#### PURPOSE

In providing SPECT phantom quality assurance images to accrediting agencies, it is not obvious whether it is preferable to submit reconstructions performed using typical clinical (CLIN) protocol processing parameters, or to follow agencies' filtered backprojection (FBP) suggestions. We applied texture analysis metrics to determine the degree to which these choices affect equipment capability assessment.

## **METHOD AND MATERIALS**

Phantom data were processed for 128 SPECT scans acquired for 32 Mcts for 10 gamma cameras, using 666-814 MBq 99mTc in cylindrical water baths with Plexiglas inserts of 6 sphere & rod sizes. Reconstructions were performed following agencies' suggestions of FBP & Hanning filtering (cutoff = 1.0) & Chang attenuation correction. Algorithms written in IDL v8.4 computed texture analysis gray-level-co-occurrence matrix (GLCM) entropy, with sphere contrast computed by fitting radial count profiles to 3rd order polynomial curves. ROC analysis established optimal discrimination thresholds using as the reference standard dichotomous visual readings of a medical imaging physicist, who graded sphere & rod visibility without knowledge of texture analysis values. The same phantom was used to collect 13 additional data sets with a dual detector SPECT camera equipped with a 4-slice non-

diagnostic CT scanner, reconstructed by FBP & by the manufacturer's default settings for clinical bone SPECT/CT protocols by OSEM (10 subsets; 2 iterations) & Butterworth filtering (cutoff = 0.5, order = 5), incorporating attenuation correction using the CT scan. GLCM computations were compared for FBP & CLIN reconstructions.

## RESULTS

Optimal criteria for best agreement with visual scores for spheres was contrast ( $81\pm1\%$  accuracy), & for rods was entropy ( $97\pm1\%$  accuracy). For the 13 new acquisitions, by there criteria, more rods would have been visible for FBP than CLIN (46% versus 39\%, p = 0.02), & more spheres (57% versus 40\%, p = 0.0003), with greater sphere contrast ( $28\pm21\%$  versus 19 $\pm18\%$ , p < 0.0001). Rod entropy & sphere entropy were significantly different for FBP & CLIN reconstructions ( $-13.5\pm3.1K$  versus  $-14.6\pm2.8K$ , p < 0.0001 &  $-3.1\pm1.4K$  versus  $-4.6\pm3.9K$ , p = 0.0001), & favored detecting rods & spheres by FBP over CLIN.

## CONCLUSION

Texture analysis can help in obtaining optimal results for equipment test data.

## **CLINICAL RELEVANCE/APPLICATION**

Texture analysis provides a useful basis for choosing among image reconstruction options.

## SSA22-06 Real-Time Deformable Image Registration for MRI-Guided Radiotherapy

Sunday, Nov. 25 11:35AM - 11:45AM Room: S103CD

Participants

Gregory C. Sharp, PhD, Boston, MA (*Presenter*) Nothing to Disclose Seyedali Mirzapourrezaei, Wichita, KS (*Abstract Co-Author*) Nothing to Disclose Thomas Mazur, St Louis, MO (*Abstract Co-Author*) Nothing to Disclose Nagarajan Kandasamy, PhD, Philadelphia, PA (*Abstract Co-Author*) Nothing to Disclose James Shackleford, PhD, Philadelphia, PA (*Abstract Co-Author*) Nothing to Disclose Ehsan Salari, Wichita, KS (*Abstract Co-Author*) Nothing to Disclose

For information about this presentation, contact:

gcsharp@partners.org

## CONCLUSION

Real-time deformable image registration is a viable strategy for tracking organs in MR-guided radiotherapy. It is a promising approach for next-generation applications including beam tracking and real-time plan optimization.

#### Background

MR-guided radiotherapy has the capability to acquire 2D cine-mode images of patient cross sections in near real time. These images are used for monitoring of patient position and motion management using respiratory gating. Beam tracking is a radiotherapy strategy where the therapy beam continuously follows the target position based on real-time sensing. To enable beam tracking, the position of the intended target and avoidance structures must be identified in real-time. This abstract investigates real-time deformable image registration as an approach for MR-guided radiotherapy.

#### **Evaluation**

Registration accuracy and speed were retrospectively evaluated on sagittal plane cine-mode video sequences from nine stomach cancer patients. The video resolution was 100 x 100 pixels, with a pixel spacing of 3.5 mm. Images were registered to a reference image at the beginning of the sequence. Accuracy was evaluated by comparing manually drawn contours of the stomach with a warped reference contour. A total of 90 images, 10 from each patient, were annotated and analyzed. Speed was measured for the registration only, with file I/O excluded. B-spline registration was performed using plastimatch, with GPU-accelerated sum of squared difference cost function, and multicore-accelerated curvature regularization. To assess real-time performance, computation time was limited to 200 milliseconds.

#### Discussion

B-spline image registration ran at 8.8 +/- 2.0 milliseconds per iteration, which allowed 22 iterations to be performed. Registration accuracy was estimated to be 2.2 +/- 1.1 mm, using the center of mass of the manually drawn contours as the standard. Dice coefficient of the stomach was found to be 0.90 +/- 0.03. Approximately 90 percent of the computation time was used to compute regularization, we estimate that implementing this routine on the GPU will allow 100 iterations to be performed within 200 milliseconds.

# SSA22-07 MR T2 \* Parameter Imaging Based on DANTE Black Blood Prepared Sequence and Modified JSENSE Reconstruction Method

Sunday, Nov. 25 11:45AM - 11:55AM Room: S103CD

Participants

Yanan Ren, Zhengzhou, China (*Presenter*) Nothing to Disclose Jingliang Cheng, MD, PhD, Zhengzhou, China (*Abstract Co-Author*) Nothing to Disclose

#### For information about this presentation, contact:

1554847793@qq.com

## CONCLUSION

Multi-contrast images can be jointly recontructed by modified Jsense method with effective removal of the residual aliasing artfact at a high acceleration factor. Accurate T2\* maps are obtained by DANTE-GRE due to its high SNR and effective blood signal supression.Phantom experiments demonstrated that the incorporation of modified Jsense and DANTE-GRE may outperform conventional multi-echo GRE T2\* mapping.

#### Background

Quantitative analysis of T2\* value is an effective tool to reflect iron content of human tissue in MRI, which are closely related to Mediterranean anemia.A new MRI pulse sequence and a modified reconstruction method were proposed to improve accuracy of T2\* measurement. Specifically, DANTE prepared sequence is selected to supress blood signals and modified reconstruction method based on JSENSE is proposed to improve image quality and reduce scan time.

#### **Evaluation**

A numerical bloch simulations were established on DANTE prepared sequence to prove the velocity sensitivity and to select parameters.Several phantom experiments completed by DANTE-GRE realized more accurate T2\* quantification with blood suppression compared with multi-echo GRE and MSDE-GRE sequence.The PSNR and HFEN were chosen to assess the quality of coil sensitivities and multi-contrast images recontructed by SENSE,Jsense and modified Jsense algorithm with acceleration factors of 2, 3 and 4. At last,ROIs in T2\* maps obtained both in phantom and vivo were evaluted between DANTE-GRE sequence and modified Jsense method with former convential methods.

#### Discussion

The phantom results validate the superiority of modified Jsense algorithm in increaseing smoothness of multi-channel coil sensitivities and decreasing artifacts of multi-contrast images at a high acceleration factor. However, images of the first echo recovered by modified JSENSE achieve lower HEEN and higher PSNR compared to the last echo which has lower SNR due to its intrinsic T2\* decay. By combining modified Jsense algorithm with DANTE-GRE sequence which could further acquire more image information and better image quanlity, more accurate T2\* maps could acquire since the artifacts originating from flowing blood are effectively supressed.

# SSA22-08 Automatic Cardiac Ventricle Segmentation from CT Images Using Fully Convolutional Neural Networks

Sunday, Nov. 25 11:55AM - 12:05PM Room: S103CD

Participants

Ryan Chamberlain, PhD, Minneapolis, MN (*Presenter*) Employee, ImBio, LLC Lauren Keith, Minneapolis, MN (*Abstract Co-Author*) Employee, ImBio, LLC; Stock options, ImBio, LLC; German Gonzalez, PhD, Cambridge, MA (*Abstract Co-Author*) Nothing to Disclose

## PURPOSE

Acute pulmonary embolism (PE) is an emergent condition with three month mortality rate of 15%. Presence of PE is most often confirmed using Computed Tomography Pulmonary Angiography (CTPA). Mortality from PE is usually caused by overload of the right ventricle. The quantification of the right ventricular to left ventricular diameter ratio has been proved to be a quantitative prognostic marker for staging acute PE. Despite strong evidence for RV/LV as a prognostic marker in PE it is not always reported because it suffers from high interobserver variability and manual effort to measure. This work investigates automating the first step in an automated RV/LV CAD tool: ventricle segmentation.

## **METHOD AND MATERIALS**

Fifty CTPA scans were used for this study (20 from cad-pe.org and 30 from a closed dataset). The ground truth segmentations were created by an imaging expert. This work developed a convolutional neural network (CNN) capable of segmenting the left and right cardiac ventricles from a 2D CT slice. The CNN was based on the U-Net. The training data consisted of 43 cases, the validation data consisted of 2 cases, and the test data consisted of 5 cases. The network was trained on 2D slices. To test the performance the CNN was passed all slices from a series and the largest morphologically connected region for each output class (RV and LV) was kept as the final segmentation. The CNN was trained with the original data and with an augmented data set where each slice passed to the network during training underwent a series of perturbations consisting of: 1) flipping, 2) noise injection, 3) deformation, and 4) random erasing.

## RESULTS

The CNN trained on the original dataset has an average Dice coefficient of 0.96 on the training data and 0.90 on the testing data. The CNN trained with data augmentation had an average Dice coefficient of 0.94 on the training data and 0.94 on the testing data.

# CONCLUSION

The CNN was able to create quality ventricle segmentations with only 43 scans in the training dataset, and the set of data augmentations significantly improved the performance on the test dataset.

## **CLINICAL RELEVANCE/APPLICATION**

Accurate reporting of RV/LV can improve the diagnosis and staging of acute PE, but it is currently underreported because of interobserver variability and high manual effort. Automating this calculation could increase the rate and quality of RV/LV reporting, thereby improving patient care in emergency departments.

# SSA22-09 Multi-institutional Deep Network for High Performance Sorting of Over 3000 AP and PA Chest Radiographs

Sunday, Nov. 25 12:05PM - 12:15PM Room: S103CD

Participants

Thomas J. Rhines, Chicago, IL (*Presenter*) Nothing to Disclose Jennie S. Crosby, BS, Chicago, IL (*Abstract Co-Author*) Nothing to Disclose Feng Li, MD, PhD, Chicago, IL (*Abstract Co-Author*) Nothing to Disclose Heber MacMahon, MD, Chicago, IL (*Abstract Co-Author*) Consultant, Riverain Technologies, LLC Stockholder, Hologic, Inc Royalties, UCTech Research support, Koninklijke Philips NV Consultant, General Electric Company Maryellen L. Giger, PhD, Chicago, IL (*Abstract Co-Author*) Stockholder, Hologic, Inc; Shareholder, Quantitative Insights, Inc; Shareholder, QView Medical, Inc; Co-founder, Quantitative Insights, Inc; Royalties, Hologic, Inc; Royalties, General Electric Company; Royalties, MEDIAN Technologies; Royalties, Riverain Technologies, LLC; Royalties, Mitsubishi Corporation; Royalties, Canon Medical Systems Corporation

#### For information about this presentation, contact:

#### tjrhines@uchicago.edu

#### PURPOSE

The classification of chest radiographs as anteroposterior (AP) or posteroanterior (PA) is important for their interpretation and any subsequent analysis and diagnosis. DICOM header information is often incomplete, and 328 of the 2364 (14%) chest radiographs acquired at our institution lacked the required information for AP/PA classification.

#### **METHOD AND MATERIALS**

Using a chest radiograph dataset from our institution, a convolutional neural network with AlexNet architecture was trained from scratch. 1475 AP and 713 PA radiographs were used, with 65% for training, 20% for step-wise validation, and 15% for testing. After training was complete, the network was tested on an independent set of 500 AP and 500 PA images from the National Institutes of Health chest radiograph dataset.

## RESULTS

The independent test set yielded an AUC of  $0.97 \pm 0.0046$ , with less than 9% (89 of 1000) of radiographs misclassified. Of the images misclassified, several were improperly oriented or included a number of radiopaque medical devices. Our institutional dataset was used for training because of its high image quality and the lack of image imprinted "AP" or "PA" labels. Many images in the NIH dataset contain imprinted AP/PA labels, prompting their exclusion from the training dataset to avoid training the network to simply look for the imprinted label for the classification.

## CONCLUSION

This model shows multi-institutional generalization of a trained network for the task of classifying AP and PA radiographs. A primary application of this network is for automated classification of the AP/PA view within the clinical workflow. The high AUC achieved demonstrates that the classification can be performed with high accuracy. Training the model took 4.5 minutes and testing 10,000 images took 130 seconds. Due to its speed, the classification technique could be applied without disruption of clinical workflow.

#### **CLINICAL RELEVANCE/APPLICATION**

To ensure appropriate classification and correct labeling of an image as AP or PA, a trained convolutional neural network can be used clinically with high accuracy and efficiency.



#### SSA23

# Radiation Oncology (Radiobiology/Science)

Sunday, Nov. 25 10:45AM - 12:15PM Room: E353A



AMA PRA Category 1 Credits ™: 1.50 ARRT Category A+ Credit: 1.75

FDA Discussions may include off-label uses.

#### Participants

Martin Colman, MD, Houston, TX (*Moderator*) Stockholder, Steward Health Care Meng X. Welliver, MD, Columbus, OH (*Moderator*) Nothing to Disclose

# Sub-Events

# SSA23-01 Brain Radiation-Induced Fatigue is Associated with Neuroinflammation and Suppression of Orexin Signaling

Sunday, Nov. 25 10:45AM - 10:55AM Room: E353A

Participants

Aaron J. Grossberg, MD, PhD, Portland, OR (*Presenter*) Nothing to Disclose Die Zhang, PhD, Houston, TX (*Abstract Co-Author*) Nothing to Disclose Wei Zhou, Houston, TX (*Abstract Co-Author*) Nothing to Disclose Connie C. Weng, Houston, TX (*Abstract Co-Author*) Nothing to Disclose Phillip S. Gross, Houston, TX (*Abstract Co-Author*) Nothing to Disclose Elisabeth G. Vichaya, PhD, Houston, TX (*Abstract Co-Author*) Nothing to Disclose Robert Dantzer, DVM,PhD, Houston, TX (*Abstract Co-Author*) Nothing to Disclose David R. Grosshans, MD, PhD, Houston, TX (*Abstract Co-Author*) Nothing to Disclose

For information about this presentation, contact:

grossber@ohsu.edu

## PURPOSE

Fatigue, the most common acute and subacute toxicity of partial or whole brain radiation therapy (WBRT), significantly decreases quality of life for patients, abrogating the benefit afforded by improved tumor control. The objective of the study is to evaluate the roles of neuroinflammation and orexin neuron activity in the pathogenesis of fatigue induced by clinically relevant WBRT fractionation.

#### **METHOD AND MATERIALS**

Adult male Sprague-Dawley rats received WBRT, 4 Gy in 5 daily fractions, or sham irradiation. Home cage locomotor activity (LMA) was continuously monitored using a photobeam system. Food intake and body weight were collected weekly. Cerebrospinal fluid (CSF) and brain sections were collected at fatigue onset, peak, and recovery. CSF orexin concentration was measured using radioimmunoassay. RNA was isolated from homogenized brain sections and inflammatory and oxidative expression patterns were evaluated using quantitative PCR. The data were compared to physician-reported fatigue, and orexin and cytokine CSF protein levels collected pre- and post-radiation from a cohort of 11 pediatric patients receiving proton radiation for primary brain cancer. Data were analyzed by t-test or 2-way ANOVA with post hoc Bonferroni corrected t-test. Significance was set at P<.05.

#### RESULTS

LMA was decreased in WBRT-treated rats starting following the first fraction and continued to decrease until reaching a nadir following the 5th and final fraction. LMA slowly recovered after that point, returning to baseline. Food intake and weight gain were significantly reduced in WBRT-treated rats, recovering to match sham rats within 2 weeks of the first fraction. The onset of fatigue is associated with widespread neuroinflammatory gene expression and decreased CSF orexin levels, which resolves as fatigue improves. Orexin levels were decreased and cytokine levels increased in CSF samples from patients for whom fatigue was recorded as a toxicity during treatment.

## CONCLUSION

Brain radiation-induced fatigue is associated with neuroinflammation and decreased orexin levels in both preclinical and clinical samples. These data provide potential therapeutic avenues to address this disabling and pervasive toxicity of brain radiation.

#### **CLINICAL RELEVANCE/APPLICATION**

Neuroinflammation and orexin signaling appear to underlie brain radiation-induced fatigue, providing potential therapeutic targets.

# SSA23-02 Translocation Frequency in Patients with Repeated CT Exposure: Comparison with CT-Naive Patients

Sunday, Nov. 25 10:55AM - 11:05AM Room: E353A

Min Hoan Moon, MD, Seoul, Korea, Republic Of (*Presenter*) Nothing to Disclose Jin Kyung Lee, Seoul, Korea, Republic Of (*Abstract Co-Author*) Nothing to Disclose Myoung Seok Lee, MD, Seoul, Korea, Republic Of (*Abstract Co-Author*) Nothing to Disclose Hyunsik Woo, MD, Seoul, Korea, Republic Of (*Abstract Co-Author*) Nothing to Disclose Sohee Oh, Seoul, Korea, Republic Of (*Abstract Co-Author*) Nothing to Disclose

#### For information about this presentation, contact:

mmhoan@gmail.com

#### PURPOSE

To compare translocation frequency between patients with repeated computed tomography (CT) exposure and CT-naïve patients and to assess the relationship between radiation exposure and translocation frequency.

## **METHOD AND MATERIALS**

This study was approved by our institutional review board. 48 cases with repeated CT exposure and 48 age- and sex-matched CTnaïve controls were prospectively enrolled in this single-institution study. Absorbed dose using dose-length product was used as a metric for radiation exposure and translocation frequency was assessed by using chromosome-specific fluorescent hybridization probes. The comparison of translocation frequency between cases and CT-naïve controls was performed by using Wilcoxon test (paired samples) and the relationship between radiation exposure and translocation frequency was assessed by partial correlation coefficient.

## RESULTS

A statistically significant difference was present in translocation frequency between cases and CT-naïve controls (P = .0003). The median translocation frequency was 7 (95% confidence interval: 6, 8) for cases and 4 (95% confidence interval: 3, 6) for controls. By using translocation frequency as the response variable and radiation exposure (accumulated, maximum, and mean) as the effect variables, statistically significant correlation was found between accumulated radiation exposure and translocation frequency (r = .4279, P = .0030).

## CONCLUSION

Chromosomal translocation was more common in patients with repeated CT exposure than CT-naïve patients, and a positive association was noted between accumulated radiation exposure and translocation frequency.

## **CLINICAL RELEVANCE/APPLICATION**

Our results added evidence favoring a non-threshold response for radiation-associated cancer induction at low-level radiation exposure in medical practice.

## SSA23-03 DNA Damage in Peripheral Blood Lymphocytes Induced By Low-Dose Chest CT: Comparison with Standard Dose Chest CT

Sunday, Nov. 25 11:05AM - 11:15AM Room: E353A

Participants

Hiroaki Sakane, MD, Hiroshima, Japan (*Presenter*) Nothing to Disclose Chiemi Sakai, Hiroshima, Japan (*Abstract Co-Author*) Nothing to Disclose Mari Ishida, Hiroshima, Japan (*Abstract Co-Author*) Nothing to Disclose Wataru Fukumoto, Hiroshima, Japan (*Abstract Co-Author*) Nothing to Disclose Satoshi Tashiro, Hiroshima, Japan (*Abstract Co-Author*) Nothing to Disclose Kazuo Awai, MD, Hiroshima, Japan (*Abstract Co-Author*) Nothing to Disclose Kazuo Awai, MD, Hiroshima, Japan (*Abstract Co-Author*) Nothing to Disclose Kazuo Awai, KD, Hiroshima, Japan (*Abstract Co-Author*) Research Grant, Canon Medical Systems Corporation; Research Grant, Hitachi, Ltd; Research Grant, Fujitsu Limited; Research Grant, Bayer AG; Research Grant, DAIICHI SANKYO Group; Research Grant, Eisai Co, Ltd; Medical Advisory Board, General Electric Company; ;

#### PURPOSE

The purpose of this study was to evaluate the DNA damage in peripheral blood lymphocytes induced by a low-dose chest CT scan using  $\gamma$ -H2AX foci as a DNA damage maker.

#### **METHOD AND MATERIALS**

We obtained institutional review board approval and the written informed consent from 217 patients, who were prospectively enrolled in this study. A total of 146 patients underwent low-dose chest CT (120 kV, 50 mAs, pitch factor 1.39), and 71 patients underwent standard-dose chest CT (120 kV, AEC, pitch factor 0.813). Blood samples were obtained before and after CT scan. Lymphocytes were isolated and stained against  $\gamma$ -H2AX (phosphorylated histone variant H2AX). The number of  $\gamma$ -H2AX foci in at least 4,000 lymphocytes was analyzed automatically with fluorescence microscopy. Significant differences between the number of foci were tested by using paired t-test, Wilcoxon test.

#### RESULTS

There were no significant difference in the character of patients between low and standard dose chest CT groups. The mean dose length product was 132 mGy·cm in low-dose CT and 455 mGy·cm in standard-dose CT groups, respectively. There was no significant difference in the baseline level of  $\gamma$ -H2AX foci between low and standard dose groups before CT examination. The numbers of  $\gamma$ -H2AX foci of patients in low-dose CT group before and after CT scan were 0.90 (standard deviation: 0.50) and 0.93 (0.51), respectively. There was no significant difference in the number of  $\gamma$ -H2AX foci before and after low-dose CT. The numbers of  $\gamma$ -H2AX foci in standard-dose CT group increased from 1.00 (0.45) to 1.07 (0.48) after CT scan. In contrast to the low dose group, the number of  $\gamma$ -H2AX foci in the standard dose group showed significant increase after CT (p=0.025).

## CONCLUSION

Radiation effect by a low-dose chest CT was too low to be detected by  $\gamma$ -H2AX assay.

# **CLINICAL RELEVANCE/APPLICATION**

v HOAN account to useful to determine the entireditation does for low does CT in lung concernation

Y-max assay may be useful to determine the optimal radiation dose for low-dose of influing cancer screening.

# SSA23-04 A Novel Molecularly Targeted Radiotherapeutic Agent (MTRT) to Deliver Immunomodulatory Radiation to Multiple Pediatric and Adult Solid Tumors

Sunday, Nov. 25 11:15AM - 11:25AM Room: E353A

Participants

Ravi Patel, MD,PhD, Madison, WI (*Presenter*) Nothing to Disclose Reinier Hernandez, MSc, Madison, WI (*Abstract Co-Author*) Nothing to Disclose Ryan Brown, Madison, WI (*Abstract Co-Author*) Nothing to Disclose Joseph Grudzinski, PhD, Madison, WI (*Abstract Co-Author*) Nothing to Disclose Peter Carlson, BS, Madison, WI (*Abstract Co-Author*) Nothing to Disclose Eduardo Aluicio-Sarduy, PhD, Madison, WI (*Abstract Co-Author*) Nothing to Disclose Jonathan Engle, PhD, Madison, WI (*Abstract Co-Author*) Nothing to Disclose Bryan Bednarz, PhD, Madison, WI (*Abstract Co-Author*) Nothing to Disclose Paul Sondel, Madison, WI (*Abstract Co-Author*) Nothing to Disclose Jamey P. Weichert, PhD, Madison, WI (*Abstract Co-Author*) Nothing to Disclose Zachary S. Morris, MD, PhD, Madison, WI (*Abstract Co-Author*) Nothing to Disclose

For information about this presentation, contact:

rpatel55@wisc.edu

#### PURPOSE

Radiation therapy (RT) has been shown in preclinical studies to enhance the efficacy of several types of immunotherapies. However, traditional external beam radiation therapy (EBRT) is typically only delivered to a few sites of disease, with larger field sizes being associated with systemic lymphopenia. Because many patients have widespread disease, it is nearly impossible for them to benefit from the efficacy enhancements afforded by immunotherapies using standard RT. Conversely, our RT delivery approach using a novel, tumor-selective form of molecularly targeted radiation therapy (MTRT), Y90-NM600, may augment tumor specific immune-priming by delivering RT to multiple sites of disease.

#### **METHOD AND MATERIALS**

Syngeneic mice were inoculated with tumors from adult and pediatric solid tumor lines B78 (melanoma), LLC (lung), MOC1 (Head and Neck), 4T1 (breast), Panc02 (Pancreas), GL261 (high grade glioma), K7M2 (Rhabdomyosarcoma), NXS2 and 9464D (neuroblastoma). Mice were injected with 250 µCi of Y86-NM600 and scanned via PET/CT at 2, 24, 48, and 72 h. Organs were then harvested for bio-distribution (BioD) via gamma scintigraphy. Another cohort of mice with bi-lateral B78 flank tumors were treated with 12 Gy EBRT to a primary tumor and anti-CTLA4 and were randomized to be treated w/wo 50 µCi MTRT. Tumor growth and survival was monitored. All mice with complete response (CR) were re-challenged with B78.

## RESULTS

PET/CT and BioD data showed preferential uptake of NM600 in all tumor lines with highest uptake in Panc02 pancreatic tumors (10fold increase of uptake in tumor compared to bone marrow, 2-fold increase compared to spleen). In our therapeutic 2-tumor trial, addition of MTRT resulted in decreased tumor growth (p < 0.05) of both primary and secondary tumors when combined with immune checkpoint inhibitor and EBRT (primary tumor) compared to a matched cohort randomized to just EBRT (primary tumor) and anti-CTLA4 alone. 50% of mice in the MTRT arm had a complete response and memory to B78 re-challenge compared to 0% in the no MTRT (EBRT + anti-CTLA4 alone) arm.

## CONCLUSION

NM600 is a novel form of MTRT that shows preferential uptake in multiple solid tumors and can deliver immunomodulatory RT to distant tumors to increase response rates to T cell checkpoint blockade.

## **CLINICAL RELEVANCE/APPLICATION**

MTRT sensitizes metastatic cancer cells to immunotherapy and improves response rates to systemic immune checkpoint blockade therapy.

## SSA23-05 Identifying the Effect of Hereditary Factors on Radiation-Induced Cardiac Toxicity Using Novel Genetic Rat Models

Sunday, Nov. 25 11:25AM - 11:35AM Room: E353A

Participants Aronne M. Schottstaedt, MS, Cleveland Heights, OH (*Presenter*) Nothing to Disclose Carmen R. Bergom, MD, PhD, Okauchee, WI (*Abstract Co-Author*) Nothing to Disclose

For information about this presentation, contact:

## ams530@case.edu

# PURPOSE

Radiation therapy is used in most cancer patients, but dose is limited by damage to normal tissue. The use of defined genetic models to assess radiation toxicity, followed by genetic mapping of radiosensitivity phenotypes, will allow for maximization of tumor dose while limiting normal tissue toxicity. In this study, we utilize consomic rats, which are genetically identical except that one chromosome is inherited from a second inbred rat strain.

# METHOD AND MATERIALS

Adult male and female Salt Sensitive (SS) rats and SS.BN3 consomic rats, (SS background with Brown Norway chromosome 3), received image-guided localized whole heart radiation at a dose of 24 Gy or 9 Gy x 5 fractions. Echocardiograms with strain analysis were performed at baseline, 3, and 5 months. The student's t-test was used to compare values. RNA-seq from left ventricle samples at 1 and 10 weeks post radiation was performed and analyzed with IPA software.

#### RESULTS

Our previous studies have demonstrated that the SS.BN3 tumors are more radiosensitive than SS tumors. In the 24 Gy study, cardiac toxicity increased in SS compared to SS.BN3 male and female rats. End diastolic volume (EDV), a measure of ventricular dilation, was elevated after radiation in SS rats (EDV: 0.62 vs 0.49 ml, p<0.01). Systolic function measured with ejection fraction (EF), and contractility measured with radial strain, were lower in SS rats at 5 months (EF: 81 vs 94%, p<0.01, radial strain: 33 vs 68%, p<0.01). Left ventricular mass was elevated at 3 months in SS rats (p<0.001), and moderate-to-large pericardial effusions were present in 6/6 SS rats compared to 1/7 SS.BN3 rats at 5 months. Similar results are seen with the 9 Gy x 5 fractions. Gene expression analysis comparing SS and SS.BN3 females showed inflammatory and mitochondrial pathways with greatly altered expression, most notably at 1 week post-radiation.

#### CONCLUSION

These data show that SS rats are more sensitive to cardiac radiation than SS.BN3 rats, demonstrating the role of heritable factors in determining cardiac radiosensitivity. Gene expression analysis identified a number of cardiac-related targets on chromosome 3 for future studies of radiation protection. Further genetic mapping will aid in narrowing the causative target(s) for potential therapies.

#### **CLINICAL RELEVANCE/APPLICATION**

This project has the potential to enhance the effectiveness and toxicity profile of radiation therapy in cancer and to delineate new therapeutic targets.

## ssA23-06 Role of Radio-Immunotherapy in the Treatment of Local and Distant Tumors in Prostate Cancer

Sunday, Nov. 25 11:35AM - 11:45AM Room: E353A

Participants

Sayeda Yasmin-Karim, Boston, MA (*Presenter*) Nothing to Disclose Wilfred Ngwa, PHD, Boston, MA (*Abstract Co-Author*) Nothing to Disclose Michele Moreau, Lowell, MA (*Abstract Co-Author*) Nothing to Disclose

## For information about this presentation, contact:

sayeda\_yasmin-karim@DFCI.Harvard.edu

#### CONCLUSION

These results suggest that the use of SRB for sustained in-situ delivery of CD40 antibody could significantly enhance the abscopal effect of radiotherapy in treating prostate adenocarcinoma.

#### Background

Metastasis is the cause of death in most cancers including prostate. It has been observed by Mole and others that radiotherapy at one site may lead to regression of metastatic cancer at other sites, which were not irradiated; this phenomenon is called 'abscopal' effect. Unfortunately, this regression is not predictable. Some studies have observed an enhancement by systemic application of immunoadjuvants, which also has limited application because of generalized adverse effect. The purpose of this study is to evaluate the enhancing the abscopal effect of radiotherapy (RT) by in-situ delivered anti-CD40 using Smart Radiation Biomaterials (SRB) in the treatment of prostate cancer where treatment in one site (location) able to cure the tumors in other locations of the body.

#### Evaluation

A syngeneic mouse model of prostate adenocarcinoma was generated in both flanks of C57/BL6 background mouse. The palpable sized tumor of right flank was treated as randomized cohorts: control, treatment with 5 Gy of RT, anti CD40 antibody (20  $\mu$ g/tumor), and in combination. Another cohort was created by sustained delivery of anti CD40 antibody using SRB where SRB material by itself demonstrates some degree of antineoplastic activity in our previous studies. A Small Animal Radiation and Research platform (SARRP) was used for image-guided RT at 220 kVp. Our result shows that in-situ application of antiCD40 antibody entited with radiation significantly enhances the effect of radiotherapy (p<0.01), whereas using the SRB for AntiCD40 delivery in situ further enhances the survival (p<0.001). Reduction of tumor volume was observed in both sides. 2 out of 5 mice showed total regression of the untreated tumors in the RT+SRB delivered AntiCD40 group.

#### Discussion

These promising findings provide a good basis for further/ongoing studies investigating RT and CD40 antibody dosing and scheduling and use of SRB for sustained in-situ delivery of such immunoadjuvants to further optimize the treatment outcomes with minimal systemic toxicities.

# SSA23-07 Imaging and Treatment of Primary and Metastasized Tumors Through Immunotherapy Using Targeted Antigen-Capturing Nanoparticles with Serum Amyloid A1 along with Radiation and PD-L1 Blockade

Sunday, Nov. 25 11:45AM - 11:55AM Room: E353A

Participants

Satoshi G. Harada, MD, Morioka, Japan (*Presenter*) Nothing to Disclose Takashi Segawa, Morioka, Japan (*Abstract Co-Author*) Nothing to Disclose Takahiro Satoh, DSc, Takasaki, Japan (*Abstract Co-Author*) Nothing to Disclose Shigeru Ehara, MD, Morioka, Japan (*Abstract Co-Author*) Nothing to Disclose Koichiro Sera, Takizawa, Japan (*Abstract Co-Author*) Nothing to Disclose

For information about this presentation, contact:

sharada@iwate-med.ac.jp

## PURPOSE

We aimed to image and treat primary and metastasized tumors in vivo using microcapsules that release antigen-capturing nanoparticles (AC-NPs) with serum amyloid A1 (SAA1) in three radiation sessions under PD-L1 blockade.

## **METHOD AND MATERIALS**

For session 1, liposome-protamine-hyaluronic acid nanoparticles (LPH-NPs) containing 5% iopamiron and 400  $\mu$ g anti-PD-L1 Ab were mixed with 1 mL 4.0% alginate, 3.0% hyaluronate, and 1  $\mu$ g/mL P-selectin solution and incubated with 0.5 mM FeCl2 with 1  $\mu$ g/mL a4B1 Ab. Microcapsules were injected intravenously (IV) into BALB/c mice with primary LM17 tumors in the left hind leg and lung metastases. After 9 h, primary tumors were exposed to 10 or 20 Gy 60Co  $\gamma$ -rays. For session 2, AC-NPs generated by nanoprecipitation of 4 mg/ml polylactic-co-glycolic acid (PLGA) and 1000 ng/ml SAA1 were mixed with the cocktail described above and sprayed into 0.5 mM FeCl2 and 1  $\mu$ g/mL anti-P-selectin Ab. Microcapsules (1  $\times$  1010) were injected IV. After 9 h, tumors were irradiated as before. For session 3, 4 cGy 60Co whole-body  $\gamma$ -rays were administered at 24 h intervals for 5 d.

## RESULTS

In session 1, anti-a4ß1 microcapsules accumulated around primary and metastatic tumors and were detected by CT. Microcapsules released P-selectin and anti-PD-L1 Ab in response to the initial irradiation. In session 2, microcapsules accumulated around the primary tumor via a P-selectin Ag-Ab reaction. PLGA AC-NPs and SAA1 were released after the second radiation dose. PLGA AC-NPs captured tumor-derived protein antigens released by the second radiation dose and transported them to SAA1-recruited and activated dendritic cells (DCs) that drove cross-priming of CD8+T cells. In session 3, primed antitumor CD8+T cells were activated by whole body radiation. These treatments significantly increased the antitumor effect (EF 1.7) and reduced metastasis by 74.3%.

## CONCLUSION

Our CT-detectable microcapsules exhibited targeted AC-NP-mediated immunotherapeutic and abscopal effects, which could be used to advance tumor diagnoses and treatments.

# **CLINICAL RELEVANCE/APPLICATION**

Targeted AC-NP-mediated immunotherapy with SAA1 directed by radiation enhanced the primary and metastatic antitumor effects of radiotherapy under PD-L1 blockade.

# SSA23-08 Evaluation in Predicting Radiotherapy Efficacy for Esophageal Carcinoma Using Magnetic Resonance Diffusion-Weighted Imaging

Sunday, Nov. 25 11:55AM - 12:05PM Room: E353A

Participants

Andu Zhang, Shijiazhuang, China (*Presenter*) Nothing to Disclose Yanfei Wang, Shijiazhuang, China (*Abstract Co-Author*) Nothing to Disclose Gaofeng Shi, MD, Shijiazhuang, China (*Abstract Co-Author*) Nothing to Disclose Qinglei Shi, Beijing, China (*Abstract Co-Author*) Employee, Siemens AG Chun Han, Shijiazhuang, China (*Abstract Co-Author*) Nothing to Disclose Hui Liu, Shijiazhuang, China (*Abstract Co-Author*) Nothing to Disclose Li Yang, MD, Shijiazhuang, China (*Abstract Co-Author*) Nothing to Disclose Ning Zhang, Shijiazhuang, China (*Abstract Co-Author*) Nothing to Disclose Ruxun Li, Shijiazhuang, China (*Abstract Co-Author*) Nothing to Disclose Tongxin Xu, Shijiazhuang, China (*Abstract Co-Author*) Nothing to Disclose

## For information about this presentation, contact:

zhangandu860520@163.com

#### PURPOSE

To evaluate magnetic resonance diffusion-weighted imaging (MR-DWI) technique in predicting the efficacy of radiotherapy for esophageal cancer

# METHOD AND MATERIALS

Two related tests were performed in this experimental study. Test 1 included 40 Eca-109 nude mice models with esophageal cancer xenogrfts (test group=24; control group=16), and Test 2 included 42 and 42 mice models in test and control groups, respectively. The test group was given a single dose of 15Gy (6MV X-rays) during radiation therapy. In Test 1, sixteen time points included at 1 day before and 1 day after radiotherapy and then very two days during radiotherapy until 29th day. In the time points, all mice models underwent MRI scan with T1WI, T2WI, and DWI. In Test 2, MRI scans were performed at seven time points until 29th day and pathology results were obtained immediately after scans. The tumor volume and ADC value were evaluated in Test 1 and ADC values were compared with pathological cell density and necrosis in Test 2

## RESULTS

Test 1, the growth doubling time was 17 days in test group and 5 days in control group. ADC values in test group rapidly increased at the 3rd day (highest at the 7th day) and then gradually decreased and returned to pre-therapy levels from the 17th day. In control group, the ADC values gradually decreased from the first day and kept at a low level from the 9th day. In Test 2, tumor cell density decreased from the 3rd day in test group compared with a gradual increased (highest at the 5th day) and then decreased in control group. Cell density in test group was lower than that in control group from the 3rd day after radiotherapy (P<0.05). ADC values were negatively correlated with cell density (rs=-0.703, p=0.000). The radio of necrosis of tumor in test group was higher than that in control group after the 3rd day (P<0.05). ADC values were positively correlated with the tumor necrosis (rs=0.658, p=0.003).

## CONCLUSION

MR-DWI values could change earlier than morphological size during radiotherapy for esophageal cancer and ADC values showed good correlations with pathology findings, which has the potential in predicting the efficacy of radiation or other therapy.

#### **CLINICAL RELEVANCE/APPLICATION**

provide theoretical basis for the rational application of this technique in clinical practice

SSA23-09 Pseudoprogression versus Progression: The Role of Diffusion MRI During Immunotherapy for Solid

## Tumor

Sunday, Nov. 25 12:05PM - 12:15PM Room: E353A

Participants Alessandra Coppola, MD, Cava Detirreni, Italy (*Presenter*) Nothing to Disclose Chiara Marigliano, MD, Milano, Italy (*Abstract Co-Author*) Nothing to Disclose Giulia Platania, MD, Gravina Di Catania, Italy (*Abstract Co-Author*) Nothing to Disclose Daniel Volterra, MD, Milan, Italy (*Abstract Co-Author*) Nothing to Disclose Francesca Travaglini, MD, Novara, Italy (*Abstract Co-Author*) Nothing to Disclose Angelo Vanzulli, MD, Segrate, Italy (*Abstract Co-Author*) Travel support, Bracco Group

For information about this presentation, contact:

alessandracoppola@hotmail.it

#### PURPOSE

The aim of our study is to evaluate the role of diffusion-weighted MR sequences in the study of patients undergoing immunotherapy for stage IV solid tumors. The study aims to identify patients with pseudoprogression by calculating ADC and to differentiate them precociously from patients with true progression.

#### **METHOD AND MATERIALS**

Between September 2017 and March 2018 were evaluated with MRI with diffusion-weighted sequences (b value up to 800) 8 patients treated with immunotherapy (4 with renal cell carcinoma, 2 with pulmonary adenocarcinoma and 2 with melanoma). 11 target abdominal lesions were considered, positioning a ROI for the calculation of ADC in MRI performed at the beginning of therapy (RMt0), at the second infusion cycle (RMt1) and concomitantly with the revaluation TC, at approximately 8- 9 weeks (RMt2) after the start of treatment. Patients were staged at t0 and re-staged at t2 with toraco-abdominale and head contrast enhanced CT (TCt1 and TCt2) and were therefore classified as: progression (PD), partial response (PR), stable disease (SD) or pseudoprogression (PP) according to immuno-RECIST criteria.

## RESULTS

Among the 8 patients evaluated, 2 died during immunotherapy (PD). Of the 6 patients on therapy, based on the immuno-RECIST criteria, 1 was considered PD, 1 PR, 3 were SD and 1 was defined in pseudoprogression (PP). The pseudoprogression is represented by a dimensional increase of the target lesion at t2. The ADC values calculated in the three MRI exams performed during immunotherapy are not significantly changed (mean ADC RMt0 0.71  $\pm$  0.14, ADC RMt1 0.91  $\pm$  0.39, ADC RMt2 0.76  $\pm$  0.16).

#### CONCLUSION

Immunotherapy in solid tumors causes a transient increase in intratumoral lymphocyte infiltrate changing cell density in the lesion. The target lesions evaluated after the start of immunotherapy showed changes both in size and ADC value. The main limitation of our study is represented by the small number of patients currently evaluated.

# **CLINICAL RELEVANCE/APPLICATION**

Despite an increase in size of target lesions in solid tumors (pseudo progression) ADC values calculated in MRI during immunotherapy are not significantly changed.



#### SSA24

## Vascular Interventional (Aortic and PAD)

Sunday, Nov. 25 10:45AM - 12:15PM Room: S502AB



AMA PRA Category 1 Credits ™: 1.50 ARRT Category A+ Credit: 1.75

FDA Discussions may include off-label uses.

#### Participants

Gordon McLennan, MD, Chagrin Falls, OH (*Moderator*) Grant, Siemens AG; Grant, Surefire Medical, Inc; Speakers Bureau, Medtronic plc; Speakers Bureau, General Electric Company; Speakers Bureau, Stryker Corporation; Advisory Board, Siemens AG; Advisory Board, Surefire Medical, Inc; Advisory Board, Stealth Medical; Advisory Board, Rene Medical, Inc; Advisory Board, F. Hoffmann-La Roche Ltd; Advisory Board, Bristol-Myers Squibb Company; Advisory Board, B. Braun Melsungen AG; Advisory Board, General Electric Company;

Dimitrios Filippiadis, MD, PhD, Athens, Greece (Moderator) Nothing to Disclose

## Sub-Events

# SSA24-01 Transarterial Computed Tomographic Angiography in Patients with Renal Function Impairment Undergoing Endovascular Aortic Repair

Sunday, Nov. 25 10:45AM - 10:55AM Room: S502AB

Participants

Giovanni F. Torsello, MD, BA, Berlin, Germany (Presenter) Nothing to Disclose

For information about this presentation, contact:

giovanni.f.torsello@gmail.com

## PURPOSE

Endovascular aneursym repair (EVAR) of aortic aneurysms is the treatment of choice in most cases. Computed tomography angiography (CTA) is crucial in the preoperative planning and postoperative surveillance. Renal function impairment secondary to high volumes of contrast media however limits pre- and postoperative assessment especially of complex aortic aneurysms. The aim of this study is to evaluate the safety and diagnostic value of a novel technique in the setting of patients undergoing EVAR.

# METHOD AND MATERIALS

Between January 2011 and August 2016, 145 patients with chronic kidney disease underwent transbrachial placement of an angiography catheter in the ascending aorta for i.a. contrast medium administration in the setting of a CTA. 45 patients with normal kidney function and aortic aneurysms were included in the analysis as a control group. Primary endpoint was the change in serum creatinine. Secondary security endpoints were access site complications and cerebrovascular accidents. Imaging quality endpoints were attenuation levels and contrast-to-noise-ratios in predefined vessels, validated by intraclass correlation coefficients.

#### RESULTS

Mean creatinine change was -.12 mg/dL, mean GFR change was 2.15% in the intervention group. There were two (1.3%) false aneurysms and one access site hematoma (0.7%). Two cerebrovascular accidents (1.3%) were transient. Transarterial CTA attenuation values varied between 228.98 ( $\pm$ 78.66) and 266.21 ( $\pm$ 110.82) Hounsfield units (HU), and 306.35 ( $\pm$ 63.27) to 321.39 ( $\pm$ 70.12) HU in the control group. The mean amount of contrast medium used in the catheter group was significantly reduced (31.70  $\pm$ 5.82 mL) compared to a standard dose of 120 mL in the control group (p = 0.001). Contrast-to-noise ratios varied between 9.1 ( $\pm$ 4.8) and 11.1 ( $\pm$ 4.4) in the different segments. Intraclass correlation coefficients between the readings were very good (0.987-0.992).

## CONCLUSION

This study demonstrates that a catheter-based transarterial computed tomographic angiography is a safe and efficacious way to evaluate patients with aortic aneurysms, both prior to and after endovascular aneurysm repair.

# **CLINICAL RELEVANCE/APPLICATION**

Transarterial CTA is a safe means of assessing complex aortic aneurysms and yields high imaging quality for preoperative assessment and postoperative follow-up in patients with decreased renal function.

# SSA24-02 Morphological Changes Within 365 Days Predict Late Adverse Events in Uncomplicated Type B Aortic Dissections

Sunday, Nov. 25 10:55AM - 11:05AM Room: S502AB

Participants Kai Higashigaito, MD, Stanford, CA (*Abstract Co-Author*) Nothing to Disclose Anna M. Sailer, MD, PhD, West Hollywood, CA (*Presenter*) Nothing to Disclose Martin J. Willemink, MD, PhD, Menlo Park, CA (Abstract Co-Author) Speakers Bureau, Koninklijke Philips NV; Research Grant, Koninklijke Philips NV

Peter Chiu, Palo Alto, CA (Abstract Co-Author) Nothing to Disclose

Michael D. Dake, MD, Stanford, CA (*Abstract Co-Author*) Scientific Advisory Board, W. L. Gore & Associates, Inc; Scientific Advisory Board, Abbott Laboratories; Research Consultant, Cook Group Incorporated; Research Consultant, TriVascular, Inc; Research Consultant, Medtronic plc; Research Consultant, Intact Vascular, Inc; Research Consultant, NOvate Medical Technologies; Research support, Cook Group Incorporated; Research support, Research support, W. L. Gore & Associates, Inc Craig Miller, Stanford, CA (*Abstract Co-Author*) Research collaboration, Edwards Lifesciences Corporation; Research collaboration, Abbott Laboratories; Research collaboration, Medtronic plc

Michael Fischbein, Stanford, CA (Abstract Co-Author) Nothing to Disclose

Dominik Fleischmann, MD, Stanford, CA (Abstract Co-Author) Research Grant, Siemens AG

# For information about this presentation, contact:

kai.higashigaito@usz.ch

#### PURPOSE

Patients with medically treated type B aortic dissection (TBAD) remain at significant risk for late adverse events (AEs). We hypothesize that not only initial morphological features, but also their change over time are associated with late AEs.

## METHOD AND MATERIALS

Baseline and 188 follow-up CT-scans (median and interquartile range: 4 years [2-5]) of 47 patients with acute uncomplicated TBAD were retrospectively reviewed. Morphologic CT imaging features were qualitatively and quantitatively assessed at baseline and each follow-up. Medical records were reviewed for late AEs, defined according to current guidelines. Predictive value of changes of morphological features (aortic diameter, size of intima tear, number of secondary tears, length of dissection, circumferential extent of false lumen and false lumen thrombosis) within 365 days for AEs was assessed using Cox proportional hazard regression with time-dependent covariates. Significant predictors were combined into a prediction model (cut-off p-value for model inclusion p<0.15)

#### RESULTS

21 AEs occurred in 47 patients. Multivariate analyses revealed following predictors for late AEs: maximum major aortic diameter: (HR=1.03[0.99-1.07] per mm increase p=0.06), number of secondary tears: (HR=1.02[0.90-1.15] per tear number increase p=0.80), area false lumen thrombosis: (HR=1.07[1.01-1.14] per mm2 increase p=0.03). The model with significant predictors showed following significant independent predictors: major aortic diameter: (HR=1.03[1.01-1.06] per mm increase p<0.01) and area false lumen thrombosis: (HR=1.07 [1.01-1.14] per mm2 increase p=0.03).

## CONCLUSION

Increase in aortic diameter and false lumen thrombosis area within 365 days after onset are both significantly associated with greater risk of late AEs.

## **CLINICAL RELEVANCE/APPLICATION**

Patients with increase of false lumen diameter and thrombosis within the first year after TBAD may benefit from shorter follow-up intervals and evaluation thereafter.

# SSA24-03 Aneurismal Sac Remodeling After Nellix Endovascular Aneurysm Sealing System (EVAS) in Patients with Abdominal Aortic Aneurysm (AAAs): A Magnetic Resonance Imaging (MRI) Study

Sunday, Nov. 25 11:05AM - 11:15AM Room: S502AB

Participants

Francesco Cilia, Rome, Italy (*Presenter*) Nothing to Disclose Nicola Galea, MD, Rome, Italy (*Abstract Co-Author*) Spouse, Employee, Merck & Co, Inc Simona Coco, Roma, Italy (*Abstract Co-Author*) Nothing to Disclose Iacopo Carbone, MD, Montreal, QC (*Abstract Co-Author*) Nothing to Disclose Marco Francone, MD,PhD, Rome, Italy (*Abstract Co-Author*) Nothing to Disclose Carlo Catalano, MD, Rome, Italy (*Abstract Co-Author*) Nothing to Disclose

For information about this presentation, contact:

nicola.galea@gmail.com

## PURPOSE

The Nellix endovascular aneurysm sealing system (EVAS) is a valid option for the treatment of infrarenal abdominal aortic aneurysm (AAAs) that has distinctive design comprising two balloon-expandable endoframes, each sorrounded by a polymer-filled endobags. This technique was conceived with the intention of reducing risk of endoleak by filling the aneurysmal lumen excluded by endoprosthesis. However the long-term impact of EVAS on sac remodeling and thrombus modification is still unclear. Our aim was to evaluate the modifications in aneurysmal sac in patients treated by EVAS for AAAs in terms of morphology and thrombus characteristics using MRI at one-year follow-up.

## **METHOD AND MATERIALS**

We enrolled 10 patients EVAS candidates for AAAs. All patients underwent MRI before, 1-week and 1-year after EVAS treatment. We determinated AAA morphological features (diameter, proximal neck, lenght, AAA sectional areas, sac volume, endoleak presence and lumen volume) and thrombus characteristics (thrombus volume and maximal thickness, T1 and T2 signal).

## RESULTS

No early or late endoleaks were observed in all patients after EVAS. We observed significant reduction of sac and thrombus volume (mean value:44.5mL Vs 40.9mL and 7.5mL Vs 3.5mL, respectively, p:0.01-0.23). Diameter and thrombus thickness did not change significantly at 1- year follow-up after EVAS (48.5mm vs 47.3mm, 12.4 vs 11.3mm, respectively, p >.05 for both). The MRI signal of thrombus showed a reduction of T1 and T2 values (mean difference: -45% and -30%, respectively, p:0.01-0.03) at the 1-year

## CONCLUSION

Filling the endobags inside the aneurysmal sac leads to the progressive reduction of thrombus volume and lowering of T1/T2 values, probably due to thrombus organization and squeezing of fluid content into collateral vessels. EVAS could be associated to an acceleration of thrombus remodeling after AAAs treatment

# **CLINICAL RELEVANCE/APPLICATION**

The accelerated thrombus remodeling, in addition to the intrinsic advantages offered by Nellix technology, could further reduce the rates of device-related complications, such as endoleak, endograft migration, component separation and sac enlargement. The positive pressure exerted by two endobags anchored to the endoprosthesis probably facilitate thrombus organization and compaction, by confering more stability to the whole system.

# SSA24-04 Remodeling of Aorta After Thoracic Endovascular Aortic Repair for Aortic Dissection

Sunday, Nov. 25 11:15AM - 11:25AM Room: S502AB

Participants

Ken Nakajima, Tsu, Japan (*Presenter*) Nothing to Disclose Noriyuki Kato, Tsu, Japan (*Abstract Co-Author*) Nothing to Disclose Takashi Hashimoto, Tsu, Japan (*Abstract Co-Author*) Nothing to Disclose Takatoshi Higashigawa, MD, Tsu, Japan (*Abstract Co-Author*) Nothing to Disclose Takafumi Ouchi, Tsu, Japan (*Abstract Co-Author*) Nothing to Disclose Shuji Chino, MD, Matsusaka, Japan (*Abstract Co-Author*) Nothing to Disclose Toshiya Tokui, Ise, Japan (*Abstract Co-Author*) Nothing to Disclose Hajime Sakuma, MD, Tsu, Japan (*Abstract Co-Author*) Nothing to Disclose Hajime Sakuma, MD, Tsu, Japan (*Abstract Co-Author*) Research Grant, Fuji Pharma Co, Ltd; Research Grant, DAIICHI SANKYO Group; Research Grant, FUJIFILM Holdings Corporation; Research Grant, Siemens AG; Research Grant, Nihon Medi-Physics Co, Ltd; Speakers Bureau, Bayer AG

## For information about this presentation, contact:

k-nakajima@clin.medic.mie-u.ac.jp

#### PURPOSE

It is well known that favorable remodeling of the aorta after thoracic endovascular aortic repair (TEVAR) does not occur and leads to enlargement of the distal aorta in some patients with aortic dissection (AD). The objective of this study is to determine the most appropriate timing of TEVAR for AD in terms of remodeling of the aorta.

## METHOD AND MATERIALS

Since March 2004 through March 2017, 99 patients with AD underwent TEVAR. Among them, 36 patients who were followed-up with CT over 1 year were included in this study. There were 28 men and 8 women. Mean age was  $66 \pm 9$  years. The diameters of the aorta, the true lumen, and the false lumen were measured at the levels of the most dilated descending aorta (level M) and the diaphragm (level D) on contrast enhanced CT. In addition, the ratio of the diameter measured on CT before TEVAR to that 1 year after TEVAR was calculated in each measurement.

## RESULTS

The cut-off interval of 2.5 months between the onset of AD and TEVAR was determined by means of a receiver operating characteristic curve in terms of existence of shrinkage of the aortic diameter at level D on 1-year follow-up CT (AUC:0.724). According to this interval, patients were divided into two groups: patients who underwent TEVAR within 2.5 months of the onset of AD (n=16, group A) and patients who underwent TEVAR over 2.5 months (n=20, group B). At level M, the diameter of the aorta and the false lumen significantly decreased and that of the true lumen significantly increased in both groups (P<0.01). At level D, the diameter of true lumen significantly increased and that of the false lumen significantly decreased in both groups (P<0.01) although there was no significant difference in the diameter of the aorta. In terms of the diameter ratio, the false lumen shrank more in group A compared to group B at both levels of M (P=0.017, CI:0.044-0.424) and D (P=0.015, CI:0.078-0.667).

## CONCLUSION

To obtain favorable remodeling of the aorta, it seems to be more effective to perform TEVAR within 2.5 months of the onset of AD.

## **CLINICAL RELEVANCE/APPLICATION**

To obtain favorable remodeling of the aorta, it seems to be more effective to perform TEVAR within 2.5 months of the onset of AD.

# SSA24-05 Early Intervention for Penetrating Aortic Ulcer Leads to Improved Outcome and Overall Survival

Sunday, Nov. 25 11:25AM - 11:35AM Room: S502AB

#### Participants

Roger T. Tomihama, MD, Loma Linda, CA (*Presenter*) Nothing to Disclose Joshua Gabel, MD, Loma Linda, CA (*Abstract Co-Author*) Nothing to Disclose Ahmed Abou-Zamzam, MD, Loma Linda, CA (*Abstract Co-Author*) Nothing to Disclose Theodore Teruya, MD, Loma Linda, CA (*Abstract Co-Author*) Nothing to Disclose Udo Oyoyo, Loma Linda, CA (*Abstract Co-Author*) Nothing to Disclose Sharon C. Kiang, MD, Loma Linda, CA (*Abstract Co-Author*) Nothing to Disclose

## PURPOSE

The natural history of penetrating aortic ulcer (PAU) has been variably described and clear guidelines are lacking. We reviewed our experience with penetrating aortic ulcers in a tertiary referral center.

#### **METHOD AND MATERIALS**

Imaging reports from January 2010 - December 2017 were retrospectively searched for the diagnosis of penetrating aortic uicer. Diagnosis was confirmed by review of imaging studies. Patient demographics, presenting symptoms, and anatomic characteristics were collected and analyzed for associations with need for surgical intervention, aortic complication, and overall survival.

## RESULTS

One hundred and six patients with PAU were identified. Locations included: 57 (53.8%) aortic arch, 24 (22.6%) descending thoracic, and 25 (23.5%) abdominal aorta. Dissection was present in 12 (11.4%) and acute rupture in 4 (3.8%) cases. At presentation 57 (53.8%) patients were symptomatic. Forty-six (43.8%) patients were evaluated by endovascular interventionalists. Thirteen (12.3%) underwent endovascular repair and 10 (10.4%) had a change in medical management. Long term follow-up was available in 30 patients for a mean 2.3 ( 2.0) years. Twenty-one (70%; 21/30) demonstrated disease stability or resolution and 9 (30%, 9/30) worsened with 3 undergoing endovascular repair. No PAU ruptured during follow-up. Patient demographics, presenting symptoms, and PAU morphology did not predict disease progression. Referral to a endovascular interventionalist at initial presentation was associated with a 40% decreased likelihood of disease progression (p=0.046) and a 30% survival advantage at LTFU (p=0.037).

## CONCLUSION

PAU disease progression occurs in 30% of patients at long-term follow up of 2.3 ( 2.0) years. All patients identified with PAU on diagnostic imaging should be referred for an evaluation and follow-up, as referral to endovascular interventionalist is associated with improved disease course and overall survival.

#### **CLINICAL RELEVANCE/APPLICATION**

Early intervention for penetrating aortic ulcer leads to improved outcome and overall survival

# SSA24-06 New 3D-Arterial Analysis Software to Evaluate Carotid Atherosclerotic Plaque in Comparison With CEUS, CTA, and Histological Examination

Sunday, Nov. 25 11:35AM - 11:45AM Room: S502AB

#### Participants

Giuseppe Schillizzi, Roma, Italy (*Presenter*) Nothing to Disclose Cantisani Vito, Rome, Italy (*Abstract Co-Author*) Nothing to Disclose Valerio Forte, MD, Rome, Italy (*Abstract Co-Author*) Nothing to Disclose Nicola Di Leo, MD, Rome, Italy (*Abstract Co-Author*) Nothing to Disclose Daniele Fresilli, Roma, Italy (*Abstract Co-Author*) Nothing to Disclose Gregorio Alagna, Rome, Italy (*Abstract Co-Author*) Nothing to Disclose Carlo Catalano, MD, Rome, Italy (*Abstract Co-Author*) Nothing to Disclose Ferdinando D'Ambrosio, Rome, Italy (*Abstract Co-Author*) Nothing to Disclose Valeria de Soccio, JD, Rome, Italy (*Abstract Co-Author*) Nothing to Disclose

#### PURPOSE

To assess the effectiveness of ultrasonographic 3D-Arterial Analysis in characterizing stenosis percentage and vulnerability of carotid plaques as compared with CEUS, CTA and histology results.

## **METHOD AND MATERIALS**

Sixty seven patients were enrolled with the following criteria: (1) asymptomatic stenosis of carotid artery >70% but <100%; or (2) recent transient ischemic attack or ischemic stroke, and ipsilateral carotid stenosis >50%. Eventually all patients underwent endarterectomy and samples were histologically assessed for instability features. 3D-Arterial Analysis provided a colour map to evaluate plaque vulnerability and a 3D volumetric stenosis evaluation. Its diagnostic performance was compared to histological examination for plaque's vulnerability and to CEUS and CTA for stenosis' grading.

#### RESULTS

Histological examination identified 47 vulnerable plaques with at least one of the following criteria: fibrous cap <200 µm, presence of lipid core, intra-plaque haemorrhage, leukocyte recruitment or angiogenesis. 3D-Arterial Analysis software, CEUS and CTA were able to detect 42, 41 and 41 of these 47 vulnerable plaques respectively, with 89%, 87% and 87% sensitivity and 100% specificity. 3D-Arterial Analysis software and CEUS were able to evaluate stenosis percentage with 88% sensitivity and 100% specificity compared to CTA, identifying 59/60 severe stenosis.

## CONCLUSION

3D-Arterial Analysis software and CEUS seem effective tools to assess plaque's vulnerability and stenosis severity, providing useful information for surgery planning.

## **CLINICAL RELEVANCE/APPLICATION**

Multiparametric ultrasound is a safe and effective modality to provide comprehensive information on carotid plaques. Further studies are needed to determine which could be its clinical role.

## SSA24-07 EZ-Access: A Novel 3D Printed Groin Puncture Device

Sunday, Nov. 25 11:45AM - 11:55AM Room: S502AB

Participants Rahmi Oklu, MD,PhD, Phoenix, AZ (*Presenter*) Nothing to Disclose Hassan Albadawi, MD, Phoenix, AZ (*Abstract Co-Author*) Nothing to Disclose

# PURPOSE

Exsanguination is the leading cause of death after vascular trauma. Resuscitative endovascular balloon occlusion of the aorta (REBOA) can control torso hemorrhage. However, adoption of this approach specifically by the military has been limited by challenges in achieving femoral artery access in austere combat environments. To address this need, we developed a novel 3D printed minimally invasive device, termed EZ-Access, to enable successful vascular access without the need for ultrasound

guidance or specialized training for use in the field by first responders.

### **METHOD AND MATERIALS**

EZ-Access was modeled using SolidWorks and 3D printed with a methacrylated resin using FormLabs2 printer. The device measured 14x2x1cm with two concave thumb rests on either side of a central plate containing 6 equidistant holes spaced at 0.8cm. The holes were fitted with a variable number of 21-gauge 7cm percutaneous entry needles followed by extensive testing. Multiple trials involved IR staff, residents, college and high school students to test success of accurate access of femoral artery using SimuLab models (Seattle, WA). Trial 1 consisted of 3 needles in alternating holes (n=40). Trial 2 used 6 sequentially placed needles (n=42). The needles within the device were inserted without ultrasound (US) guidance, two fingerbreadths lateral to the pubic symphysis. The device was angled along the groin crease and the needles entered the skin at a 45 degrees. After each puncture, US was used to confirm vessel entry. A control trial was also performed using standard single-entry access needle (n=5) by staff IR. Statistical analysis performed using Prism software (P=0.05).

# RESULTS

The control trial demonstrated vessel entry rate of 20%. Using 3 alternating needles, successful vessel entry increased to 40% (p=0.396). With 6 sequential needles, vessel entry success significantly increased to 100% (p<0.001) regardless of operator experience.

### CONCLUSION

EZ-Access has demonstrated overwhelming success in obtaining consistent percutaneous vascular access in a simulated clinical scenario independent of the operator's experience without the need for imaging guidance. The device has promising applications in pre-hospital resuscitation.

### **CLINICAL RELEVANCE/APPLICATION**

Access into arterial system can be challenging especially in austere environments; EZ-Access may lead to a higher use of REBOA and improve outcomes.

# SSA24-08 Effect of Rosuvastatin and Aspirin Therapy for Abdominal Aortic Atherosclerotic Plaque in Rabbits: A Magnetic Resonance Imaging Study

Sunday, Nov. 25 11:55AM - 12:05PM Room: S502AB

Participants

Mingmei Li, MMed, Shenzhen, China (*Presenter*) Nothing to Disclose Juan Huang, MMed, Beijing, China (*Abstract Co-Author*) Nothing to Disclose Rong Huang, MD, Shenzhen, China (*Abstract Co-Author*) Nothing to Disclose Guanxun Cheng, MD, PhD, Shenzhen, China (*Abstract Co-Author*) Nothing to Disclose Yan Song, MD, Beijing, China (*Abstract Co-Author*) Nothing to Disclose

### For information about this presentation, contact:

Immbetter@163.com

# PURPOSE

To evaluate the therapeutic effect of rosuvastatin, aspirin and two-drug combination on atherosclerotic plaque by conventional magnetic resonance imaging, explore its inhibition of inflammatory cells.

# METHOD AND MATERIALS

160 New Zealand rabbits were given endothelial denudation combined with a cholesterol-enriched diet to induce abdominal aortic atherosclerosis. all rabbits were assigned randomly to control group (high fat diet), group A (high fat diet with aspirin), group T(high fat diet with rosuvastatin) and group AT(high fat diet with aspirin as well as rosuvastatin), 40 for each group. Four groups of animals were divided randomly into 1 week, 2 weeks 1month and 2 months subgroup. All rabbits underwent MR scan. Specimens of abdominal aorta were obtained within 24 hours after MR scan, afterwards HE stain and macrophages RAM - 11 ICH staining was performed. Using software CASCADE quantitatively analyse abdominal aorta MRI, to acquire the wall standardized(NWI). Using the software Image-Pro Plus quantitatively analyse the RAM-11 ICH Image. Through compare NWI of group A, T, AT with control group at different time, study the changes of NWI, the number of plaque macrophages after drug treatment.

#### RESULTS

1) At four time points, the NWI of A, T and AT group is lower than the control group. At 1 week,1 month,2 month, the difference was statistically significant (P < 0.05). At 2 weeks, there was no significant difference (P > 0.05). 2) At four time points, the arterial intima gradually thickened in the control group over time.1month and 2 months, rendering the appearance of foam cell aggregation, lipid drops calm, disordered arrangement of collagen fiber hyperplasia. At each time point, the degree of arterial intimal thickening in group A,T,AT was less than that in the control group, and the accumulation of foam cells and deposition of lipid droplets were decreased compared with the control group.3)At 2 months, the macrophage of plaque with group A,T,AT were all decreased compared with the control group.

#### CONCLUSION

1) Rosuvastatin, aspirin and two drug combination can restrain plaque load, reduce inflammatory response. MR can response the inhibition, thus MR can be used in the evaluation of drug therapy. 2)Rosuvastatin combined aspirin can better reduce plaque load, reduce the number of macrophages.

#### **CLINICAL RELEVANCE/APPLICATION**

Black blood MR technology can be used to evaluate the effect of drugs on plaque treatment.

# SSA24-09 18F-FDG Uptake as a Predictive Factor for Late Aortic Enlargement in Subacute Aortic Dissection

Sunday, Nov. 25 12:05PM - 12:15PM Room: S502AB

Participants Takatoshi Higashigawa, MD, Tsu, Japan (*Presenter*) Nothing to Disclose Noriyuki Kato, Tsu, Japan (*Abstract Co-Author*) Nothing to Disclose Yasutaka Ichikawa, MD, Tsu, Japan (*Abstract Co-Author*) Nothing to Disclose Takashi Hashimoto, Tsu, Japan (*Abstract Co-Author*) Nothing to Disclose Ken Nakajima, Tsu, Japan (*Abstract Co-Author*) Nothing to Disclose Takafumi Ouchi, Tsu, Japan (*Abstract Co-Author*) Nothing to Disclose Shuji Chino, MD, Matsusaka, Japan (*Abstract Co-Author*) Nothing to Disclose Masahiro Inagaki, Ise, Japan (*Abstract Co-Author*) Nothing to Disclose Koji Hirano, Ise, Japan (*Abstract Co-Author*) Nothing to Disclose Toshiya Tokui, Ise, Japan (*Abstract Co-Author*) Nothing to Disclose Hajime Sakuma, MD, Tsu, Japan (*Abstract Co-Author*) Nothing to Disclose Group; Research Grant, FUJIFILM Holdings Corporation; Research Grant, Siemens AG; Research Grant, Nihon Medi-Physics Co, Ltd; Speakers Bureau, Bayer AG

#### PURPOSE

Purpose: Although previous study demonstrated that greater uptake of 18F fluoro-2-deoxy-D-glucose (FDG) in the dissected aortic wall was significantly associated with an increased risk for adverse aortic events in acute aortic dissection (AD), clinical assessment in subacute aortic dissection remains unexplored. This study was aimed to clarify the relationship of 18F-FDG uptake and late aortic enlargement in medically treated patients with subacute AD.

### METHOD AND MATERIALS

Materials and Methods: A total of 16 medically treated patients with subacute AD (age: 69±9, 2 Stanford type and 14 type B) were prospectively enrolled in this study. PET/CT images were acquired 60 minutes after 18F-FDG injection in all patients. All patients underwent 18F-FDG PET/CT between 2 weeks and 4 months from the onset of aortic dissection. In all examinations, 10-mm circular regions of interest were drawn at the site of the dissected aortic wall with maximal focal 18F-FDG uptake. Areas with maximal focal 18F-FDG uptake were visually detected and the maximal standardized uptake value (SUV) was measured. The maximal SUV was divided by the blood-pool SUV, yielding a target-to-background ratio (TBR) for dissected aortic segment.

#### RESULTS

Results: During a median follow up of 21 (range 12-28) months, surgical repair was required in 4 patients due to aortic enlargement. In these patients, aortic diameter enlarged by more than 10mm compared to that of the onset. There was significant difference in TBR between patients undergoing surgical repair and the other patients (p=0.012). With TBR of 1.8 as cutoff level for the predictor of aortic enlargement, the sensitivity, specificity, and positive and negative predictive value, accuracy, and odds ratio were 75%, 75%, 50%, 90%, 75%, and 9.0, respectively.

#### CONCLUSION

Conclusion: Greater uptake of 18F-FDG in subacute AD was significantly associated with an increased risk for aortic enlargement. 18F-FDG PET/CT may be useful for predicting the unfavorable aortic enlargement in medically treated patients with subacute AD.

#### **CLINICAL RELEVANCE/APPLICATION**

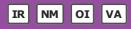
(dealing with 18F-FDG PET/CT) 'Greater uptake of 18F-FDG in subacute aortic dissection was significantly associated with an increased risk for aortic enlargement.'



#### SSA25

# Vascular Interventional (Chemo-Embolization and Radio-Embolization)

Sunday, Nov. 25 10:45AM - 12:15PM Room: S503AB



AMA PRA Category 1 Credits ™: 1.50 ARRT Category A+ Credit: 1.75

#### Participants

Kevin Kim, BA, Arcadia, CA (Moderator)

#### Sub-Events

# SSA25-01 Nomogram and Artificial Neural Network for Prognostic Performance on the Albumin-Bilirubin Grade for HCC Undergoing TACE

Sunday, Nov. 25 10:45AM - 10:55AM Room: S503AB

#### Awards

#### **Trainee Research Prize - Medical Student**

Participants

Binyan Zhong, MD, PhD, Nanjing, China (*Presenter*) Nothing to Disclose Caifang Ni, MD, PhD, Suzhou, China (*Abstract Co-Author*) Nothing to Disclose JianSong Ji, MD, Hangzhou, China (*Abstract Co-Author*) Nothing to Disclose Guowen Yin, MD, Nanjing, China (*Abstract Co-Author*) Nothing to Disclose Gao-Jun Teng, MD, Nanjing, China (*Abstract Co-Author*) Nothing to Disclose

# For information about this presentation, contact:

byzhongir@sina.com

### PURPOSE

The albumin-bilirubin (ALBI) grade is a newly raised objective liver function assessment tool as well as an emerging alternative of the Child-Turcotte-Pugh (CTP) grade in hepatocellular carcinoma (HCC). We aimed to construct ALBI and CTP grades based nomograms as well as develop an artificial neural network (ANN) to compare the prognostic performance of these two grades.

# METHOD AND MATERIALS

This multicentric retrospective study included all patients with HCC who underwent TACE monotherapy as initial treatment between January 2008 and December 2016 at four institutions. In the training cohort, independent risk factors associated with overall survival (OS) were identified by univariate and multivariate Cox proportional hazards analyses. The prognostic nomograms and ANN were then established in the training cohort and validated in the two validation cohorts.

#### RESULTS

Totally, 838 patients (548, 115, and 175 in the training cohort and validation cohorts 1 and 2, respectively) were included. The median OS was 10.4, 15.7, and 9.2 months in the training cohort and validation cohorts 1 and 2, respectively. In the training cohort, independent risk factors were identified as: higher Eastern Cooperative Oncology Group (ECOG) grade, portal vein tumor thrombosis (PVTT), extrahepatic spread (exclude PVTT), higher ALBI/CTP grade, a-fetoprotein level greater than 200 ng/mL, multiple tumors, and tumor size larger than 5 cm. The ALBI and CTP grades based nomograms were then established separately, and showed comparable prognostic performance when assessed externally in two independent validation cohorts (C-index in validation cohort 1: 0.823 vs. 0.802, P =0.417; in validation cohort 2: 0.716 vs. 0.729, P =0.793). ANN showed that ALBI grade had higher importance on survival prediction than CTP grade.

### CONCLUSION

The ALBI grade outperforms the CTP grade on survival prediction for HCC patients who undergo TACE. Considering the easy application, the ALBI grade should be regarded as an alternative to CTP grade.

# **CLINICAL RELEVANCE/APPLICATION**

The ALBI grade should be regarded as an alternative to CTP grade about prognostic prediction for HCC underwent TACE.

# SSA25-02 Predicting Patient Survival After TACE for HCC Using a Neural Network: A Promising Tool

#### Sunday, Nov. 25 10:55AM - 11:05AM Room: S503AB

Participants

Roman Kloeckner, MD, Mainz, Germany (*Presenter*) Advisory Board, Guerbet SA; Advisory Board, Bristol-Myers Squibb Company; Advisory Board, Sirtex Medical Ltd; Speaker, Guerbet SA; Speaker, Sirtex Medical Ltd Aline Maehringer-Kunz, MD, Mainz, Germany (*Abstract Co-Author*) Nothing to Disclose Christoph Dueber, MD, Mainz, Germany (*Abstract Co-Author*) Nothing to Disclose Franziska Wagner, Mainz, Germany (*Abstract Co-Author*) Nothing to Disclose Arndt Weinmann, Mainz, Germany (*Abstract Co-Author*) Nothing to Disclose Sandra Koch, Mainz, Germany (*Abstract Co-Author*) Nothing to Disclose Bettina Baessler, MD, Cologne, Germany (*Abstract Co-Author*) Nothing to Disclose Daniel Pinto dos Santos, MD, Cologne, Germany (*Abstract Co-Author*) Nothing to Disclose

# For information about this presentation, contact:

Roman.Kloeckner@gmail.com

#### PURPOSE

Transarterial chemoembolization (TACE) is the standard of care for intermediate stage hepatocellular carcinoma (HCC). Nevertheless, even for experienced investigators it can be challenging to decide when to repeat and when to stop TACE-treatment. To objectify treatment decisions, several scoring systems have been developed, e.g. ART, ABCR, and SNACOR. However, the predictive ability was only poor-moderate in several attempts of external validation. Therefore, our aim was to develop a survival prediction model for patients with intermediate stage HCC undergoing TACE using novel machine learning algorithms.

#### **METHOD AND MATERIALS**

For this retrospective analysis, we included 792 patients who underwent TACE for HCC at our tertiary referral centre between 01/2005-01/2017. Clinical parameters were acquired from the institutions clinical registry and laboratory system. Radiological response was evaluated in consensus by two board certified radiologists experienced in HCC imaging. Consecutively, we built an artificial neural network, which included all parameters used by the aforementioned clinical risk scoring systems (i.e. ART-, ABCR-, and SNACOR-score): baseline BCLC stage, alpha-fetoprotein level, tumour size and number, as well as change of Child-Pugh stage, AST, and radiological response after the first TACE.

#### RESULTS

With ten-fold cross validation, the neural network showed a promising performance at predicting one-year survival with an area under the ROC curve of 0.69 and a positive predictive value of 78.6%. This outperforms other established risk stratification scores such as ART, ABCR, and SNACOR.

#### CONCLUSION

Neural networks could prove superior in predicting patient survival after TACE for HCC compared to other commonly used scoring systems. Inclusion of additional parameters in the prediction model is likely to further increase its performance.

### **CLINICAL RELEVANCE/APPLICATION**

Once established, such novel prediction models could easily be deployed in clinical routine and help in determining optimal patient care.

# SSA25-03 Experimental Study on Transarterial Administration of Bevacizumab Combined with Transarterial Chemoembolization in Rats with Hepatocellular Carcinoma

Sunday, Nov. 25 11:05AM - 11:15AM Room: S503AB

Participants

Jun Qian, Wuhan, China (*Abstract Co-Author*) Nothing to Disclose Kun Qian, Wuhan, China (*Presenter*) Nothing to Disclose Ping Han, MD, Wuhan, China (*Abstract Co-Author*) Nothing to Disclose Chuansheng Zheng, Wuhan, China (*Abstract Co-Author*) Nothing to Disclose Thomas J. Vogl, MD, PhD, Frankfurt, Germany (*Abstract Co-Author*) Nothing to Disclose Elsie Oppermann, Frankfurt, Germany (*Abstract Co-Author*) Nothing to Disclose Qi Wang, Wuhan, China (*Abstract Co-Author*) Nothing to Disclose

#### For information about this presentation, contact:

qianjun\_whuh@aliyun.com

#### PURPOSE

To evaluate the effects of transarterial administration of Bevacizumab (Avastin), an inhibitor of vascular endothelial growth factor (VEGF), combined with transarterial chemoembolization (TACE) to treat hepatocellular carcinoma in rats.

#### **METHOD AND MATERIALS**

Subcapsular implantation of a solid Morris hepatoma 3924A (2 mm3) in the liver was carried out in 20 male ACI rats. Animal subjects were assigned to group based on which treatment-drugs were injected into the hepatic artery: group A: TACE (mitomycin C + lipiodol + degradable starch microspheres) + bevacizumab; group B: TACE alone. Tumor volumes of the post-treatment (V2) and pre-treatment tumor (V1) were assessed by magnetic resonance imaging (MRI) and the mean ratio (V2/V1) was calculated. Immunohistochemical expression of MMP-9 and VEGF in the tumor was semi-quantified in all rats.

# RESULTS

The rate of tumor implantation reached 100 % in all the rats receiving tumor implantation with Morris hepatoma 3924A. None of the animals died during implantation or interventional therapy. A total of 20 individual HCC tumors were observed with unenhanced MR imaging in the livers of 20 rats (100%) before treatment. After different interventional treatments, intrahepatic metastases developed in one of the 10 rats in group B. The mean value of the volume ratios [V2 (postreatment /V1 (pretreatment] were 1.6649  $\pm$  0.1255 in group A, and 3.0061  $\pm$  0.1910 in group B, respectively. Significant differences of mean volume ratio (V2/V1) were observed between the two groups using an unpaired t test (P<0.0001) (Fig.1) (Fig.2). The angiogenesis of tumor was evaluated using anti-VEGF antibodies, and the metastasis of tumor was assessed using anti-MMP-9 antibody. MMP-9 and VEGF were expressed in all specimens. The immunoexpression of these proteins was confirmed by the presence of red cytoplasmic staining in tumor cells. Higher expressions of MMP-9 (4.9  $\pm$  0.199) and VEGF (4.2  $\pm$  0.79) in hepatocellular carcinoma were observed in the group B (TACE alone) than the MMP-9 (1.9  $\pm$  0.733) and VEGF (2.9  $\pm$  0.678) in group A (TACE + Bevacizumab). Statistical significance was calculated using Wilcoxon signed ranked test (both P<0.0020) (Tab.1) (Fig3).

### CONCLUSION

Transarterial administration of bevacizumab combined with TACE noticeably inhibit the growth of hepatic carcinoma and intrahepatic metastases in rats.

# **CLINICAL RELEVANCE/APPLICATION**

# N/A

# SSA25-04 Tc-99m-MAA Lung Shunt Fraction Studies Prior to Y-90 Radioembolization Have Limited Utility in Non-Hepatocellular Carcinoma Malignancies

Sunday, Nov. 25 11:15AM - 11:25AM Room: S503AB

Participants

Mohammad Elsayed, MD, Atlanta, GA (*Presenter*) Nothing to Disclose Jonathan Martin, MD, Atlanta, GA (*Abstract Co-Author*) Nothing to Disclose Alexander Dabrowiecki, MD, Tucker, GA (*Abstract Co-Author*) Nothing to Disclose Daryl T. Goldman, MD, New Orleans, LA (*Abstract Co-Author*) Nothing to Disclose Razan Faraj, MS, Atlanta, GA (*Abstract Co-Author*) Nothing to Disclose James T. Mcmahon, BS, Atlanta, GA (*Abstract Co-Author*) Nothing to Disclose Richard Duszak JR, MD, Atlanta, GA (*Abstract Co-Author*) Nothing to Disclose Michal Horny, PhD, Atlanta, GA (*Abstract Co-Author*) Nothing to Disclose Janice M. Newsome, MD, Alexandria, VA (*Abstract Co-Author*) Nothing to Disclose Zachary Bercu, MD, Atlanta, GA (*Abstract Co-Author*) Speaker, Terumo Medical Corporation; Grant, Coulter Translational Program, Steerable Robotic Guidewire

#### For information about this presentation, contact:

mohammad.elsayed@emory.edu

# PURPOSE

Lung shunt fraction (LSF) studies using Technetium-99m macro aggregated albumin (Tc-99m-MAA) are routinely performed prior to Yttrium-90 (Y90) radioembolization in all eligible patients regardless of underlying malignancy. This study evaluates the utility of performing Tc-99m-MAA lung shunt fraction studies in patients with hepatocellular carcinoma (HCC) compared to those with non-HCC liver tumors.

# METHOD AND MATERIALS

A multi-hospital retrospective analysis of all pre-Y90 Tc-99m-MAA LSF studies between November 2012 to March 2018 was performed. Patient records were evaluated for age, gender, LSF, and underlying malignancy. Tc-99m-MAA studies were evaluated for mean LSF and were compared between HCC and non-HCC cases (p=.05).

#### RESULTS

A total of 734 Tc-99m-MAA studies were identified among 653 patients. Among these cases 368 (50.1%) involved HCC, 112 (15.3%) colorectal cancer metastatic to liver, 89 (12.1%) neuroendocrine tumor metastatic to liver, 59 (8.0%) cholangiocarcinoma, 27 (3.7%) breast cancer metastatic to liver, and the remaining 79 cases (10.7%) involved other primary malignancies metastatic to liver. The mean LSF of non-HCC cases, 7.4%, was significantly lower than the mean LSF of HCC cases, 11.7% (p=0.0001). There was only one non-HCC case in which a Y-90 radioembolization was not pursued due to high LSF (69.3%), a case of metastatic GIST to liver, in which large scale shunting through the 8 cm mass was grossly apparent on the angiogram. This is compared to at least 37 HCC cases (mean LSF 35.1%) in which LSF was too high to pursue radioembolization.

#### CONCLUSION

Tc-99m-MAA LSF is low among patients with liver malignancies that are not HCC. This study indicates that pre-Y90 Tc-99m-MAA studies have limited utility in non-HCC liver malignancies.

#### **CLINICAL RELEVANCE/APPLICATION**

Patients with non-HCC liver malignancies may only require a consolidated single procedure selective Y-90 radioembolization without prior Tc-99m-MAA nuclear medicine scan.

# SSA25-05 Post-Radioembolization Lung Shunt Fraction Assessment of Yttrium-90 Microspheres with Digital Photon Counting PET/CT: Intra-Individual Comparison with Conventional Photomultiplier Tube-Based PET/CT

Sunday, Nov. 25 11:25AM - 11:35AM Room: S503AB

Participants

Chadwick L. Wright, MD, PhD, Lewis Center, OH (*Presenter*) Nothing to Disclose Katherine Binzel, PhD, Columbus, OH (*Abstract Co-Author*) Nothing to Disclose Evan J. Wuthrick, MD, Columbus, OH (*Abstract Co-Author*) Nothing to Disclose Eric D. Miller, MD, PhD, Columbus, OH (*Abstract Co-Author*) Nothing to Disclose Piotr J. Maniawski, MSc, Cleveland, OH (*Abstract Co-Author*) Employee, Koninklijke Philips NV Michael V. Knopp, MD, PhD, Columbus, OH (*Abstract Co-Author*) Nothing to Disclose Jun Zhang, PhD, Columbus, OH (*Abstract Co-Author*) Nothing to Disclose

# PURPOSE

The purpose of this study is to assess the clinical feasibility and estimate 90Y microsphere lung shunt fraction (LSF) following radioembolization using both digital photon counting PET detector (dPET) and conventional photomultiplier tube-based PET detector (cPET) technologies and compare to pre-radioembolization 99mTc macro-aggregated albumin (MAA) LSF.

#### **METHOD AND MATERIALS**

In a Phase I intra-individual comparison trial, pre-radioembolization 99mTc MAA was performed in 8 patients who were then treated with 90Y glass microspheres for hepatic malignancies/metastases. Investigational 90Y dPET/CT (Vereos, Philips) and cPET/CT (Gemini, Philips) imaging of the lungs and liver was performed in each patient (4 - 50 hrs following radioembolization). Intra-individual comparison of PET image quality and volumetric assessment of intrahepatic radioactivity was performed by a blinded reader panel. 99mTc MAA LSF was routinely calculated using planar scintigraphy. PET estimation of 90Y LSF was performed using MIMVista (MIM Software).

# RESULTS

All patients had evaluable MAA and 90Y PET images for qualitative assessment of radioactivity distribution. Qualitatively, dPET enabled more precise localization of 90Y radioactivity when compared with cPET. Quantitatively, 90Y-treated liver volumes were consistently smaller with dPET than cPET (660 +/-429 mL for dPET and 944 +/- 595 mL for cPET). There were no instances of significant 90Y microspheres shunting outside of the liver or in the lungs. PET estimation of 90Y LSF was consistently and significantly less (dPET was 0.1 +/- 0.2 % and cPET was 0.2 +/- 0.3 %) than MAA LSF (7 +/- 5 %, P < 0.001).

# CONCLUSION

There remains an unmet clinical need to improve the quantification of 90Y biodistribution following radioembolization. These results demonstrate the feasibility of 90Y LSF assessment using new dPET and cPET approaches that may identify patients with smaller or larger than anticipated LSFs.

### **CLINICAL RELEVANCE/APPLICATION**

Digital PET technologies may enable new quantitative methodologies for 90Y-dosimetry and improve our understanding of vascular shunting in various liver malignancies/metastases.

# SSA25-06 Hepatocellular Carcinoma Prognostication Survival Based on Scoring System Developed and Validated on Combined Milieu Intérieur and Milieu Extérieur

Sunday, Nov. 25 11:35AM - 11:45AM Room: S503AB

Participants

Rehan Ali, MBBS, Forest Park, IL (*Presenter*) Nothing to Disclose Ahsun Riaz, MD, Chicago, IL (*Abstract Co-Author*) Nothing to Disclose Ahmed Gabr, MD, MBBCh, Chicago, IL (*Abstract Co-Author*) Nothing to Disclose Ronald A. Mora, MD, Chicago, IL (*Abstract Co-Author*) Nothing to Disclose Samdeep Mouli, MD, Chicago, IL (*Abstract Co-Author*) Nothing to Disclose Robert J. Lewandowski, MD, Chicago, IL (*Abstract Co-Author*) Nothing to Disclose Robert J. Lewandowski, MD, Chicago, IL (*Abstract Co-Author*) Consultant, BTG International Ltd; Advisory Board, Boston Scientific Corporation; Consultant, Cook Group Incorporated; Advisory Board, ABK Biomedical Inc; Advisory Board, Accurate Medical; Consultant, C. R. Bard, Inc;

Riad Salem, MD, MBA, Chicago, IL (*Abstract Co-Author*) Research Consultant, BTG International Ltd; Research Grant, BTG International Ltd; Consultant, Eisai Co, Ltd; Consultant, Exelixis, Inc; Consultant, Bristol-Myers Squibb Company; Consultant, Dove; ;

# PURPOSE

To explore role of routine laboratory parameters in prediction of overall survival (OS) for hepatocellular carcinoma (HCC) treated with transartrerial radioembolization (TARE) and develop/validate a prognostic scoring system.

# METHOD AND MATERIALS

With IRB approval, we selected all HCC patients who received TARE and had alpha-fetoprotein (AFP)>100 ng/dl at baseline. Routine labs [neutrophil-lymphocyte (N/L) (inflammatory-immune response), albumin-bilirubin (ALBI) grade (liver function), and AFP (tumor marker)] were measured at baseline and at 1, 3 and 6 month post-TARE Landmarks. Univariate/multivariate analyses were performed to evaluate OS predictability of these parameters. Scoring systems were developed based on baseline imaging (including PVT, metastases, ascites, portal hypertension); baseline labs and labs at respective landmark (including ALBI and AFP). Cohort was divided randomly into two groups: Predicting Group and Validating Group. This scoring was investigated and validated in the predictability of HCC. Using this score, time-dependent receiver operating characteristics (ROC) were evaluated with survival outcomes at each landmark.

# RESULTS

345/401, 238/401, and 167/401 patients had laboratory parameters available at the 1, 3, and 6 month Landmarks, respectively. ALBI score and AFP response were significant OS prognosticators at all Landmarks. Laboratory Score [ALBI+(0.3xLnAFP)] was developed to predict OS from these Landmarks in the Predicting Group and was internally validated. For developing and validating groups; at 1-month landmark, 1-year survival was 69% and 71%, at 3-month landmark (p<0.001), 1-year survival was 72% and 66%, at 6-month landmark (p<0.001), 1-year survival was 78% and 82% respectively (p<0.001). Area under ROCs were correlative with significant survival prognostication.

# CONCLUSION

Post-therapeutic AFP response and ALBI scores are easily calculable values from routinely performed blood tests. Our proposed Laboratory Score combines post-therapeutic ALBI score with AFP response and is independent of imaging findings. Following TARE, changes in labs can predict survival earlier even in absence of apparent imaging response.

### **CLINICAL RELEVANCE/APPLICATION**

For HCC survival, imaging response is standard but it may take time. As per our study, laboratory values can also surrogate the HCC survival with earlier results and outcomes.

# SSA25-07 Prospective Randomized FAST I Trial: Evaluation of Tumor Response of Colorectal Liver Metastases after Transarterial Chemoembolization with Two Different Protocols Using MRI

Sunday, Nov. 25 11:45AM - 11:55AM Room: S503AB

# Participants

Thomas J. Vogl, MD, PhD, Frankfurt, Germany (*Presenter*) Nothing to Disclose Christian Marko, Frankfurt, Germany (*Abstract Co-Author*) Nothing to Disclose Marcel C. Langenbach, MD, Frankfurt, Germany (*Abstract Co-Author*) Nothing to Disclose Marc Harth, MD, Frankfurt am Main, Germany (*Abstract Co-Author*) Nothing to Disclose Nour-Eldin A. Nour-Eldin, MD,PhD, Frankfurt Am Main, Germany (*Abstract Co-Author*) Nothing to Disclose Renate M. Hammerstingl, MD, Frankfurt Am Main, Germany (*Abstract Co-Author*) Nothing to Disclose Tatjana Gruber-Rouh, Frankfurt Am Main, Germany (*Abstract Co-Author*) Nothing to Disclose

#### For information about this presentation, contact:

T.Vogl@em.uni-frankfurt.de

#### PURPOSE

To prospectively evaluate therapy response of third-line transarterial chemoembolization (TACE) for colorectal liver metastases with either degradable starch microspheres (DSM) or Lipiodol (cTACE) using regular and diffusion MRI.

#### **METHOD AND MATERIALS**

In total, 50 patients (35 males, 15 females, mean 62 years, range 40-79) underwent TACE. They were randomly assigned into two groups: group A receiving DSM and group B receiving Lipiodol as embolization agents. Chemotherapy consisted of a combination of Cisplatin, Irinotecan, Mitomycin. Therapy response was evaluated using MRI with diffusion imaging and unenhanced MRI sequences, which were performed before each of the three TACE cycles to obtain tumor volume and apparent diffusion coefficient (ADC). In addition, contrast-enhanced MRI sequences were performed before the first and after the last TACE cycle. Local tumor response was evaluated using the RECIST criteria and survival data were analyzed using the Kaplan-Meier estimator.

### RESULTS

Evaluation using the RECIST 1.1 criteria showed partial response (PR) in 33% of cases, stable disease (SD) in 13% of cases, and progressive disease (PD) in 53% of cases in the cTACE group while the DSM group showed 23% cases of PR, 59% cases of SD, and 18% cases of PD. Over the course of the therapy, the DSM group showed a statistically significant reduction in the average tumor volume (p=0.006). A statistically significant difference in tumor response was not found between the cTACE and DSM groups (p=0.37). Maximum ADC values after the last MRI session correlated significantly with therapy response (p=0.005), pre-treatment ADC values, however, did not (p=0.34). Median survival in the cTACE group was 13 months and 16 months in the DSM group.

#### CONCLUSION

A statistically significant reduction in tumor volume was found in the DSM group. No significant difference in tumor response was found comparing the Lipiodol and DSM group. Maximum ADC values may be used to assess therapy response after completion of one or more TACE cycles.

# **CLINICAL RELEVANCE/APPLICATION**

Both the Lipiodol and DSM group show similar results with greater tumor volume reduction for the DSM group.

# SSA25-08 Liver Transplantation Following Yttrium-90 Radioembolization: A Comprehensive Report of Short and Long-Term Outcomes of a 170-Patient Cohort

Sunday, Nov. 25 11:55AM - 12:05PM Room: S503AB

Participants

Ahmed Gabr, MD, MBBCh, Chicago, IL (*Presenter*) Nothing to Disclose
Rehan Ali, MBBS, Forest Park, IL (*Abstract Co-Author*) Nothing to Disclose
Ronald A. Mora, MD, Chicago, IL (*Abstract Co-Author*) Nothing to Disclose
Ali Al Asadi, BS, Chicago, IL (*Abstract Co-Author*) Nothing to Disclose
Karen Grace, RN, Chicago, IL (*Abstract Co-Author*) Nothing to Disclose
Nadine Abouchaleh, BA, Chicago, IL (*Abstract Co-Author*) Nothing to Disclose
Samdeep Mouli, MD, Chicago, IL (*Abstract Co-Author*) Nothing to Disclose
Samdeep Mouli, MD, Chicago, IL (*Abstract Co-Author*) Nothing to Disclose
Samdeep Mouli, MD, Chicago, IL (*Abstract Co-Author*) Nothing to Disclose
Robert J. Lewandowski, MD, Chicago, IL (*Abstract Co-Author*) Consultant, BTG International Ltd; Advisory Board, Boston Scientific
Consultant, C. R. Bard, Inc;
Riad Salem, MD, MBA, Chicago, IL (*Abstract Co-Author*) Research Consultant, BTG International Ltd; Research Grant, BTG
International Ltd; Consultant, Eisai Co, Ltd; Consultant, Exelixis, Inc; Consultant, Bristol-Myers Squibb Company; Consultant, Dove;

;

#### For information about this presentation, contact:

ahmed.gabr@northwestern.edu

#### PURPOSE

To report short and long-term outcomes of liver transplantation (LT) for hepatocellular carcinoma (HCC) patients bridged or downstaged by Y90 radioembolization

#### **METHOD AND MATERIALS**

Between 2004 and 2017, 170 HCC patients underwent LT after receiving Y90. Patients were staged using the United Network of Organ Sharing (UNOS) staging system at the times of their Y90 and LT. Early post-operative outcomes were recorded. Recurrence-free survival (RFS) and overall survival (OS) were calculated using Kaplan Meier Method.

#### RESULTS

170 patients underwent LT after Y90, with a median time to LT of 7.4 months (IQR: 4.4-10.3). Only 1 patient grade 3 albumin (<3 gm/dl) toxicities and 9 patetients had grade 3 bilirubin toxicities could be attributed to Y90.138 patients were successfully bridged to LT (maintained within Milan criteria) while 11 patients were down-staged to Milan criteria. 12 (7%) developed post-operative complications. Three-month mortality rate after LT was 6/170 (3.5%). 75 (44%), 49 (29%) and 46 (27%) patients showed complete, extensive and partial tumor necrosis on explants pathologic assessment. Three, five and ten-year OS rates were 86%, 80%, and 56% respectively. 20 patients developed recurrence, with 3, 5 and 10-year RFS rates of 79%, 67% and 40%. Median RFS was 119 (95%CI: 68-119) months. There were no significant differences in OS or RFS for bridged or downstaged patients. There was significant difference in terms of number of recurrences and RFS between patients who had complete or extensive necrosis vs patients who had partial necrosis (p<0.0001).

#### CONCLUSION

Y90 can be used as a locoregional therapy that permits bridging or downtaging to LT. LT after Y90 represents a curative treatment for HCC with excellent OS rates comparable to LT for non-malignant causes. Patients who achieved extensive or complete necrosis have better recurrence free survival outcomes.

#### **CLINICAL RELEVANCE/APPLICATION**

Y90 has proven to be not only beneficial for HCC patients with bridging or downstaging to LT but also with good tumor response pre-LT and prolonged recurrence free survival post-LT.

# SSA25-09 Predicting Treatment Response of Primary and Secondary Lung Neoplasms to Transpulmonay Chemoembolization (TPCE) and Transarterial Chemoperfusion (TACP) Using Diffusion-Weighted MRI (DWI): Value of Pretreatment Apparent Diffusion Coefficient (ADC)

Sunday, Nov. 25 12:05PM - 12:15PM Room: S503AB

Participants

Thomas J. Vogl, MD, PhD, Frankfurt, Germany (*Presenter*) Nothing to Disclose A. T. Hoppe, Frankfurt, Germany (*Abstract Co-Author*) Nothing to Disclose Tatjana Gruber-Rouh, Frankfurt Am Main, Germany (*Abstract Co-Author*) Nothing to Disclose Nour-Eldin A. Nour-Eldin, MD,PhD, Frankfurt Am Main, Germany (*Abstract Co-Author*) Nothing to Disclose

# For information about this presentation, contact:

T.Vogl@em.uni-frankfurt.de

#### PURPOSE

To examine predictive value of apparent diffusion coefficients (ADC) derived from diffusion-weighted MR imaging (DWI) in patients with unresectable primary and secondary lung cancer undergoing transpulmonary chemoembolization (TPCE) and transarterial chemoperfusion (TACP) treatment.

#### **METHOD AND MATERIALS**

31 patients with 42 lesions (non-small cell lung cancer (NSCLC) n=13; and lung metastases n=18) underwent examination with DWI prior to first treatment and one month thereafter. Lesion diameter and volume were measured at the beginning and end of each treatment cycle (mean 3.1 procedures per patient) in about 4-week intervals between January 2014 and December 2017. Decreases by at least 30% regarding tumor volume were classified as partial response (PR), an increase by 20% or more was defined as progressive disease (PD), while remaining lesions were categorized as stable disease (SD).

# RESULTS

The PR group contained 9 lesions (NSCLC n=8; metastasis n=1), mean pretreatment ADC was 1.164 x 10-3 mm2/s, increase in mean ADC after first intervention was 32.9%. The PD group had 14 lesions (NSCLC n=1; metastases n=13), mean pretreatment ADC was 1.418 x 10-3 mm2/s, increase in mean ADC was 5.0%. Difference between ADC changes in the response groups was significant p<0.01). Lesion pretreatment ADC recorded fair diagnostic value for predicting response (AUC 0.774). Applying a threshold ADC increase of 20.71%, response can be predicted with a sensitivity and specificity of 88% and 78%, respectively (AUC 0.838). In primary lung cancer lesions, correlation of ADC changes with changes in tumor diameter and volume of -0.87 and -0.66, respectively. In metastatic lesions, correlation coefficients were -0.18 and -0.35.

#### CONCLUSION

A correlation was documented between early increases in ADC and tumor size reduction. Furthermore, responding lesions showed lower pretreatment ADC. DWI seems a suitable method for response prediction. The findings correlated better with primary lung cancer than with lung metastases.

#### **CLINICAL RELEVANCE/APPLICATION**

DWI provides the interventionalist with information going beyond morphological tumor aspects and response prediction assists in prioritising treatment locations in patients with multiple lesions



#### VSPD01

#### **Pediatric Series: Neuroradiology**

Sunday, Nov. 25 10:45AM - 12:15PM Room: S406A



AMA PRA Category 1 Credits ™: 1.50 ARRT Category A+ Credit: 1.75

#### Participants

Manu S. Goyal, MD, MSc, Saint Louis, MO (*Moderator*) Nothing to Disclose Arastoo Vossough, MD, PhD, Philadelphia, PA (*Moderator*) Consultant, Banyan Biomarkers, Inc

### For information about this presentation, contact:

goyalm@wustl.edu

Sub-Events

#### VSPD01-01 Pediatric Brain Imaging in Neurofibromatosis-1

Sunday, Nov. 25 10:45AM - 11:05AM Room: S406A

Participants

Manu S. Goyal, MD, MSc, Saint Louis, MO (Presenter) Nothing to Disclose

For information about this presentation, contact:

goyalm@wustl.edu

#### LEARNING OBJECTIVES

1) Learn the clinical role and indications for brain MRI in children with suspected NF1. 2) Identify the typical features of optic pathway gliomas in NF1. 3) Identify the typical features of non-optic pathway gliomas in NF1. 4) Identify the typical non-neoplastic findings on brain MRI in NF1.

# VSPD01-02 White Matter Microstructural Changes in the Cases of Tuberous Sclerosis: Evaluation by Neurite Orientation Dispersion and Density Imaging (NODDI) Compared with Conventional Diffusion Tensor Method

Sunday, Nov. 25 11:05AM - 11:15AM Room: S406A

Participants

Toshiaki Taoka, MD, PhD, Nagoya, Japan (*Presenter*) Nothing to Disclose Noriko Aida, MD, Yokohama, Japan (*Abstract Co-Author*) Nothing to Disclose Yuta Fujii, Yokohama, Japan (*Abstract Co-Author*) Nothing to Disclose Hisashi Kawai, Nagoya, Japan (*Abstract Co-Author*) Nothing to Disclose Toshiki Nakane, Nagoya, Japan (*Abstract Co-Author*) Nothing to Disclose Shinji Naganawa, MD, Nagoya, Japan (*Abstract Co-Author*) Nothing to Disclose

#### For information about this presentation, contact:

ttaoka@med.nagoya-u.ac.jp

#### PURPOSE

Neurite orientation dispersion and density imaging (NODDI) is an advanced diffusion imaging technique that provides detailed information on tissue microstructure of the brain. Intracellular volume fraction (Ficv) image is one of the products of NODDI which is a marker of neurite density. We accessed the Ficv images in the tuberous sclerosis (TS) cases and evaluated the changes in the white matter microstructure in comparison with fractional anisotropy (FA) images by conventional diffusion tensor method.

#### **METHOD AND MATERIALS**

Twelve cases of TS and eight controls were evaluated. Diffusion datasets of 20 axes motion proving gradients were acquired with b=1000 and 2000 s/mm2 by a 3T clinical scanner, and analyzed with NODDI Matlab toolbox. Ficvf images were accessed as well as FA images. We analyzed (1) qualitative scoring method comparing the areas with and without cortical tuber, (2) quantitative analysis to acquire VoxTh ratio which is a ratio of the number of voxels lower than the value of thalamus to the total voxels, and (3) Tract-Based Spatial Statistics (TBSS) method compared to controls.

#### RESULTS

(1) On qualitative analysis, Ficv images showed lower value especially in the areas with cortical tuber. These changes could be seen not only in the area with cortical tuber, but the area without them. While, FA images showed hyperintensity in the white matter regardless of the existence of cortical tuber. (2) On histogram analysis, VoxTh ratio were smaller on Ficv images than on FA images. (3) On TBSS analysis, Ficv images of TS complex showed statistically significant lower values compared to controls in the area with subcortical or gyral white matter.

#### CONCLUSION

In conventional diffusion tensor method, decreases of FA, which might represent lower packing density of unmyelinated axonal fibers, were not prominent in the TS cases. While, Ficvf from NODDI showed significant decrease, which might reflect the lack of maturation with thin non-myelinated fibers, especially in the areas with cortical tuber in the TS cases.

### **CLINICAL RELEVANCE/APPLICATION**

In conventional diffusion tensor method, decreases of FA, which might represent lower packing density of unmyelinated axonal fibers, were not prominent in the TS cases. While, Ficvf from NODDI showed significant decrease, which might reflect the lack of maturation with thin non-myelinated fibers, especially in the areas with cortical tuber in the TS cases.

### VSPD01-03 Can Advanced MR Imaging predict Molecular Subgroups of Medulloblastoma?

Sunday, Nov. 25 11:15AM - 11:25AM Room: S406A

Participants

Nadezhda Plakhotina, MD, Saint-Petersburg, Russia (*Presenter*) Nothing to Disclose Elida Vazquez, MD, Barcelona, Spain (*Abstract Co-Author*) Nothing to Disclose Ignacio Delgado, MD, Barcelona, Spain (*Abstract Co-Author*) Nothing to Disclose Angel Sanchez-Montanez, MD, Barcelona, Spain (*Abstract Co-Author*) Nothing to Disclose Elena Martinez, Barcelona, Spain (*Abstract Co-Author*) Nothing to Disclose Anna Llort, Barcelona, Spain (*Abstract Co-Author*) Nothing to Disclose Gemma Burcet Rodriguez, MD, Barcelona, Spain (*Abstract Co-Author*) Nothing to Disclose

### For information about this presentation, contact:

evazquez@vhebron.net

# PURPOSE

As preoperative MR characterization of medulloblastoma into groups parallel to those established by molecular diagnosis may be valuable for oncologists, our purpose was to determine whether advanced MR imaging patterns of medulloblastoma can correlate with the diverse molecular groups used as a basis for treating this condition.

#### **METHOD AND MATERIALS**

Twenty-nine patients, mean age 4.74 (1-15 years), 10 (34.5%) female and 19 (65.5%) male, with a confirmed diagnosis of medulloblastoma, underwent structural and advanced pretreatment MRI of the brain and spine (1.5 or 3T magnets), including diffusion imaging, MR spectroscopy, ASL perfusion, and dynamic enhanced perfusion, in our tertiary pediatric center (January 2010-December 2017) and were retrospectively reviewed. One neuroradiology research fellow and 2 experienced pediatric neuroradiologists reviewed the MR images. The MRI findings of each tumor were recorded on a structured list of possible features (eg, location, morphology, enhancement, type of perfusion, diffusion restriction, ADC measurements, spectroscopy metabolite abnormalities).

# RESULTS

In accordance with the new molecular classification, these tumors are now being assigned to molecular subgroups: wingless (WNT), sonic hedgehog (SHH), group 3, and group 4. As a work in progress, the MRI features from the advanced techniques, mainly perfusion and spectroscopy, are undergoing statistical analysis to determine which parameters are useful for predicting the various medulloblastoma molecular subgroups. As an example, the figure shows four different patients with medulloblastoma demonstrating diverse cerebral blood volumes and spectroscopy patterns.

#### CONCLUSION

Advanced MRI techniques, together with the conventional findings, contribute to assessing the diagnosis of medulloblastoma; in addition, our findings to date suggest that some MRI features can predict a particular molecular subgroup, with implications for management.

#### **CLINICAL RELEVANCE/APPLICATION**

Advanced MRI techniques may be useful to classify medulloblastoma patients into molecular subgroups, which are relevant for therapy strategies, with tailored subgroup-specific treatments.

# VSPD01-04 Differentiation of High-Grade and Low-Grade Pediatric Brain Tumors Using Mono-exponential, Biexponential, and Stretched Exponential Diffusion-weighted Imaging

Sunday, Nov. 25 11:25AM - 11:35AM Room: S406A

Participants

Stephen F. Kralik, MD, Indianapolis, IN (*Presenter*) Nothing to Disclose Jeremy S. Cardinal, MD, Indianapolis, IN (*Abstract Co-Author*) Nothing to Disclose Sean C. Dodson, MD, Indianapolis, IN (*Abstract Co-Author*) Nothing to Disclose Chang Y. Ho, MD, Indianapolis, IN (*Abstract Co-Author*) Nothing to Disclose

#### For information about this presentation, contact:

steve.kralik@gmail.com

#### PURPOSE

The purpose of this study was to assess the diagnostic performance of parameters obtained from mono-exponential, biexponential, and stretched exponential diffusion-weighted imaging (DWI) for differentiating low-grade and high-grade pediatric brain tumors.

#### **METHOD AND MATERIALS**

Pediatric patients with brain tumors were evaluated at initial presentation with diffusion-weighted imaging using 8 b values (0-800

s/mm2) at 3T. The apparent diffusion coefficient (ADC), true diffusion coefficient (D), pseudo-diffusion coefficient (D\*), perfusion fraction (f), and alpha were calculated by fitting the mono-exponential, bi-exponential model and stretched exponential methods. Histogram analysis of ADC, D, D\*, f, and alpha values from tumor volumetric region of interest were compared between low-grade tumors, World Health Organization (WHO) grade 1 and 2, and high-grade tumors, WHO grade 3 and 4.

### RESULTS

A total of 36 patients (mean age 7.4 years, range 0-17 years; 23 males, 9 females) were evaluated. There were 17 low grade tumors and 19 high grade tumors. The volumetric mean tumor ADC (1.45 +/- 0.36 vs 1.01 +/- 0.33 x 10-3 mm2/s, P=0.001), D (1.32 +/- 0.31 vs 0.90 +/- 0.29 x 10-3 mm2/s, P<0.001), D\* (6.21 +/- 3.59 vs 17.1 +/- 6.97 x 10-3 mm2/s, P<0.0001), and alpha (0.93 +/- 0.03 vs 0.86 +/- 0.04, P<0.0001) were significantly different between the low grade group compared to the high grade group. The f was not statistically significant (0.07 +/- 0.02 vs 0.08 +/- 0.03, P=0.49). Receiver operating characteristic analysis for the mean volumetric tumor demonstrated maximum area under the curve, sensitivity and specificity of 0.85, 83%, 79% for ADC, 0.84, 87%, 79% for D, 0.91, 87%, 93% for D\*, 0.57, 20%, 100% for f, and 0.90, 89%, 86% for alpha.

### CONCLUSION

Biexponential, and stretched exponential diffusion parameters obtained from multiple b value DWI may outperform the ADC for differentiation of low-grade and high-grade pediatric brain tumors.

### **CLINICAL RELEVANCE/APPLICATION**

The addition of multiple b value diffusion weighted imaging may improve diagnosis of low grade versus high grade tumors in pediatric patients with brain tumors.

# VSPD01-05 Histogram Analysis of Apparent Diffusion Coefficients May Predict Molecular Subgroups of Medulloblastoma in Children

Sunday, Nov. 25 11:35AM - 11:45AM Room: S406A

Participants

Weijian Wang, Zhengzhou, China (*Presenter*) Nothing to Disclose Jingliang Cheng, Zhengzhou, China (*Abstract Co-Author*) Nothing to Disclose Yong Zhang, DO, Zhengzhou, China (*Abstract Co-Author*) Nothing to Disclose

For information about this presentation, contact:

weijianwang520@163.com

#### PURPOSE

The aim is to verify if ADC histogram is able to predict new subgroups of medulloblastoma.

### METHOD AND MATERIALS

Sixty-five patients with diagnosis of medulloblastoma(30 classic, 8 desmoplastic/nodular, 7 extensive nodularity, 20 large cell/anaplastic), with pretreatment MR imaging, histologic, genomic characterisation after surgery, were retrospectively selected. ADC maps were coregistered with T1WI post-contrast and T2WI images. Drawing the region of interest(ROI) on the maximum level of ADC maps and going on histogram analysis, these two steps are all performed on the software named Mazda.We used the Mann-Whitney test to evaluate the capacity of histogram parameters to discriminate among paired medulloblastoma subgroups.

# RESULTS

Desmoplastic/nodular and extensive nodularity were detected no statistical significance. A trend in differences was found between classic and large cell/anaplastic. 9 texture parameters using histogram extracted, with statistical significance (mean,variance,1 percent,10 percent). ROC curve analysis of the 10th percentile yielded the best area under the ROC curve (AUC; 0.96), sensitivity of 98%, and specificity of 96%, with a cutoff value of 90.

#### CONCLUSION

The study shows histograms analysis of apparent diffusion coefficient can provide reliably objective basis for molecular subgroups of medulloblastoma in children.

# **CLINICAL RELEVANCE/APPLICATION**

Histogram is a kind of the texture analysis which is non-invasive, ROI can include the entire range of tumor, we can get a histogram data by calculating all the voxel of the tumor volume , the results is more objective and has less error.

# VSPD01-06 Cerebral Blood Flow and Marrow Diffusion Alterations in Children with Sickle Cell Anemia After Bone Marrow Transplant and Transfusion

Sunday, Nov. 25 11:45AM - 11:55AM Room: S406A

Participants

Matt Whitehead, MD, Washington, DC (*Presenter*) Nothing to Disclose Anilawan Smitthimedhin, Bangken Bangkok, Thailand (*Abstract Co-Author*) Nothing to Disclose Jennifer Webb, Washington, DC (*Abstract Co-Author*) Nothing to Disclose Eman S. Mahdi, MD, MBChB, Washington, DC (*Abstract Co-Author*) Nothing to Disclose Zarir P. Khademian, MD, PhD, Washington , DC (*Abstract Co-Author*) Nothing to Disclose Jessica Carpenter, Washington, DC (*Abstract Co-Author*) Nothing to Disclose Bonmyong Lee, MD, Baltimore, MD (*Abstract Co-Author*) Nothing to Disclose Allistari Abraham, Washington, DC (*Abstract Co-Author*) Nothing to Disclose

### For information about this presentation, contact:

MWhitehe@childrensnational.org

#### PURPOSE

Hematopoietic bone marrow hyperplasia and hyperperfusion are compensatory mechanisms in sickle cell anemia (SCA). We have observed changes in marrow diffusion and ASL perfusion values in SCA following bone marrow transplant (BMT), potentially representing biomarkers of a favorable therapeutic response. We aim to compare ASL perfusion and marrow diffusion/ADC values in SCA patients prior to and after BMT or transfusion.

# METHOD AND MATERIALS

All consecutive brain MRIs performed over 6 years at an academic children's hospital in SCA patients were reviewed. Those lacking ASL and cases with disease processes that would affect ASL perfusion values were excluded. Quantitative marrow diffusion values were obtained from the occipital and sphenoid bones. Quantitative pseudo-continuous ASL perfusion values (ml/100g tissue/min) were determined by interrogating each of the following bilateral territories: MCA, ACA, and PCA. Thereafter, average whole brain perfusion was estimated. Each territory, whole brain average CBF, and marrow ADC values were compared for changes in the same patient prior to and after either BMT or transfusion, and over time. BMT and transfusion groups were then compared to one another. Two-tailed paired and unpaired student T tests were utilized where appropriate; P <0.05 was considered significant.

# RESULTS

Fifty-three exams from 17 BMT patients (follow-up 0-4 years) and 29 brain MR examinations from 9 transfusion patients (follow-up 1-5 years) were included. ADC values significantly increased in the sphenoid wing (0.97x10-3 to 1.59x10-3; P=0.025) and occipital marrow following BMT in contrast to transfusion patients (P>0.83). Whole brain mean CBF significantly decreased following BMT, from 77.39+/-13.78 to 60.39+/-13.62 (1st scan; P=0.00004), and did not significantly change thereafter. CBF did not significantly change following the 1st transfusion (81.11+/-12.23 to 80.25+/-8.27, P=0.47) or after subsequent transfusions. There was no significant difference in mean CBF between the BMT and transfusions groups prior to intervention (P=0.22).

### CONCLUSION

Improved CBF and marrow diffusion eventuate following bone marrow transplantation in children with SCA. In contrast, no significant alteration in CBF or marrow diffusion was found in SCA patients that underwent transfusion therapy.

# **CLINICAL RELEVANCE/APPLICATION**

ASL perfusion and quantitative marrow diffusion values are useful post-therapeutic imaging biomarkers.

# VSPD01-07 Pediatric Neuroimaging in Vascular Neurocutaneous Syndromes

Sunday, Nov. 25 11:55AM - 12:15PM Room: S406A

#### Participants

Arastoo Vossough, MD, PhD, Philadelphia, PA (Presenter) Consultant, Banyan Biomarkers, Inc

# **LEARNING OBJECTIVES**

1) Classify the various pediatric vascular neurocutaneous syndromes. 2) Identify the major clinical features of select vascular neurocutaneous syndromes. 3) Describe the main imaging features and differential diagnoses of select vascular neurocutaneous syndromes.



#### RCA11

# Radiology Search and Analytics Software Tools for Clinical and Practice Quality Optimization (Hands-on)

Sunday, Nov. 25 11:00AM - 12:30PM Room: S401AB

IN

AMA PRA Category 1 Credits ™: 1.50 ARRT Category A+ Credit: 1.75

#### **Participants**

Safwan Halabi, MD, Stanford, CA (*Moderator*) Nothing to Disclose Safwan Halabi, MD, Stanford, CA (*Presenter*) Nothing to Disclose Matthew P. Lungren, MD, Palo Alto, CA (*Presenter*) Nothing to Disclose

### For information about this presentation, contact:

safwan.halabi@stanford.edu

# **LEARNING OBJECTIVES**

Become familiar with available search and analytics tools that can be used to promote clinical and practice quality optimization.
 Apply common search and analytics techniques to extract meaningful clinical and practice data.
 Understand the tools and resources needed to develop your practice's search and analytics strategy for performance improvement.



### RCB11

Teaching Congenital Heart Morphology with 3D Print Models II: Understanding Surgical Procedures in Congenital Heart Diseases with Illustrations and 3D Print Models (Hands-on)

Sunday, Nov. 25 11:00AM - 12:30PM Room: S401CD



AMA PRA Category 1 Credits ™: 1.50 ARRT Category A+ Credit: 1.75

### Participants

Shi-Joon Yoo, MD, Toronto, ON (*Presenter*) Owner, 3D HOPE Medical; CEO, IMIB-CHD; Spouse, CEO, 3D PrintHeart; Cynthia K. Rigsby, MD, Chicago, IL (*Presenter*) Nothing to Disclose Rajesh Krishnamurthy, MD, Columbus, OH (*Presenter*) Nothing to Disclose Whal Lee, MD, PhD, Seoul, Korea, Republic Of (*Presenter*) Nothing to Disclose Andreas Giannopoulos, MD, Zurich, Switzerland (*Presenter*) Nothing to Disclose Hyun Woo Goo, MD, Seoul, Korea, Republic Of (*Presenter*) Nothing to Disclose Lorna Browne, MD, FRCR, Aurora, CO (*Presenter*) Nothing to Disclose

#### For information about this presentation, contact:

crigsby@luriechildrens.org

# LEARNING OBJECTIVES

1) Understand the terms used in describing the pathology of criss-cross heart and related conditions. 2) Understand the pathologic and surgical anatomy of various forms of criss-cross heart and related conditions. 3) Develop ideas how to image the patients with criss-cross heart and related conditions for surgical management.

# ABSTRACT

Congenital heart diseases are the most common significant birth defects requiring surgical treatment in the majority of cases. Understanding of pathologic anatomy is crucial in surgical decision and performing optimal surgical procedures. Learning cardiac morphology has relied on the pathologic specimens removed from dead patients or at the time of transplantation. However, the pathologic specimens are rare and hardly represent the whole spectrum of diseases. 3D print models from the CT and MR angiograms of the patients with congenital heart disease are great resources for teaching and can revolutionize education. In this hands-on session, 3D print models of hearts will be used for comprehensive understanding of comlex morphology of criss-cross or twisted hearts, superofinferior ventricles and topsy-turvy hearts. The session will consist of 15-minute introductory lecture, 60minute hands-on observation and 15-minute discussion and evaluation. Experts on congenital heart disease pathology will be available for guidance and answering questions throughout the session.

### **Honored Educators**

Presenters or authors on this event have been recognized as RSNA Honored Educators for participating in multiple qualifying educational activities. Honored Educators are invested in furthering the profession of radiology by delivering high-quality educational content in their field of study. Learn how you can become an honored educator by visiting the website at: https://www.rsna.org/Honored-Educator-Award/ Rajesh Krishnamurthy, MD - 2017 Honored Educator



#### RCC11

# Case Review: Lung-RADS - Bring Your Own Device (Hands-on)

Sunday, Nov. 25 11:00AM - 12:30PM Room: S402AB



AMA PRA Category 1 Credits ™: 1.50 ARRT Category A+ Credit: 0

# Participants

Ella A. Kazerooni, MD, Ann Arbor, MI (*Presenter*) Nothing to Disclose Elizabeth Lee, MD, Ann Arbor, MI (*Presenter*) Nothing to Disclose Jared D. Christensen, MD, Durham, NC (*Presenter*) Advisory Board, Riverain Technologies, LLC Maria D. Martin, MD, Madison, WI (*Presenter*) Nothing to Disclose Brett M. Elicker, MD, San Francisco, CA (*Presenter*) Nothing to Disclose

### LEARNING OBJECTIVES

1) Describe patient risk factors for lung cancer and current requirements for patients to be eligible for lung cancer screening based on the coverage decision outlined by the Centers for Medicare and Medicaid Services. 2) Explain the rational for each category used in Lung-RADS. 3) Apply Lung-RADS to case examples and recommend appropriate follow up.

#### ABSTRACT

Participants will review cases on their own devices and answer questions. The cases will then be reviewed by the presenters. Note: this activity is best done on a laptop or tablet. Although phones will work, their small size limits optimal image view. Lung-RADS was established in 2014 as a means to standardized reporting and management in high-risk patients undergoing screening for lung cancer with low dose CT. This workshop will begin with an approximately 20 minute review of the National Lung Screening Trial (NLST) and other supporting evidence for the efficacy of screening, recommendations for screening as per the U.S. Preventative Services Task Force and the coverage decision by the Centers for Medicare and Medicaid Services. Additionally, concepts regarding the structure and rational for Lung-RADS will be highlighted. After a didactic portion, participants will review cases independently on their own devices. Faculty support will be available throughout the room to answer individual questions. Following this, cases will be reviewed by the presenters in order to highlight key concepts in the use of Lung-RADS. This session will focus on the application of Lung-RADS including: recognizing important imaging features and applying findings to assign the correct Lung-RADS category. Attendees will be given tips and tools to help with use of Lung-RADS and requirements for establishments of a lung cancer screening program.

#### **Honored Educators**

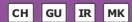
Presenters or authors on this event have been recognized as RSNA Honored Educators for participating in multiple qualifying educational activities. Honored Educators are invested in furthering the profession of radiology by delivering high-quality educational content in their field of study. Learn how you can become an honored educator by visiting the website at: https://www.rsna.org/Honored-Educator-Award/ Ella A. Kazerooni, MD - 2014 Honored Educator



### VSIO11

Interventional Oncology Series: Lung, Kidney and Bone

Sunday, Nov. 25 1:30PM - 6:00PM Room: S405AB



ARRT Category A+ Credits: 5.00 AMA PRA Category 1 Credits M: 4.25

**FDA** Discussions may include off-label uses.

#### Participants

Christos S. Georgiades, MD, PhD, Baltimore, MD (*Moderator*) Consultant, Galil Medical Ltd Sean M. Tutton, MD, Milwaukee, WI (*Moderator*) Medical Director, Benvenue Medical, Inc; Consultant, Benvenue Medical, Inc; Researcher, Siemens AG; Consultant, BTG International Ltd

#### For information about this presentation, contact:

g\_christos@hotmail.com

#### LEARNING OBJECTIVES

1) To understand the physics and physiology relevant to the main ablation modalities as applied to different target organs. 2) To become updated on the currrent evidence for kidney, lung and MSK tumor ablation. 3) To learn how to anticipate and mitigate potential complications related tolung, kidney and MSK ablations. 4) To learn techniques (including tackling challenging cases) that maximize oncologic outcomes.

# Sub-Events

### VSI011-01 Keynote and Series Opening: Interventional Oncology-The 4th Pillar of Cancer Care

Sunday, Nov. 25 1:30PM - 1:55PM Room: S405AB

Participants

William S. Rilling, MD, Milwaukee, WI (*Presenter*) Research support, B. Braun Melsungen AG; Research support, Sirtex Medical Ltd; Research support, Siemens AG; Consultant, B. Braun Melsungen AG; Consultant, Cook Group Incorporated ; Consultant, Terumo Corporation; Advisory Board, Terumo Corporation

#### VSI011-02 Physics of MW, RF and Cryoablation: Clinically Relevant Parameters

Sunday, Nov. 25 1:55PM - 2:15PM Room: S405AB

#### Participants

Christos S. Georgiades, MD, PhD, Baltimore, MD (Presenter) Consultant, Galil Medical Ltd

# **LEARNING OBJECTIVES**

To understand the physical principles behind the common ablation modalities (RFA, Microwave, Cryoablation, HIFU, IRE etc)To understand how physiological parameters can affect the efficacy of the ablation modalityTo be able to select the appropriate ablation modality for each specific case and optimize outcomes

#### LEARNING OBJECTIVES

1) Comprehend clinically relevant physical parameters of microwave, radiofrequency, and cryoablation technologies. 2) Apply the most appropriate thermal ablative technique for a patient.

### VSI011-03 Lung Cancer Ablation: Techniques to Optimize Outcome and Current Evidence

Sunday, Nov. 25 2:15PM - 2:35PM Room: S405AB

#### Participants

William H. Moore, MD, Port Washington, NY (Presenter) Consultant, Merck & Co, Inc; Consultant, BTG International Ltd;

#### **LEARNING OBJECTIVES**

1) Discuss Ablative Mechanism Understand Patient/Lesion selection Comparison of RFA/MVA/Cryo. 2) Review and describe outcomes including adverse events, local control, and survival abscopal effect.

### VSI011-05 Complications of Lung Ablation and Mitigating Actions

Sunday, Nov. 25 2:45PM - 3:05PM Room: S405AB

Participants

Stephen B. Solomon, MD, New York, NY (*Presenter*) Research Grant, General Electric Company; Consultant, Johnson & Johnson; Consultant, BTG International Ltd;

1) To review the complications associated with lung ablation and offer suggestions and approaches that would mitigate them.

# VSI011-06 XRT versus Ablation with Curative Intent: Patient Selection and Outcomes

Sunday, Nov. 25 3:05PM - 3:25PM Room: S405AB

Participants

Kelvin K. Hong, MD, Baltimore, MD (*Presenter*) Scientific Advisory Board, Boston Scientific Corporation Scientific Advisory Board, BTG International Ltd Research support, Merit Medical Systems, Inc

# LEARNING OBJECTIVES

1) The current available data will be reviewed and contextualized.

# ABSTRACT

Patients with early stage, non operable lung cancers suffer from local progression as the primary cause of failure. SBRT and thermal ablation (such as RFA) are promising non operative therapeutic options. At present, there are no radomized comparisons between SBRT or RFA, nor direct clinical comparisons- and no prospective trial is underway. It is difficult for cancer specialists to decide between the two, and it is not definitive which provides superior undisputable outcomes.

# VSI011-07 Renal Cancer Ablation: Patient, Tumor Selection, Techniques and Current Evidence

Sunday, Nov. 25 3:25PM - 3:45PM Room: S405AB

#### Participants

Debra A. Gervais, MD, Boston, MA (Presenter) Nothing to Disclose

### LEARNING OBJECTIVES

1) To review selection criteria for renal tumor ablation cases. 2) To review reported effectiveness of the most common renal tumor ablation modalities and techniques.

### **Honored Educators**

Presenters or authors on this event have been recognized as RSNA Honored Educators for participating in multiple qualifying educational activities. Honored Educators are invested in furthering the profession of radiology by delivering high-quality educational content in their field of study. Learn how you can become an honored educator by visiting the website at: https://www.rsna.org/Honored-Educator-Award/ Debra A. Gervais, MD - 2012 Honored Educator

# VSIO11-08 Percutaneous Microwave Ablation versus Laparoscopic Partial Nephrectomy for cT1a Renal Cell Carcinoma: A 12-Year Inception Cohort Study with 1955 Patients

Sunday, Nov. 25 3:45PM - 3:55PM Room: S405AB

Participants

Jie Yu, Beijing, China (*Presenter*) Nothing to Disclose Ping Liang, PhD, Beijing, China (*Abstract Co-Author*) Nothing to Disclose Xiaoling Yu, Md, PhD, Beijing, China (*Abstract Co-Author*) Nothing to Disclose Zhigang Cheng, Beijing, China (*Abstract Co-Author*) Nothing to Disclose Zhiyu Han, Beijing, China (*Abstract Co-Author*) Nothing to Disclose Fangyi Liu, MD, Beijing, China (*Abstract Co-Author*) Nothing to Disclose

For information about this presentation, contact:

jiemi301@163.com

### PURPOSE

While partial nephrectomy (PN) is considered the standard approach for cT1a renal cell carcinoma (RCC). Objective of the study is to compare outcomes between percutaneous MWA (PMWA) and laparoscopic PN (LPN) for cT1a RCC.

# METHOD AND MATERIALS

We performed a prospective study of patients who underwent either PMWA or LPN for cT1a RCC (<=4cm) between April 2006 and November 2017. To reduce the inherent biases of the study, PMWA and LPN groups were matched on the basis of key variables: tumor size and number, Charlson comorbidity index (CCI), age, pathology, preoperative serum creatinine, preoperative estimated glomerular filtration rate (C) and gender. The matching algorithm was 1:1 genetic matching with no replacement. The risk of having a post-treatment complication and percent drop in eGFR, as well as the risks of local tumor progress (LTP), distant metastasis, and cancer-specific mortality, were compared between groups using logistic, linear, and Fine-and-Gray competing risk regression models.

### RESULTS

The cohort included 1955 patients (PMWA: 185; LPN: 1770) with a median follow-up of 40.6 mo (interquartile range 25.1, 63.4). After matching, there was no significant difference between the PMWA and LPN groups for tumor size (2.3 vs 2.3 cm; p = 0.86), age (63.2 vs 60.4 yr; p = 0.07), tumor location (p = 0.68) and pathology classification (p = 1.0). But PMWA group had higher CCI (4 vs 1; p<0.001), preoperative creatinine (84.4 vs 74.2 mg/dl; p<0.001) and preoperative eGFR (119.5 vs 106.8 ml/min/1.73m2; p = 0.002). There were significant differences between PMWA and LPN in percentage drop in eGFR at discharge (mean: 6% vs 17.9%; p = 0.002) and major complication (mean: 2.2% vs 4.9%; p = 0.16). Likewise, no significant differences were noted in LTP (3.2% vs 0.5%; p = 0.06), distant metastases (4.3% vs 4.3%; p = 1.0), or 5-year cancer-specific mortality (p = 0.68). But LPN group needed longer operative time(29.4 vs 108.1 min; p<0.001), more estimated blood loss(4.0 vs 50 ml; p<0.001).

### CONCLUSION

Our study found no significant difference in complications, renal function outcomes, and oncologic outcomes between PMWA and LPN for patients with cT1a RCC. Validation in a larger multi-institutional analysis may be warranted.

#### **CLINICAL RELEVANCE/APPLICATION**

PMWA with less invasion should be reserved for patients with imperative indications for nephron-sparing surgery who cannot be subjected to the risks of more invasive LPN.

### VSI011-09 Complications of Renal Ablation and Mitigating Actions

Sunday, Nov. 25 4:05PM - 4:25PM Room: S405AB

Participants

Shane A. Wells, MD, Madison, WI (Presenter) Consultant, Johnson & Johnson

#### For information about this presentation, contact:

swells@uwhealth.org

### LEARNING OBJECTIVES

1) Differentiate expected imaging findings and complications on imaging performed immediately after renal mass ablation. 2) Differentiate expected imaging findings and complications on follow-up imaging. 3) Develop strategies to mitigate procedure-related complications.

# VSIO11-10 Usefulness of a Modified RENAL Nephrometry Score in Predicting Renal Function after Cryotherapy for Renal Mass

Sunday, Nov. 25 4:25PM - 4:35PM Room: S405AB

#### Participants

Yoshiki Asayama, MD, Fukuoka, Japan (*Presenter*) Nothing to Disclose Akihiro Nishie, MD, Fukuoka, Japan (*Abstract Co-Author*) Nothing to Disclose Yasuhiro Ushijima, MD, Fukuoka, Japan (*Abstract Co-Author*) Nothing to Disclose Koichiro Morita, Fukuoka, Japan (*Abstract Co-Author*) Nothing to Disclose Seiichiro Takao, Fukuoka, Japan (*Abstract Co-Author*) Nothing to Disclose Hiroshi Honda, MD, Fukuoka, Japan (*Abstract Co-Author*) Nothing to Disclose Daisuke Kakihara, Fukuoka, Japan (*Abstract Co-Author*) Nothing to Disclose Keisuke Ishimatsu, MD, Fukuoka, Japan (*Abstract Co-Author*) Nothing to Disclose Kousei Ishigami, MD, Fukuoka, Japan (*Abstract Co-Author*) Nothing to Disclose Nobuhiro Fujita, MD, Ph, Fukuoka, Japan (*Abstract Co-Author*) Nothing to Disclose

### PURPOSE

We investigated the application of the modified RENAL nephrometry (MRN) score system for predicting post-cryotherapy renal function in T1 renal mass patients.

#### **METHOD AND MATERIALS**

A total of 75 patients with a T1 renal mass were enrolled. The MRN score is based on the tumor size (radius, R), the tumor's exophytic/endophytic properties (E), the tumor's nearness to the collecting system (N), the anterior/posterior location of the kidney (A), and the location relative to the polar lines (L). The change in the estimated glomerular filtration rate ( $\Delta$ eGFR) was calculated as follows:  $\Delta$ eGFR= 100 ([pretreatment eGFR - eGFR at 6 months after cryotherapy]/pretreatment eGFR). Based on the  $\Delta$ eGFR results, we classified the patients into two groups: the preserved renal function group ( $\Delta$ eGFR <10%, n=44) and the impaired group ( $\Delta$ eGFR >=10%, n=31). We analyzed the relationship between the MRN score and the  $\Delta$ eGFR and the chronic kidney disease (CKD) stage.

#### RESULTS

The mean  $\Delta$ eGFR for all patients was 5.5%. The preserved group's MRN scores (5.8±0.3) were significantly lower than those of the impaired group (7.4±0.3) (p<0.001). With the MRN score cutoff value set at 7 points, the following values for predicting impaired status were obtained: 67.7% sensitivity, 72.7% specificity, 61.8% positive predictive value (PPV), 76.1% negative predictive value (NPV), and 70.7% accuracy. Those of predicting a down-stage of CKD status were 92.9% sensitivity, 67.2% specificity, 39.4% PPV, 97.6% NPV, and 72% accuracy.

### CONCLUSION

The modified RENAL nephrometry score may be useful in predicting renal function after renal cryotherapy.

# **CLINICAL RELEVANCE/APPLICATION**

(dealing with renal function after cryoablation for renal mass) Our newly proposed modified RENAL nephrometory score may be useful for predicting impairment of renal function (especially in CKD down-stages) with high sensitivity and a high negative predictive value and is recommended as a part of a pretreatment workup.

#### VSI011-11 Bone Ablation and Augmentation Outside the Spine

Sunday, Nov. 25 4:35PM - 4:55PM Room: S405AB

Participants

Sean M. Tutton, MD, Milwaukee, WI (*Presenter*) Medical Director, Benvenue Medical, Inc; Consultant, Benvenue Medical, Inc; Researcher, Siemens AG; Consultant, BTG International Ltd

### LEARNING OBJECTIVES

1) Better understand the various ablative modalities available including their specific differences and relative benefits and limitations in certain clinical scenarios. 2) Be familiarized with the existing literature supporting ablative therapies.

# VSI011-12 Interventional Oncology Palliative Treatment for Bone Metastases: Technique and Outcomes

### Participants

Steven Yevich, MD, MPH, Houston, TX (Presenter) Scientific Advisory Committee, Siemens AG; Scientific Advisor, Endocare, Inc

# VSIO11-13 Advanced Image Optimization Using Metal Artifact Reduction and Dual-Energy Processing to Improve Visualization of Therapeutic Ice Ball Margins During Cryoablation of Musculoskeletal Metastases

Sunday, Nov. 25 5:15PM - 5:25PM Room: S405AB

Participants Ethan Y. Lin, MD, Houston, TX (*Abstract Co-Author*) Nothing to Disclose Gouthami Chintalapani, Hoffman Estates, IL (*Abstract Co-Author*) Nothing to Disclose Rahul A. Sheth, MD, Boston, MA (*Abstract Co-Author*) Nothing to Disclose Steven Y. Huang, MD, Houston, TX (*Abstract Co-Author*) Nothing to Disclose Steven Yevich, MD, MPH, Houston, TX (*Presenter*) Scientific Advisory Committee, Siemens AG; Scientific Advisor, Endocare, Inc

For information about this presentation, contact:

SYevich@mdanderson.org

### PURPOSE

Evaluate combined metal artifact reduction (MAR) and monoenergetic spectral analysis by dual energy computed tomography (DECT) for assessment of ice ball ablation margins during cryoablation of musculoskeletal (MSK) metastases.

### METHOD AND MATERIALS

We retrospectively evaluated image with greatest cryoprobe metallic artifact from CT-guided cryoablation of MSK metastases (Somatom Edge 128 slice, Siemens Healthineers, Germany) in 9 patients (11 lesions, 8:3 bone:soft tissue adjacent to bone) from November 2017 to March 2018. Low and high KV images from DECT acquisition were first reconstructed with iterative MAR, then processed by monoenergetic spectral analysis. MAR+DECT monoenergetic images at 60KeV, 90KeV, and 120KeV were compared to corresponding DECT-only monoenergetic images, MAR-only composite CT images, and composite CT images at 120KV. All images were qualitatively ranked by 3 board-certified radiologists for visualization of ice ball margins and least amount of metal artifact in front of and adjacent to cryoprobe. Quantitative evaluation of contrast to noise ratio (CNR) was measured between ice adjacent to probes and soft tissue or bone at DECT 60, 90, and 120 KeV with and without MAR. Wilcoxon Signed Ranks test was used to compare CNR at the same KeV setting.

#### RESULTS

The combined MAR+DECT at 120KeV and 90KeV were first and second most preferred for least metal artifact in front of and adjacent to probe respectively, with DECT-only at 120KeV ranked third. For ice ball margin assessment, MAR+DECT at 90KeV and 120KeV and DECT-only at 120KeV were most preferred in order. Overall, both DECT-only at 120KeV and MAR+DECT at 120KeV were most preferred images, followed by MAR-only images. Composite CT image at 120KeV that mimics standard CT acquisition was least preferred image. CNR in soft tissue at 90KeV showed a significant difference between DECT with and without MAR (DECT + MAR 2.6  $\pm$  1.8 vs. DECT 2.0  $\pm$  1.3, p < 0.05).

### CONCLUSION

Combination of MAR and DECT analysis shows improved visualization for MSK cryoablation compared to standard CT acquisition, MAR-only, or DECT-only images.

# CLINICAL RELEVANCE/APPLICATION

Advanced image processing with combination of metal artifact reduction and dual energy CT may provide a real clinical advantage to delineate ice ball margins during MSK cryoablation.

### VSI011-14 Specific Augmentation Choices and Examples for Malignant Bone Lesions

Sunday, Nov. 25 5:25PM - 5:45PM Room: S405AB

Participants

Alexios Kelekis, MD, PhD, Athens, Greece (*Presenter*) Medical Advisory Board, BTG International Ltd; Medical Advisory Board, Merit Medical Systems, Inc; Research Grant, Mindray Medical

For information about this presentation, contact:

akelekis@med.uoa.gr

#### LEARNING OBJECTIVES

1) Identify the different type of malignant bone lesions associated with Augmentation. 2) Classify the available support systems for Augmentation. 3) Assess and recommend proper lesion management and Augmentation technique.

# VSI011-15 Tumor Board: Techniques and Challenging Cases in Lung, Kidney and Bone

Sunday, Nov. 25 5:45PM - 6:00PM Room: S405AB



# **Interstitial Lung Disease: Update 2018**

Sunday, Nov. 25 2:00PM - 3:30PM Room: S406A

# СНСТ

AMA PRA Category 1 Credits <sup>™</sup>: 1.50 ARRT Category A+ Credit: 1.75

#### Participants

David A. Lynch, MBBCh, Denver, CO (*Moderator*) Research support, Siemens AG; Research Consultant, PAREXEL International Corporation; Research Consultant, Boehringer Ingelheim GmbH; Research Consultant, F. Hoffmann-La Roche Ltd; Research Consultant, Veracyte, Inc;

#### Sub-Events

# RC101A Pulmonary Fibrosis

Participants

David A. Lynch, MBBCh, Denver, CO (*Presenter*) Research support, Siemens AG; Research Consultant, PAREXEL International Corporation; Research Consultant, Boehringer Ingelheim GmbH; Research Consultant, F. Hoffmann-La Roche Ltd; Research Consultant, Veracyte, Inc;

# LEARNING OBJECTIVES

1) Understand the radiologic differential diagnosis of fibrotic lung disease. 2) Become familiar with the most recent diagnostic criteria for usual interstitial pneumonia (UIP) on CT. 3) Understand the significance of 'early interstitial abnormality' on CT.

# RC101B Hypersensitivity Pneumonitis

Participants

Santiago E. Rossi, MD, Buenos Aires City, Argentina (*Presenter*) Advisory Board, Boehringer Ingelheim GmbH; Speaker, Boehringer Ingelheim GmbH; Royalties, Springer Nature

# For information about this presentation, contact:

santirossi@cdrossi.como

# LEARNING OBJECTIVES

1) Review the most common imaging findings of hypersensitivity pneumonitis (HP) (case-based). 2) Describe clinical manifestations of HP. 3) Identify proposed classification of HP.

### **Honored Educators**

Presenters or authors on this event have been recognized as RSNA Honored Educators for participating in multiple qualifying educational activities. Honored Educators are invested in furthering the profession of radiology by delivering high-quality educational content in their field of study. Learn how you can become an honored educator by visiting the website at: https://www.rsna.org/Honored-Educator-Award/ Santiago E. Rossi, MD - 2015 Honored Educator

# RC101C Smoking-Related Interstitial Lung Diseases

Participants

Carolina A. Souza, MD, Ottawa, ON (*Presenter*) Consultant, Pfizer Inc; Consultant, Boehringer Ingelheim GmbH; Consultant, AstraZeneca PLC; Speaker, Pfizer Inc; Speaker, Boehringer Ingelheim GmbH; Speaker, F. Hoffmann-La Roche Ltd; Speaker, AstraZeneca PLC; Advisory Board, AstraZeneca PLC

# For information about this presentation, contact:

csouza@toh.on.ca

# LEARNING OBJECTIVES

1) Describe the spectrum of smoking-related interstitial lung diseases and their clinical manifestations. 2) Recognize the highresolution CT appearances of smoking-related lung diseases. 3) Identify the most common imaging differential diagnoses of smoking-related interstitial lung diseases.

### RC101D Sarcoidosis

Participants

Lacey Washington, MD, Durham, NC (Presenter) Consultant, Novartis AG

# **LEARNING OBJECTIVES**

1) Review the classic clinical and imaging manifestations and common complications of thoracic sarcoidosis. 2) Review less well known clinical features and imaging findings.

# RC101E Quantification of Interstitial Lung Diseases

Participants

Joseph Jacob, MBBS, MRCP, London, United Kingdom (*Presenter*) Consultant, Boehringer Ingelheim GmbH; Consultant, F. Hoffmann-La Roche Ltd

# For information about this presentation, contact:

j.jacob@ucl.ac.uk

### LEARNING OBJECTIVES

1) Understand why computer analysis of CT imaging has relevance in interstitial lung diseases. 2) Understand the limitations of visual CT scoring. 3) Understand the various quantitative analytic techniques/tools. 4) Become aware of the latest results achieved by quantitative tools in predicting outcome across the various interstitial lung diseases.



Radiology Stewardship in the Transition to High-Value Practice: A Primer for Resident and Faculty Education, Engagement, and Effectiveness

Sunday, Nov. 25 2:00PM - 3:30PM Room: S502AB



AMA PRA Category 1 Credits ™: 1.50 ARRT Category A+ Credit: 0

#### Participants

Pamela T. Johnson, MD, Baltimore, MD (Moderator) Consultant, Oliver Wyman

For information about this presentation, contact:

PamelaJohnson@jhmi.edu

# LEARNING OBJECTIVES

1) Education: Understand the principles of healthcare value and how to design a curriculum for radiology trainees; a) Understand what is value and why it is important; b) Understand the 3Cs: cost, charges, and collections; c) Introduction to CMS quality driven reimbursement; d) Introduction to a value-driven outcomes model. 2) Engagement: Learn about how to engage residents and faculty in quality improvement; a) Explain principles of QI initiatives; b) Define value in QI initiatives; c) Detect QI opportunities that improve value; d) Apply QI principles to initiatives. 3) Effectiveness: design & assessment of a successful value-based performance improvement initiative; a) Understand the importance of cross-specialty consensus for appropriate use criteria; b) Recognize the role of cross-specialty education and resources (online modules, lectures, cases conferences, etc.); c) Learn how to create and distribute provider feedback reports and they drive performance; d) Understand how to create and distribute provider feedback reports and they drive performance; end use the pre- and post-interventional variables to measure (utilization, appropriateness, safety outcomes, cost reductions, charge reductions, etc.)

# Sub-Events

# RC102A Education: Value Economics Curriculum to Integrate into Healthcare Economics Milestone

### Participants

Yoshimi Anzai, MD, Salt Lake City, UT (Presenter) Nothing to Disclose

For information about this presentation, contact:

yoshimi.anzai@hsc.utah.edu

# LEARNING OBJECTIVES

1) To learn difference in changes, collection, and cost. 2) Determine the cost of care from various perspective. 3) To learn how to measure the internal cost of patient care and imaging services.

#### Active Handout:Yoshimi Anzai

http://abstract.rsna.org/uploads/2018/18001108/2018 high value education rc102a.pdf

#### **Honored Educators**

Presenters or authors on this event have been recognized as RSNA Honored Educators for participating in multiple qualifying educational activities. Honored Educators are invested in furthering the profession of radiology by delivering high-quality educational content in their field of study. Learn how you can become an honored educator by visiting the website at: https://www.rsna.org/Honored-Educator-Award/ Yoshimi Anzai, MD - 2014 Honored Educator

# RC102B Engagement: Proposed Resident Quality Improvement Initiatives to Improve Value

Participants Annemarie Relyea-Chew, JD,MS, Seattle, WA (*Presenter*) Nothing to Disclose

# For information about this presentation, contact:

archew@uw.edu

#### LEARNING OBJECTIVES

1) Explain principles of QI initiatives. 2) Define value in QI initiatives. 3) Detect QI opportunities that improve value. 4) Apply QI principles to initiatives.

# RC102C Effectiveness: Value-based Quality Improvement Plan for Residents, Fellows, and Faculty

Participants Pamela T. Johnson, MD, Baltimore, MD (*Presenter*) Consultant, Oliver Wyman

# LEARNING OBJECTIVES

1) Effectiveness: design & assessment of a successful value-based performance improvement initiative; a) Understand the importance of cross-specialty consensus for appropriate use criteria; b) Recognize the role of cross-specialty education and resources (online modules, lectures, cases conferences, etc.); c) Learn how to create and distribute provider feedback reports and they drive performance; d) Understand how to create and distribute provider feedback reports and they drive performance; e) Learn about the pre- and post-interventional variables to measure (utilization, appropriateness, safety outcomes, cost reductions, charge reductions, etc.)

# **Honored Educators**

Presenters or authors on this event have been recognized as RSNA Honored Educators for participating in multiple qualifying educational activities. Honored Educators are invested in furthering the profession of radiology by delivering high-quality educational content in their field of study. Learn how you can become an honored educator by visiting the website at: https://www.rsna.org/Honored-Educator-Award/ Pamela T. Johnson, MD - 2016 Honored Educator



# Rapid Fire: 80 Cardiac Cases in 80 Minutes

Sunday, Nov. 25 2:00PM - 3:30PM Room: S406B



AMA PRA Category 1 Credits ™: 1.50 ARRT Category A+ Credit: 1.75

FDA Discussions may include off-label uses.

#### Participants

Suhny Abbara, MD, Dallas, TX (*Moderator*) Royalties, Reed Elsevier; Institutional research agreement, Koninklijke Philips NV; Institutional research agreement, Siemens AG

#### Sub-Events

# RC103A Thoracic Vascular: 20 Cases

Participants Sachin S. Saboo, MD, FRCR, Dallas, TX (*Presenter*) Nothing to Disclose

For information about this presentation, contact:

saboo\_100@yahoo.com

# LEARNING OBJECTIVES

1) Describe key imaging features of twenty interesting thoracic vascular cases. 2) Assess significance of these imaging findings with respect to management.

#### **Honored Educators**

Presenters or authors on this event have been recognized as RSNA Honored Educators for participating in multiple qualifying educational activities. Honored Educators are invested in furthering the profession of radiology by delivering high-quality educational content in their field of study. Learn how you can become an honored educator by visiting the website at: https://www.rsna.org/Honored-Educator-Award/ Sachin S. Saboo, MD, FRCR - 2017 Honored Educator

# RC103B Cardiothoracic Oncology: 20 Cases

Participants

Eric E. Williamson, MD, Rochester, MN (Presenter) Nothing to Disclose

### For information about this presentation, contact:

williamson.eric@mayo.edu

### LEARNING OBJECTIVES

1) Describe the imaging features seen in the most common benign and malignant cardiac masses.

# RC103C Pericardium: 20 Cases

Participants Seth J. Kligerman, MD, Denver, CO (*Presenter*) Nothing to Disclose

### For information about this presentation, contact:

skligerman@ucsd.edu

#### **LEARNING OBJECTIVES**

1) Review various acute and chronic inflammatory conditions that involve the pericardium on CT and MRI. 2) Show various benign and malignant masses that involve the pericardial on CT and MRI. 3) Discuss differential diagnosis and methods of differentiation.

# RC103D Coronary Arteries and Myocardium: 20 Cases

Participants

Jacobo Kirsch, MD, Weston, FL (Presenter) Nothing to Disclose

For information about this presentation, contact:

kirschj@ccf.org

#### **LEARNING OBJECTIVES**

1) To review the imaging manifestations of common and uncommon ischemic and non-ischemic cardiac pathologies.

#### **Honored Educators**

Presenters or authors on this event have been recognized as RSNA Honored Educators for participating in multiple qualifying educational activities. Honored Educators are invested in furthering the profession of radiology by delivering high-quality educational content in their field of study. Learn how you can become an honored educator by visiting the website at: https://www.rsna.org/Honored-Educator-Award/ Jacobo Kirsch, MD - 2013 Honored Educator



### Opportunistic CT Screening for Osteoporosis, Sarcopenia, and Adiposity

Sunday, Nov. 25 2:00PM - 3:30PM Room: E450B



AMA PRA Category 1 Credits ™: 1.50 ARRT Category A+ Credit: 1.75

#### Participants

Robert D. Boutin, MD, Davis, CA (Director) Nothing to Disclose

#### For information about this presentation, contact:

rdboutin@ucdavis.edu

llenchik@wakehealth.edu

#### LEARNING OBJECTIVES

1) Discuss proposed CT-based definitions of osteoporosis, sarcopenia, and adiposity. 2) Review the potential for clinical impact when using routine CT to screen for osteoporosis, sarcopenia, and adiposity. 3) Highlight practical pearls and pitfalls for diagnostic imagers using opportunistic CT.

#### ABSTRACT

Non-communicable diseases are now "the world's main killer" [WHO, 2011]. The pandemics of osteoporosis, sarcopenia, and adiposity continue to grow globally as populations age. With more than 100 million CT exams performed annually worldwide, how might CT be used to screen patients efficiently for body composition derangements? This course focuses on the rapidly evolving field of "opportunistic" CT screening for the value-added diagnosis of osteoporosis, sarcopenia, and adiposity, with an emphasis on the clinical consequences of diagnostic imaging, as well as practical pearls and pitfalls.

### Sub-Events

# RC104A Opportunistic CT: Boom or Bust

Participants Leon Lenchik, MD, Winston-Salem, NC (*Presenter*) Nothing to Disclose

For information about this presentation, contact:

llenchik@wakehealth.edu

#### LEARNING OBJECTIVES

1) Define opportunistic CT screening.

# RC104B Muscle CT: Value-added Assessment for Sarcopenia

Participants

Robert D. Boutin, MD, Davis, CA (Presenter) Nothing to Disclose

# LEARNING OBJECTIVES

1) Discuss clinical and CT-based definitions of sarcopenia. 2) Review the potential clinical impact of screening for sarcopenia at the point of imaging care. 3) Highlight practical pearls and pitfalls for diagnostic imagers using opportunistic CT to screen for sarcopenia.

#### ABSTRACT

This session will focus on the state-of-art imaging of sarcopenia and provide a clinical context by discussing the epidemiology, pathophysiology, consequences, and future directions in the field of sarcopenia. Our goal is to provide radiologists with the foundation needed to help evaluate patients affected by this clinically relevant and increasingly common diagnosis.

# RC104C Bone CT: Opportunities for Osteoporosis

#### Participants

Robert J. Ward, MD, Boston, MA (Presenter) Nothing to Disclose

For information about this presentation, contact:

### robert.ward@tufts.edu

# LEARNING OBJECTIVES

1) To apply currently available CT technologies, both retrospective and prospective, for the identification of patients at risk for osteoporosis in their daily practice.

# RC104D Fat CT: From Research to Patient Care

Participants Miriam A. Bredella, MD, Boston, MA (*Presenter*) Nothing to Disclose

For information about this presentation, contact:

mbredella@mgh.harvard.edu

### LEARNING OBJECTIVES

1) Be familiar with assessment of abdominal and intermuscular fat compartments and fat depots in the head and neck using CT. 2) Understand the effects of different fat compartments on cardiometabolic risk. 3) Be familiar with the bone-fat connection.

### RC104E Machine Learning for Body Composition

Participants

Martin Torriani, MD, Lincoln, MA (Presenter) Nothing to Disclose

For information about this presentation, contact:

mtorriani@mgh.harvard.edu

# LEARNING OBJECTIVES

1) Understand basic concepts of artificial intelligence and machine learning. 2) Understand how such techniques can extract body composition data from images. 3) Discuss other applications of machine learning in body composition.

# RC104F Osteosarcopenic Obesity: Why Bother

Participants Leon Lenchik, MD, Winston-Salem, NC (*Presenter*) Nothing to Disclose

For information about this presentation, contact:

llenchik@wakehealth.edu

### **LEARNING OBJECTIVES**

1) Define osteosarcopenic obesity.



### Update on Imaging in Dementia

Sunday, Nov. 25 2:00PM - 3:30PM Room: E451A



AMA PRA Category 1 Credits ™: 1.50 ARRT Category A+ Credit: 1.75

#### **Participants**

Cyrus Raji, MD, PhD, St. Louis, MO (*Moderator*) Consultant, Brainreader ApS Jody L. Tanabe, MD, Aurora, CO (*Moderator*) Nothing to Disclose

#### For information about this presentation, contact:

cyrusraji@gmail.com

jody.tanabe@ucdenver.edu

### LEARNING OBJECTIVES

1) Enhance radiologist understanding in current clinical applications of structural and functional hippocampal imaging in Alzheimer's disease. 2) Overview MR imaging findings in non-Alzheimer's causes of dementia such as Creutzfeldt-Jakob disease and normal pressure hydrocephalus. 3) Update radiologists about neuronuclear techniques in Alzheimer's disease such as FDG PET and amyloid PET. 4) Overview correlative structural and functional neuroimaging findings in the neuropsychological characterization of dementia with a focus on non-Alzheimer's dementia such as frontal temporal dementia.

#### Sub-Events

### RC105A Advanced Hippocampal Neuroimaging in Alzheimer's Disease

#### Participants

Michael M. Zeineh, PhD, MD, Stanford, CA (Presenter) Research funded, General Electric Company; Consultant, Biogen Idec Inc

#### LEARNING OBJECTIVES

1) Describe the benefits of advanced forms of imaging (e.g. 7T MRI, DTI, fMRI). 2) Identify major issues around neuroimaging in AD. C) Appraise potential benefits of advanced neuroimaging in AD.

# RC105B Non-Alzheimer's Causes of Dementia: Focus on CJD and NPH

Participants Leo P. Sugrue, MD, PhD, San Francisco, CA (*Presenter*) Nothing to Disclose

# LEARNING OBJECTIVES

1) To use clinical history to narrow the dementia differential. 2) To identify imaging findings in CJD. 3) To recognize CJD mimics. 4) To identify imaging findings in NPH. 5) To explain the difference between NPH and communicating hydrocephalus.

# RC105C Neuronuclear Imaging in Alzheimer's with FDG and Amyloid PET

Participants

James M. Mountz, MD, PhD, Pittsburgh, PA (Presenter) Nothing to Disclose

For information about this presentation, contact:

mountzjm@upmc.edu

# LEARNING OBJECTIVES

1) To describe the physiologic characteristics of F-18 FDG and Amyloid imaging binding agents as it's related to imaging findings in dementia. 2) To explain the imaging methods and scan findings that are obtained in normal and Alzheimer's disease patients as compared to normal controls. 3) To show imaging characteristics in other dementias that have cognitive symptomatology which are similar to those of patients with Alzheimer's disease.

# RC105D The Clinical Classifications, Diagnostic Dilemmas, and the Impetus for Imaging Biomarkers in Dementia

Participants

John L. Ulmer, MD, Milwaukee, WI (*Presenter*) Stockholder, Prism Clinical Imaging, Inc; Medical Advisory Board, General Electric Company

# For information about this presentation, contact:

julmer@mcw.edu

# LEARNING OBJECTIVES

1) To familiarize with current classification of Alzheimer's Disease and Frontotemporal Lobe Degeneration. 2) Come to know the challenges faced by Neurologist and Neuropsychologist in diagnosing dementias. 3) Understand potential for imaging biomarkers in supporting diagnosis of Alzheimer's Disease and Frontotemporal lobe dementias.

# Active Handout:John L. Ulmer

http://abstract.rsna.org/uploads/2018/18002521/Clinical Classifications, Diagnostic Dilemmas RC105D.pdf



### **The Cranial Nerves**

Sunday, Nov. 25 2:00PM - 3:30PM Room: S402AB

# HN NR

AMA PRA Category 1 Credits <sup>™</sup>: 1.50 ARRT Category A+ Credit: 1.75

#### For information about this presentation, contact:

shatzkes@hotmail.com

#### Sub-Events

# RC106A Cranial Nerves 1 through 6 Minus 5

Participants

Ilona M. Schmalfuss, MD, Gainesville, FL (Presenter) Nothing to Disclose

### For information about this presentation, contact:

schmai@radiology.ufl.edu

#### LEARNING OBJECTIVES

1) Describe the location and course of cranial nerves 1, 2, 3, 4, and 6 and their relation to pertinent adjacent anatomical structures. 2) Analyze CT or MR imaging studies to determine the most likely diagnosis causing the neuropathy.

# RC106B The Trigeminal Nerve

Participants

Deborah L. Reede, MD, Brooklyn, NY (Presenter) Nothing to Disclose

### LEARNING OBJECTIVES

1) Identify the location of the trigeminal nerve on cross-sectional imaging. 2) Describe clinical and imaging findings of common pathologies that involve the nerve. 3) Recommend imaging protocols based on clinical findings.

#### RC106C Cranial Nerves 7 and 8

Participants

Phillip R. Chapman, MD, Birmingham, AL (Presenter) Nothing to Disclose

# LEARNING OBJECTIVES

1) Discuss the relevant anatomy of the 7th (Facial) and 8th (Vestibulocochlear) cranial nerves, particularly in the cerebellopontine angle and internal auditory canal. 2) Outline the relatively complex course of the facial nerve through the temporal bone. 3) Briefly describe function of the facial nerve and vestibulocochlear nerves. 4) Present clinical cases that demonstrate the utilization of MRI and CT in pathologic conditions of the 7th and 8th cranial nerves.

# RC106D Cranial Nerves 9 through 12

Participants Ashok Srinivasan, MD, Canton, MI (*Presenter*) Nothing to Disclose

For information about this presentation, contact:

ashoks@med.umich.edu

# LEARNING OBJECTIVES

1) To review applied anatomy and imaging techniques pertaining to cranial nerves 9 through 12. 2) To discuss imaging features of pathologies involving cranial nerves 9 through 12.



Advances in Imaging of Small Incidental Renal Masses (Including Cancers): Implications for Management

Sunday, Nov. 25 2:00PM - 3:30PM Room: E353B



AMA PRA Category 1 Credits ™: 1.50 ARRT Category A+ Credit: 1.75

# Participants

Matthew S. Davenport, MD, Ann Arbor, MI (*Moderator*) Nothing to Disclose Nicole M. Hindman, MD, New York, NY (*Presenter*) Nothing to Disclose Matthew S. Davenport, MD, Ann Arbor, MI (*Presenter*) Nothing to Disclose Nicola Schieda, MD, Ottawa, ON (*Presenter*) Nothing to Disclose Stuart G. Silverman, MD, Brookline, MA (*Presenter*) Nothing to Disclose

### For information about this presentation, contact:

nschieda@toh.on.ca

sgsilverman@partners.org

matdaven@med.umich.edu

nicole.hindman@nyumc.org

# LEARNING OBJECTIVES

1) Recommend appropriate management for the incidental renal mass using the latest guidelines. 2) Generate a comprehensive evaluation of indeterminate renal masses using a novel structured report. 3) Predict malignant subtypes of renal cancers (and differentiate from benign masses) using new developments in CT and MRI. 4) Manage small renal masses, including select renal cancers, with active surveillance based on imaging and biopsy.



# Imaging of Musculoskeletal Injuries (Interactive Session)

Sunday, Nov. 25 2:00PM - 3:30PM Room: E451B



AMA PRA Category 1 Credits ™: 1.50 ARRT Category A+ Credit: 1.75

#### Participants

Manickam Kumaravel, MD, FRCR, Houston, TX (Moderator) Nothing to Disclose

#### LEARNING OBJECTIVES

1) The learner will be exposed to a wide gamut of common and uncommon presentation of soft tissue and subtle bony injuries of the ankle and hind foot. Injuries will be elucidated with CT and MRI. 2) Understand in depth the normal anatomy of the ankle and hind foot on CT and MRI. 3) Appreciate subtle and catastrophic injury patterns of the ankle and hind foot. 4) Evaluate post-operative imaging. 5) Effectively utilize CT and MRI in management of patients with ankle and hind foot injuries. 6) To understand the anatomy and biomechanics of hip joint. 2) To recognize easily missed injuries. 7) To review common hip injuries. 8) Describe normal elbow anatomy. 9) Identify subtle and catastrophic injury patterns to elbow. 10) Recommend CT or MR when appropriate. 11) Detect imaging abnormalities commonly seen in the hand and wrist in the emergency setting. 12) Identify commonly encountered hand and wrist pathology in the emergency setting. 13) Recommend appropriate follow up for various findings in the hand and wrist in the emergency setting.

#### **GENERAL INFORMATION**

This interactive session will use RSNA Diagnosis Live<sup>™</sup>. Please bring your charged mobile wireless device (phone, tablet or laptop) to participate.

# Sub-Events

#### RC108A Ankle & Hindfoot

Participants Manickam Kumaravel, MD, FRCR, Houston, TX (*Presenter*) Nothing to Disclose

# For information about this presentation, contact:

manickam.kumaravel@uth.tmc.edu

#### LEARNING OBJECTIVES

1) The learner will be exposed to a wide gamut of common and uncommon presentation of soft tissue and subtle bony injuries of the ankle and hind foot. Injuries will be elucidated with CT and MRI. 2) Understand in depth the normal anatomy of the ankle and hind foot on CT and MRI. 2) Appreciate subtle and catastrophic injury patterns of the ankle and hind foot. 3) Evaluate post-operative imaging. 4) Effectively utilize CT and MRI in management of patients with ankle and hind foot injuries.

#### RC108B Hip

Participants Bharti Khurana, MD, Boston, MA (*Presenter*) Nothing to Disclose

### For information about this presentation, contact:

bkhurana@bwh.harvard.edu

### LEARNING OBJECTIVES

1) To understand the anatomy and biomechanics of hip joint. 2) To recognize easily missed injuries. 3) To review common hip injuries.

#### **Honored Educators**

Presenters or authors on this event have been recognized as RSNA Honored Educators for participating in multiple qualifying educational activities. Honored Educators are invested in furthering the profession of radiology by delivering high-quality educational content in their field of study. Learn how you can become an honored educator by visiting the website at: https://www.rsna.org/Honored-Educator-Award/ Bharti Khurana, MD - 2014 Honored EducatorBharti Khurana, MD - 2018 Honored Educator

# RC108C Elbow

Participants

Claire K. Sandstrom, MD, Seattle, WA (*Presenter*) Royalties, Cambridge University Press; Spouse, Advisory Board, BTG International Ltd;

#### **LEARNING OBJECTIVES**

1) Deceribe normal allow anatoms 2) Identify cubile and estactrophic injury nattoms to allow 2) Decommond CT or MD when

1) Describe normal endow anatomy. 2) Identity subcle and catastrophic injury patterns to endow. 5) Recommend of or MR when appropriate.

# RC108D Wrist & Hand

Participants Jonathan A. Flug, MD, MBA, Phoenix, AZ (*Presenter*) Nothing to Disclose

# For information about this presentation, contact:

flug.jonathan@mayo.edu

### LEARNING OBJECTIVES

1) Detect imaging abnormalities commonly seen in the hand and wrist in the emergency setting. 2) Identify commonly encountered hand and wrist pathology in the emergency setting. 3) Recommend appropriate follow up for various findings in the hand and wrist in the emergency setting.



# Abbreviated/Faster MRI Abdominal Pelvic Protocols

Sunday, Nov. 25 2:00PM - 3:30PM Room: S102CD



AMA PRA Category 1 Credits ™: 1.50 ARRT Category A+ Credit: 1.75

FDA Discussions may include off-label uses.

#### Participants

Judy Yee, MD, Bronx, NY (Moderator) Research Grant, EchoPixel, Inc; Research Grant, Koninklijke Philips NV;

For information about this presentation, contact:

jyee@montefiore.org

#### Sub-Events

# RC109A Hepatocellular Carcinoma Screening

Participants

Claude B. Sirlin, MD, San Diego, CA (*Presenter*) Research Grant, Gilead Sciences, Inc; Research Grant, General Electric Company; Research Grant, Siemens AG; Research Grant, Bayer AG; Research Grant, ACR Innovation; Research Grant, Koninklijke Philips NV; Research Grant, Celgene Corporation; Consultant, General Electric Company; Consultant, Bayer AG; Consultant, Boehringer Ingelheim GmbH; Consultant, AMRA AB; Consultant, Fulcrum Therapeutics; Consultant, IBM Corporation; Consultant, Exact Sciences Corporation; Advisory Board, AMRA AB; Advisory Board, Guerbet SA; Advisory Board, VirtualScopics, Inc; Speakers Bureau, General Electric Company; Author, Medscape, LLC; Author, Resoundant, Inc; Lab service agreement, Gilead Sciences, Inc; Lab service agreement, ICON plc; Lab service agreement, Intercept Pharmaceuticals, Inc; Lab service agreement, Shire plc; Lab service agreement, Takeda Pharmaceutical Company Limited; Lab service agreement, sanofi-aventis Group; Lab service agreement, Johnson & Johnson; Lab service agreement, NuSirt Biopharma, Inc ; Contract, Epigenomics; Contract, Arterys Inc

### For information about this presentation, contact:

csirlin@ucsd.edu

#### LEARNING OBJECTIVES

1) Explain the need for HCC screening in adults with cirrhosis. 2) Explain the limitations of ultrasound for HCC screening in adults with cirrhosis, in particular adults with overweight or obesity. 3) Explain one approach for abbreviated MRI for HCC screening as a potential alternative to ultrasound.

### RC109B Pancreatic IPMN Evaluation and Follow-up

Participants

Ivan Pedrosa, MD, Dallas, TX (Presenter) Nothing to Disclose

For information about this presentation, contact:

ivan.pedrosa@utsouthwestern.edu

### LEARNING OBJECTIVES

1) Describe the epidemiology of pancreatic cysts and the clinical outcomes in patients with this condition. 2) Explain the basis of a succinct but comprehensive MRI protocol for evaluation and follow up of pancreatic cysts. 3) Describe new MRI technologies that allow for a marked decreased in total exam time.

# RC109C MR Enterography

Participants Michael S. Gee, MD, PhD, Boston, MA (*Presenter*) Nothing to Disclose

For information about this presentation, contact:

#### msgee@mgh.harvard.edu

#### **LEARNING OBJECTIVES**

1) To comprehend the indications for MR enterography. 2) To apply structured interpretation and reporting of MR enterography studies. 3) To apply new techniques for decreasing MR enterography scan time.

#### RC109D Rectal Cancer Staging

Participants Marc J. Gollub, MD, New York, NY (*Presenter*) Nothing to Disclose gollubm@mskcc.org

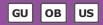
### LEARNING OBJECTIVES

1) Understand the technical and quality requirements to result in a diagnostic rectal MRI. 2) Develop an approach to interpreting images to cover key staging questions. 3) Arrive at an accurate T-category and N-category using known criteria. 4) Describe CRM, tumor location w/r/t the sphincter apparatus and the peritoneal reflection. 5) Be aware of limitations in baseline staging.



### Second and Third Trimester Obstetrical Ultrasound

Sunday, Nov. 25 2:00PM - 3:30PM Room: N228



AMA PRA Category 1 Credits <sup>™</sup>: 1.50 ARRT Category A+ Credit: 1.75

### LEARNING OBJECTIVES

1) Understand how measurements can be used in obstetrical ultrasound. 2) Know which measurements should be used routinely in obstetrical ultrasound. 3) Know how to determine gestational age and estimate fetal weight. 4) To diagnose placenta previa. 5) To diagnose vasa previa. 6) To diagnose morbidly adherent placenta. 6) Identify chorionicity and amnionicity in multiple gestations. 7) Detect complications of monochorionic placentation. 8 Identify those cases that need referral for prenatal intervention.

#### Sub-Events

# RC110A OB Measurements

Participants Peter M. Doubilet, MD, PhD, Boston, MA (*Presenter*) Nothing to Disclose

For information about this presentation, contact:

pdoubilet@bwh.harvard.edu

### LEARNING OBJECTIVES

1) Understand how measurements can be used in obstetrical ultrasound. 2) Know which measurements should be used routinely in obstetrical ultrasound. 3) Know how to determine gestational age and estimate fetal weight.

#### **Active Handout:Peter Michael Doubilet**

http://abstract.rsna.org/uploads/2018/18000732/OB measurements RC110A.pdf

# RC110B Pregnancy Support Structures: Placenta and Umbilical Cord

Participants Paula J. Woodward, MD, Salt Lake City, UT (*Presenter*) Editor, Reed Elsevier

#### For information about this presentation, contact:

paula.woodward@hsc.utah.edu

### LEARNING OBJECTIVES

1) To diagnose placenta previa. 2) To diagnose vasa previa. 3) To diagnose morbidly adherent placenta.

#### ABSTRACT

The placenta and umbilical cord are quite literally the lifeline for the developing fetus. Abnormalities in either can adversely affect the pregnancy and pose a significant risk of morbidity or mortality to either the fetus or mother at the time of delivery.

### RC110C Multiple Gestations

Participants

Anne M. Kennedy, MD, Salt Lake City, UT (Presenter) Author with royalties, Reed Elsevier

# LEARNING OBJECTIVES

1) Identify chorionicity and amnionicity in multiple gestations. 2) Detect complications of monochorionic placentation. 3) Identify those cases that need referral for prenatal intervention.

### Active Handout: Anne M. Kennedy

http://abstract.rsna.org/uploads/2018/18000734/RSNA 2018 Twins Refresher Course FINAL RC110C.pdf

# **Honored Educators**

Presenters or authors on this event have been recognized as RSNA Honored Educators for participating in multiple qualifying educational activities. Honored Educators are invested in furthering the profession of radiology by delivering high-quality educational content in their field of study. Learn how you can become an honored educator by visiting the website at: https://www.rsna.org/Honored-Educator-Award/ Anne M. Kennedy, MD - 2016 Honored EducatorAnne M. Kennedy, MD - 2018 Honored Educator



#### **Update on Radionuclide Therapies**

Sunday, Nov. 25 2:00PM - 3:30PM Room: S505AB



AMA PRA Category 1 Credits <sup>™</sup>: 1.50 ARRT Category A+ Credit: 1.75

**FDA** Discussions may include off-label uses.

#### Sub-Events

# RC111A New Guidelines for I-131 Therapy of Thyroid Cancer

Participants

Don C. Yoo, MD, E Greenwich, RI (Presenter) Consultant, Endocyte, Inc

# For information about this presentation, contact:

dyoo@lifespan.org

## **LEARNING OBJECTIVES**

1) Describe why thyroid cancer is increasing. 2) Review guidelines for the use of I-131 in the treatment of thyroid cancer. 3) Review the controversies in thyroid cancer treatment.

#### ABSTRACT

The purpose of this educational activity is to review the reasons why the incidence of thyroid cancer has risen so rapidly over the last 40 years and discuss the role of radioiodine ablation in patients with thyroid cancer. Issues that will be discussed include controversies in the extent of thyroid surgery and the appropriate use of radioiodine ablation in patients with thyroid cancer which is controversial in low risk and intermediate risk patients. The incidence of thyroid cancer in the United States has almost tripled since the early 1970s with unchanged mortality principally due to overdiagnosis. The extent of surgery performed for thyroid cancer is controversial especially in small cancers but only patients with complete thyroidectomy are candidates for radioiodine ablation. Recently lower doses of I-131 have been shown to be effective for radioiodine ablation of remnant thyroid tissue after thyroidectomy. High risk patients will benefit from radioidine ablation with decreased recurrence and improved mortality. Radioidine ablation in low risk patients is very controversial and has not been shown to improve mortality.

# RC111B Lu177-DOTATATE Therapy for Neuroendocrine Tumors

Participants

Salvador Borges-Neto, MD, Durham, NC (Presenter) Grant, General Electric Company

#### For information about this presentation, contact:

borge001@mc.duke.edu

## **LEARNING OBJECTIVES**

1) Learn the objectives and indications of the Lu-177 DOTATATE treatment. 2) Learn the short term and long term side effects of the Lu-177 treatment. 3) Learn how to set up this treatment modality at one's center.

# RC111C Hepatic Artery Infusion Therapy with Y90 Microspheres

Participants

Charles Y. Kim, MD, Durham, NC (Presenter) Consultant, Merit Medical Systems, Inc; Consultant, Cook Group Incorporated

## LEARNING OBJECTIVES

1) Review range of malignancies treated with Y90 microsphere infusion. 2) Discuss the types of Y90 therapy and dosimetric considerations. 3) Describe the procedures and technical steps involved in Y90 therapy. 4) Recognize pertinent scintigraphic findings associated with Y90 therapy.

#### ABSTRACT

Intra-arterial Yttrium-90 (Y90) therapy is an important treatment modality for a variety of hepatic tumors. While numerous types of embolotherapies are employed by interventional radiologists for treatment of cancer, Y90 therapy is unique in its multimodality and multi-procedural nature. Not only does this treatment effect rely on deposited ionizing radiation therapy, but scintigraphic imaging is also an integral component of treatment. Two types of Y90 therapies are available, made by two different manufacturers. The differences between the two types are subtle, but there are differences in administration and manufacturer-recommended dosimetric calculation. These various differences will be highlighted. Y90 therapy is comprised of several steps and is frequently subclassified into a 'planning' phase and 'treatment' phase. In the planning phase, detailed angiographic imaging is performed to delineate arterial anatomy , determine tumoral distributions, and redistribute vascular flow if indicated. Scintigraphic imaging is an integral component of this planning phase, in order to help identify angiographically occult arterial anomalies, confirm appropriate infusion site, and to quantify the hepatopulmonary shunt fraction. From this information, as well as other factors, the appropriate treatment doses can be determined. In the treatment phase(s), the Y90 dose is administered to the appropriate portions of the

liver with subsequent scintigraphic imaging for confirmation.



## **CTA for TAVR and Other Aortic Valve Replacements**

Sunday, Nov. 25 2:00PM - 3:30PM Room: N230B



AMA PRA Category 1 Credits ™: 1.50 ARRT Category A+ Credit: 1.75

#### Participants

Jonathon A. Leipsic, MD, Vancouver, BC (*Moderator*) Speakers Bureau, General Electric Company; Speakers Bureau, Edwards Lifesciences Corporation; Consultant, Heartflow, Inc; Consultant, Circle Cardiovascular Imaging Inc; Consultant, Edwards Lifesciences Corporation; Consultant, Neovasc Inc; Consultant, Samsung Electronics Co, Ltd; Consultant, Koninklijke Philips NV; Consultant, Arineta Ltd; Consultant, Pi-Cardia Ltd;

Jean Jeudy JR, MD, Baltimore, MD (Moderator) Nothing to Disclose

#### For information about this presentation, contact:

jleipsic@providencehealth.bc.ca

jjeudy@som.umaryland.edu

#### Sub-Events

#### RC112A Pre-TAVR CT Imaging Protocols

#### Participants

Stefan L. Zimmerman, MD, Ellicott City, MD (*Presenter*) Project consultant, Siemens Healthcare; Research grant, American Heart Association;

#### **LEARNING OBJECTIVES**

1) To review CT imaging requirements for TAVR planning. 2) To provide an overview of default acquisition protocols to ensure robust CT image quality with various CT systems. 3) To provide tips and tricks of how to image challenging patients with renal failure or atrial fibrillation.

#### **Honored Educators**

Presenters or authors on this event have been recognized as RSNA Honored Educators for participating in multiple qualifying educational activities. Honored Educators are invested in furthering the profession of radiology by delivering high-quality educational content in their field of study. Learn how you can become an honored educator by visiting the website at: https://www.rsna.org/Honored-Educator-Award/ Stefan L. Zimmerman, MD - 2012 Honored EducatorStefan L. Zimmerman, MD - 2015 Honored Educator

# RC112B CTA for Sizing Transcatheter Heart Valves

#### Participants

Jonathon A. Leipsic, MD, Vancouver, BC (*Presenter*) Speakers Bureau, General Electric Company; Speakers Bureau, Edwards Lifesciences Corporation; Consultant, Heartflow, Inc; Consultant, Circle Cardiovascular Imaging Inc; Consultant, Edwards Lifesciences Corporation; Consultant, Neovasc Inc; Consultant, Samsung Electronics Co, Ltd; Consultant, Koninklijke Philips NV; Consultant, Arineta Ltd; Consultant, Pi-Cardia Ltd;

## For information about this presentation, contact:

jleipsic@providencehealth.bc.ca

# LEARNING OBJECTIVES

1) Discuss the importance of reproducible and accurate annular anatomical definition. 2) Define the meaning of oversizing in device selection and the role that capture and sealing have to optimize clinical outcomes. 3) Discuss the importance of appropriate sizing to optimize clinical outcomes.

#### **Honored Educators**

Presenters or authors on this event have been recognized as RSNA Honored Educators for participating in multiple qualifying educational activities. Honored Educators are invested in furthering the profession of radiology by delivering high-quality educational content in their field of study. Learn how you can become an honored educator by visiting the website at: https://www.rsna.org/Honored-Educator-Award/ Jonathon A. Leipsic, MD - 2015 Honored Educator

#### RC112C Aortic Valve Assessment in the Post-TAVR Patient

Participants

Jean Jeudy JR, MD, Baltimore, MD (Presenter) Nothing to Disclose

For information about this presentation, contact:

# RC112D CT for the Evaluation of Surgical Bioprostheses

Participants

Dominika Sucha, MD, PhD, Utrecht, Netherlands (Presenter) Nothing to Disclose

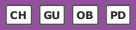
# LEARNING OBJECTIVES

1) To understand differences in surgical bioprostheses and learn to appreciate normal CT findings after surgical implantation. 2) To review the underlying pathology in biovalve dysfunction and the role of CT. 3) To learn what the surgeon and cardiologist want to know for clinical decision-making. 4) To discuss latest literature and developments.



# Pediatric Series: Fetal/Neonatal Imaging

Sunday, Nov. 25 2:00PM - 3:30PM Room: E352



AMA PRA Category 1 Credits ™: 1.50 ARRT Category A+ Credit: 1.75

#### **Participants**

Amy R. Mehollin-Ray, MD, Pearland, TX (*Moderator*) Nothing to Disclose Carol E. Barnewolt, MD, Boston, MA (*Moderator*) Nothing to Disclose

For information about this presentation, contact:

armeholl@texaschildrens.org

Sub-Events

# RC113-01 Imaging of Congenital Lung Malformation

Sunday, Nov. 25 2:00PM - 2:20PM Room: E352

Participants

Amy R. Mehollin-Ray, MD, Pearland, TX (Presenter) Nothing to Disclose

For information about this presentation, contact:

armeholl@texaschildrens.org

## LEARNING OBJECTIVES

1) Describe the various types of congenital lung malformations and characteristic prenatal imaging findings. 2) Understand the pathophysiology of abnormal lung development and how it impacts lesion appearance and behavior. 3) Discuss the management implications for appropriate prospective designation of lesions based on imaging.

# RC113-02 Quantitative Assessment of Posterior Fossa Malformations in Fetal MRI

Sunday, Nov. 25 2:20PM - 2:30PM Room: E352

Participants

Gregor O. Dovjak, MD, Vienna, Austria (*Presenter*) Nothing to Disclose Mariana G. Diogo, MD, Lisboa, Portugal (*Abstract Co-Author*) Nothing to Disclose Gerlinde Gruber, Vienna, Austria (*Abstract Co-Author*) Nothing to Disclose Peter C. Brugger, MD, PhD, Vienna, Austria (*Abstract Co-Author*) Nothing to Disclose Daniela Prayer, MD, Vienna, Austria (*Abstract Co-Author*) Nothing to Disclose Gregor Kasprian, MD, Vienna, Austria (*Abstract Co-Author*) Nothing to Disclose

## For information about this presentation, contact:

Gregor.Dovjak@meduniwien.ac.at

# PURPOSE

Assessment of posterior fossa malformations with fetal MRI after screening ultrasound is frequently demanded. Recently it has been shown, that fetal vermian lobules can be evaluated in detail by fetal neuroimaging. This fetal MRI study aimed to systematically segment rhombencephalic structures in common posterior fossa anomalies. The aim of the study was to determine which of the quantitative parameters is suitable to distinguish between a favorable and a less favorable outcome group.

# METHOD AND MATERIALS

Group 1 (29 cases) included prenatal cases with a favorable outcome (Blake's pouch and Megacisterna magna) with a gestational age (GA) of  $26.18\pm4.72$  (mean GA  $\pm$  standard deviation). Group 2 (33 cases, GA of  $23.38\pm5.29$ ) included the classical Dandy Walker malformation and other cystic posterior fossa malformations, known to be associated with a less favorable neurocognitive outcome. The number of vermian lobules, the brainstem-vermian angle, vermian and brainstem area (in mm<sup>2</sup>) and the vermis-brainstem ratio were assessed using an optimal T2-weighted median sagittal slice (resolution ranging from .57/.57/3.3 to 1.17/1.17/4.4). The parameters were compared with two-sided t-tests between the two groups.

## RESULTS

All evaluated parameters were significantly different between the two groups. The number of lobules was  $5.69\pm0.95$  (mean  $\pm$  standard deviation) in group 1 vs  $3.91\pm1.31$  in group 2 (p<0.001). The brainstem-vermian angle also differed significantly with 7.93 $\pm10.86$  vs 72.24 $\pm27.52$  (p<0.001). The vermian size was 118.68 $\pm66.83$  vs 54.41 $\pm34.41$  (p<0.001). The brainstem size was 174.97 $\pm69.24$  vs 121.65 $\pm51.62$  (p=0.002). The vermis-brainstem ratio was 64.24 $\pm16.47$  vs 42.22 $\pm11.96$  (p<0.001).

#### CONCLUSION

Resinctem and vermian hiematry provide objective and quantitative measures, which significantly differ hetween favorable and pon-

favorable neurodevelopmental outcome groups. Assessment of vermian lobulation (number and morphology) allows further characterization of cystic posterior fossa malformations, given optimal fetal MR imaging conditions.

## **CLINICAL RELEVANCE/APPLICATION**

Due to the functional importance of the brainstem and the cerebellar vermis, fetal MR based biometry is a promising tool in the prognostic assessment of hindbrain malformations.

## RC113-03 Fetal Cardiac MRI in the Evaluation of Double and Right Aortic Arch

Sunday, Nov. 25 2:30PM - 2:40PM Room: E352

Participants

Su-Zhen Dong, MD,PhD, Shanghai, China (*Presenter*) Nothing to Disclose Ming Zhu, Shanghai, China (*Abstract Co-Author*) Nothing to Disclose

For information about this presentation, contact:

dongsuzhen@126.com

## PURPOSE

Right aortic arch (RAA) refers to a congenital abnormal position of the aortic arch to the right of the trachea. The aim of this study was to evaluate the feasibility of fetal cardiac magnetic resonance (CMR) in the assessment of fetal double and right aortic arch.

#### **METHOD AND MATERIALS**

This retrospective review included 148 pregnant women (21-32 weeks gestation mean 24 weeks) referred to a children's hospital for a fetal cardiac MRI from June 2005 to December 2017 due to the finding of a cardiovascular anomaly by fetal echocardiogram (echo) performed by a cardiologist or due to a technically limited echo. CMR was performed using 1.5T or 3.0 T unit. Sequences included steady-state free-precession (SSFP); non gated SSFP cine, single-shot turbo spin echo (SSTSE) and non-gated phase contrast (PC) cine sequences. Sequences included transverse fetal thorax, and four-chamber, short-axis, coronal and oblique sagittal planes of the fetal heart when possible. The radiologists were not blinded to the echo findings. Echo and CMR findings were compared with postnatal imaging and/or surgery.

#### RESULTS

Anomalies identified by CMR included double aortic arch (DAA) (n=36), right aortic arch (RAA) with aberrant left subclavian artery (LSCA) (n=52), RAA with mirror image branching (n=48), RAA with right ductus arteriosus (RDA) (n=6, 4 with other cardiovascular defects), RAA with mirror image branching with retroesophageal ductus (n=6). 93.8% (45/48) RAA with mirror image branching had additional congenital intracardiac anomalies better seen by fetal echo. The remaining were not associated with additional congenital heart defect. 75.7% (112/148) arch anomalies were correctly diagnosed by fetal echo, while Fetal CMR was correct in 87.8% (130/148). 18 arch anomalies were missed by fetal echo but identified by MRI and confirmed postnatally, echos were technically limited in 6 cases due to maternal obesity, oligohydramnios, fetal position, twins. The cases echo missed/misdignosed included DAA (n=7), RAA with aberrant LSCA (n=4), RAA with mirror image branching (n=1), RAA with RDA (n=3), RAA with mirror image branching with retroesophageal ductus (n=3).

#### CONCLUSION

Fetal cardiac MRI can provide additional diagnostic information for fetal DAA and RAA and can be a useful adjunct.

#### **CLINICAL RELEVANCE/APPLICATION**

Fetal cardiac MRI can provide accurate diagnostic information for fetal DAA and RAA and is recommended as an adjunct to fetal echocardiography.

# RC113-04 MR Imaging of Retroplacental Clear Space during the Course of Gestation in Pregnant Mice

Sunday, Nov. 25 2:40PM - 2:50PM Room: E352

#### Participants

Andrew A. Badachhape, PhD, Houston, TX (*Presenter*) Nothing to Disclose Ketan B. Ghaghada, PhD, Houston, TX (*Abstract Co-Author*) Research Consultant, Alzeca Biosciences, LLC Igor Stupin, Houston, TX (*Abstract Co-Author*) Nothing to Disclose Mayank Srivastava, PhD, Houston, TX (*Abstract Co-Author*) Nothing to Disclose Laxman Devkota, PhD, Houston, TX (*Abstract Co-Author*) Nothing to Disclose Verghese George, MBBS, Houston, TX (*Abstract Co-Author*) Nothing to Disclose Eric Tanifum, PhD, Houston, TX (*Abstract Co-Author*) Consultant, Alzeca Bioscoences, LLC Ananth Annapragada, PhD, Houston, TX (*Abstract Co-Author*) Stockholder, Alzeca Biosciences, LLC Stockholder, Sensulin, LLC Stockholder, Abbott Laboratories Stockholder, Johnson & Johnson

#### For information about this presentation, contact:

badachha@bcm.edu

#### PURPOSE

Visualization of the retroplacental clear space is critical for the diagnosis of invasive placentation. In this pre-clinical study, we evaluated MR imaging of the retroplacental clear space during the course of gestation in a mouse model using a liposomal-Gd contrast agent that has been shown to not penetrate the placental barrier.

# **METHOD AND MATERIALS**

In vivo studies were performed in pregnant C57BL/6 mice (8-10 week age at start of pregnancy). MR imaging was performed on a 1T permanent magnet scanner. Imaging was performed at five time points during the second half of gestation (e10.5, e12.5, e14.5, e16.5, and e18.5 days). At each time point, pre-contrast and post-contrast images were acquired using a T1-weighted (T1w) 3D

gradient-recalled echo (GRE) sequence. Post-contrast images were acquired following intravenous administration of high T1 relaxivity liposomal-Gd (0.1 mmol Gd/kg). Images were reviewed by a radiologist and scored for the visualization of the retroplacental clear space. Contrast-to-noise ratio (CNR) were determined to quantify the visualization of the retroplacental clear space in T1w images.

#### RESULTS

Contrast-enhanced T1w images enabled the visualization of both the placenta and retroplacental clear space. The shape of the placenta at the earliest time point (e10.5) was indicative of the development phase; however, during the later imaging time points, the placenta transformed into the typical round to oval disk shape. Although the retroplacental clear space was visible at all time points, radiologist review for feature conspicuity indicated partial visibility at the first imaging time point (e10.5) and improved visibility during the mid to later stages of gestation. The CNR, determined from the analysis of retroplacental space and adjacent placenta, varied between  $12\pm3$  at e10.5 to  $24\pm6$  at e18.5.

# CONCLUSION

Contrast-enhanced MR imaging using a liposomal-Gd contrast agent enabled clear visualization of the retroplacental space in a pregnant mouse model starting as early as e12.5 day of gestation.

#### **CLINICAL RELEVANCE/APPLICATION**

Visualization of the retroplacental clear space at the early stages of pregnancy using a liposomal-Gd blood-pool contrast agent may enable early detection of invasive placentation.

# RC113-05 Personalized Management of Fetuses with Congenital Diaphragmatic Hernia with the Help of Fetal MRI

Sunday, Nov. 25 2:50PM - 3:00PM Room: E352

#### Participants

Florian Prayer, MD, Vienna, Austria (*Presenter*) Nothing to Disclose Dieter Bettelheim, Vienna, Austria (*Abstract Co-Author*) Nothing to Disclose Michael Weber, Vienna, Austria (*Abstract Co-Author*) Nothing to Disclose Gerlinde Gruber, Vienna, Austria (*Abstract Co-Author*) Nothing to Disclose Georg Langs, Vienna, Austria (*Abstract Co-Author*) Nothing to Disclose Gregor Kasprian, MD, Vienna, Austria (*Abstract Co-Author*) Nothing to Disclose Daniela Prayer, MD, Vienna, Austria (*Abstract Co-Author*) Nothing to Disclose Peter C. Brugger, MD, PhD, Vienna, Austria (*Abstract Co-Author*) Nothing to Disclose

# PURPOSE

Fetal MRI-based diaphragmatic segmentation in fetuses with congenital diaphragmatic hernia (CDH) has the potential to provide information regarding diaphragmatic defect typology and extent as well as three dimensional visualization of the diaphragmatic defect to the pediatric surgeon even during intrauterine life. This retrospective pilot study aims to determine the feasibility of fetal MRI-based manual diaphragmatic segmentation.

#### **METHOD AND MATERIALS**

22 CDH cases (gestational week 21 to 38) who had fetal MRI and diaphragmatic repair surgery performed were retrospectively identified. Manual segmentation of the fetal diaphragm and the diaphragmatic defect was performed based on routine T2-weighted TSE sequences using ITK-Snap. Surface area measurements of the diaphragm and the diaphragmatic defect were utilized to calculate diaphragmatic defect to thoracic aperture ratios. Three dimensional visualization of the fetal diaphragm was used to assign CDH typology according to Kardon et al. (Dis Model Tech 2017). Results were compared to data from surgery reports. CDH typology, diaphragmatic defect to thoracic aperture ratios, and use of patch for diaphragmatic repair were analyzed using descriptive statistics.

# RESULTS

Fetal MRI-based diaphragmatic segmentation was feasible in 90.91% (20/22) of CDH cases. In two cases excessive fetal movement did not allow segmentation. CDH typology based on three dimensional visualization of the fetal diaphragm was in accordance with information extracted from surgery reports. All CDH cases with a diaphragmatic defect to thoracic aperture ratio of more than 0.4 received diaphragmatic patch repair.

#### CONCLUSION

Routine fetal MRI-based diaphragmatic segmentation is possible in a majority of cases. Surface area measurements of the fetal diaphragm and the diaphragmatic defect may allow prediction of optimal diaphragmatic repair technique. In conclusion, this new method has the potential to provide personalized management of CDH cases.

# **CLINICAL RELEVANCE/APPLICATION**

The proposed new method can be applied on routine fetal MRI data and can provide CDH typology, extent of diaphragmatic defect, diaphragmatic defect to thoracic aperture ratio, and three dimensional visualizations to the managing team already at a stage of fetal development. Fetal MRI-based personalization of management in CDH cases is indispensable in a time of intensive research regarding tissue engineering-based therapy of CDH.

# RC113-06 Fast Temperature Mapping of the Fetal Brain During Routine 3T Fetal MR Imaging

Sunday, Nov. 25 3:00PM - 3:10PM Room: E352

Participants

Jason G. Parker, PhD, Indianapolis, IN (*Presenter*) Nothing to Disclose Emily E. Diller, MS, Indianapolis, IN (*Abstract Co-Author*) Nothing to Disclose Chang Y. Ho, MD, Indianapolis, IN (*Abstract Co-Author*) Nothing to Disclose Rupa Radhakrishnan, MD, Cincinnati, OH (*Abstract Co-Author*) Nothing to Disclose Brandon P. Brown, MD, MA, Indianapolis, IN (*Abstract Co-Author*) Nothing to Disclose

#### For information about this presentation, contact:

#### brpbrown@iupui.edu

#### PURPOSE

To develop and evaluate a rapid technique capable of quantifying the effects of RF-heating on the fetal brain during normal clinical MR scanning.

## METHOD AND MATERIALS

Patients Sixteen (16) pregnant female patients underwent clinical fetal MRI at 3T. Normal scan sequences included T1, T2, DWI, and T2\* sequences, and had a total scan time less than 60 mins. <u>Scanning sequence</u> To monitor potential heating of the fetus during MRI, temperature maps were acquired at the beginning (scan 1), mid-point (scan 2), and end of each fetal MRI (scan 3) session using a custom phase-based thermometry sequence. The thermometry sequence was designed to exploit the temperature dependence of the proton resonance frequency using a gradient-echo echo-planar imaging (GRE-EPI) technique with TR/TE: 150/8.3ms, 256x256 matrix, 5mm slice thickness, and 1mm gap. TE was chosen to maximize the SNR of brain tissue. The total acquisition time of the MR thermometry sequence was 4.3 seconds and required no special procedures to be performed by the technologist. All imaging was performed with an abdominal phased-array surface coil. <u>Image Processing</u> Phase unwrapping was performed for each acquisition using a magnitude-sorted list, multi-clustering phase unwrapping algorithm, and temperature maps were then created from the phase difference images. The mean, maximum, and standard deviation of a single whole brain ROI was calculated from the temperature maps for each patient. <u>Analysis</u> 2-way one-sample t-tests were used to investigate significant temperature changes in the ROIs at scan 2 and scan 3 compared to scan 1. A 2-way paired t-test was used to evaluate the absolute change in temperature between scan 2 and scan 3.

## RESULTS

At 3T magnetic field strengths, the maximum temperature in the brain increased significantly from scan 1 to scan 2 by an average of  $0.42 \pm .24$  °C (p=4.5\*10-6) and from scan 1 to scan 3 by an average of  $0.48 \pm .30$  °C (p=1.16\*10-5). A significant difference between scan 2 and scan 3 was not found (p=.084).

#### CONCLUSION

We have demonstrated the clinical application of a fast, MR-based temperature mapping method to monitor RF-heating of the fetal brain during routine clinical imaging.

# CLINICAL RELEVANCE/APPLICATION

RF-heating of the fetus during fetal MRI carries a theoretical risk of harm to the developing fetal brain, and this technique allows a practical method to monitor heating effects in vivo.

# RC113-07 Perinatal Imaging of the Airway

Sunday, Nov. 25 3:10PM - 3:30PM Room: E352

#### Participants

Carol E. Barnewolt, MD, Boston, MA (Presenter) Nothing to Disclose

#### LEARNING OBJECTIVES

1) To define the nature of basic congenital airway abnormalities. 2) To identify general malformation categories that may require special attention at the time of delivery. 3) To help the attendee develop a perinatal imaging strategy, with the goal of optimizing the chances of prompt airway access, in settings where challenges may be expected.



# Interventional Course (Interactive Session)

Sunday, Nov. 25 2:00PM - 3:30PM Room: S403A

IR

AMA PRA Category 1 Credits ™: 1.50 ARRT Category A+ Credit: 1.75

**FDA** Discussions may include off-label uses.

## Participants

Steven M. Zangan, MD, Chicago, IL (*Presenter*) Nothing to Disclose Rakesh C. Navuluri, MD, Chicago, IL (*Presenter*) Nothing to Disclose Kush R. Desai, MD, Chicago, IL (*Presenter*) Speakers Bureau, Cook Group Incorporated; Consultant, Cook Group Incorporated; Consultant, The Spectranetics Corporation; Consultant, AngioDynamics, Inc; Consultant, Boston Scientific Corporation

# For information about this presentation, contact:

kdesai007@northwestern.edu

RNavuluri@radiology.bsd.uchicago.edu

## **LEARNING OBJECTIVES**

1) Recognize vascular and non-vascular conditions and their image-guided treatment in the chest, abdomen and pelvis.

#### **GENERAL INFORMATION**

This interactive session will use RSNA Diagnosis Live<sup>™</sup>. Please bring your charged mobile wireless device (phone, tablet or laptop) to participate.



## **Screening for Breast Cancer**

Sunday, Nov. 25 2:00PM - 3:30PM Room: E353C

# BR

AMA PRA Category 1 Credits ™: 1.50 ARRT Category A+ Credit: 1.75

#### **Participants**

Jennifer A. Harvey, MD, Charlottesville, VA (*Moderator*) Stockholder, Hologic, Inc; Research Grant, Volpara Health Technologies Limited; Stockholder, Volpara Health Technologies Limited;

For information about this presentation, contact:

jharvey@virginia.edu

zuleyml@upmc.edu

#### Sub-Events

# RC115A Screening Data: Where Are We?

Participants

Debra L. Monticciolo, MD, Temple, TX (Presenter) Nothing to Disclose

# LEARNING OBJECTIVES

1) To review key data for breast cancer screening from randomized controlled trials and observational studies. 2) To understand the risks and benefits of mammography screening for the woman of average risk. 3) To understand the differences between various screening recommendations.

## RC115B Risk Models

Participants

Jennifer A. Harvey, MD, Charlottesville, VA (*Presenter*) Stockholder, Hologic, Inc; Research Grant, Volpara Health Technologies Limited; Stockholder, Volpara Health Technologies Limited;

#### For information about this presentation, contact:

jharvey@virginia.edu

#### LEARNING OBJECTIVES

1) Cite pros and cons of different risk models in use. 2) Describe how risk models can be used in practice. 3) List which patients at risk may not be identified using risk models.

# RC115C Personalized Screening Paradigms

Participants Wendie A. Berg, MD, PhD, Pittsburgh, PA (*Presenter*) Nothing to Disclose

#### For information about this presentation, contact:

wendieberg@gmail.com

#### **LEARNING OBJECTIVES**

1) Distinguish and define average risk, intermediate risk, and high-risk populations. 2) Understand existing recommendations for supplemental screening beyond mammography and/or screening at an earlier age. 3) Discuss potential strategies for elective supplemental screening and expected outcomes.



# Experiencing Radiology: Patients' Perspectives (Sponsored by RSNA Public Information Committee)

Sunday, Nov. 25 2:00PM - 3:30PM Room: E350

# PR

AMA PRA Category 1 Credits ™: 1.50 ARRT Category A+ Credit: 1.75

#### Participants

Mary C. Mahoney, MD, Cincinnati, OH (*Moderator*) Nothing to Disclose Jennifer L. Kemp, MD, Denver, CO (*Presenter*) Advisory Board, Koninklijke Philips NV James V. Rawson, MD, Boston, MA (*Presenter*) Nothing to Disclose Brian Godish, Elgin, IL (*Presenter*) Nothing to Disclose

## For information about this presentation, contact:

jkemp@divrad.com

## LEARNING OBJECTIVES

1) To understand the mission and goals of RSNA's *Radiology Cares: The Art of Patient-centered Practice* and ACR's *Imaging 3.0* campaigns. 2) To assess your radiology practice model and realign it to focus on value over volume. 3) To learn tactics to put the concepts of patient-centeredness and value vs. volume into practice. 4) To understand your patients' perspectives as they navigate through the healthcare continuum, especially as it relates to radiology.

#### ABSTRACT

In many healthcare facilities and institutions, the culture and actual practice of radiology have marginalized the patient. Today the call to practice patient-centered care is one of the primary drivers of change within the radiology community. The benefits include improvded patient care, improved communication between radiologists and their patients and referring physicians, and greater awareness of the essential role that radiologists play in patients' overall healthcare. The RSNA's *Radiology Cares* and ACR's *Imaging 3.0* campaigns were launched to provide tools to move the radiology profession to focus on patient-centeredness and to help transform the way radiology is practiced. This course, presented in the style of a TED Talk, will offer insights into the radiology patient mindset and describe tools to bring the concept of patient-centeredness into practice.

#### **Honored Educators**

Presenters or authors on this event have been recognized as RSNA Honored Educators for participating in multiple qualifying educational activities. Honored Educators are invested in furthering the profession of radiology by delivering high-quality educational content in their field of study. Learn how you can become an honored educator by visiting the website at: https://www.rsna.org/Honored-Educator-Award/ James V. Rawson, MD - 2017 Honored Educator



Emerging Technology: Contrast Enhanced Ultrasound - Update 2018

Sunday, Nov. 25 2:00PM - 3:30PM Room: S504CD



FDA Discussions may include off-label uses.

#### Participants

David T. Fetzer, MD, Dallas, TX (*Moderator*) Researcher, Koninklijke Philips NV; Consultant, Koninklijke Philips NV; Consultant, Siemens AG; Speakers Bureau, Koninklijke Philips NV; ;

## For information about this presentation, contact:

david.fetzer@utsouthwestern.edu

## **LEARNING OBJECTIVES**

1) Briefly introduce contrast-enhanced ultrasound (CEUS) imaging techniques, and the pharmacology of these unique agents. 2) Discuss how to start a contrast-enhanced ultrasound service in your practice. 3) Highlight how CEUS has been adopted by the ACR LI-RADS as a technique for the definitive diagnosis of HCC. 4) Explore how CEUS can enhance ultrasound-guided procedures, and may be used to monitor tumors following ablation. 5) Consider the major emerging possibilities of microbubble-directed molecular imaging and targeted therapies.

# ABSTRACT

Contrast-enhanced ultrasound (CEUS) has been recognized world-wide as a robust tool that can be applied in a variety of clinical situations, particularly given its high safety profile. With the recent FDA approval of one agent for use in liver imaging in adults, and hepatic and urological imaging in pediatrics, there has been increased acceptance and use of these techniques throughout the country. However, CEUS is not limited to the liver-the use of ultrasound contrast in a range of pathologies and situations is also possible and with a variety of agents, off-label. This session will cover the opportunities and challenges in CEUS, including a brief introduction into these unique contrast agents and the imaging techniques utilized; how to start a CEUS serviceline in your practice; how CEUS has been adopted by LI-RADS in the definitive diagnosis on HCC; how contrast may be used as a problem-solving tool and in ultrasound-guided procedures; and finally where CEUS techniques and agents may be headed in the future.

#### Sub-Events

# RC117A CEUS: A Brief Overview

#### Participants

David T. Fetzer, MD, Dallas, TX (*Presenter*) Researcher, Koninklijke Philips NV; Consultant, Koninklijke Philips NV ; Consultant, Siemens AG; Speakers Bureau, Koninklijke Philips NV; ;

#### For information about this presentation, contact:

david.fetzer@utsouthwestern.edu

# LEARNING OBJECTIVES

1) Briefly introduce ultrasound microbubble agent formulation and pharmacology. 2) Discuss the unique imaging techniques required for contrast-enhanced ultrasound (CEUS). 3) Highlight ultrasound contrast agent safety profile and contraindications.

# RC117B CEUS: Starting a Practice from Scratch

Participants Shuchi K. Rodgers, MD, Philadelphia, PA (*Presenter*) Nothing to Disclose

## For information about this presentation, contact:

## rodgerss@einstein.edu

# LEARNING OBJECTIVES

1) List the steps to start a contrast enhanced ultrasound service from scratch. 2) Describe the implementation process at a large academic center. 3) Explain CEUS tips and lessons learned from a beginner.

# RC117C CEUS: Liver Imaging and LI-RADS

Participants

Yuko Kono, MD, PhD, San Diego, CA (*Presenter*) Equipment support, Canon Medical Systems Corporation; Equipment support, General Electric Company; Contrast agent support, Lantheus Medical Imaging, Inc; Contrast agent support, Bracco Group

#### For information about this presentation, contact:

#### LEARNING OBJECTIVES

1) Understand CEUS LI-RADS will standardize technique, data collection interpretation and reporting of CEUS exams on patients at risk for HCC. 2) Describe differences of CEUS from CT/MRI. 3) Lean how to apply new CEUS LIRADS v2017 algorithm with interactive case examples.

# RC117D CEUS: Monitoring Response to Ablative Therapies

Participants

Stephanie R. Wilson, MD, Calgary, AB (*Presenter*) Equipment support, Koninklijke Philips NV; Equipment support, Siemens AG; Equipment support, Samsung Electronics Co, Ltd; Research support, Koninklijke Philips NV; Research support, Lantheus Medical Imaging, Inc; Speaker, Samsung Electronics Co, Ltd

## For information about this presentation, contact:

stephanie.wilson@ahs.ca

#### LEARNING OBJECTIVES

1) Recognize CEUS features of residual/recurrent tumor following ablative therapies. 2) Perform CEUS examinations directed at showing tumor enhancement within or AP-related to the treatment sites. 3) Identify the strengths of CEUS for these evaluations related to contrast agent sensitivity and real time dynamic scanning.

# **RC117E** CEUS: Molecular Imaging and Targeted Therapies

Participants

Andrej Lyshchik, MD, PhD, Philadelphia, PA (*Presenter*) Research support, Bracco Group; Advisory Board, Bracco Group; Research support, General Electric Company; Research support, Siemens AG; Research support, Canon Medical Systems Corporation; Speaker, SonoScape Co, Ltd

# LEARNING OBJECTIVES

1) Discuss pre-clinical and translational applications of molecular ultrasound using targeted microbubble contrast agents.



## Tumor Imaging Metrics: Is it Time to Invest in a Service?

Sunday, Nov. 25 2:00PM - 3:30PM Room: S504AB



AMA PRA Category 1 Credits ™: 1.50 ARRT Category A+ Credit: 1.75

FDA Discussions may include off-label uses.

#### Participants

Michelle S. Ginsberg, MD, New York, NY (Moderator) Nothing to Disclose

#### Sub-Events

## RC118A Current Response Assessment Tools in Clinical Trials

Participants

Les R. Folio, MPH,DO, Bethesda, MD (Presenter) Institutional research agreement, Carestream Health, Inc

For information about this presentation, contact:

Les.Folio@nih.gov

# LEARNING OBJECTIVES

 Comprehend objective tumor assessment criteria, such as RECIST 1.1, in a variety of clinical trials. 2) Exploit existing and evolving PACS along with other available image processing tools to improve tumor assessment consistency and workflow efficiency.
 Optimize radiology report value with more consistent tumor quantification.

#### ABSTRACT

Cancer patients enrolled in clinical trials require objective imaging criteria (e.g. RECIST 1.1) rarely included (in the US) in routine radiologists' clinical reports. With oncologists' need for consistent target lesion selection and measurements many cancer centers have tumor assessment core labs consisting of various radiology personnel dedicated to image processing for consistent tumor measurements, organ/lesion segmentation for volumetric quantification, display (3D) and/or density/texture analysis. There are a variety of approaches and challenges to successfully support oncologists' needs for consistent quantification. This presentation addresses the balance between measurements made in PACS that are included in radiology reports and those that are used in objective tumor assessments by core labs supporting oncologists. By comprehending the tumor assessment requirements and process, radiology reports can be more valuable to oncologists when target lesion selection and measurements are concordant with oncologists' records used to assess therapeutic response. Consistent application of existing and evolving tools, such as line, twodiameter and volumetric segmentations, can improve report value and radiology services to include tumor imaging core labs. Understanding tumor assessment terminology (e.g. response categories, such as 'Stable Disease' or 'Partial Response') can also enhance report value while minimizing the need to addend reports. A familiar example involves using words in the impression such as 'disease progression' or 'stable disease' where radiologists are usually not aware of pertinent information. For example, may not know the previously established target lesions, the criteria used, baseline date or nadir. Without this information, progressive or stable disease often cannot be concluded. Between radiologists and oncologists, communication beyond the standard radiology report can further improve with use of PACS tools such as key images and bookmark tables to label target lesions while also establishing a workflow with more consistent and concordant measurements. Improved efficiency can result from minimizing duplication in disparate systems where data does not automatically transfer (e.g. from PACS to RIS to EMR to cancer database).

RC118B Developing Robust Imaging Biomarkers for Use in Drug Development

Participants

Nina Tunariu, MD, Sutton, United Kingdom (Presenter) Nothing to Disclose

# For information about this presentation, contact:

nina.tunariu@icr.ac.uk

# LEARNING OBJECTIVES

1) To be able to understand and differentiate different types of imaging biomarkers. 2) Achieve an understanding of the use and value of imaging-based biomarkers in the various phases of clinical drug development. 3) Have a better understanding of the barriers and opportunities for using robust quantitative imaging biomarkers in oncological drug development.

# RC118C Should Every Radiology Department Invest in a Quantitative Imaging Lab?

Participants

Gordon J. Harris, PhD, Boston, MA (*Presenter*) Medical Advisory Board, Fovia, Inc; Member, IQ Medical Imaging LLC; Member, Precision Imaging Metrics, LLC; ;

For information about this presentation, contact:

gjharris@partners.org

#### LEARNING OBJECTIVES

1) Assess the pros and cons of establishing a Quantitative Imaging Lab for clinical trials image assessments. 2) Explain to Radiology Department leadership the benefits of establishing a Quantitative Imaging Lab. 3) Specify the requirements and evaluate options for implementing a Quantitative Imaging Lab.

## ABSTRACT

Managing oncology clinical trials imaging assessments can be very challenging, especially with the increasing complexity of protocols and modifications to tumor response criteria. Maintaining protocol compliance and keeping up with criteria changes can be difficult. Furthermore, all trial data must be assessed accurately and be available for data locks, monitoring visits, and audits. These challenges can be addressed through a Quantitative Imaging Lab that provides quality reviews, adequate training, and consistent tumor metrics data. This presentation will discuss our experience in developing such a service, the Tumor Imaging Metrics Core (TIMC) as a shared resource of the Dana-Farber/Harvard Cancer Center, as well as our informatics and image assessment platform that we developed to manage this complex workflow, Precision Imaging Metrics. The TIMC uses this web-based platform to manage over 1,000 active clinical trials and performs over 15,000 time point image assessments per year. In addition, seven NCI-designated Cancer Centers around the US have implemented the Precision Imaging Metrics platform to manage their clinical trials image assessments. In this presentation, we will discuss the pros and cons for a radiology department to implement a Quantitative Imaging Lab for managing clinical trials image assessments.



Near Misses and Errors in Diagnostic Radiology and Radiation Oncology: What to Do Next?

Sunday, Nov. 25 2:00PM - 3:30PM Room: S404AB



AMA PRA Category 1 Credits ™: 1.50 ARRT Category A+ Credit: 1.75

#### Participants

Abhishek A. Solanki, MD, Maywood, IL (*Moderator*) Consultant, Blue Earth Diagnostics Ltd Advisory Board, Blue Earth Diagnostics Ltd

#### Sub-Events

# RC120A Radiation Incidents in Diagnostic Radiology: What is the Role of the Physicist?

#### Participants

Christopher H. Cagnon, PhD, Los Angeles, CA (Presenter) Nothing to Disclose

# LEARNING OBJECTIVES

Identify areas of risk or potential staff and patient harm that may involve the diagnostic physicist. 2) Review emerging arenas of potential responsibility for the diagnostic physicist including regulatory and accreditation requirements, patient consults, and institutional priorities. 3) Discuss strategies for navigating gaps between responsibility and control from the physicist perspective.
 Review practices and preventative measures that can control and mitigate potential problems and risk. 5) Actions that can/should be taken by the physicist in the event of emergencies or accidents.

# RC120B Radiation Incidents in Radiation Oncology: What Does the Physicist Do Next?

Participants

Eric Ford, PhD, Seattle, WA (Presenter) Nothing to Disclose

For information about this presentation, contact:

eford@uw.edu

#### **LEARNING OBJECTIVES**

1) Understand the basics of investigating a near-miss or incident event including root-cause analysis. 2) Appreciate how incident learning data can inform the QA procedures of physicists. 3) Learn the new recommendations related to the physics review of plans and charts.

# ABSTRACT

Near-miss and incident events in healthcare provide an opportunity for learning and improving care. Here I focus on practical aspects of this process as it relates to the medical physicist in radiation oncology. I will briefly review the basics structure of incident learning and how and incident investigation is conducted using root cause analysis. Data and experience from incident learning can inform the QA procedures that physicists perform and, in particular, the review of plans and charts be a physicist prior to treatment. I will review the new recommendations are emerging around this practice which are informed by incident reports from national and international systems.

# RC120C Radiation Incidents in Diagnostic Radiology: What Does the Diagnostic Radiologist Do Next?

Participants Kimberly E. Applegate, MD, MS, Lexington, KY (*Presenter*) Nothing to Disclose

For information about this presentation, contact:

keapple@uky.edu

# LEARNING OBJECTIVES

1) To examine diagnostic radiology settings to ensure radiation incidents do not occur. 2) To develop a plan of action for post radiation incident evaluation. 3) To reflect on processes such as quality control, assurance, and PQI training, with a short list of resources.

# RC120D Radiation Incidents in Radiation Oncology: What Does the Radiation Oncologist Do Next?

Participants

Naomi R. Schechter, MD, Los Angeles, CA (Presenter) Nothing to Disclose

#### LEARNING OBJECTIVES

1) Describe strategies for responding to variety of potential near misses and errors in radiation oncology department 2) Describe strategies for learning from near misses and errors in radiation oncology department for purposes of quality improvement and prevention of future errors.

## ABSTRACT

In a radiation oncology department, incidents can range from minor to severe. We take them all seriously. Due to our many checks and balances, it is unusual for an error to reach the patient. In the rare case that an error does reach the patient, most can be corrected for, with minimal if any harm to the patient. Our goal is to learn from every incident, review our processes and continually improve the delivery of radiation therapy to prevent futureerrors from occurring.

# Active Handout:Naomi Rachel Schechter

http://abstract.rsna.org/uploads/2018/18001717/RSNA 2018 Radiation Incidents RC120D.pdf



# Advances in CT: Technologies, Applications, Operations-Quantitative CT (QIBA)

Sunday, Nov. 25 2:00PM - 3:30PM Room: E351



AMA PRA Category 1 Credits ™: 1.50 ARRT Category A+ Credit: 1.75

#### Participants

Ehsan Samei, PhD, Durham, NC (*Coordinator*) Research Grant, General Electric Company; Research Grant, Siemens AG; Advisory Board, medInt Holdings, LLC; License agreement, 12 Sigma Technologies; License agreement, Gammex, Inc Lifeng Yu, PhD, Chicago, IL (*Coordinator*) Nothing to Disclose

## ABSTRACT

CT has become a leading medical imaging modality, thanks to its superb spatial and temporal resolution to depict anatomical details. New advances have enabled extending the technology to depict physiological information. This has enabled a wide and expanding range of clinical applications. These advances are highlighted in this multi-session course. The course offers a comprehensive and topical depiction of these advances with material covering CT system innovations, CT operation, CT performance characterization, functional and quantitative applications, and CT systems devised for specific anatomical applications. The sessions include advances in CT system hardware and software, CT performance optimization, CT practice management and monitoring, spectral CT techniques, quantitative CT techniques, functional CT methods, and special CT use in breast, musculoskeletal, and interventional applications.

# Sub-Events

## RC121A Volumetry

Participants

Michael F. McNitt-Gray, PhD, Los Angeles, CA (Presenter) Institutional research agreement, Siemens AG; ;;;;

# LEARNING OBJECTIVES

1) Understand the role of lesion volumetry in CT, especially in the setting of oncologic imaging. 2) Understand the basic methods in lesion volumetry. 3) Understand the factors that influence the measurement of lesion volume in CT.

# RC121B Material Identification

Participants

Daniele Marin, MD, Durham, NC (Presenter) Research support, Siemens AG

## LEARNING OBJECTIVES

1) Review different dual-energy CT imaging techniques for material identification. 2) Provide an overview of clinically available applications of material identification using dual-energy CT. 3) Identify factors that can affect the reproducibility of quantitative measurements of material composition using dual-energy CT.

# **RC121C** Texture Characterization

#### Participants

Samuel G. Armato III, PhD, Chicago, IL (*Presenter*) Consultant, Aduro Biotech, Inc; Consultant, Boehringer Ingelheim GmbH Maryellen L. Giger, PhD, Chicago, IL (*Presenter*) Stockholder, Hologic, Inc; Shareholder, Quantitative Insights, Inc; Shareholder, QView Medical, Inc; Co-founder, Quantitative Insights, Inc; Royalties, Hologic, Inc; Royalties, General Electric Company; Royalties, MEDIAN Technologies; Royalties, Riverain Technologies, LLC; Royalties, Mitsubishi Corporation; Royalties, Canon Medical Systems Corporation

#### For information about this presentation, contact:

m-giger@uchicago.edu

s-armato@uchicago.edu

## **LEARNING OBJECTIVES**

1) Understand the concept of texture-based image characterization. 2) Identify radiologic tasks in CT that could benefit from image texture analysis. 3) Describe the limitations of these techniques.



Anatomical MR Imaging for Radiotherapy Planning and Guidance

Sunday, Nov. 25 2:00PM - 3:30PM Room: S103AB



AMA PRA Category 1 Credits ™: 1.50 ARRT Category A+ Credit: 1.75

**FDA** Discussions may include off-label uses.

#### Participants

Kristy K. Brock, PhD, Houston, TX (Moderator) License agreement, RaySearch Laboratories AB

#### Sub-Events

# RC122A State of the Art in Anatomical MR Imaging

Participants

Aradhana M. Venkatesan, MD, Houston, TX (Presenter) Research Grant, Canon Medical Systems Corporation;

# RC122B Clinical Need for Anatomical MR Imaging in Radiation Therapy

Participants

Cynthia Menard, MD, Montreal, QC (Presenter) Nothing to Disclose

# LEARNING OBJECTIVES

1) Understand the various roles of MRI in radiotherapy practice. 2) Identify pitfalls in integrating MRI in radiotherapy planning. 3) Describe anatomical sites where the integration of MRI is established as standard-care.

# RC122C Technical Challenges in the Integration of Anatomical MR Imaging into Radiotherapy

Participants

Carri Glide-Hurst, PHD, Detroit, MI (*Presenter*) Researcher, ViewRay, Inc; Research Consultant, Koninklijke Philips NV; Researcher, Koninklijke Philips NV; Researcher, Modus Medical Devices Inc; Equipment support, Medspira, LLC; Equipment support, QFix

#### LEARNING OBJECTIVES

To understand the unique imaging challenges and benefits for incorporating MRI into radiation therapy treatment planning.
 To describe the magnetic resonance simulation (MR-SIM) process to yield images that are more robust for radiation therapy planning.
 To describe emerging technologies in MR-only treatment planning and MR-guided radiation therapy and opportunities for collaboration between imaging and radiation therapy colleagues.



# **ACR Accreditation Updates I**

Sunday, Nov. 25 2:00PM - 3:30PM Room: N226

PH

AMA PRA Category 1 Credits ™: 1.50 ARRT Category A+ Credit: 1.75

#### **Participants**

James M. Kofler JR, PhD, Jacksonville, FL (Coordinator) Nothing to Disclose

#### **LEARNING OBJECTIVES**

1) Learn new and updated information for the ACR CT imaging accreditation program. 2) Become familiar with the requirements for the ACR MRI accreditation program. 3) Learn updated information on the ACR Nuclear Mediciant and PET accreditation program.

## Sub-Events

# RC123A ACR CT Accreditation Update

Participants Jessica Clements, MS, Monrovia, CA (*Presenter*) Nothing to Disclose

## For information about this presentation, contact:

jessicaclements@gmail.com

#### LEARNING OBJECTIVES

1) To understand the requirements of the ACR CT accreditation program, including updates to the QC manual and accreditation process.

# **Active Handout:Jessica Clements**

http://abstract.rsna.org/uploads/2018/18001926/2018 Nov 25 RSNA ACR CT Update RC123A.pdf

# RC123B ACR MRI Accreditation Update

Participants

Donna M. Reeve, MS, Houston, TX (Presenter) Nothing to Disclose

# LEARNING OBJECTIVES

1) Provide an overview of the current ACR MRI and Breast MRI Accreditation Program requirements. 2) Present recent changes to the MRI programs and updates to guidance documents. 3) Discuss how to prepare for a site visit.

## Active Handout:Donna M. Reeve

http://abstract.rsna.org/uploads/2018/18001927/RSNA 2018 ACR MRI Update Reeve Handout RC123B.pdf

# RC123C ACR Nuclear Medicine and PET Accreditation Update

Participants

Beth A. Harkness, MS, Detroit, MI (Presenter) Nothing to Disclose

#### LEARNING OBJECTIVES

1) Describe the requirements of the Nuclear Medicine and PET ACR accreditation programs. 2) Describe physics testing and QC requirements. 3) List common pitfalls in the accreditation process.

## ABSTRACT

The ACR Nuclear Medicine (NM) and PET Accreditation program is a means of demonstrating that the department is performing quality imaging studies. The program itself evolves to address the current state of nuclear and PET imaging and comments from users. This presentation will review the current status of the physics requirements for this process.

## Active Handout:Beth A. Harkness

http://abstract.rsna.org/uploads/2018/18001928/Update on Nuclear Medicine Accreditation 2018 RSNA RC123C.pdf



# The Best of RADIOLOGY in 2018: The Editors of RADIOLOGY Keep You Up to Date

Sunday, Nov. 25 2:00PM - 3:30PM Room: E353A



AMA PRA Category 1 Credits ™: 1.50 ARRT Category A+ Credit: 1.75

**FDA** Discussions may include off-label uses.

#### Sub-Events

## RC124A Review of 2018: New Research That Should Impact Your Practice

Participants

David A. Bluemke, MD, PhD, Bethesda, MD (Presenter) Nothing to Disclose

#### For information about this presentation, contact:

dbluemke@rsna.org

## **LEARNING OBJECTIVES**

1) Identify key publications over the past year that may affect your clinical practice. 2) Evaluate new research developments in the field of radiological imaging. 3) Describe new developments in radiology that may affect the management of your patients.

#### ABSTRACT

RADIOLOGY is the leading journal for publications leading to new, important and translatable discoveries in imaging research. In the past year, there continue to be basic developments in radiology, as well as new guidelines and clinical trials in imaging that affect your practice. Overall trends for new scientific studies reflect an increasing number of clinical trials being submitted from around the world in addition to those of North America. Publications from Europe have been prominent in recent years, but new research programs from countries such as Japan, South Korea and China are developing quickly. Large numbers of study subjects in clinical trials are now common, and tends to result in more robust demonstration of the efficacy of imaging interventions. Artificial intelligence applications are becoming commonplace in our publications, as are radiomics studies with increasing large numbers of study subjects. This seminar will highlight the results of key publications in the past year that are most likely to affect your practice in the near future, as well as presenting novel topics that are likely to be important to the field over the next 5 years.

## RC124B Innovations in Cardiothoracic Imaging in 2018

Participants

Albert De Roos, MD, Leiden, Netherlands (Presenter) Nothing to Disclose

#### For information about this presentation, contact:

a.de\_roos@lumc.nl

#### **LEARNING OBJECTIVES**

1) Key publications in cardiothoracic imaging 2018 will be highlighted.

## ABSTRACT

Cardiothoracic manuscripts are frequently introducing new technology, acquisition techniques and clinical evaluation. Major advances in cardiothoracic imaging over the last year published in Radiology will be discussed for their innovation and potential impact.

## RC124C Research and Innovations in Breast Imaging in 2018

Participants Linda Moy, MD, New York, NY ( $\ensuremath{\textit{Presenter}}\xspace$ ) Nothing to Disclose

#### For information about this presentation, contact:

linda.moy@nyumc.org

## LEARNING OBJECTIVES

1) To highlight key publications on breast imaging over the past year. 2) To discuss the implications of these publications for patient care

## RC124D New Developments in Neuroimaging in 2018

Participants Birgit B. Ertl-Wagner, MD, Toronto, ON (*Presenter*) Spouse, Stockholder, Siemens AG; ;

# LEARNING OBJECTIVES

1) Identify key publications over the past year that may affect your clinical practice. 2) Evaluate new research developments in the field of radiological imaging. 3) Describe new developments in radiology that may affect the management of your patients.



# Medical Physics 3.0: Re-envisioning Medical Physics in the Era of Value-based and Precision Healthcare

Sunday, Nov. 25 2:00PM - 3:30PM Room: S103CD

# PH

AMA PRA Category 1 Credits ™: 1.50 ARRT Category A+ Credit: 1.75

## Participants

Todd Pawlicki, PhD, La Jolla, CA (Presenter) Nothing to Disclose

Ehsan Samei, PhD, Durham, NC (*Presenter*) Research Grant, General Electric Company; Research Grant, Siemens AG; Advisory Board, medInt Holdings, LLC; License agreement, 12 Sigma Technologies; License agreement, Gammex, Inc

# LEARNING OBJECTIVES

1) Understand the broad trajectory of advances in the contribution of medical physics to human health. 2) Understand the attributes of excellent in clinical physics. 3) Outline processes to position physicists to have the competence and the confidence to fulfill their unique calling as scientific agents of precision and innovation in healthcare.



# Radiologist Peer-Review and Peer Learning-Options, Best Practices, and Future Directions

Sunday, Nov. 25 2:00PM - 3:30PM Room: S403B



AMA PRA Category 1 Credits ™: 1.50 ARRT Category A+ Credit: 1.75

## Participants

Jay K. Pahade, MD, New Haven, CT (*Moderator*) Consultant, General Electric Company David B. Larson, MD, MBA, Stanford, CA (*Presenter*) Grant, Siemens AG ; Grant, Koninklijke Philips NV Danny C. Kim, MD, New York, NY (*Presenter*) Nothing to Disclose

# **LEARNING OBJECTIVES**

1) To provide a brief review on radiologist peer review history, practices and discuss implementation of a department wide peer review conference. 2) To review methods of peer review and peer learning through IT improvements, institutional consensus criteria development, and creation of Rad-Path modules. 3) To discuss new methods addressing peer review with an emphasize on peer learning principles and quality improvement. 4) To allow open discussion with audience members on the pro's and con's of current peer review practices and changes to expect in the future.

#### **Honored Educators**

Presenters or authors on this event have been recognized as RSNA Honored Educators for participating in multiple qualifying educational activities. Honored Educators are invested in furthering the profession of radiology by delivering high-quality educational content in their field of study. Learn how you can become an honored educator by visiting the website at: https://www.rsna.org/Honored-Educator-Award/ David B. Larson, MD - 2014 Honored EducatorDavid B. Larson, MD - 2018 Honored Educator



MR Imaging of the Female Pelvis for Planning Fertility Preservation Therapy and the Appearance of the Pelvis Post Therapy (Interactive Session)

Sunday, Nov. 25 2:00PM - 3:30PM Room: S404CD



AMA PRA Category 1 Credits ™: 1.50 ARRT Category A+ Credit: 1.75

#### Participants

Hero K. Hussain, MD, Ann Arbor, MI (Moderator) Nothing to Disclose

# LEARNING OBJECTIVES

1) Discuss the spectrum of benign uterine and adnexal pathology. 2) Describe the fertility sparing procedures that can be performed for such conditions. 3) Explain the role of MRI in planning for these procedures. 4) To become familiar with most current various treatment options for gynecologic malignancies as well as expected imaging appearance of post treatment female pelvis. 5) To understand the expected and some unexpected imaging appearances as well as common pitfalls. 6) Appreciate low risk imaging features of adnexal masses, supporting potential management with surveillance, cystectomy, or oophorectomy rather than complete surgical staging. 7) Recognize imaging features of non myoinvasive endometrial cancer, for both diagnosis and surveillance if managed conservatively. 8) Understand imaging guidelines supporting surgical choice of trachelectomy in cervical cancer. 9) To become familiar with most current various treatment options for gynecologic malignancies as well as expected imaging appearance of post treatment female pelvis. 10) To understand the expected and some unexpected imaging appearance of post treatment female pelvis. 10) To understand the expected and some unexpected imaging appearances as well as common pitfalls.

#### Sub-Events

# RC129A MR Imaging for Planning Fertility Preservation Therapy in Benign Gynecologic Diseases

#### Participants

Jessica B. Robbins, MD, Madison, WI (Presenter) Nothing to Disclose

# LEARNING OBJECTIVES

1) Discuss the spectrum of benign uterine and adnexal pathology. 2) Describe the fertility sparing procedures that can be performed for such conditions. 3) Explain the role of MRI in planning for these procedures.

## Active Handout:Jessica B. Robbins

http://abstract.rsna.org/uploads/2018/18001116/RSNA 2018 benign pelvis RC129A.pdf

# RC129B MR Imaging of the Pelvis Post Therapy of Benign Gynecologic Conditions

Participants

Susan M. Ascher, MD, Washington, DC (Presenter) Nothing to Disclose

## LEARNING OBJECTIVES

1) To become familiar with most current various treatment options for gynecologic malignancies as well as expected imaging appearance of post treatment female pelvis. 2) To understand the expected and some unexpected imaging appearances as well as common pitfalls.

# RC129C MR Imaging for Planning Fertility Preservation Therapy in Gynecologic Malignancies

Participants

Katherine E. Maturen, MD, Ann Arbor, MI (*Presenter*) Royalties, Reed Elsevier; Royalties, Wolters Kluwer nv; Consultant, Allena Pharmaceuticals, Inc;

## For information about this presentation, contact:

kmaturen@umich.edu

## LEARNING OBJECTIVES

1) Appreciate low risk imaging features of adnexal masses, supporting potential management with surveillance, cystectomy, or oophorectomy rather than complete surgical staging. 2) Recognize imaging features of non myoinvasive endometrial cancer, for both diagnosis and surveillance if managed conservatively. 3) Understand imaging guidelines supporting surgical choice of trachelectomy in cervical cancer.

## **Honored Educators**

Presenters or authors on this event have been recognized as RSNA Honored Educators for participating in multiple qualifying educational activities. Honored Educators are invested in furthering the profession of radiology by delivering high-quality educational content in their field of study. Learn how you can become an honored educator by visiting the website at: https://www.rsna.org/Honored-Educator-Award/ Katherine E. Maturen, MD - 2014 Honored Educator

# RC129D MR Imaging of the Pelvis Post Therapy of Gynecologic Malignancies

Participants Liina Poder, MD, Mill Valley, CA (*Presenter*) Nothing to Disclose

For information about this presentation, contact:

liina.poder@ucsf.edu

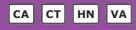
# LEARNING OBJECTIVES

1) To become familiar with most current various treatment options for gynecologic malignancies as well as expected imaging appearance of post treatment female pelvis. 2) To understand the expected and some unexpected imaging appearances as well as common pitfalls.



## **CTA from Head to Toe**

Sunday, Nov. 25 2:00PM - 3:30PM Room: S503AB



AMA PRA Category 1 Credits ™: 1.50 ARRT Category A+ Credit: 1.75

#### Participants

Christopher Lee, MD, Los Angeles, CA (Moderator) Nothing to Disclose

#### For information about this presentation, contact:

christopher.lee.1@med.usc.edu

## **LEARNING OBJECTIVES**

1) Describe techniques for CTA of the neck, upper and lower extremities. 2) Distinguish common artifacts on CTA of these anatomic regions. 3) Evaluate protocol/scanner modifications for optimal CTA imaging. 4) Formulate a CTA protocol to optimally image acute aortic syndrome. 5) Distinguish the imaging appearances and pitfalls of acute aortic syndrome. 6) Summarize the important measurements that help guide therapy. 7) Describe pre-procedural patient preparation including appropriate patient selection, contraindications, and beta-blockade. 8) Evaluate peri-procedural issues including vasodilation, continued heart rate control, and breathholding. 9) Evaluate Image acquisition including radiation dose reduction techniques and technique choice. 10) Describe postprocedural complications including contrast reactions and their management.

#### Sub-Events

#### RC131A Head and Neck CTA

Participants

Participants

Alexander Lerner, MD, Los Angeles, CA (Presenter) Research Grant, Koninklijke Philips NV; Research Grant, Bracco Group

## LEARNING OBJECTIVES

1) Describe techniques for CTA of the neck, upper and lower extremities. 2) Distinguish common artifacts on CTA of these anatomic regions. 3) Evaluate protocol/scanner modifications for optimal CTA imaging.

# RC131B Aortic CTA

Christopher Lee, MD, Los Angeles, CA (Presenter) Nothing to Disclose

#### For information about this presentation, contact:

christopher.lee.1@med.usc.edu

## LEARNING OBJECTIVES

1) Formulate a CTA protocol to optimally image acute aortic syndrome. 2) Distinguish the imaging appearances and pitfalls of acute aortic syndrome. 3) Summarize the important measurements that help guide therapy.

# ABSTRACT

Acute aortic syndrome (AAS) represents the triad of aortic dissection, intramural hematoma, and penetrating atherosclerotic ulcer. Imaging with CTA is essential for the accurate diagnosis of AAS. CTA protocols should optimally image the aorta while minimizing radiation exposure and intravenous contrast administration. Newer CT technology can reduce radiation dose and contrast delivery while preserving image quality. Minimally invasive treatment of acute aortic syndrome with thoracic endovascular aortic repair (TEVAR) has become increasingly popular.

## RC131C Cardiac CTA

Participants Cameron Hassani, MD, Los Angeles, CA (*Presenter*) Nothing to Disclose

For information about this presentation, contact:

ch602nyc@gmail.com

# LEARNING OBJECTIVES

1) Describe pre-procedural patient preparation including appropriate patient selection, contraindications, and beta-blockade. 2) Evaluate peri-procedural issues including vasodilation, continued heart rate control, and breathholding. 3) Evaluate Image acquisition including radiation dose reduction techniques and technique choice. 4) Describe postprocedural complications including contrast reactions and their management.

#### **Honored Educators**

Presenters or authors on this event have been recognized as RSNA Honored Educators for participating in multiple qualifying educational activities. Honored Educators are invested in furthering the profession of radiology by delivering high-quality educational content in their field of study. Learn how you can become an honored educator by visiting the website at: https://www.rsna.org/Honored-Educator-Award/ Cameron Hassani, MD - 2018 Honored Educator



## **Qualities of a Successful Leader**

Sunday, Nov. 25 2:00PM - 3:30PM Room: N227B

LM

AMA PRA Category 1 Credits ™: 1.50 ARRT Category A+ Credit: 1.75

#### **Participants**

James A. Brink, MD, Boston, MA (Moderator) Nothing to Disclose

#### For information about this presentation, contact:

yoshimi.anzai@hsc.utah.edu

## **LEARNING OBJECTIVES**

1) Develop an understanding of the essential traits and skills required for a leader to be successful, i.e. traits and states. 2) Develop an understanding of the common errors made by leaders in academic and private practices enabling the attendee to obtain the 'learnings' without the 'lumps. 3) Acquire the skills of succession planning needed to ensure that the success of your organization is sustainable over time and leadership transitions. (This course is part of the Leadership Track)

#### Sub-Events

# RC132A Life Lessons for Successful Leadership

Participants

James A. Brink, MD, Boston, MA (Presenter) Nothing to Disclose

# LEARNING OBJECTIVES

1) To understand the importance of emotional intelligence in for successful leadership. 2) To explore the relationship between communication style and the effectiveness of leadership. 3) To consider techniques that elevate the level of respect and trust in an organization.

# RC132B Key Concepts for Successful Leadership

Participants

Jonathan S. Lewin, MD, Atlanta, GA (Presenter) Nothing to Disclose

## LEARNING OBJECTIVES

View learning objectives under main course title. (This course is part of the Leadership Track)

#### **Honored Educators**

Presenters or authors on this event have been recognized as RSNA Honored Educators for participating in multiple qualifying educational activities. Honored Educators are invested in furthering the profession of radiology by delivering high-quality educational content in their field of study. Learn how you can become an honored educator by visiting the website at: https://www.rsna.org/Honored-Educator-Award/ Jonathan S. Lewin, MD - 2012 Honored Educator

# RC132C Leadership: Understanding the Organizational Culture

Participants

N. Reed Dunnick, MD, Ann Arbor, MI (Presenter) Royalties, Wolters Kluwer nv; Editor, Reed Elsevier

#### LEARNING OBJECTIVES

1) Recognize historical examples of leaders, in addition to how you can recognize and emulate their favorable characteristics that draw you to their leadership attributes. 2) Understand an overview of leadership references, where and how to access the same, how the related body of knowledge has evolved, and current perspectives concerning leaders and leadership. (This course is part of the Leadership Track)



# MR Imaging-guided Breast Biopsy (Hands-on)

Sunday, Nov. 25 2:00PM - 3:30PM Room: E260



AMA PRA Category 1 Credits ™: 1.50 ARRT Category A+ Credit: 1.75

# Participants

Manisha Bahl, MD, MPH, Boston, MA (Presenter) Nothing to Disclose Rosalind P. Candelaria, MD, Houston, TX (Presenter) Nothing to Disclose Sarah M. Friedewald, MD, Chicago, IL (Presenter) Consultant, Hologic, Inc; Research Grant, Hologic, Inc; Brian Johnston, MD, Gilbert, AZ (Presenter) Nothing to Disclose Jennifer R. Kohr, MD, Seattle, WA (Presenter) Nothing to Disclose Lizza Lebron, MD, West Harrison, NY (Presenter) Nothing to Disclose Diana L. Lam, MD, Seattle, WA (Presenter) Grant, General Electric Company Santo Maimone IV, MD, Jacksonville, FL (Presenter) Research Consultant, GRAIL Inc Cecilia L. Mercado, MD, New York, NY (Presenter) Nothing to Disclose Bethany L. Niell, MD, PhD, Tampa, FL (*Presenter*) Nothing to Disclose Jessica H. Porembka, MD, Dallas, TX (*Presenter*) Nothing to Disclose Elissa R. Price, MD, San Francisco, CA (Presenter) Nothing to Disclose Jean M. Seely, MD, Ottawa, ON (Presenter) Nothing to Disclose Toma Omofoye, MD, Houston, TX (Presenter) Nothing to Disclose Gaiane M. Rauch, MD, PhD, Houston, TX (Presenter) Nothing to Disclose Roberta M. Strigel, MD, Madison, WI (Presenter) Research support, General Electric Company Jocelyn A. Rapelyea, MD, Washington, DC (Presenter) Speakers Bureau, General Electric Company; Consultant, Transmed7; Ryan W. Woods, MD, MPH, Madison, WI (Presenter) Nothing to Disclose Beatriu Reig, MD, New York, NY (Presenter) Nothing to Disclose Erin I. Neuschler, MD, Chicago, IL (Presenter) Research Grant, Seno Medical Instruments, Inc; Speaker, Northwest Imaging Forums, Inc; ; ;

## For information about this presentation, contact:

jessica.porembka@utsouthwestern.edu

rstrigel@uwhealth.org

mbahl1@mgh.harvard.edu

jeseely@toh.ca

rwoods@uwhealth.org

jrapelyea@mfa.gwu.edu

dllam@uw.edu

gmrauch@mdanderson.org

sarah.friedewald@nm.org

## LEARNING OBJECTIVES

1) Explain why MR-guided breast biopsy is needed for patient care. 2) Identify relative and absolute contraindications to MR-guided breast biopsy. 3) Describe criteria for MR-guided breast biopsy patient selection. 4) Debate risks and benefits of pre-biopsy targeted ultrasound for suspicious MRI findings. 5) Understand the basic MR-guided biopsy procedure, protocol and requirements for appropriate coil, needle and approach selection. 6) Manage patients before, during and after MR-guided breast biopsy. 7) Define the benefits and limitations of MR-guided vacuum assisted breast biopsy. 8) Apply positioning and other techniques to challenging combinations of lesion location and patient anatomy for successful MR-guided biopsy.

#### ABSTRACT

This course is intended to provide basic didactic instruction and hands-on experience for MR-guided breast biopsy. Because of the established role of breast MRI in the evaluation of breast cancer through screening and staging, there is a proven need for MR-guided biopsy of the abnormalities that can only be identified at MRI. This course will be devoted to the understanding and identification of: 1) appropriate patient selection 2) optimal positioning for biopsy 3) target selection and confirmation 4) various biopsy technologies and techniques 5) potential problems and pitfalls and 6) radiology/pathology concordance. Participants will spend 30 minutes in didactic instruction followed by 60 minutes practicing MR-guided biopsy using provided phantoms. Various combinations of full size state-of-the-art breast MRI coils, biopsy localization equipment and needles from multiple different vendors will be available for hands-on practice. Some stations will have monitors loaded with targeting software. Expert breast imagers from around the world will be at each of 10 stations to provide live coaching, tips, techniques and advice.

#### Active Handout: Roberta Marie Strigel

http://abstract.rsna.org/uploads/2018/4426451/Strigel-RSNA-MRIBx-2018-Handout RC150.pdf



Nerve Ultrasound Based on a Regional Approach: Hip to Knee (Hands-on)

Sunday, Nov. 25 2:00PM - 3:30PM Room: E264



AMA PRA Category 1 Credits ™: 1.50 ARRT Category A+ Credit: 1.75

# Participants

Jon A. Jacobson, MD, Ann Arbor, MI (Presenter) Research Consultant, BioClinica, Inc; Advisory Board, General Electric Company; Advisory Board, Koninklijke Philips NV; Royalties, Reed Elsevier Kenneth S. Lee, MD, Madison, WI (Presenter) Grant, General Electric Company Research support, SuperSonic Imagine Research support, Johnson & Johnson Consultant, Echometrix, LLC Royalties, Reed Elsevier J. Antonio Bouffard, MD, Detroit, MI (Presenter) Nothing to Disclose Marnix T. van Holsbeeck, MD, Detroit, MI (Presenter) Minor stockholder, Koninklijke Philips NV; Minor stockholder, General Electric Company; Stockholder, MedEd3D; Grant, Siemens AG; Grant, General Electric Company; Joseph H. Introcaso, MD, Neenah, WI (Presenter) Nothing to Disclose Viviane Khoury, MD, Philadelphia, PA (Presenter) Nothing to Disclose Marina Kislyakova, MD, Moscow, Russia (Presenter) Nothing to Disclose Ximena L. Wortsman, MD, Santiago, Chile (Presenter) Nothing to Disclose Federico Zaottini, Genova, Italy (Presenter) Nothing to Disclose Ghiyath Habra, MD, Troy, MI (Presenter) Nothing to Disclose Lodewijk J. van Holsbeeck, MD, Lansing, MI (Presenter) Nothing to Disclose Carlo Martinoli, MD, Genova, Italy (Presenter) Nothing to Disclose Etienne Cardinal, MD, Montreal, QC (Presenter) Nothing to Disclose Humberto G. Rosas, MD, Madison, WI (Presenter) Nothing to Disclose David P. Fessell, MD, Ann Arbor, MI (Presenter) Nothing to Disclose Girish Gandikota, MBBS , Ann Arbor, MI (Presenter) Nothing to Disclose

For information about this presentation, contact:

viviane.khoury@uphs.upenn.edu

jjacobsn@umich.edu

carlo.martinoli@unige.it

mkisliakova@yandex.ru

klee2@uwhealth.org

# LEARNING OBJECTIVES

1) Familiarize course participants with the ultrasound appearance of nerves and the scanning techniques used to image them about the hip and knee. 2) Emphasize the ultrasound anatomy of the femoral, sciatic and peroneal nerves and their divisional branches at their common sites of entrapment. 3) Learn the technique to image some minor nerves in their course throughout the proximal lower extremity, such as the lateral and posterior femoral cutaneous, the obturator, the saphenous and the sural. 4) Outline the range of clinical conditions where ultrasound is appropriate as the primary imaging modality for nerve assessment.

#### ABSTRACT

In recent years, ultrasound of the musculoskeletal and peripheral nervous systems is becoming an increasingly imaging tool with an expanding evidence base to support its use. However, the operator dependent nature and level of technical expertise required to perform an adequate ultrasound assessment means that appropriate training is required. For this purpose, the present course will demonstrate the basic principles of musculoskeletal ultrasound with a special focus on nerves of the proximal lower extremity (hip to knee). The standardized techniques of performing an adequate ultrasound study of the femoral, lateral and posterior femoral cutaneous, obturator, peroneal, saphenous, sciatic, sural nerves and their divisional branches will be illustrated. The hands-on workshops will provide the opportunity to interactively discuss the role of ultrasound in this field with expert instructors. Participants will be encouraged to directly scan model patients. A careful ultrasound approach with thorough understanding of soft-tissue planes and extensive familiarity with anatomy are prerequisites for obtaining reliable information regarding the affected structure and the site and nature of the disease process affecting it.

## Active Handout:Carlo Martinoli

http://abstract.rsna.org/uploads/2018/4404504/Handouts Nerves Ultrasound Based RC152.pdf

## **Honored Educators**

Presenters or authors on this event have been recognized as RSNA Honored Educators for participating in multiple qualifying educational activities. Honored Educators are invested in furthering the profession of radiology by delivering high-quality educational content in their field of study. Learn how you can become an honored educator by visiting the website at: https://www.rsna.org/Honored-Educator-Award/ Jon A. Jacobson, MD - 2012 Honored EducatorJon A. Jacobson, MD - 2017 Honored Educator



# Deep Learning in Radiology: How Do We Do It?

Sunday, Nov. 25 2:00PM - 3:30PM Room: E450A



AMA PRA Category 1 Credits ™: 1.50 ARRT Category A+ Credit: 1.75

#### Participants

Luciano M. Prevedello, MD, MPH, Dublin, OH (Moderator) Nothing to Disclose

#### LEARNING OBJECTIVES

1) Learn what Deep Learning is and how it may be applied to Radiology. 2) Understand the challenges and benefits of creating a laboratory dedicated to machine learning in Radiology. 3) Be exposed to several applied examples of Deep Learning in Radiology at different institutions.

#### Sub-Events

## RC153A Ohio State University Experience

Participants

Luciano M. Prevedello, MD, MPH, Dublin, OH (Presenter) Nothing to Disclose

## LEARNING OBJECTIVES

1) Describe the existing infrastructure to handle pixel and non pixel data at our institution for translational research in machine learning. 2) Learn some applications of Deep Learning in Radiology through examples.

# RC153B Stanford University Experience

Participants

Curtis P. Langlotz, MD,PhD, Menlo Park, CA (*Presenter*) Advisory Board, Nuance Communications, Inc; Shareholder, whiterabbit.ai; Advisory Board, whiterabbit.ai; Shareholder, Nines.ai; Consultant, Nines.ai; Shareholder, TowerView Health; Research Grant, Koninklijke Philips NV; Research Grant, Siemens AG; Research Grant, Alphabet Inc;

# LEARNING OBJECTIVES

1) Consider the types of clinical problems that are best suited to machine learning solutions. 2) Understand how 'deep' neural networks work, and the technology and people needed for a successful program. 3) Learn about the type of work performed by an artificial intelligence laboratory focused on medical imaging and computer vision. 4) Analyze the key technologies needed to create large annotated training data sets.

# RC153C Mayo Clinic Rochester Experience

Participants

Bradley J. Erickson, MD, PhD, Rochester, MN (*Presenter*) Stockholder, OneMedNet Corporation; Stockholder, VoiceIt Technologies, LLC; Stockholder, FlowSigma;

## For information about this presentation, contact:

bje@mayo.edu

# LEARNING OBJECTIVES

1) Describe Mayo experience with deep learning radiomics technology.



## Leveraging IT to Optimize Quality in Radiology

Sunday, Nov. 25 2:00PM - 3:30PM Room: N229



AMA PRA Category 1 Credits ™: 1.50 ARRT Category A+ Credit: 1.75

#### **Participants**

Paul J. Chang, MD, Chicago, IL (*Moderator*) Co-founder, Koninklijke Philips NV; Researcher, Koninklijke Philips NV; Researcher, Bayer AG; Advisory Board, Aidoc Ltd; Advisory Board, EnvoyAI; Advisory Board, Inference Analytics

# Sub-Events

# RC154A IHE and Beyond: Improving Radiology Quality through IT Interoperability

#### Participants

Tessa S. Cook, MD, PhD, Philadelphia, PA (Presenter) Royalties, Osler Institute

#### For information about this presentation, contact:

tessa.cook@uphs.upenn.edu

## LEARNING OBJECTIVES

1) Discuss the importance of interoperability of health IT systems within and beyond radiology. 2) Discuss how IHE efforts can promote this interoperability. 3) Describe other interoperability efforts to improve communication of health IT systems.

# RC154B Business Intelligence and Analytics: Dashboards, Scorecards, and Beyond

#### Participants

Paul J. Chang, MD, Chicago, IL (*Presenter*) Co-founder, Koninklijke Philips NV; Researcher, Koninklijke Philips NV; Researcher, Bayer AG; Advisory Board, Bayer AG; Advisory Board, Aidoc Ltd; Advisory Board, EnvoyAI; Advisory Board, Inference Analytics

## LEARNING OBJECTIVES

1) The technical steps required to develop and implement dashboards and scorecards (including data/state aggregation, semantic normalization, modeling, data mining, and presentation) will be discussed. 2) Specific strategies and technologies that can be used to create dashboards and scorecards (including HL7, DICOM, ETL, web services, and SOA) will be illustrated. 3) Strategies to create a sustainable and agile architecture to support advanced business intelligence and analytics (BIA) tools will be explored.

#### ABSTRACT

Current and near future requirements and constraints will require radiology practices to continuously improve and demonstrate the value they add to the enterprise. Merely "managing the practice" will not be sufficient; groups will be required to compete in an environment where the goal will be measurable improvements in efficiency, productivity, quality, and safety. Although the phrase "one cannot improve a process unless one can measure it" is a familiar platitude, it is an increasingly important and relevant concept. The proper leveraging of formal Business Intelligence and Analytics (BIA) is a critical, absolutely essential strategy for any radiology group. Although currently underutilized, concepts such as Key Performance Indicators (KPIs), tactical dashboards, and strategic scorecards, should be familiar tools for radiology groups attempting to "navigate disruption."

# RC154C Leveraging IT to Optimize Quality in Radiology

#### Participants

Paul J. Chang, MD, Chicago, IL (*Presenter*) Co-founder, Koninklijke Philips NV; Researcher, Koninklijke Philips NV; Researcher, Bayer AG; Advisory Board, Bayer AG; Advisory Board, Aidoc Ltd; Advisory Board, EnvoyAI; Advisory Board, Inference Analytics

# LEARNING OBJECTIVES

1) Discuss how modern radiology quality expectations require a greater degree of "meaningful innovation" in imaging IT and informatics. 2) Introduced to examples of next generation IT tools and models that can help achieve both improved efficiency and quality. 3) Describe how and why radiology must redefine and re-engineer itself in order to fully take advantage of these next generation electronic based practice tools. The impact these changes in practice management can have on quality, workflow efficiency, and productivity will be discussed.

#### ABSTRACT

Radiology practices have benefited from the adoption of electronic-based information technology, especially with respect to practice efficiency. However, there is great opportunity to further leverage information technology to significantly improve quality within the radiology practice. However, electronic tools, such as PACs, RIS, and speech recognition (along with their associated workflow), are still relatively immature and arguably support only "commodity-level" capability. There is a critical need for a new generation of "meaningful innovation" in radiology IT that will allow radiology to maximize value to patients and other stakeholders by significantly improving both efficiency and quality. Radiologists must be "value innovators" who maximally leverage information technology to ensure their relevance and value to patient care through measureable improvements in quality, efficiency, and safety.



#### RCA12

# Technologies for Creating Educational Content and Teaching Files (Hands-on)

Sunday, Nov. 25 2:00PM - 3:30PM Room: S401AB



AMA PRA Category 1 Credits ™: 1.50 ARRT Category A+ Credit: .50

## Participants

Harprit S. Bedi, MD, Boston, MA (Moderator) Nothing to Disclose

# Sub-Events

# **RCA12A Podcasting and Screencasting for Teaching**

Participants

Mahesh M. Thapa, MD, Seattle, WA (Presenter) Nothing to Disclose

# RCA12B ePublishing

Participants Michael L. Richardson, MD, Seattle, WA (*Presenter*) Nothing to Disclose

# LEARNING OBJECTIVES

Be familiar with pros and cons of ePublishing in general.
 Be aware of several free ePublishing programs and where to find them.
 Be aware of the ramifications of digital rights management and book pricing.
 Know how to convert an eBook into a physical paper book as needed.

#### **Honored Educators**

Presenters or authors on this event have been recognized as RSNA Honored Educators for participating in multiple qualifying educational activities. Honored Educators are invested in furthering the profession of radiology by delivering high-quality educational content in their field of study. Learn how you can become an honored educator by visiting the website at: https://www.rsna.org/Honored-Educator-Award/ Michael L. Richardson, MD - 2013 Honored EducatorMichael L. Richardson, MD - 2015 Honored Educator

# RCA12C Incorporating the iPad in Resident Education: Using Mobile Technology to Improve the Way We Teach

Participants Harprit S. Bedi, MD, Boston, MA (*Presenter*) Nothing to Disclose



#### RCB12

RSNA Diagnosis Live Interactive and Mobile Device Integrated Audience Response: Tips, Tricks, and How to Get Started (Hands-on)

Sunday, Nov. 25 2:00PM - 3:30PM Room: S401CD



AMA PRA Category 1 Credits ™: 1.50 ARRT Category A+ Credit: 0

#### **Participants**

Christopher G. Roth, MD,MS, Philadelphia, PA (*Moderator*) Nothing to Disclose Christopher G. Roth, MD,MS, Philadelphia, PA (*Presenter*) Nothing to Disclose Sandeep P. Deshmukh, MD, Philadelphia, PA (*Presenter*) Nothing to Disclose

For information about this presentation, contact:

christopher.roth@jefferson.edu

## LEARNING OBJECTIVES

1) Appreciate the higher receptiveness of interactive content by adult learners compared with traditional didactic techniques. 2) Understand the basic operational features of the Diagnosis Live audience participation authoring tool, including the types of questions offered and how to embed them into PowerPoint presentations. 3) Learn how to manage the Diagnosis Live administrator portal and launch and run interactive games and review analytics regarding student performance.



#### RCC12

Core Cybersecurity for Imaging Departments and Imagers: Threats, Vulnerabilities and Best Practices Part 1

Sunday, Nov. 25 2:00PM - 3:30PM Room: S501ABC



AMA PRA Category 1 Credits ™: 1.50 ARRT Category A+ Credit: 1.75

#### Participants

Christopher J. Roth, MD, Raleigh, NC (Moderator) Nothing to Disclose

# LEARNING OBJECTIVES

1) Understand the changing environment of network and internet connected devices and software. 2) Be aware of the motivations and tactics of current threat actors. 3) Understand common security issues found in medical devices. 4) Know simple actions that can decrease risk. 5) Understand the vulnerabilities of imaging system modalities to security and privacy breaches. 6) Determine ways to protect and secure imaging systems from internal and external threats. 7) Describe institutional best-practices to maintain protection yet provide necessary accessibility for imaging modalities.

# ABSTRACT

All imaging department devices are potential sites of risk for cybersecurity attack. Such attacks have compromised enterprise data security, modality function, patient health data, and ongoing patient care. This session will describe common insider and outsider threats, and highest yield steps for mitigation at small and large imaging sites.

#### Sub-Events

# RCC12A Sounding the Alarm in Healthcare Cybersecurity: Escalating Threats to Patient Health

Participants

James Whitfill, MD, Scottsdale, AZ (Presenter) President, Lumetis LLC

## LEARNING OBJECTIVES

1) Understand the changing environment of network and internet connected devices and software. 2) Be aware of the motivations and tatics of current threat actors. 3) Understand common security issues found in medical devices. 4) Know simple actions that can decrease risk. 5) Understand the steps to implement a medical device security program.

#### ABSTRACT

Medical devices are increasingly becoming dependent on technology and network connectivity, at a time that the electronic environment is becoming more dangerous. Because of this medical devices and systems can become easy targets for attackers attempting to access PHI, disrupt patient care or even harm a patient. When tested, these devices have been shown to have multiple vulnerabilities. These vulnerabilities range from hardcoded passwords, publically available service passwords and no encryption of patient data. Because of this institutions using these devices need to work with their vendors to improve the security of medical devices and take actions themselves to help protect their environment and patients. There are simple steps to decrease your risk and ways, even with limited resources and skills, to start to evaluate medical devices at your institution.

# RCC12B The Bare Minimum Cybersecurity Hygiene for Radiologists

Participants

Christopher J. Roth, MD, Raleigh, NC (Presenter) Nothing to Disclose

#### LEARNING OBJECTIVES

1) Appreciate the anatomy of a typical healthcare advanced persistent threat cyberattack. 2) Learn the underpinnings and impact of typical protections including anti-malware, multi-factor authentication, personal device managers, firewalls, encryption, password managers, URL and attachment screeners, popup blockers, physical data protections, and identity theft protection. 3) Understand high yield procurement, contingency planning, auditing, training, and hiring next steps. 4) Realize that health care entities will never be completely private or secure, and there is a balance of functionality, efficiency, and care process that must be understood against privacy and security protections.

# RCC12C Knowing if Your Imaging Systems are Secure and Keeping Them That Way

Participants

J. Anthony Seibert, PhD, Sacramento, CA (Presenter) Advisory Board, Bayer AG

For information about this presentation, contact:

jaseibert@ucdavis.edu

#### **LEARNING OBJECTIVES**

1) Appreciate the evolving landscape of cyberthreats to healthcare and Radiology. 2) Understand the different targeting strategies used by cyber attackers. 3) Realize imaging system security weaknesses and everyone's responsibilities to keep systems safe.



## PS12

# **Sunday Afternoon Plenary Session**

Sunday, Nov. 25 4:00PM - 5:45PM Room: Arie Crown Theater



# Participants

Vijay M. Rao, MD, Philadelphia, PA (Presenter) Nothing to Disclose

#### Sub-Events

# PS12A Report of the RSNA Research and Education Foundation

Participants

N. Reed Dunnick, MD, Ann Arbor, MI (Presenter) Royalties, Wolters Kluwer nv; Editor, Reed Elsevier

# PS12B Image Interpretation Session

Participants

Donald P. Frush, MD, Durham, NC (*Moderator*) Nothing to Disclose John Eng, MD, Cockeysville, MD (*Introduction*) Nothing to Disclose Laura W. Bancroft, MD, Orlando, FL (*Presenter*) Author with royalties, Wolters Kluwer nv; Speaker, World Class CME; Editor, Thieme Medical Publishers, Inc; Travel support, Thieme Medical Publishers, Inc ; ; Matthew S. Davenport, MD, Ann Arbor, MI (*Presenter*) Nothing to Disclose Tomas C. Franquet, MD, Barcelona, Spain (*Presenter*) Nothing to Disclose R. Paul Guillerman, MD, Houston, TX (*Presenter*) Consultant, Guerbet SA Christopher P. Hess, MD, PhD, Mill Valley, CA (*Presenter*) Nothing to Disclose Andrea Laghi, MD, Rome, Italy (*Presenter*) Nothing to Disclose Elizabeth A. Morris, MD, New York, NY (*Presenter*) Nothing to Disclose Pamela K. Woodard, MD, Saint Louis, MO (*Presenter*) Research agreement, Siemens AG; Research, Eli Lilly and Company; Research, F. Hoffmann-La Roche Ltd; ; ; ; ; ;

For information about this presentation, contact:

woodardp@wustl.edu



#### RCA13

# 3D/VR/AR Imaging: Staying on the Cutting Edge of Brain Anatomy/Pathology (Hands-on)

Sunday, Nov. 25 4:00PM - 5:30PM Room: S401AB



AMA PRA Category 1 Credits ™: 1.50 ARRT Category A+ Credit: 0

# Participants

Komal B. Shah, MD, Houston, TX (*Presenter*) Nothing to Disclose Maria Gule-Monroe, MD, Houston, TX (*Presenter*) Nothing to Disclose Melissa M. Chen, MD, Houston, TX (*Presenter*) Nothing to Disclose Jill V. Hunter, MD, Houston, TX (*Presenter*) Author with royalties, Wolters Kluwer nv Halyna Pokhylevych, MD, Lviv, Ukraine (*Presenter*) Nothing to Disclose Donald F. Schomer, MD, Fountain Hills, AZ (*Presenter*) Stockholder, Vertos Medical, Inc Stockholder, Sinopsys Surgical, Inc Vinodh A. Kumar, MD, Houston, TX (*Presenter*) Nothing to Disclose

## For information about this presentation, contact:

halia1309@gmail.com

# ABSTRACT

Brain Atlas/VR/AR imaging: Staying on the Cutting Edge of Brain Anatomy/Pathology This hands-on workshop will demonstrate an advanced brain atlas which fuses with a patient's MR brain imaging. Attendees will be able to navigate a patient's brain with 3D googles using Virtual Reality (VR) technology. Augmented Reality (AR) technology will also be presented. The atlas presented has extensive data related to brain anatomy, vasculature and function. It can map white fiber tracts when conventional DTI cannot be generated as a result of tumor or vasogenic edema. The atlas also takes into account tumor mass effect by deforming adjacent anatomical structures. Given its 3D capability, this tool has been used in neurosurgical pre-operative planning cases. Intraoperatively, the atlas has been successfully fused to neuronavigation systems to aid in real time surgical guidance. The atlas also has been very useful for radiation treatment planning. It supports individualized medicine, through the generation of videos related to the patient's brain tumor assisting patient education.



#### RCC13

## **Overview of Medical 3D Printing**

Sunday, Nov. 25 4:00PM - 5:30PM Room: S501ABC



AMA PRA Category 1 Credits ™: 1.50 ARRT Category A+ Credit: 1.75

## Participants

Jane S. Matsumoto, MD, Rochester, MN (*Moderator*) Nothing to Disclose William J. Weadock, MD, Ann Arbor, MI (*Moderator*) Owner, Weadock Software, LLC

#### LEARNING OBJECTIVES

1) Understand basic 3D printing technology. 2) Learn the history of 3D printing in medicine. 3) Describe steps in production of anatomic models. 4) List current clinical, educational and research applications of 3D printing of imaging data. 5) Learn about potential future opportunities.

#### ABSTRACT

There has been growing interest and involvement in 3D printing of anatomic models in the last few years. There are increasing reports in the literature on the usefulness of models in multiple specialty areas for surgical planning. This technology is rapidly developing with faster, less expensive and more versatile printers. It is within the reach of most radiology departments to establish some level of 3D printing service in response to surgical need. Imaging is at the center of the 3D printing and radiology offers the best home for it for many reasons. This process depends on acquisition of high resolution imaging data, segmenation by staff knowledgeable in imaging and anatomy and pathology and an embedded quality control program. Physical anatomic models created from an individual's own imaging studies offer improved comprehension of an individual's complex anatomy as an aid in presurgical planning. They are also impactful for patient education and informed consent. Models are being integrated into medical education programs and are used for procedural training simulation. Overall this developing field of medical 3D printing of imaging data offers radiology an opportunity for a unique value added service for patient care and for medical education.

#### Sub-Events

# RCC13A Medical 3D Printing for Radiology: A View to the Future

Participants

Jane S. Matsumoto, MD, Rochester, MN (Presenter) Nothing to Disclose

# LEARNING OBJECTIVES

1) Teach the steps required to build hallow vascular phantoms which could be used for flow and endovascular procedure simulations. 2) Demonstrate how 3D printed phantoms could be used for angiography radiomics. 3) Demonstrate the benefit of using 3D printed cardiovascular phantoms to test endovascular devices. 4) Demonstrate the benefit of using 3D printed cardiovascular phantoms for pre-treatment simulations in high risk surgery patients.

# ABSTRACT

Patient specific vascular phantoms manufactured using 3D printing can be a valuable tool for device testing, software validation and endovascular treatment planning. Traditional vascular phantoms are made from one material and they are a simplification of the patient anatomy. They model one artery, rarely included branching arteries and the arterial wall mechanical properties are not properly modeled. In addition, inclusion of pathologies such as atherosclerotic plaques or surrounding anatomical structures is practically inexistent. These simple patient specific models can be used to evaluate endovascular devices, validate software or simulate interventions but their simplicity could misguide the user about the true clinical situations. New advancements in multimaterial 3D printing allow development of phantoms replicating complex vascular systems and vascular disease which can mimic mechanical properties of the vessels and physiological aspects of the blood flow. In this presentation we will present how to design complex vascular phantoms which includes significant distal vasculature and vascular lesions such as atherosclerotic plaques and aneurysms. We will show various applications of the phantoms to study device behavior and software validation. For diagnostic software validation, we will demonstrate how such phantoms could be used for angiography radiomics research. In the second part of the lecture, we will present the use of the patient specific vascular phantoms for treatment planning of vascular diseases such as abdominal aortic aneurysms with the Fenestrated Endo Vascular Aortic Repair device. We will show how significant surgery outcome improvementwas achieved in twelve patients undergoing pre-treatment simulation using patient specific phantoms.

# RCC13B Research Applications of 3D Printing

Participants

Ciprian N. Ionita, PhD, Buffalo, NY (*Presenter*) Grant, Canon Medical Systems Corporation; Grant, Stratasys, Ltd; Grant, Medtronic plc;

#### **LEARNING OBJECTIVES**

1) Discuss current clinical applications of 3D printing. 2) Describe major 3D printing technologies. 3) Identify workflows appropriate for clinical 3D printing. 4) Develop a program for quality assessment of medical 3D-printed models.

#### ABSTRACT

 Medical 3D printing is emerging as a clinically relevant imaging tool that is currently being used in directing preoperative and intraoperative planning in many surgical specialties. These life-sized models of human anatomy and pathology and patient-specific implants and surgical guides to facilitate the required procedures are fabricated using data from standard imaging modalities such as CT, MRI, echocardiography and rotational angiography. Printed models are suitable for planning both surgical and minimally invasive procedures. Major specialties that use these models and surgical aides are vascular, thoracic and orthopedic surgery services, as well as increasingly neurosurgery and interventional radiology. In a number of these specialties added value has been reported toward improving outcomes, minimizing peri-operative risk, and helping develop new procedures such as transcatheter mitral valve replacements. Anatomic models enable surgeons and interventional radiologists to assimilate information more quickly than image review, choose the optimal surgical approach, and perform a procedure more safely and in a shorter time.Finally, patient-specific 3D-printed implants are also beginning to appear and may have significant impact on cosmetic and life-saving procedures in the future. In summary, medical 3D printing is rapidly evolving and may be a potential game-changer that radiologists are ideally-suited to deliver.

# RCC13C Overview of Clinical Applications

Participants

Dimitris Mitsouras, PhD, Boston, MA (Presenter) Research Grant, Canon Medical Systems Corporation;

#### **Honored Educators**

Presenters or authors on this event have been recognized as RSNA Honored Educators for participating in multiple qualifying educational activities. Honored Educators are invested in furthering the profession of radiology by delivering high-quality educational content in their field of study. Learn how you can become an honored educator by visiting the website at: https://www.rsna.org/Honored-Educator-Award/ Frank J. Rybicki III, MD, PhD - 2016 Honored Educator

# RCC13D Contemporary Issues in 3D Printing

Participants

Frank J. Rybicki III, MD, PhD, Ottawa, ON (Presenter) Medical Director, Imagia Cybernetics Inc

#### For information about this presentation, contact:

frybicki@toh.ca

#### LEARNING OBJECTIVES

1. To understand the rationale for the creation of the RSNA Special Interest Group (SIG) in 3D Printing 2. To review the accomplishments of the SIG and why these achievements are important 3. To define the different roles of medical professionals in 3D printing 4. To review the challenges in 3D printing and anatomic modeling, particularly as it relates to physican professional and technical reimbursement.

#### ABSTRACT

This presentation will describe and detail the important features of modern 3D printing (medical modeling, anatomic modeling) and provide an outline for the future direction of this practice in the medical sector.